Supplementary Information

Evolution of Multicomponent [Pd_2ABCD] Cages

Kai Wu,[1,2] Elie Benchimol,[1] Ananya Baksi[1,3] and Guido H. Clever[1]*

[1]*Department of Chemistry and Chemical Biology, TU Dortmund University, Otto-Hahn-Str. 6, 44227 Dortmund, Germany.*

[2]*Present address: Department of Chemistry, University of Cambridge, Lensfield Road, Cambridge, CB2 1EW, UK.*

[3]*Present address: Department of Chemistry, Jadavpur University, Kolkata-700032, West Bengal, India.*

E-mail: guido.clever@tu-dortmund.de

Homepage: www.clever-lab.de

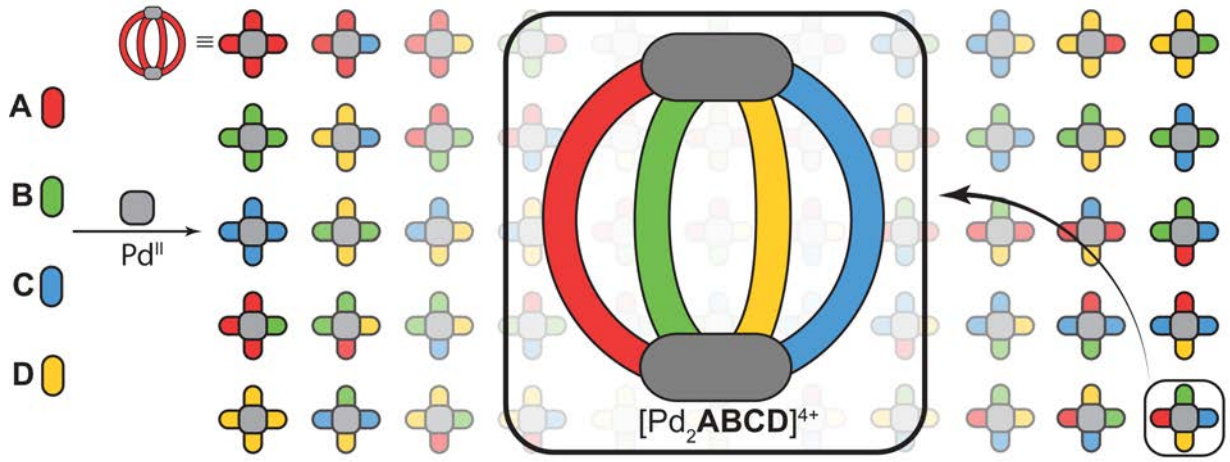

Supplementary Scheme 1 | Statistical outcome of the self-assembly of four different, but fully interchangeable, banana-shaped, bis-monodentate ligands **A**, **B**, **C** and **D** with two square-planar Pd(II) cations without any stereochemical control, leading to a maximum of 55 possible lantern-shaped [Pd_2L_4] cages (all shown in top view; a desired Pd_2**ABCD** product is highlighted and shown in side view).

1. Materials and measurements

Unless otherwise stated, all chemicals were obtained from commercial sources and used as received.

Compound 2,7-dibromo-9-methyl-9H-carbazole,[1] 2,7-dibromo-9-methyl-9H-fluorene,[2] ligands **A**,[3] **B^0**,[4] **B**,[5] **C**,[6] **D**,[7] and **D^4**,[8] were prepared according to literature procedures. Gel permeation chromatography (GPC) purification of ligands were performed on a JAI 9210-II NEXT GPC System with a JAIGEL HH-2/HH-1 column combination running with $CHCl_3$ (HPLC grade). High-resolution Electrospray ionization (ESI) mass spectra were recorded on Bruker ESI timsTOF (electrospray ionization-trapped ion mobility-time of flight) and Compact mass spectrometers. All samples were diluted with spectroscopy grade CH_3CN (1:10). NMR experiments were measured on Bruker AVANCE III 500, 600 or 700 MHz spectrometers. Chemical shifts for ^1H and ^{13}C are reported in ppm with residual solvent as reference: acetonitrile (1.94 ppm for ^1H, 1.32 ppm for ^{13}C), DMSO (2.50 ppm for ^1H, 39.52 ppm for ^{13}C). Abbreviations for the multiplicity of ^1H NMR signals were indicated as following: s: singlet, d: doublet, t: triplet, dd: doublet of doublets; dt: doublet of triplets; m: multiplet, br: broad.

2. Synthesis of ligands

2.1. Synthesis of 10-(8-(3,6-diiodo-9H-carbazol-9-yl)octyl)-2,7-diiodoacridin-9(10H)-one (D^3)

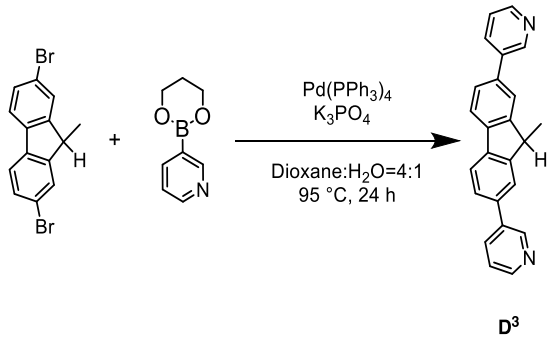

D^3

Scheme S1. Synthesis of ligand D^3

To a mixture of 2,7-dibromo-9-methyl-9H-fluorene (507 mg, 1.5 mmol), 3-(1,3,2-dioxaborinan-2-yl)pyridine (734 mg, 4.5 mmol) and K_3PO_4 (1.15 mg, 5.4 mmol) were added 1,4-dioxane (30 mL) and water (7.5 mL). The resulting mixture was thoroughly degassed and $Pd(PPh_3)_4$ (104 mg, 0.09 mmol) were added under N_2 atmosphere. After stirring at 95 °C overnight, the mixture was allowed to cool down to room temperature and 30 mL of dichloromethane were added. The solution was washed with brine (3 × 15 mL) and dried over Na_2SO_4. The solvent was removed under vacuum, affording an orange powder. The crude product was purified through column chromatography (silica) using ethyl acetate as eluent and further purified by gel permeation chromatography (GPC) using chloroform as eluent, to afford 245 mg of **D^3** as white powder. Yield: 49 %.

^{1}H NMR (600 MHz, 298 K, CD_3CN) δ 9.0 – 8.9 (m, 2H), 8.6 (dd, J = 4.8, 1.6 Hz, 2H), 8.1 (ddd, J = 7.9, 2.5, 1.6 Hz, 2H), 8.0 (d, J = 7.8 Hz, 2H), 7.9 (dt, J = 1.7, 0.8 Hz, 2H), 7.7 (ddd, J = 7.9, 1.8, 0.7 Hz, 2H), 7.5 (ddd, J = 7.9, 4.8, 0.9 Hz, 2H), 4.1 (q, J = 7.5 Hz, 1H), 1.6 (d, J = 7.4 Hz, 3H).

^{13}C NMR (151 MHz, 298 K, CD_3CN) δ 151.5, 149.4, 149.1, 140.8, 137.9, 137.4, 135.2, 127.3, 124.7, 124.0, 121.8, 43.5, 18.5.

HR-ESI MS (CH_3CN) *m/z*: $[M+H]^+$ calc. for $C_{24}H_{19}N_2$, 335.1548; found 335.1544.

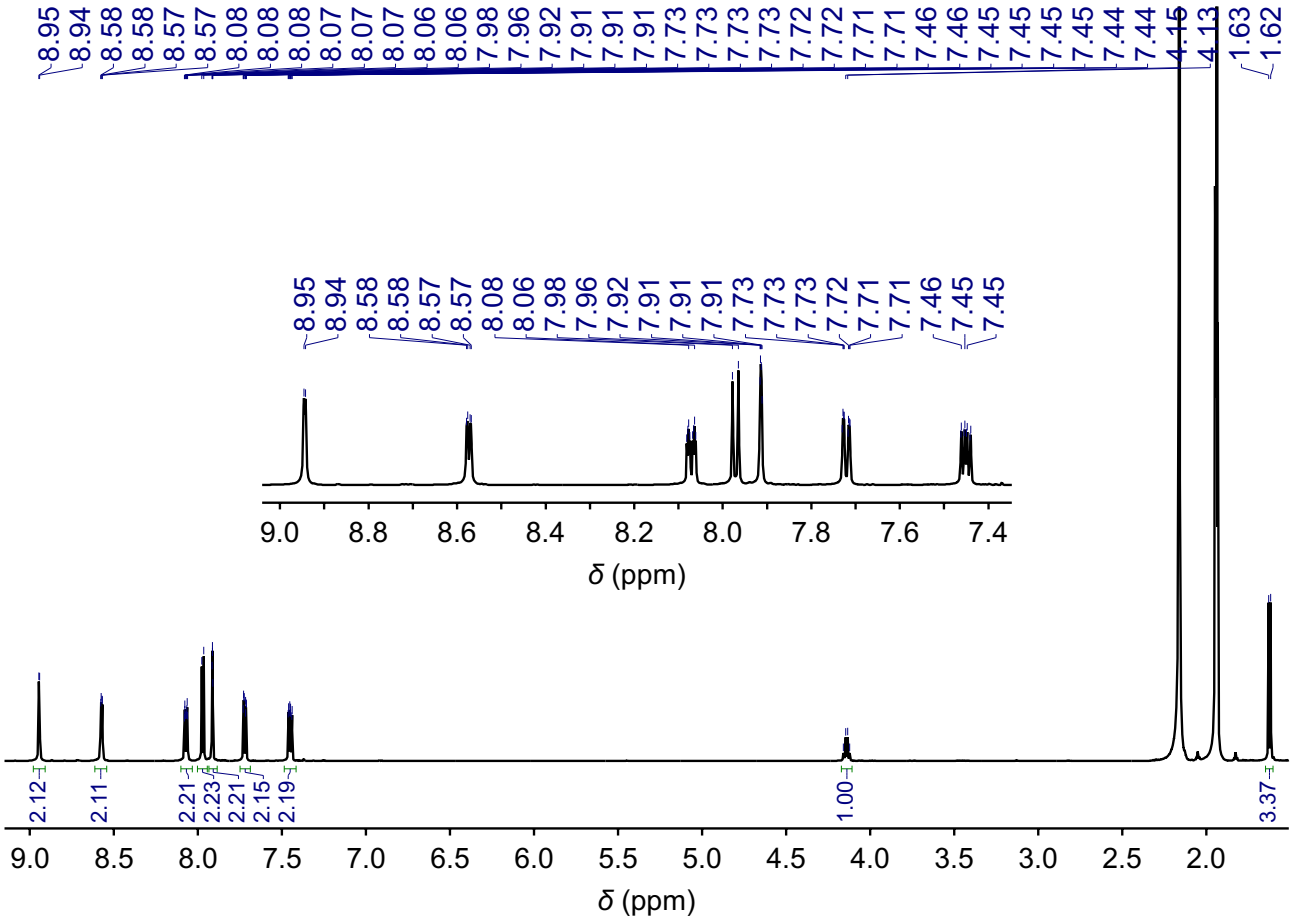

Supplementary Figure 1 | ^{1}H NMR spectrum (600 MHz, 298 K, CD_3CN) of ligand **D^3**.

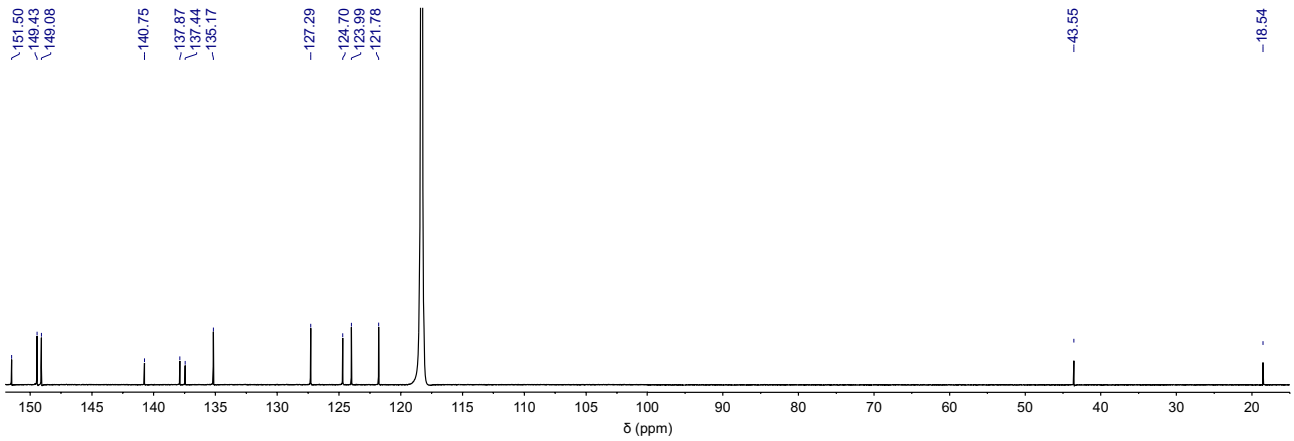

Supplementary Figure 2 | ^{13}C NMR spectrum (151 MHz, 298 K, CD_3CN) of ligand **D^3**.

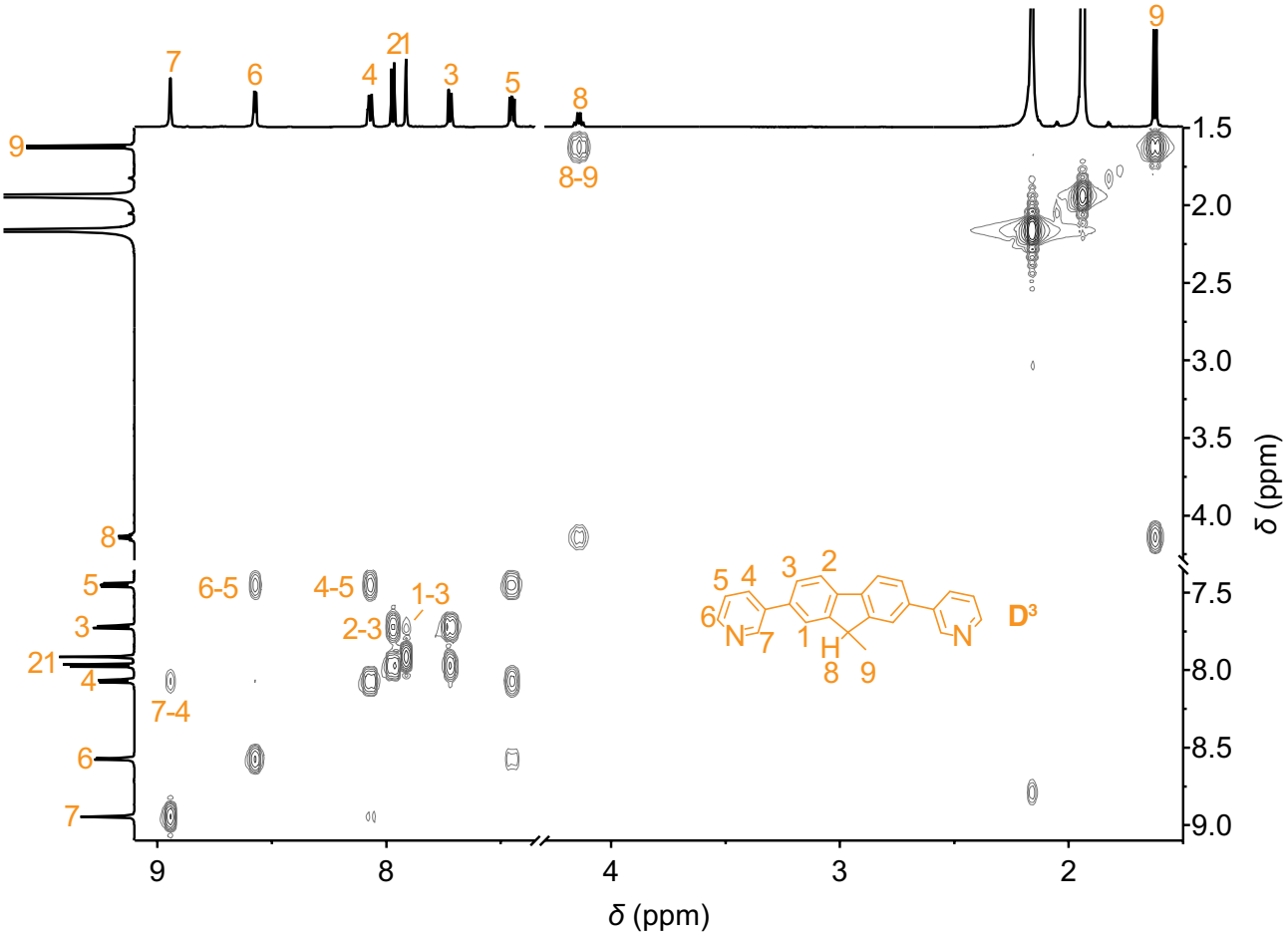

Supplementary Figure 3 | Partial ^{1}H–^{1}H COSY spectrum (600 MHz, 298 K, CD_3CN) of ligand **D³**.

2.2. Synthesis of 2,7-di(pyridin-3-yl)-9H-carbazole (D¹)

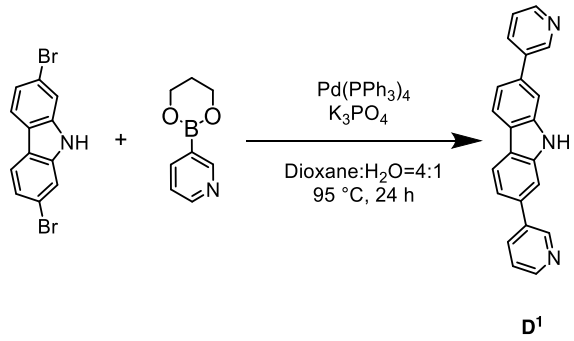

D¹

Scheme S2. Synthesis of ligand D¹

Ligand **D¹** was synthesized in a similar procedure as **D³** by using 2,7-dibromo-9H-carbazole as starting material instead. Yield: 79 %.

^{1}H NMR (700 MHz, 298 K, CD_3CN) δ 9.6 (s, 1H), 9.0 (dd, J = 2.4, 0.8 Hz, 2H), 8.6 (dd, J = 4.7, 1.6 Hz, 2H), 8.2 (d, J = 8.0 Hz, 2H), 8.1 (ddd, J = 7.8, 2.4, 1.6 Hz, 2H), 7.8 (d, J = 1.5 Hz, 2H), 7.5 (dd, J = 8.1, 1.6 Hz, 2H), 7.5 (ddd, J = 7.8, 4.7, 0.8 Hz, 2H).

^{13}C NMR (151 MHz, 298 K, CD_3CN) δ 149.1, 142.0, 138.0, 136.6, 135.4, 124.7, 123.3, 121.9, 119.6, 110.4.

HR-ESI MS (CH_3CN) *m/z*: $[M+H]^+$ calc. for $C_{22}H_{16}N_3$, 322.1344; found 322.1347.

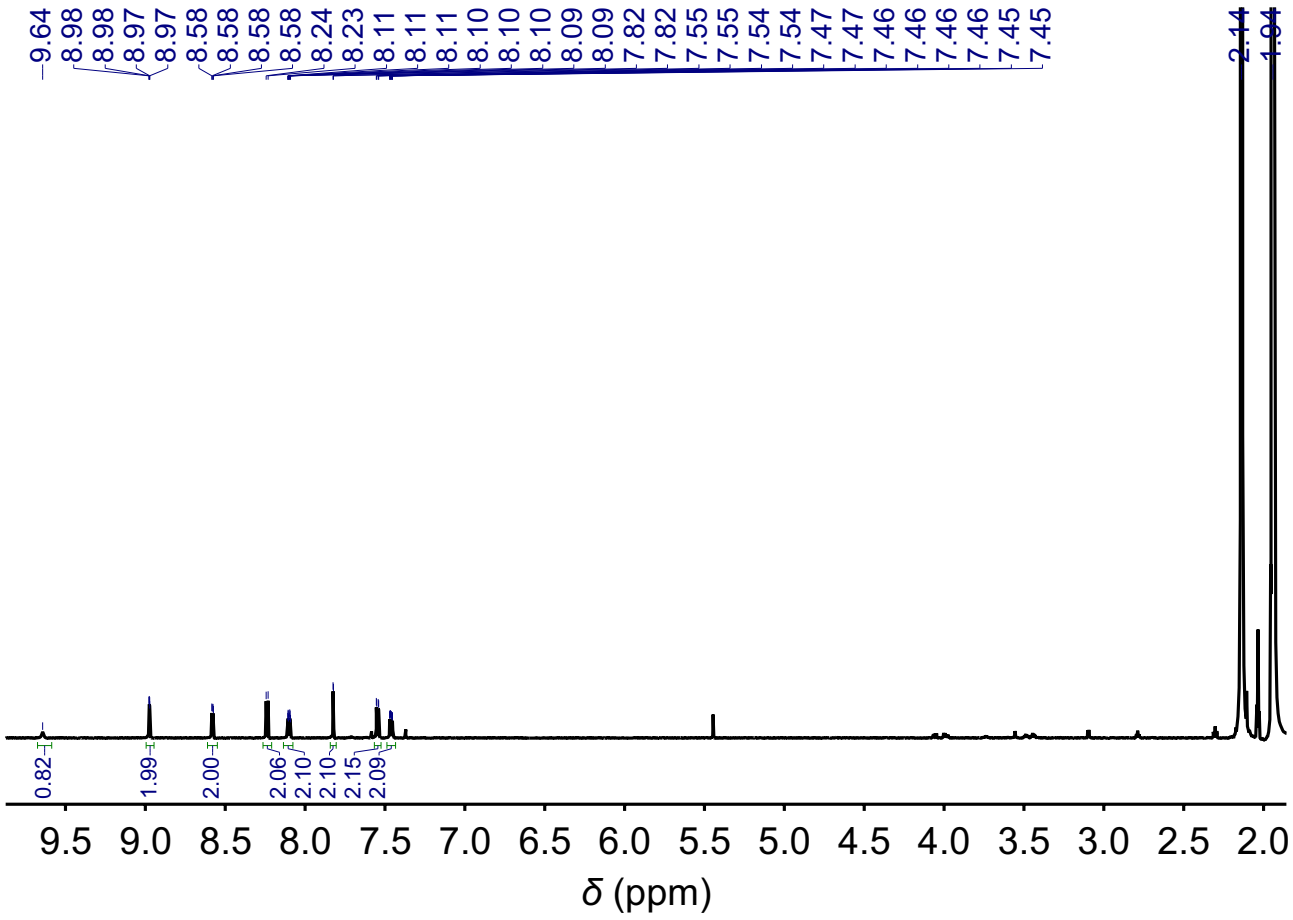

Supplementary Figure 4 | ^{1}H NMR spectrum (600 MHz, 298 K, CD_3CN) of ligand **D^3**.

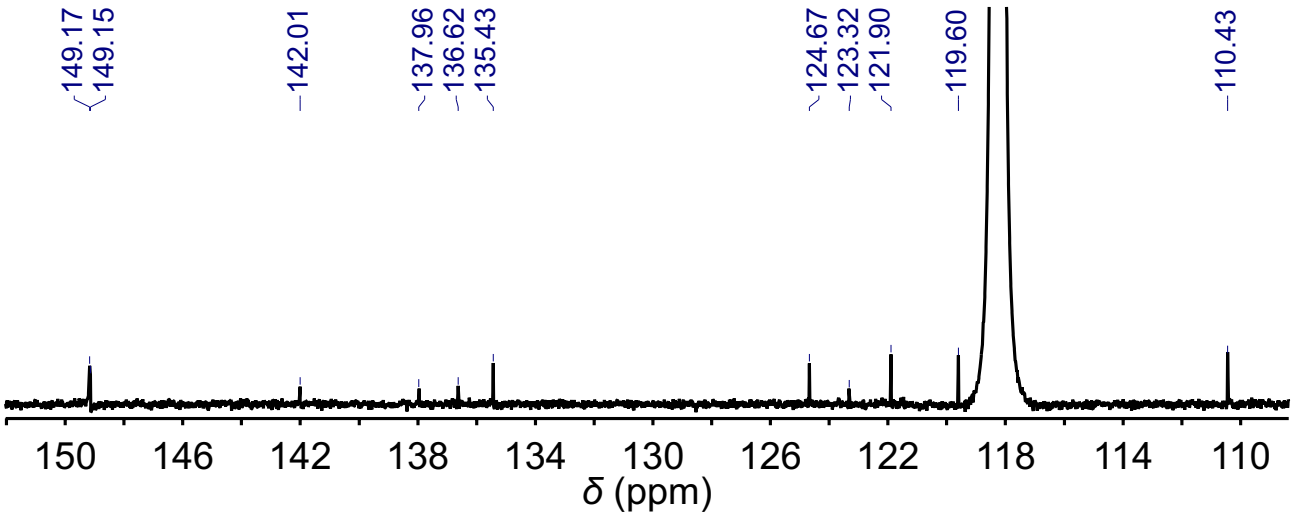

Supplementary Figure 5 | ^{13}C NMR spectrum (151 MHz, 298 K, CD_3CN) of ligand **D^3**.

2.3. Synthesis of 9-methyl-2,7-di(pyridin-3-yl)-9H-carbazole (D^2)

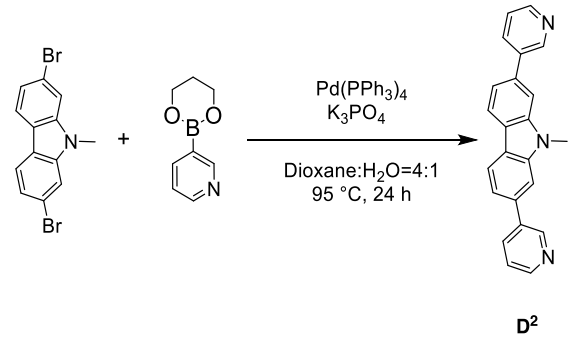

D^2

Scheme S3. Synthesis of ligand D^2

Ligand **D^2** was synthesized in a similar procedure as **D^3** by using 2,7-dibromo-9-methyl-9H-carbazole as starting material instead. Yield: 82 %.

^{1}H NMR (700 MHz, 298 K, CD_3CN) δ 9.0 (dd, J = 2.4, 0.9 Hz, 2H), 8.6 (dd, J = 4.7, 1.6 Hz, 2H), 8.3 (dd, J = 8.0, 0.7 Hz, 2H), 8.2 (ddd, J = 7.9, 2.5, 1.6 Hz, 2H), 7.9 – 7.8 (m, 2H), 7.6 (dd, J = 8.0, 1.6 Hz, 2H), 7.5 (ddd, J = 7.8, 4.8, 0.9 Hz, 2H), 4.0 (s, 3H).

^{13}C NMR (176 MHz, 298 K, CD_3CN) δ 149.4, 149.3, 143.3, 138.0, 136.8, 135.5, 124.7, 123.0, 122.0, 119.4, 108.6, 29.87.

HR-ESI MS (CH_3CN) *m/z*: $[M+H]^+$ calc. for $C_{23}H_{18}N_3$, 336.1501; found 336.1509.

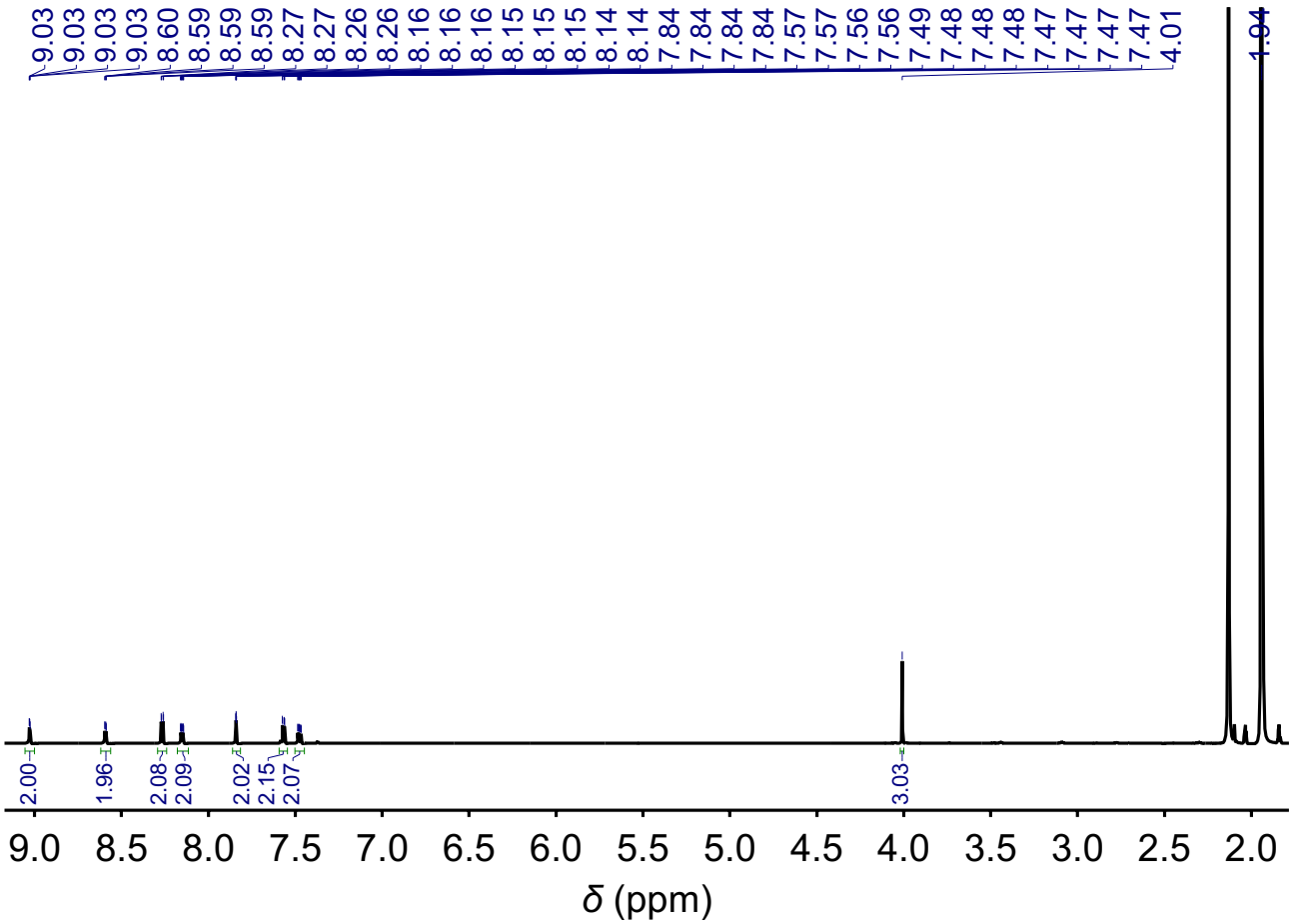

Supplementary Figure 6 | ^{1}H NMR spectrum (600 MHz, 298 K, CD_3CN) of ligand **D^2**.

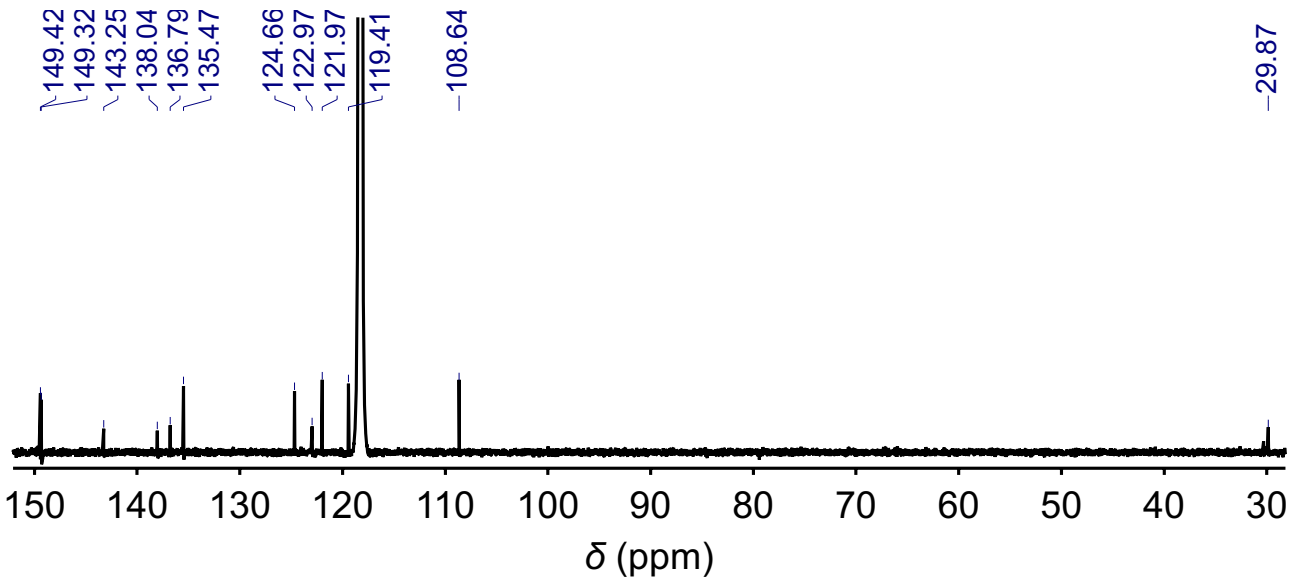

Supplementary Figure 7 | ^{13}C NMR spectrum (151 MHz, 298 K, CD_3CN) of ligand **D²**.

3. Self-assembly of cages

Homoleptic cages $Pd_2\mathbf{A}_4$,[3] $Pd_2\mathbf{B}^0_4$,[4] $Pd_2\mathbf{B}_4$,[9] $Pd_3\mathbf{C}_6$,[6] $Pd_3\mathbf{D}_6$,[7] and heteroleptic cage $Pd_2\mathbf{B}^0_2\mathbf{C}_2$,[6] were prepared according to literature procedures. The synthesis of all other homo- and heteroleptic cages is described in the following.

3.1. Ligand library for multicomponent cages

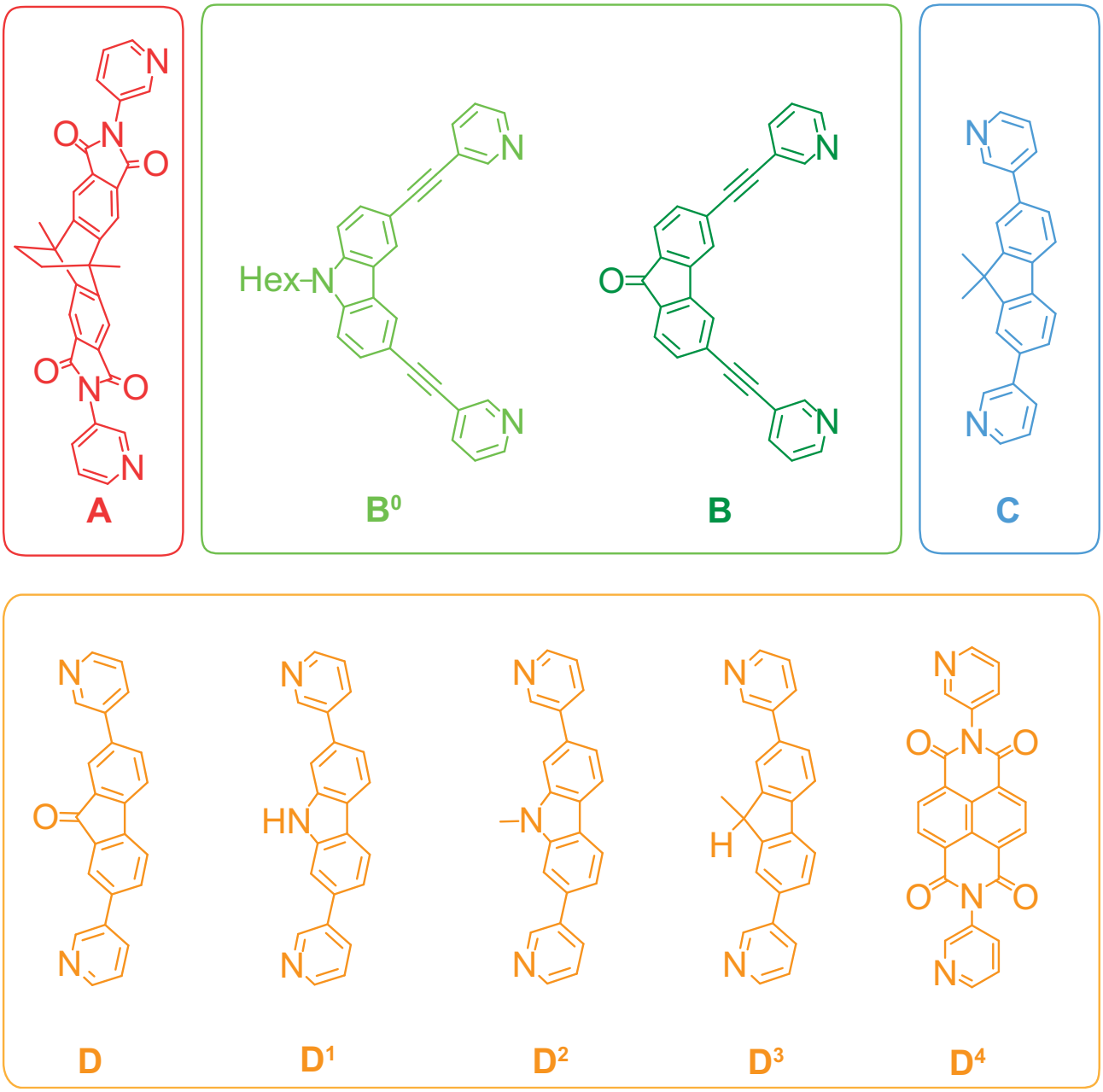

3.2. Self-assembly of homoleptic cages

3.2.1. Self-assembly of homoleptic cage $Pd_4\mathbf{D^1}_8$

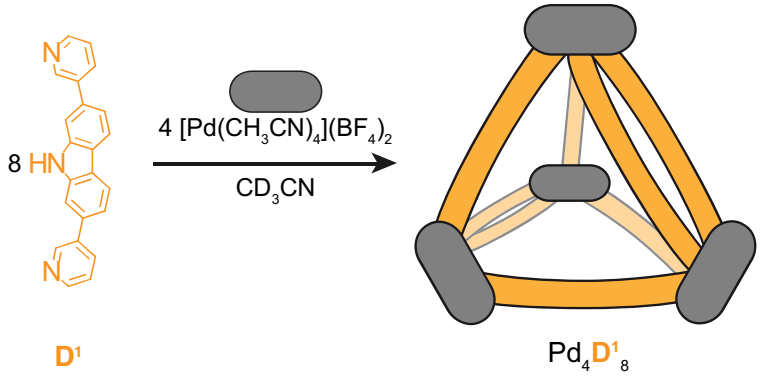

To a suspension of $\mathbf{D^1}$ (240 µL, 3 mM, 0.72 µmol) in CD_3CN were added a stock solution of $[Pd(CH_3CN)_4](BF_4)_2$ (24 µL, 15 mM/CD_3CN, 0.36 µmol) and 186 µL additional CD_3CN. The mixture was heated at 80 °C for 8 h to give a solution containing the shown tetrahedral cage as only identifiable assembly product.

^{1}H NMR (500 MHz, 298 K, CD_3CN) δ 9.92 (s, 4H), 9.84 (s, 8H), 9.73 (d, J = 2.2 Hz, 12H), 9.12 (d, J = 5.6 Hz, 8H), 8.98 (d, J = 5.6 Hz, 8H), 8.54 (d, J = 8.3 Hz, 8H), 8.40 (s, 8H), 8.35 (d, J = 8.3 Hz, 8H), 8.29 (d, J = 8.0 Hz, 8H), 8.11 (d, J = 8.2 Hz, 8H), 7.90 (d, J = 8.2 Hz, 8H), 7.80 (s, 8H), 7.74 (dd, J = 8.2, 5.6 Hz, 8H), 7.63 (dd, J = 8.1, 5.6 Hz, 8H), 7.44 (dd, J = 8.4, 1.6 Hz, 8H).

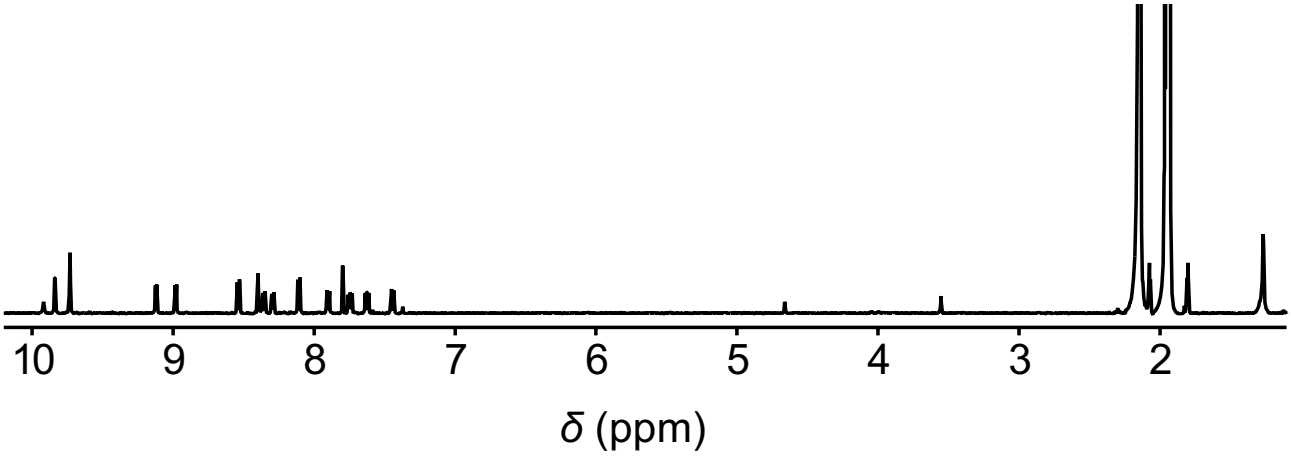

Supplementary Figure 8 | ^{1}H NMR spectrum (500 MHz, 298 K, CD_3CN) of homoleptic cage $Pd_4\mathbf{D^1}_8$.

^{13}C NMR (151 MHz, 298 K, CD_3CN) δ 150.28, 150.22, 149.97, 149.43, 142.37, 142.23, 141.85, 141.24, 140.01, 139.67, 133.83, 133.56, 128.60, 128.23, 124.46, 124.34, 122.90, 122.76, 119.74, 119.69, 111.04, 110.27.

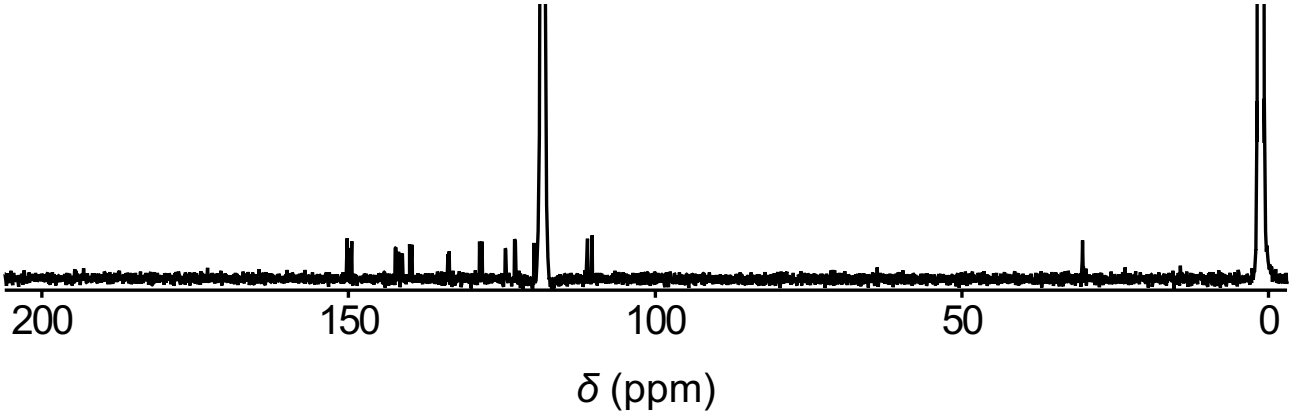

Supplementary Figure 9 | ^{13}C NMR spectrum (151 MHz, 298 K, CD_3CN) of homoleptic cage $Pd_4\mathbf{D^1}_8$.

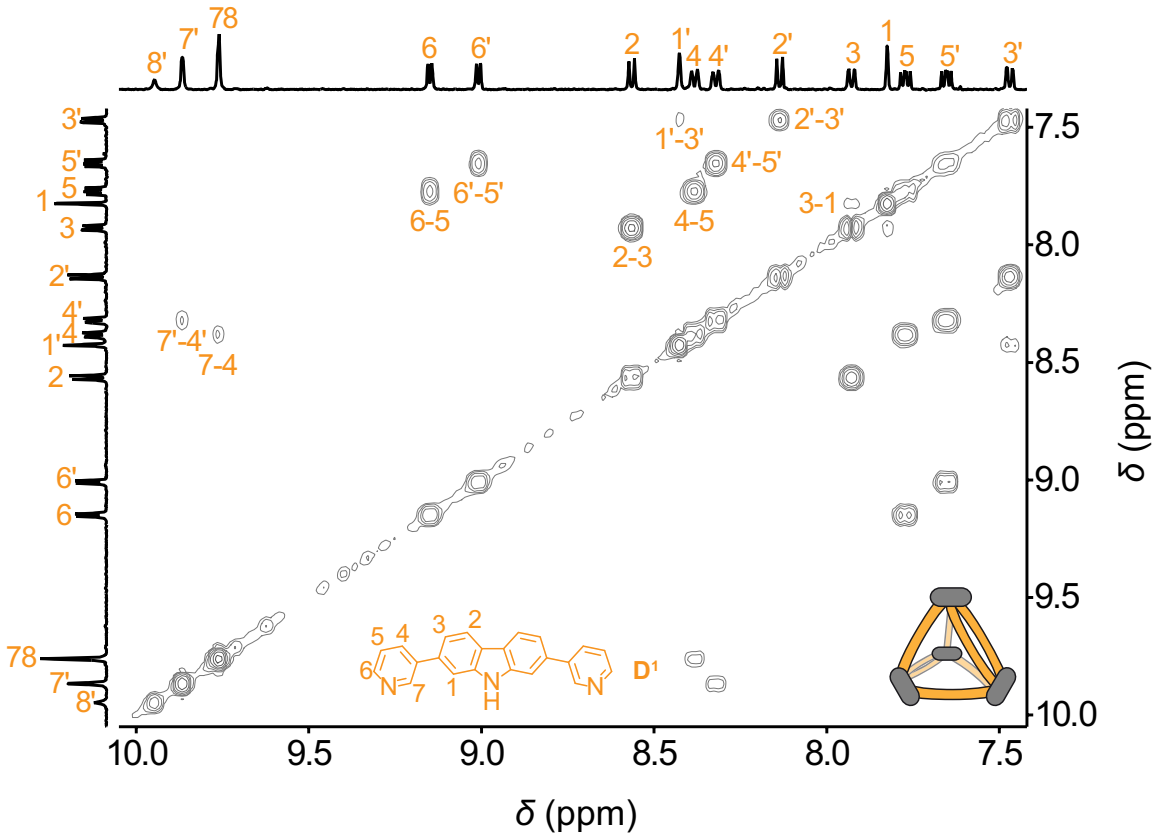

Supplementary Figure 10 | Partial ^{1}H–^{1}H COSY spectrum (500 MHz, 298 K, CD_3CN) of homoleptic cage $Pd_4\mathbf{D^1}_8$.

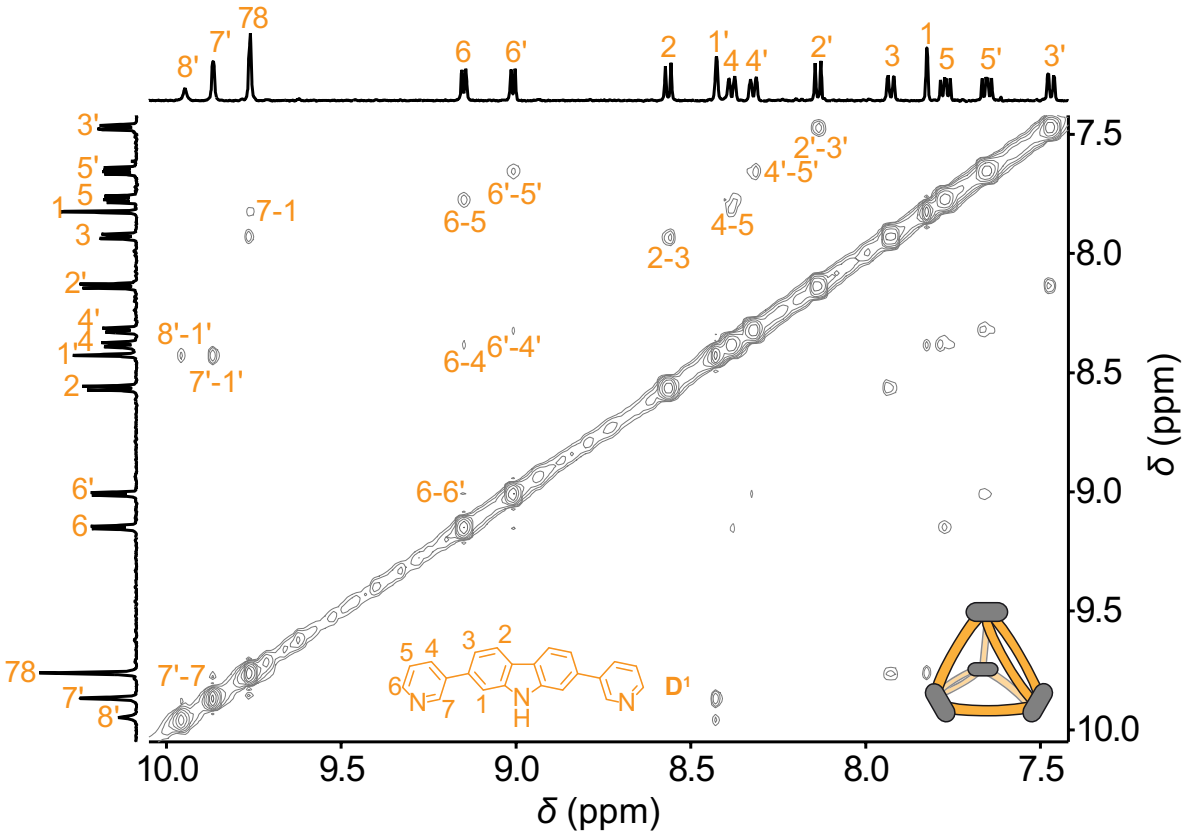

Supplementary Figure 11 | Partial ^{1}H–^{1}H NOESY spectrum (500 MHz, 298 K, CD_3CN) of homoleptic cage $Pd_4\mathbf{D^1}_8$.

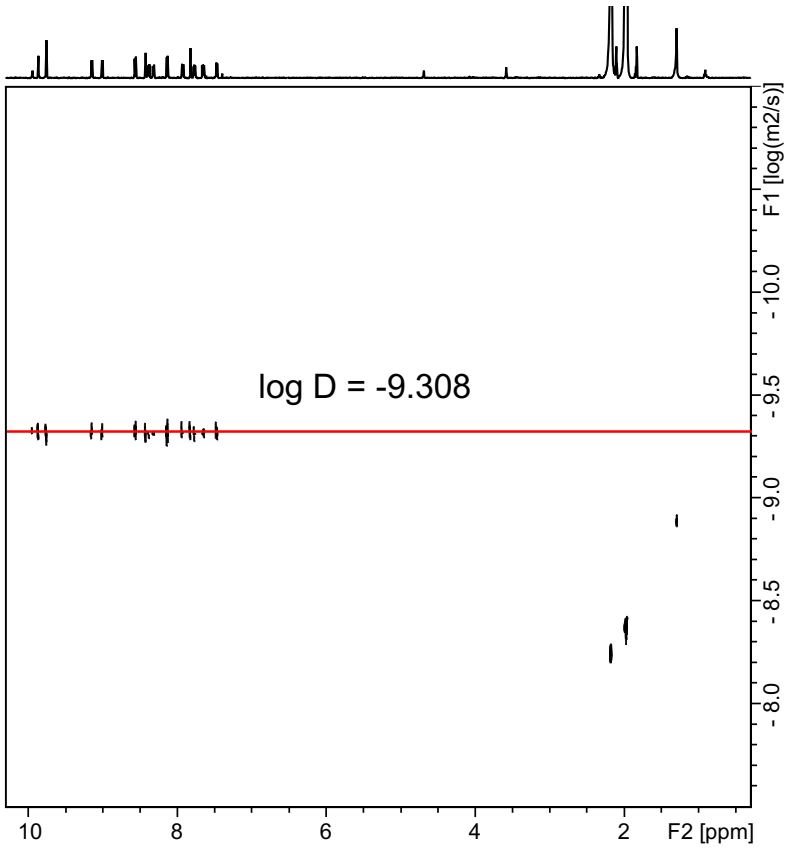

Supplementary Figure 12 | ^{1}H DOSY spectrum (500 MHz, 298 K, 298 K, CD_3CN) of homoleptic cage $Pd_4\mathbf{D^1}_8$. Diffusion coefficient for $Pd_4\mathbf{D^1}_8$: D = 4.920 × 10^{-10} m^2s^{-1}, log *D* = −9.308, r = 13.3 Å.

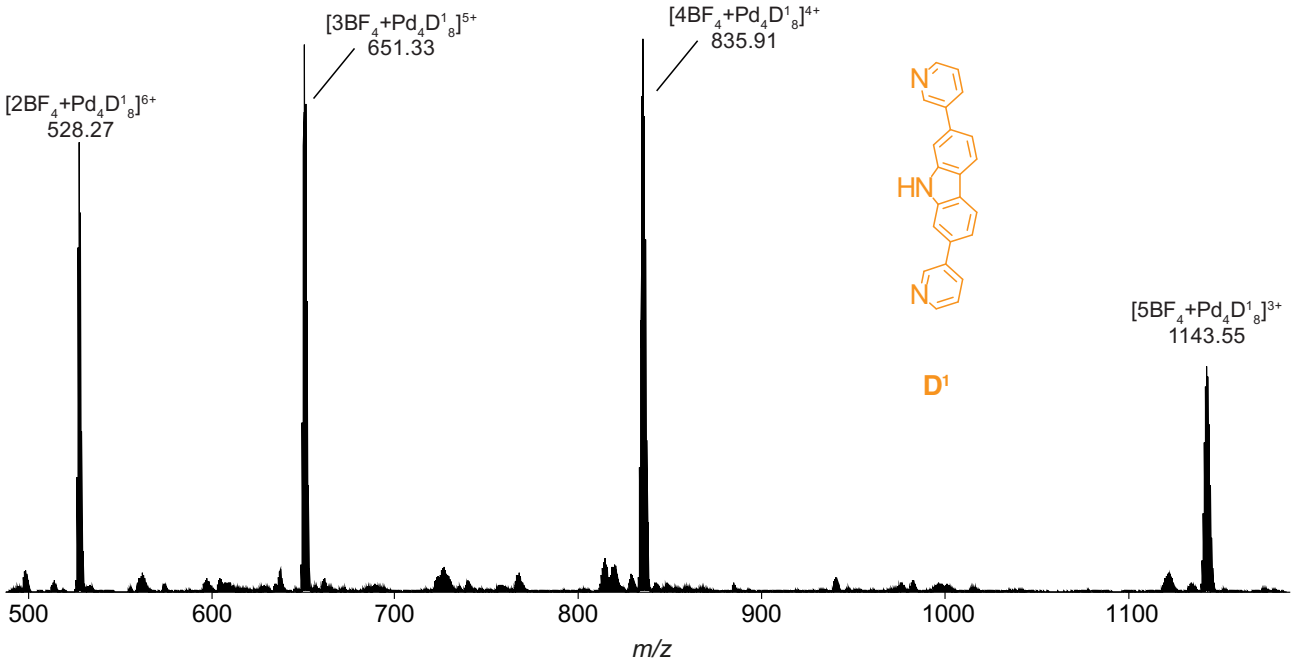

Supplementary Figure 13 | HR-ESI mass spectrum of homoleptic cage $Pd_4\mathbf{D^1}_8$.

3.2.2. Self-assembly of homoleptic $Pd_3D^2{}_6/Pd_4D^2{}_8$ ring/cage mixture

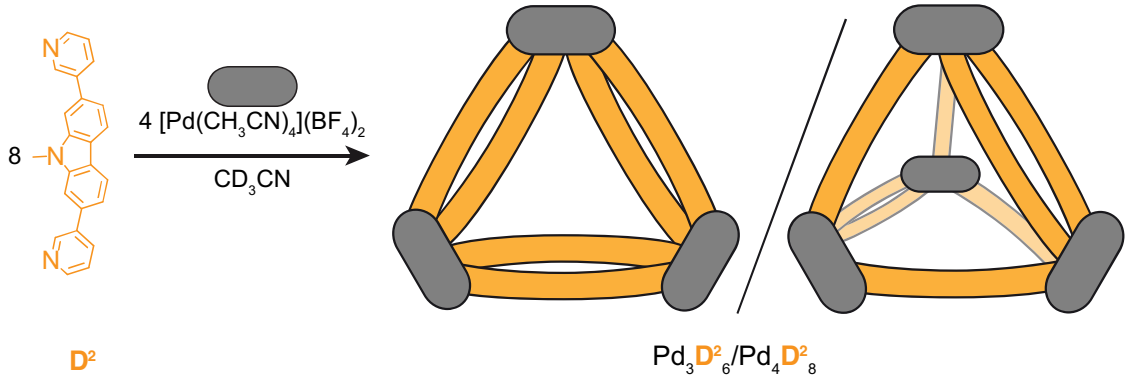

To a suspension of $\mathbf{D^2}$ (240 µL, 3 mM, 0.72 µmol) in CD_3CN were added a stock solution of $[Pd(CH_3CN)_4](BF_4)_2$ (24 µL, 15 mM/CD_3CN, 0.36 µmol) and 186 µL additional CD_3CN. The mixture was heated at 80 °C for 8 h to give a mixture containing a 3-membered ring and a tetrahedral cage in a ratio of 8:7.

^{1}H NMR (600 MHz, 298 K, CD_3CN) δ 10.01 (d, J = 2.1 Hz, 7H), 9.96 – 9.93 (m, 7H), 9.91 (d, J = 2.1 Hz, 12H), 9.24 (dt, J = 5.8, 1.7 Hz, 19H), 9.19 (dd, J = 5.8, 1.3 Hz, 7H), 8.58 (d, J = 8.3 Hz, 7H), 8.46 (dt, J = 8.5, 1.6 Hz, 7H), 8.26 (ddt, J = 7.9, 6.2, 1.7 Hz, 19H), 8.23 (d, J = 8.1 Hz, 12H), 8.11 (d, J = 8.1 Hz, 7H), 8.04 (dd, J = 8.3, 1.6 Hz, 7H), 8.03 – 8.01 (m, 7H), 7.87 – 7.85 (m, 12H), 7.84 (d, J = 1.6 Hz, 7H), 7.76 (dd, J = 8.3, 5.7 Hz, 7H), 7.73 (dd, J = 8.1, 5.7 Hz, 12H), 7.68 (dd, J = 8.1, 5.6 Hz, 7H), 7.45 (dd, J = 8.1, 1.6 Hz, 12H), 7.34 (dd, J = 8.2, 1.6 Hz, 7H), 3.92 (s, 10.5H), 3.79 (s, 10.5H), 3.72 (s, 18H).

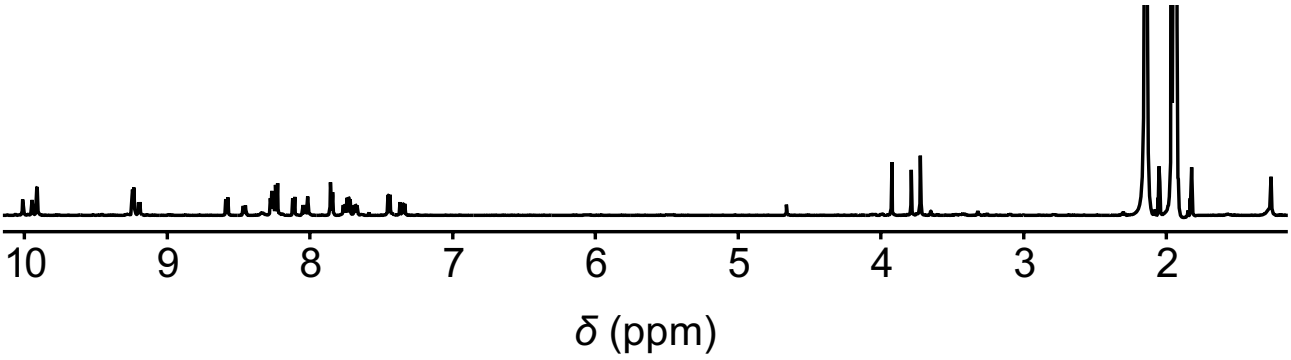

Supplementary Figure 14 | ^{1}H NMR spectrum (600 MHz, 298 K, CD_3CN) of homoleptic $Pd_3\mathbf{D^2}_6/Pd_4\mathbf{D^2}_8$ ring/cage mixture (ring:tetrahedron = 8:7).

^{13}C NMR (151 MHz, 298 K, CD_3CN) δ 150.51, 150.28, 150.22, 150.03, 149.85, 149.71, 143.51, 143.16, 143.13, 142.49, 142.46, 141.63, 140.48, 139.98, 139.80, 134.39, 134.08, 133.62, 128.46, 128.28, 128.14, 124.05, 123.74, 123.51, 123.00, 122.71, 122.57, 120.43, 119.74, 119.47, 108.98, 108.90, 108.69, 30.36, 29.96, 29.21.

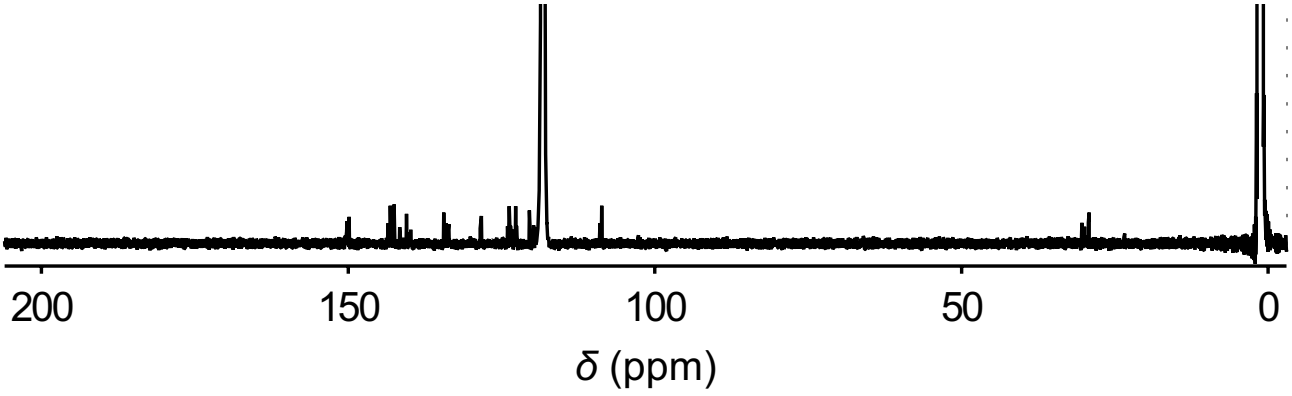

Supplementary Figure 15 | ^{13}C NMR spectrum (151 MHz, 298 K, CD_3CN) of homoleptic $Pd_3\mathbf{D^2}_6/Pd_4\mathbf{D^2}_8$ ring/cage mixture.

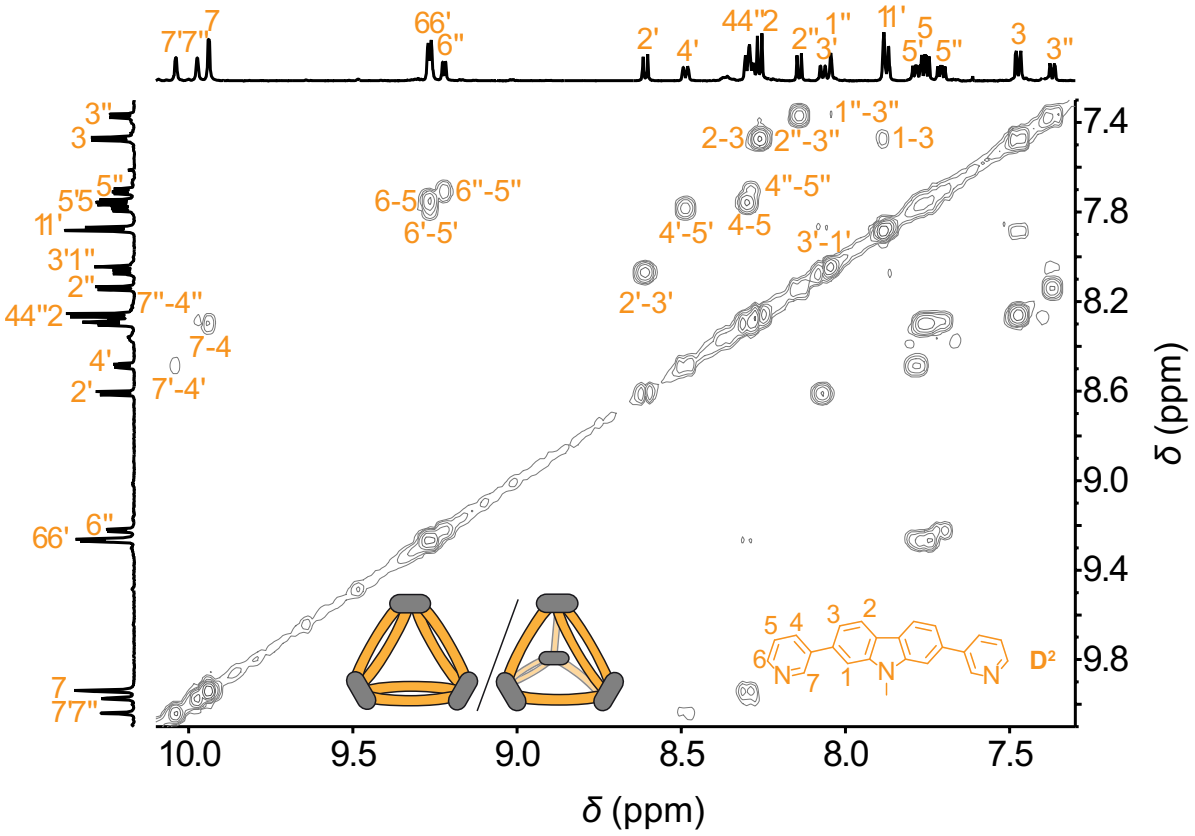

Supplementary Figure 16 | Partial ^{1}H–^{1}H COSY spectrum (500 MHz, 298 K, CD_3CN) of homoleptic $Pd_3\mathbf{D^2}_6$/$Pd_4\mathbf{D^2}_8$ ring/cage mixture.

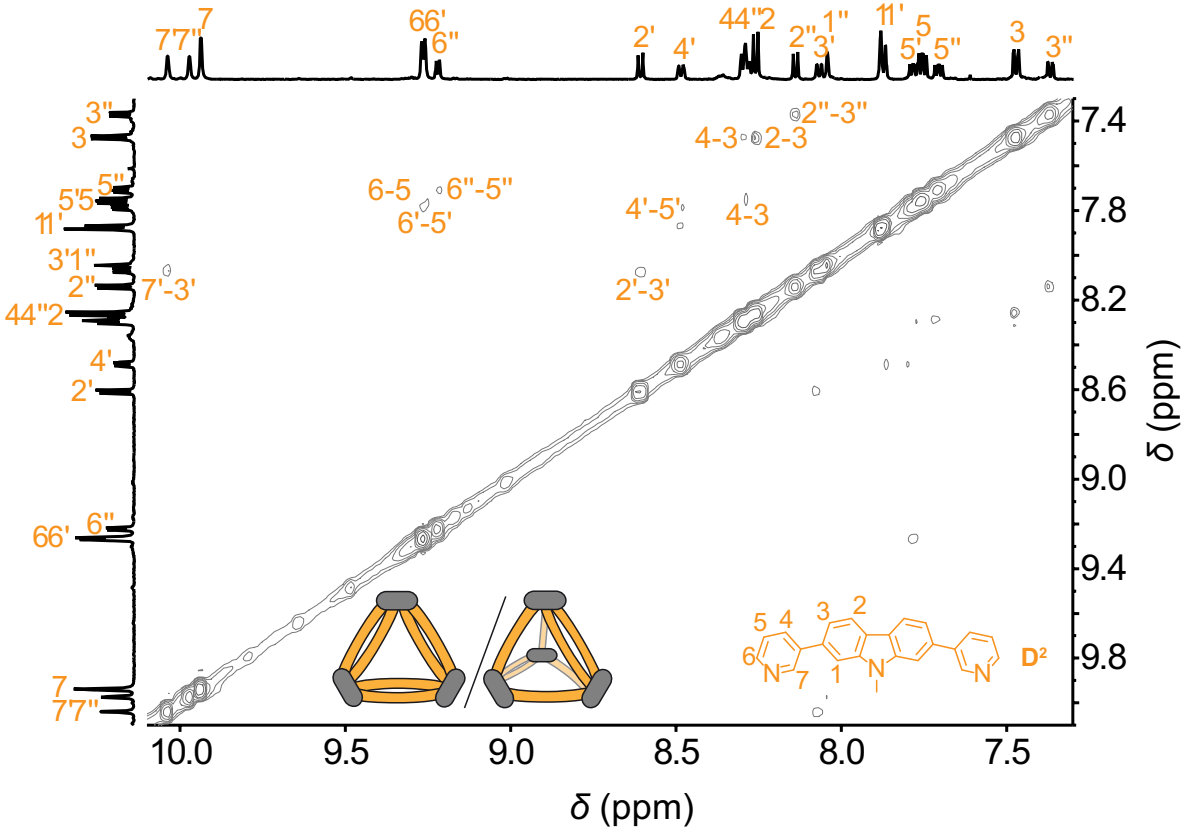

Supplementary Figure 17 | Partial ^{1}H–^{1}H NOESY spectrum (500 MHz, 298 K, CD_3CN) of homoleptic $Pd_3\mathbf{D^2}_6$/$Pd_4\mathbf{D^2}_8$ ring/cage mixture.

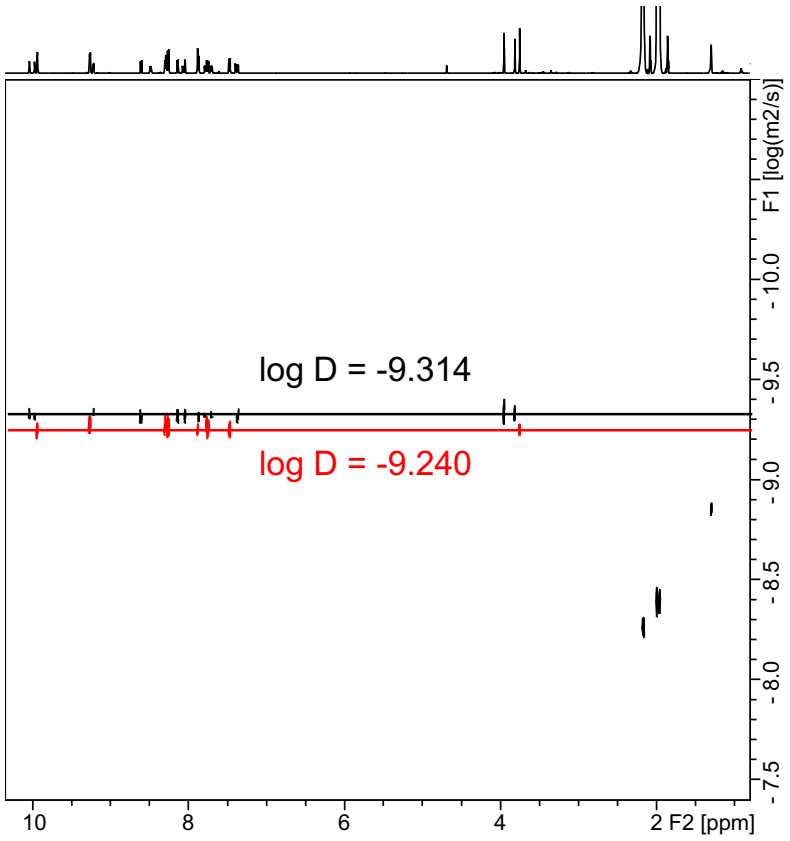

Supplementary Figure 18 | ^{1}H DOSY spectrum (500 MHz, 298 K, 298 K, CD_3CN) of homoleptic $Pd_3\mathbf{D^2}_6$/$Pd_4\mathbf{D^2}_8$ ring/cage mixture. Diffusion coefficient for $Pd_3\mathbf{D^2}_6$: D = 5.754 × 10^{-10} m^2s^{-1}, log *D* = −9.240, r = 11.4 Å; $Pd_4\mathbf{D^2}_8$: D = 4.853 × 10^{-10} m^2s^{-1}, log *D* = −9.314, r = 13.5 Å

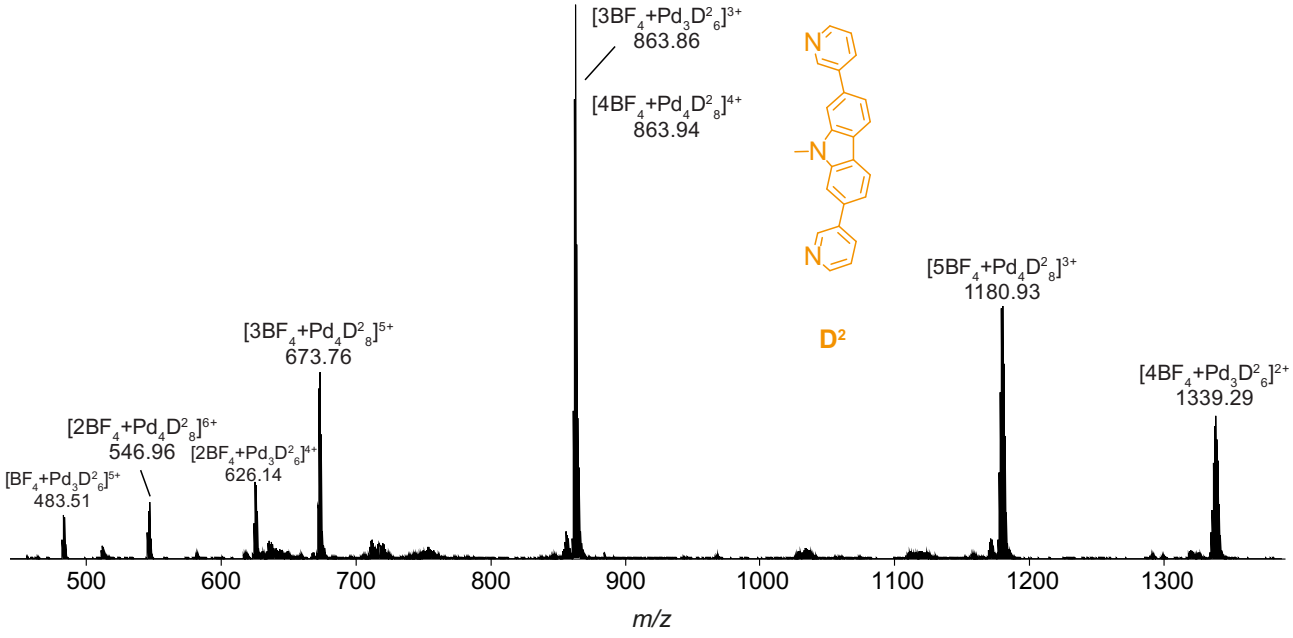

Supplementary Figure 19 | HR-ESI mass spectrum of homoleptic $Pd_3\mathbf{D^2}_6$/$Pd_4\mathbf{D^2}_8$ ring/cage mixture.

3.2.3. Self-assembly of homoleptic $Pd_3D^3{}_6/Pd_4D^3{}_8$ ring/cage mixture

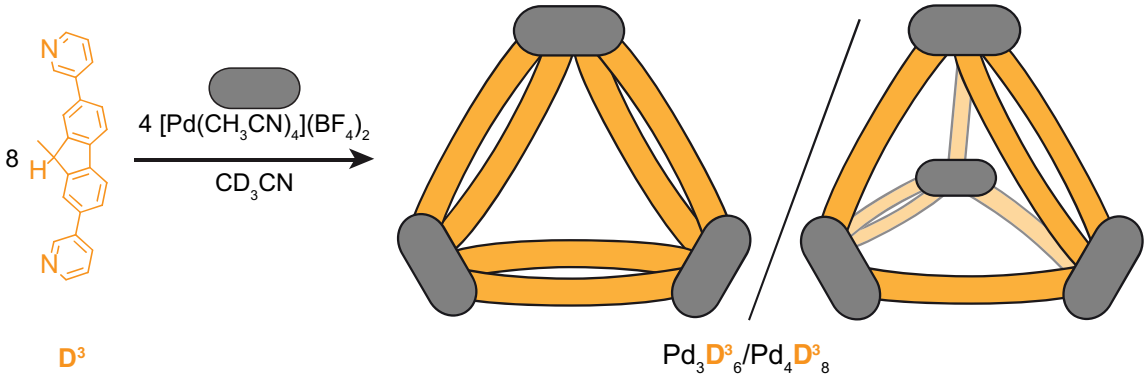

To a suspension of $\mathbf{D^3}$ (240 µL, 3 mM, 0.72 µmol) in CD_3CN were added a stock solution of $[Pd(CH_3CN)_4](BF_4)_2$ (24 µL, 15 mM/CD_3CN, 0.36 µmol) and 186 µL additional CD_3CN. The mixture was heated at 80 °C for 8 h to give a mixture of 3-membered rings and tetrahedral cages, each consisting of numerous diastereomers with respect to the relative positions of the central methyl substituents at the ligands. Due to the convoluted NMR spectrum of this mixture of diastereomers, the ring:cage ratio could not be quantified.

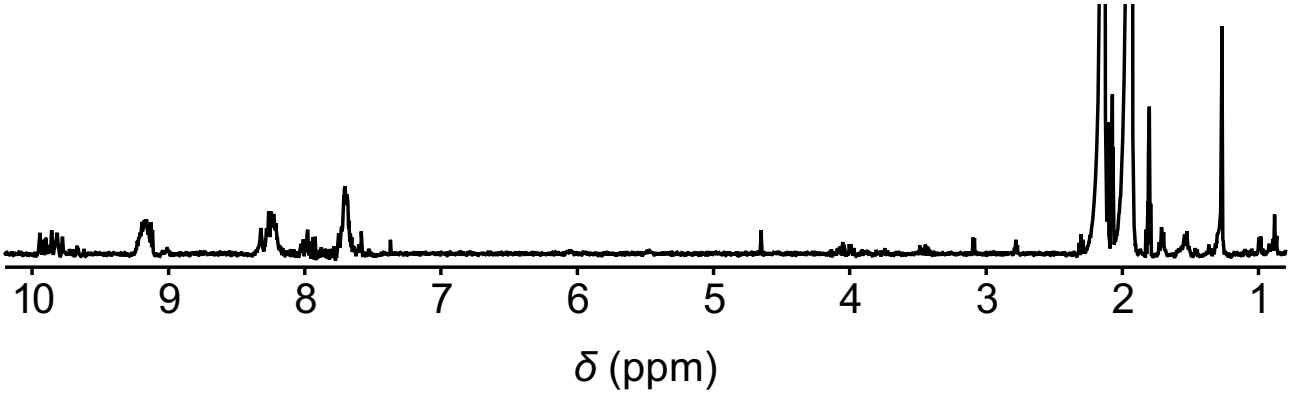

Supplementary Figure 20 | ^1H NMR spectrum (600 MHz, 298 K, CD_3CN) of homoleptic $Pd_3\mathbf{D^4}_6/Pd_4\mathbf{D^4}_8$ ring/cage mixture.

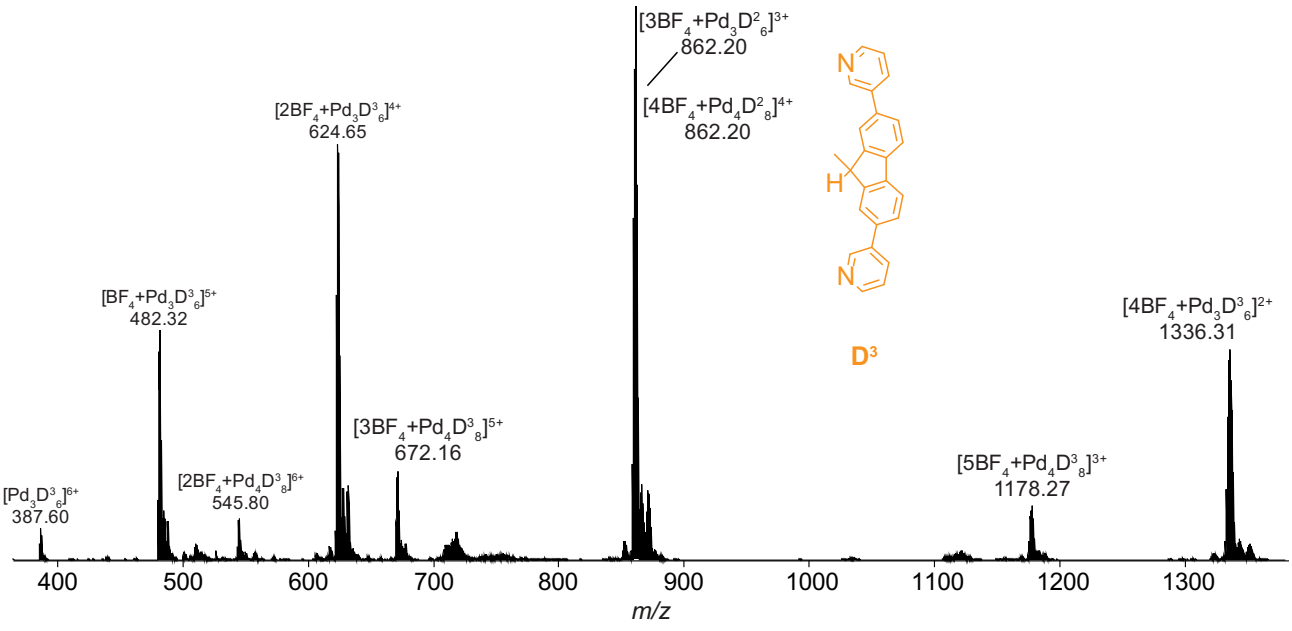

Supplementary Figure 21 | HR-ESI mass spectrum of homoleptic $Pd_3\mathbf{D^3}_6/Pd_4\mathbf{D^3}_8$ ring/cage mixture.

3.2.4. Self-assembly of homoleptic $Pd_3D^4_6/Pd_4D^4_8$ ring/cage mixture

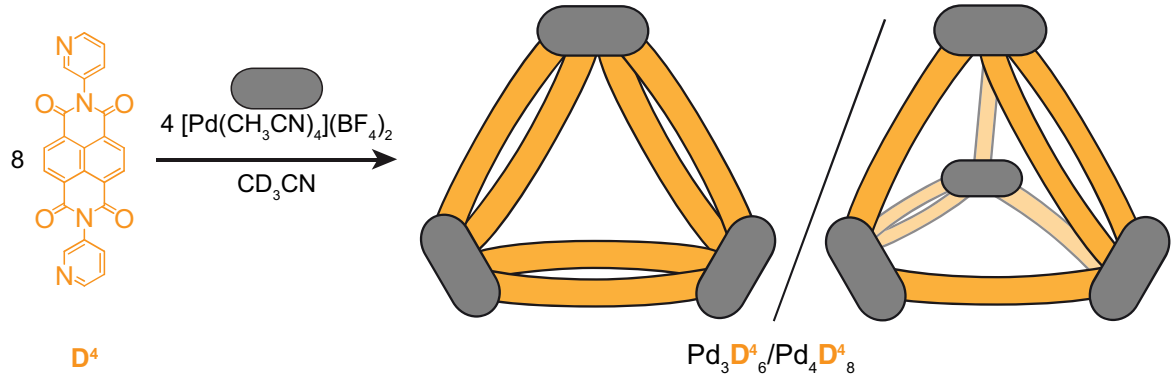

To a suspension of **D⁴** (240 µL, 3 mM, 0.72 µmol) in CD_3CN were added a stock solution of $[Pd(CH_3CN)_4](BF_4)_2$ (24 µL, 15 mM/CD_3CN, 0.36 µmol) and 186 µL additional CD_3CN. The mixture was heated at 80 °C for 8 h to give a mixture containing a 3-membered ring and a tetrahedral cage in a ratio of 4:11.

^{1}H NMR (600 MHz, 298 K, CD_3CN) δ 9.42 (dd, J = 5.9, 1.3 Hz, 22H), 9.41 – 9.37 (m, 12H), 9.18 (s, 12H), 9.15 (d, J = 2.2 Hz, 22H), 9.02 (dd, J = 6.0, 1.2 Hz, 22H), 8.91 (d, J = 2.2 Hz, 22H), 8.76 (s, 44H), 8.58 (s, 68H), 8.24 (ddd, J = 8.4, 2.1, 1.3 Hz, 22H), 8.23 – 8.18 (m, 34H), 8.04 (dd, J = 8.4, 5.7 Hz, 22H), 7.95 (dd, J = 8.1, 5.9 Hz, 12H), 7.84 (dd, J = 8.3, 5.8 Hz, 22H).

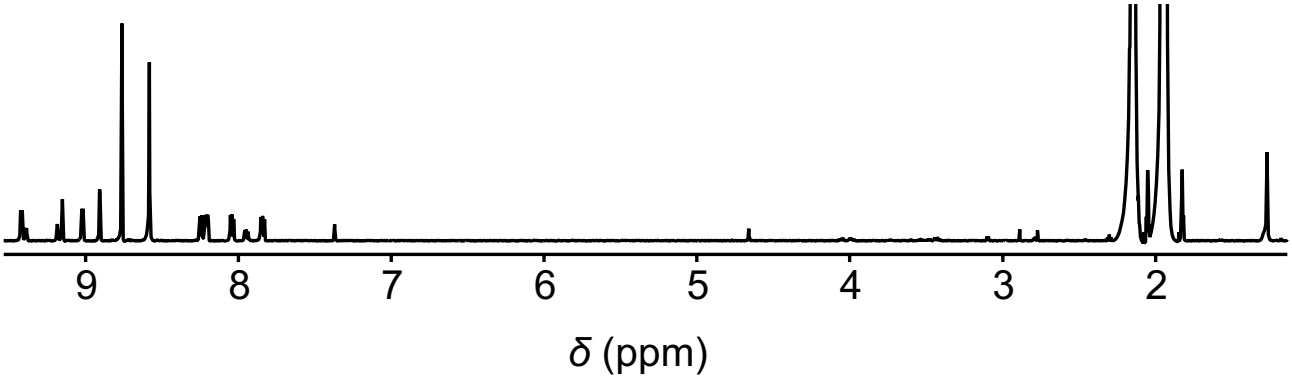

Supplementary Figure 22 | ^{1}H NMR spectrum (600 MHz, 298 K, CD_3CN) of homoleptic $Pd_3D^4_6/Pd_4D^4_8$ mixture (ring:tetrahedron = 4:11).

^{13}C NMR (151 MHz, 298 K, CD_3CN) δ 163.36, 163.34, 163.18, 163.02, 152.69, 152.29, 152.09, 151.72, 151.63, 151.35, 143.14, 135.77, 135.69, 135.03, 132.31, 132.13, 129.54, 128.91, 128.40, 128.14, 127.89, 127.80, 127.73, 127.60.

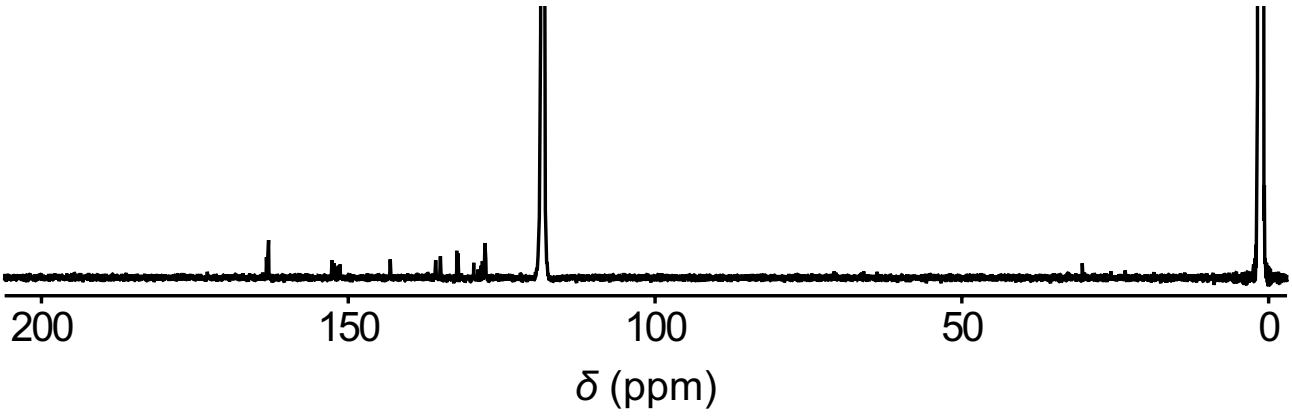

Supplementary Figure 23 | ^{13}C NMR spectrum (151 MHz, 298 K, CD_3CN) of homoleptic $Pd_3D^4_6/Pd_4D^4_8$ ring/cage mixture.

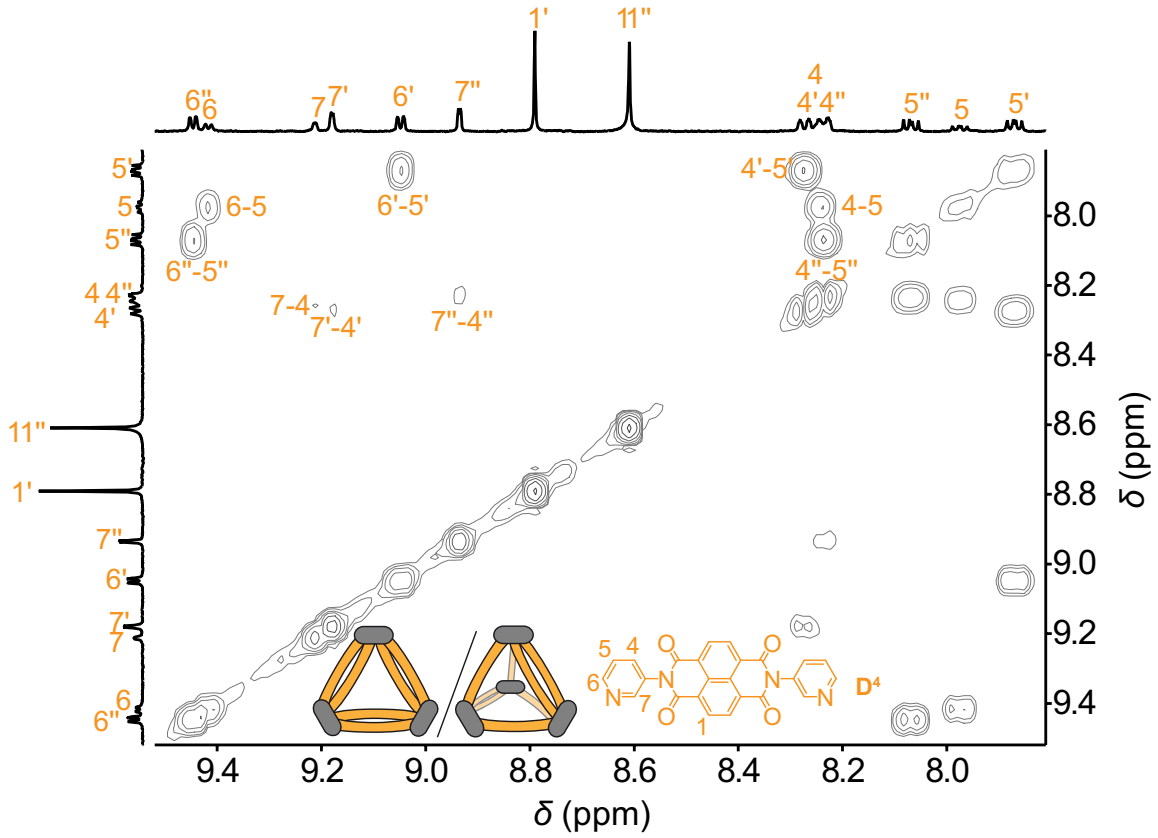

Supplementary Figure 24 | Partial ^{1}H–^{1}H COSY spectrum (500 MHz, 298 K, CD_3CN) of homoleptic $Pd_3\mathbf{D}^{4}{}_6$/$Pd_4\mathbf{D}^{4}{}_8$ ring/cage mixture.

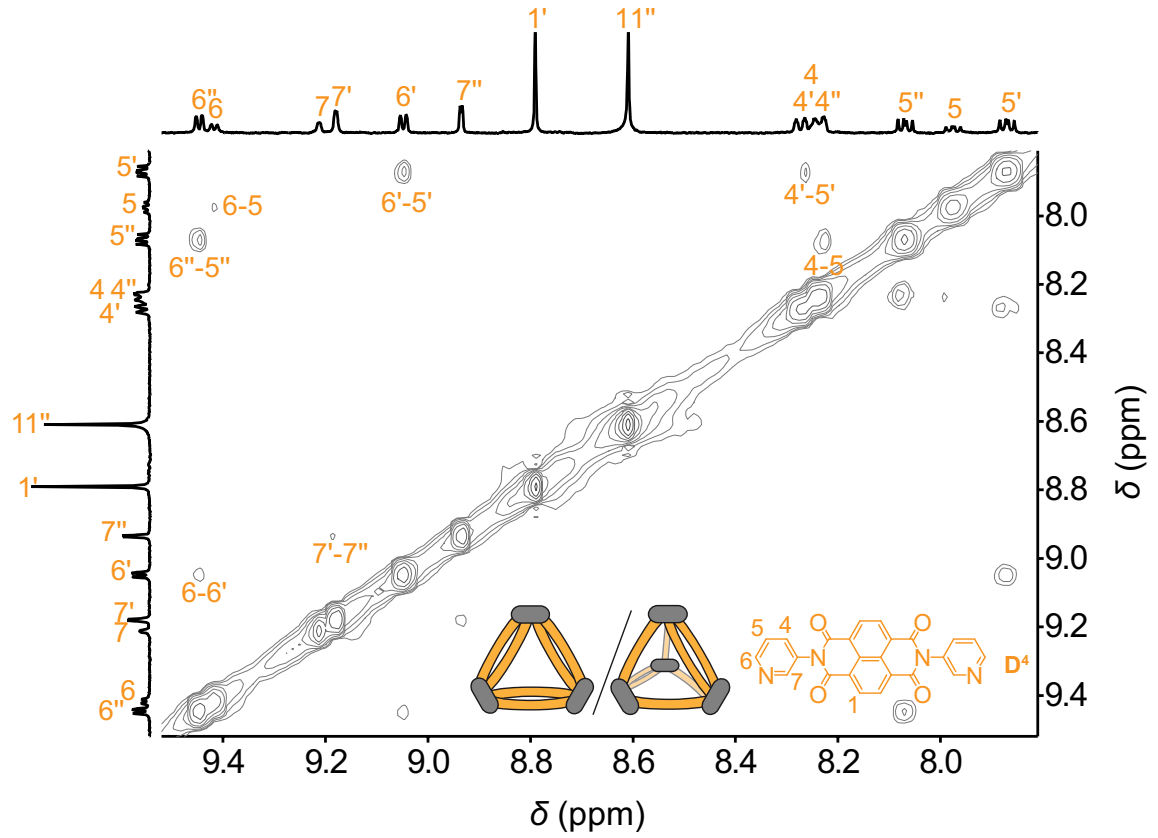

Supplementary Figure 25 | Partial ^{1}H–^{1}H NOESY spectrum (500 MHz, 298 K, CD_3CN) of homoleptic $Pd_3\mathbf{D}^{4}{}_6$/$Pd_4\mathbf{D}^{4}{}_8$ ring/cage mixture.

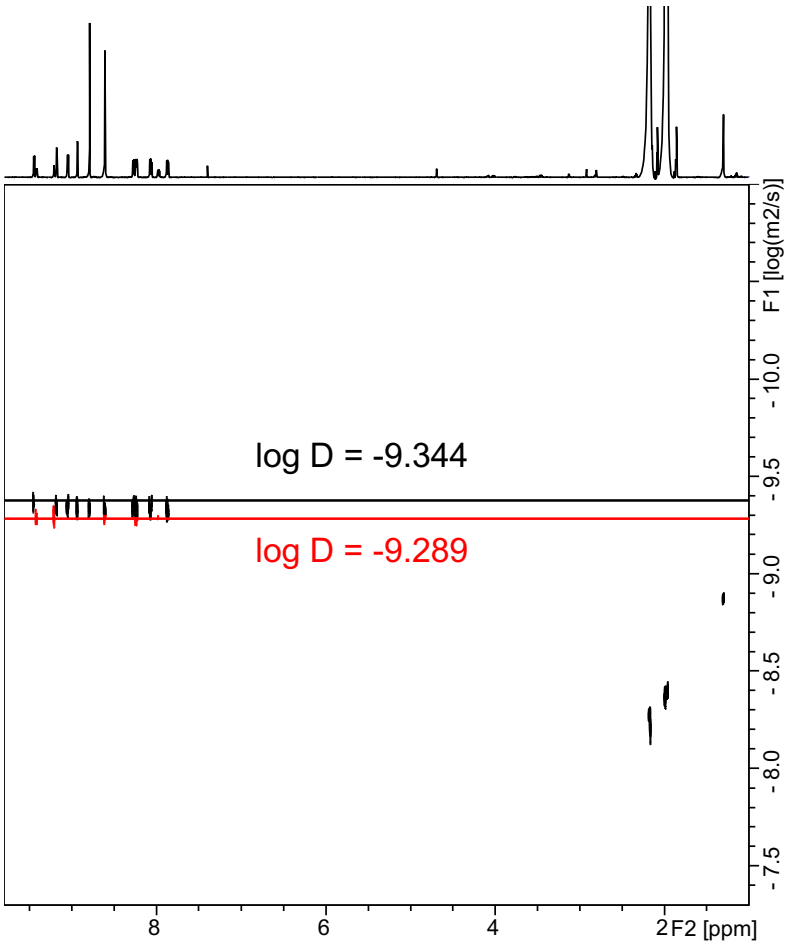

Supplementary Figure 26 | ^{1}H DOSY spectrum (500 MHz, 298 K, 298 K, CD_3CN) of homoleptic $Pd_3\mathbf{D^4}_6$/$Pd_4\mathbf{D^4}_8$ ring/cage mixture. Diffusion coefficient for $Pd_3\mathbf{D^4}_6$: D = 5.140 × 10^{-10} m^2s^{-1}, log *D* = −9.289, r = 12.7 Å; $Pd_4\mathbf{D^4}_8$: D = 4.529 × 10^{-10} m^2s^{-1}, log *D* = −9.344, r = 14.4 Å

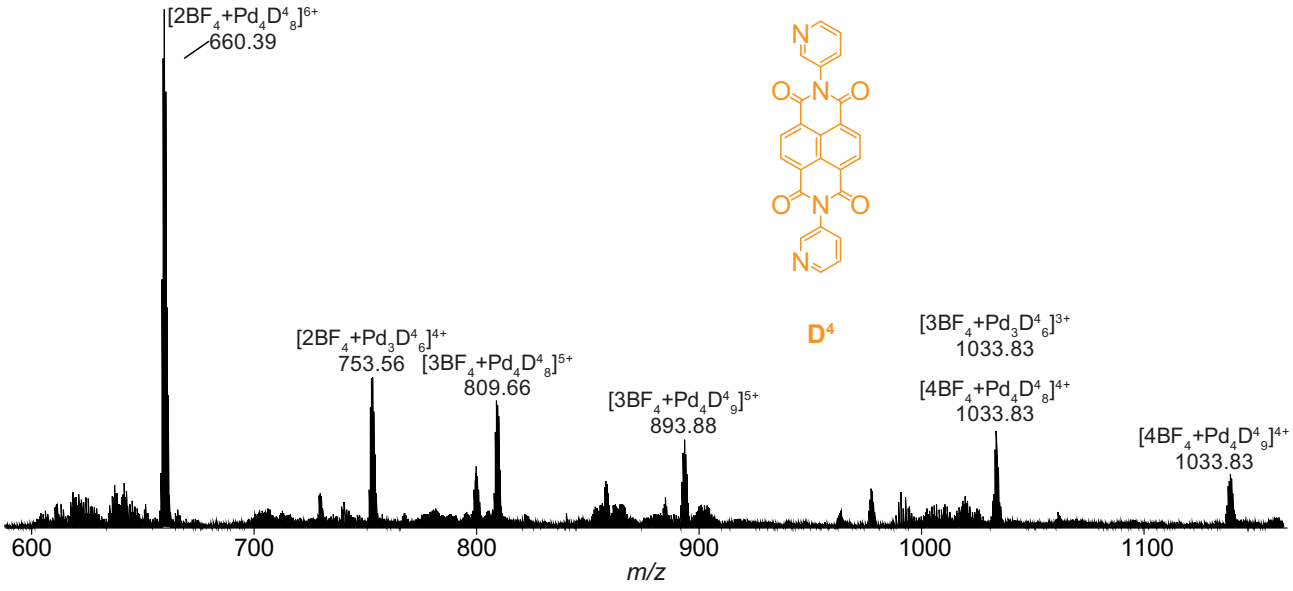

Supplementary Figure 27 | HR-ESI mass spectrum of homoleptic $Pd_3\mathbf{D^4}_6$/$Pd_4\mathbf{D^4}_8$ ring/cage mixture.

3.3. Evolution of heteroleptic cage Pd_2**ABCD**

In the following, the reactions of pairs of different ligands, followed by triples and all quadruples of ligands with Pd(II) cations are described in a systematic way, leading to a number of heteroleptic cages that pave the way to understanding the non-statistical assembly of the ultimately desired Pd_2**ABCD** system as a non-statistical (one out of 55 possible) integrative self-assembly product.

Note: Cases leading to (more or less) statistical assembly outcome are introduced by "Self-assembly with ligands." in the respective heading while reactions leading to clearly defined heteroleptic species denote the formula of this species in their heading.

*3.3.1. Self-assembly with ligands **A** and **B***

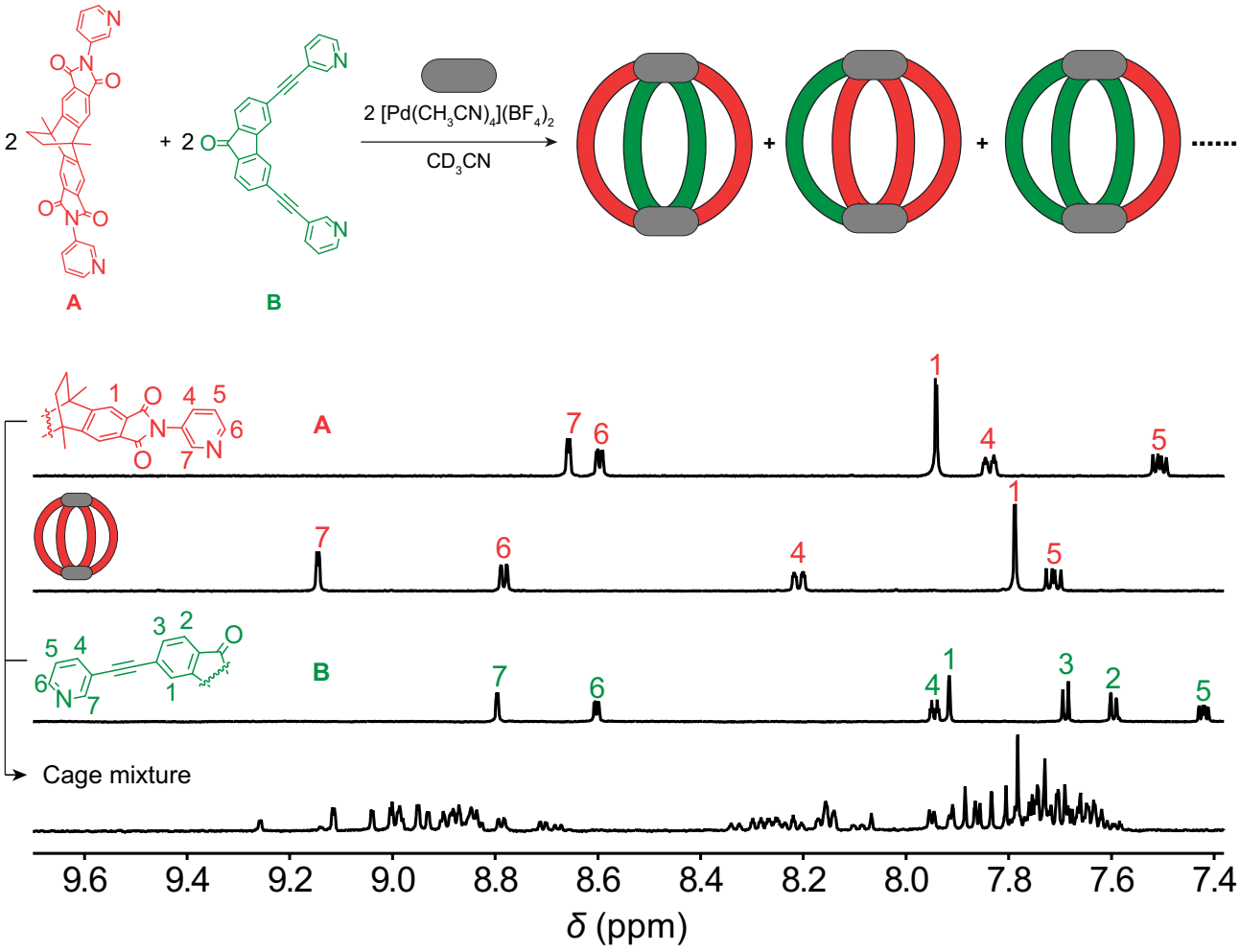

Supplementary Figure 28 | Partial ^{1}H NMR spectra (500 MHz, 298 K, CD_3CN) comparing the Pd(II)-mediated self-assembly of ligand **A** alone with the assembly of a mixture of ligands **A** and **B** (ratio Pd(II):**A**:**B** = 1:1:1).

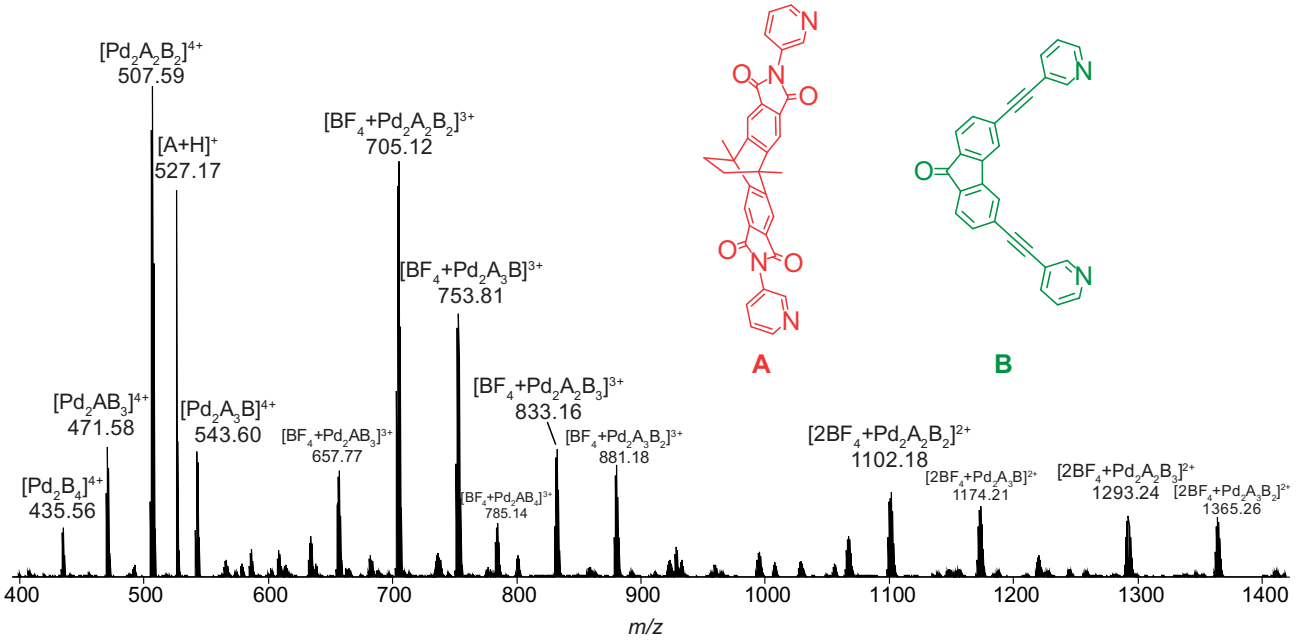

Supplementary Figure 29 | HR-ESI mass spectrum of the self-assembly with ligands **A** and **B** (ratio Pd(II):**A**:**B** = 1:1:1).

*3.3.2. Self-assembly with ligands **C** and **D***

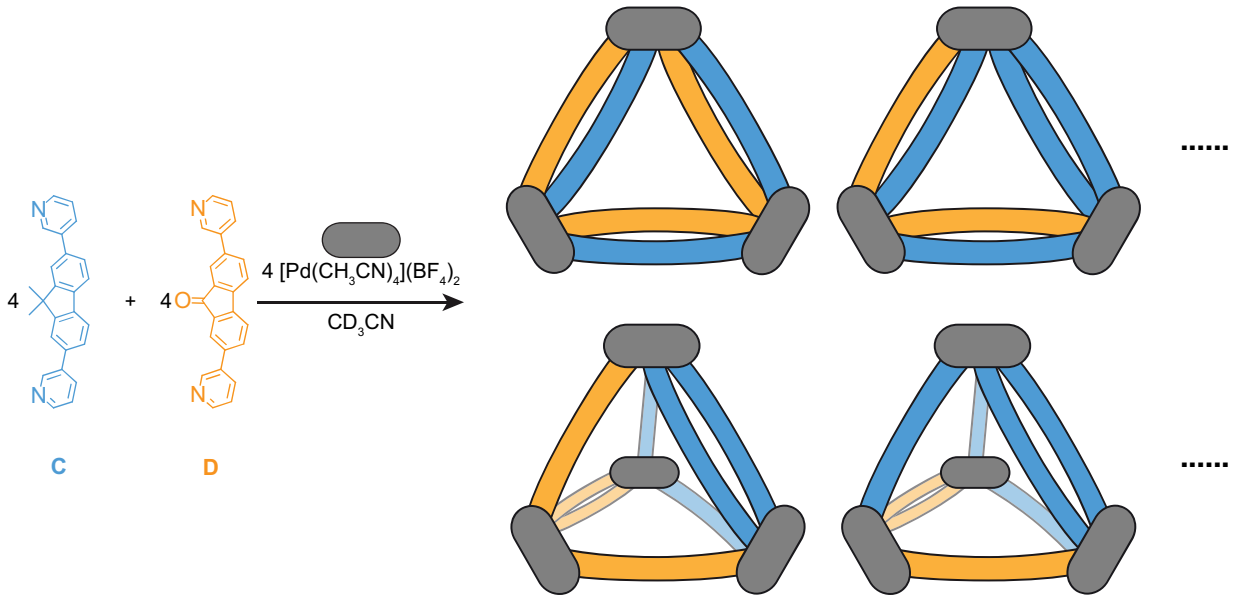

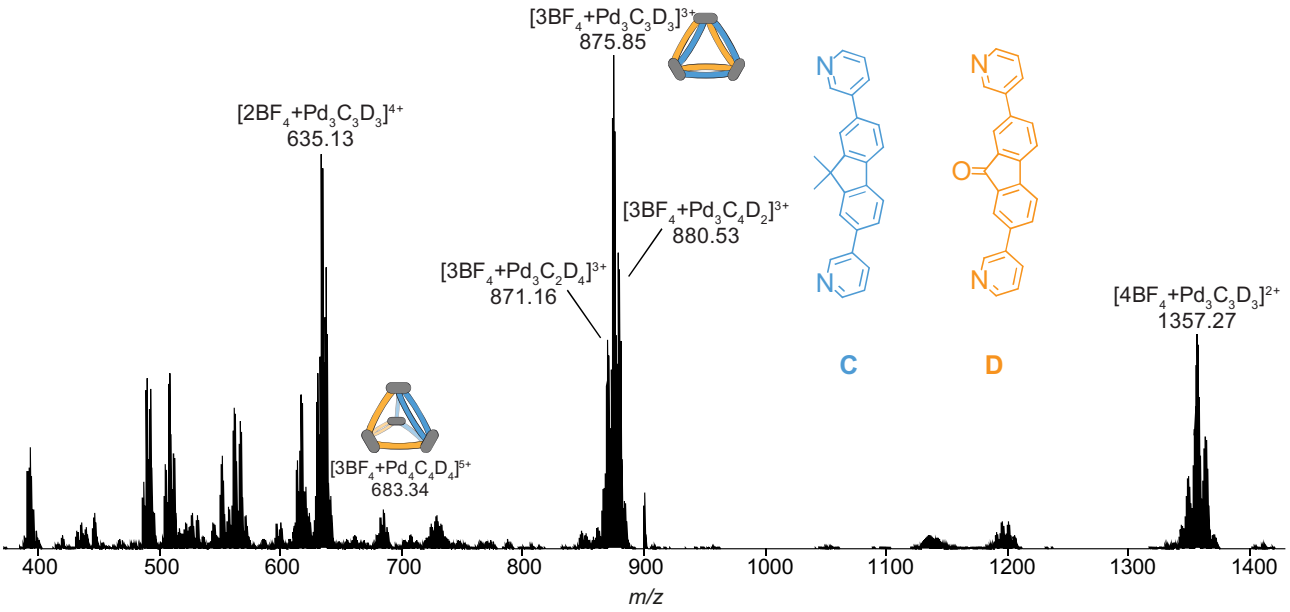

Supplementary Figure 30 | HR-ESI mass spectrum of the self-assembly with ligands **C** and **D**.

3.3.3. Self-assembly of heteroleptic cage $Pd_2\mathbf{B}_2\mathbf{C}_2$

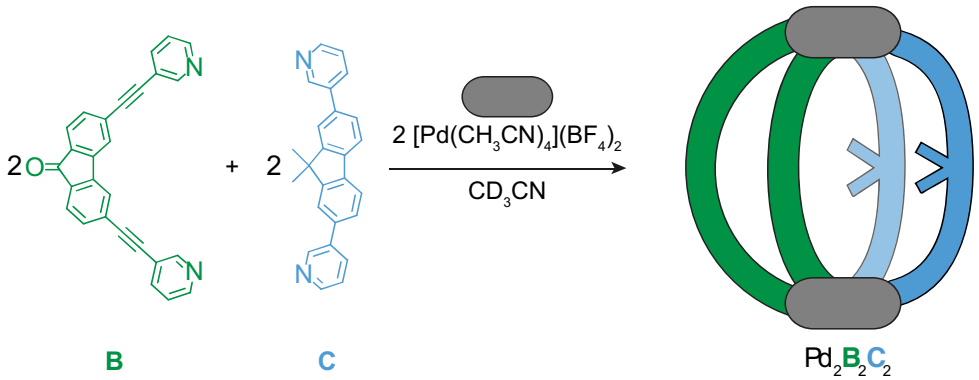

To a solution of **C** (120 µL, 3 mM, 0.36 µmol) and a suspension of **B** (120 µL, 3 mM, 0.36 µmol) in CD_3CN were added a stock solution of $[Pd(CH_3CN)_4](BF_4)_2$ (24 µL, 15 mM/CD_3CN, 0.36 µmol) and 186 µL additional CD_3CN. The mixture was heated in an NMR tube at 80 °C for 8 h to give a 0.4 mM cage solution containing the shown cage as only identifiable assembly product.

^{1}H NMR (500 MHz, 298 K, CD_3CN) δ 9.55 (d, J = 2.0 Hz, 4H), 9.43 (d, J = 1.8 Hz, 4H), 9.12 (dd, J = 5.9, 1.4 Hz, 4H), 9.02 (d, J = 5.8 Hz, 4H), 8.25 – 8.21 (m, 4H), 8.18 (dt, J = 8.1, 1.6 Hz, 4H), 7.95 (d, J = 7.7 Hz, 4H), 7.77 (s, 4H), 7.72 – 7.64 (m, 16H), 7.57 (d, J = 1.7 Hz, 4H), 7.49 (dd, J = 7.8, 1.7 Hz, 4H), 1.63 (s, 6H), 1.29 (s, 6H).

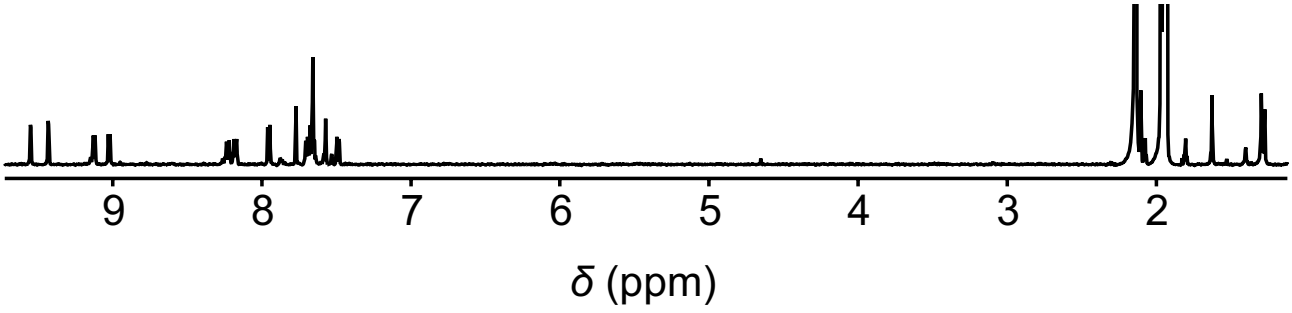

Supplementary Figure 31 | ^{1}H NMR spectrum (500 MHz, 298 K, CD_3CN) of heteroleptic cage $Pd_2\mathbf{B}_2\mathbf{C}_2$.

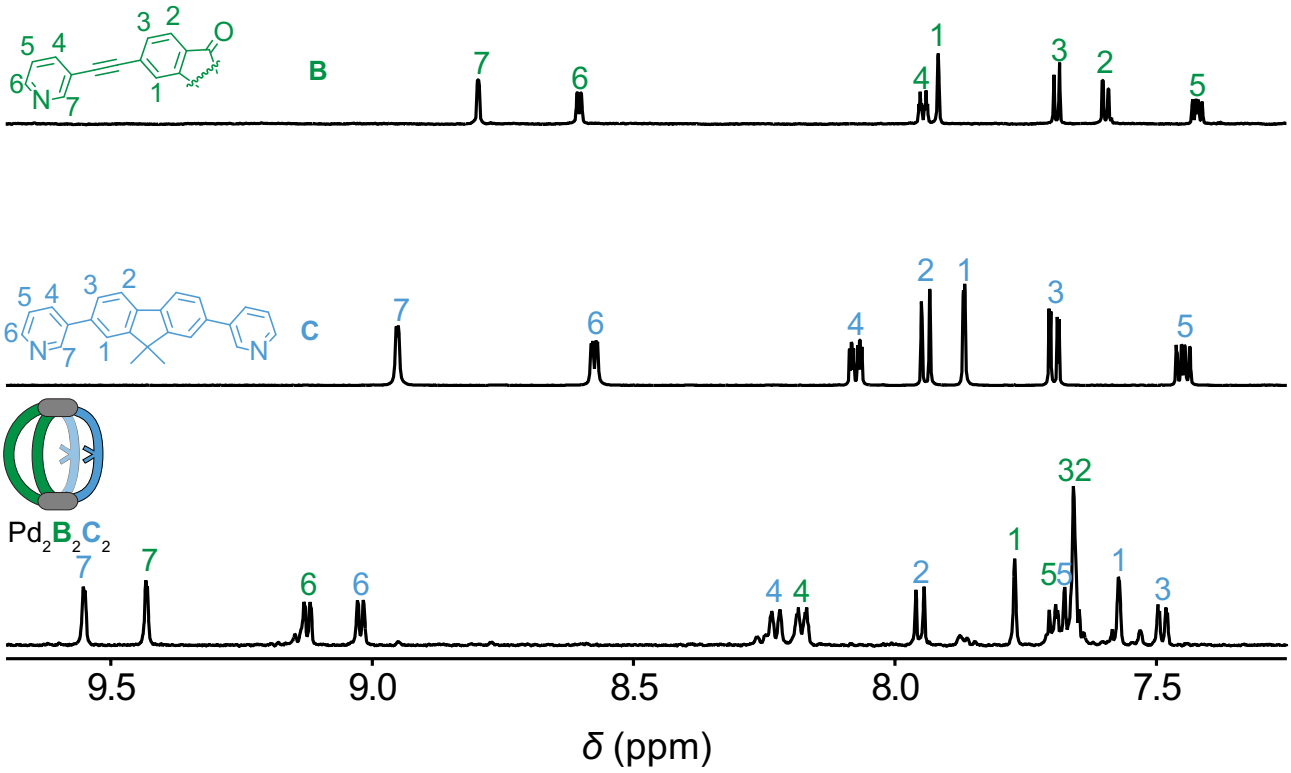

Supplementary Figure 32 | Partial ^{1}H NMR spectrum (500 MHz, 298 K, CD_3CN) comparison of ligand **B** (top), ligand **C** (middle), and heteroleptic cage $Pd_2\mathbf{B}_2\mathbf{C}_2$ (bottom).

^{13}C NMR (176 MHz, 298 K, CD_3CN) δ 192.17, 156.86, 153.88, 151.25, 150.58, 150.16, 144.76, 144.73, 143.14, 140.66, 139.71, 136.11, 135.99, 135.52, 128.95, 128.87, 128.44, 128.31, 125.24, 124.25, 123.74, 122.93, 122.70, 95.43, 87.58, 48.26, 29.84, 25.86.

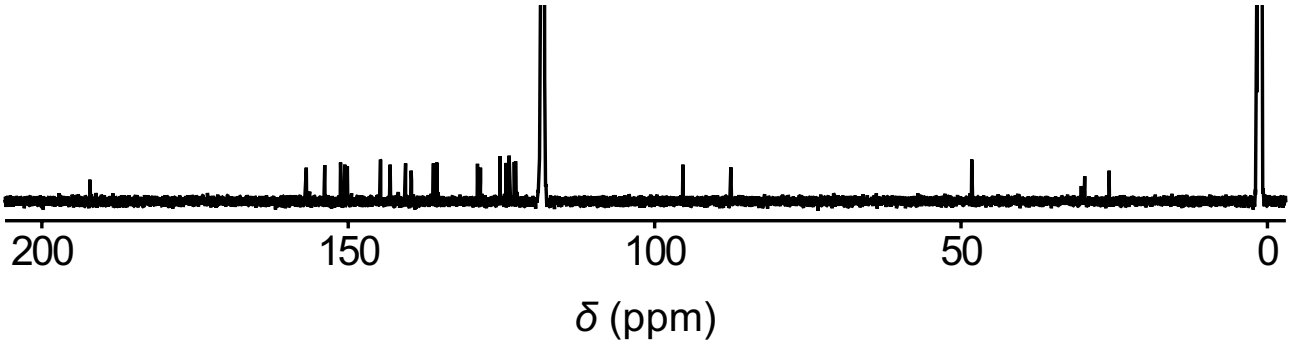

Supplementary Figure 33 | ^{13}C NMR spectrum (176 MHz, 298 K, CD_3CN) of heteroleptic cage $Pd_2\mathbf{B}_2\mathbf{C}_2$.

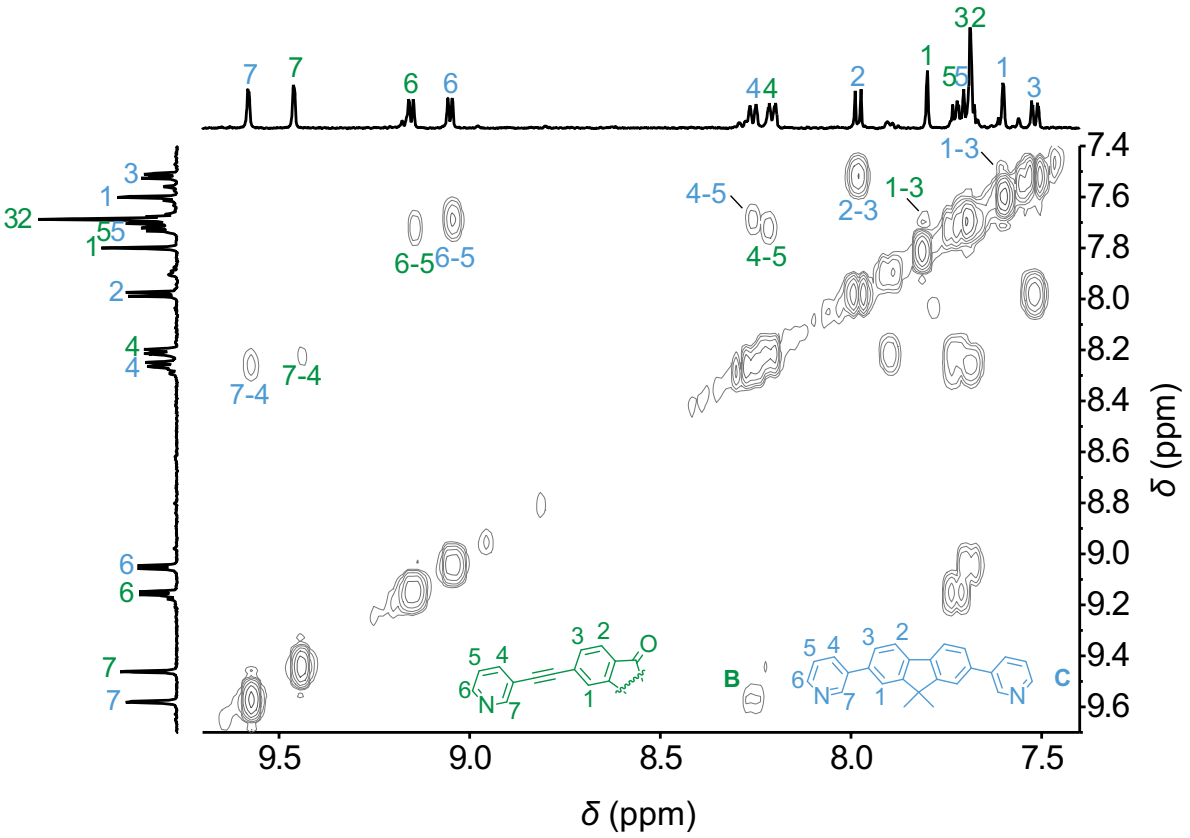

Supplementary Figure 34 | Partial ^{1}H–^{1}H COSY spectrum (500 MHz, 298 K, CD_3CN) of heteroleptic cage $Pd_2\mathbf{B}_2\mathbf{C}_2$.

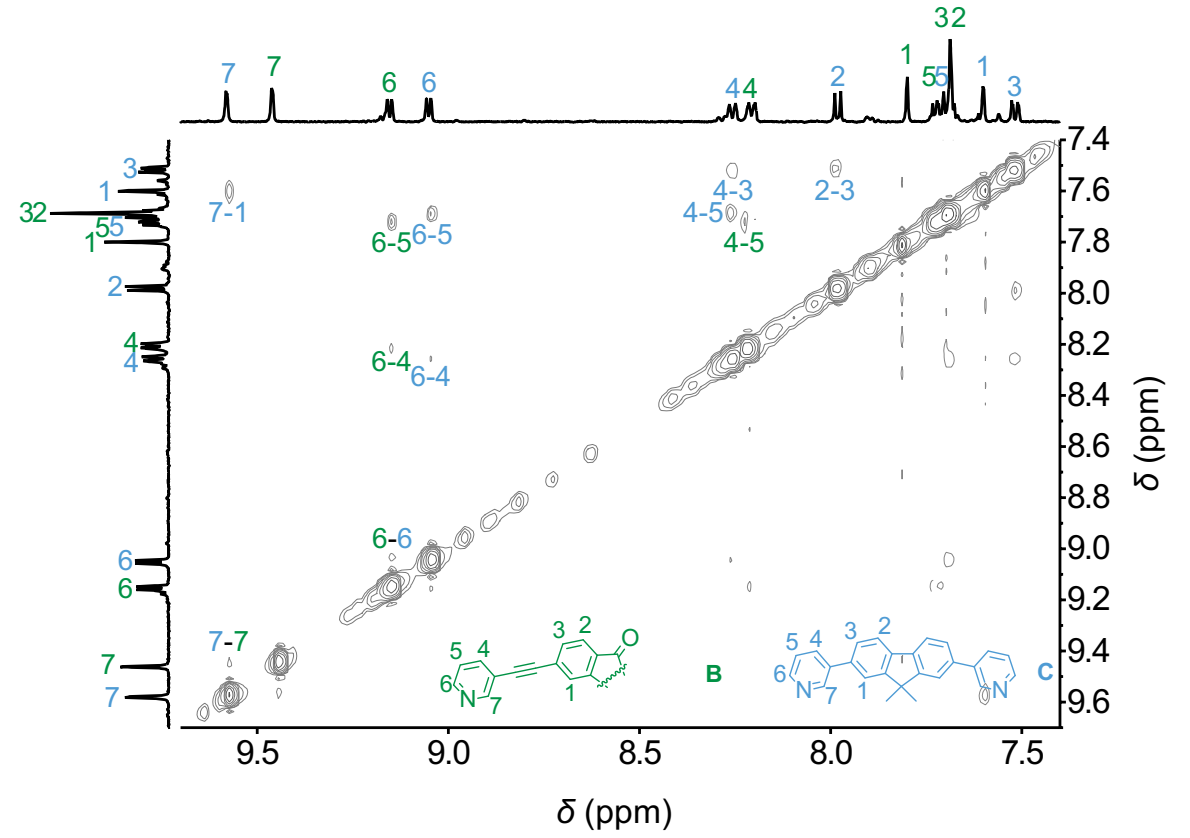

Supplementary Figure 35 | Partial ^{1}H–^{1}H NOESY spectrum (500 MHz, 298 K, CD_3CN) of heteroleptic cage $Pd_2\mathbf{B}_2\mathbf{C}_2$.

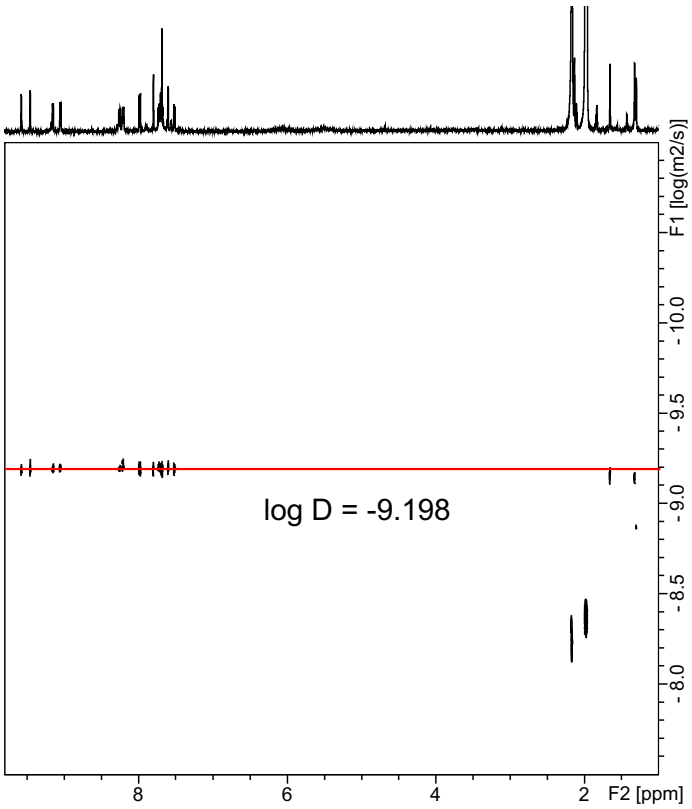

Supplementary Figure 36 | ^{1}H DOSY spectrum (500 MHz, 298 K, CD_3CN) of heteroleptic cage $Pd_2\mathbf{B}_2\mathbf{C}_2$. Diffusion coefficient for $Pd_2\mathbf{B}_2\mathbf{C}_2$: D = 6.34 × 10^{-10} m^2s^{-1}, log *D* = −9.198, r = 10.3 Å.

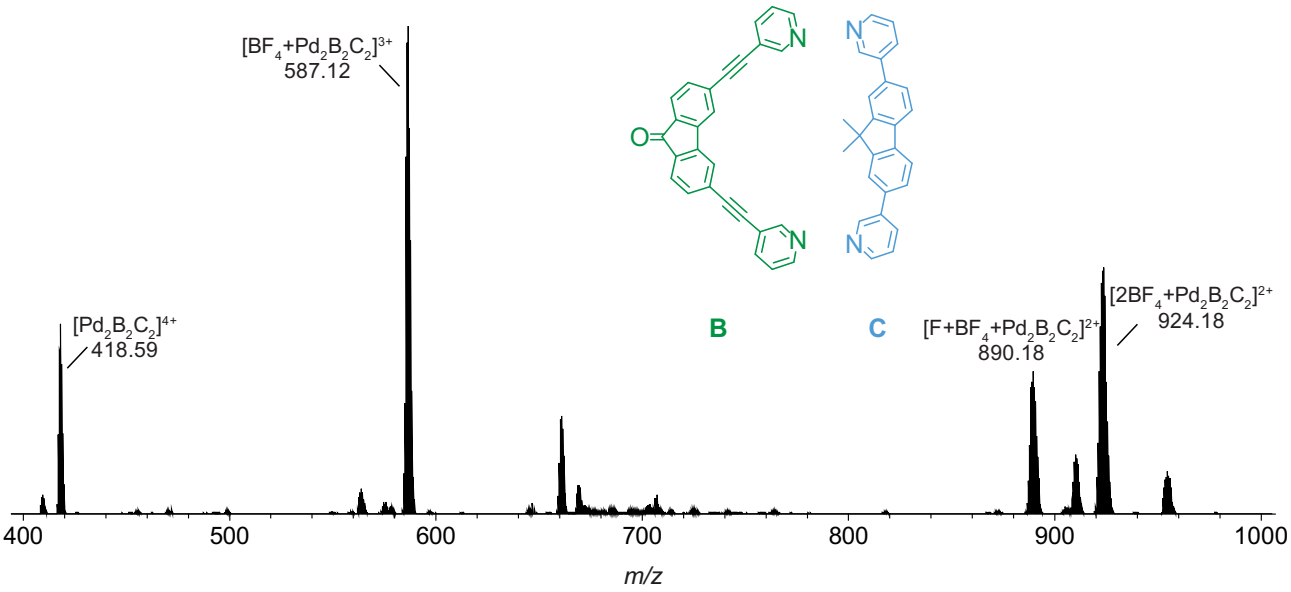

Supplementary Figure 37 | HR-ESI mass spectrum of heteroleptic cage $Pd_2\mathbf{B}_2\mathbf{C}_2$.

3.3.4. Self-assembly of heteroleptic cage $Pd_2\mathbf{B}_2\mathbf{D}_2$

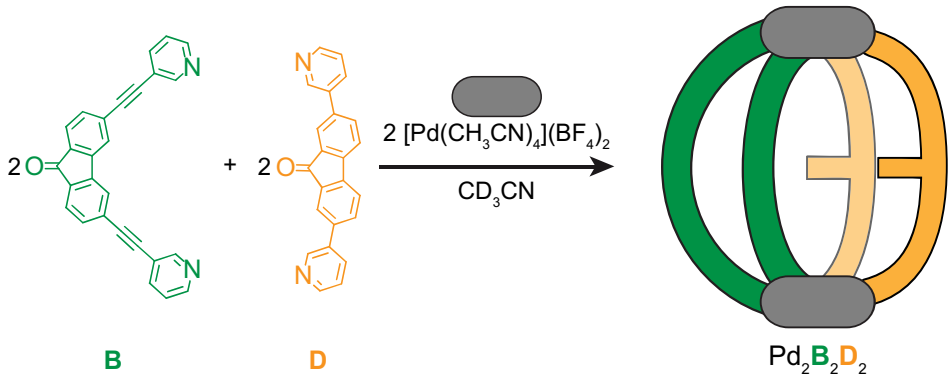

To a solution of **D** (120 µL, 3 mM, 0.36 µmol) and a suspension of **B** (120 µL, 3 mM, 0.36 µmol) in CD_3CN were added a stock solution of $[Pd(CH_3CN)_4](BF_4)_2$ (24 µL, 15 mM/CD_3CN, 0.36 µmol) and 186 µL additional CD_3CN. The mixture was heated in an NMR tube at 80 °C for 8 h to give a 0.4 mM cage solution containing the shown cage as only identifiable assembly product.

^{1}H NMR (500 MHz, 298 K, CD_3CN) δ 9.82 (d, J = 2.1 Hz, 4H), 9.33 (d, J = 1.8 Hz, 4H), 9.17 (dd, J = 5.9, 1.4 Hz, 4H), 8.99 (dd, J = 5.8, 1.3 Hz, 4H), 8.26 (dt, J = 8.4, 1.5 Hz, 4H), 8.20 (dt, J = 8.1, 1.6 Hz, 4H), 8.11 (d, J = 1.8 Hz, 4H), 7.87 – 7.84 (m, 4H), 7.82 (dd, J = 7.7, 1.8 Hz, 4H), 7.79 (t, J = 1.1 Hz, 4H), 7.72 – 7.65 (m, 16H).

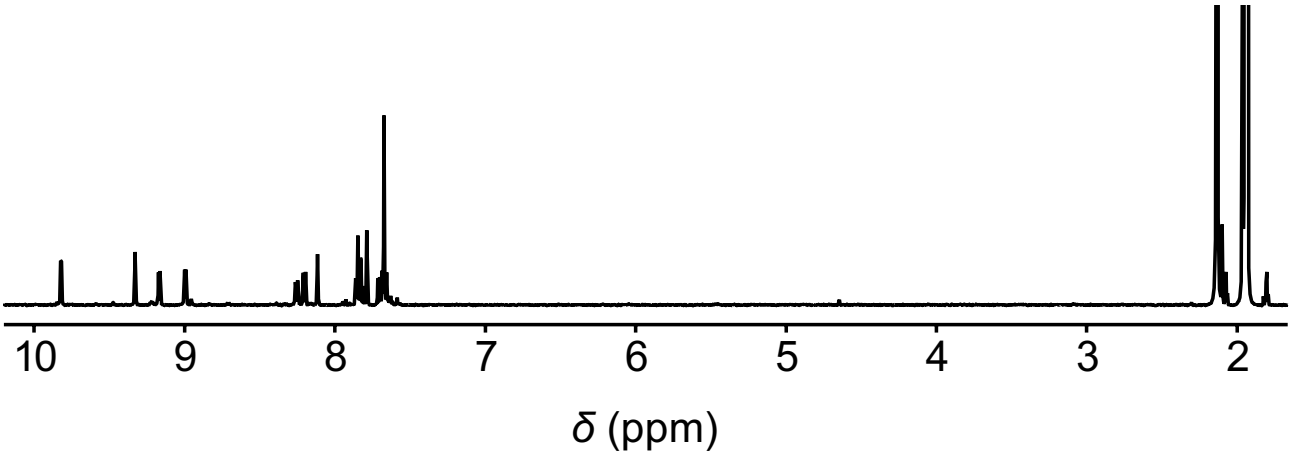

Supplementary Figure 38 | ^{1}H NMR spectrum (500 MHz, 298 K, CD_3CN) of heteroleptic cage $Pd_2\mathbf{B}_2\mathbf{D}_2$.

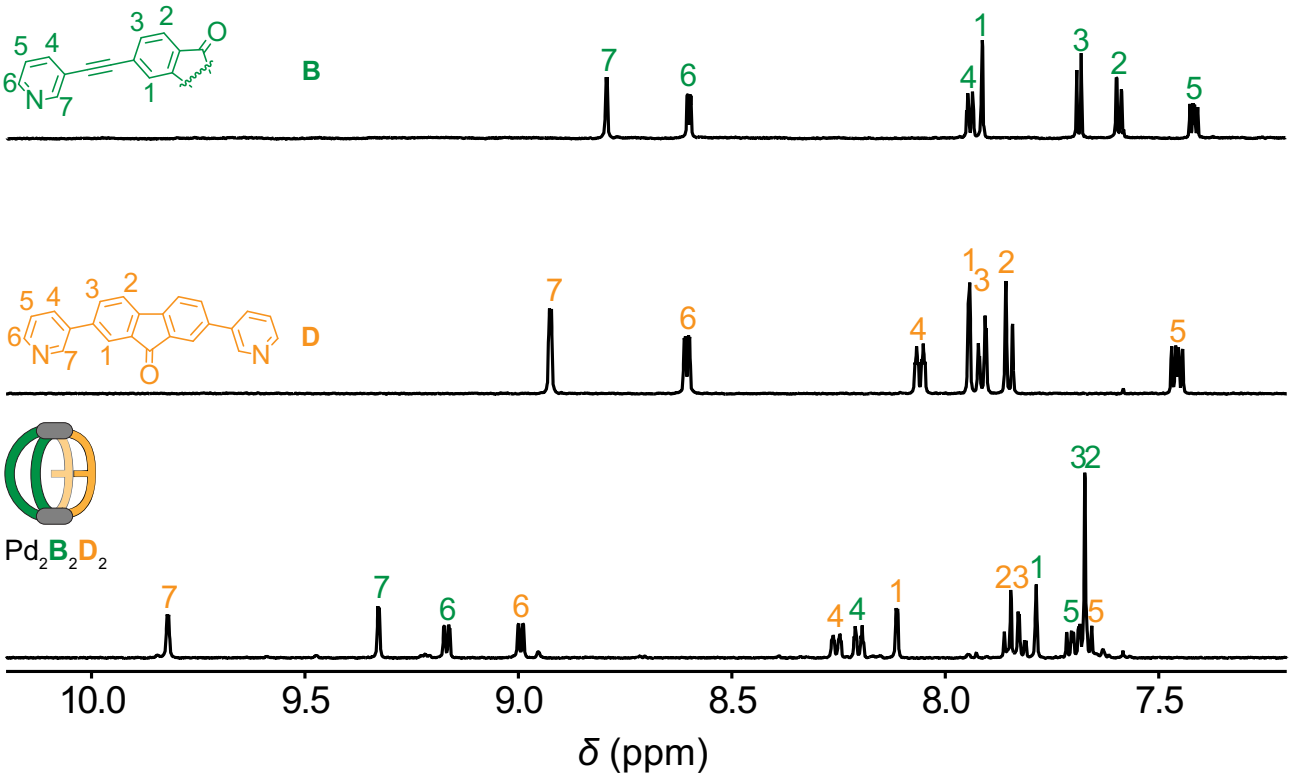

Supplementary Figure 39 | Partial ^{1}H NMR spectrum (500 MHz, 298 K, CD_3CN) comparison of ligand **B** (top), ligand **D** (middle), and heteroleptic cage $Pd_2\mathbf{B}_2\mathbf{D}_2$ (bottom).

^{13}C NMR (151 MHz, 298 K, CD_3CN) δ 193.18, 192.16, 153.14, 151.61, 150.68, 150.09, 145.59, 145.06, 144.74, 140.44, 138.86, 137.14, 137.13, 136.38, 135.57, 135.07, 128.76, 128.68, 128.42, 125.27, 124.53, 123.60, 95.69, 87.83.

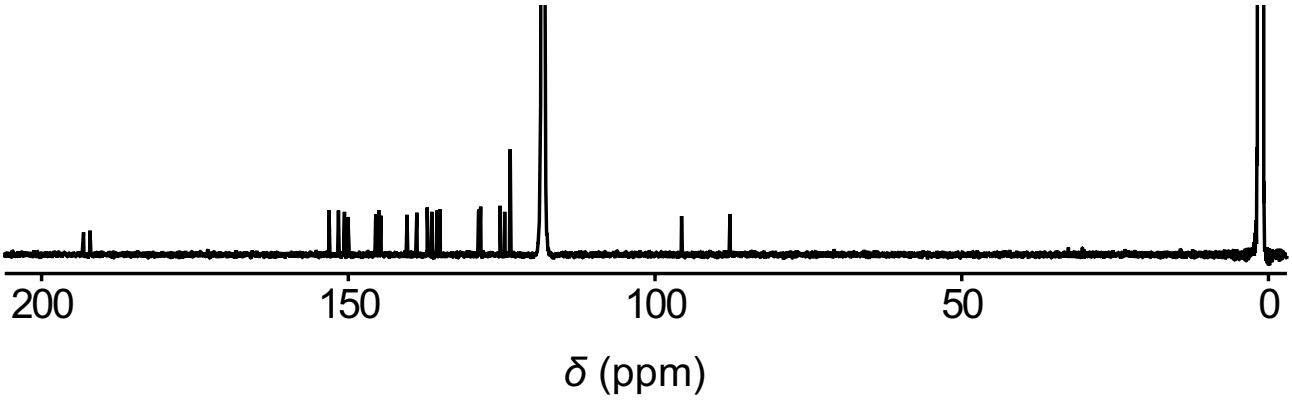

Supplementary Figure 40 | ^{13}C NMR spectrum (151 MHz, 298 K, CD_3CN) of heteroleptic cage $Pd_2\mathbf{B}_2\mathbf{D}_2$.

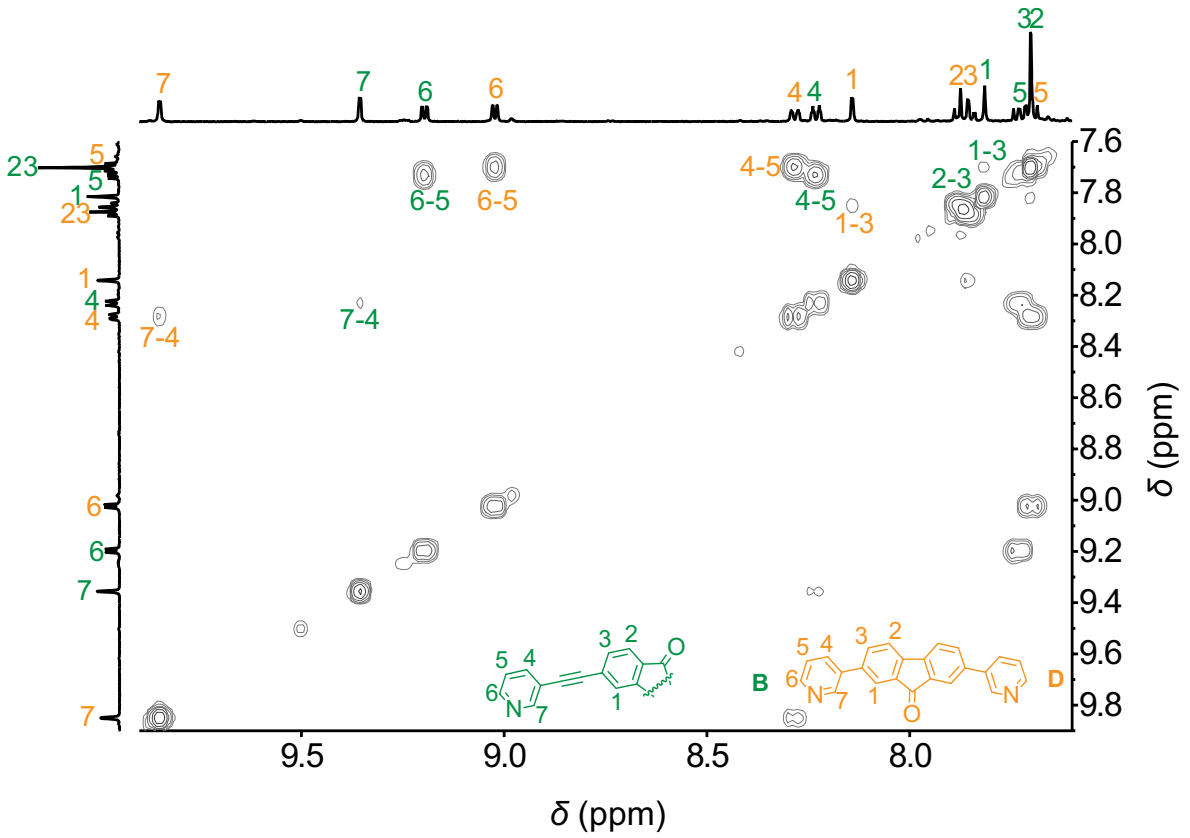

Supplementary Figure 41 | Partial ^{1}H–^{1}H COSY spectrum (500 MHz, 298 K, CD_3CN) of heteroleptic cage $Pd_2\mathbf{B}_2\mathbf{D}_2$.

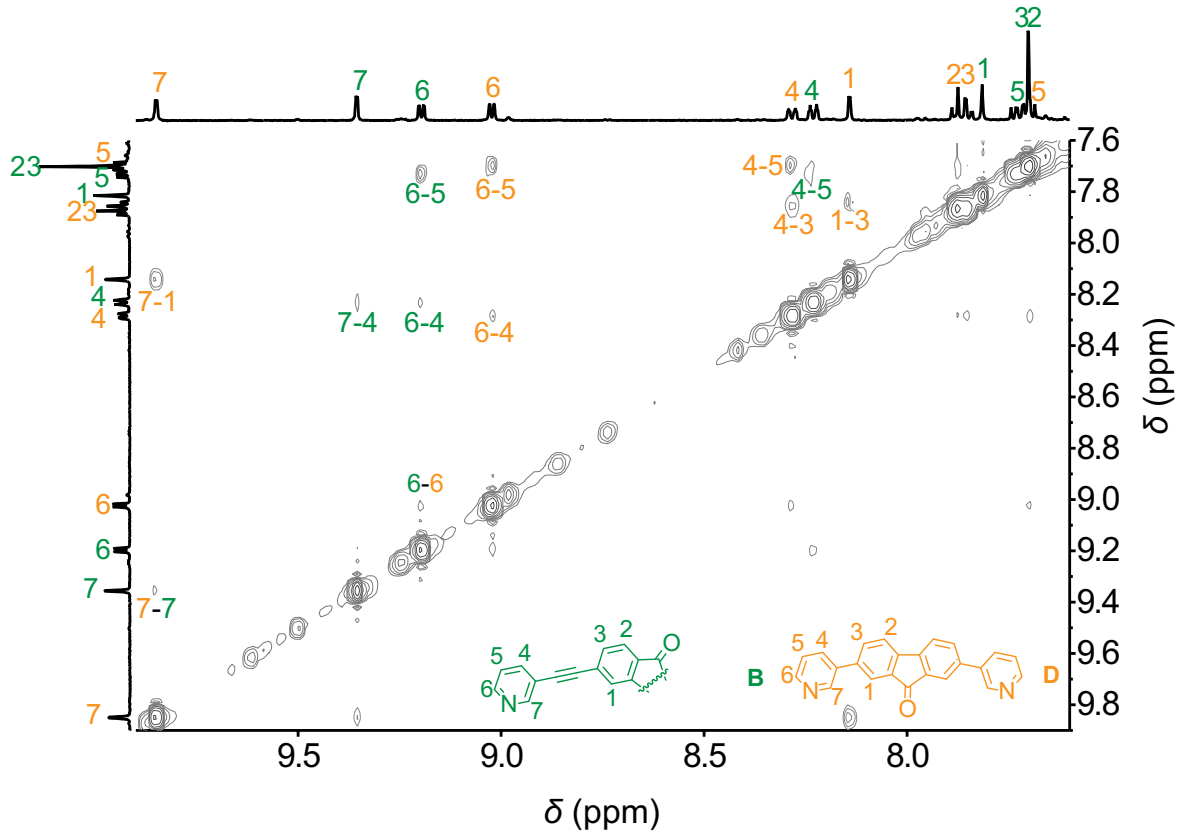

Supplementary Figure 42 | Partial ^{1}H–^{1}H NOESY spectrum (500 MHz, 298 K, CD_3CN) of heteroleptic cage $Pd_2\mathbf{B}_2\mathbf{D}_2$.

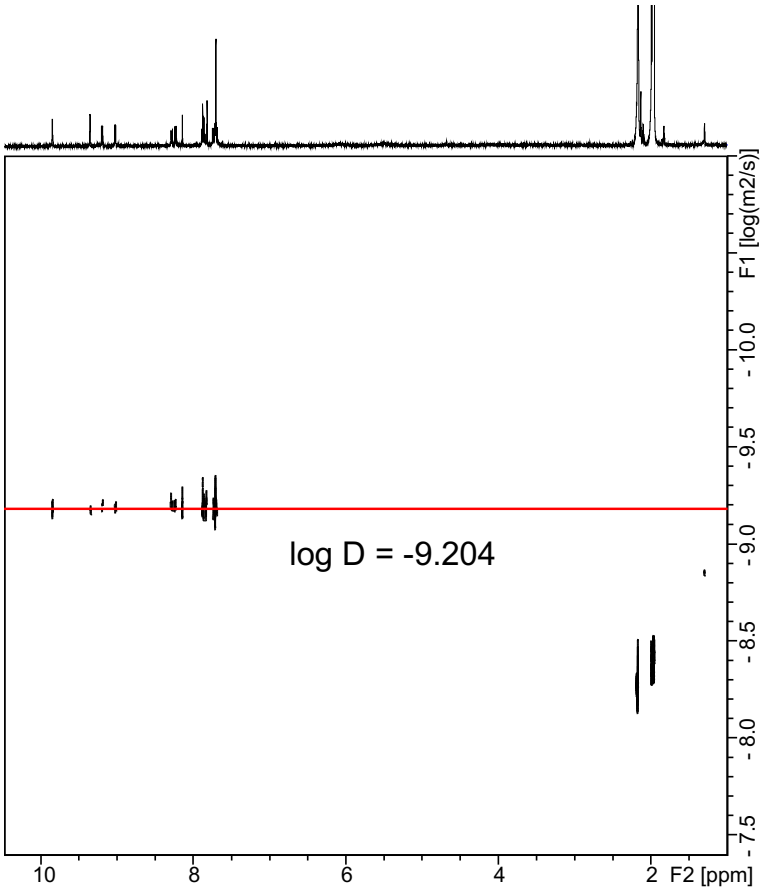

Supplementary Figure 43 | ^{1}H DOSY spectrum (500 MHz, 298 K, CD_3CN) of heteroleptic cage $Pd_2\mathbf{B}_2\mathbf{D}_2$. Diffusion coefficient for $Pd_2\mathbf{B}_2\mathbf{D}_2$: D = 6.25 × 10^{-10} m^2s^{-1}, log *D* = −9.204, r = 10.5 Å.

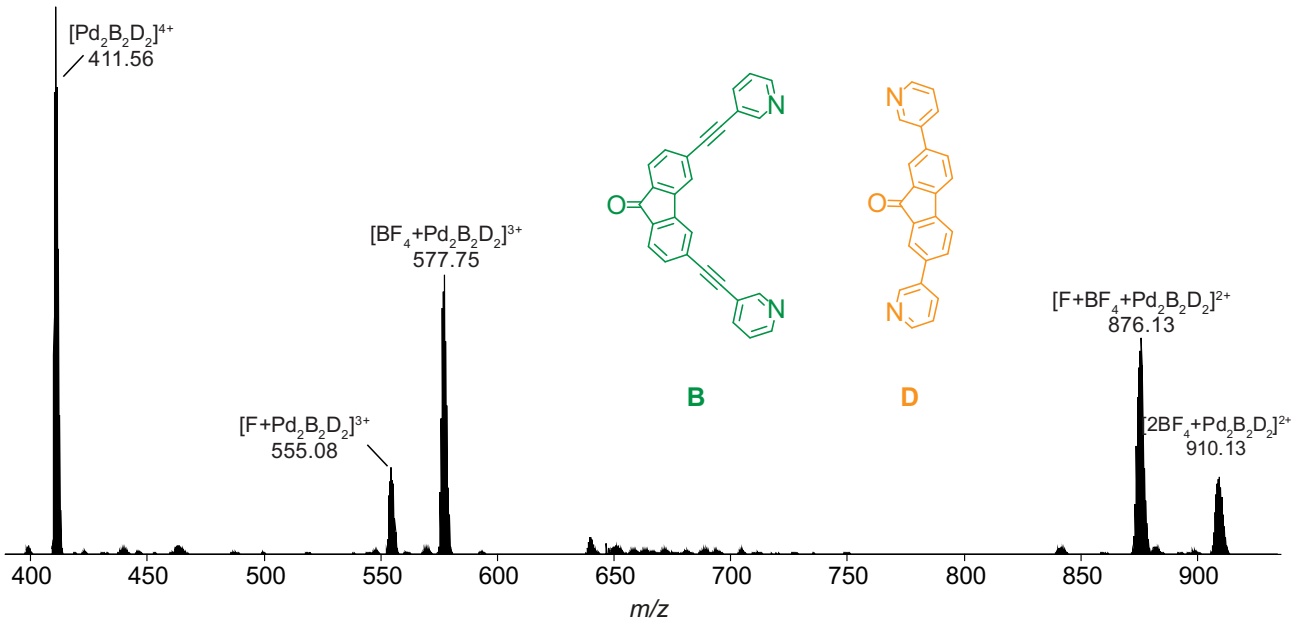

Supplementary Figure 44 | HR-ESI mass spectrum of heteroleptic cage $Pd_2\mathbf{B}_2\mathbf{D}_2$.

*3.3.5. Self-assembly of heteroleptic cage Pd_2**B**$_2$**CD***

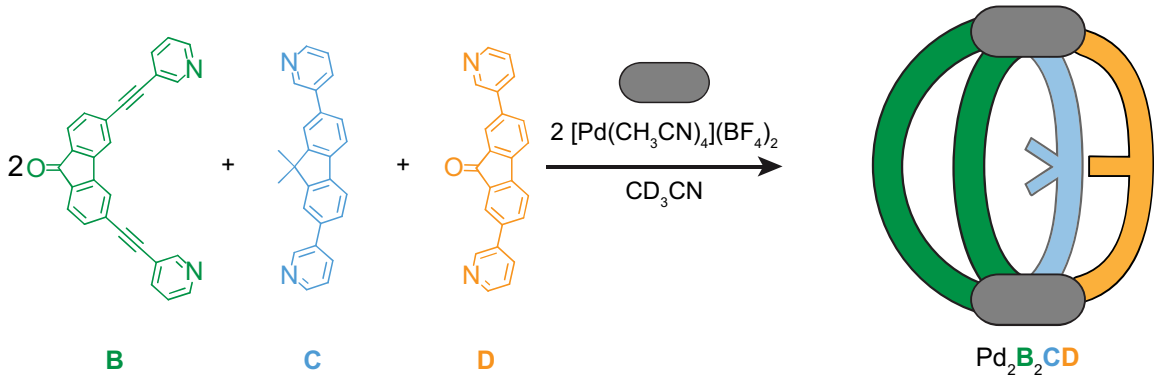

To a solution of **C** (60 µL, 3 mM, 0.18 µmol) and **D** (60 µL, 3 mM, 0.18 µmol), a suspension of **B** (120 µL, 3 mM, 0.36 µmol) were added a stock solution of $[Pd(CH_3CN)_4](BF_4)_2$ (24 µL, 15 mM/CD_3CN, 0.36 µmol) and 186 µL additional CD_3CN. The mixture was heated at 80 °C for 8 h to give a 0.4 mM solution containing the shown cage as predominant species.

^{1}H NMR (500 MHz, 298 K, CD_3CN) δ 9.94 (s, 2H), 9.49 (s, 2H), 9.46 (s, 2H), 9.20 (s, 2H), 9.18 (d, J = 5.7 Hz, 2H), 9.13 (d, J = 5.8 Hz, 4H), 8.95 (d, J = 5.3 Hz, 2H), 8.61 (s, 2H), 8.35 (d, J = 7.9 Hz, 2H), 8.23 (d, J = 8.1 Hz, 2H), 8.18 (d, J = 8.1 Hz, 2H), 8.15 (d, J = 8.1 Hz, 2H), 7.98 (d, J = 7.7 Hz, 2H), 7.94 – 7.89 (m, 4H), 7.82 (s, 2H), 7.78 – 7.70 (m, 4H), 7.70 – 7.65 (m, 10H), 7.62 (d, J = 1.7 Hz, 4H), 7.52 (d, J = 7.6 Hz, 2H), 7.22 (s, 2H), 1.27 (s, 3H), 0.62 (s, 3H).

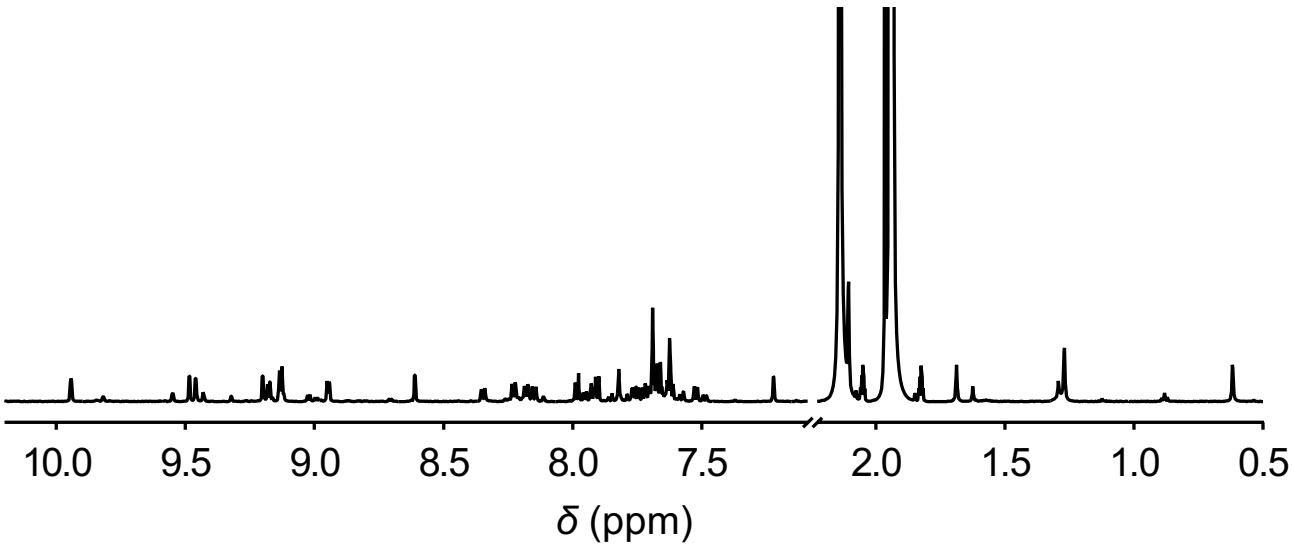

Supplementary Figure 45 | ^{1}H NMR spectrum (500 MHz, 298 K, CD_3CN) of heteroleptic cage Pd_2**B**$_2$**CD**.

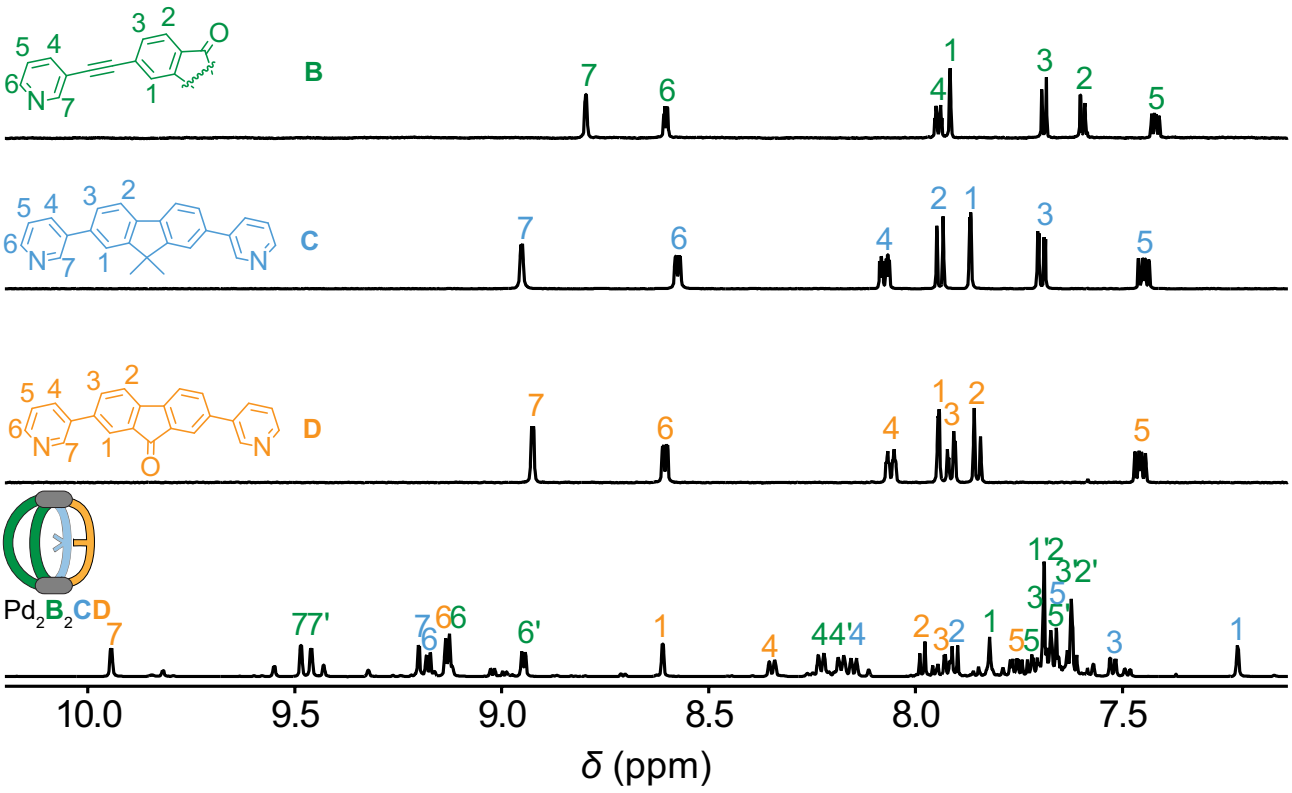

Supplementary Figure 46 | Partial ^{1}H NMR spectrum (500 MHz, 298 K, CD_3CN) comparison of ligand **B** (green), ligand **C** (blue), ligand **D** (yellow) and heteroleptic cage Pd_2**B**$_2$**CD** (bottom).

^{13}C NMR (151 MHz, 298 K, CD_3CN) δ 194.01, 192.13, 172.94, 155.99, 153.80, 152.90, 151.54, 151.40, 150.87, 150.28, 150.02, 146.01, 145.09, 144.80, 144.73, 142.19, 140.90, 140.29, 139.28, 139.09, 137.89, 137.13, 136.49, 136.29, 136.24, 135.75, 135.61, 135.45, 128.81, 128.71, 128.50, 128.40, 128.07, 125.32, 125.18, 124.54, 124.43, 124.18, 123.94, 123.66, 123.58, 123.23, 122.91, 95.75, 95.51, 87.97, 87.61, 46.84, 30.36, 26.91.

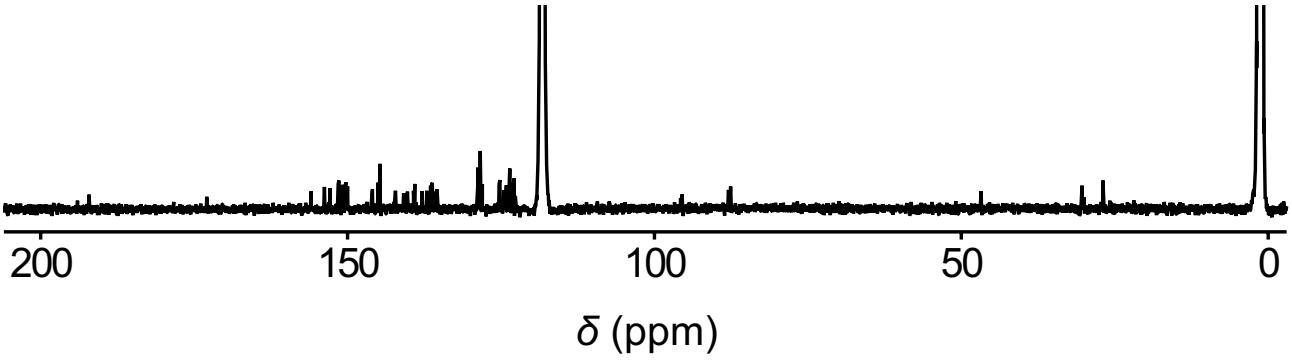

Supplementary Figure 47 | ^{13}C NMR spectrum (151 MHz, 298 K, CD_3CN) of heteroleptic cage Pd_2**B**$_2$**CD.**

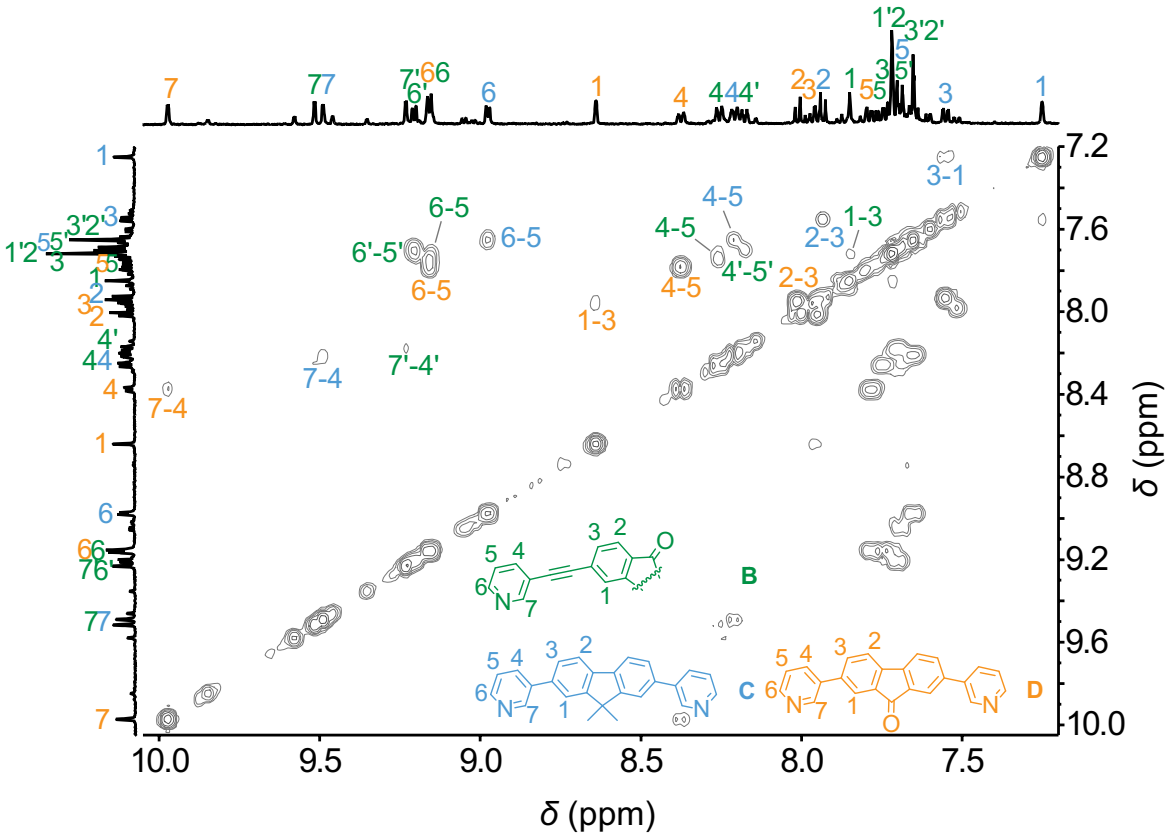

Supplementary Figure 48 | Partial ^{1}H–^{1}H COSY spectrum (500 MHz, 298 K, CD_3CN) of heteroleptic cage Pd_2**B**$_2$**CD**.

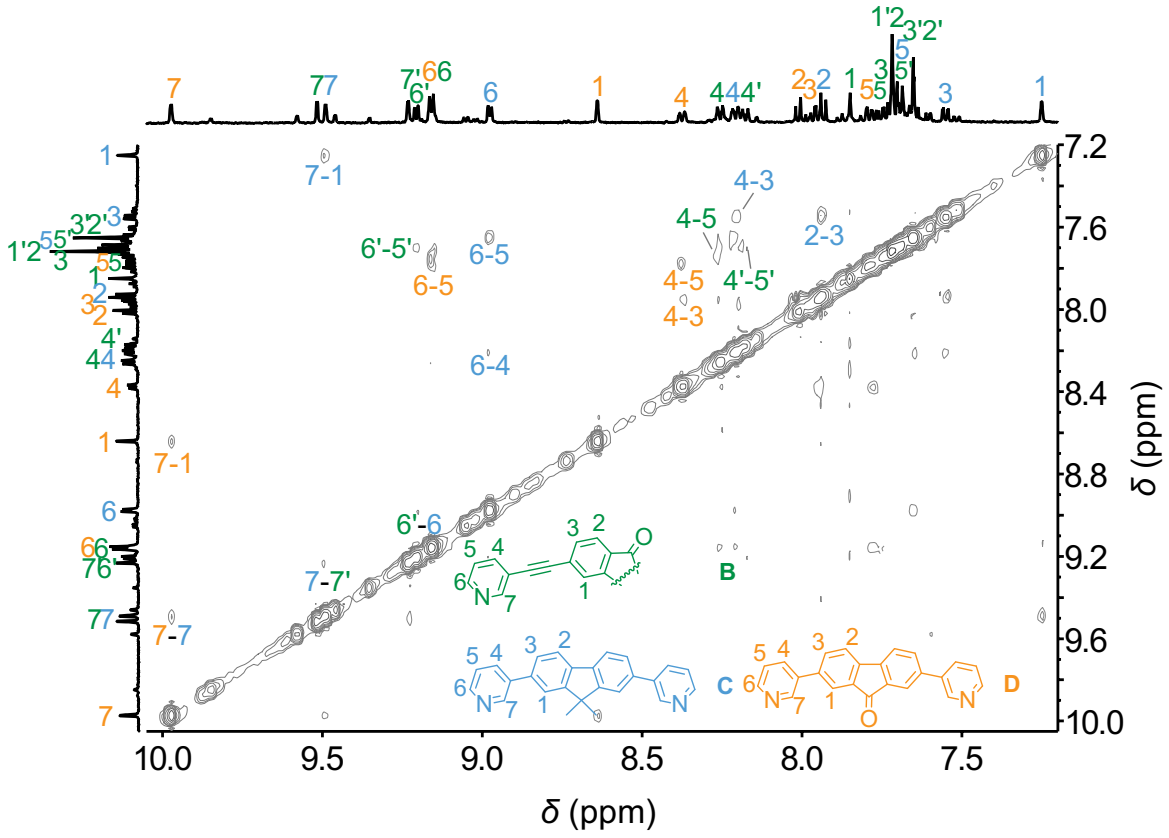

Supplementary Figure 49 | Partial ^{1}H–^{1}H NOESY spectrum (500 MHz, 298 K, CD_3CN) of heteroleptic cage Pd_2**B**$_2$**CD**.

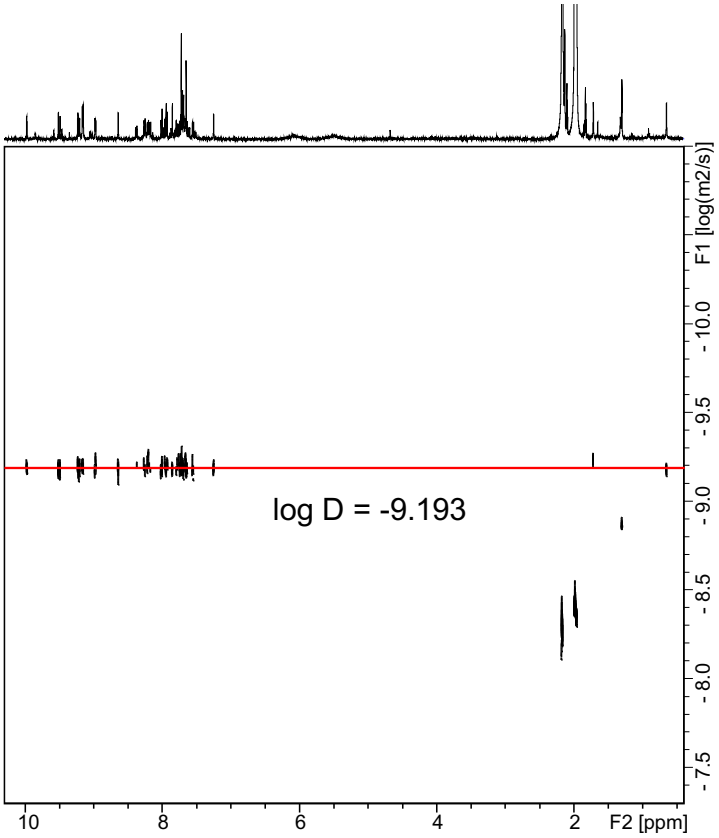

Supplementary Figure 50 | ^{1}H DOSY spectrum (500 MHz, 298 K, CD_3CN) of heteroleptic cage Pd_2**B**$_2$**CD**. Diffusion coefficient for Pd_2**B**$_2$**CD**: D = 6.412 × 10^{-10} m^2s^{-1}, log *D* = −9.193, r = 10.2 Å.

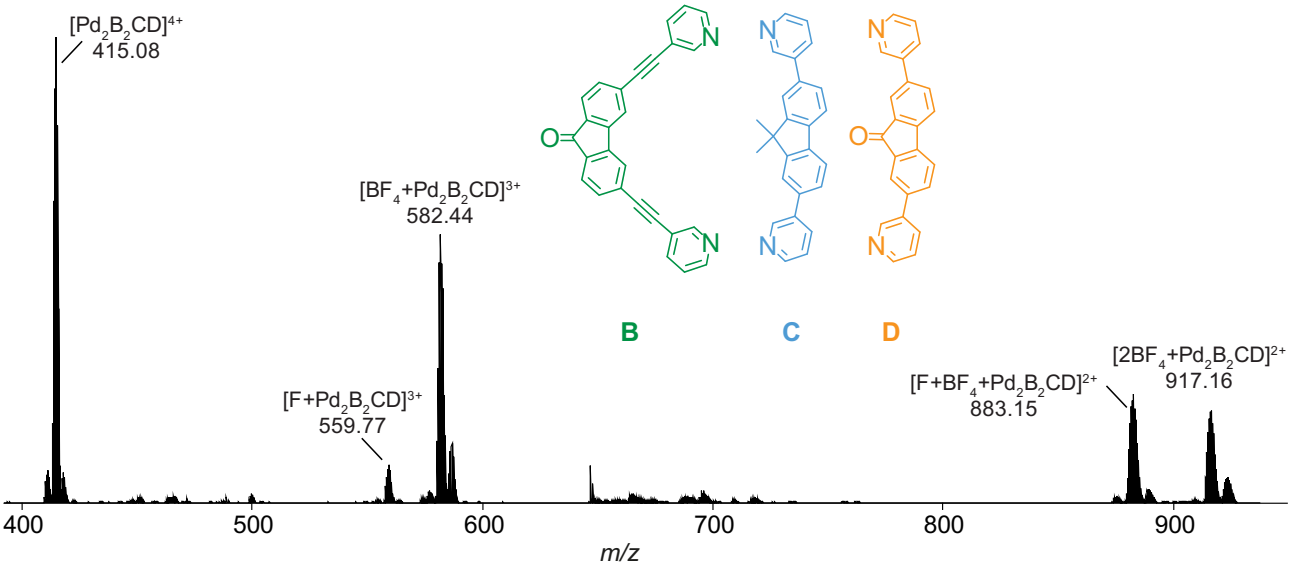

Supplementary Figure 51 | HR-ESI mass spectrum of heteroleptic cage Pd_2**B**$_2$**CD.**

3.3.6. Self-assembly of heteroleptic cage $Pd_2A_2C_2$

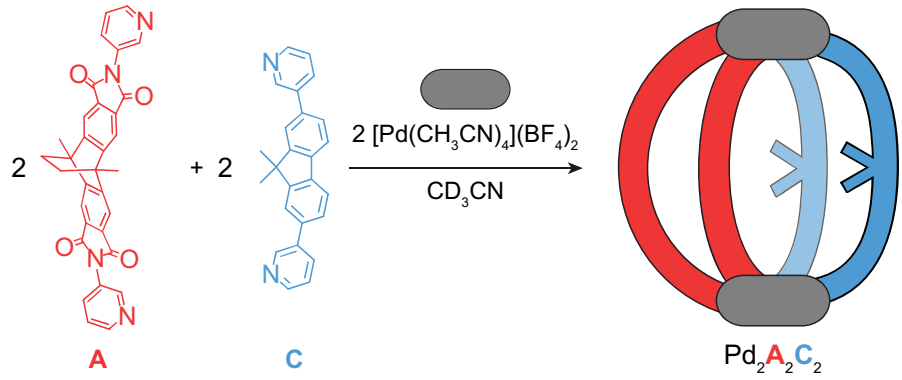

To a solution of **A** (120 µL, 3 mM, 0.36 µmol) in CD_3CN and **C** (120 µL, 3 mM, 0.36 µmol) were added a stock solution of $[Pd(CH_3CN)_4](BF_4)_2$ (24 µL, 15 mM/CD_3CN, 0.18 µmol) and 186 µL additional CD_3CN. The mixture was heated at 80 °C for 8 h to give a 0.4 mM cage solution containing the shown cage as predominant species.

^{1}H NMR (500 MHz, 298 K, CD_3CN) δ 9.29 (s, 4H), 9.07 (s, 4H), 9.06 – 9.04 (m, 4H), 8.98 (d, J = 5.7 Hz, 4H), 8.27 – 8.24 (m, 4H), 8.10 – 8.07 (m, 4H), 7.88 (m, 8H), 7.82 (dd, J = 8.3, 5.8 Hz, 4H), 7.73 (s, 4H), 7.63 (dd, J = 8.0, 5.7 Hz, 4H), 7.49 (dd, J = 7.8, 1.8 Hz, 4H), 7.43 (s, 4H), 2.19 (s, 6H), 2.04 (s, 6H), 1.43 (m, 8H), 1.04 (s, 12H).

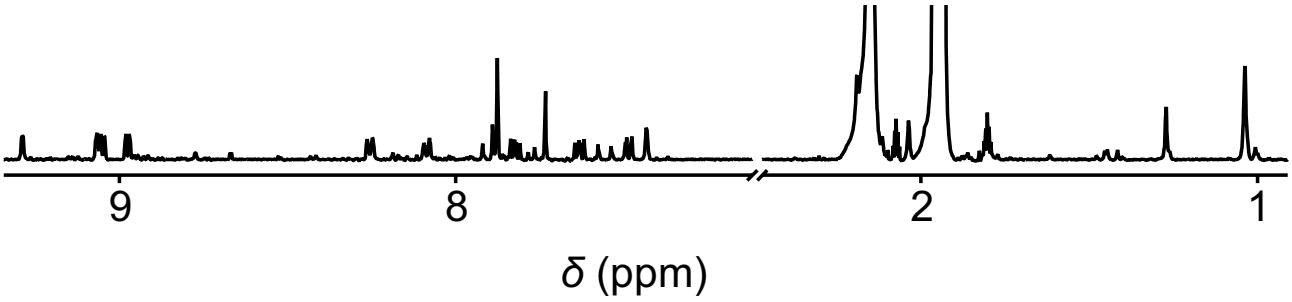

Supplementary Figure 52 | ^{1}H NMR spectrum (500 MHz, 298 K, CD_3CN) of heteroleptic cage $Pd_2A_2D_2$.

^{13}C NMR (151 MHz, 298 K, CD_3CN) δ 167.14, 166.75, 156.50, 154.82, 154.53, 151.00, 150.60, 150.58, 150.23, 143.25, 140.34, 140.23, 139.68, 135.95, 131.96, 130.56, 130.46, 128.85, 128.73, 128.20, 122.90, 122.38, 117.57, 47.73, 45.47, 45.22, 34.68, 34.49, 29.92, 25.90, 18.75, 18.62.

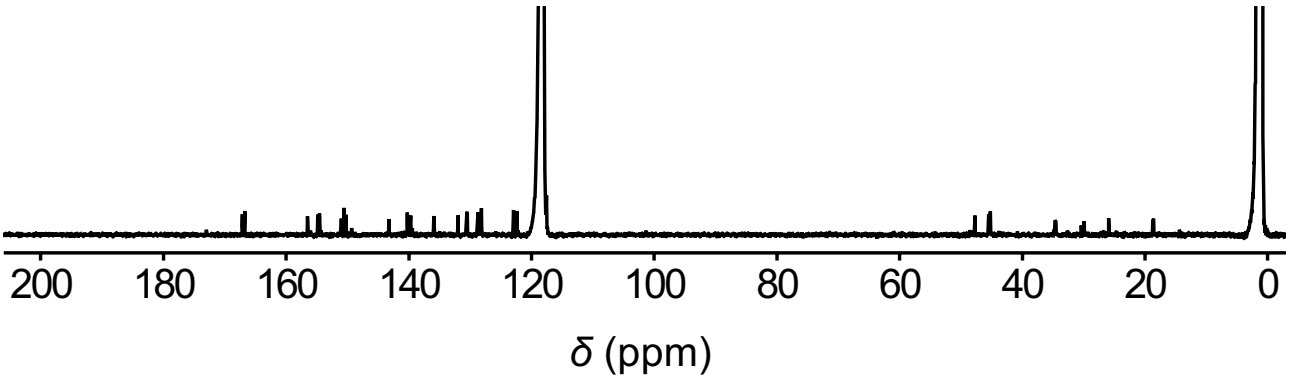

Supplementary Figure 53 | ^{13}C NMR spectrum (151 MHz, 298 K, CD_3CN) of heteroleptic cage $Pd_2A_2C_2$.

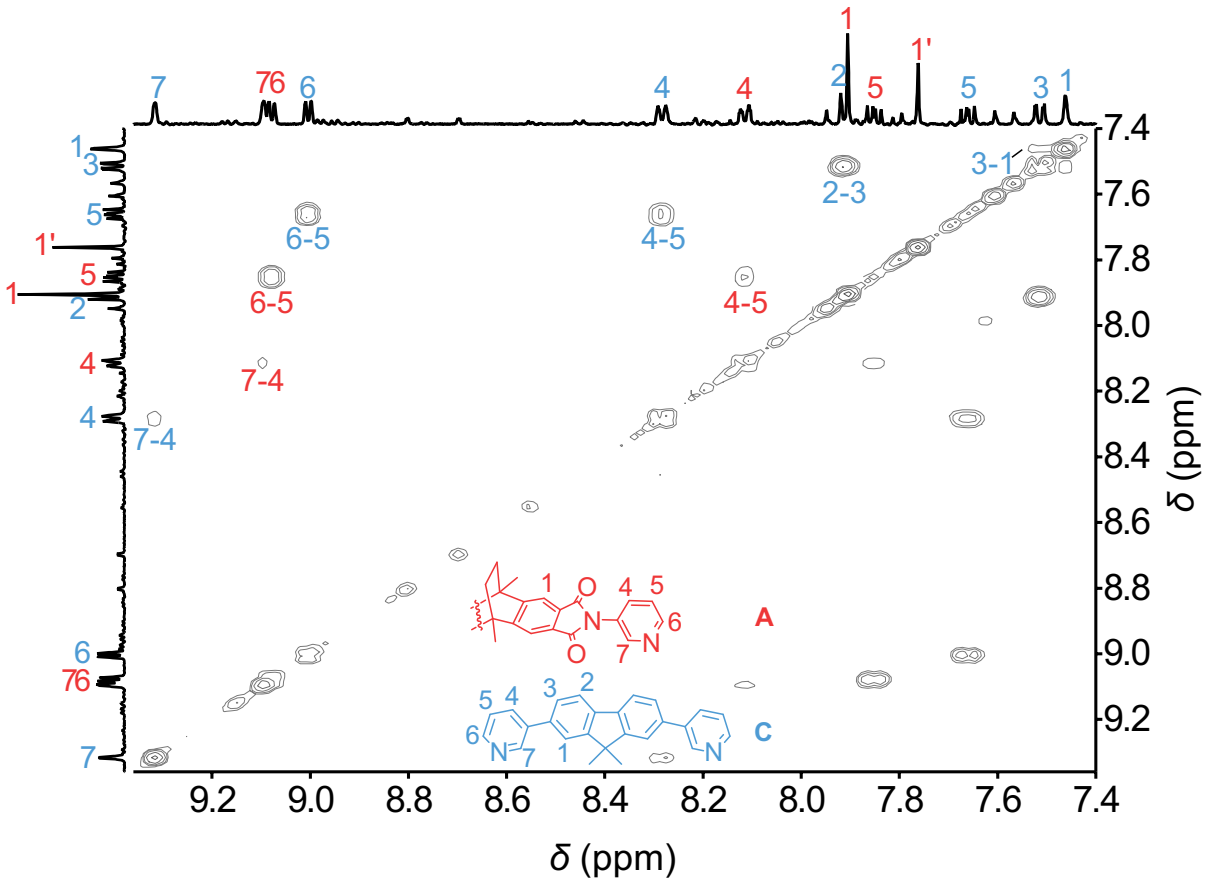

Supplementary Figure 54 | Partial ^{1}H–^{1}H COSY spectrum (500 MHz, 298 K, CD_3CN) of heteroleptic cage $Pd_2\mathbf{A}_2\mathbf{C}_2$.

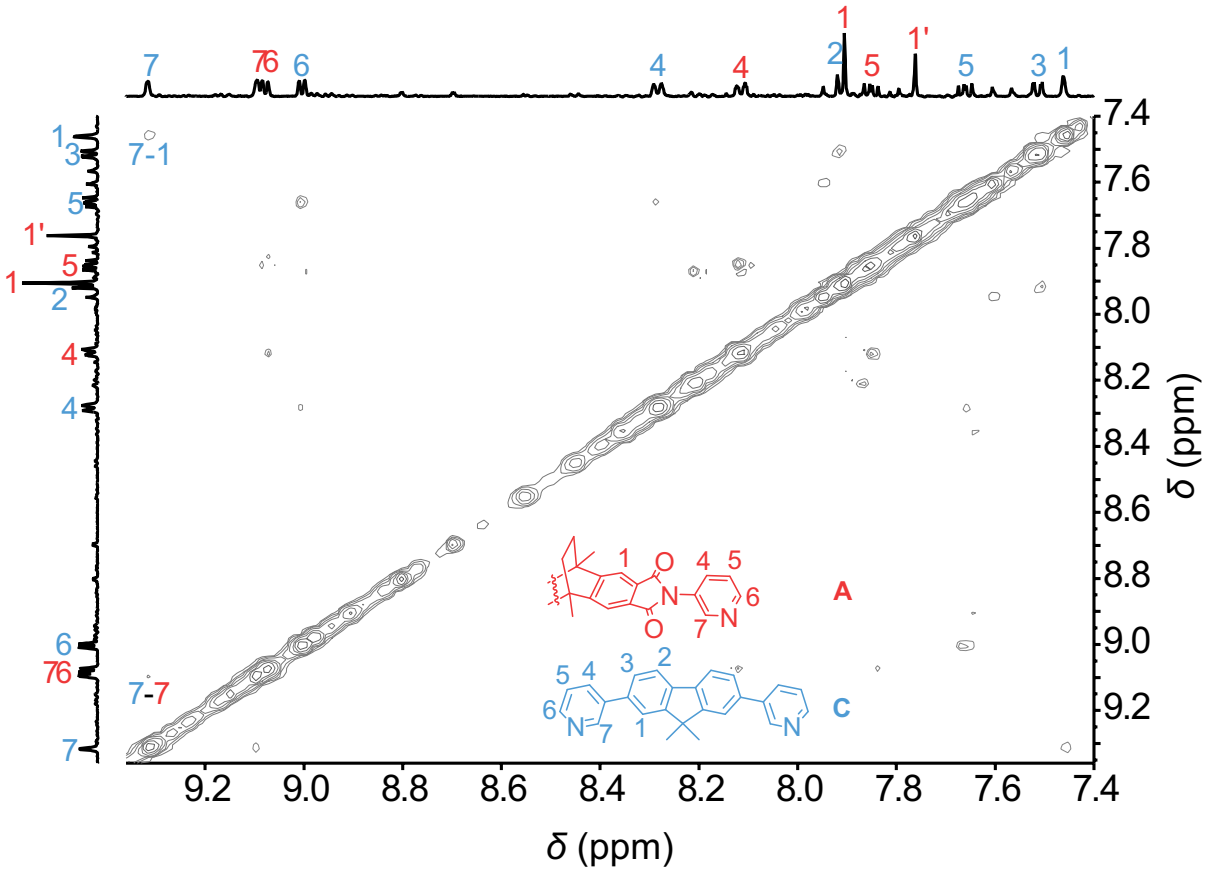

Supplementary Figure 55 | Partial ^{1}H–^{1}H NOESY spectrum (500 MHz, 298 K, CD_3CN) of heteroleptic cage $Pd_2\mathbf{A}_2\mathbf{C}_2$.

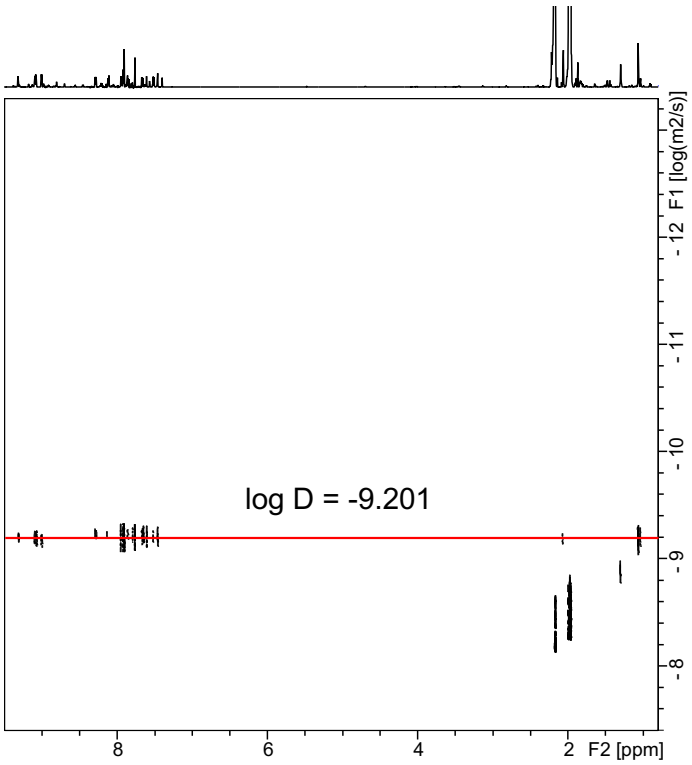

Supplementary Figure 56 | ^{1}H DOSY spectrum (500 MHz, 298 K, CD_3CN) of heteroleptic cage $Pd_2\mathbf{A}_2\mathbf{C}_2$. Diffusion coefficient for $Pd_2\mathbf{A}_2\mathbf{C}_2$: D = 6.295 × 10^{-10} m^2s^{-1}, log *D* = −9.201, r = 10.4 Å.

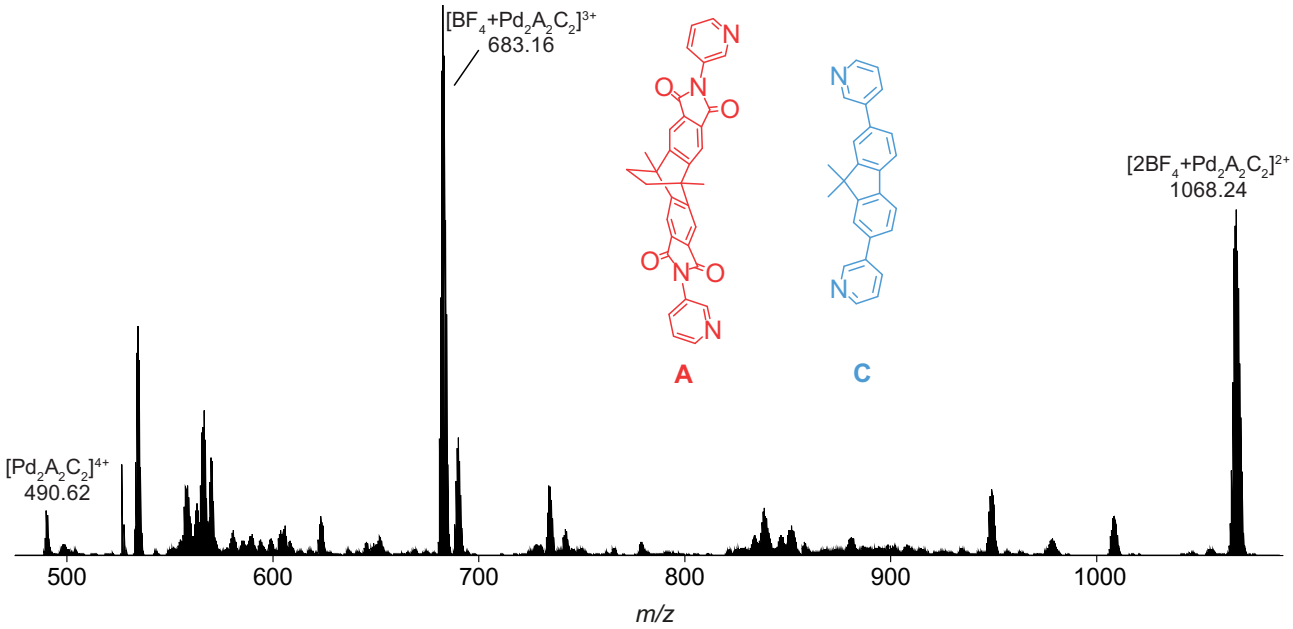

Supplementary Figure 57 | HR-ESI mass spectrum of heteroleptic cage $Pd_2\mathbf{A}_2\mathbf{C}_2$.

3.3.7. Self-assembly of heteroleptic cage $Pd_2A_2D_2$

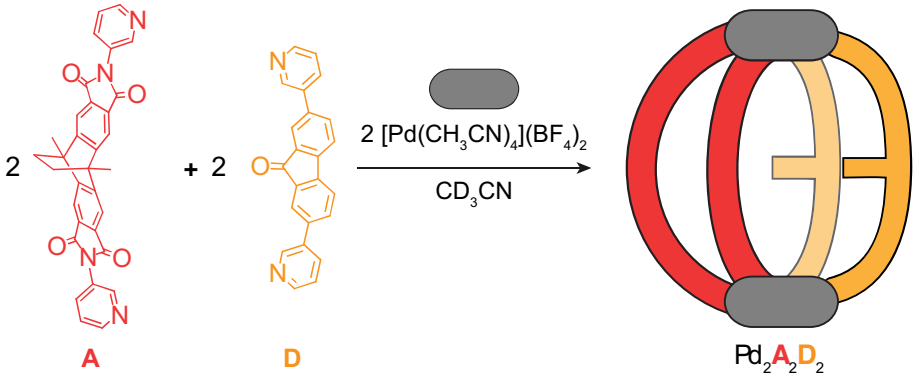

To a solution of **D** (120 µL, 3 mM, 0.36 µmol) in CD_3CN and a suspension of **A** (120 µL, 3 mM, 0.36 µmol) were added a stock solution of $[Pd(CH_3CN)_4](BF_4)_2$ (24 µL, 15 mM/CD_3CN, 0.18 µmol) and 186 µL additional CD_3CN. The mixture was heated at 80 °C for 8 h to give a 0.4 mM cage solution containing the shown cage as predominant species.

^{1}H NMR (500 MHz, 298 K, CD_3CN) δ 9.51 (d, J = 2.0 Hz, 4H), 9.16 (d, J = 2.2 Hz, 4H), 8.94 (dd, J = 5.9, 1.3 Hz, 4H), 8.92 (dd, J = 5.8, 1.2 Hz, 4H), 8.25 (dt, J = 8.1, 1.6 Hz, 4H), 8.11 (ddd, J = 8.2, 2.2, 1.3 Hz, 4H), 7.90 (s, 4H), 7.83 – 7.78 (m, 12H), 7.74 (dd, J = 7.7, 1.8 Hz, 4H), 7.63 (q, J = 2.5 Hz, 8H), 2.19 (s, 6H), 1.96 (s, 6H), 1.76 (m, 8H).

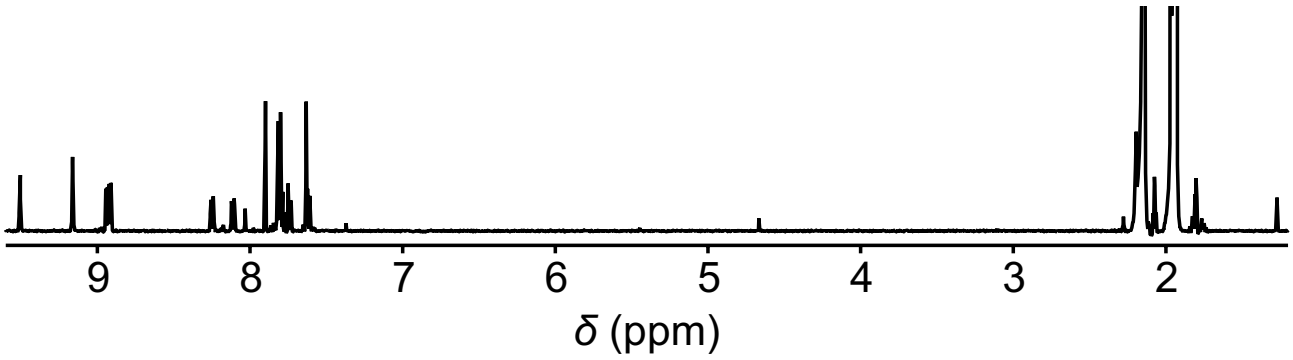

Supplementary Figure 58 | ^{1}H NMR spectrum (500 MHz, 298 K, CD_3CN) of heteroleptic cage $Pd_2A_2D_2$.

^{13}C NMR (151 MHz, 298 K, CD_3CN) δ 192.55, 167.27, 167.08, 166.68, 154.58, 154.35, 151.01, 150.69, 150.11, 145.42, 141.62, 139.32, 139.01, 137.70, 136.65, 135.87, 131.73, 130.56, 130.44, 128.64, 128.22, 124.17, 122.90, 117.58, 45.42, 44.97, 34.98, 34.49, 18.68, 18.57.

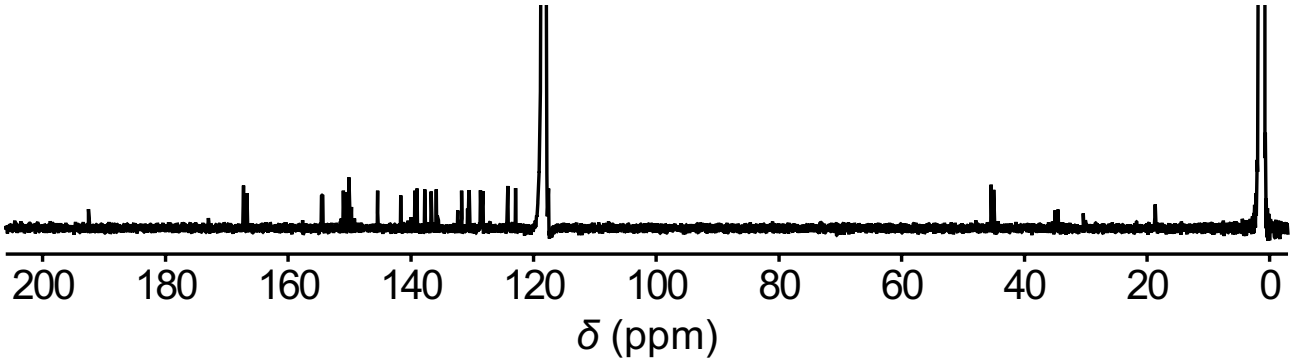

Supplementary Figure 59 | ^{13}C NMR spectrum (151 MHz, 298 K, CD_3CN) of heteroleptic cage $Pd_2A_2D_2$.

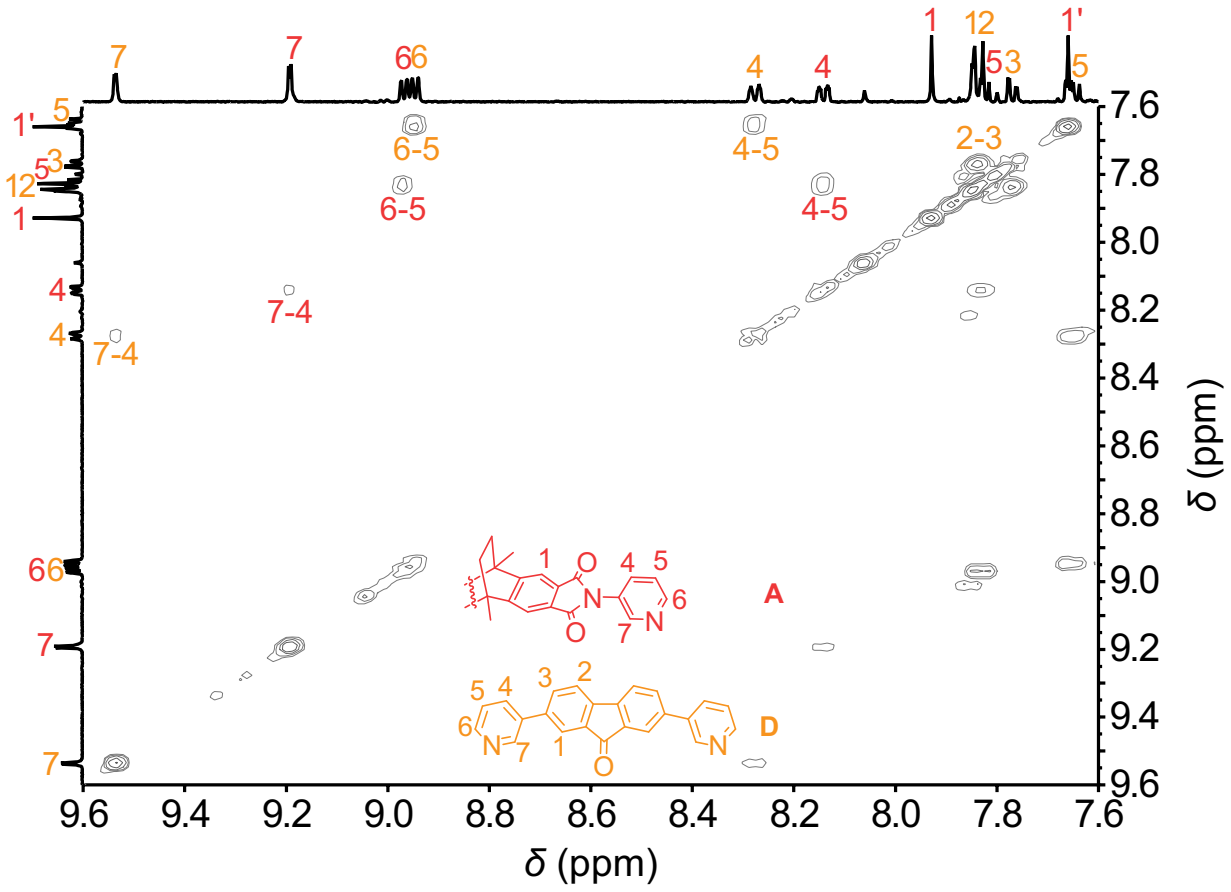

Supplementary Figure 60 | Partial ^{1}H–^{1}H COSY spectrum (500 MHz, 298 K, CD_3CN) of heteroleptic cage $Pd_2\mathbf{A}_2\mathbf{D}_2$.

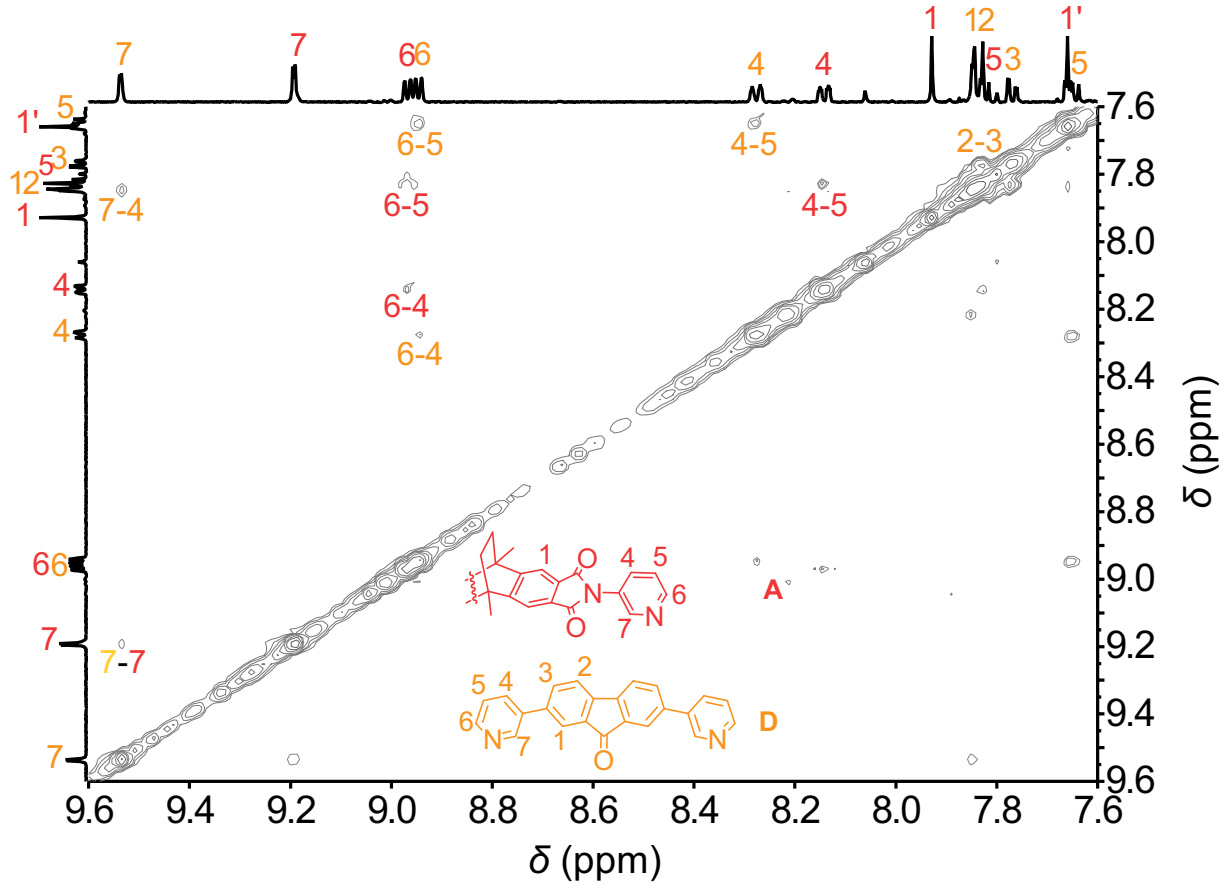

Supplementary Figure 61 | Partial ^{1}H–^{1}H NOESY spectrum (500 MHz, 298 K, CD_3CN) of heteroleptic cage $Pd_2\mathbf{A}_2\mathbf{D}_2$.

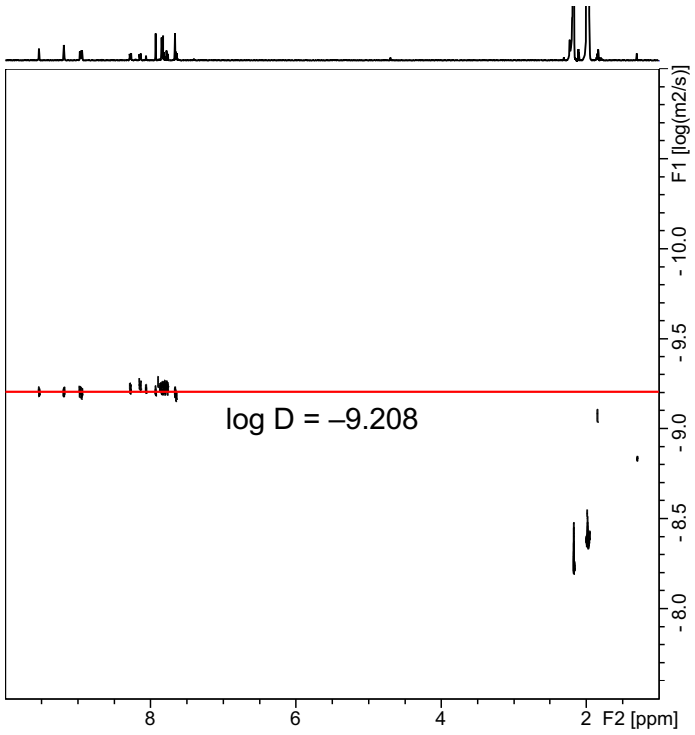

Supplementary Figure 62 | ^{1}H DOSY spectrum (500 MHz, 298 K, CD_3CN) of heteroleptic cage $Pd_2\mathbf{A}_2\mathbf{D}_2$. Diffusion coefficient for $Pd_2\mathbf{A}_2\mathbf{D}_2$: D = 6.194 × 10^{-10} m^2s^{-1}, log *D* = −9.208, r = 10.6 Å.

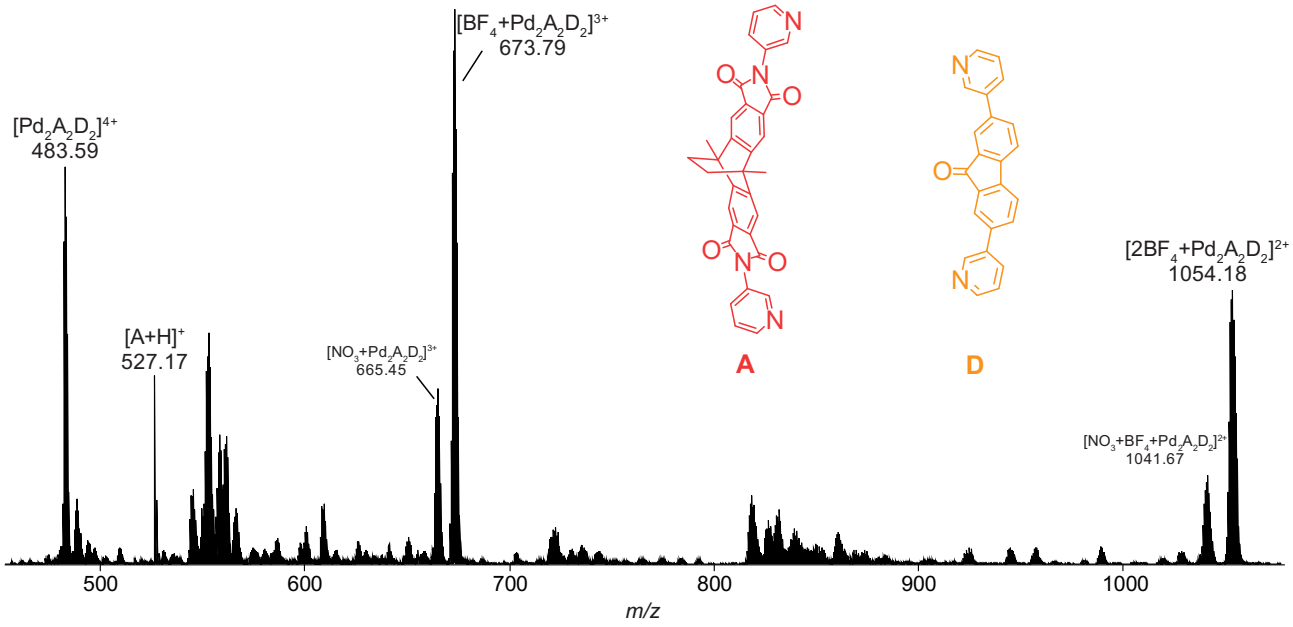

Supplementary Figure 63 | HR-ESI mass spectrum of heteroleptic cage $Pd_2\mathbf{A}_2\mathbf{D}_2$.

3.3.8. Self-assembly of heteroleptic cage Pd_2A_2CD

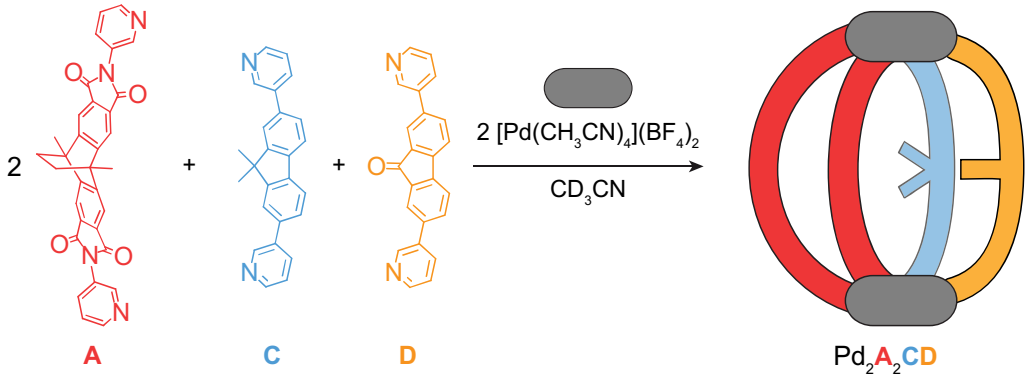

To a solution of **A** (120 µL, 3 mM, 0.36 µmol), **C** (60 µL, 3 mM, 0.18 µmol) and a suspension of **D** (60 µL, 3 mM, 0.18 µmol) in CD_3CN and were added a stock solution of $[Pd(CH_3CN)_4](BF_4)_2$ (24 µL, 15 mM/CD_3CN, 0.36 µmol) and 186 µL additional CD_3CN. The mixture was heated at 80 °C for 8 h to give a 0.4 mM cage solution containing the shown cage as predominant species.

^{1}H NMR (700 MHz, 298 K, CD_3CN) δ 9.73 (d, J = 2.1 Hz, 2H), 9.36 (d, J = 2.2 Hz, 2H), 9.24 (d, J = 2.0 Hz, 2H), 9.03 (dd, J = 6.1, 1.3 Hz, 2H), 9.00 (dd, J = 6.0, 1.2 Hz, 2H), 8.98 (d, J = 2.2 Hz, 2H), 8.87 (dd, J = 6.0, 1.2 Hz, 2H), 8.78 (dd, J = 5.9, 1.3 Hz, 2H), 8.36 (ddd, J = 7.9, 2.0, 1.3 Hz, 2H), 8.35 – 8.33 (m, 2H), 8.23 (ddd, J = 8.2, 2.2, 1.2 Hz, 2H), 8.15 – 8.12 (m, 2H), 8.05 – 8.01 (m, 4H), 7.93 (dd, J = 7.6, 0.6 Hz, 2H), 7.83 – 7.78 (m, 8H), 7.74 (s, 2H), 7.72 (s, 2H), 7.71 – 7.68 (m, 2H), 7.61 – 7.60 (m, 2H), 7.59 – 7.56 (m, 2H), 7.51 (dd, J = 7.7, 1.8 Hz, 2H), 6.99 (d, J = 1.8 Hz, 2H), 2.28 (s, 3H), 2.08 (s, 3H), 2.05 (s, 3H), 1.93 (s, 3H), 1.76 – 1.72 (m, 8H), 0.91 (s, 3H), 0.44 (s, 3H).

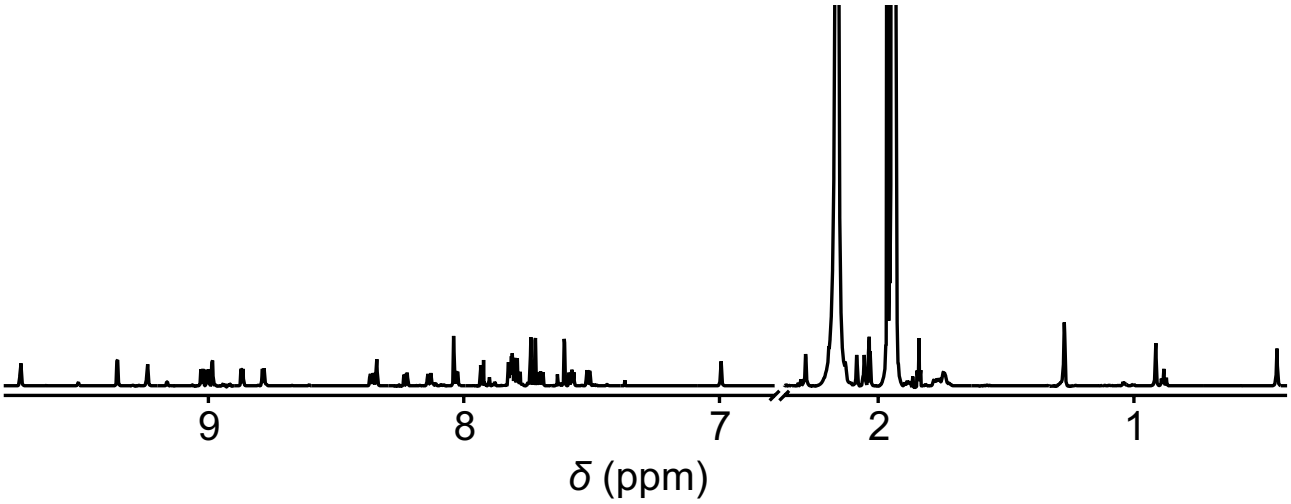

Supplementary Figure 64 | ^{1}H NMR spectrum (500 MHz, 298 K, CD_3CN) of heteroleptic cage $Pd_2\mathbf{A}_2\mathbf{D}_2$.

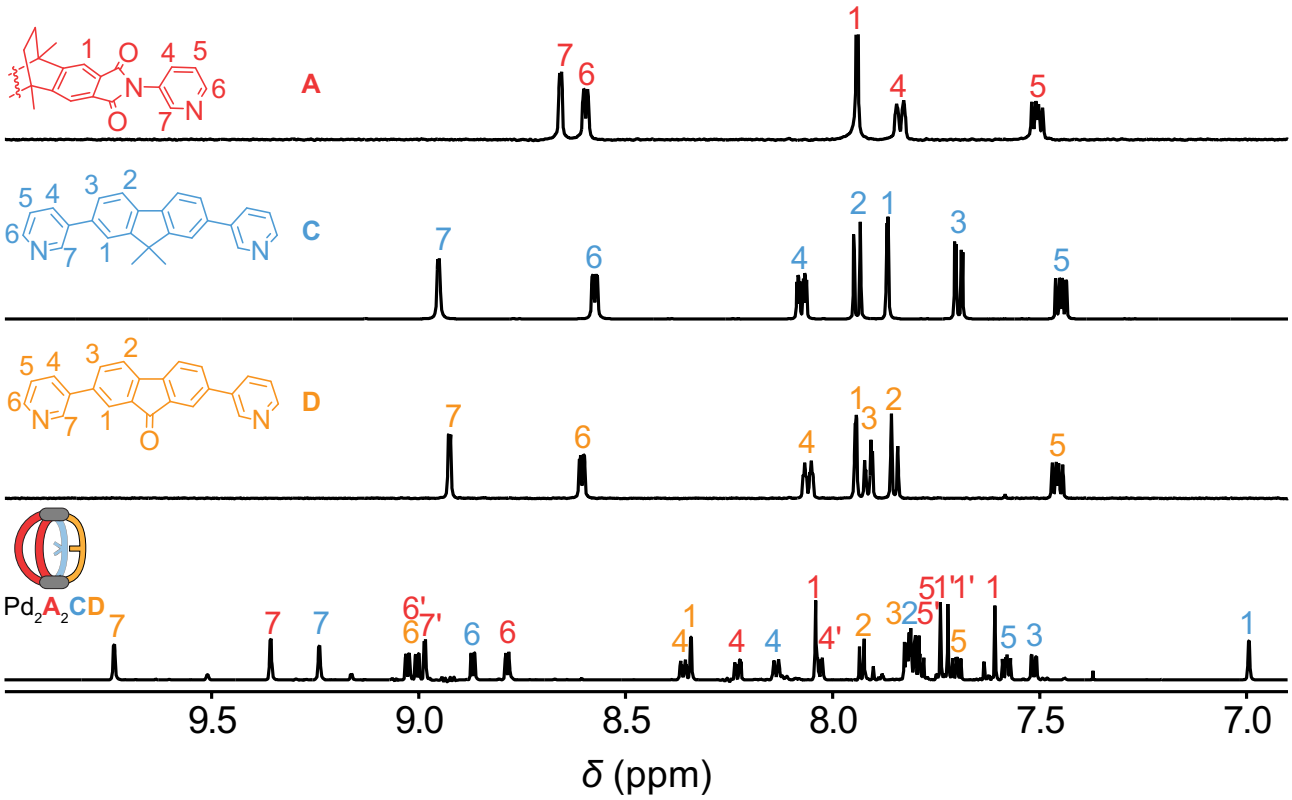

Supplementary Figure 65 | Partial ^{1}H NMR spectrum (700 MHz, 298 K, CD_3CN) comparison of ligand **A** (red), ligand **C** (blue), ligand **D** (yellow) and heteroleptic Pd_2**A**$_2$**CD**.

^{13}C NMR (176 MHz, 298 K, CD_3CN) δ 192.83, 172.98, 167.61, 167.12, 166.90, 166.79, 166.74, 166.61, 155.76, 154.75, 154.58, 154.52, 154.37, 154.27, 154.19, 151.36, 150.62, 150.45, 150.34, 150.22, 150.05, 149.91, 149.32, 145.82, 142.33, 140.09, 139.88, 139.79, 139.45, 139.17, 138.60, 138.41, 136.97, 136.79, 135.57, 132.05, 131.68, 130.64, 130.45, 128.73, 128.50, 128.25, 127.88, 124.68, 123.33, 123.10, 122.13, 117.56, 117.52, 46.64, 45.59, 45.35, 45.14, 44.98, 35.00, 34.83, 34.76, 34.69, 34.48, 30.36, 30.30, 30.07, 29.99, 29.77.

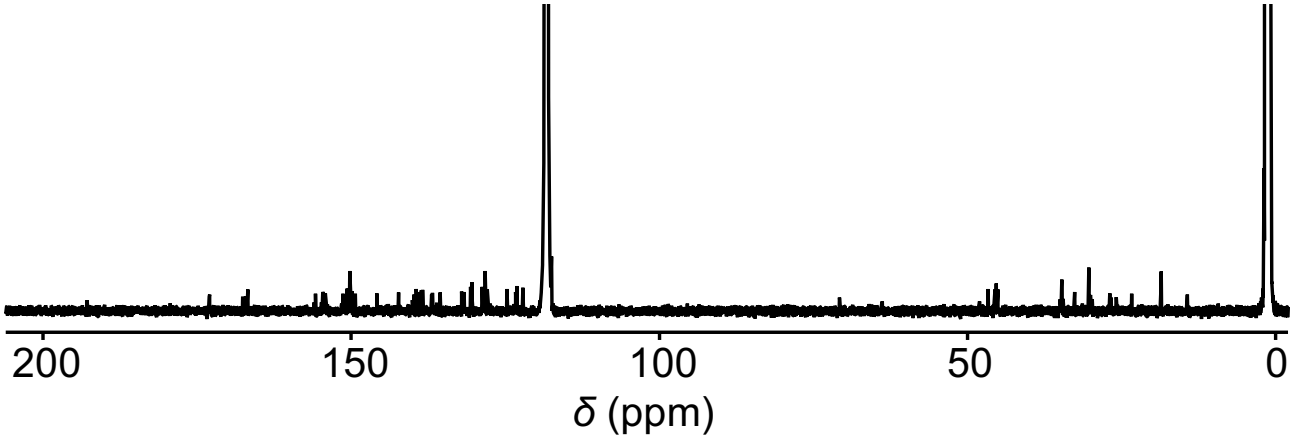

Supplementary Figure 66 | ^{13}C NMR spectrum (151 MHz, 298 K, CD_3CN) of heteroleptic cage Pd_2**A**$_2$**CD**.

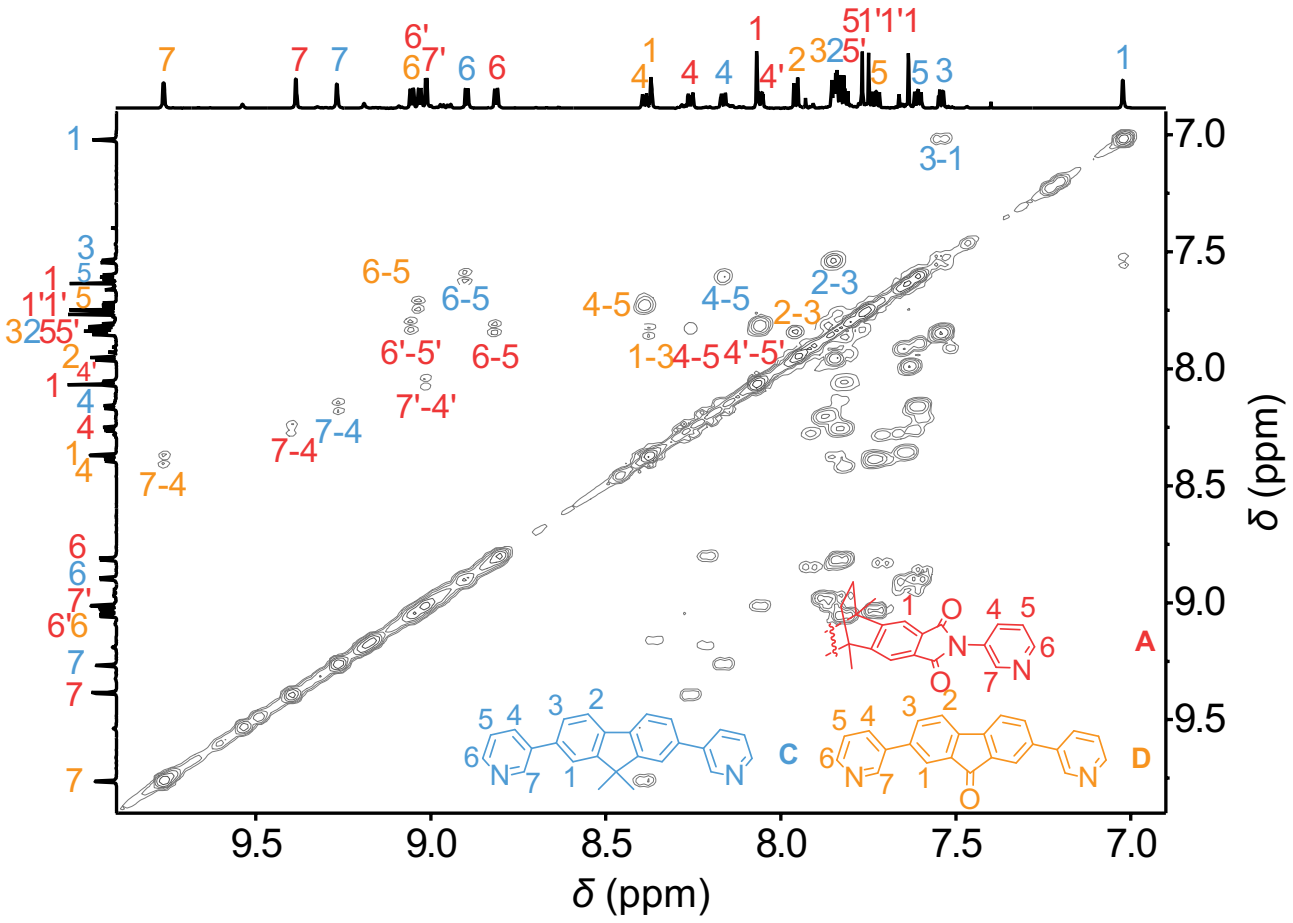

Supplementary Figure 67 | Partial ^{1}H–^{1}H COSY spectrum (500 MHz, 298 K, CD_3CN) of heteroleptic cage $Pd_2\mathbf{A}_2\mathbf{CD}$.

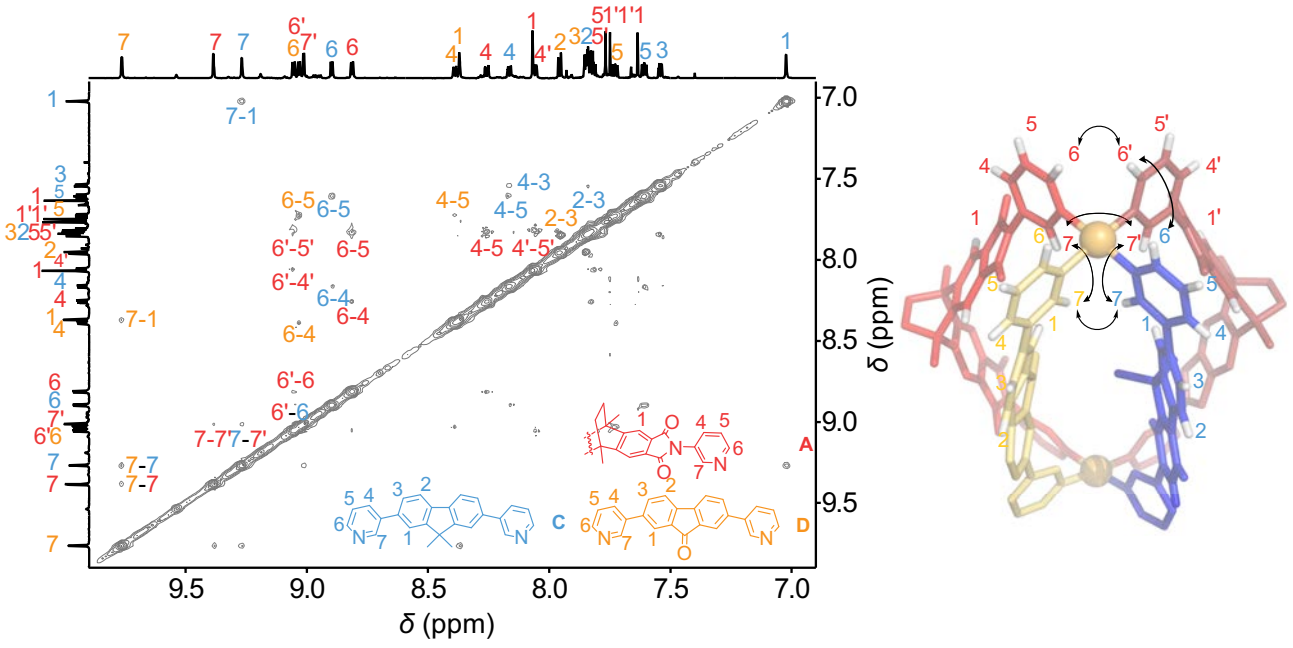

Supplementary Figure 68 | Partial ^{1}H–^{1}H NOESY spectrum (500 MHz, 298 K, CD_3CN) of heteroleptic cage $Pd_2\mathbf{A}_2\mathbf{CD}$. The composition of this heteroleptic cage is supported by a single crystal X-ray structure (details see below). The found NOE contacts in solution are in full accordance with the X-ray structure results.

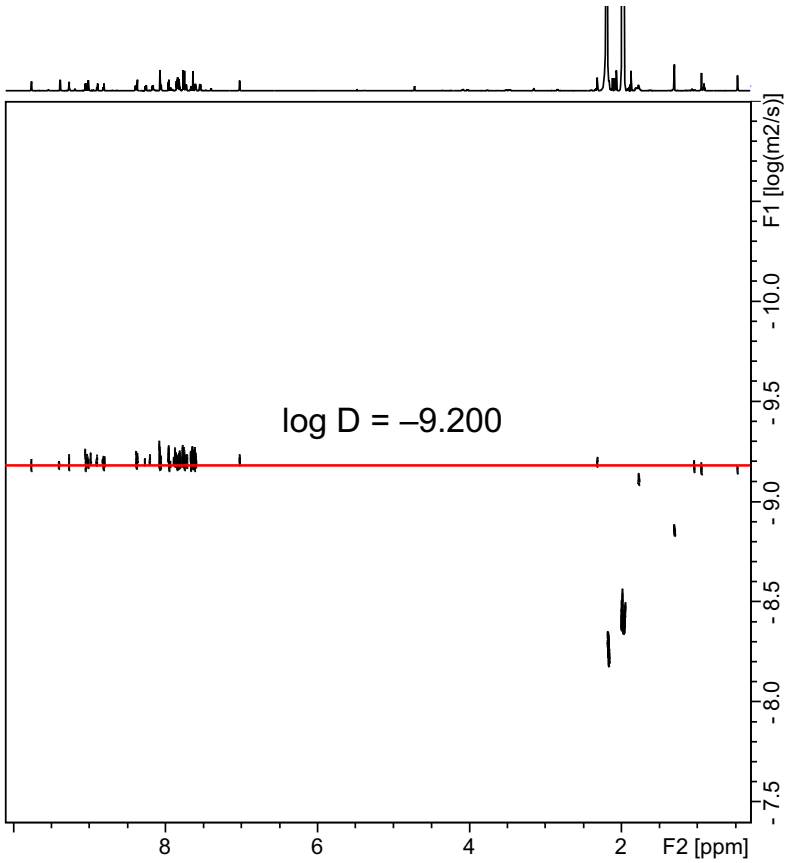

Supplementary Figure 69 | ^{1}H DOSY spectrum (500 MHz, 298 K, CD_3CN) of heteroleptic cage Pd_2**A**$_2$**CD**. Diffusion coefficient for Pd_2**A**$_2$**CD**: D = 6.317 × 10^{-10} m^2s^{-1}, log *D* = –9.200, r = 10.3 Å.

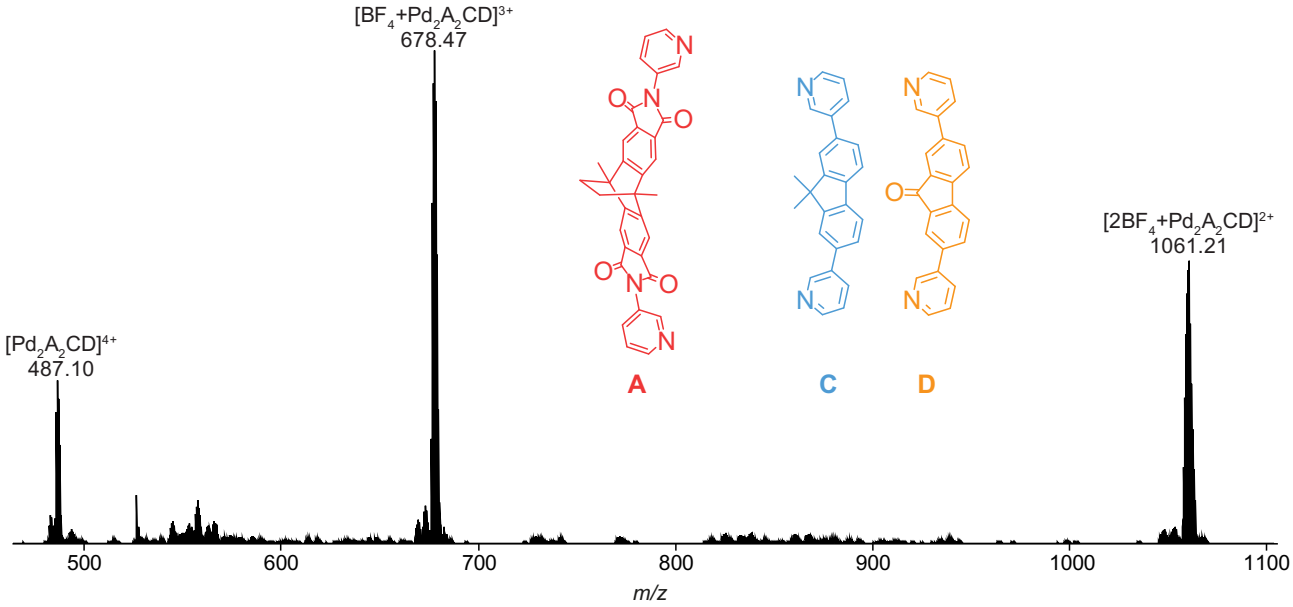

Supplementary Figure 70 | HR-ESI mass spectrum of heteroleptic cage Pd_2**A**$_2$**CD**.

*3.3.9. Self-assembly of heteroleptic cage Pd_2**ABC**$_2$*

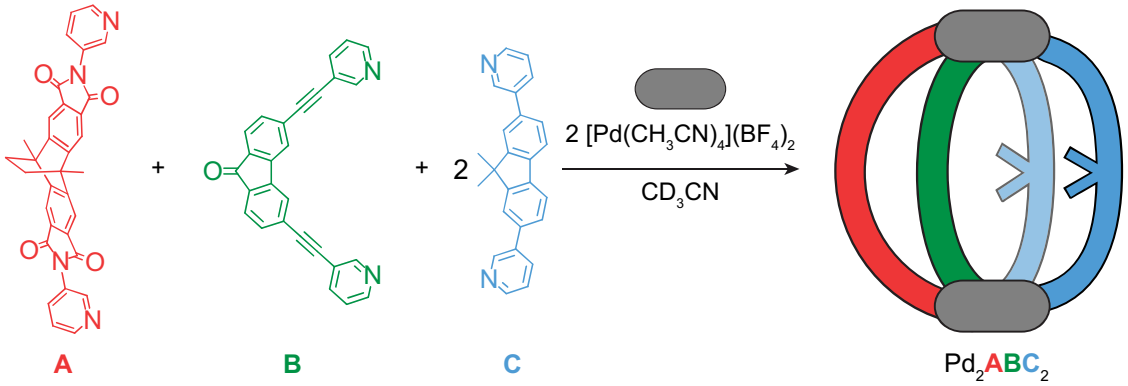

To a solution of **A** (60 µL, 3 mM, 0.18 µmol), **B** (60 µL, 3 mM, 0.18 µmol), **C** (120 µL, 3 mM, 0.36 µmol) was added a stock solution of $[Pd(CH_3CN)_4](BF_4)_2$ (24 µL, 15 mM/CD_3CN, 0.36 µmol) and additional 186 µL CD_3CN. The mixture was heated at 80 °C for 8 h to give a 0.4 mM cage solution with Pd_2**ABC**$_2$ as predominant species besides small amounts of Pd_2**A**$_2$**C**$_2$.

^{1}H NMR (700 MHz, 298 K, CD_3CN) δ 9.70 (d, J = 2.0 Hz, 2H), 9.25 (d, J = 2.2 Hz, 2H), 9.20 (d, J = 2.0 Hz, 2H), 9.18 (dd, J = 5.9, 1.4 Hz, 2H), 9.14 (d, J = 1.8 Hz, 2H), 9.05 – 9.02 (m, 2H), 9.00 (dd, J = 5.9, 1.2 Hz, 2H), 8.84 – 8.80 (m, 2H), 8.37 (dt, J = 7.8, 1.4 Hz, 2H), 8.15 – 8.10 (m, 6H), 8.08 (dd, J = 7.6, 4.7 Hz, 2H), 7.97 (s, 2H), 7.96 (d, J = 1.5 Hz, 2H), 7.91 (s, 2H), 7.84 – 7.81 (m, 2H), 7.76 – 7.69 (m, 6H), 7.66 – 7.61 (m, 4H), 7.60 – 7.57 (m, 4H), 7.42 (t, J = 1.0 Hz, 2H), 7.38 (dd, J = 7.7, 1.8 Hz, 2H), 7.02 (d, J = 1.8 Hz, 2H), 2.16 (s, 3H), 2.13 (s, 3H), 1.63 (d, J = 8.8 Hz, 3H), 1.58 (s, 3H), 0.96 (s, 3H), 0.86 (s, 3H).

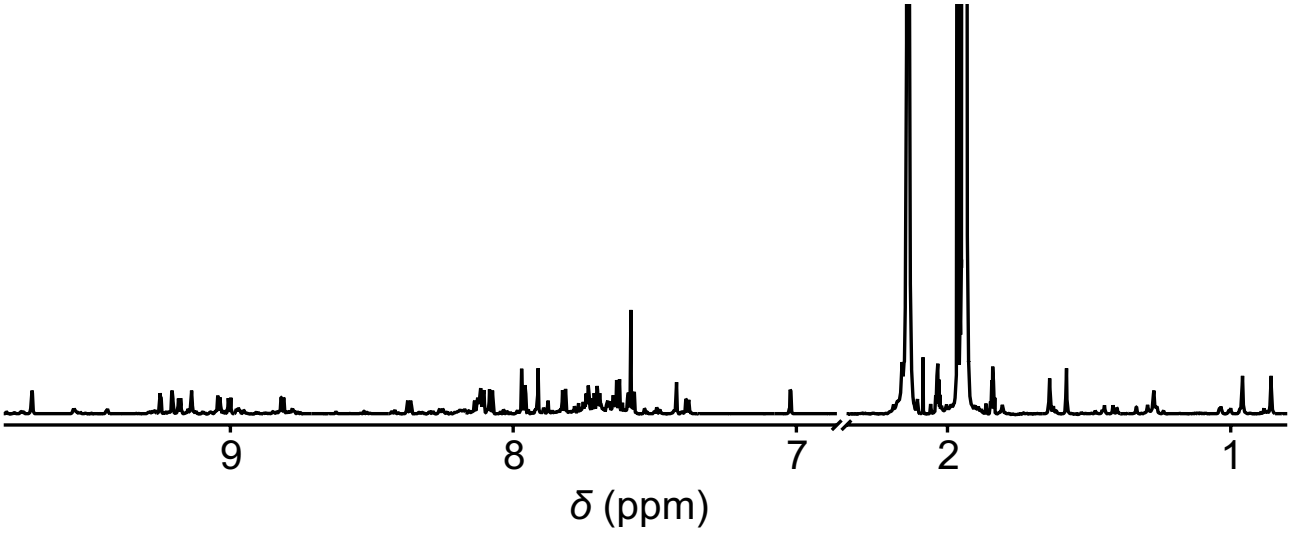

Supplementary Figure 71 | ^{1}H NMR spectrum (700 MHz, 298 K, CD_3CN) of heteroleptic cage Pd_2**ABC**$_2$.

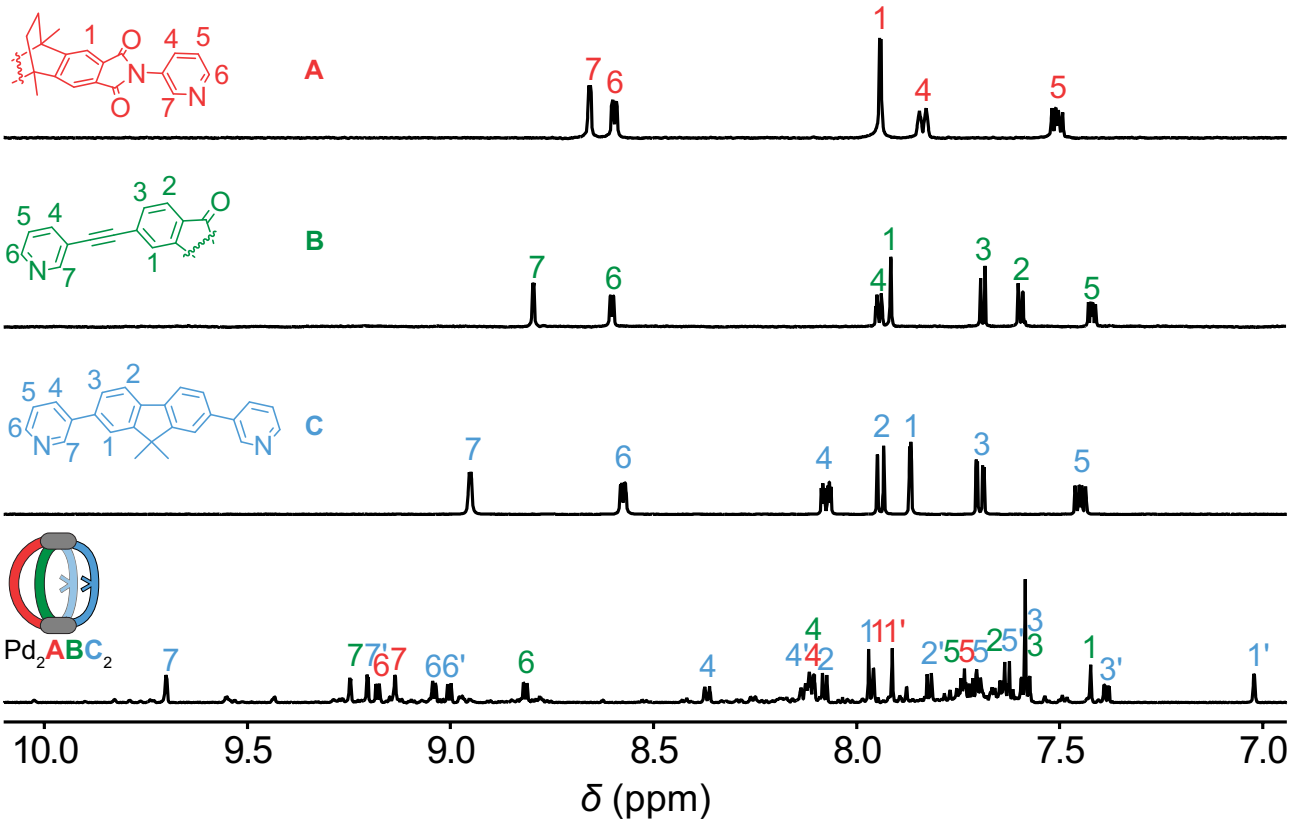

Supplementary Figure 72 | Partial ^{1}H NMR spectrum (700 MHz, 298 K, CD_3CN) comparison of ligands **A** (red), **B** (green), **C** (blue), heteroleptic cage Pd_2**ABC**$_2$.

^{13}C NMR (151 MHz, 298 K, CD_3CN) δ 192.19, 167.31, 166.97, 156.85, 156.33, 155.14, 154.98, 154.07, 150.95, 150.86, 150.77, 150.76, 150.69, 150.23, 149.77, 144.71, 144.63, 144.11, 142.42, 140.90, 140.17, 140.01, 139.93, 139.39, 136.43, 135.98, 135.87, 135.44, 132.27, 130.85, 130.72, 129.53, 128.51, 128.43, 128.37, 128.33, 128.20, 125.08, 123.94, 123.81, 123.21, 122.73, 122.65, 122.60, 117.57, 95.19, 87.32, 79.15, 48.60, 47.16, 45.63, 45.46, 34.54, 34.38, 33.84, 27.93, 27.00, 23.96, 18.79, 18.59.

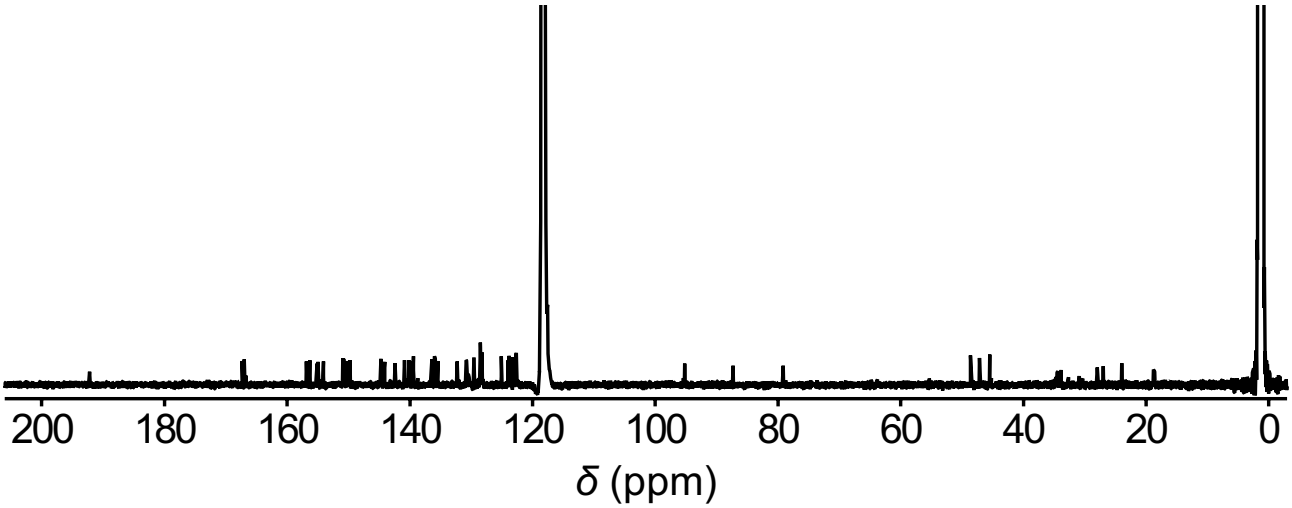

Supplementary Figure 73 | ^{13}C NMR spectrum (151 MHz, 298 K, CD_3CN) of heteroleptic cage Pd_2**ABC**$_2$.

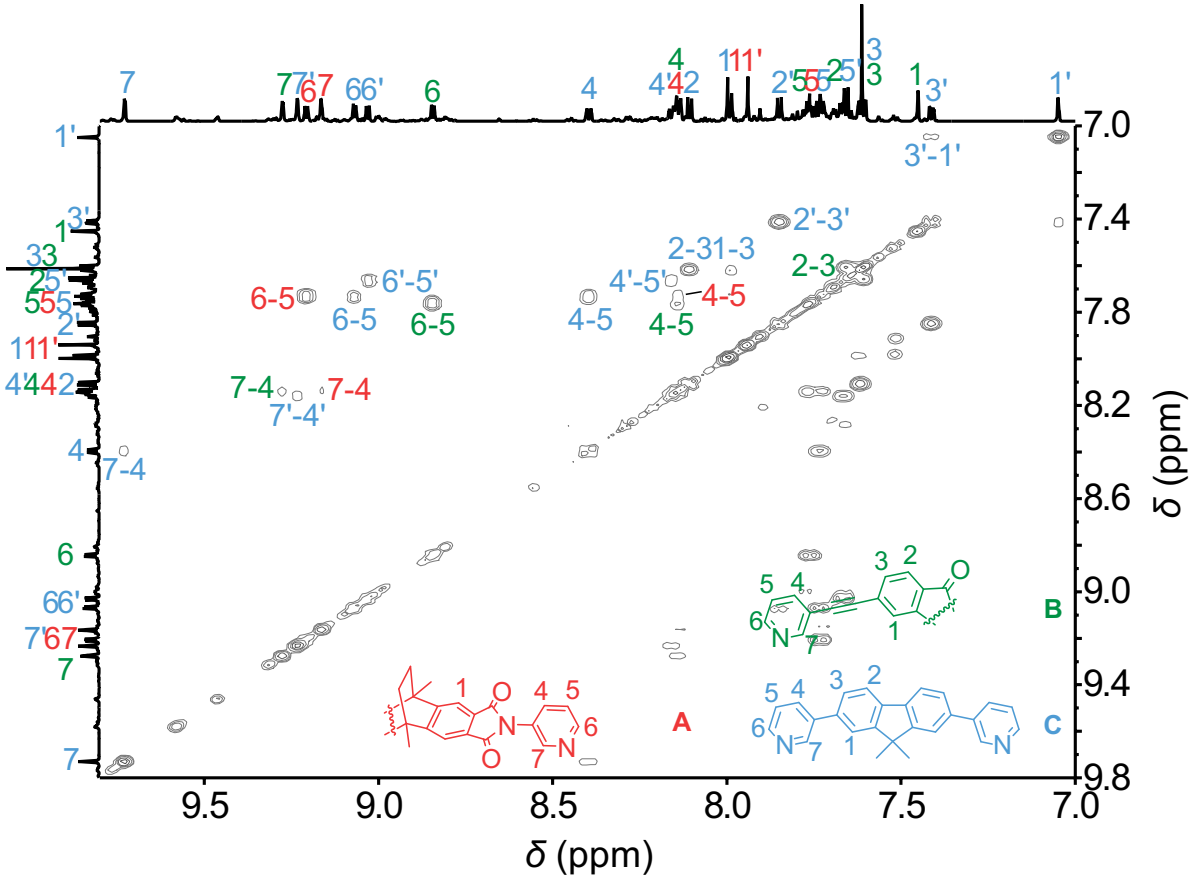

Supplementary Figure 74 | Partial ^{1}H–^{1}H COSY spectrum (500 MHz, 298 K, CD_3CN) of heteroleptic cage Pd_2**ABC**$_2$.

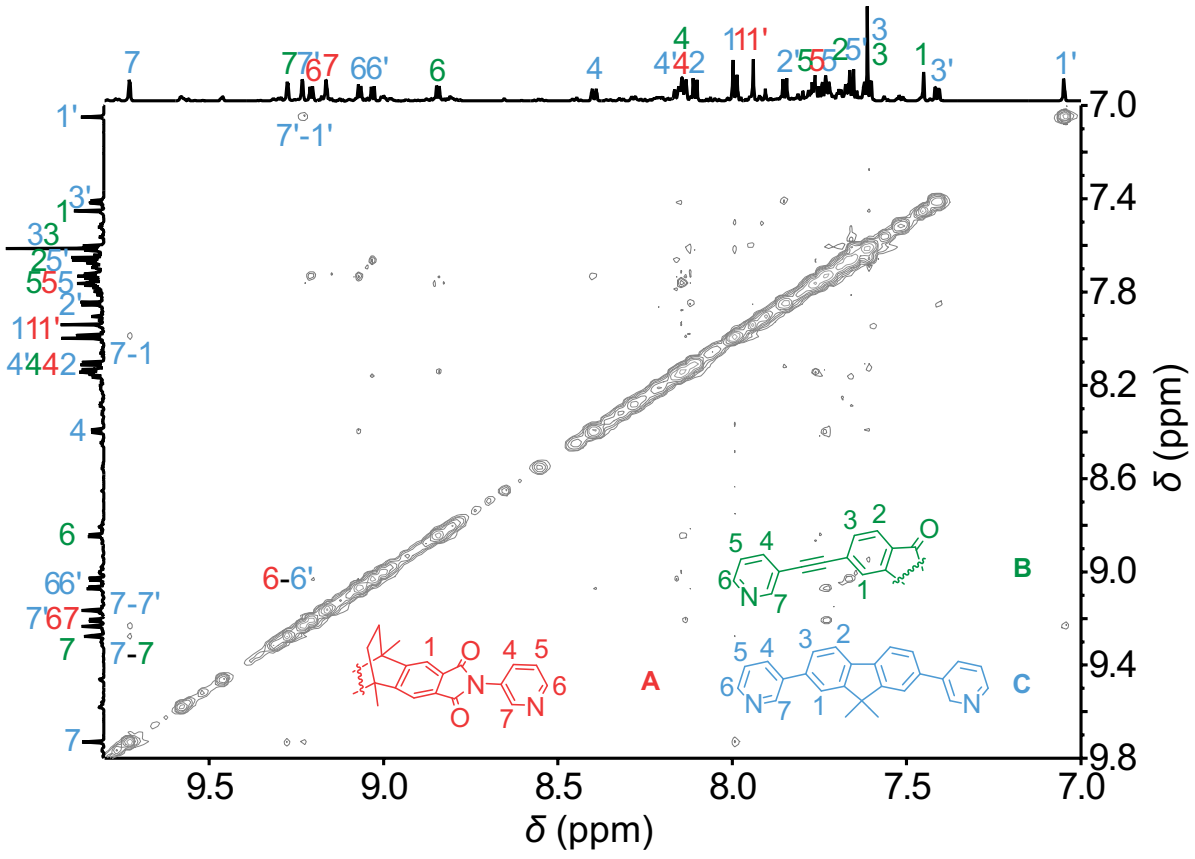

Supplementary Figure 75 | Partial ^{1}H–^{1}H NOESY spectrum (500 MHz, 298 K, CD_3CN) of heteroleptic cage Pd_2**ABC**$_2$. (The correlation between 7 and 7' of ligand **C** confirmed the two ligands **C** are in cis- arrangement.)

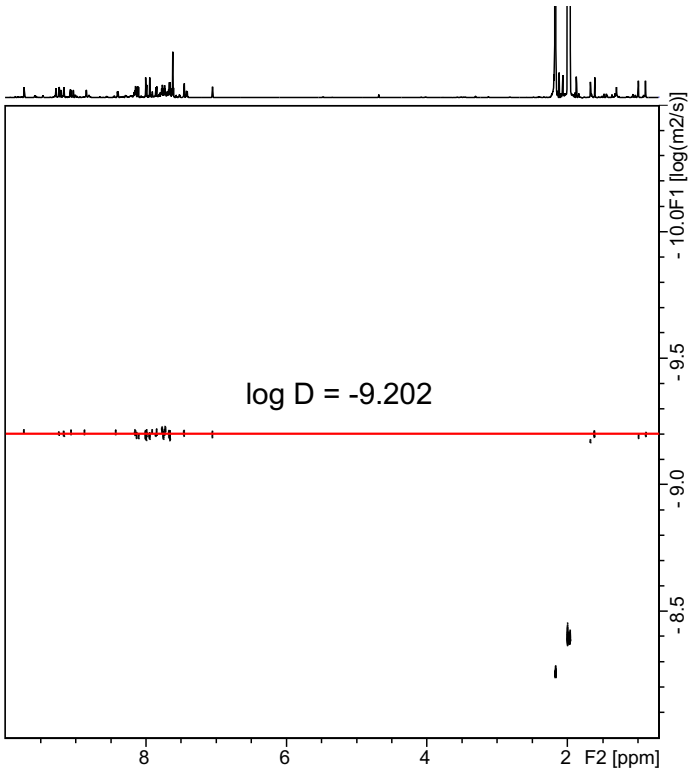

Supplementary Figure 76 | ^{1}H DOSY spectrum (500 MHz, 298 K, CD_3CN) of heteroleptic cage Pd_2**ABC**$_2$. Diffusion coefficient for Pd_2**ABC**$_2$: D = 6.282 × 10^{-10} m^2s^{-1}, log *D* = −9.202, r = 10.4 Å.

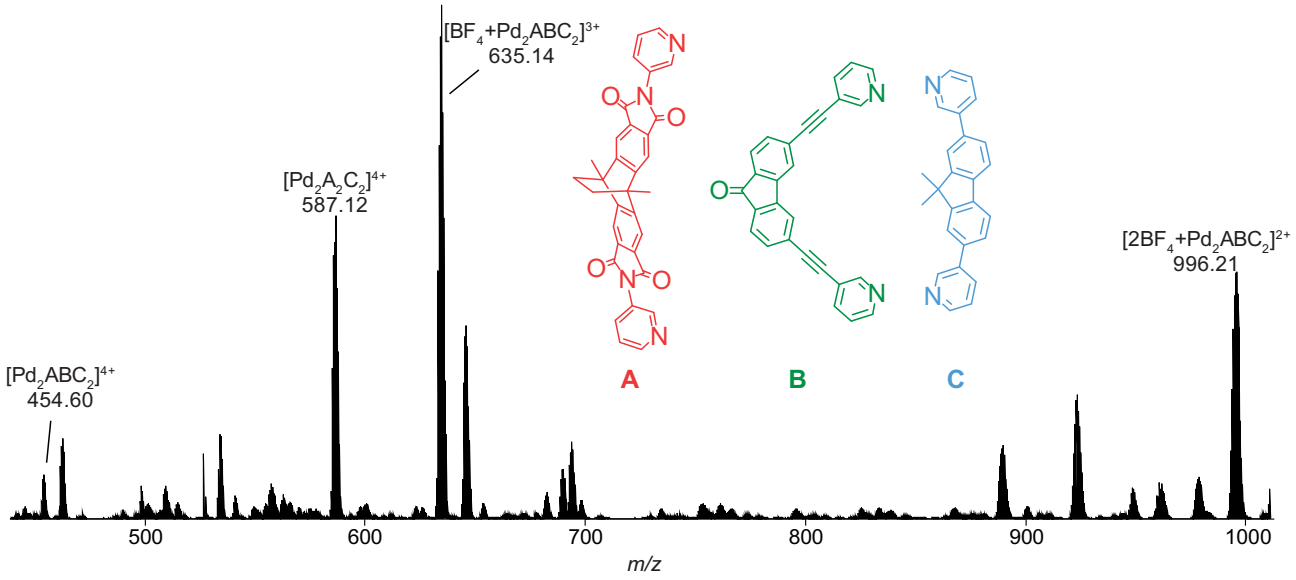

Supplementary Figure 77 | HR-ESI mass spectrum of heteroleptic cage Pd_2**ABC**$_2$.

*3.3.10. Self-assembly of heteroleptic cage Pd2**ABD**$_2$*

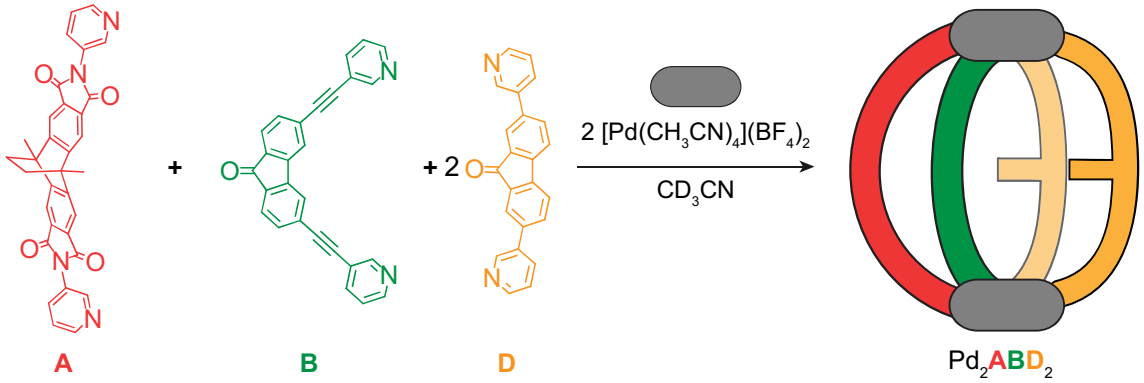

To a solution of **A** (60 µL, 3 mM, 0.18 µmol), **B** (60 µL, 3 mM, 0.18 µmol), **D** (120 µL, 3 mM, 0.36 µmol) was added a stock solution of [Pd(CH3CN)4](BF4)2 (24 µL, 15 mM/CD3CN, 0.36 µmol) and additional 186 µL CD3CN. The mixture was heated at 80 °C for 8 h to give a 0.4 mM cage solution with heteroleptic cage Pd$_2$**ABD**$_2$ as predominant species besides small amounts of Pd$_2$**B**$_2$**D**$_2$.

1H NMR (700 MHz, 298 K, CD3CN) δ 9.83 (d, J = 2.0 Hz, 2H), 9.61 (d, J = 2.1 Hz, 2H), 9.34 (d, J = 2.0 Hz, 2H), 9.29 (d, J = 2.2 Hz, 2H), 9.15 (d, J = 5.3 Hz, 2H), 8.98 (d, J = 5.8 Hz, 2H), 8.93 (d, J = 6.0 Hz, 2H), 8.77 (d, J = 5.9 Hz, 2H), 8.34 (q, J = 3.5, 2.9 Hz, 4H), 8.17 (t, J = 6.4 Hz, 4H), 8.14 (dt, J = 8.6, 1.6 Hz, 2H), 7.88 (d, J = 7.6 Hz, 2H), 7.83 (s, 2H), 7.81 (s, 2H), 7.78 (d, J = 7.5 Hz, 2H), 7.76 – 7.72 (m, 6H), 7.72 – 7.61 (m, 12H), 7.59 (d, J = 1.7 Hz, 2H), 2.05 (s, 3H), 2.01 (s, 3H), 1.81 (b, 4H).

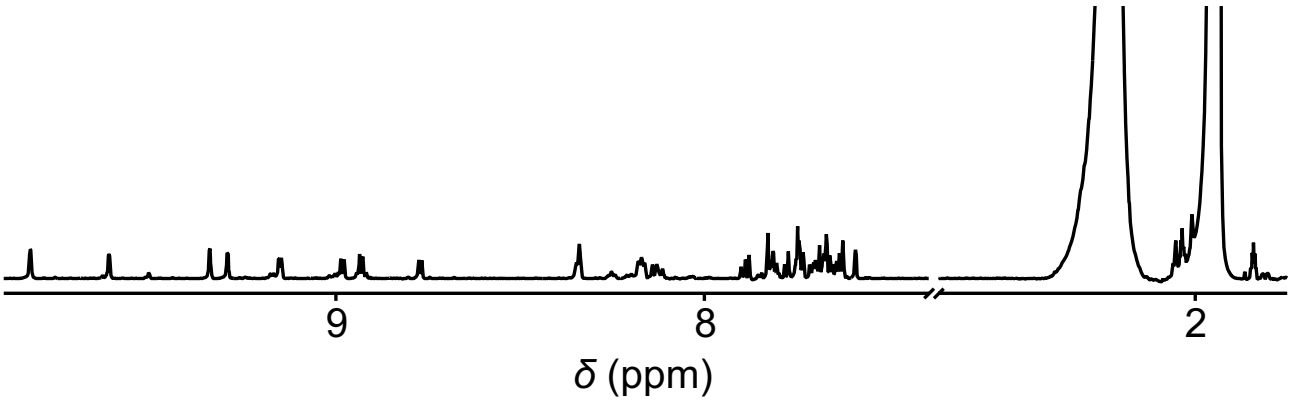

Supplementary Figure 78 | 1H NMR spectrum (700 MHz, 298 K, CD3CN) of heteroleptic cage Pd2**ABD**$_2$.

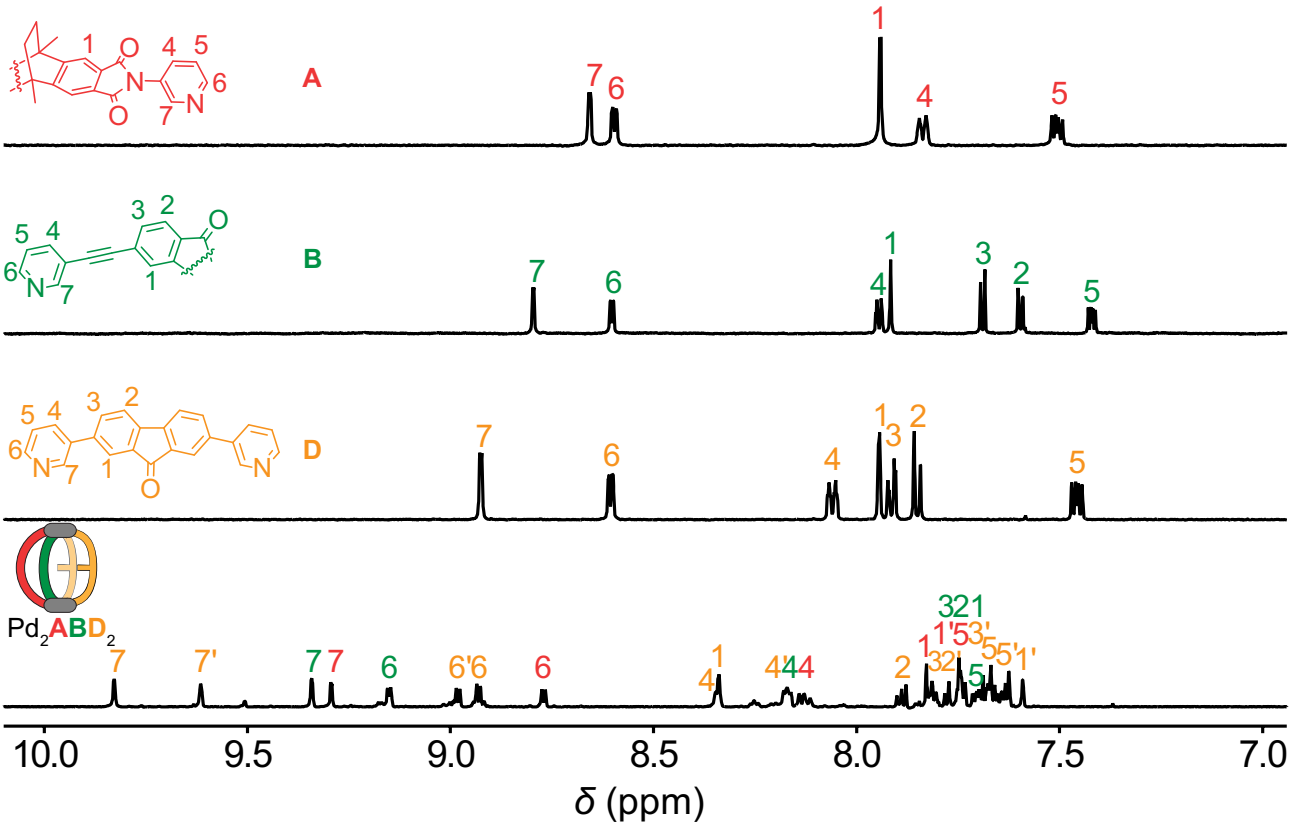

Supplementary Figure 79 | Partial ^{1}H NMR spectrum (700 MHz, 298 K, CD_3CN) comparison of ligands **A** (red), **B** (green), **D** (yellow), heteroleptic cage Pd_2**ABD**$_2$.

^{13}C NMR (151 MHz, 298 K, CD_3CN) δ 192.04, 187.09, 172.99, 167.34, 167.03, 154.58, 153.24, 150.91, 150.75, 145.80, 143.84, 142.37, 141.63, 140.32, 139.14, 138.93, 138.58, 137.60, 137.44, 137.24, 136.38, 135.41, 135.18, 132.55, 131.93, 128.52, 128.40, 128.37, 125.38, 124.18, 124.06, 123.50, 123.40, 123.07, 122.96, 111.56, 98.10, 83.52, 45.26, 45.10, 32.15, 30.36, 27.36, 23.21.

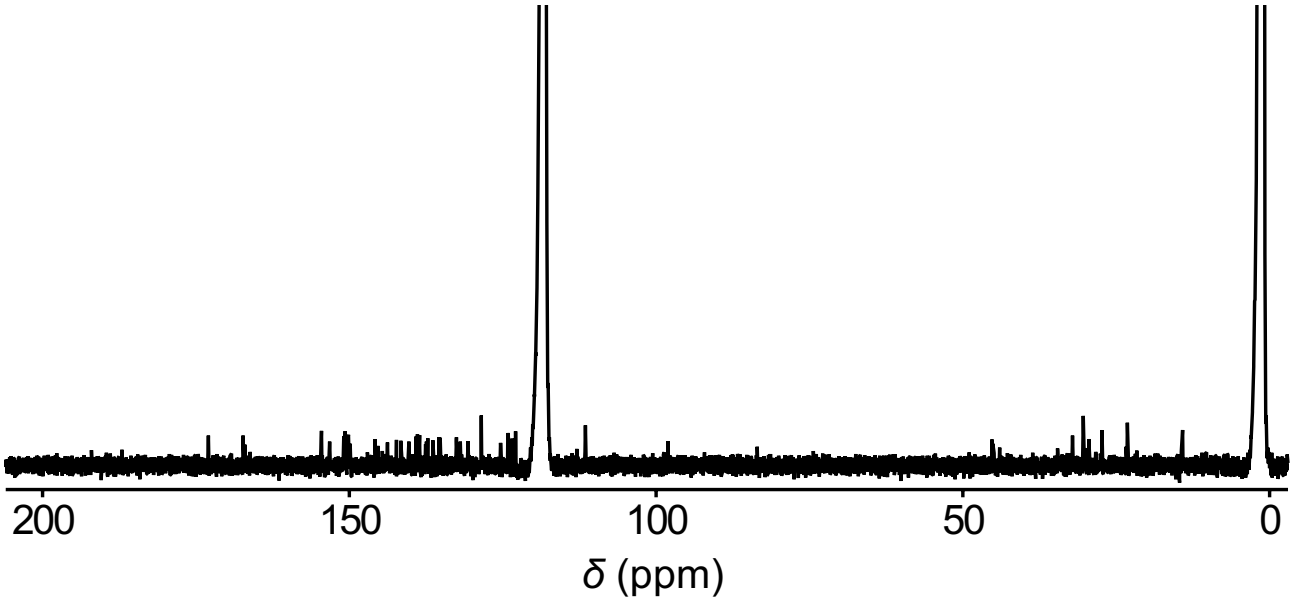

Supplementary Figure 80 | ^{13}C NMR spectrum (151 MHz, 298 K, CD_3CN) of heteroleptic cage Pd_2**ABD**$_2$.

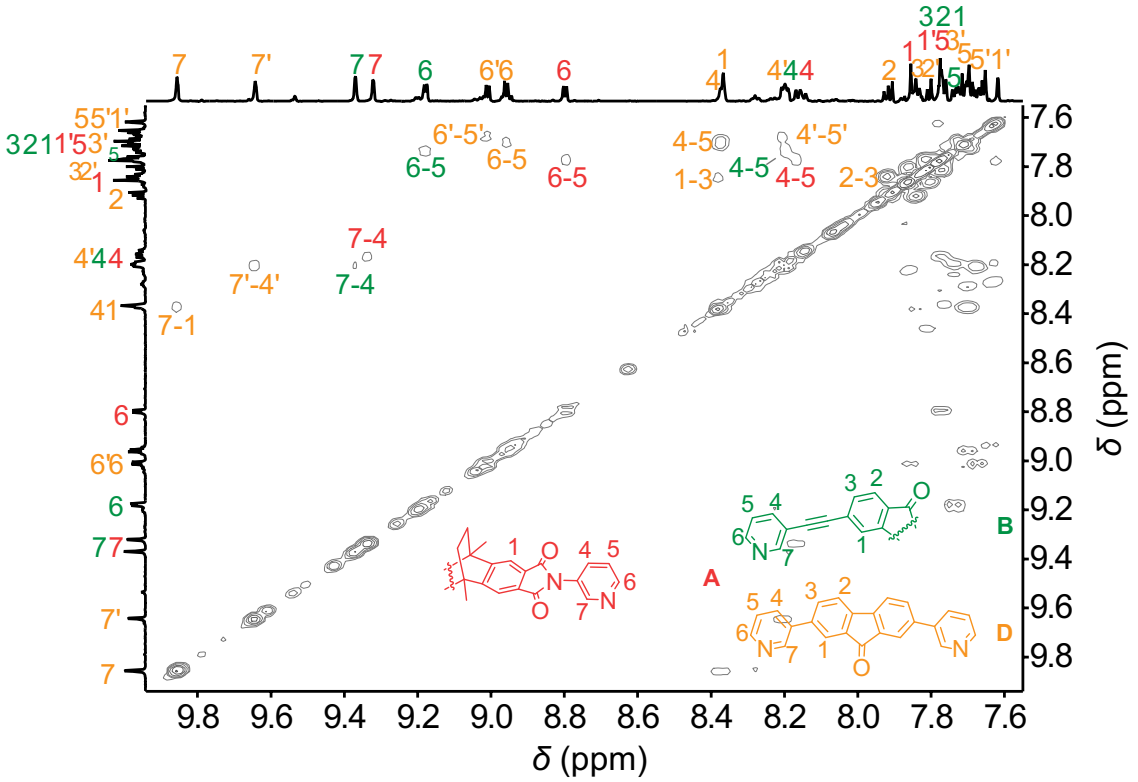

Supplementary Figure 81 | Partial ^{1}H–^{1}H COSY spectrum (500 MHz, 298 K, CD_3CN) of heteroleptic cage Pd_2**ABD**$_2$.

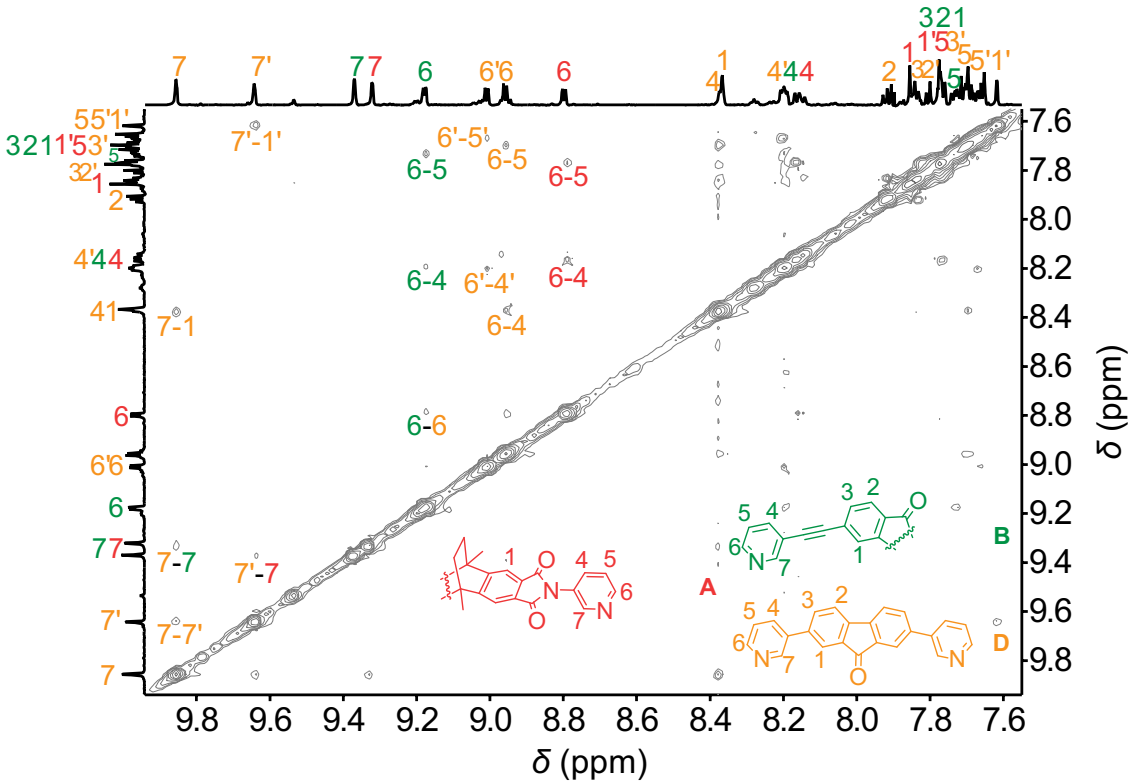

Supplementary Figure 82 | Partial ^{1}H–^{1}H NOESY spectrum (500 MHz, 298 K, CD_3CN) of heteroleptic cage Pd_2**ABD**$_2$. (The correlation between 7 and 7’ of ligand **D** confirmed the two ligands **D** are in cis- arrangement.)

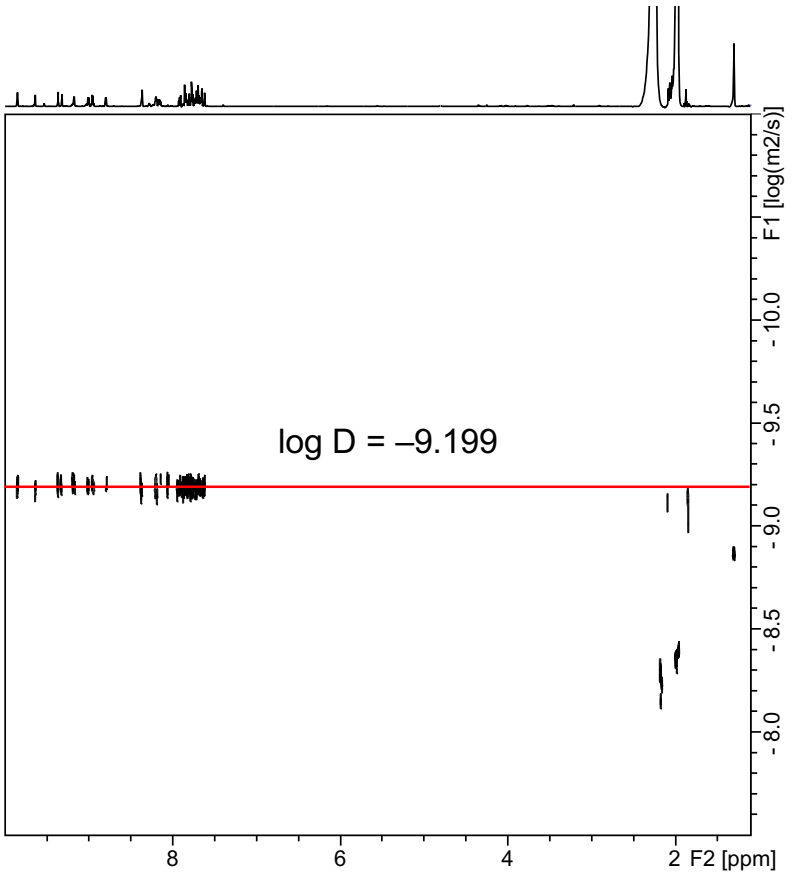

Supplementary Figure 83 | ^{1}H DOSY spectrum (500 MHz, 298 K, CD_3CN) of heteroleptic cage Pd_2**ABD**$_2$. Diffusion coefficient for Pd_2**ABD**$_2$: D = 6.316 × 10^{-10} m^2s^{-1}, log *D* = −9.199, r = 10.3 Å.

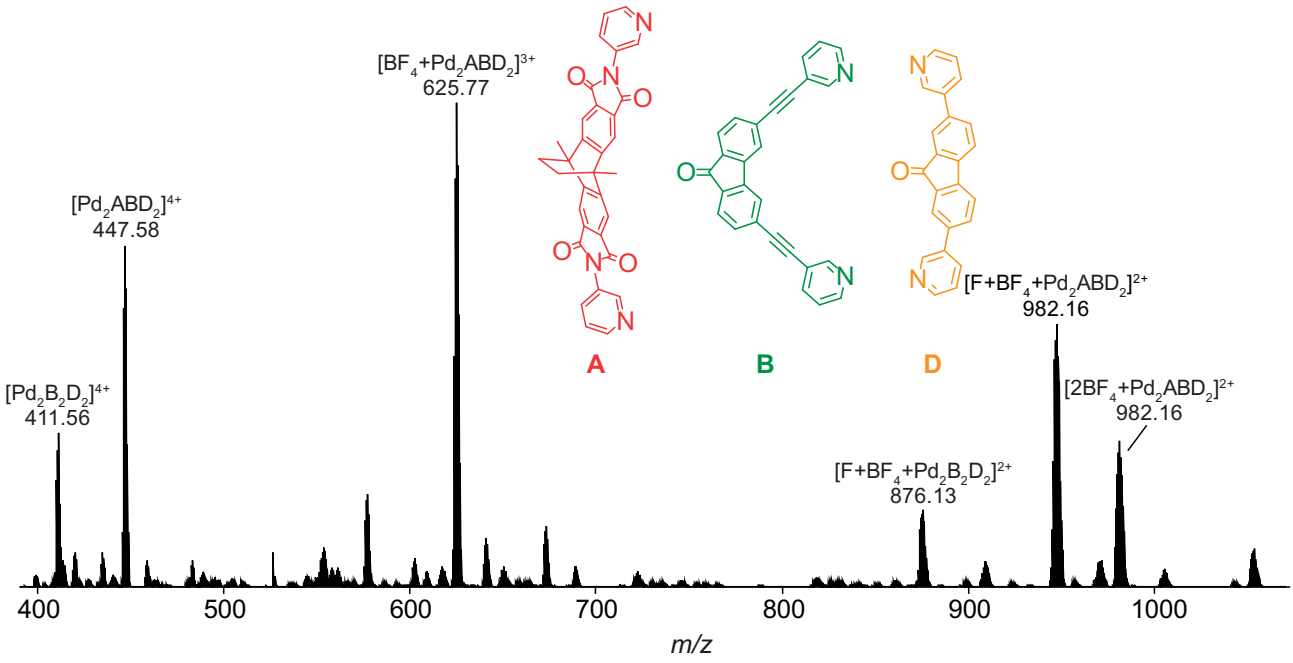

Supplementary Figure 84 | HR-ESI mass spectrum of heteroleptic cage Pd_2**ABD**$_2$.

*3.3.11. Self-assembly of heteroleptic cage Pd₂**ABCD***

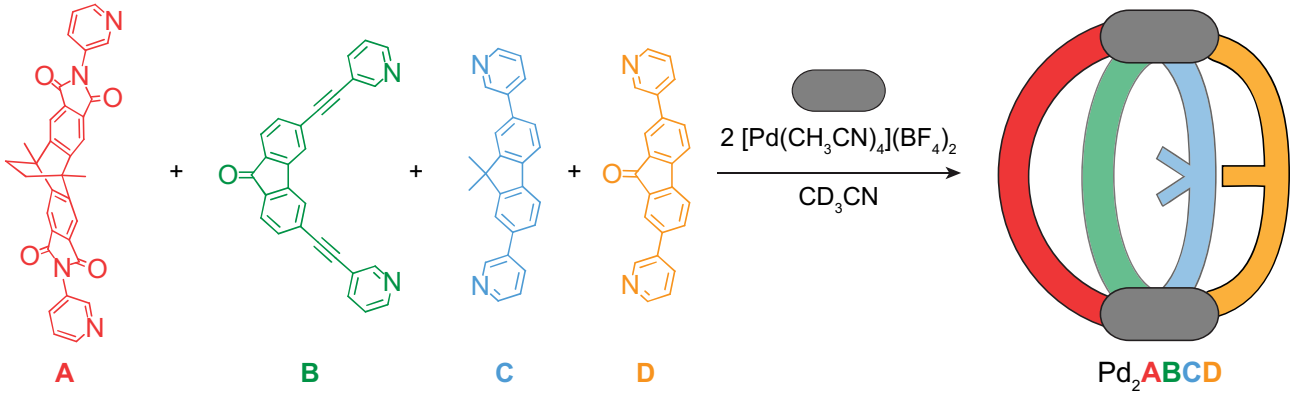

To a solution of **A** (60 µL, 3 mM, 0.18 µmol), **C** (60 µL, 3 mM, 0.18 µmol) and a suspension of **B** (60 µL, 3 mM, 0.18 µmol), **D** (60 µL, 3 mM, 0.18 µmol) were added a stock solution of $[Pd(CH_3CN)_4](BF_4)_2$ (24 µL, 15 mM/CD_3CN, 0.36 µmol) and additional 186 µL CD_3CN. The mixture was heated in an NMR tube at 80 °C for 8 h to give a 0.4 mM cage solution containing the shown cage as predominant species.

^{1}H NMR (700 MHz, 298 K, CD_3CN) δ 9.89 (d, *J* = 2.1 Hz, 2H), 9.38 (t, *J* = 2.7 Hz, 4H), 9.25 (d, *J* = 1.9 Hz, 2H), 9.16 (d, *J* = 5.9 Hz, 2H), 9.02 (d, *J* = 5.8 Hz, 2H), 8.97 (d, *J* = 5.8 Hz, 2H), 8.71 (d, *J* = 6.0 Hz, 2H), 8.53 (d, *J* = 1.8 Hz, 2H), 8.40 (d, *J* = 7.8 Hz, 2H), 8.17 – 8.10 (m, 4H), 8.00 (d, *J* = 7.5 Hz, 2H), 7.90 – 7.86 (m, 4H), 7.85 (d, *J* = 7.7 Hz, 2H), 7.79 (s, 2H), 7.75 – 7.69 (m, 6H), 7.65 – 7.61 (m, 4H), 7.61 – 7.59 (m, 2H), 7.48 (s, 2H), 7.46 (dd, *J* = 7.6, 1.8 Hz, 2H), 7.09 (d, *J* = 1.8 Hz, 2H), 2.12 (s, 3H), 1.97 (s, 3H), 1.81 (s, 4H), 1.32 (s, 3H), 0.55 (s, 3H).

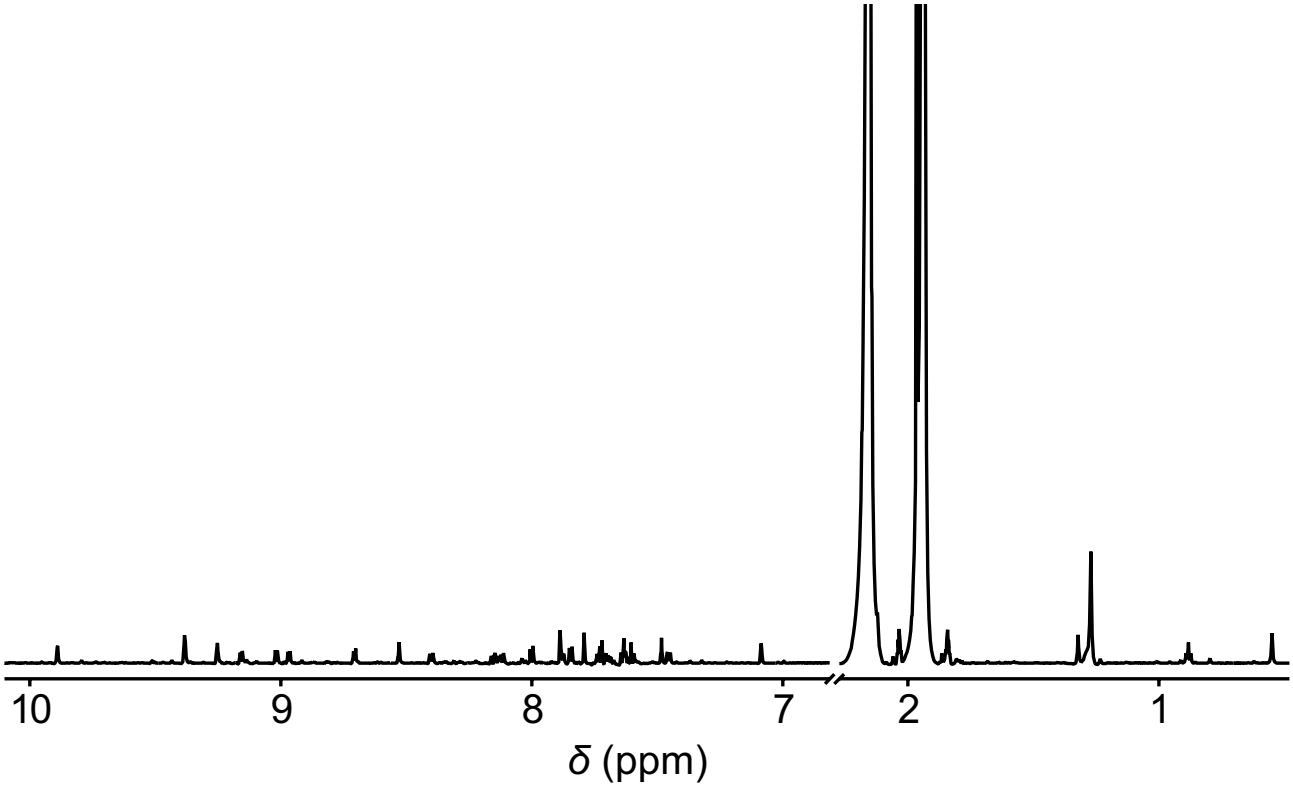

Supplementary Figure 85 | ^{1}H NMR spectrum (700 MHz, 298 K, CD_3CN) of heteroleptic cage Pd₂**ABCD**.

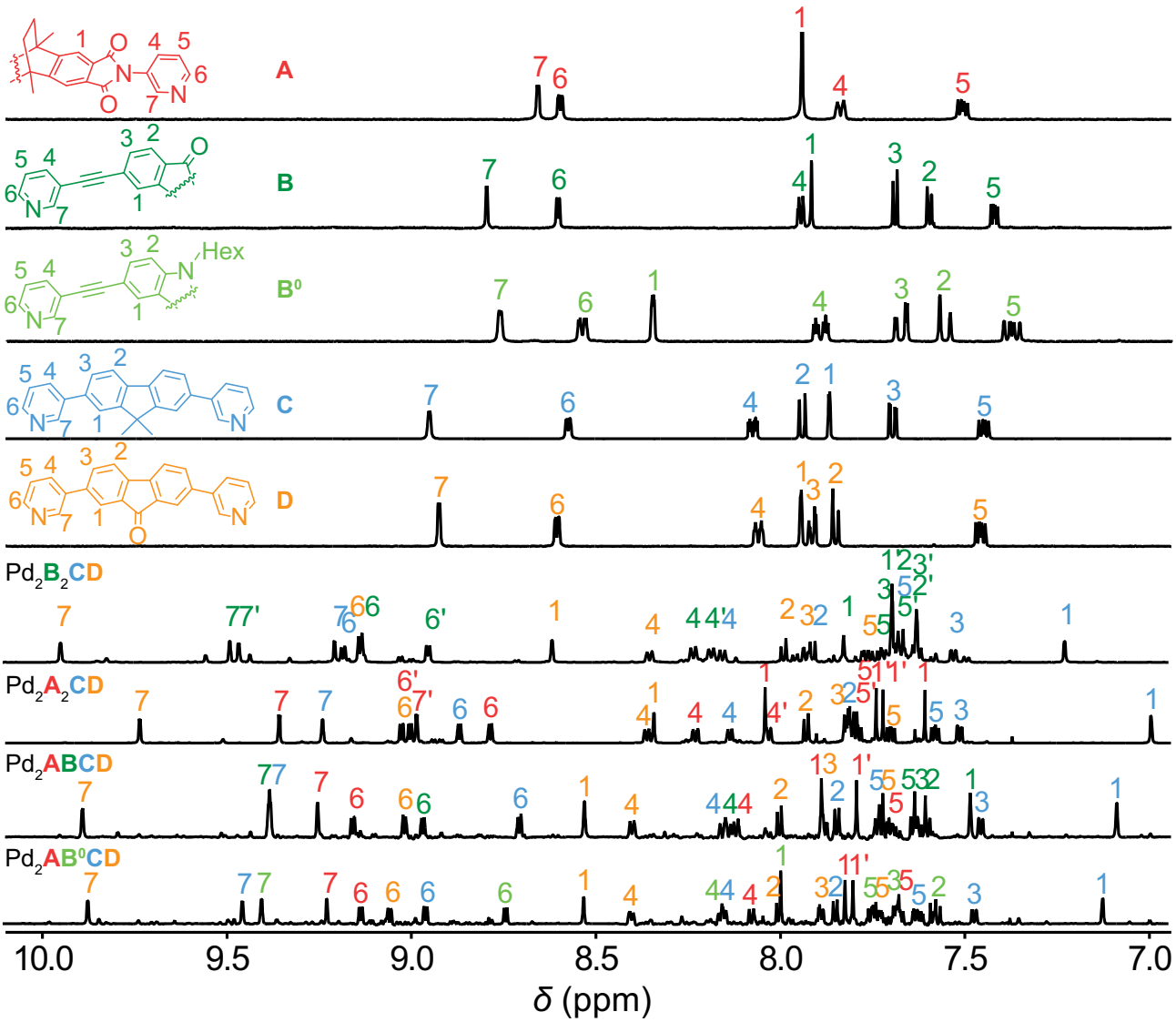

Supplementary Figure 86 | Partial ^{1}H NMR spectrum (700 MHz, 298 K, CD_3CN) comparison of ligands **A** (red), **B** (green), **B^{0}** (pale green), **C** (blue), **D** (yellow), and heteroleptic cages Pd_2**B**$_2$**CD**, Pd_2**A**$_2$**CD**, Pd_2**ABCD** and Pd_2**AB^{0}CD**.

^{13}C NMR (151 MHz, 298 K, CD_3CN) δ 194.28, 192.81, 173.03, 167.76, 167.65, 167.11, 166.94, 154.71, 154.63, 153.97, 151.26, 151.15, 150.50, 150.43, 150.32, 149.86, 149.83, 145.99, 144.74, 142.35, 142.03, 140.18, 139.66, 139.08, 138.48, 138.42, 137.29, 136.69, 136.23, 135.69, 135.46, 131.86, 130.66, 130.58, 128.69, 128.49, 128.38, 128.34, 127.92, 125.13, 124.89, 124.07, 123.64, 123.44, 123.05, 122.69, 117.56, 95.28, 87.38, 46.85, 45.04, 32.64, 30.37, 27.10, 23.39, 18.75, 14.39.

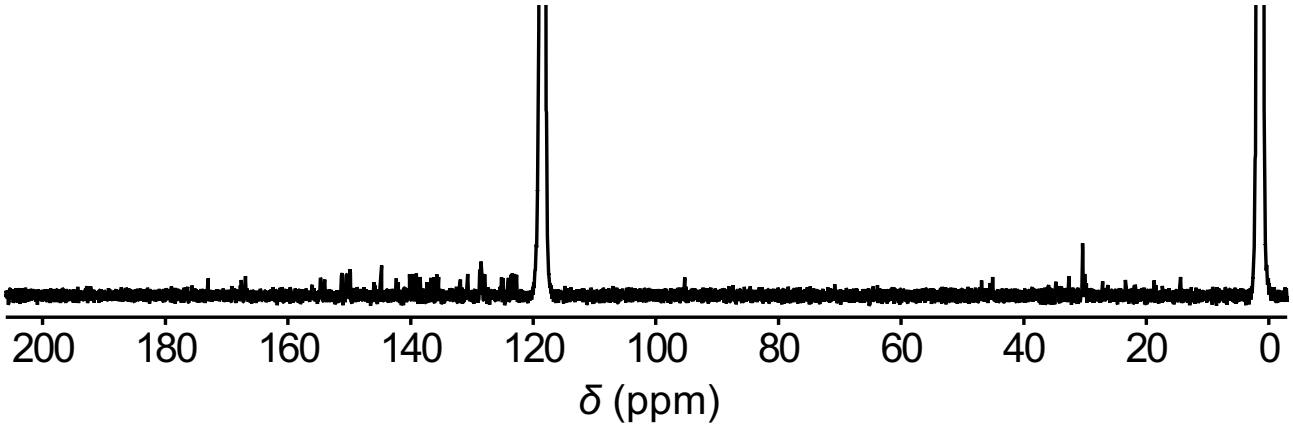

Supplementary Figure 87 | ^{13}C NMR spectrum (151 MHz, 298 K, CD_3CN) of heteroleptic cage Pd_2**ABCD**.

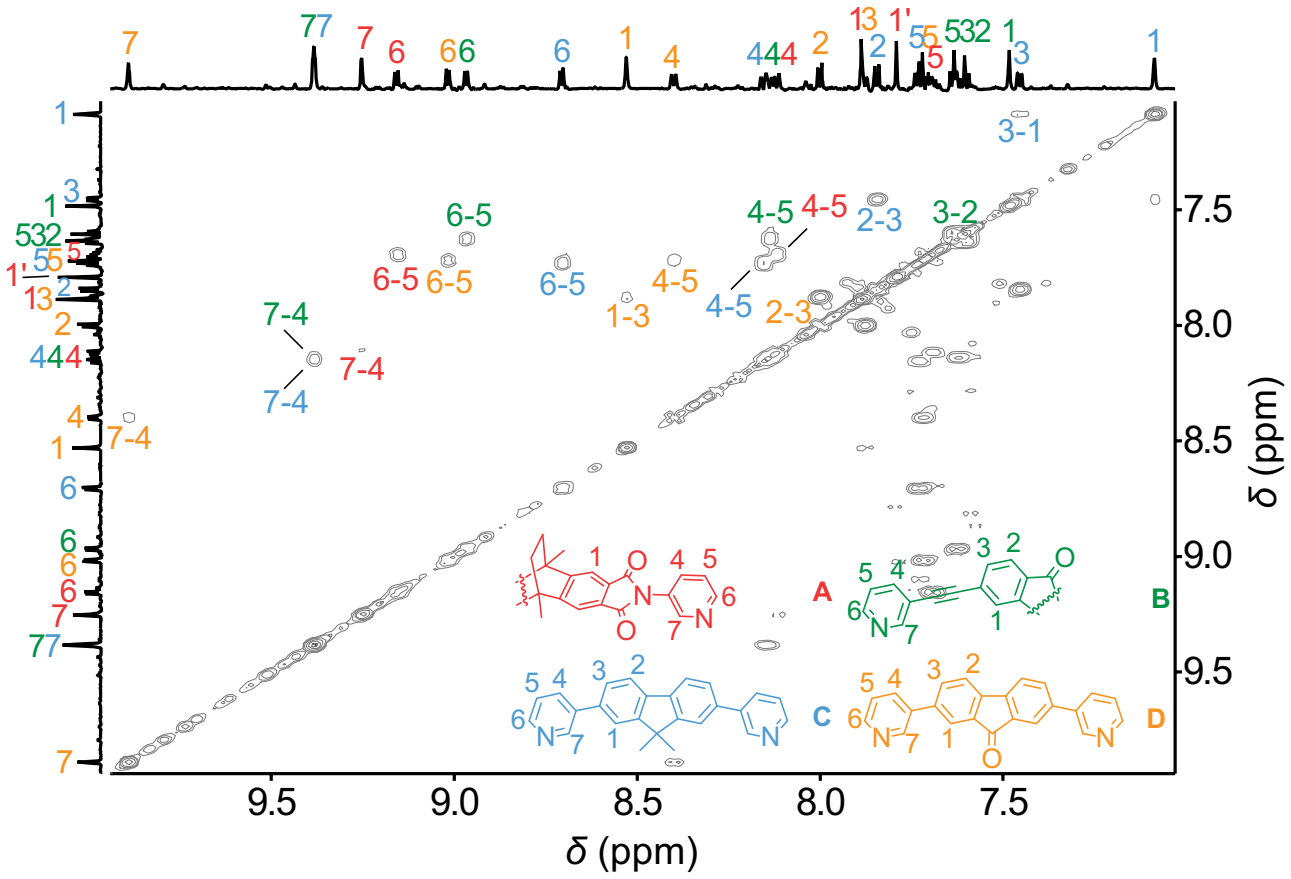

Supplementary Figure 88 | Partial ^{1}H–^{1}H COSY spectrum (500 MHz, 298 K, CD_3CN) of heteroleptic cage Pd_2**ABCD**.

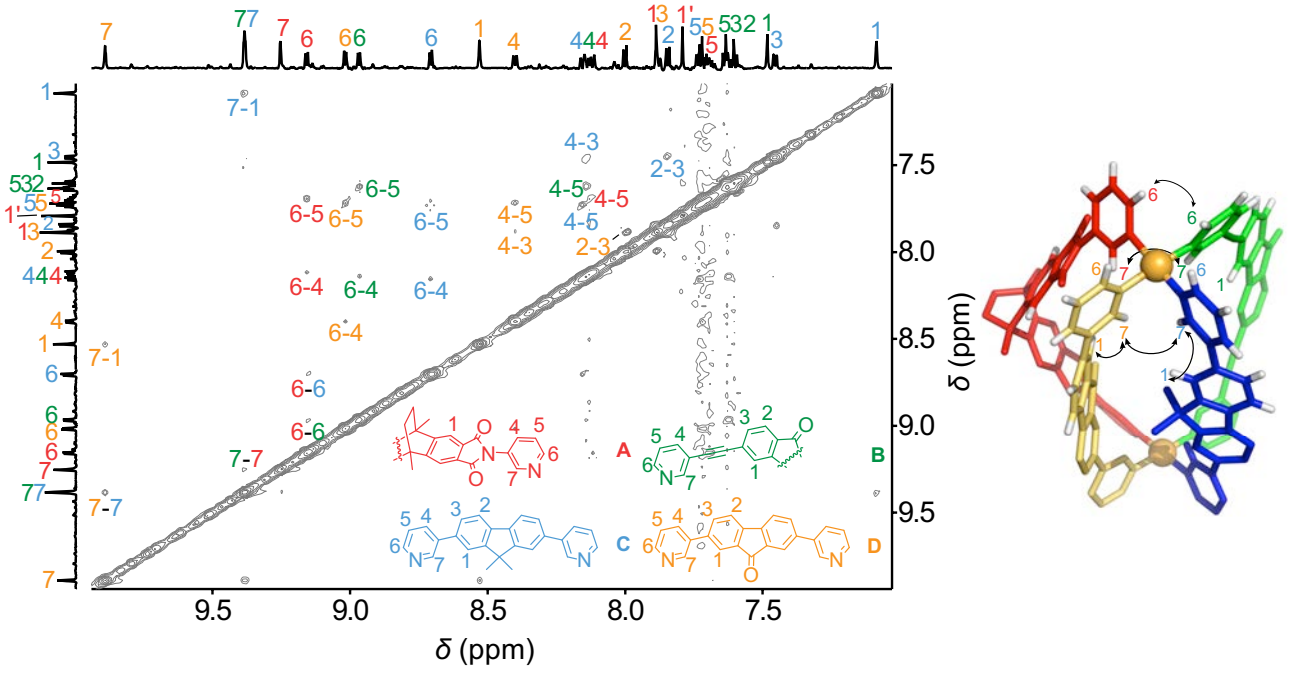

Supplementary Figure 89 | Partial ^{1}H–^{1}H NOESY spectrum (500 MHz, 298 K, CD_3CN) of heteroleptic cage Pd_2**ABCD**. The composition of this heteroleptic cage is supported by a single crystal X-ray structure (details see below). The found NOE contacts in solution are in full accordance with the X-ray structure results.

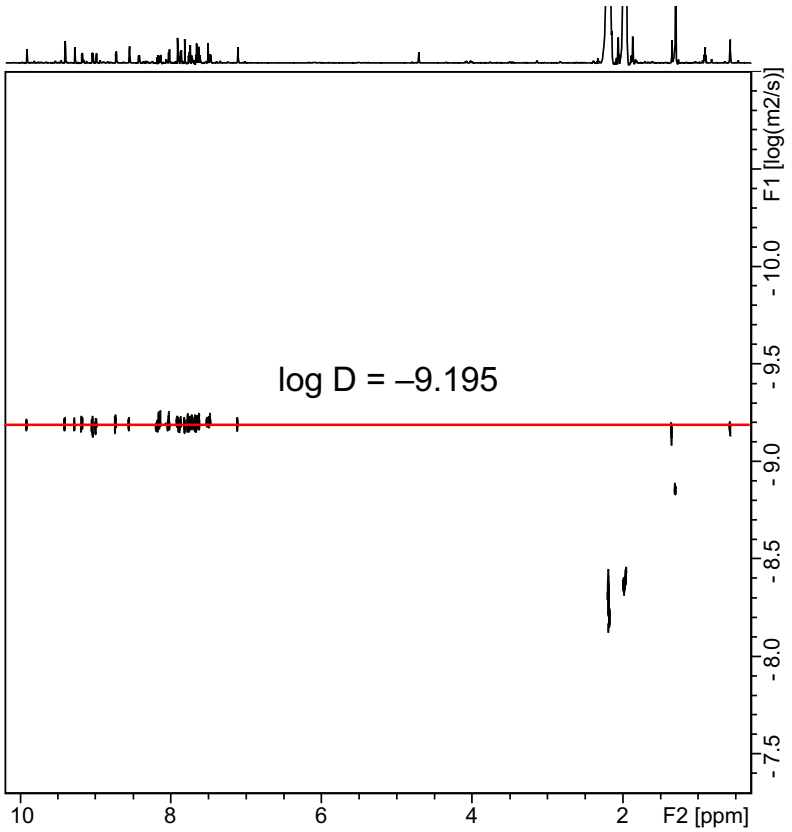

Supplementary Figure 90 | ^{1}H DOSY spectrum (500 MHz, 298 K, CD_3CN) of heteroleptic cage Pd_2**ABCD**. Diffusion coefficient for Pd_2**ABCD**: D = 6.384 × 10^{-10} m^2s^{-1}, log *D* = −9.195, r = 10.2 Å.

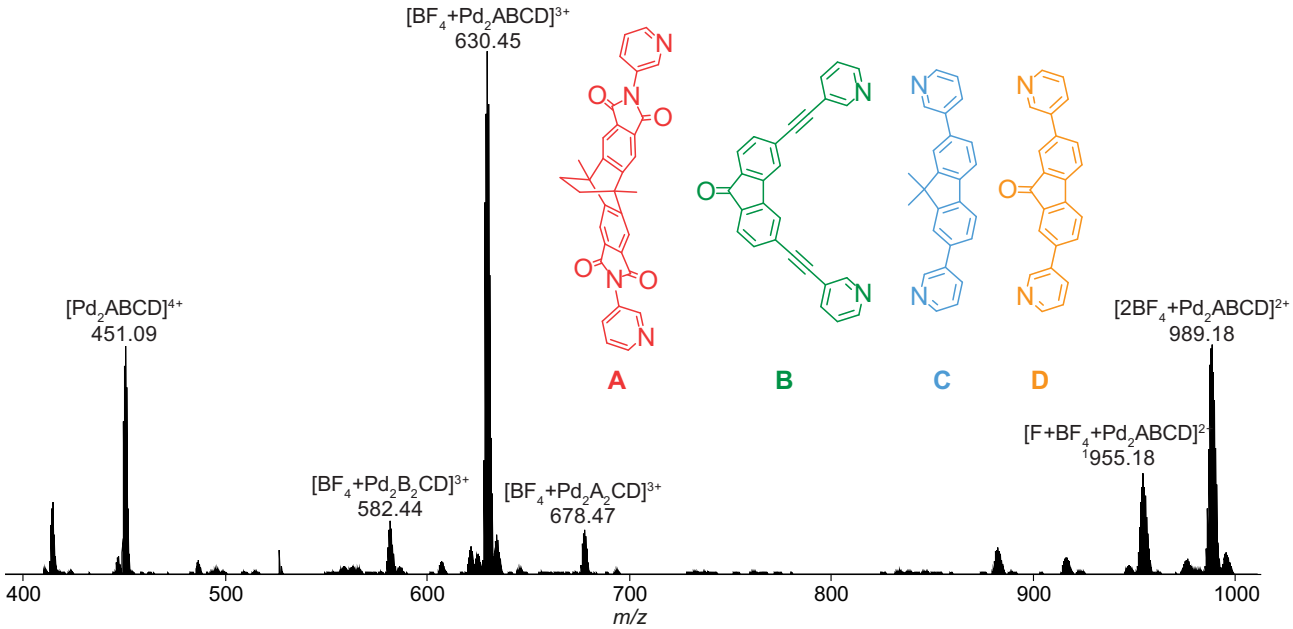

Supplementary Figure 91 | HR-ESI mass spectrum of heteroleptic cage Pd_2**ABCD**.

3.4. Evolution of heteroleptic cage Pd_2AB^0CD

3.4.1. Self-assembly of heteroleptic cage $Pd_2B^0{}_2D_2$

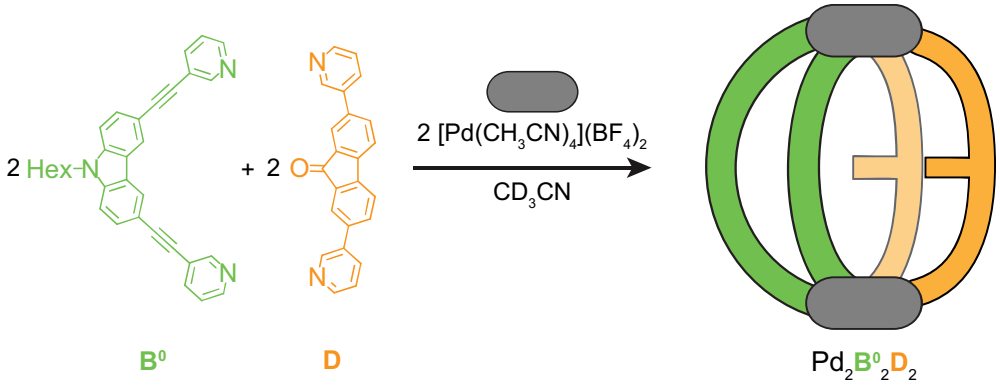

To a suspension of **D** (100 µL, 7 mM, 0.7 µmol) and $\mathbf{B^0}$ (100 µL, 7 mM, 0.7 µmol) in CD_3CN were added a stock solution of $[Pd(CH_3CN)_4](BF_4)_2$ (47 µL, 15 mM/CD_3CN, 0.7 µmol) and 253 µL additional CD_3CN. The mixture was heated in an NMR tube at 80 °C for 8 h to give a 0.7 mM cage solution containing the shown cage as predominant species.

^{1}H NMR (500 MHz, 298 K, CD_3CN) δ 9.86 (d, J = 2.1 Hz, 4H), 9.34 (d, J = 2.0 Hz, 4H), 9.12 (dd, J = 6.0, 1.4 Hz, 4H), 9.00 (dd, J = 5.7, 1.2 Hz, 4H), 8.31 – 8.28 (m, 4H), 8.26 (dt, J = 8.1, 1.6 Hz, 4H), 8.18 (d, J = 1.8 Hz, 4H), 8.14 (dt, J = 8.0, 1.6 Hz, 4H), 7.88 – 7.82 (m, 8H), 7.74 – 7.72 (m, 4H), 7.70 – 7.65 (m, 8H), 7.60 – 7.57 (m, 4H), 4.33 (t, J = 7.1 Hz, 4H), 1.76 (t, J = 7.1 Hz, 4H), 1.18 (m, 12H), 0.74 (t, J = 7.1 Hz, 6H).

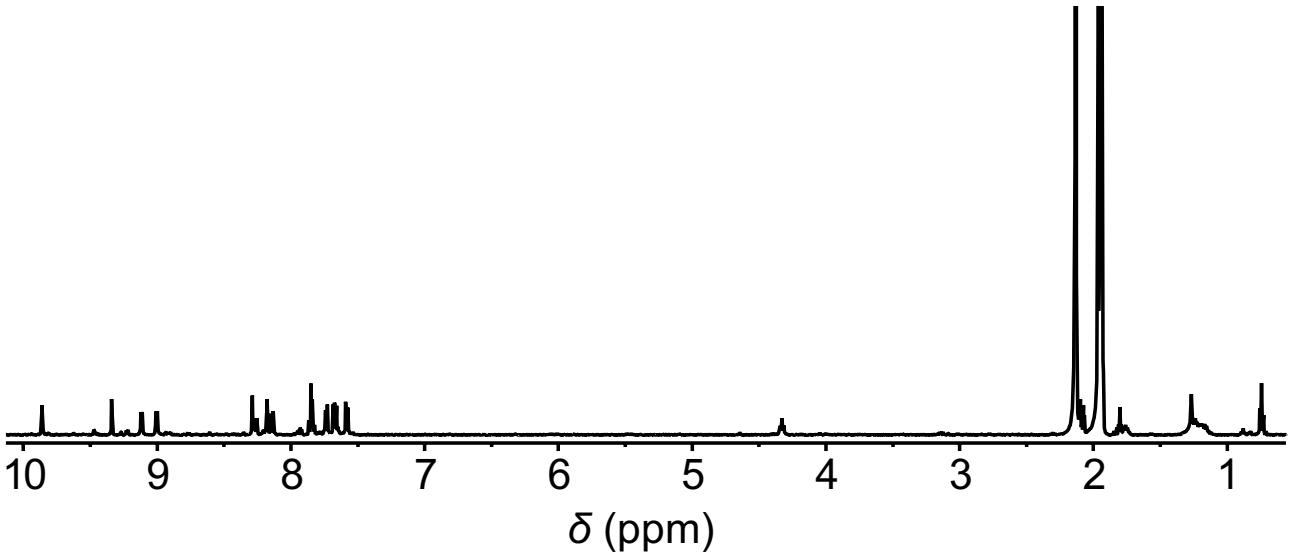

Supplementary Figure 92 | ^{1}H NMR spectrum (500 MHz, 298 K, CD_3CN) of heteroleptic cage $Pd_2B^0{}_2D_2$.

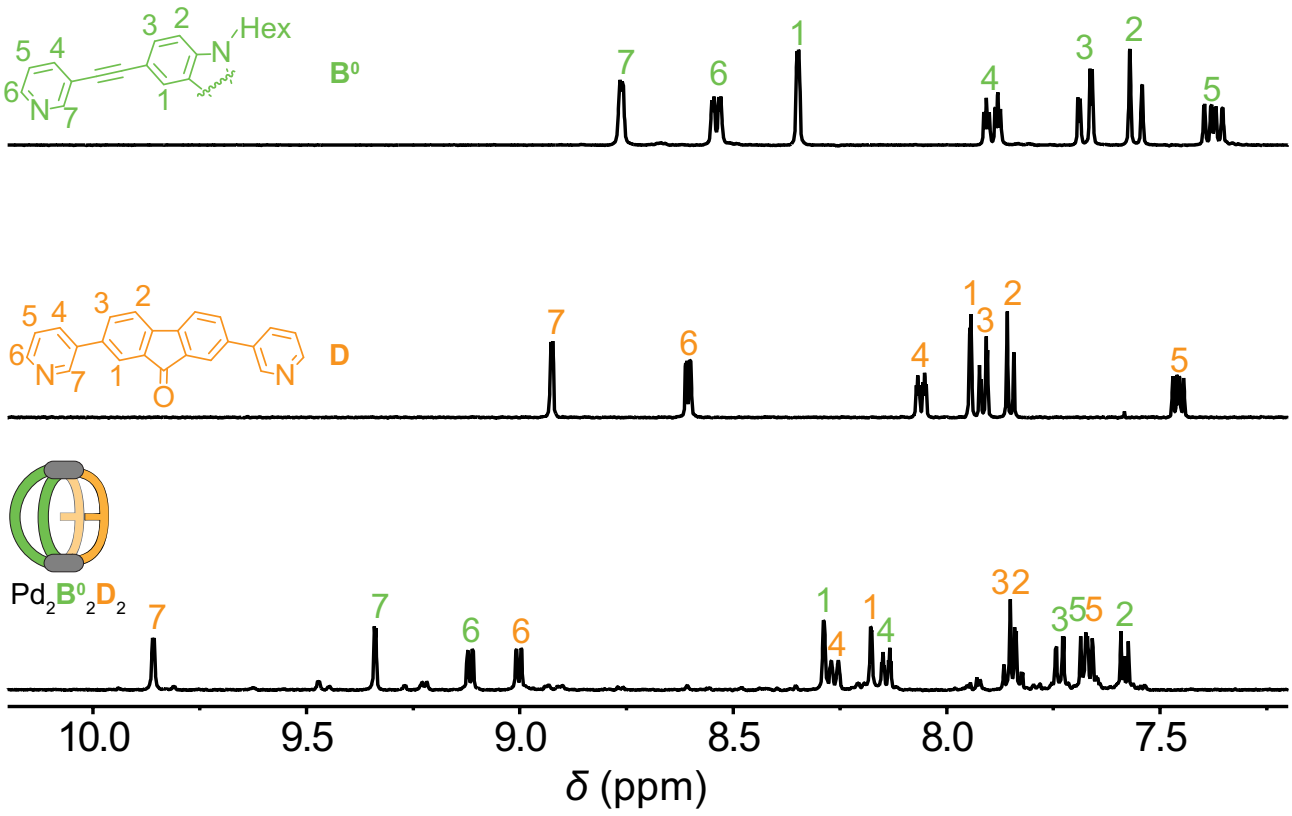

Supplementary Figure 93 | Partial ^{1}H NMR spectrum (500 MHz, 298 K, CD_3CN) comparison of ligand $\mathbf{B^0}$ (top), ligand **D** (middle), and heteroleptic cage $Pd_2\mathbf{B^0}_2\mathbf{D}_2$ (bottom).

^{13}C NMR (176 MHz, 298 K, CD_3CN) δ 152.60, 150.74, 150.35, 149.93, 145.60, 144.04, 142.40, 138.90, 137.20, 137.16, 135.09, 132.48, 128.65, 128.35, 125.69, 124.25, 123.60, 123.05, 112.89, 111.59, 98.33, 83.71, 32.08, 30.37, 29.40, 27.26, 23.14, 14.12.

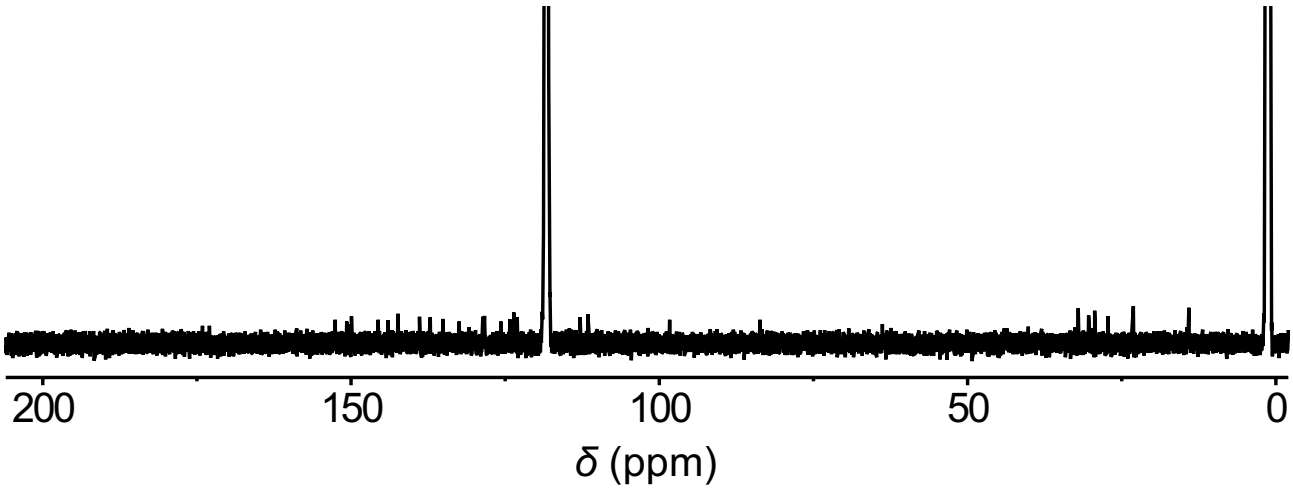

Supplementary Figure 94 | ^{13}C NMR spectrum (176 MHz, 298 K, CD_3CN) of heteroleptic cage $Pd_2\mathbf{B^0}_2\mathbf{D}_2$.

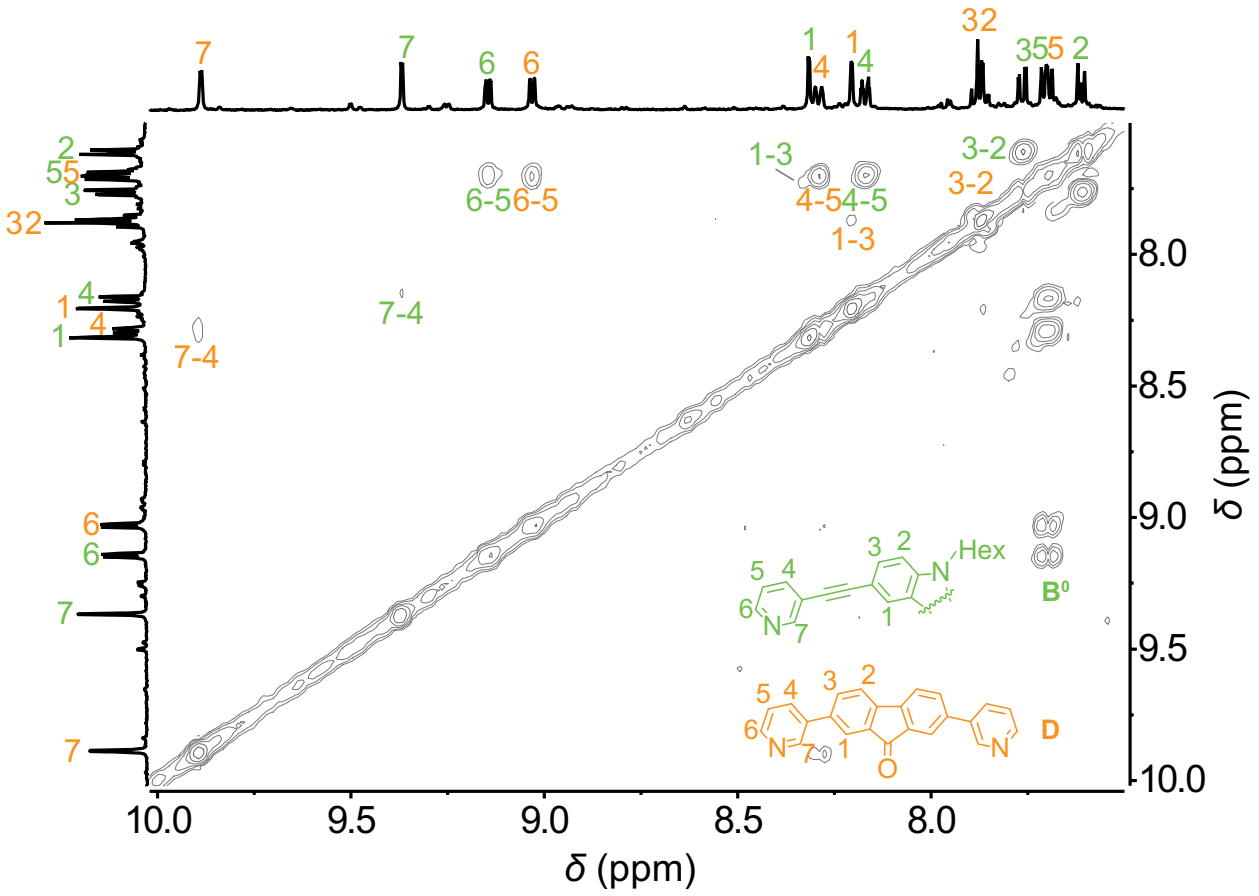

Supplementary Figure 95 | Partial ^{1}H–^{1}H COSY spectrum (500 MHz, 298 K, CD_3CN) of heteroleptic cage $Pd_2\mathbf{B}^{0}_{2}\mathbf{D}_2$.

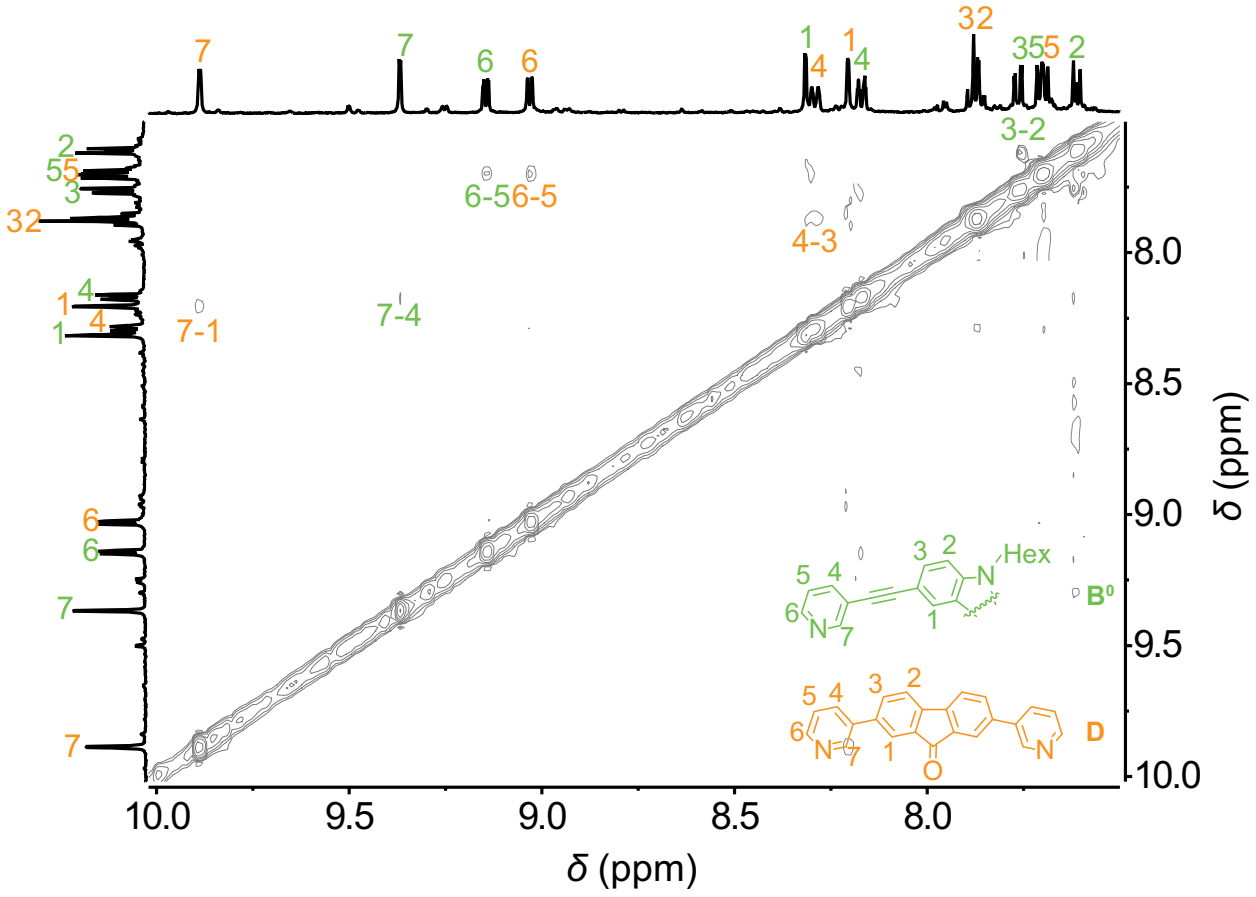

Supplementary Figure 96 | Partial ^{1}H–^{1}H NOESY spectrum (500 MHz, 298 K, CD_3CN) of heteroleptic cage $Pd_2\mathbf{B}^{0}_{2}\mathbf{D}_2$.

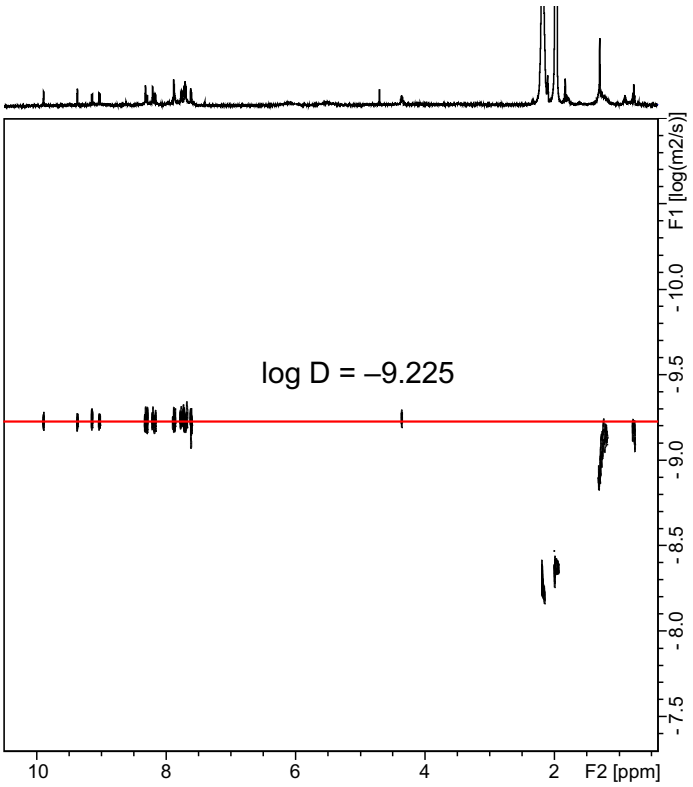

Supplementary Figure 97 | ^{1}H DOSY spectrum (500 MHz, 298 K, CD_3CN) of heteroleptic cage $Pd_2\mathbf{B^0}_2\mathbf{D}_2$. Diffusion coefficient for $Pd_2\mathbf{B^0}_2\mathbf{D}_2$: D = 5.96 × 10^{-10} m^2s^{-1}, log *D* = −9.225, r = 11.0 Å.

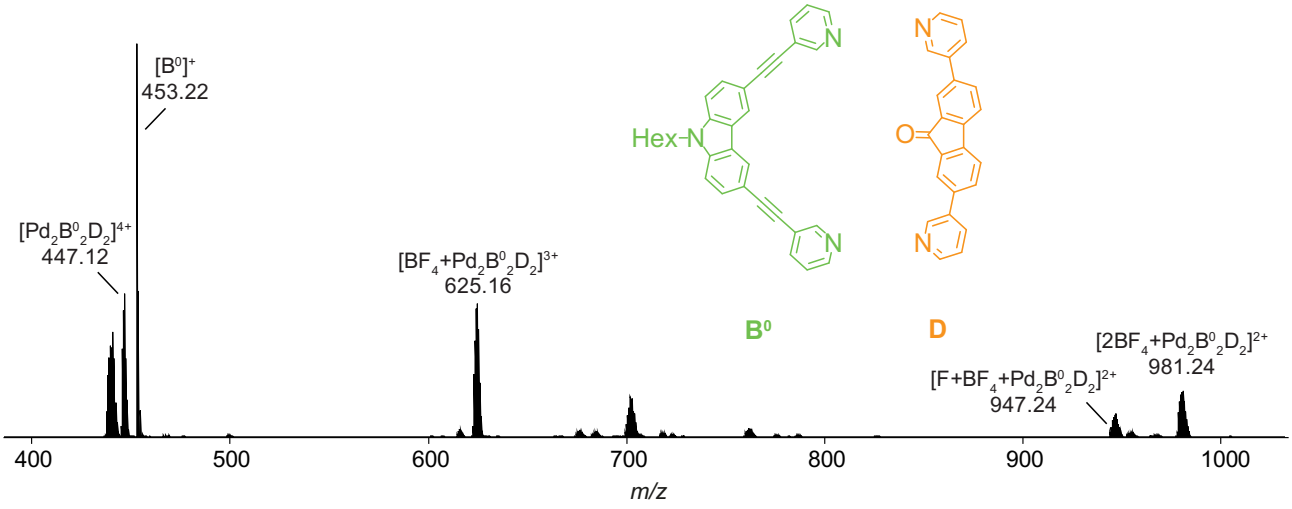

Supplementary Figure 98 | HR-ESI mass spectrum of heteroleptic cage $Pd_2\mathbf{B^0}_2\mathbf{D}_2$.

3.4.2. Self-assembly of heteroleptic cage $Pd_2B^0{}_2CD$

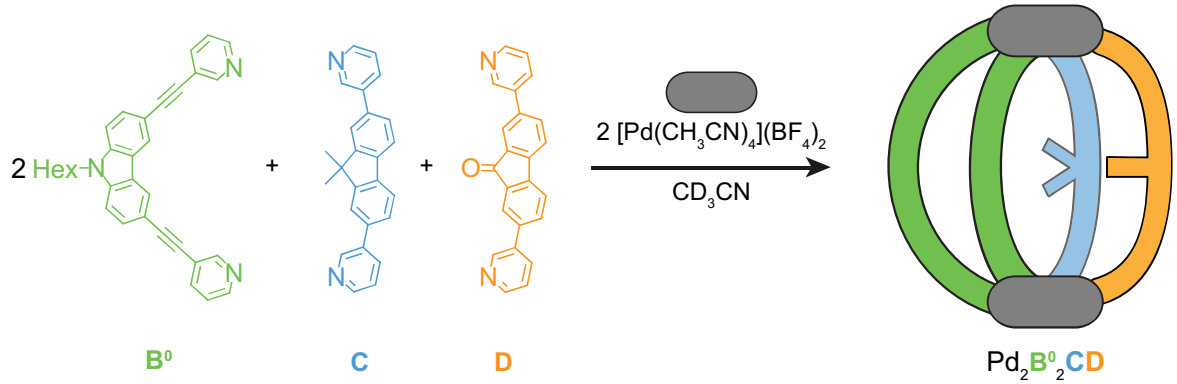

To a solution of **B^0** (200 µL, 3 mM, 0.6 µmol), **C** (100 µL, 3 mM, 0.3 µmol) and **D** (100 µL, 3 mM, 0.3 µmol) were added a stock solution of $[Pd(CH_3CN)_4](BF_4)_2$ (40 µL, 15 mM/CD_3CN, 0.6 µmol) and 60 µL additional CD_3CN,. The mixture was heated in an NMR tube at 80 °C for 8 h to give a 0.6 mM cage solution containing the shown cage as predominant species.

^{1}H NMR (600 MHz, 298 K, CD_3CN) δ 9.99 – 9.94 (m, 2H), 9.51 (d, *J* = 2.0 Hz, 2H), 9.47 (d, *J* = 1.8 Hz, 2H), 9.20 – 9.16 (m, 2H), 9.12 (ddt, *J* = 6.9, 4.0, 2.1 Hz, 4H), 9.10 (dd, *J* = 6.0, 1.3 Hz, 2H), 8.97 (d, *J* = 5.8 Hz, 2H), 8.67 (d, *J* = 1.8 Hz, 2H), 8.37 – 8.32 (m, 4H), 8.23 (d, *J* = 1.6 Hz, 2H), 8.18 (ddd, *J* = 5.9, 4.6, 2.9 Hz, 4H), 8.09 (dt, *J* = 8.0, 1.7 Hz, 2H), 7.99 (d, *J* = 7.6 Hz, 2H), 7.94 (dd, *J* = 7.6, 1.8 Hz, 2H), 7.90 (d, *J* = 7.7 Hz, 2H), 7.78 – 7.73 (m, 4H), 7.71 – 7.67 (m, 4H), 7.64 (ddd, *J* = 11.7, 7.8, 5.8 Hz, 4H), 7.59 (d, *J* = 7.2 Hz, 2H), 7.56 – 7.52 (m, 4H), 7.29 – 7.25 (m, 2H), 4.35 (t, *J* = 7.1 Hz, 2H), 4.30 (t, *J* = 7.1 Hz, 2H), 1.78 (s, 3H), 1.75 (dd, *J* = 18.5, 7.6 Hz, 4H), 1.26 – 1.12 (m, 12H), 0.74 (dt, *J* = 15.6, 7.1 Hz, 6H), 0.63 (s, 3H).

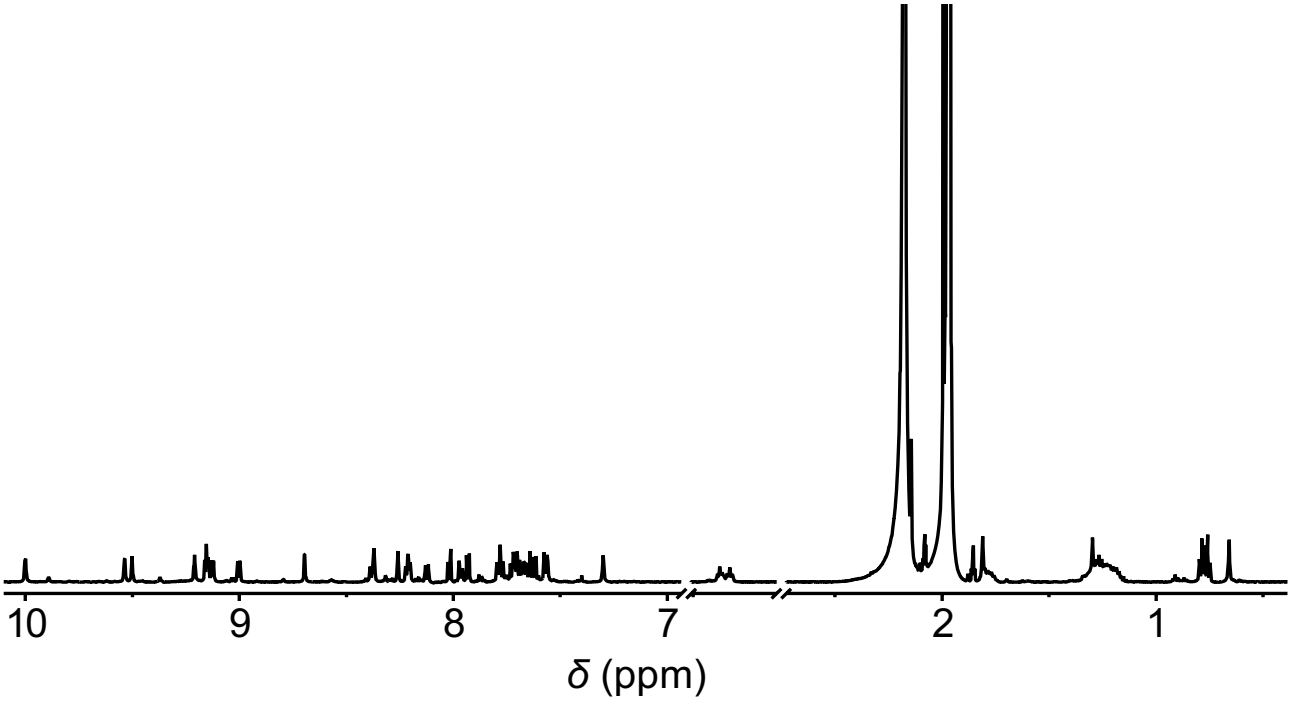

Supplementary Figure 99 | ^{1}H NMR spectrum (600 MHz, 298 K, CD_3CN) of heteroleptic cage $Pd_2B^0{}_2CD$.

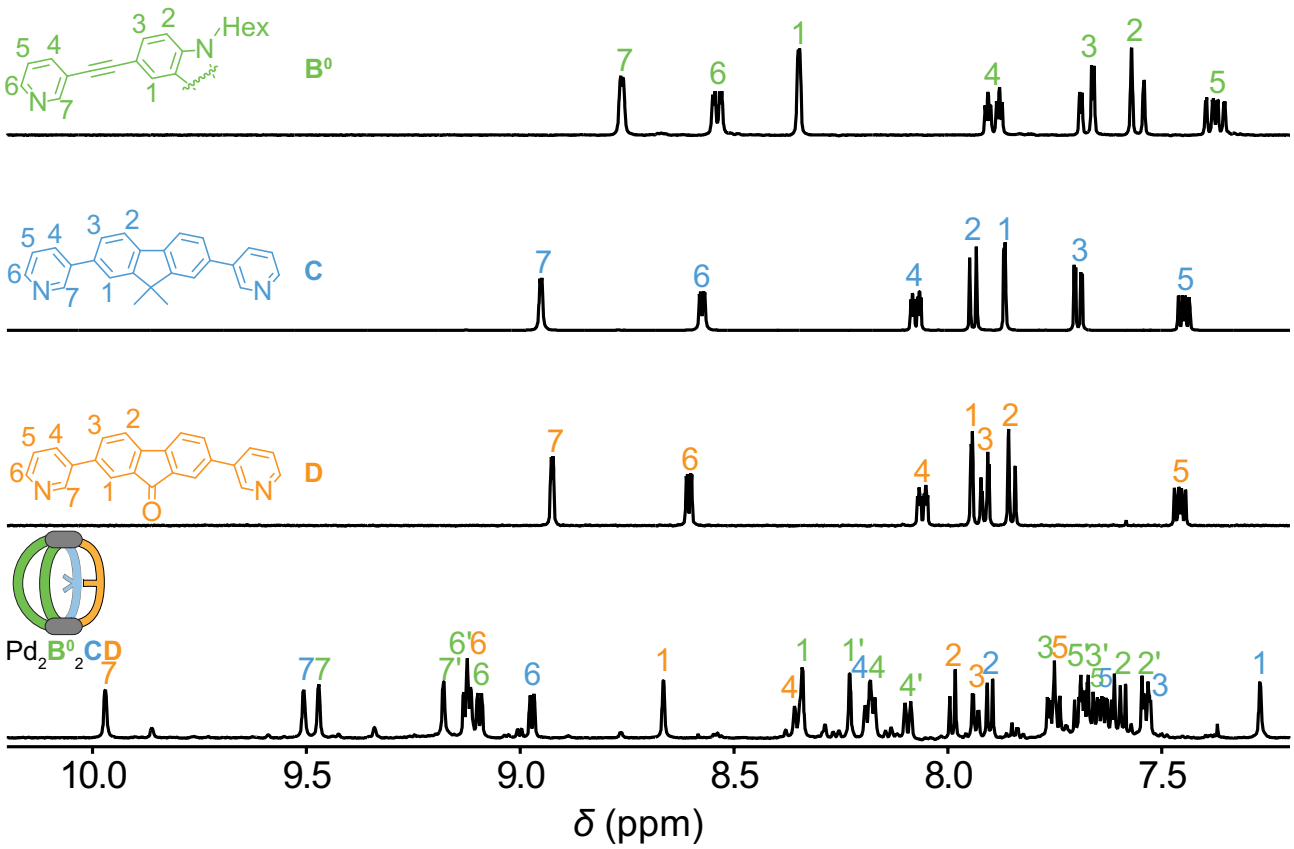

Supplementary Figure 100 | Partial ^{1}H NMR spectrum (600 MHz, 298 K, CD_3CN) comparison of ligand **B⁰** (top), ligand **C** (upper middle), ligand **D** (lower middle) and heteroleptic cage Pd_2**B⁰**$_2$**CD** (bottom).

^{13}C NMR (151 MHz, 298 K, CD_3CN) δ 194.26, 172.98, 166.33, 155.98, 153.27, 152.30, 150.95, 150.23, 150.20, 150.16, 150.09, 146.03, 144.02, 143.90, 142.43, 142.27, 142.15, 140.92, 140.33, 139.31, 139.11, 137.94, 137.14, 136.59, 135.77, 132.41, 132.31, 128.76, 128.47, 128.06, 125.67, 125.60, 124.48, 124.14, 124.09, 123.94, 123.20, 123.07, 123.03, 122.94, 112.97, 112.79, 111.65, 111.47, 98.40, 98.14, 83.86, 83.46, 46.88, 44.02, 43.98, 32.07, 29.39, 27.25, 14.13, 14.11.

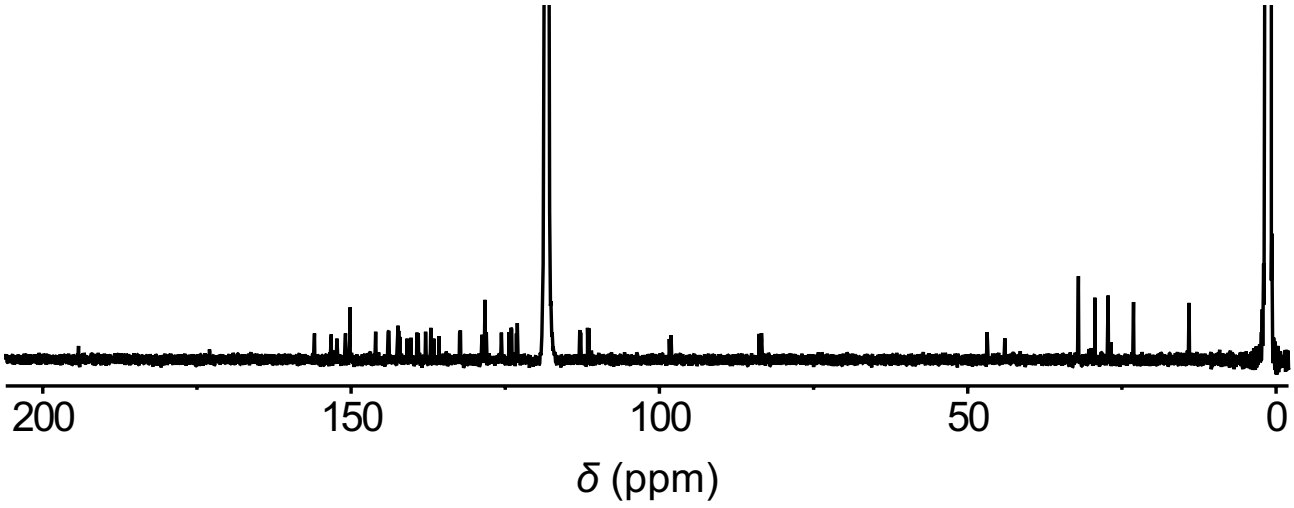

Supplementary Figure 101 | ^{13}C NMR spectrum (151 MHz, 298 K, CD_3CN) of heteroleptic cage Pd_2**B⁰**$_2$**CD**.

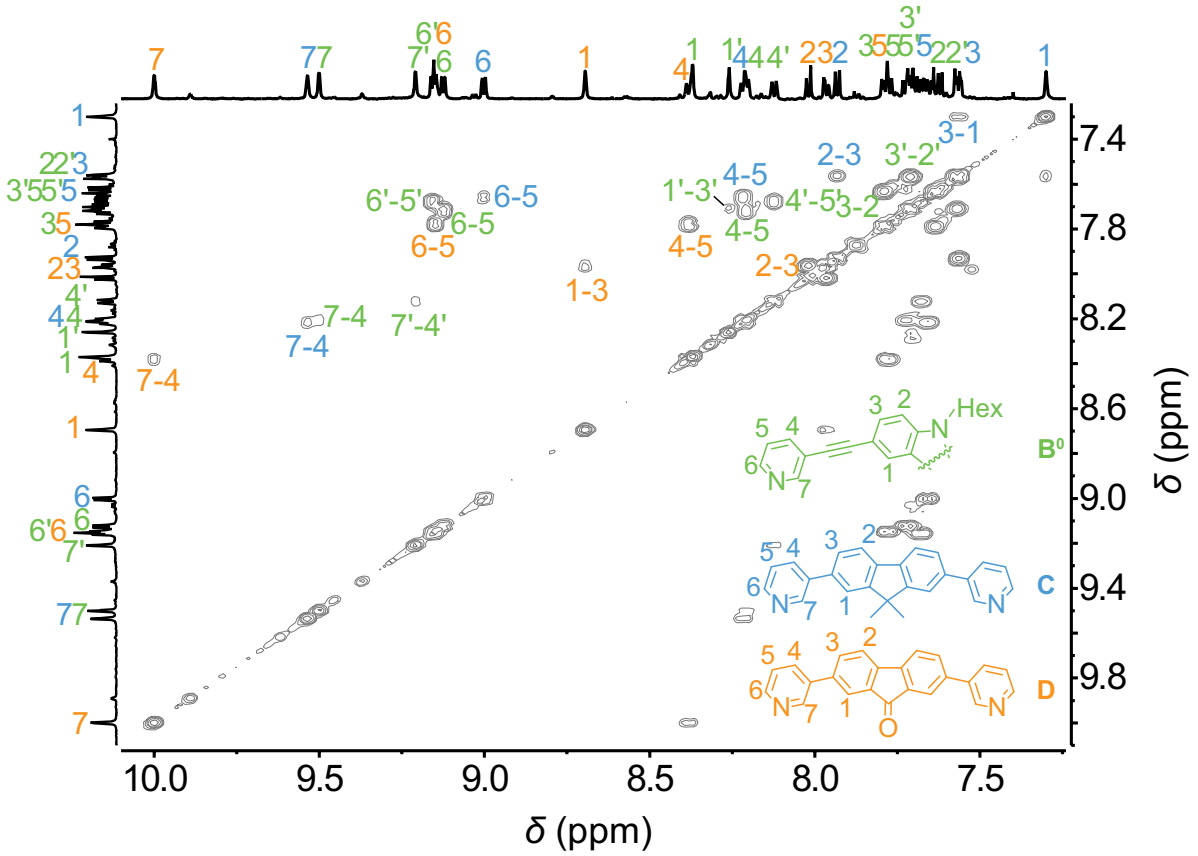

Supplementary Figure 102 | Partial ^{1}H–^{1}H COSY spectrum (500 MHz, 298 K, CD_3CN) of heteroleptic cage $Pd_2\mathbf{B^0}_2\mathbf{CD}$.

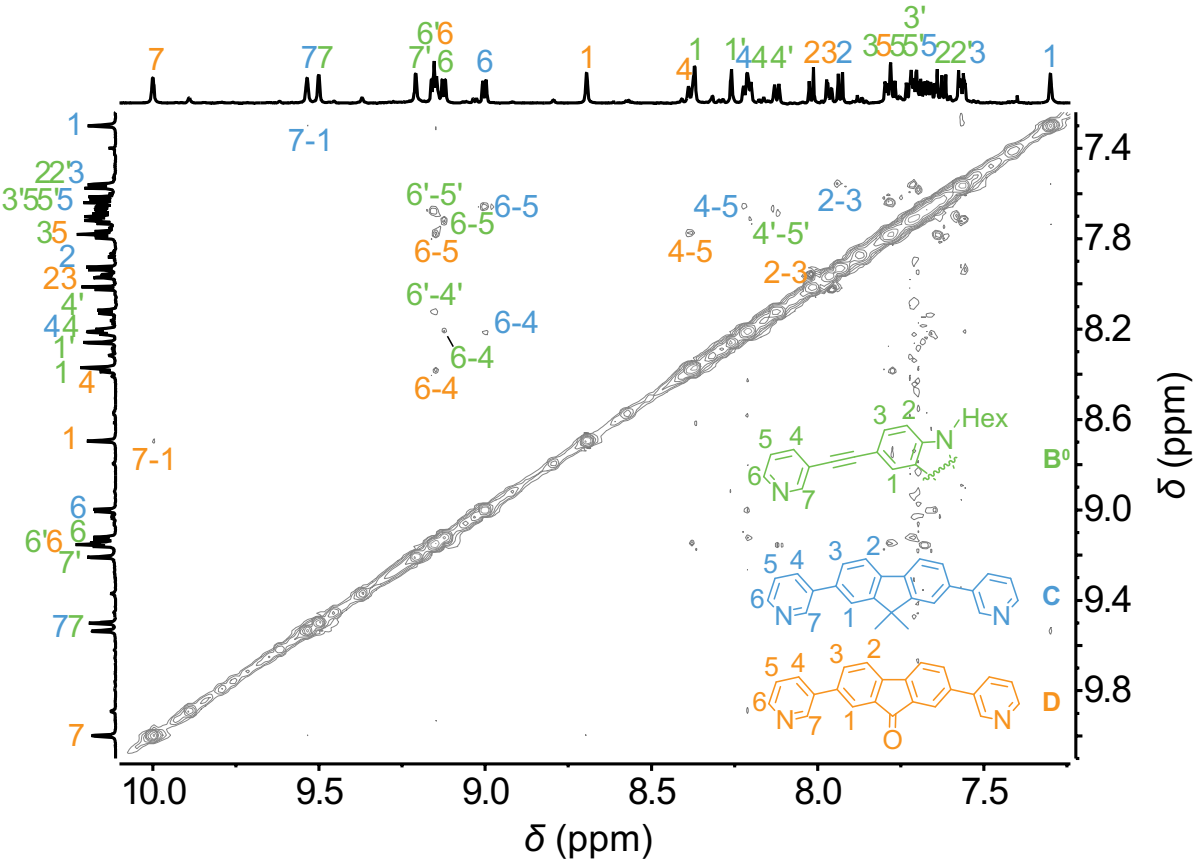

Supplementary Figure 103 | Partial ^{1}H–^{1}H NOESY spectrum (500 MHz, 298 K, CD_3CN) of heteroleptic cage $Pd_2\mathbf{B^0}_2\mathbf{CD}$.

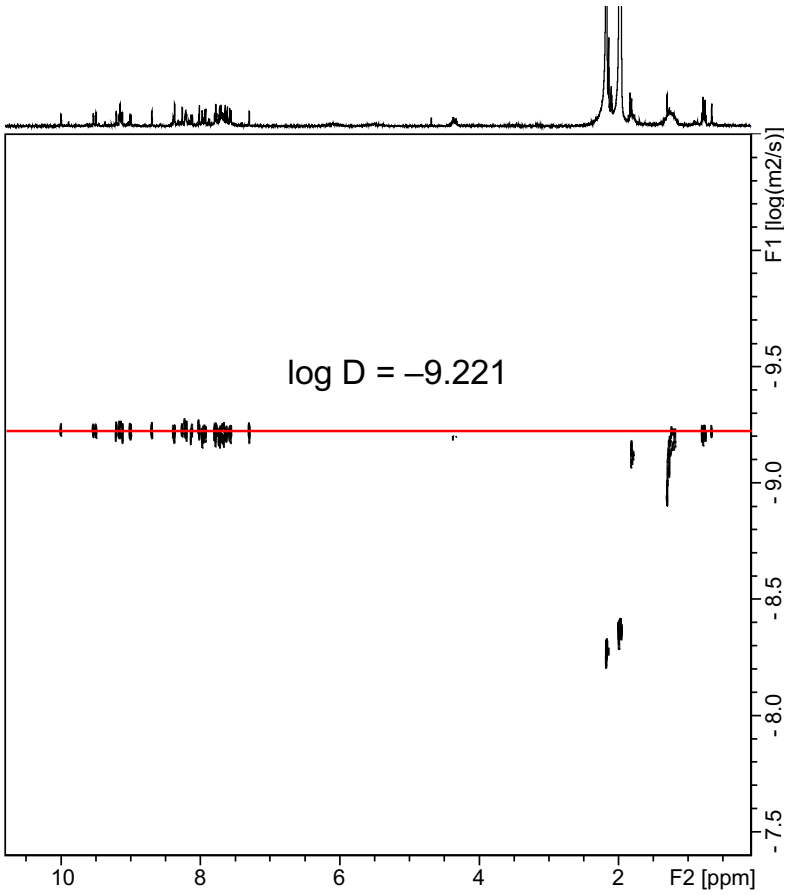

Supplementary Figure 104 | ^{1}H DOSY spectrum (500 MHz, 298 K, CD_3CN) of heteroleptic cage $Pd_2\mathbf{B^0}_2\mathbf{CD}$. Diffusion coefficient for $Pd_2\mathbf{B^0}_2\mathbf{CD}$: D = 6.012 × 10^{-10} m^2s^{-1}, log *D* = −9.221, r = 10.9 Å.

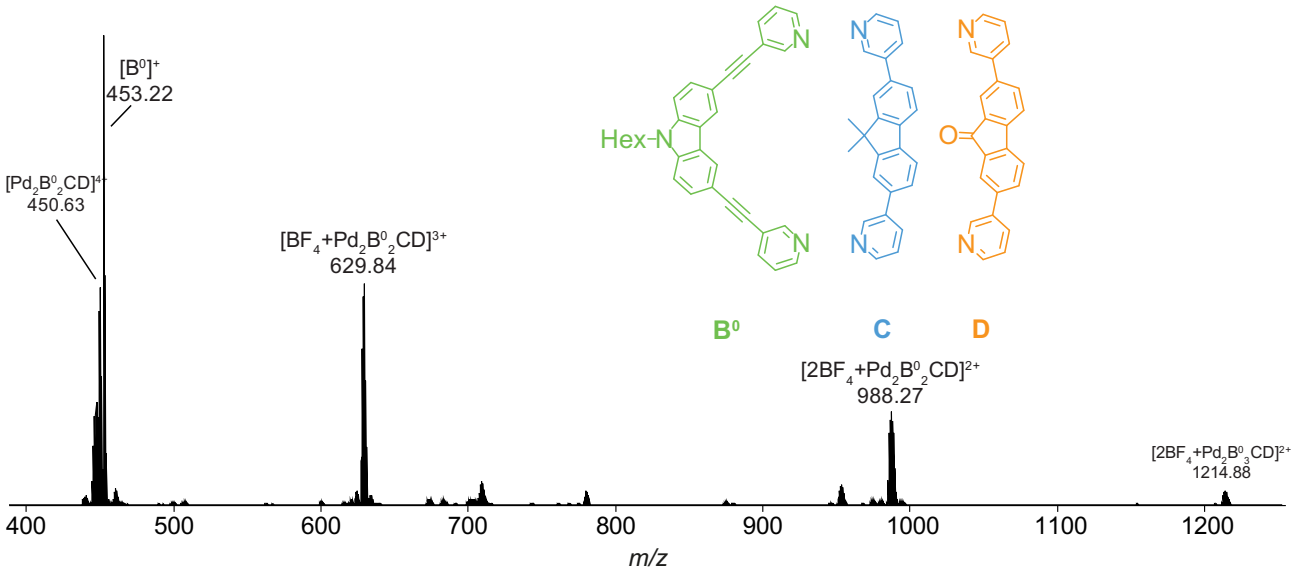

Supplementary Figure 105 | HR-ESI mass spectrum of heteroleptic cage $Pd_2\mathbf{B^0}_2\mathbf{CD}$.

3.4.3. Self-assembly of heteroleptic cage $Pd_2AB^0C_2$

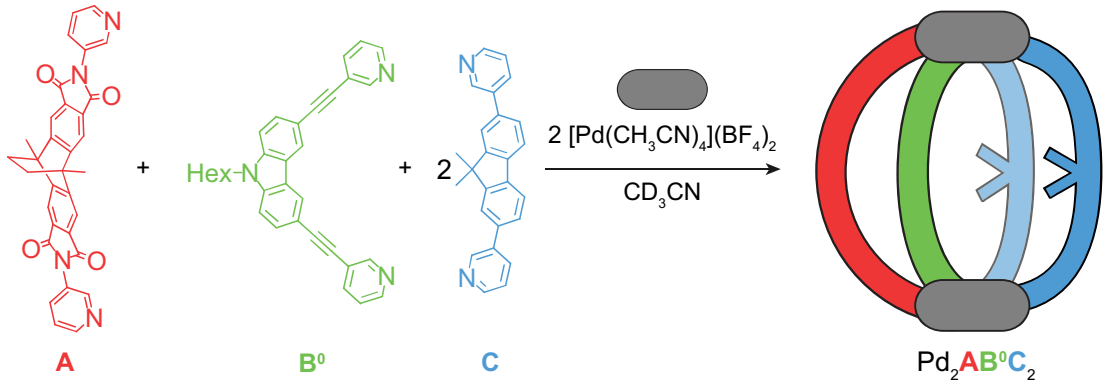

To a solution of **A** (60 µL, 3 mM, 0.18 µmol), **B^0** (60 µL, 3 mM, 0.18 µmol), **C** (120 µL, 3 mM, 0.36 µmol) was added a stock solution of $[Pd(CH_3CN)_4](BF_4)_2$ (24 µL, 15 mM/CD_3CN, 0.36 µmol) and additional 186 µL CD_3CN. The mixture was heated at 80 °C for 8 h to give a 0.4 mM cage solution with Pd_2**AB^0C_2** as predominant species and some impurities.

^{13}C NMR (151 MHz, 298 K, CD_3CN) δ 173.08, 167.34, 166.99, 156.85, 156.34, 156.16, 155.09, 154.94, 153.51, 150.87, 150.73, 150.69, 150.59, 150.32, 150.21, 150.08, 149.82, 149.77, 149.31, 144.07, 143.77, 142.47, 142.27, 140.90, 140.23, 140.02, 139.99, 139.43, 138.12, 135.85, 132.26, 132.10, 130.87, 130.75, 129.50, 128.44, 128.39, 128.20, 124.41, 122.91, 122.70, 122.66, 122.60, 117.56, 112.66, 111.37, 97.90, 83.18, 63.81, 48.62, 47.21, 45.60, 45.44, 45.35, 45.14, 45.09, 44.00, 34.69, 32.13, 30.37, 27.31, 23.86, 23.19.

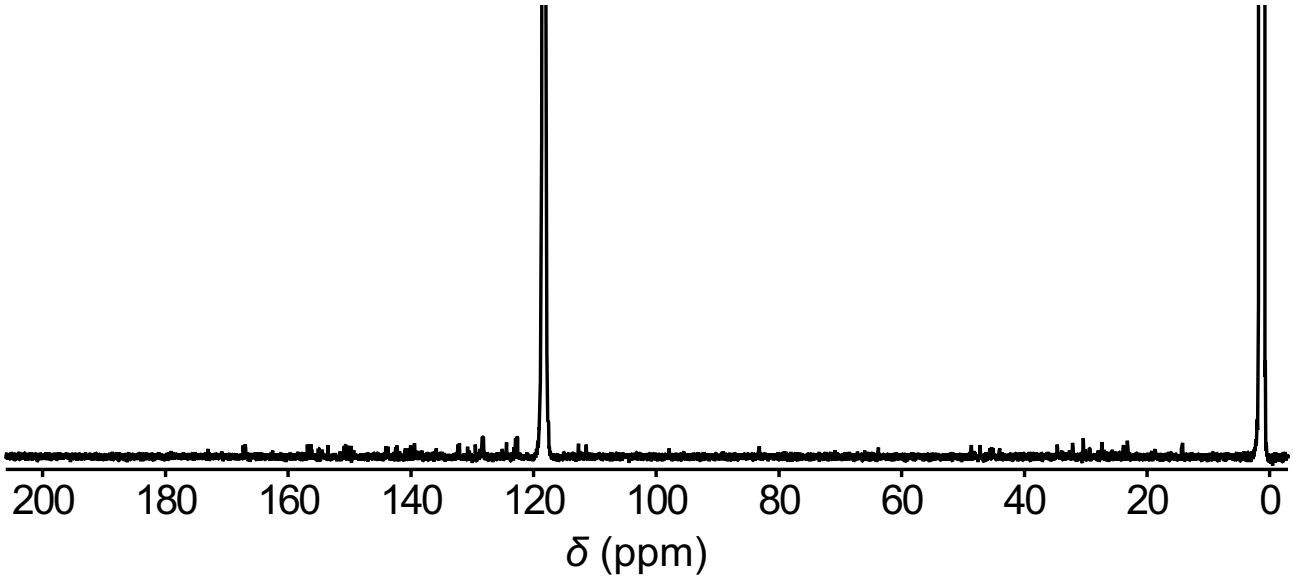

Supplementary Figure 106 | ^{13}C NMR spectrum (176 MHz, 298 K, CD_3CN) of heteroleptic cage Pd_2**AB^0C_2**. The ^{13}C signals are quite weak, even using long measurement time, thus less than expected number of signals were observed.

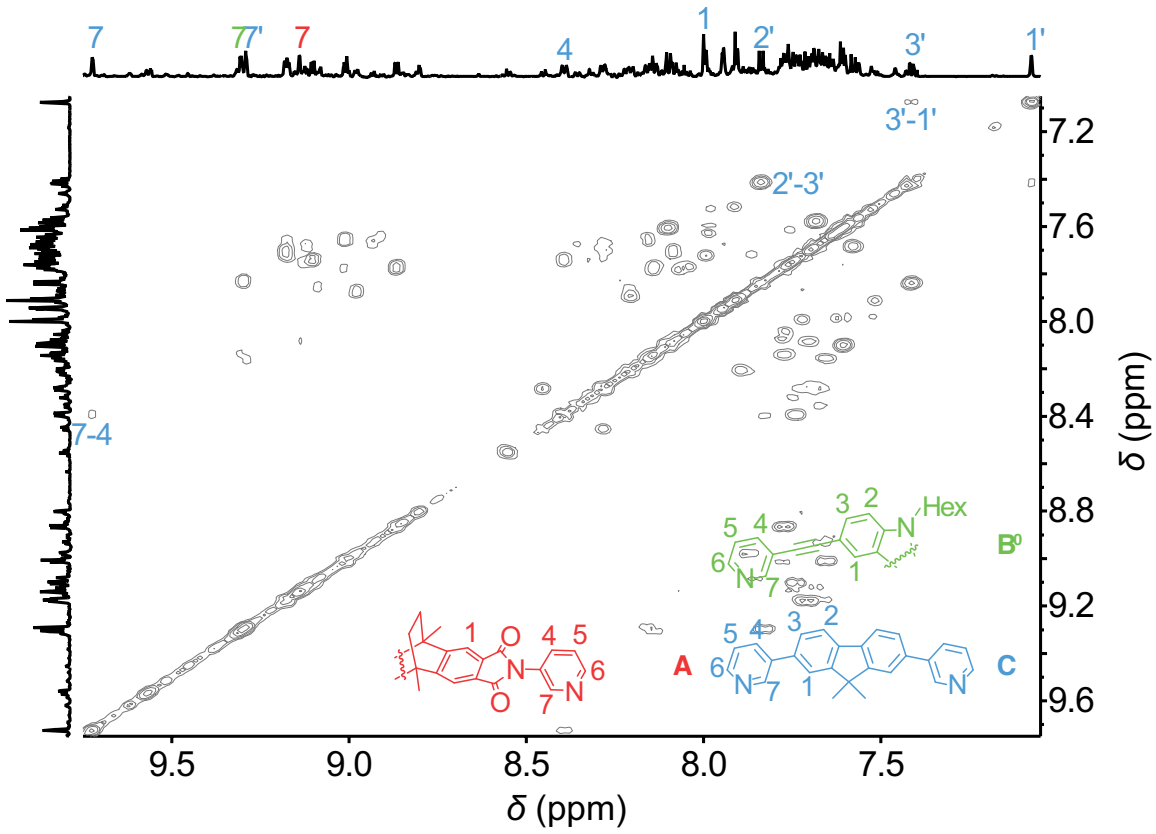

Supplementary Figure 107 | Partial ^{1}H–^{1}H COSY spectrum (500 MHz, 298 K, CD_3CN) of heteroleptic cage Pd_2**AB^{0}C**$_2$. The formation of heteroleptic cage Pd_2**AB^{0}C**$_2$ was not exclusive, resulting in a complicated NMR with some impurity, thus only some key protons are assigned.

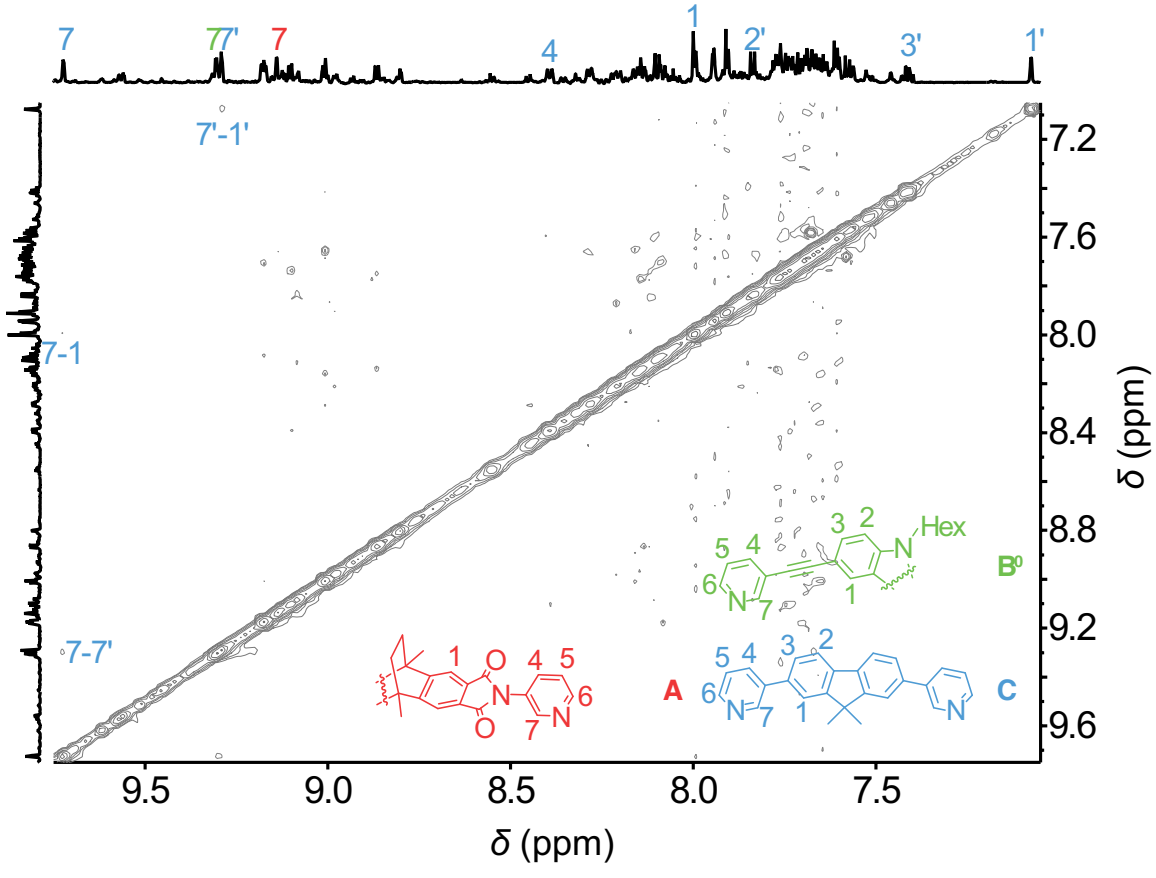

Supplementary Figure 108 | Partial ^{1}H–^{1}H NOESY spectrum (500 MHz, 298 K, CD_3CN) of heteroleptic cage Pd_2**AB^{0}C**$_2$.

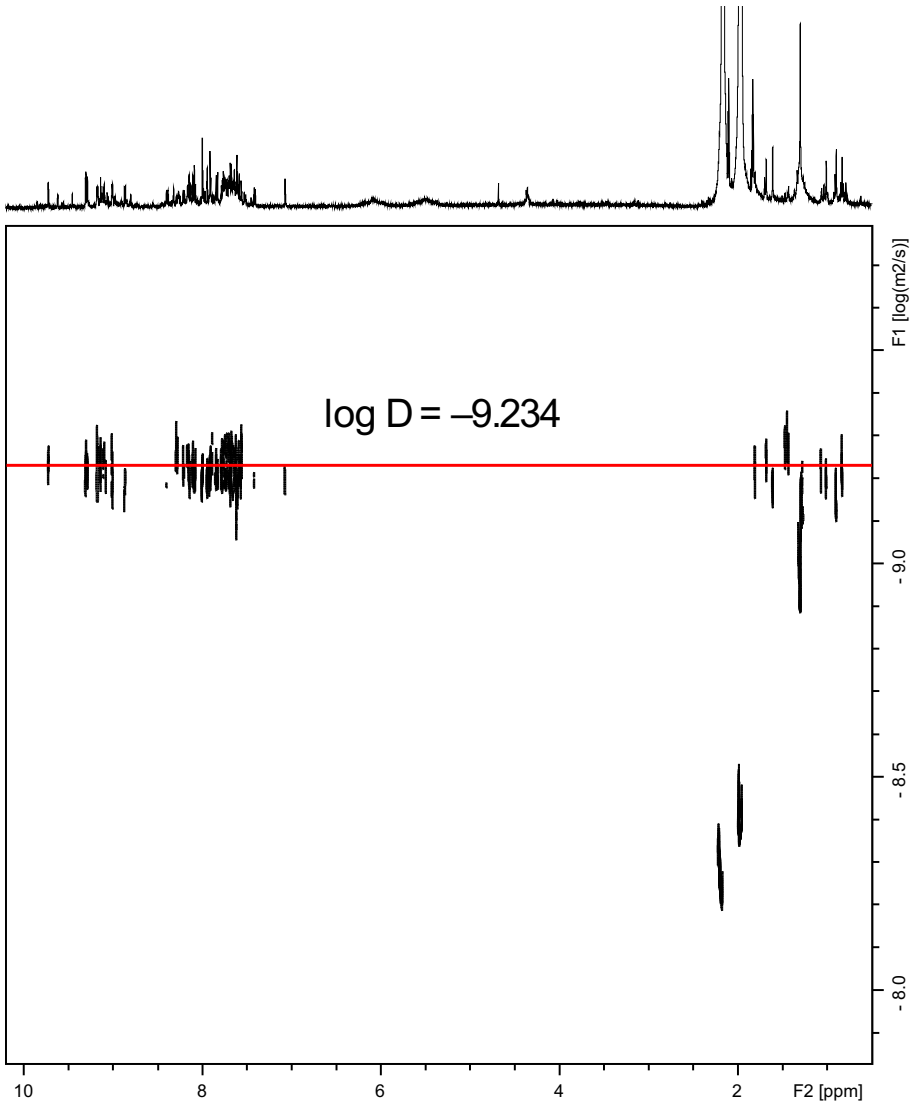

Supplementary Figure 109 | ^{1}H DOSY spectrum (500 MHz, 298 K, CD_3CN) of heteroleptic cage $Pd_2\mathbf{AB^0}_2\mathbf{C}_2$. Diffusion coefficient for $Pd_2\mathbf{AB^0}_2\mathbf{C}_2$: D = 5.834 × 10^{-10} m^2s^{-1}, log *D* = –9.234, r = 11.2 Å.

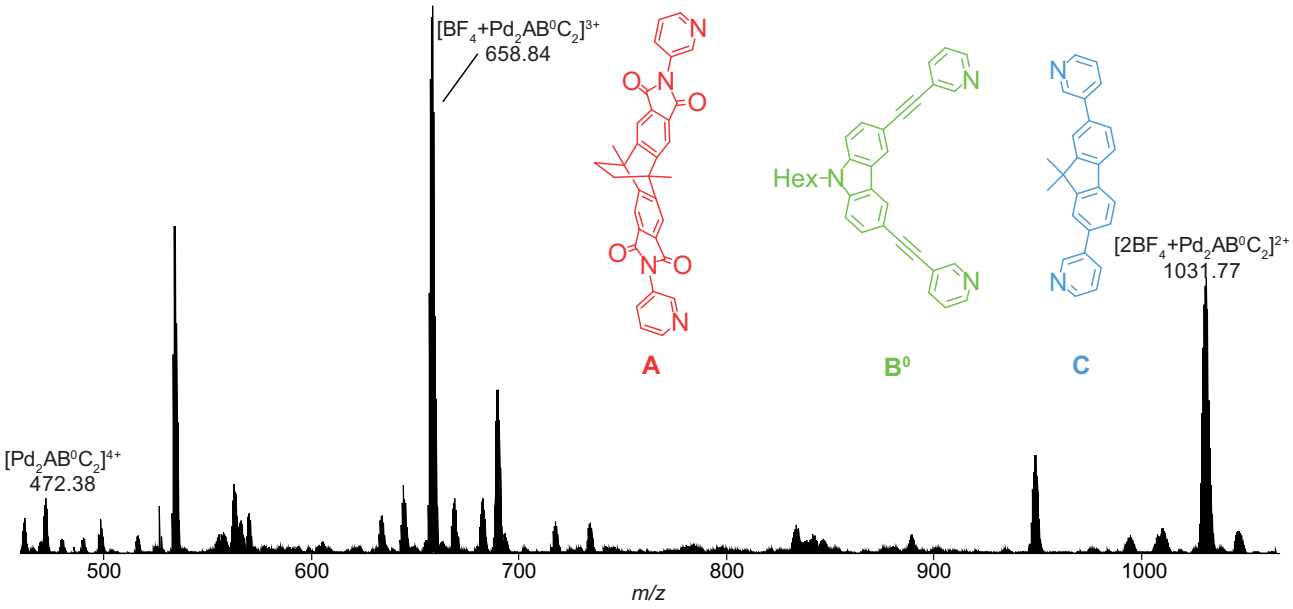

Supplementary Figure 110 | HR-ESI mass spectrum of heteroleptic cage $Pd_2\mathbf{AB^0}\mathbf{C}_2$.

3.4.4. Self-assembly of heteroleptic cage $Pd_2AB^0D_2$

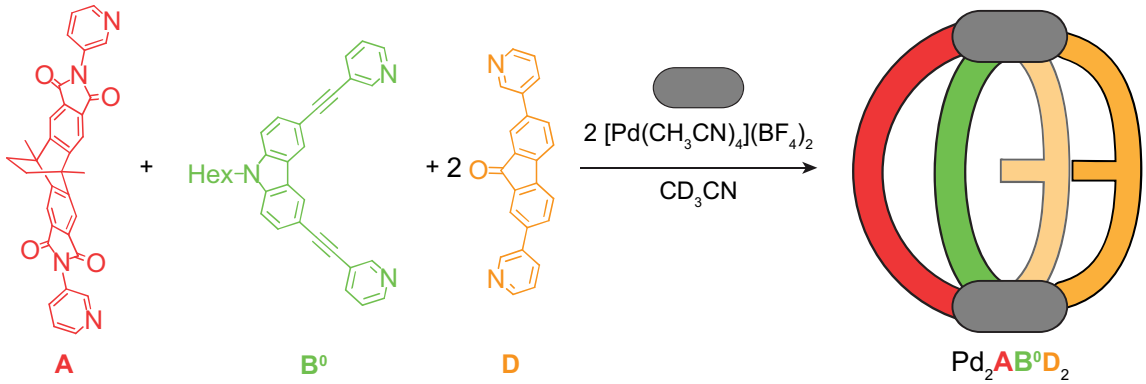

To a solution of **A** (60 µL, 3 mM, 0.18 µmol), **B⁰** (60 µL, 3 mM, 0.18 µmol), **D** (120 µL, 3 mM, 0.36 µmol) was added a stock solution of $[Pd(CH_3CN)_4](BF_4)_2$ (24 µL, 15 mM/CD_3CN, 0.36 µmol) and additional 186 µL CD_3CN. The mixture was heated at 80 °C for 8 h to give a 0.4 mM cage solution containing the shown cage as predominant species.

^{1}H NMR (700 MHz, 298 K, CD_3CN) δ 9.83 – 9.81 (m, 2H), 9.68 (d, J = 2.1 Hz, 2H), 9.34 (t, J = 2.7 Hz, 2H), 9.33 – 9.30 (m, 2H), 9.12 (d, J = 5.7 Hz, 2H), 8.96 (dd, J = 6.0, 2.6 Hz, 4H), 8.81 (d, J = 5.9 Hz, 2H), 8.39 – 8.36 (m, 2H), 8.34 (d, J = 7.6 Hz, 2H), 8.20 – 8.16 (m, 2H), 8.16 – 8.10 (m, 4H), 7.87 (d, J = 7.5 Hz, 2H), 7.82 – 7.80 (m, 2H), 7.79 – 7.71 (m, 14H), 7.68 (dd, J = 7.9, 5.7 Hz, 4H), 7.63 (q, J = 8.2, 7.4 Hz, 6H), 4.37 (t, J = 7.2 Hz, 2H), 2.01 (s, 3H), 1.88 (s, 3H), 1.82 (m, 4H), 1.23 (m, 4H), 0.81 (t, J = 7.1 Hz, 3H).

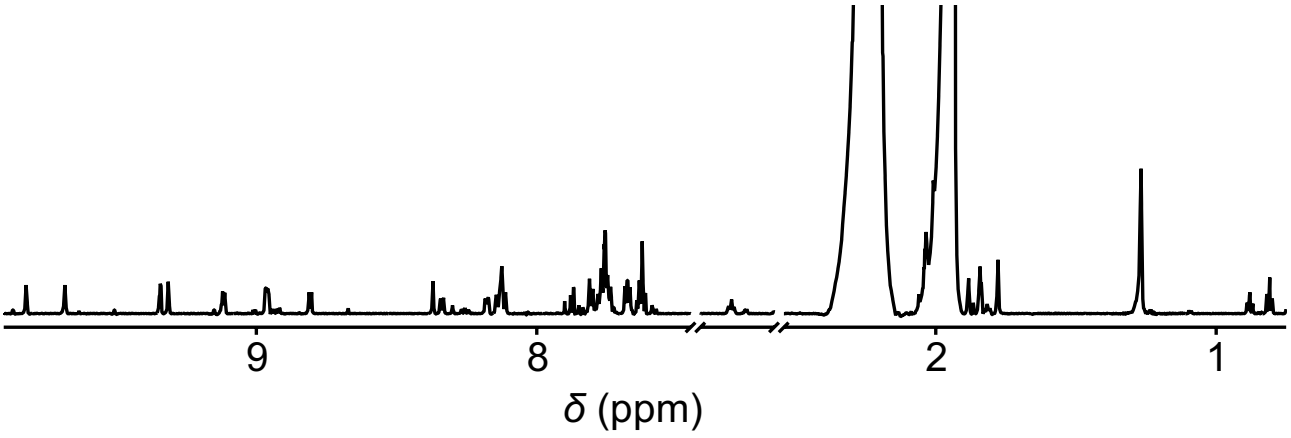

Supplementary Figure 111 | ^{1}H NMR spectrum (700 MHz, 298 K, CD_3CN) of heteroleptic cage $Pd_2AB^0D_2$.

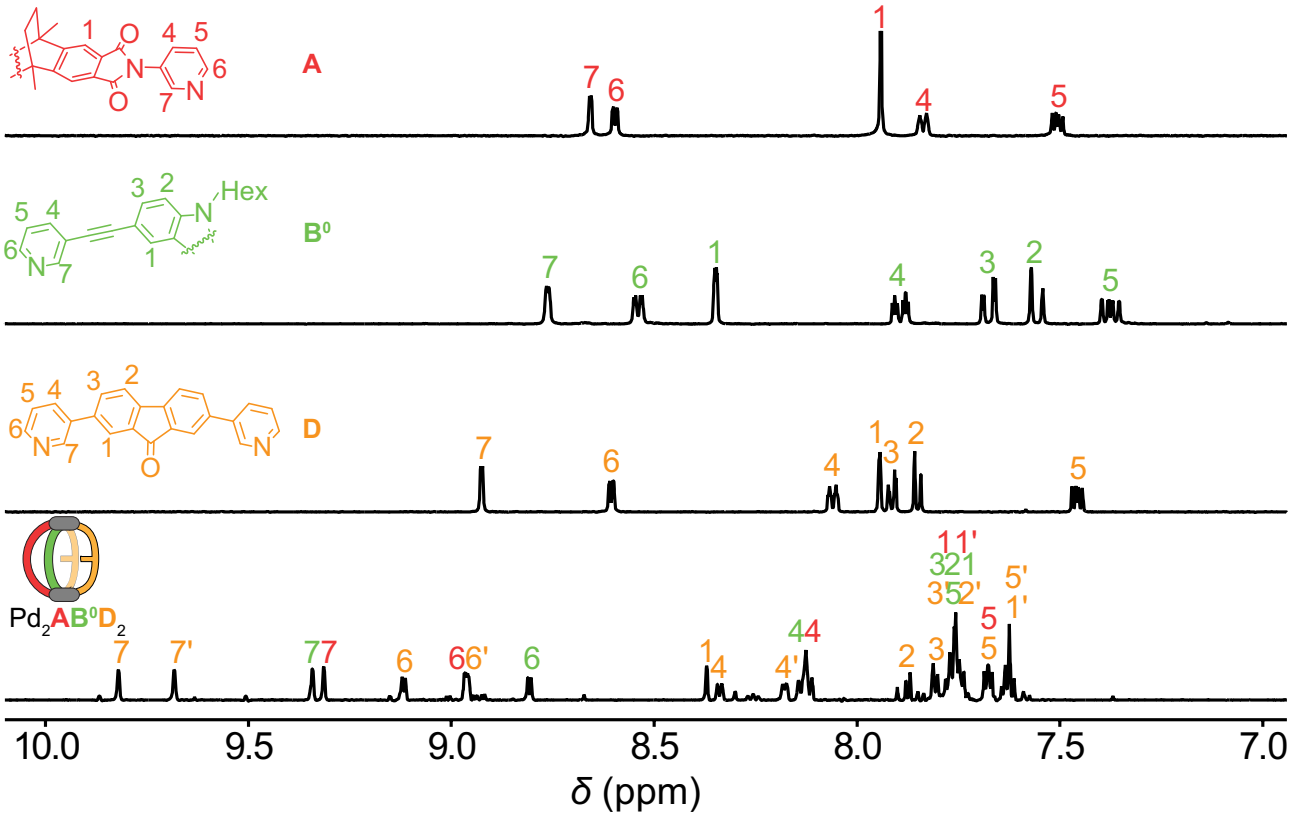

Supplementary Figure 112 | Partial ^{1}H NMR spectrum (700 MHz, 298 K, CD_3CN) comparison of ligands **A** (red), **B^0** (pale green), **D** (yellow), heteroleptic cage Pd_2**AB^{0}D**$_2$.

^{13}C NMR (151 MHz, 298 K, CD_3CN) δ 192.21, 192.00, 172.99, 167.36, 166.99, 154.66, 154.58, 153.89, 151.39, 150.93, 150.68, 150.32, 150.16, 150.01, 145.85, 145.30, 144.81, 144.76, 142.10, 141.84, 140.30, 139.20, 138.91, 138.58, 137.56, 137.52, 137.27, 136.45, 136.32, 135.55, 135.53, 135.22, 131.90, 130.67, 130.61, 128.84, 128.56, 128.45, 128.37, 125.24, 124.28, 124.17, 123.51, 123.41, 122.91, 117.78, 110.81, 95.38, 87.64, 45.35, 45.08, 34.42, 32.64, 30.37, 30.19, 30.07, 25.68, 23.39, 18.72, 18.42, 14.38.

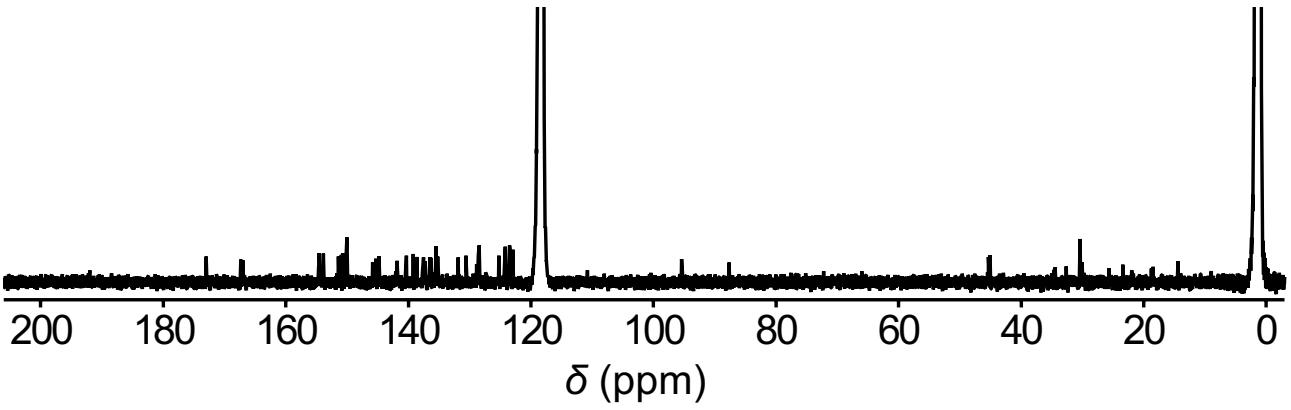

Supplementary Figure 113 | ^{13}C NMR spectrum (176 MHz, 298 K, CD_3CN) of heteroleptic cage Pd_2**AB^{0}D**$_2$.

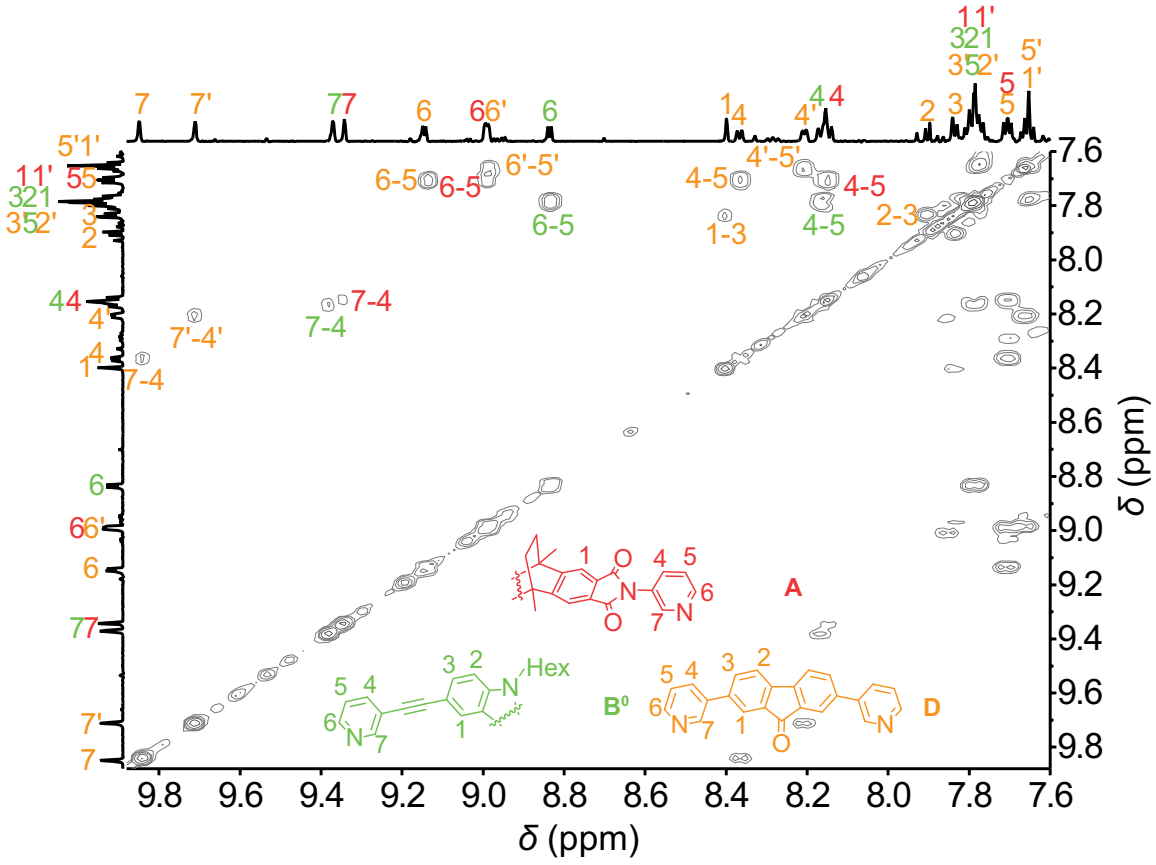

Supplementary Figure 114 | Partial ^{1}H–^{1}H COSY spectrum (500 MHz, 298 K, CD_3CN) of heteroleptic cage Pd_2**AB⁰D**$_2$.

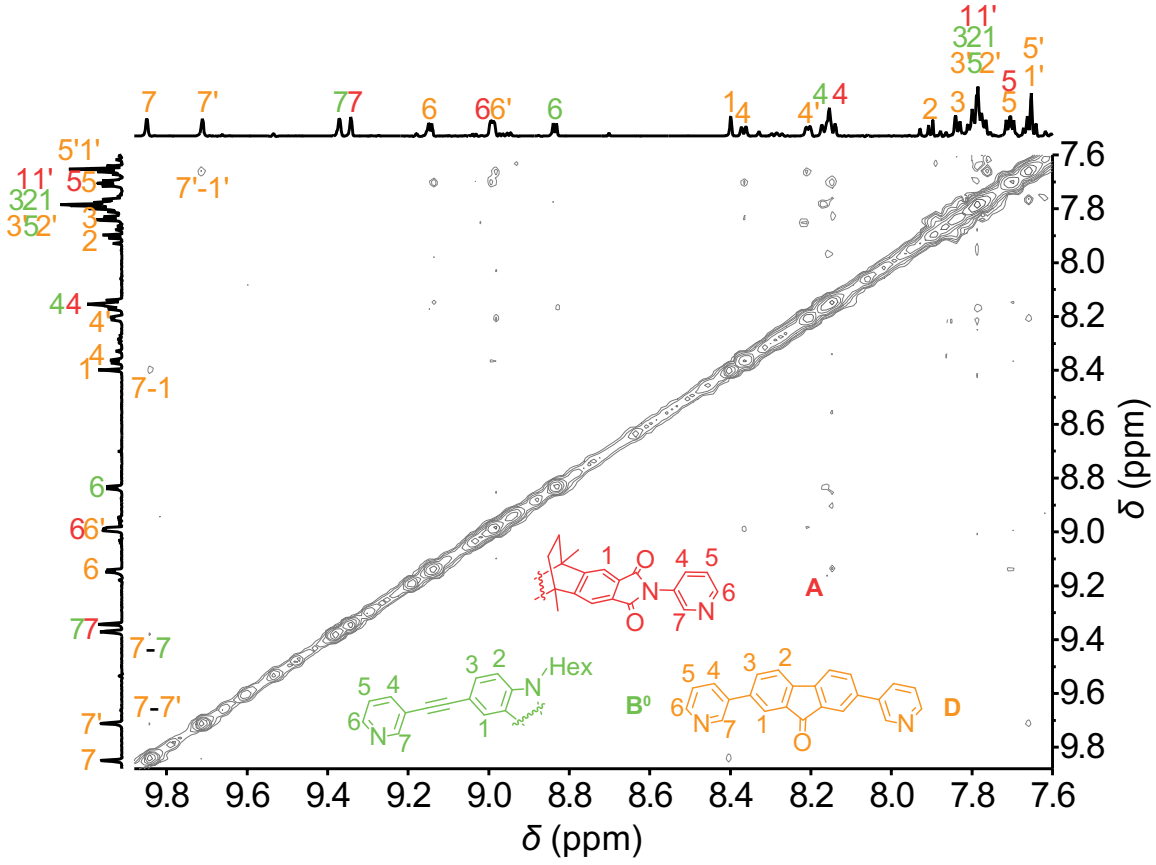

Supplementary Figure 115 | Partial ^{1}H–^{1}H NOESY spectrum (500 MHz, 298 K, CD_3CN) of heteroleptic cage Pd_2**AB⁰D**$_2$.

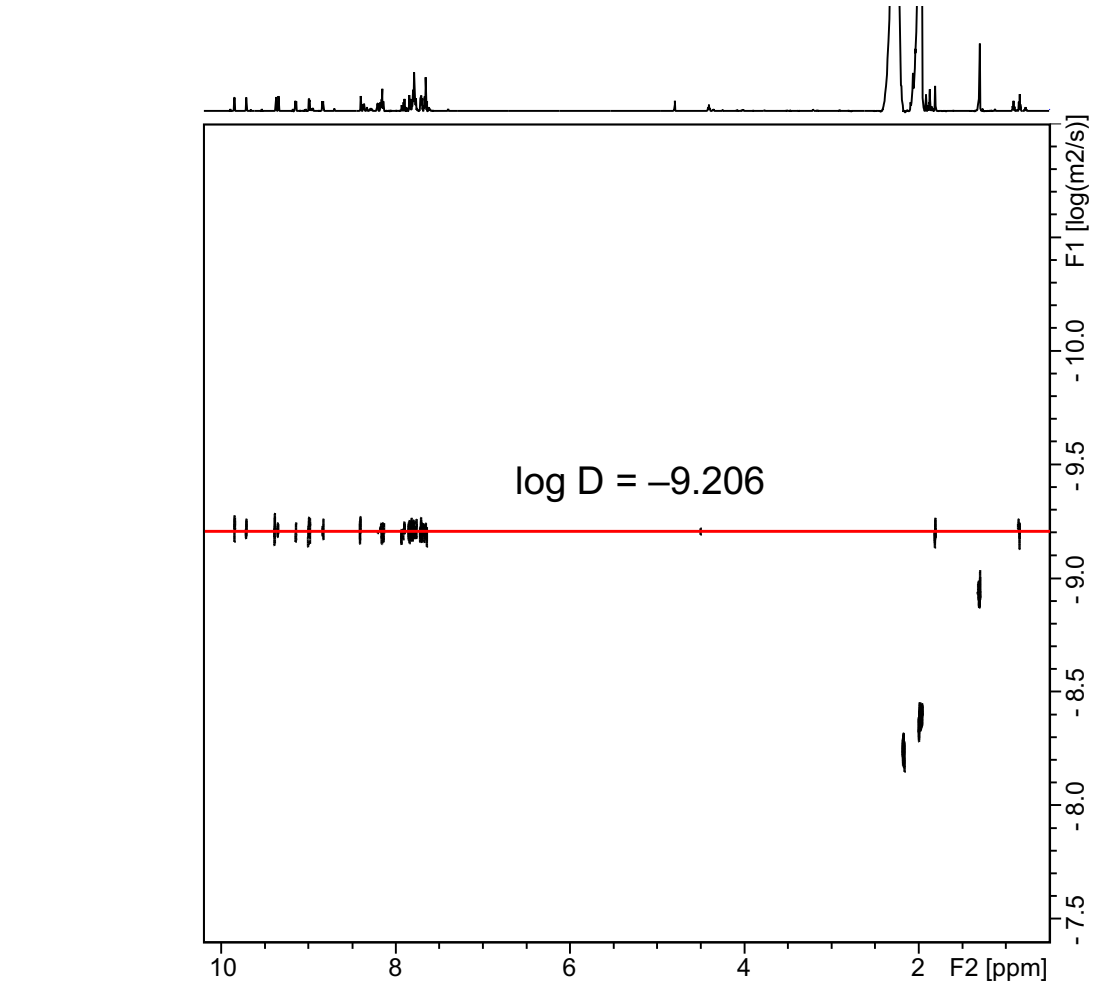

Supplementary Figure 116 | ^{1}H DOSY spectrum (500 MHz, 298 K, CD_3CN) of heteroleptic cage Pd_2**AB^{0}D**$_2$. Diffusion coefficient for Pd_2**AB^{0}D**$_2$: D = 6.223 × 10^{-10} m^2s^{-1}, log *D* = −9.206, r = 10.5 Å.

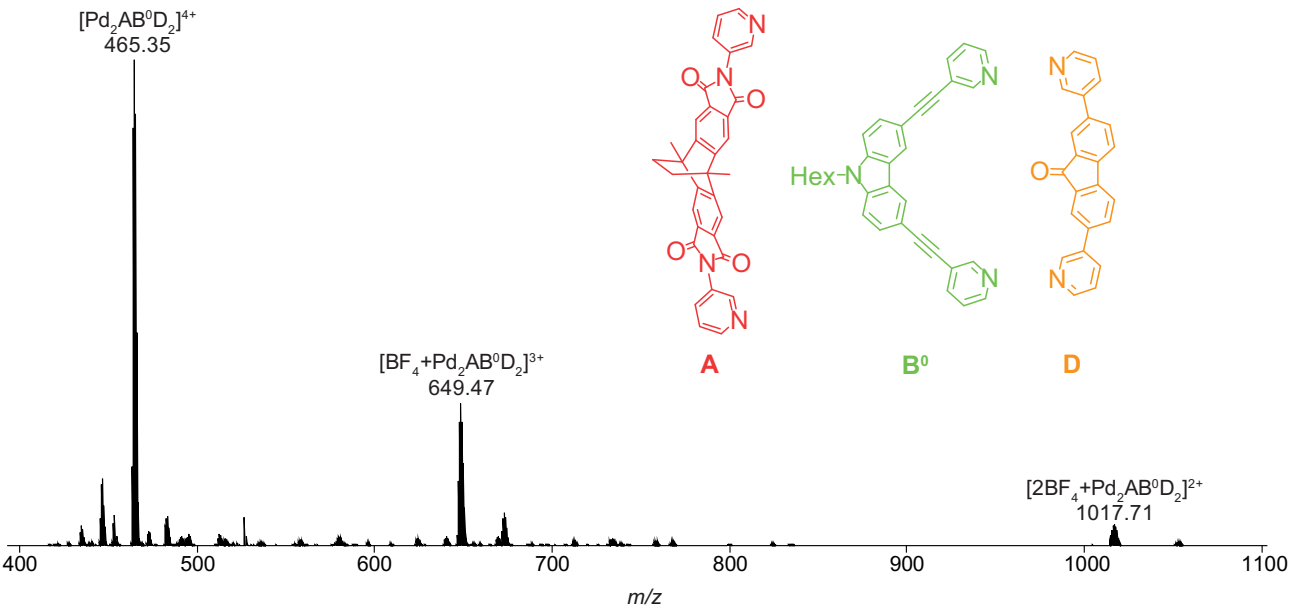

Supplementary Figure 117 | HR-ESI mass spectrum of heteroleptic cage Pd_2**AB^{0}D**$_2$.

3.4.5. Self-assembly of heteroleptic cage Pd_2AB^0CD

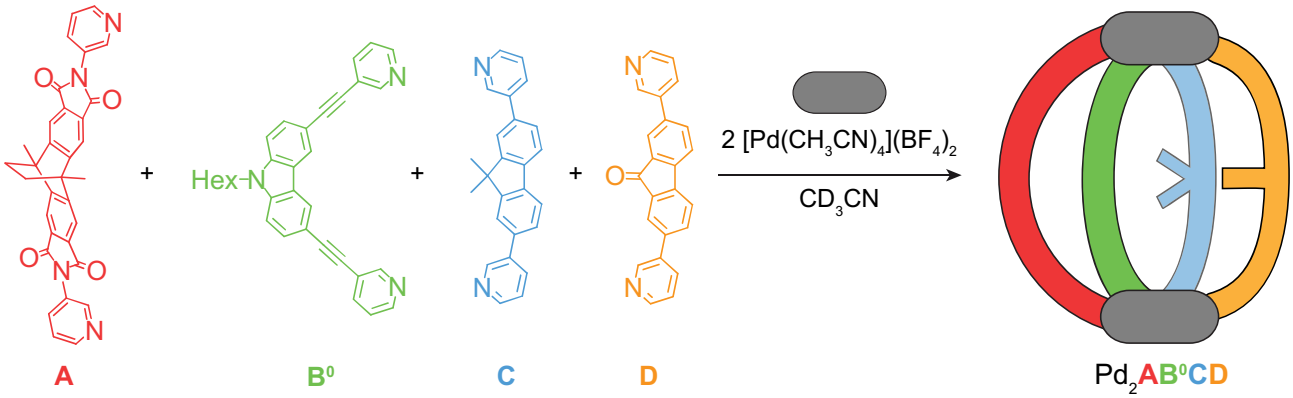

To a solution of **A** (60 µL, 3 mM, 0.18 µmol), **B⁰** (60 µL, 3 mM, 0.18 µmol), **C** (60 µL, 3 mM, 0.18 µmol) and a suspension of **D** (60 µL, 3 mM, 0.18 µmol) was added a stock solution of $[Pd(CH_3CN)_4](BF_4)_2$ (24 µL, 15 mM/CD_3CN, 0.36 µmol) and additional 186 µL CD_3CN. The mixture was heated at 80 °C for 8 h to give a 0.4 mM cage solution containing the shown cage as predominant species.

^{1}H NMR (700 MHz, 298 K, CD_3CN) δ 9.87 (d, *J* = 2.0 Hz, 2H), 9.45 (d, *J* = 2.1 Hz, 2H), 9.40 (d, *J* = 2.2 Hz, 2H), 9.22 (d, *J* = 1.8 Hz, 2H), 9.13 (dd, *J* = 5.8, 1.3 Hz, 2H), 9.06 – 9.04 (m, 2H), 8.95 (dd, *J* = 6.0, 1.2 Hz, 2H), 8.74 (dd, *J* = 6.0, 1.3 Hz, 2H), 8.53 (d, *J* = 1.8 Hz, 2H), 8.41 – 8.38 (m, 2H), 8.17 – 8.13 (m, 4H), 8.07 (dt, *J* = 8.0, 1.6 Hz, 2H), 8.01 – 7.98 (m, 4H), 7.89 – 7.87 (m, 2H), 7.84 (d, *J* = 7.6 Hz, 2H), 7.82 (s, 2H), 7.80 (s, 2H), 7.76 – 7.71 (m, 4H), 7.69 – 7.66 (m, 4H), 7.64 – 7.61 (m, 2H), 7.58 – 7.55 (m, 2H), 7.47 (dd, *J* = 7.7, 1.8 Hz, 2H), 7.12 (d, *J* = 1.8 Hz, 2H), 4.34 (t, *J* = 7.2 Hz, 2H), 1.98 (s, 3H), 1.97 (s, 3H), 1.80 – 1.76 (m, 6H), 1.38 (s, 3H), 1.23 (m, 6H), 0.80 (t, *J* = 7.1 Hz, 3H), 0.55 (s, 3H).

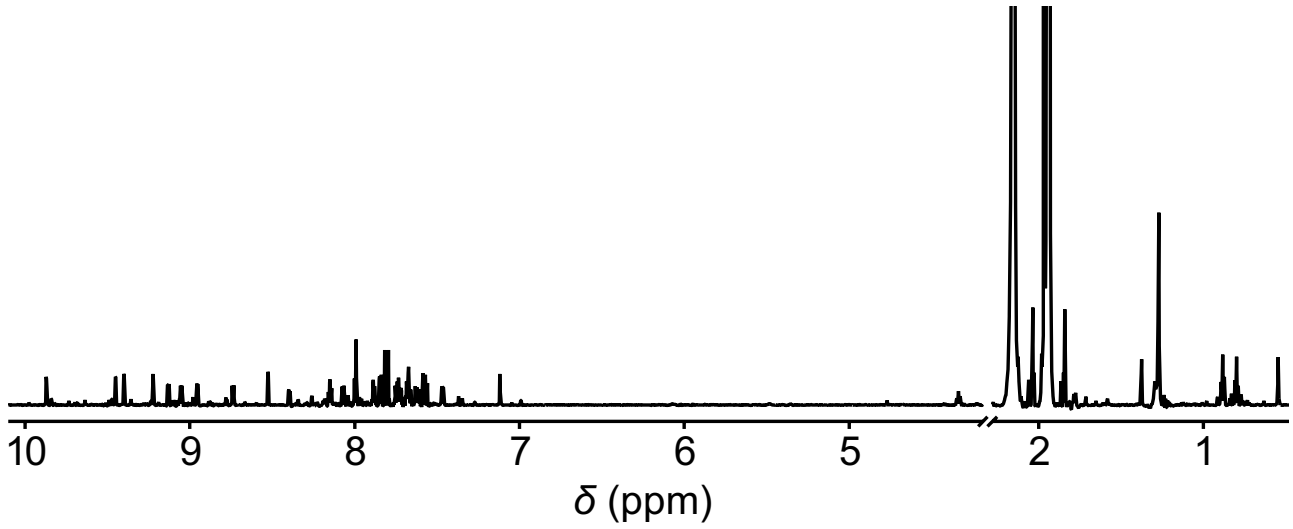

Supplementary Figure 118 | ^{1}H NMR spectrum (700 MHz, 298 K, CD_3CN) of heteroleptic cage Pd_2AB^0CD.

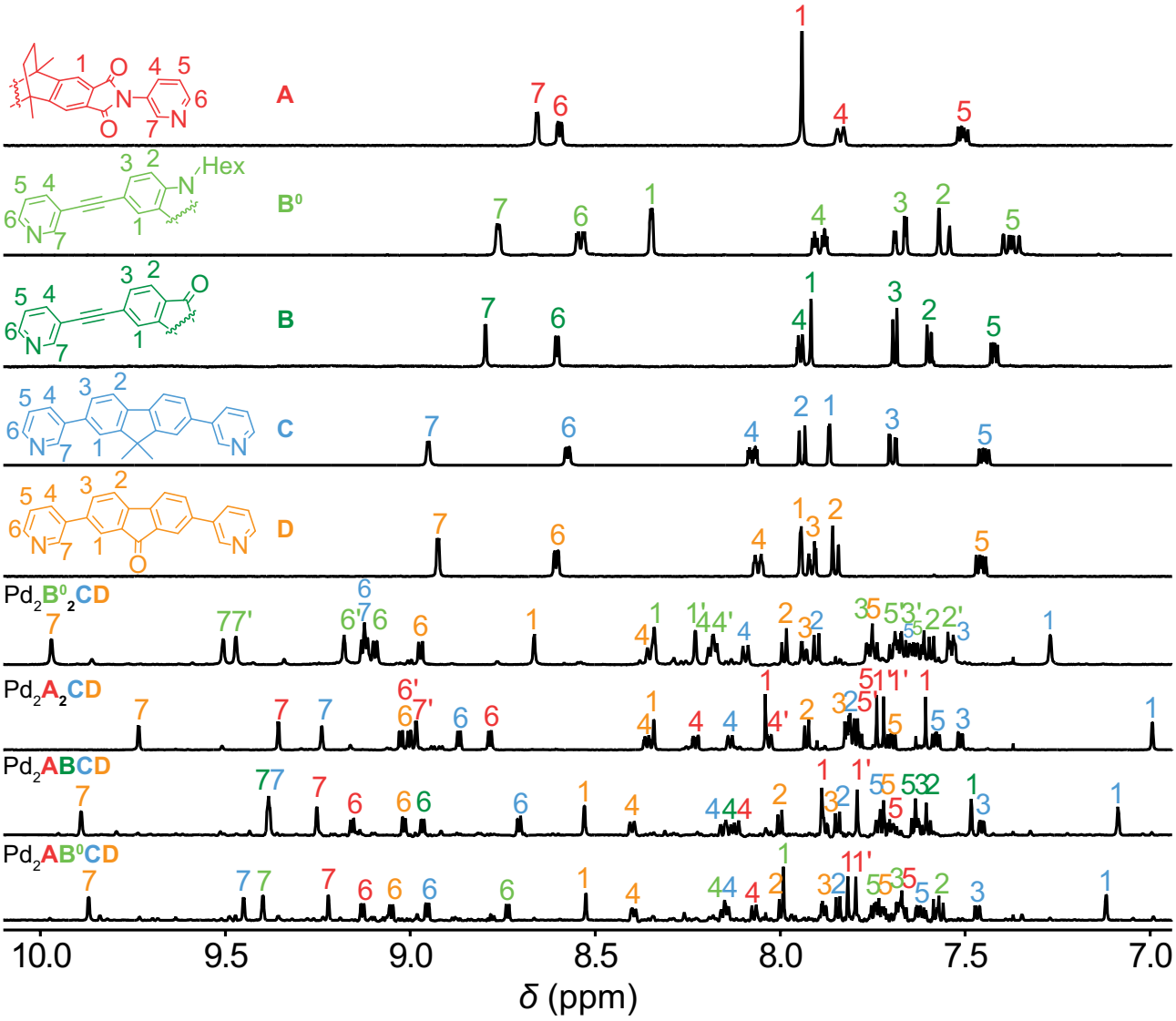

Supplementary Figure 119 | Partial ^{1}H NMR spectrum (700 MHz, 298 K, CD_3CN) comparison of ligands **A** (red), **B^0** (green), **B** (deep green), **C** (blue), **D** (yellow), and heteroleptic cages Pd_2**B$^0_2$CD**, Pd_2**A$_2$CD**, Pd_2**ABCD** and Pd_2**AB^{0}CD**.

^{13}C NMR (176 MHz, 298 K, CD_3CN) δ 192.93, 173.04, 167.62, 166.97, 156.10, 155.93, 154.69, 154.63, 153.38, 151.24, 150.44, 150.35, 150.23, 150.02, 149.81, 145.98, 143.83, 142.30, 142.23, 142.07, 140.27, 139.64, 139.13, 138.50, 138.39, 137.28, 136.68, 135.68, 132.32, 131.88, 130.69, 130.60, 128.43, 127.93, 125.80, 125.30, 124.82, 124.26, 123.47, 123.04, 122.70, 112.81, 111.44, 98.03, 83.26, 70.82, 66.02, 63.83, 46.90, 45.37, 45.07, 34.70, 32.65, 32.14, 30.37, 27.34, 26.24, 25.69, 23.40, 23.19, 14.39, 14.19.

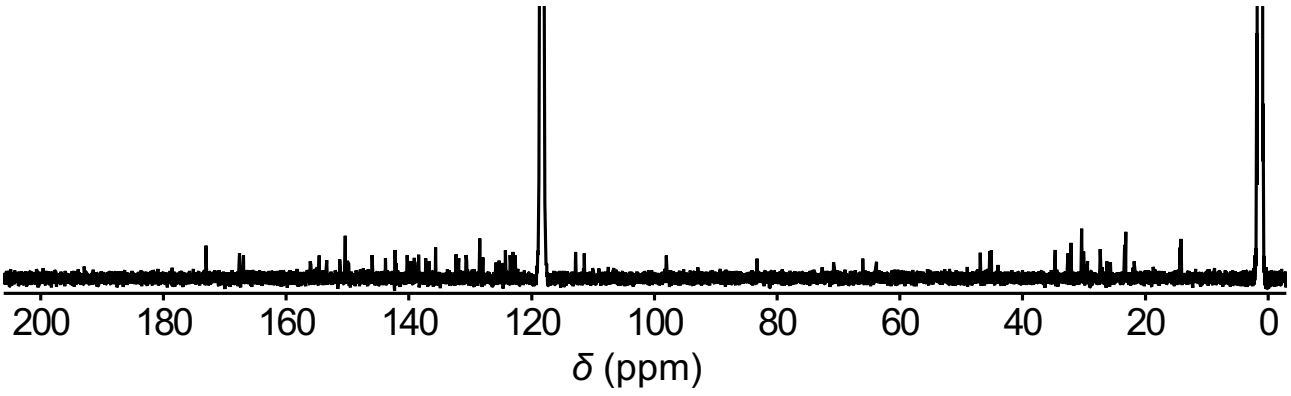

Supplementary Figure 120 | ^{13}C NMR spectrum (176 MHz, 298 K, CD_3CN) of heteroleptic cage Pd_2**AB^{0}CD**.

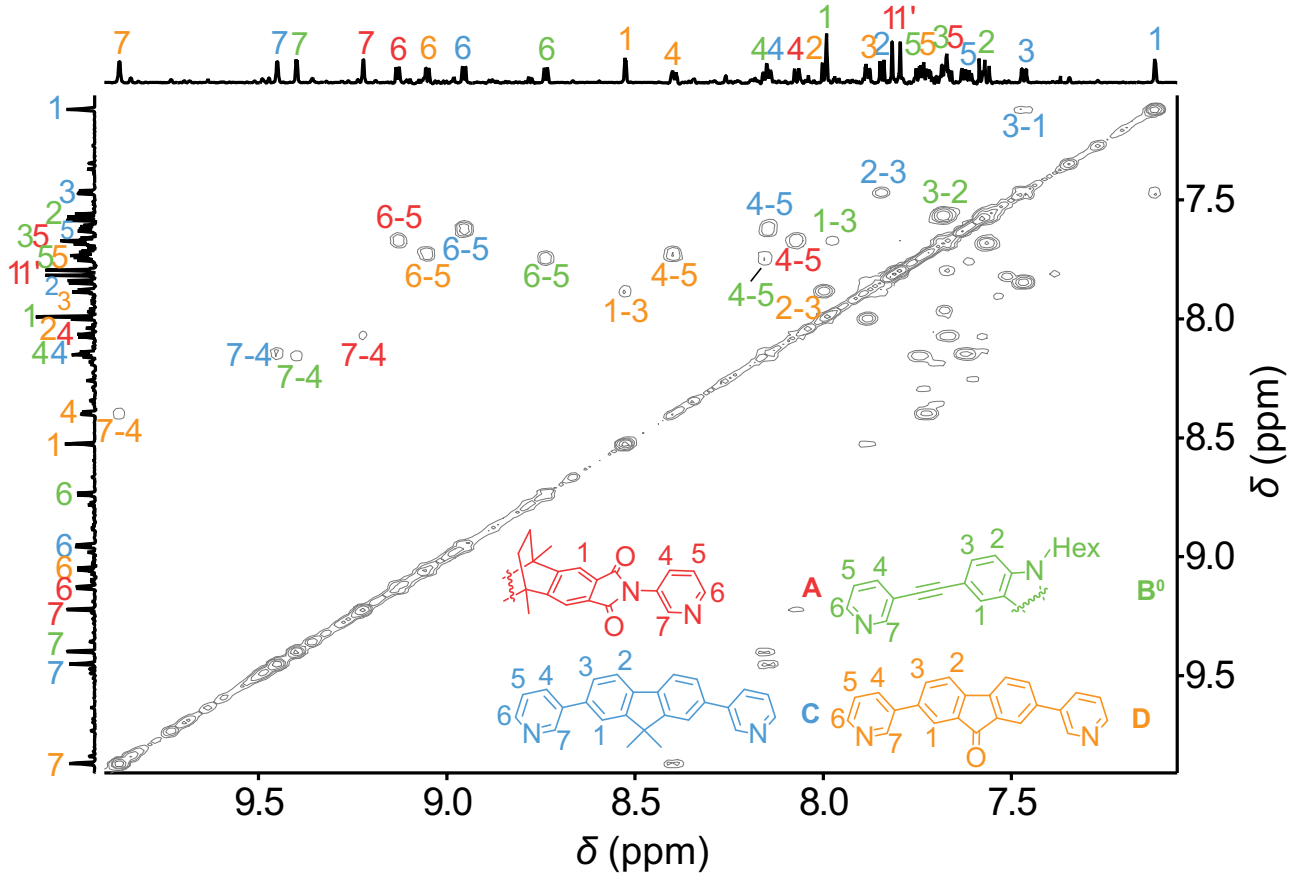

Supplementary Figure 121 | Partial ^{1}H–^{1}H COSY spectrum (500 MHz, 298 K, CD_3CN) of heteroleptic cage Pd_2**AB^{0}CD**.

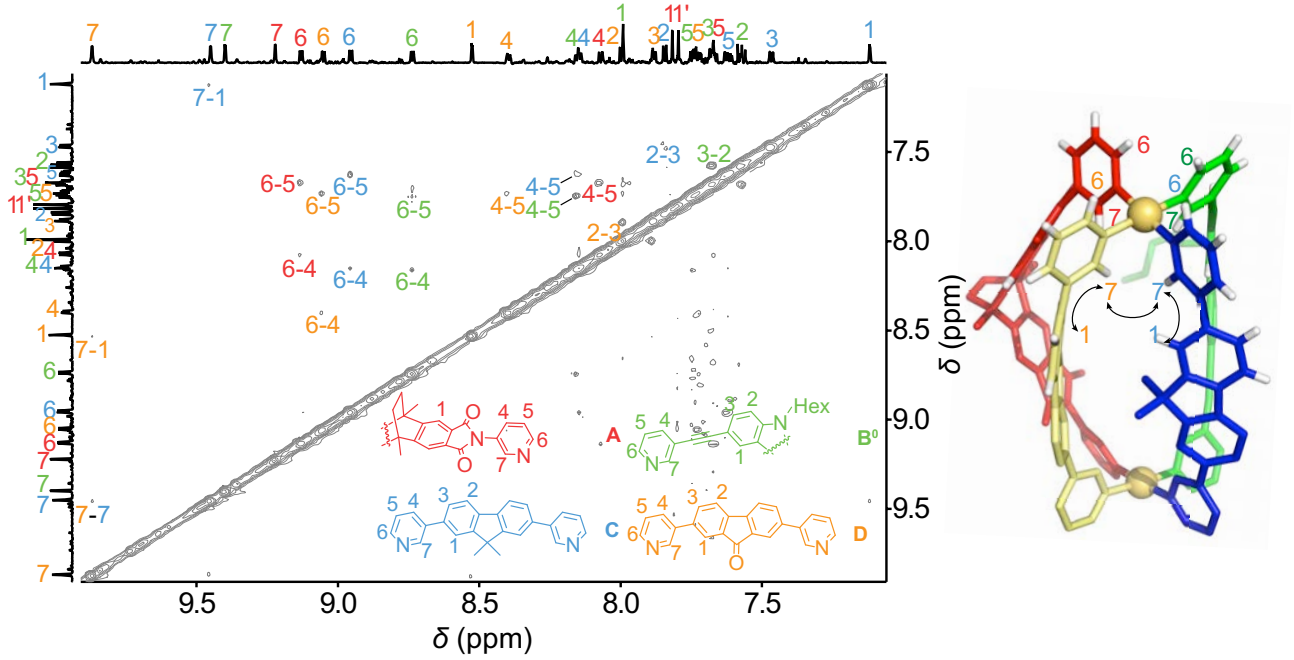

Supplementary Figure 122 | Partial ^{1}H–^{1}H NOESY spectrum (500 MHz, 298 K, CD_3CN) of heteroleptic cage Pd_2**AB^{0}CD**. The composition of this heteroleptic cage is supported by a single crystal X-ray structure (details see below). The found NOE contacts in solution are in full accordance with the X-ray structure results.

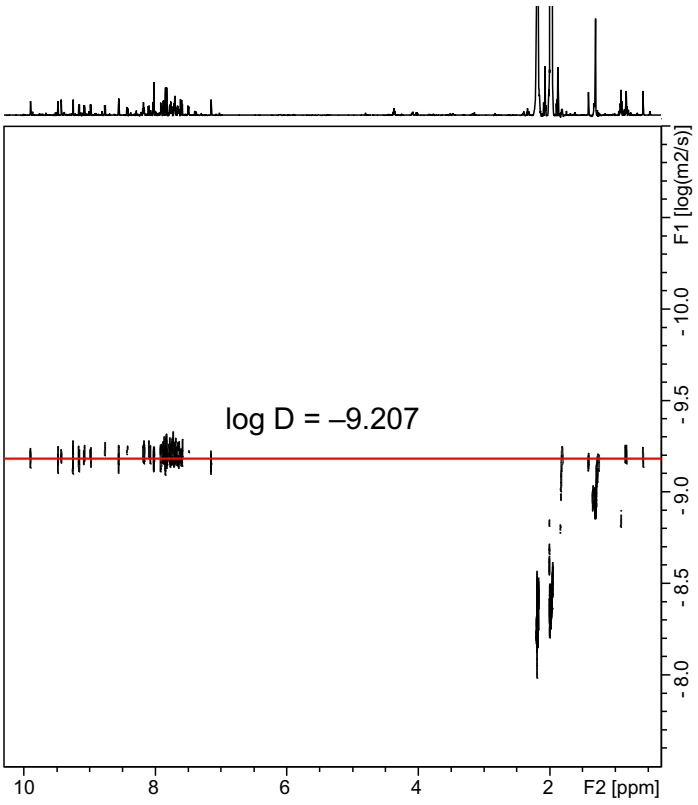

Supplementary Figure 123 | ^{1}H DOSY spectrum (500 MHz, 298 K, CD_3CN) of heteroleptic cage Pd_2**AB^{0}CD**. Diffusion coefficient for Pd_2**AB^{0}CD**: D = 6.209 × 10^{-10} m^2s^{-1}, log *D* = −9.207, r = 10.5 Å.

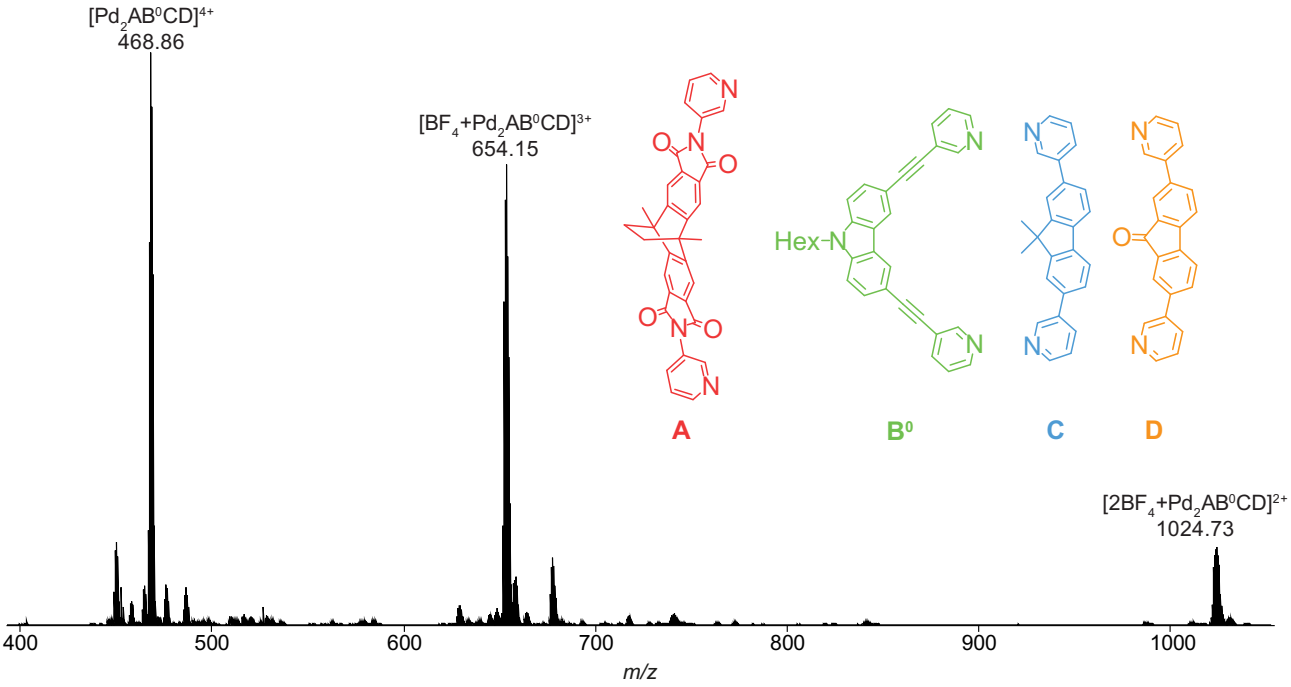

Supplementary Figure 124 | HR-ESI mass spectrum of heteroleptic cage Pd_2**AB^{0}CD**.

3.5. Modulation of interligand C-H···π interactions in heteroleptic cages

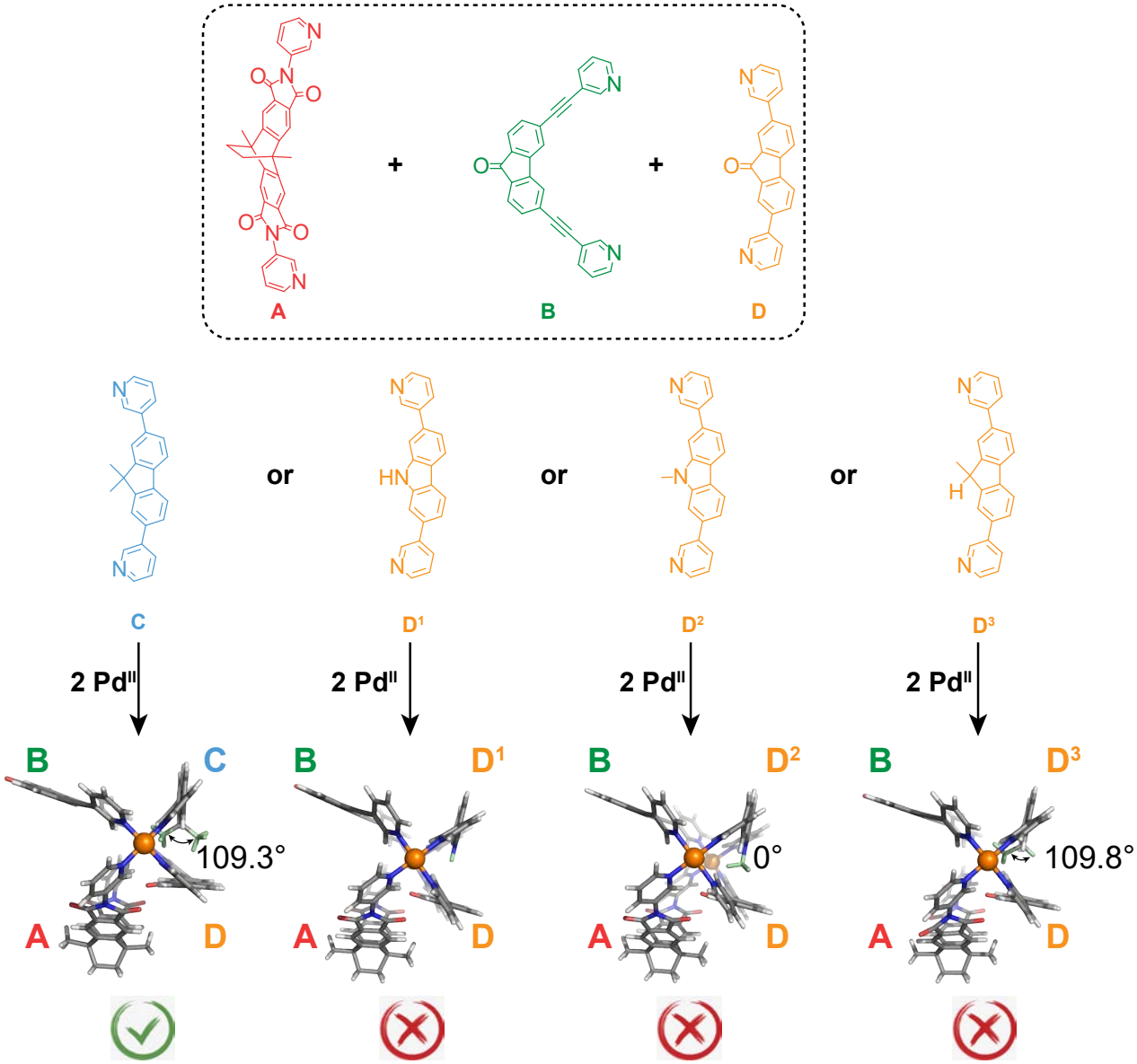

Supplementary Figure 125 | PM6 optimized models (X-ray crystal structure in the case of Pd_2**ABCD)** showing the modulation of interligand C-H···π interactions by keeping ligands **A**, **B** and **D** the same but only modifying the dimethyl motif of ligand **C**, i.e. using ligands **D**^{1}, **D**^{2}, **D**^{3} to replace ligand **C**. Self-assembly control experiments shown in the following confirmed that only the ligand combination **A**, **B**, **C** plus **D** results in the selective and exclusive formation of one species in solution, corroborating that both of the methyl groups on ligand **C** are crucial to the integrative self-sorting yielding cage Pd_2**ABCD** as a single, thermodynamic product. Note, however, that while a single crystal X-ray structure of the third cage (Pd_2**ABD**^{2}**D**) could be obtained (see below), this ligand combination does not lead to clean self-sorting in solution.

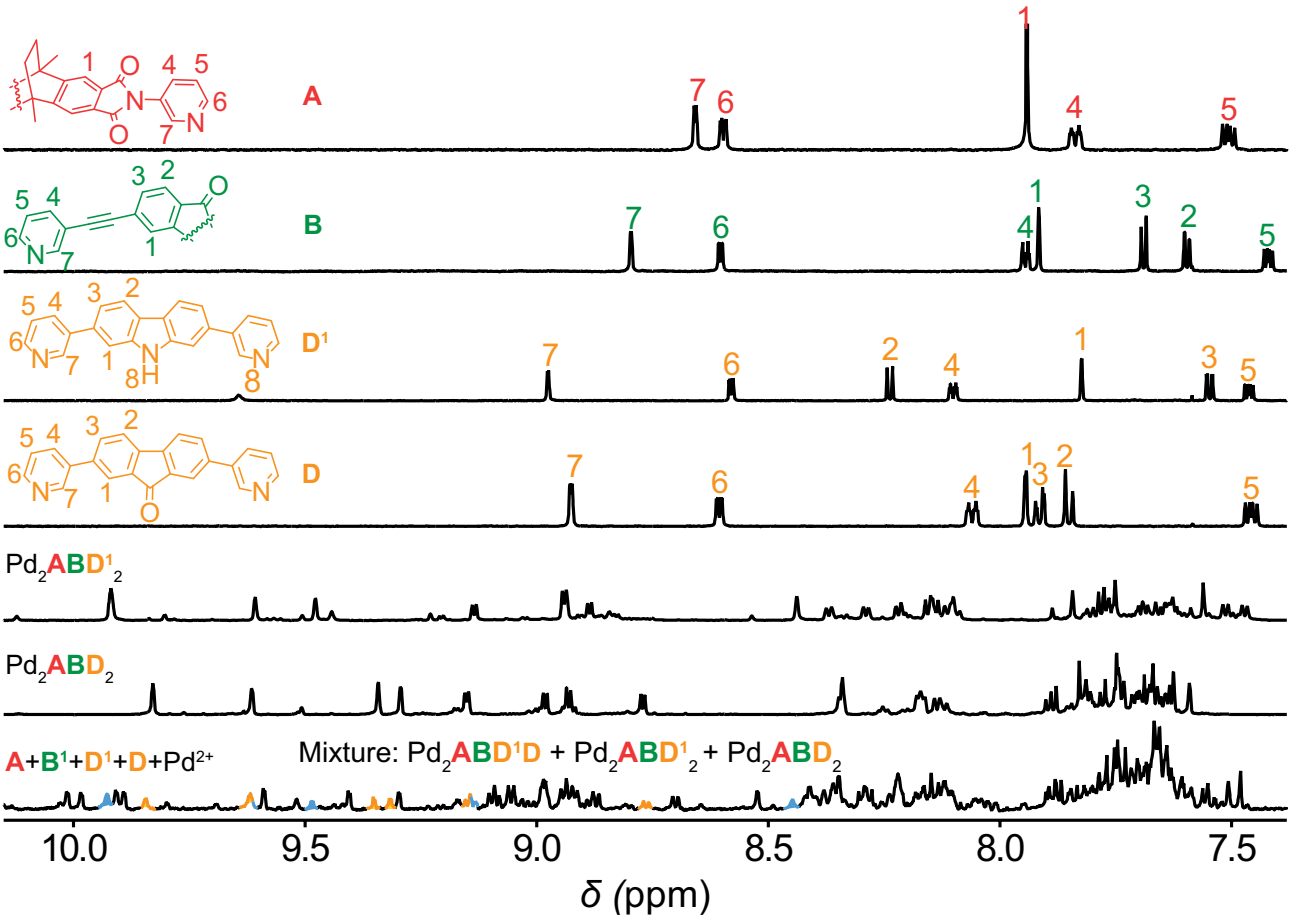

Supplementary Figure 126 | Partial ^{1}H NMR spectrum (700 MHz, 298 K, CD_3CN) comparison of ligands **A** (red), **B** (green), **D^1** (yellow), **D** (yellow), heteroleptic cages Pd_2**ABD^1**$_2$, Pd_2**ABD**$_2$ and the convoluted cage mixture resulting from the combination of ligands **A**, **B**, **D^1** and **D** (bottom), showing, that this combination does not yield a cage composed of four different ligands as a single species, in contrast the mixture of ligands **A**, **B**, **C** and **D**, as shown in Supp. Fig. 86.

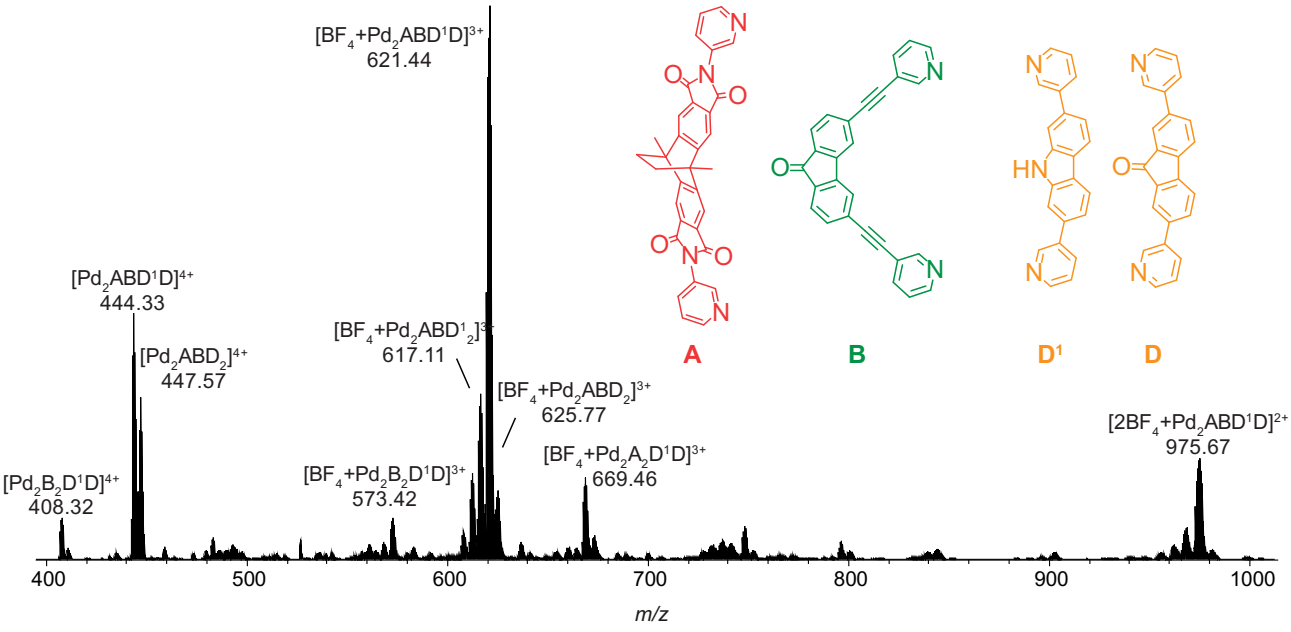

Supplementary Figure 127 | HR-ESI mass spectrum of cage assembly with ligands **A**, **B**, **D^1**, **D** and Pd^{II}.

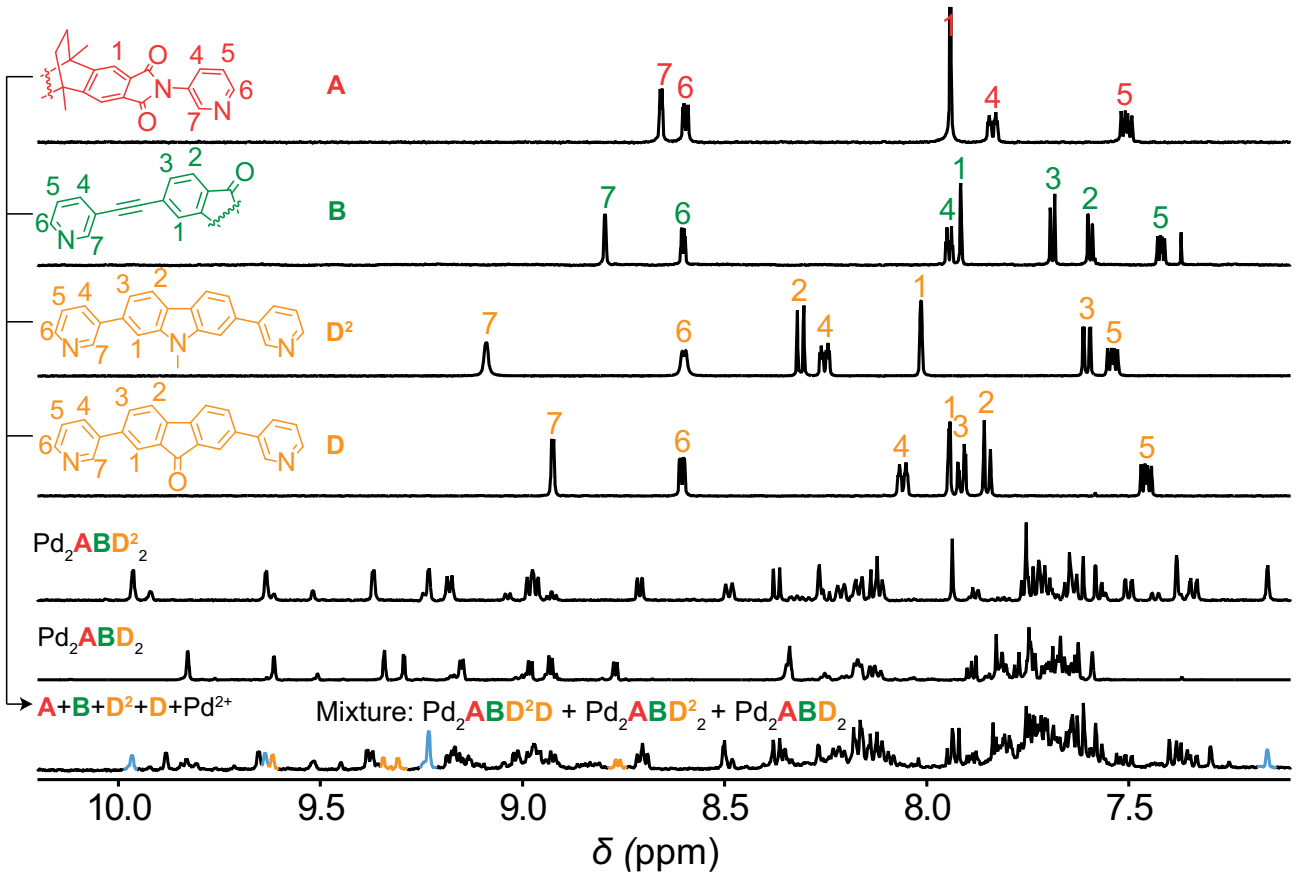

Supplementary Figure 128 | Partial ^{1}H NMR spectrum (700 MHz, 298 K, CD_3CN) comparison of ligands **A** (red), **B** (green), **D²** (yellow), **D** (yellow), heteroleptic cages Pd_2**ABD²**$_2$, Pd_2**ABD**$_2$ and cage the convoluted cage mixture resulting from the combination of ligands **A**, **B**, **D²** and **D** (bottom), showing, that this combination does not yield a cage composed of four different ligands as a single species, in contrast the mixture of ligands **A**, **B**, **C** and **D**, as shown in Supp. Fig. 86.

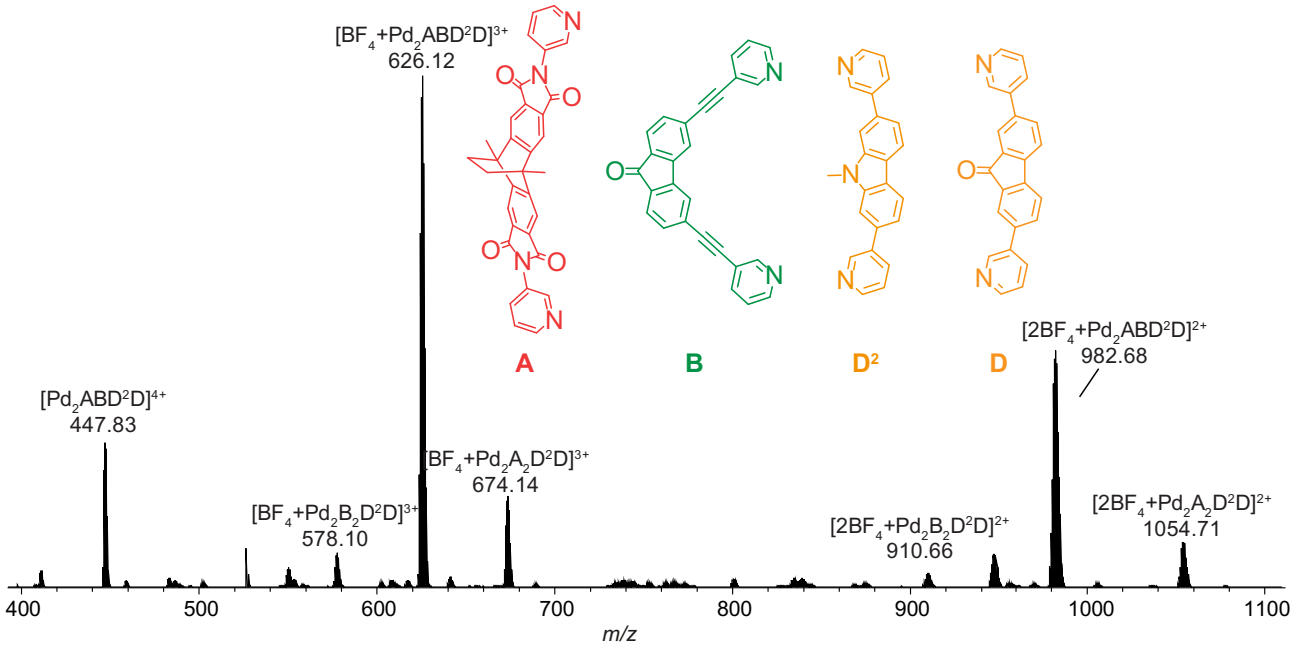

Supplementary Figure 129 | HR-ESI mass spectrum of cage assembly with ligands **A, B, D², D** and Pd^{II}.

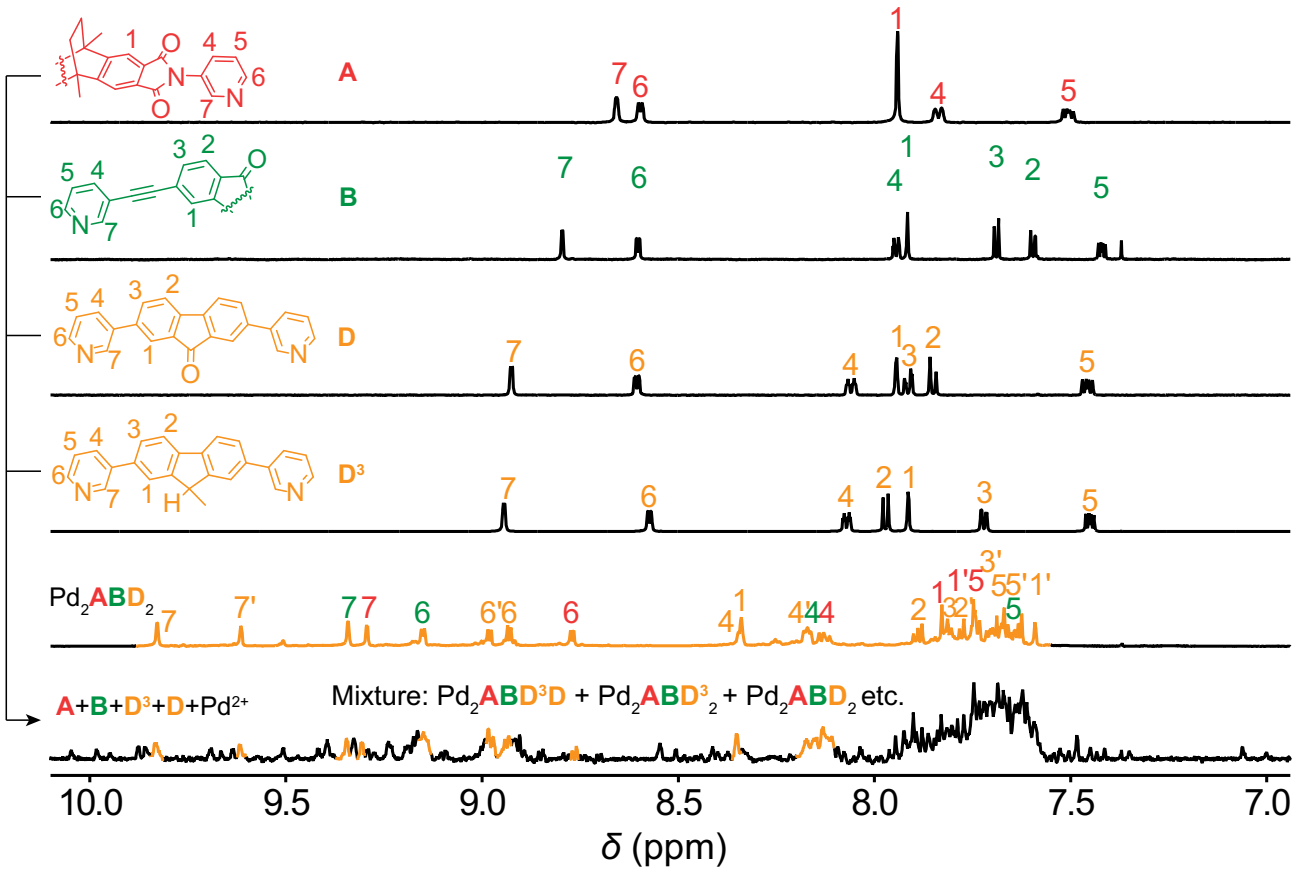

Supplementary Figure 130 | Partial ^{1}H NMR spectrum (700 MHz, 298 K, CD_3CN) comparison of ligands **A** (red), **B** (green), **D** (yellow), **D³** (yellow), heteroleptic cage Pd_2**ABD**$_2$ and cage the convoluted cage mixture resulting from the combination of ligands **A**, **B**, **D³** and **D** (bottom), showing, that this combination does not yield a cage composed of four different ligands as a single species, in contrast the mixture of ligands **A**, **B**, **C** and **D**, as shown in Supp. Fig. 86.

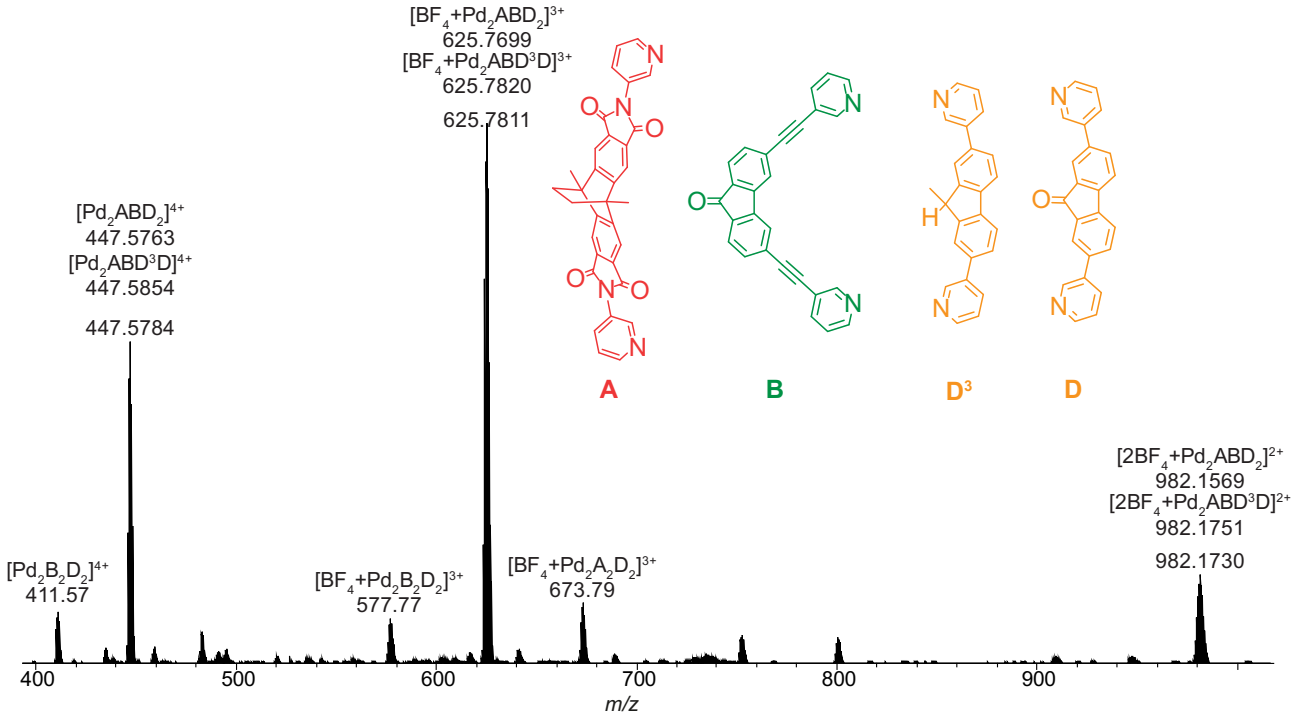

Supplementary Figure 131 | HR-ESI mass spectrum of cage assembly with ligands **A**, **B**, **D³**, **D** and Pd^{II} (the molecular weight of ligands **D³**, **D** are very close, some MS signals are overlapped).

3.6. Evolution of heteroleptic cage Pd_2ABCD^1

3.6.1. Self-assembly of heteroleptic cage $Pd_2A_2D^1_2$

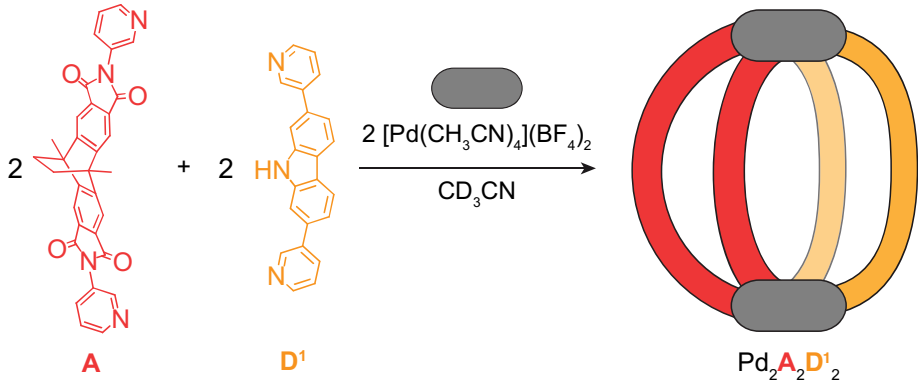

To a solution of **A** (120 µL, 3 mM, 0.36 µmol) in CD_3CN and $\mathbf{D^1}$ (120 µL, 3 mM, 0.36 µmol) were added a stock solution of $[Pd(CH_3CN)_4](BF_4)_2$ (24 µL, 15 mM/CD_3CN, 0.36 µmol) and 186 µL additional CD_3CN. The mixture was heated at 80 °C for 8 h to give a 0.4 mM cage solution containing the shown cage as predominant species.

^{1}H NMR (700 MHz, 298 K, CD_3CN) δ 9.80 (d, J = 2.1 Hz, 4H), 9.22 (d, J = 2.2 Hz, 4H), 8.94 (dd, J = 5.9, 1.3 Hz, 4H), 8.86 (s, 2H), 8.83 (dd, J = 5.8, 1.2 Hz, 4H), 8.34 (dt, J = 7.9, 1.7 Hz, 4H), 8.18 – 8.13 (m, 8H), 8.08 (d, J = 1.6 Hz, 4H), 7.89 (s, 4H), 7.83 – 7.79 (m, 4H), 7.60 (dd, J = 8.0, 5.8 Hz, 4H), 7.59 (s, 4H), 7.49 (dd, J = 8.2, 1.7 Hz, 4H), 2.19 (s, 6H), 1.96 (s, 6H), 1.82 (b, 8H).

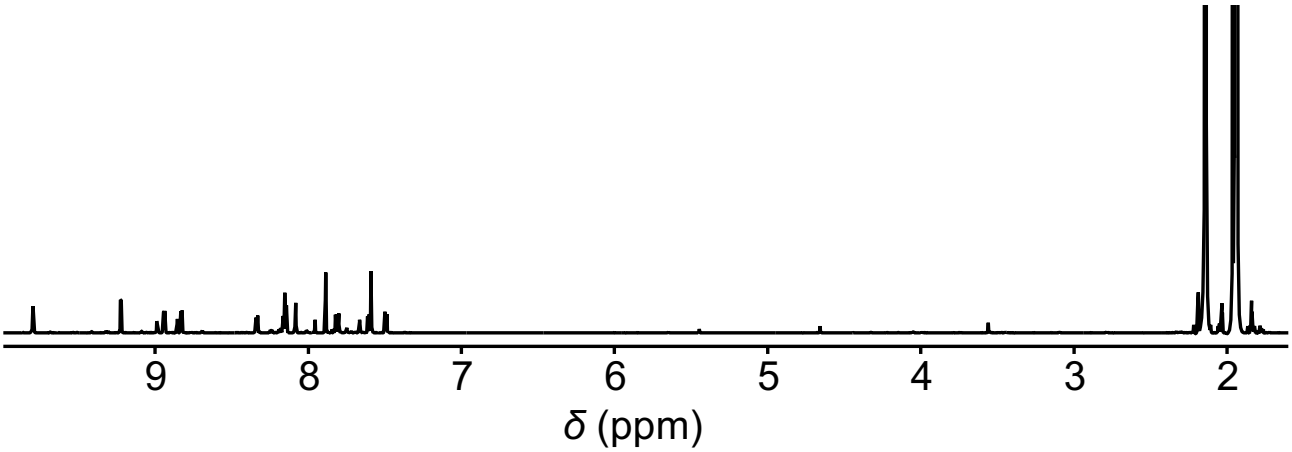

Supplementary Figure 132 | ^{1}H NMR spectrum (700 MHz, 298 K, CD_3CN) of heteroleptic cage $Pd_2\mathbf{A}_2\mathbf{D^1}_2$.

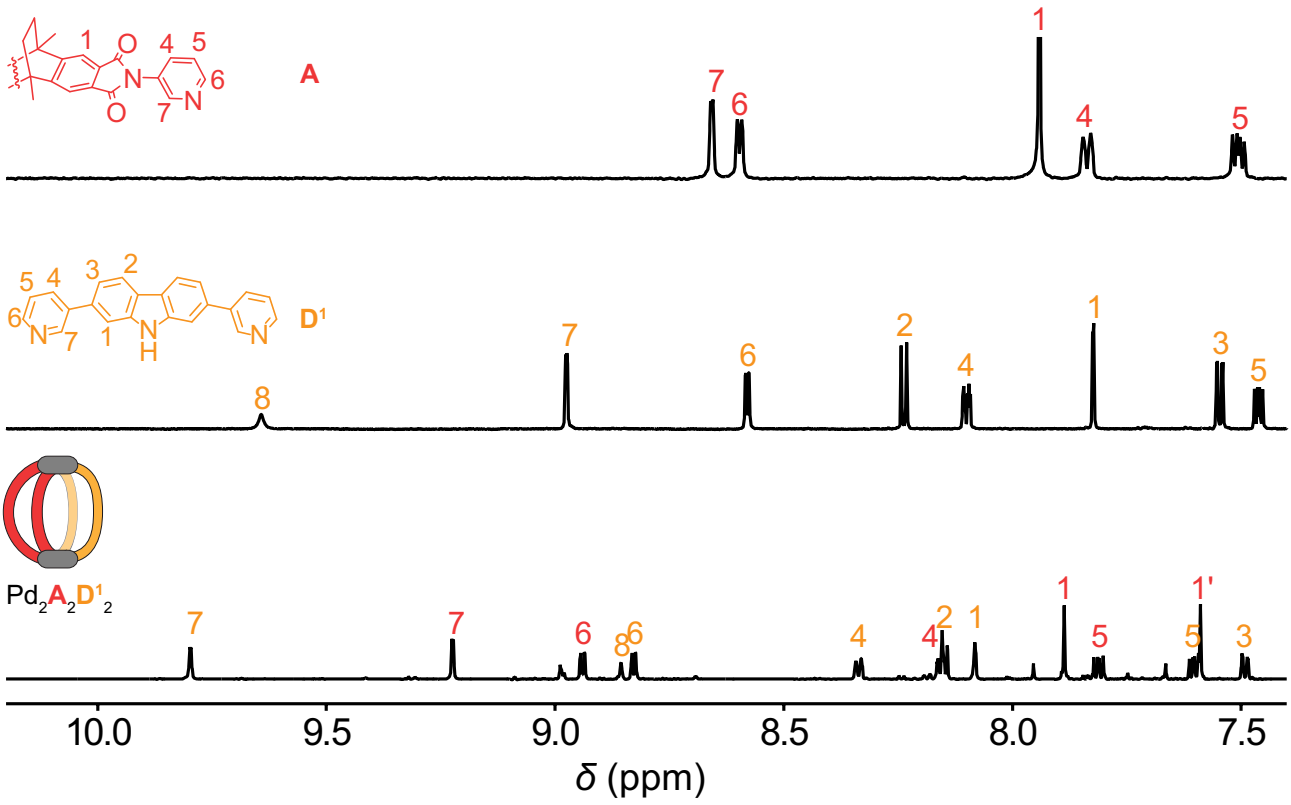

Supplementary Figure 133 | Partial ^{1}H NMR spectrum (700 MHz, 298 K, CD_3CN) comparison of ligand **A** (red), ligand **D^{1}** (yellow) and heteroleptic cage $Pd_2\mathbf{A}_2\mathbf{D}^{1}_2$.

^{13}C NMR (176 MHz, 298 K, CD_3CN) δ 166.86, 166.68, 154.56, 154.47, 150.55, 150.35, 150.22, 149.62, 142.26, 141.83, 139.27, 139.13, 133.51, 132.24, 130.48, 130.40, 128.68, 128.29, 124.40, 122.51, 119.72, 117.81, 117.76, 110.81, 45.31, 45.08, 34.71, 34.56, 18.69, 18.52.

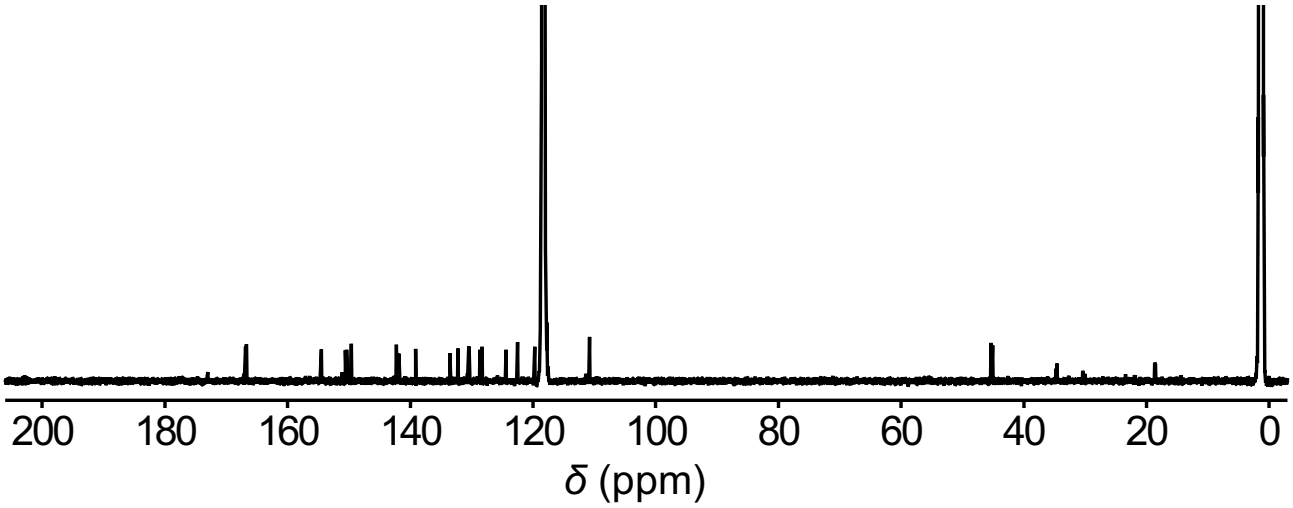

Supplementary Figure **134** | ^{13}C NMR spectrum (176 MHz, 298 K, CD_3CN) of heteroleptic cage $Pd_2\mathbf{A}_2\mathbf{D}^{1}_2$.

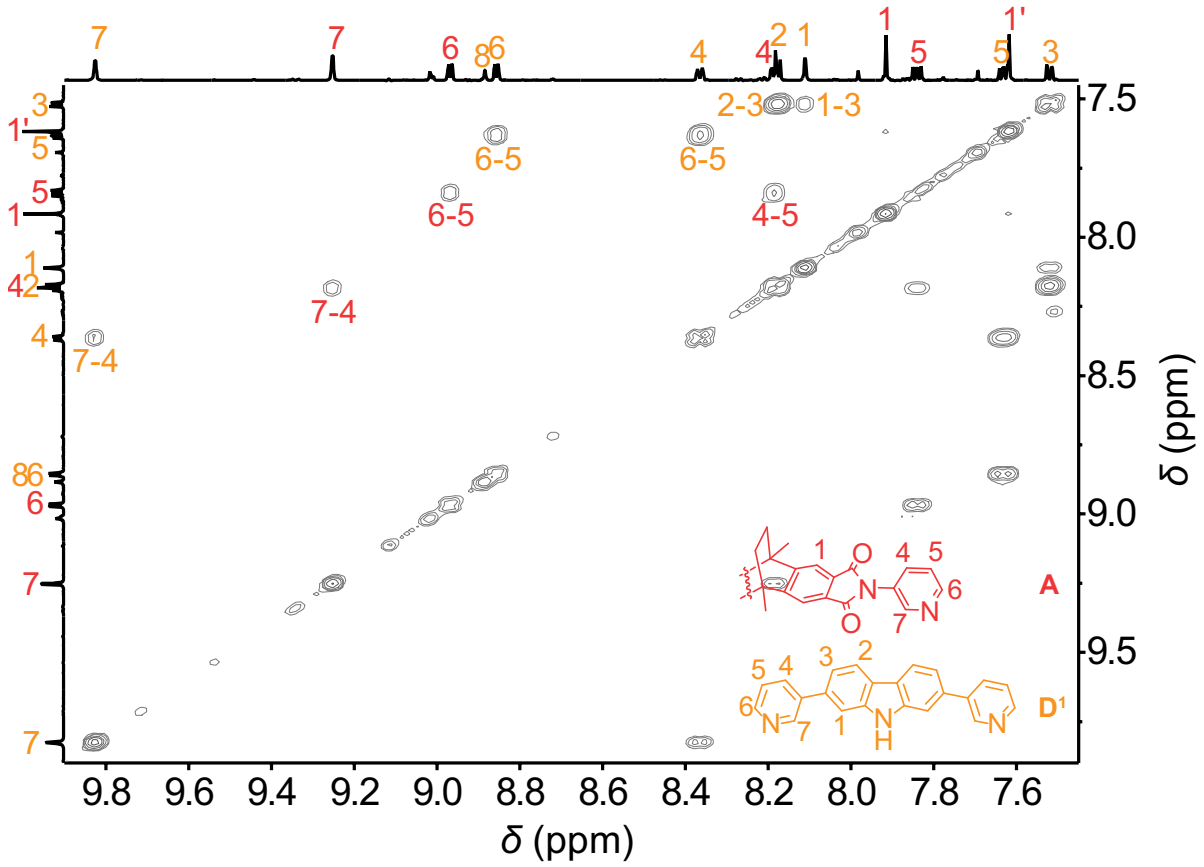

Supplementary Figure 135 | Partial ^{1}H–^{1}H COSY spectrum (500 MHz, 298 K, CD_3CN) of heteroleptic cage $Pd_2\mathbf{A}_2\mathbf{D}^{1}_2$.

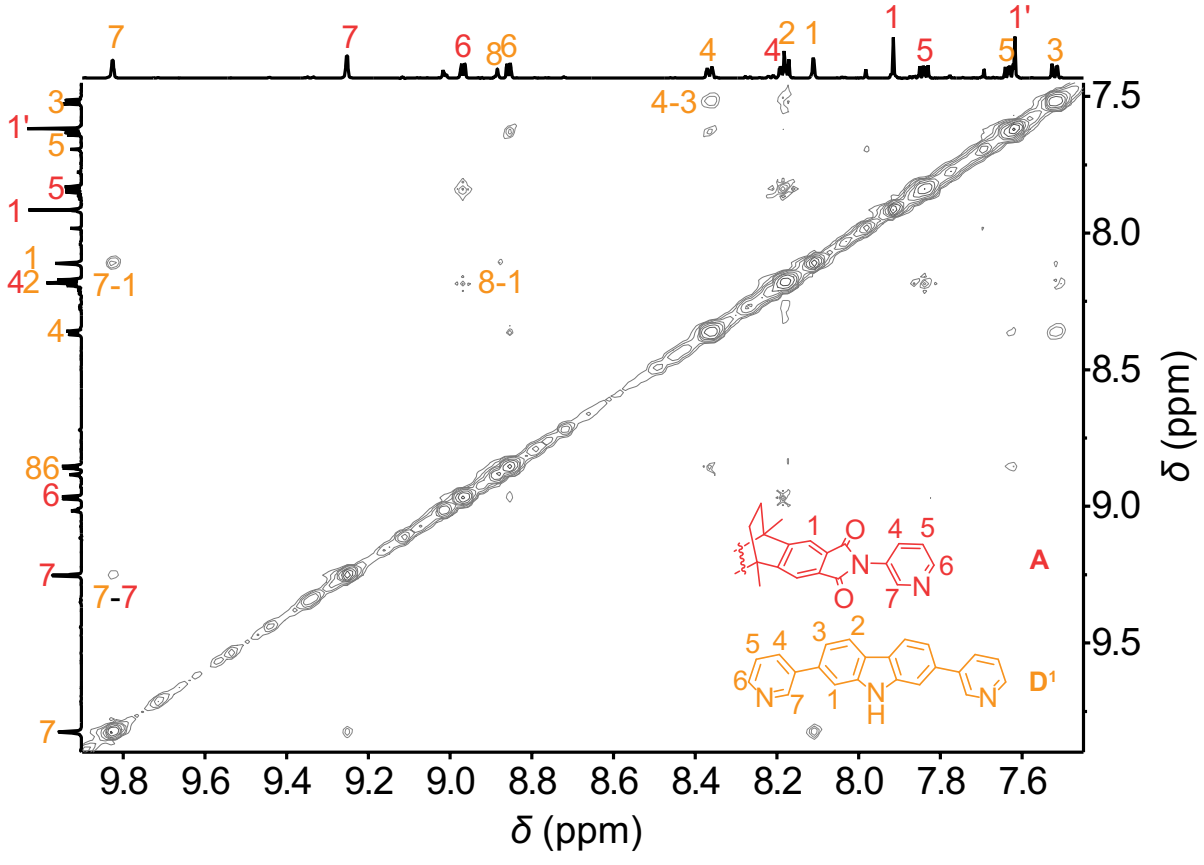

Supplementary Figure 136 | Partial ^{1}H–^{1}H NOESY spectrum (500 MHz, 298 K, CD_3CN) of heteroleptic cage $Pd_2\mathbf{A}_2\mathbf{D}^{1}_2$.

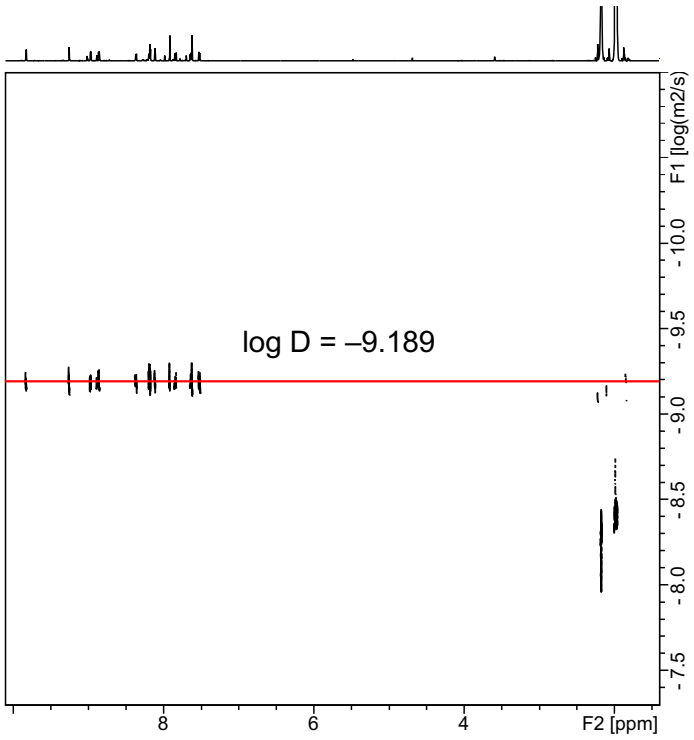

Supplementary Figure 137 | ^{1}H DOSY spectrum (500 MHz, 298 K, CD_3CN) of heteroleptic cage $Pd_2\mathbf{A}_2\mathbf{D}^1_2$. Diffusion coefficient for $Pd_2\mathbf{A}_2\mathbf{D}^1_2$: D = 6.471 × 10^{-10} m^2s^{-1}, log *D* = −9.189, r = 10.1 Å.

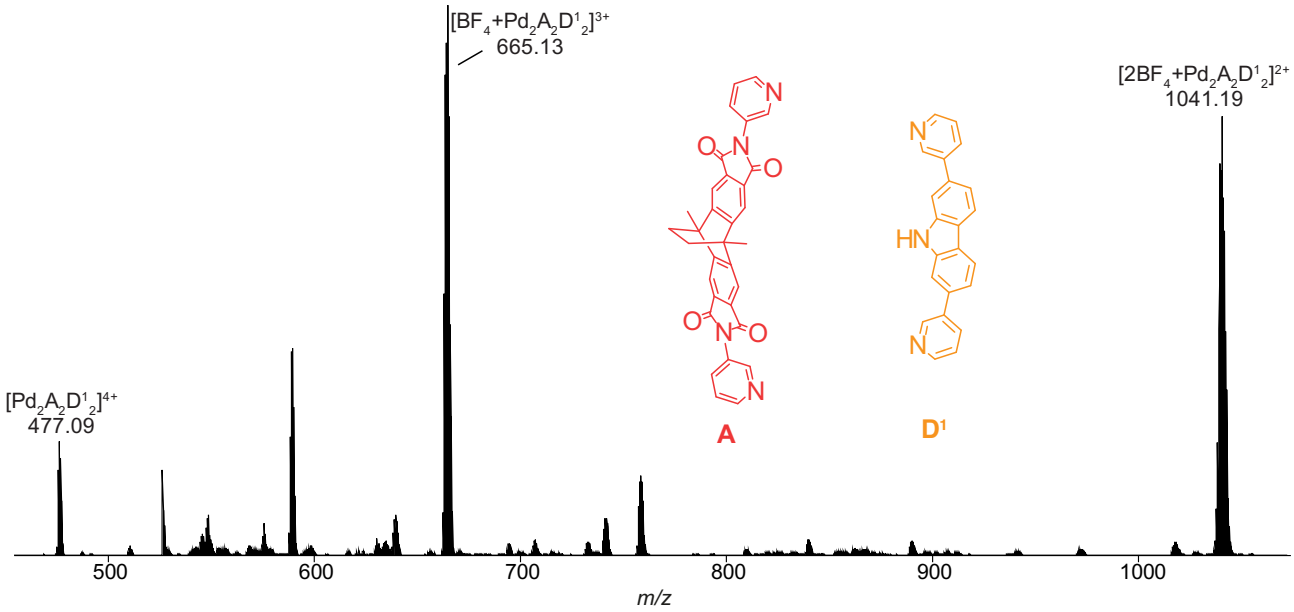

Supplementary Figure 138 | HR-ESI mass spectrum of heteroleptic cage $Pd_2\mathbf{A}_2\mathbf{D}^1_2$.

3.6.2. Self-assembly of heteroleptic cage $Pd_2B_2D^1_2$

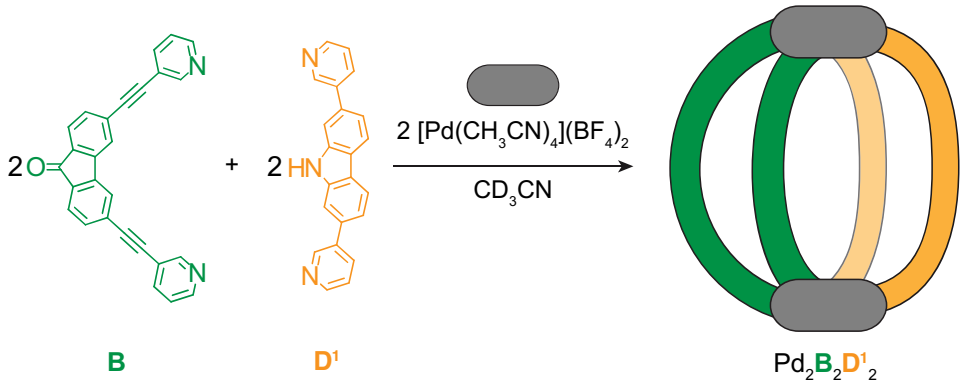

To a solution of **D¹** (120 µL, 3 mM, 0.36 µmol) in CD_3CN and a suspension of **B** (120 µL, 3 mM, 0.36 µmol) were added a stock solution of $[Pd(CH_3CN)_4](BF_4)_2$ (24 µL, 15 mM/CD_3CN, 0.36 µmol) and 186 µL additional CD_3CN. The mixture was heated at 80 °C for 8 h to give a 0.4 mM cage solution containing the shown cage as predominant species.

^{1}H NMR (700 MHz, 298 K, CD_3CN) δ 10.11 (d, J = 2.1 Hz, 4H), 9.52 (s, 2H), 9.49 (d, J = 1.9 Hz, 4H), 9.20 (dd, J = 6.0, 1.4 Hz, 4H), 8.90 (dd, J = 5.9, 1.2 Hz, 4H), 8.52 (d, J = 1.7 Hz, 4H), 8.36 (ddd, J = 8.2, 2.0, 1.0 Hz, 4H), 8.23 – 8.18 (m, 8H), 7.81 (t, J = 1.0 Hz, 4H), 7.70 (ddd, J = 7.9, 6.0, 0.7 Hz, 4H), 7.67 (q, J = 1.3, 0.8 Hz, 8H), 7.65 – 7.62 (m, 4H), 7.56 (dd, J = 8.2, 1.7 Hz, 4H).

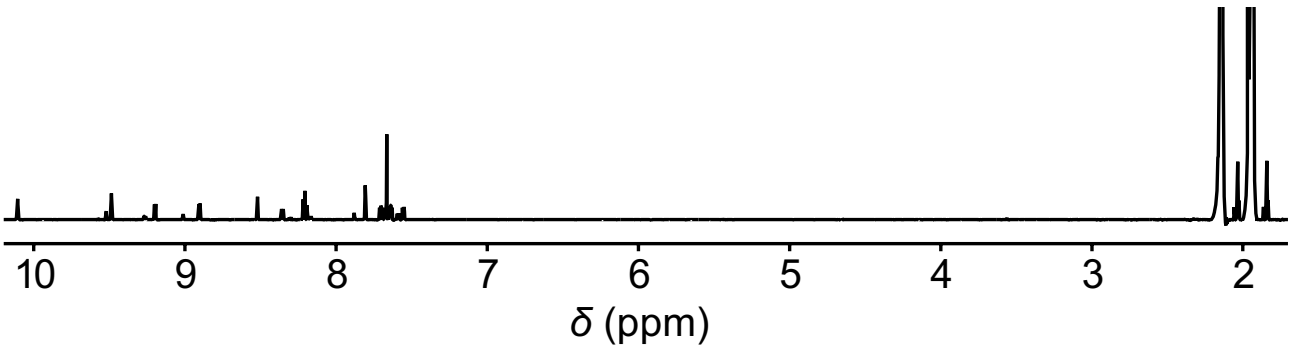

Supplementary Figure 139 | ^{1}H NMR spectrum (700 MHz, 298 K, CD_3CN) of heteroleptic cage $Pd_2B_2D^1_2$.

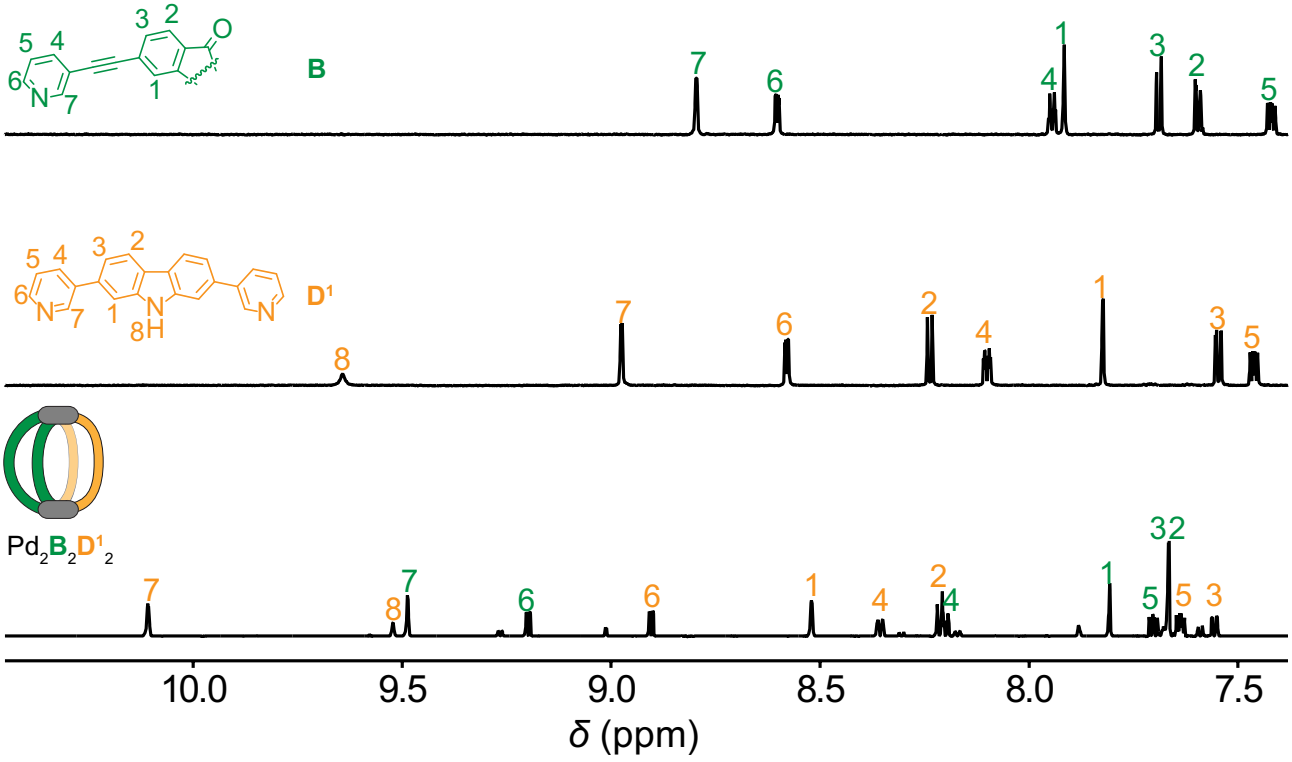

Supplementary Figure 140 | Partial ^{1}H NMR spectrum (700 MHz, 298 K, CD_3CN) comparison of ligand **B** (green), ligand **D^{1}** (yellow) and heteroleptic cage $Pd_2\mathbf{B}_2\mathbf{D}^{1}_2$.

^{13}C NMR (176 MHz, 298 K, CD_3CN) δ 195.22, 186.98, 179.14, 172.96, 165.64, 153.93, 153.10, 150.00, 149.67, 146.90, 146.60, 141.08, 138.75, 135.50, 133.42, 128.86, 128.60, 128.39, 125.80, 124.76, 123.16, 119.41, 110.68, 94.52, 87.52.

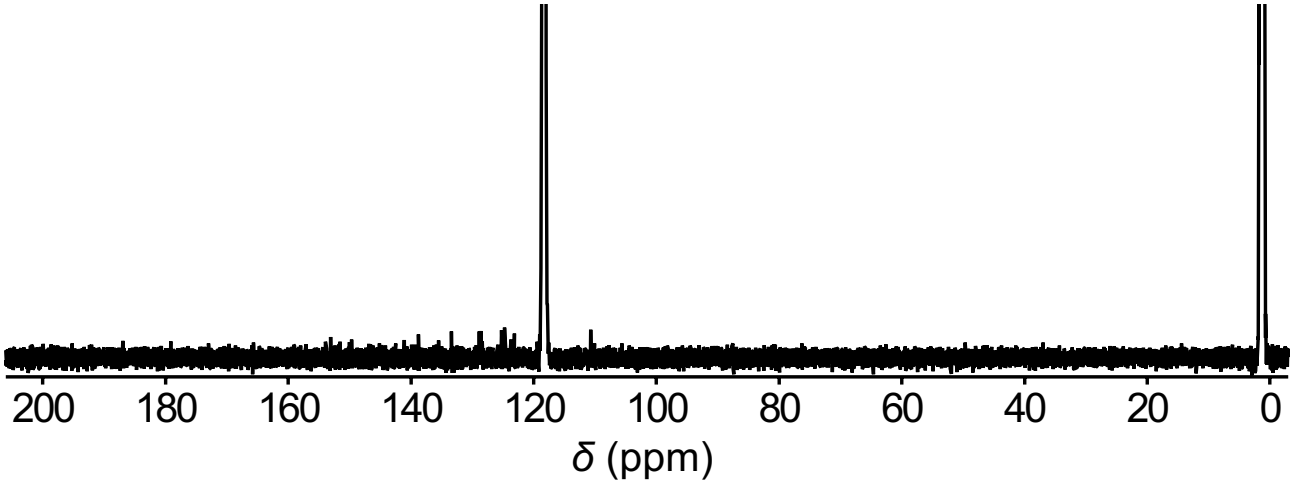

Supplementary Figure 141 | ^{13}C NMR spectrum (176 MHz, 298 K, CD_3CN) of heteroleptic cage $Pd_2\mathbf{B}_2\mathbf{D}^{1}_2$.

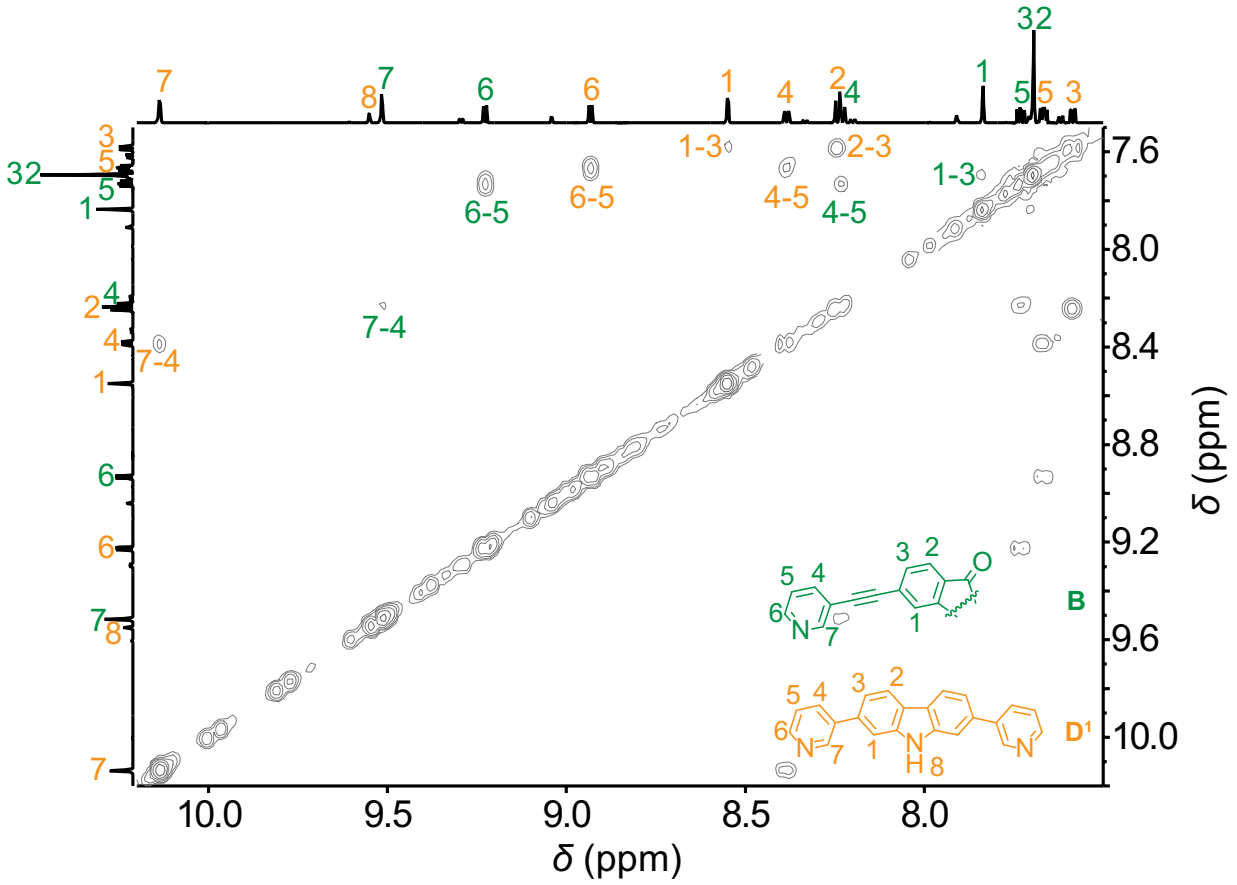

Supplementary Figure 142 | Partial ^{1}H–^{1}H COSY spectrum (500 MHz, 298 K, CD_3CN) of heteroleptic cage $Pd_2\mathbf{B}_2\mathbf{D}^{1}_2$.

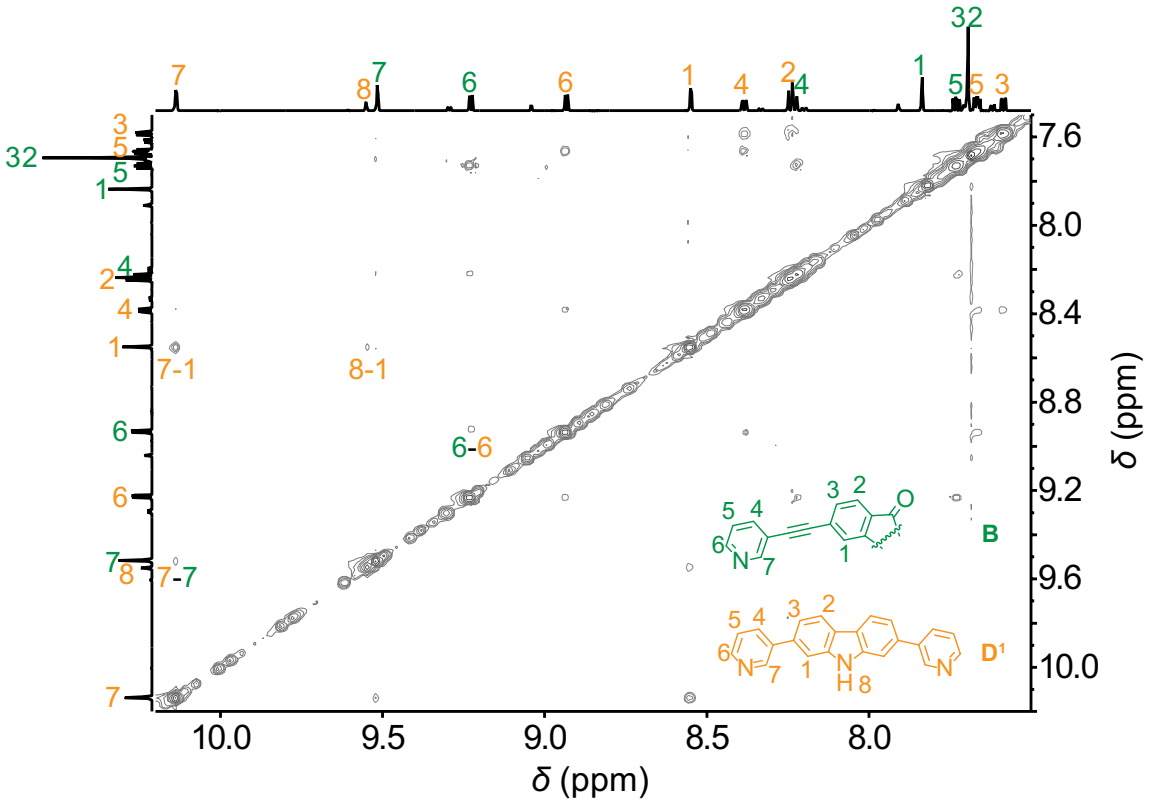

Supplementary Figure 143 | Partial ^{1}H–^{1}H NOESY spectrum (500 MHz, 298 K, CD_3CN) of heteroleptic cage $Pd_2\mathbf{B}_2\mathbf{D}^{1}_2$.

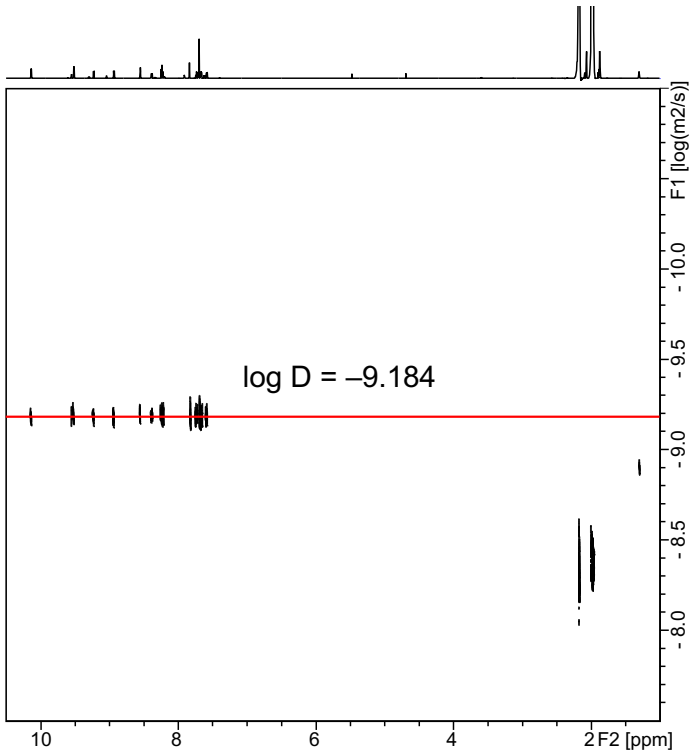

Supplementary Figure 144 | ^{1}H DOSY spectrum (500 MHz, 298 K, CD_3CN) of heteroleptic cage $Pd_2\mathbf{B}_2\mathbf{D}^{1}_2$**.** Diffusion coefficient for $Pd_2\mathbf{B}_2\mathbf{D}^{1}_2$: D = 6.546 × 10^{-10} m^2s^{-1}, log *D* = −9.184, r = 10.0 Å.

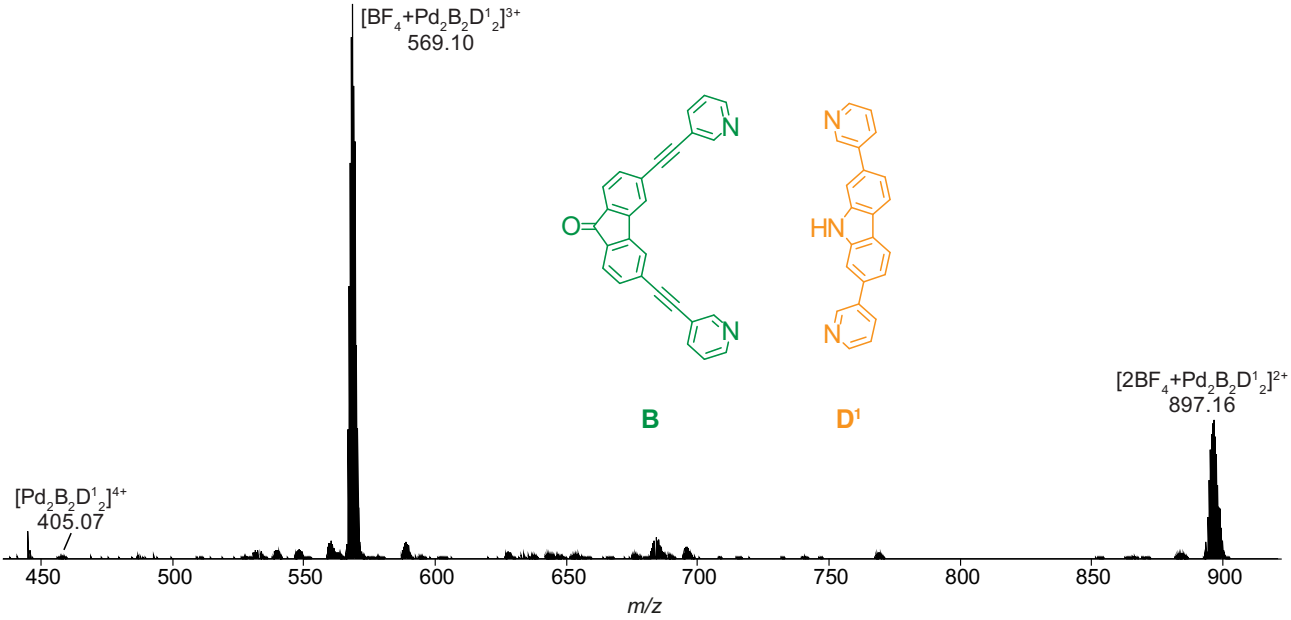

Supplementary Figure 145 | HR-ESI mass spectrum of heteroleptic cage $Pd_2\mathbf{B}_2\mathbf{D}^{1}_2$**.**

3.6.3. Self-assembly of heteroleptic cage $Pd_2A_2CD^1$

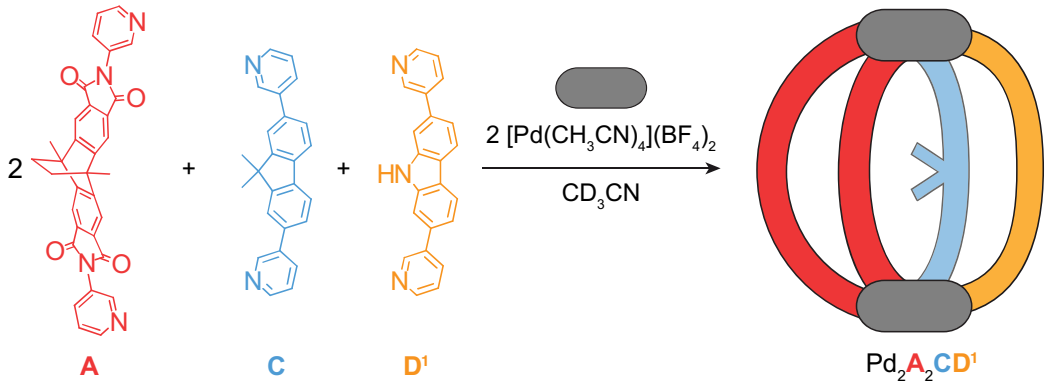

To a solution of **C** (60 µL, 3 mM, 0.18 µmol) and **D^1** (60 µL, 3 mM, 0.18 µmol) in CD_3CN and **A** (120 µL, 3 mM, 0.36 µmol) were added a stock solution of $[Pd(CH_3CN)_4](BF_4)_2$ (24 µL, 15 mM/CD_3CN, 0.36 µmol) and 186 µL additional CD_3CN. The mixture was heated at 80 °C for 8 h to give a 0.4 mM cage solution containing the shown cage as predominant species.

^{1}H NMR (700 MHz, 298 K, CD_3CN) δ 9.76 (d, J = 2.0 Hz, 2H), 9.52 (s, 1H), 9.33 (d, J = 2.2 Hz, 2H), 9.26 (d, J = 2.0 Hz, 2H), 9.07 (dd, J = 5.9, 1.3 Hz, 2H), 9.04 (d, J = 2.2 Hz, 2H), 8.93 (dd, J = 5.9, 1.2 Hz, 2H), 8.89 (dd, J = 5.8, 1.2 Hz, 2H), 8.75 (dd, J = 6.0, 1.2 Hz, 2H), 8.46 (dt, J = 7.9, 1.6 Hz, 2H), 8.28 (d, J = 7.9 Hz, 2H), 8.27 (d, J = 1.5 Hz, 2H), 8.25 (ddd, J = 8.3, 2.3, 1.3 Hz, 2H), 8.10 (dt, J = 7.9, 1.6 Hz, 2H), 8.06 (ddd, J = 8.3, 2.3, 1.3 Hz, 2H), 8.02 (s, 2H), 7.80 (m, 4H), 7.75 (s, 2H), 7.73 (d, J = 7.6 Hz, 2H), 7.67 (dd, J = 7.9, 5.8 Hz, 2H), 7.63 (s, 2H), 7.59 (s, 2H), 7.59 – 7.57 (m, 2H), 7.48 (dd, J = 7.9, 1.7 Hz, 2H), 7.43 (dd, J = 7.7, 1.8 Hz, 2H), 6.93 (d, J = 1.8 Hz, 2H), 2.26 (s, 3H), 2.07 (s, 3H), 2.02 (s, 3H), 1.75 (b, 8H), 1.74 (s, 3H), 0.94 (s, 3H), -0.22 (s, 3H).

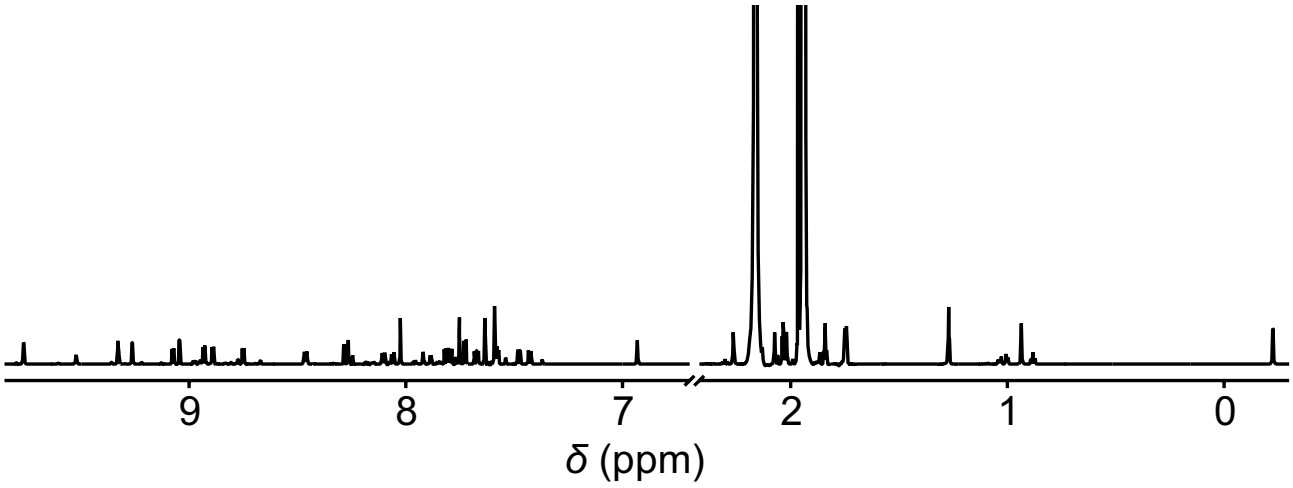

Supplementary Figure 146 | ^{1}H NMR spectrum (700 MHz, 298 K, CD_3CN) of heteroleptic cage Pd_2**A**$_2$**CD^1**.

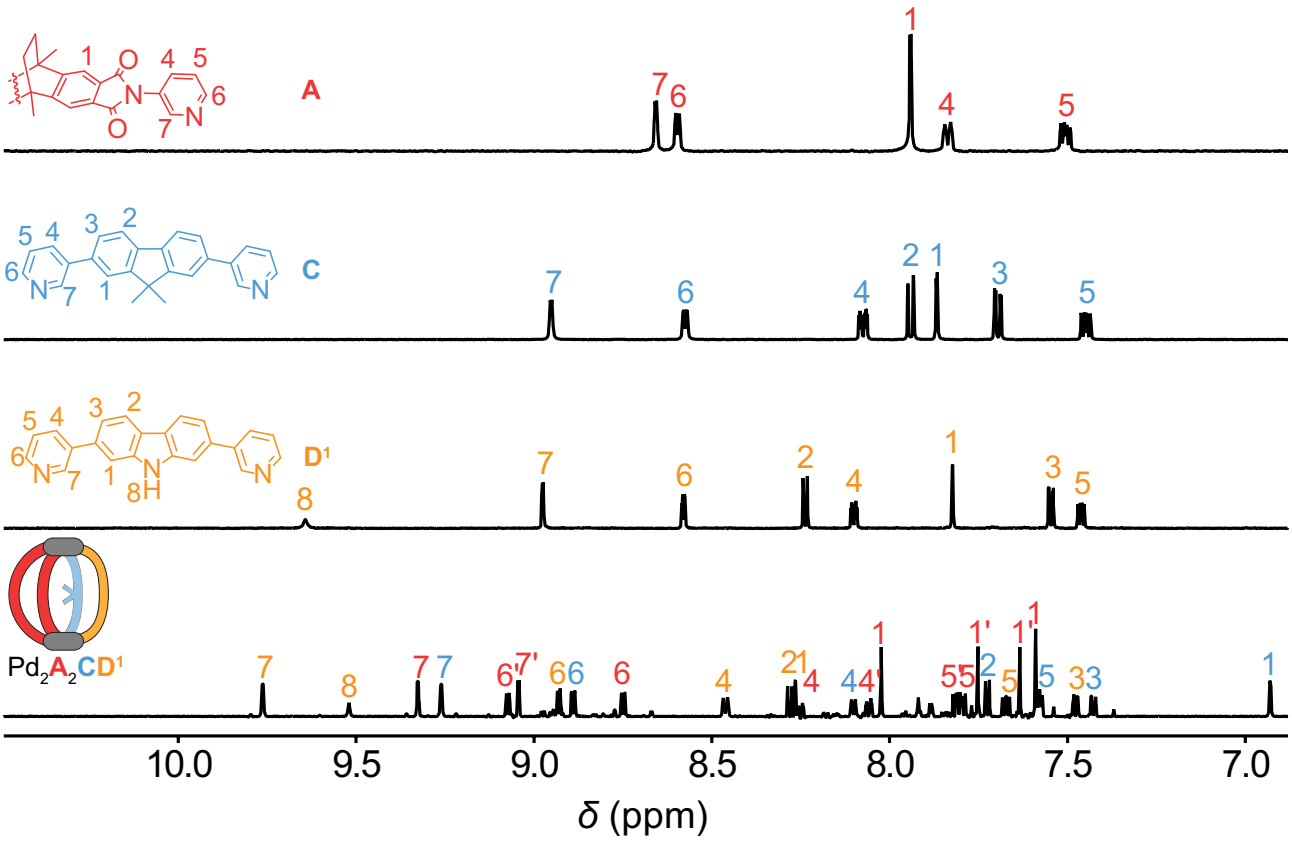

Supplementary Figure 147 | Partial ^{1}H NMR spectrum (700 MHz, 298 K, CD_3CN) comparison of ligand **A** (red), ligand **C** (blue), ligand **D**^{1} (yellow) and heteroleptic cage Pd_2**A**$_2$**CD**^{1}.

^{13}C NMR (151 MHz, 298 K, CD_3CN) δ 167.29, 166.91, 166.80, 166.55, 156.12, 154.67, 154.52, 154.42, 154.37, 150.64, 150.42, 150.30, 150.19, 150.10, 149.96, 144.00, 142.81, 142.02, 139.85, 139.80, 139.46, 139.15, 138.64, 135.46, 134.71, 132.16, 131.75, 130.98, 130.49, 130.38, 130.27, 128.82, 128.38, 128.31, 128.28, 128.16, 127.41, 124.92, 122.94, 122.46, 122.29, 120.64, 117.77, 117.67, 117.40, 111.45, 46.31, 45.52, 45.14, 45.09, 44.94, 34.89, 34.81, 34.69, 34.61, 30.36, 25.84, 18.74, 18.66, 18.48, 18.42.

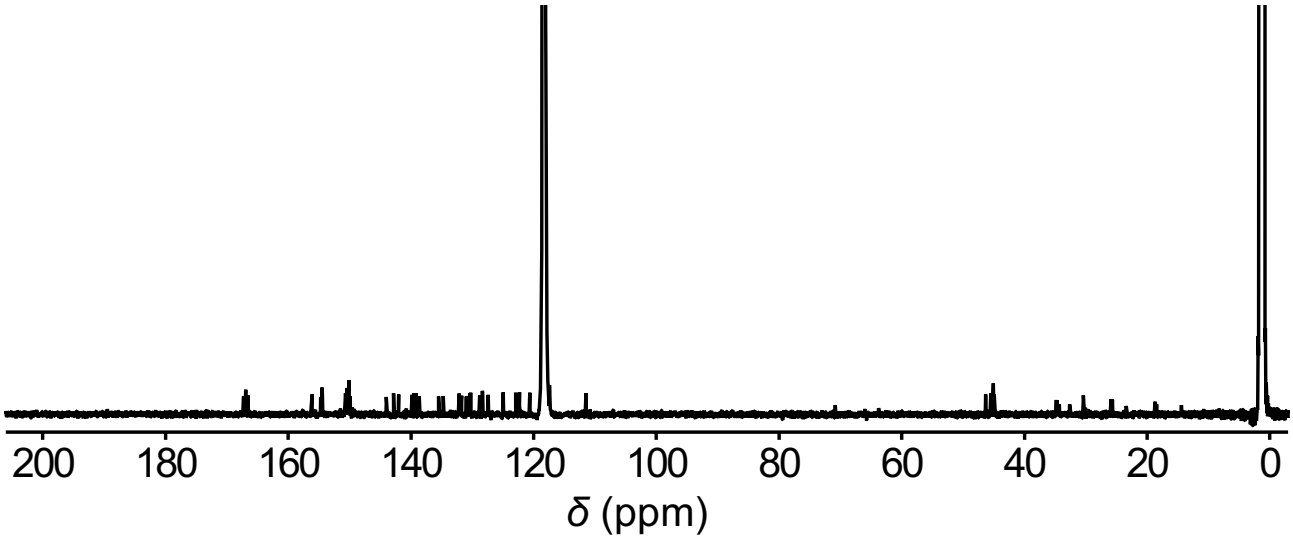

Supplementary Figure 148 | ^{13}C NMR spectrum (151 MHz, 298 K, CD_3CN) of heteroleptic cage Pd_2**A**$_2$**CD**^{1}.

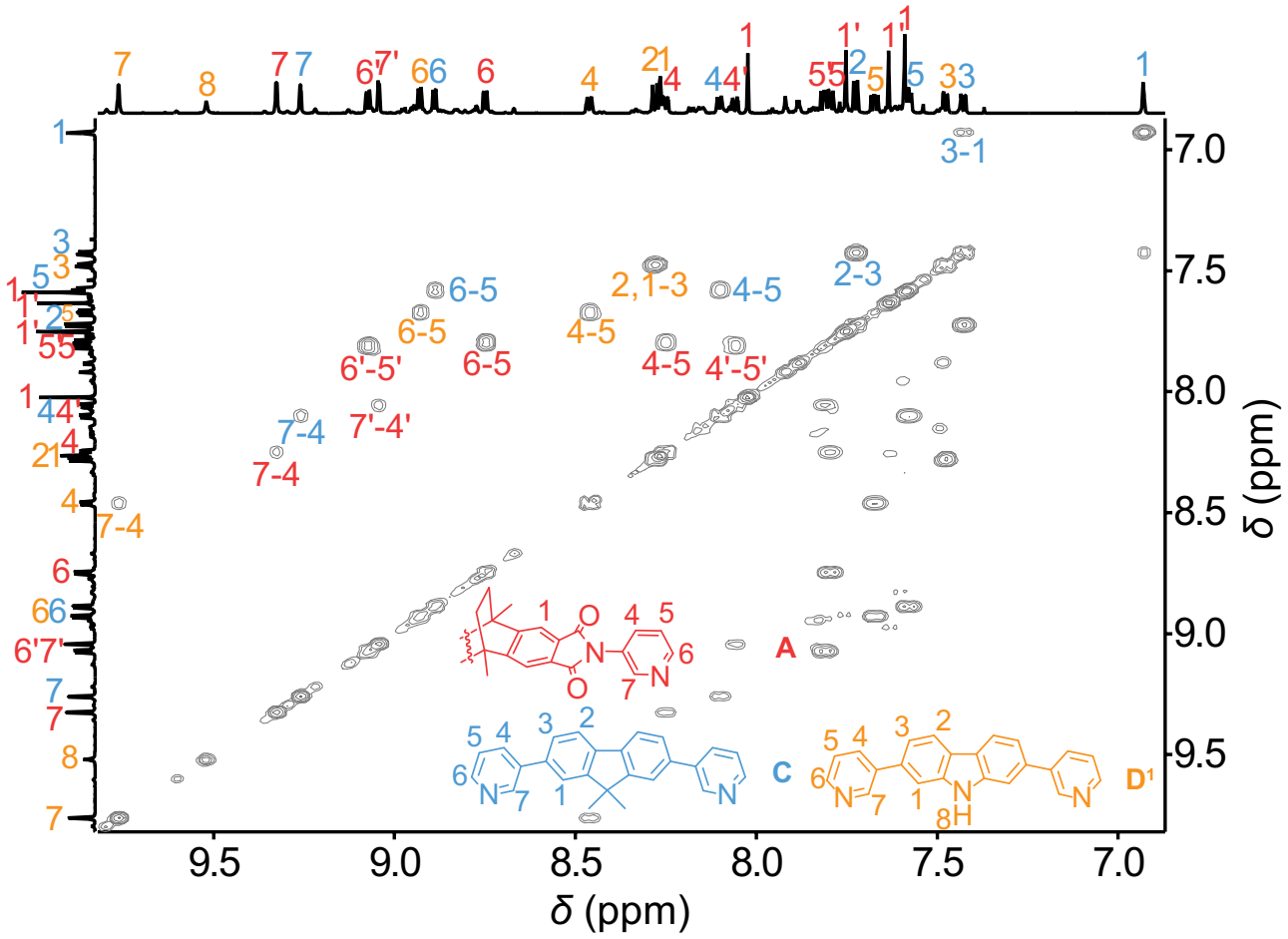

Supplementary Figure 149 | Partial ^{1}H–^{1}H COSY spectrum (500 MHz, 298 K, CD_3CN) of heteroleptic cage $Pd_2\mathbf{A}_2\mathbf{CD}^1$.

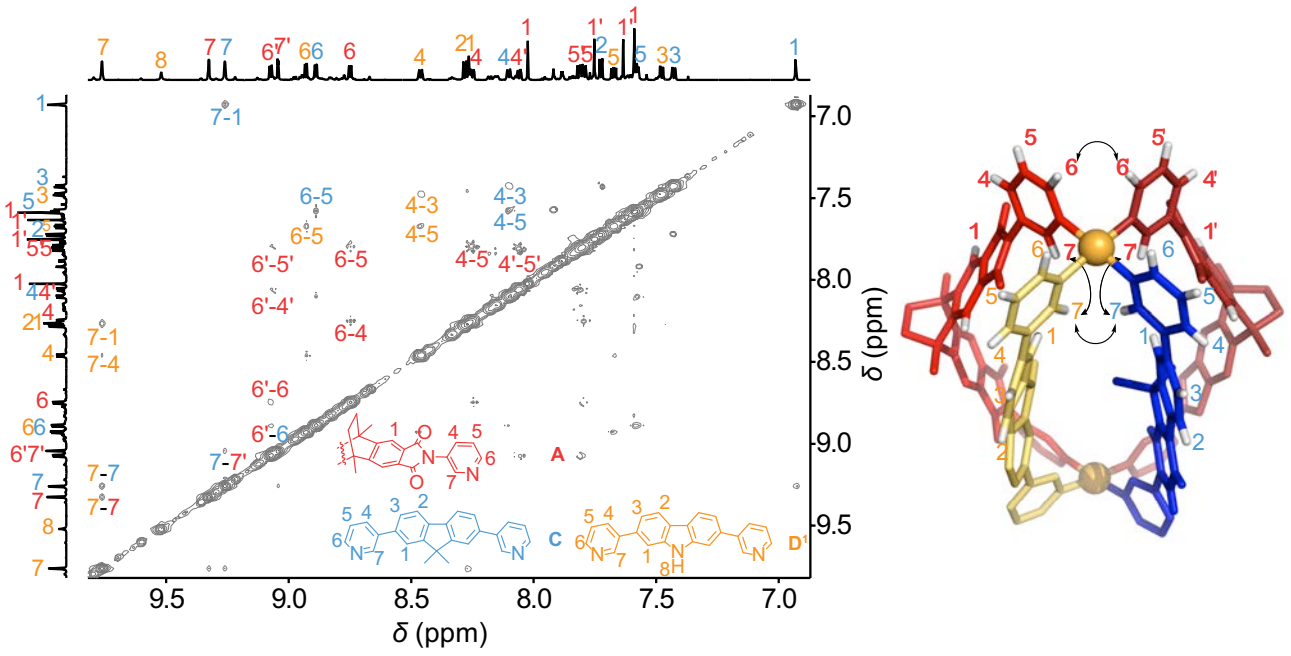

Supplementary Figure 150 | Partial ^{1}H–^{1}H NOESY spectrum (500 MHz, 298 K, CD_3CN) of heteroleptic cage $Pd_2\mathbf{A}_2\mathbf{CD}^1$.

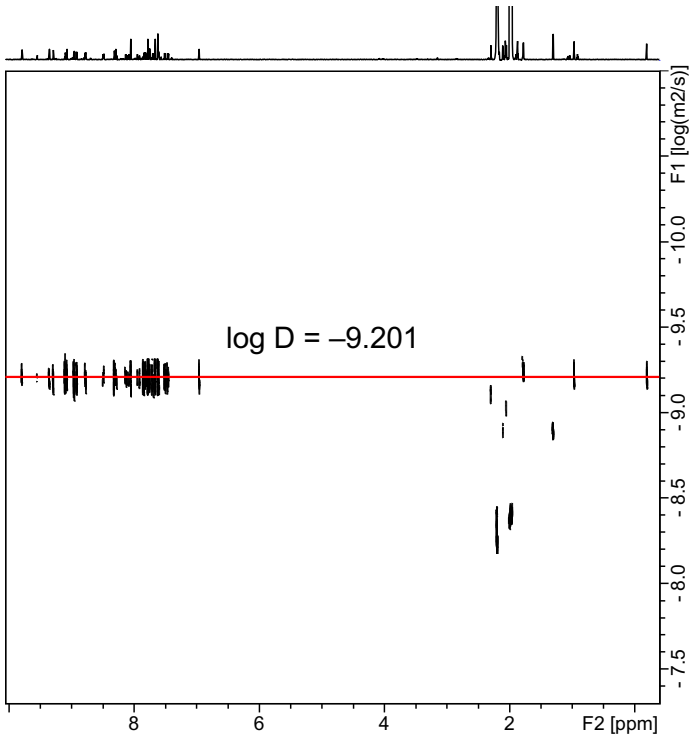

Supplementary Figure 151 | ^{1}H DOSY spectrum (500 MHz, 298 K, CD_3CN) of heteroleptic cage $Pd_2\mathbf{A}_2\mathbf{CD}^{\mathbf{1}}$. Diffusion coefficient for $Pd_2\mathbf{A}_2\mathbf{CD}^{\mathbf{1}}$: D = 6.295 × 10^{-10} m^2s^{-1}, log *D* = −9.201, r = 10.4 Å.

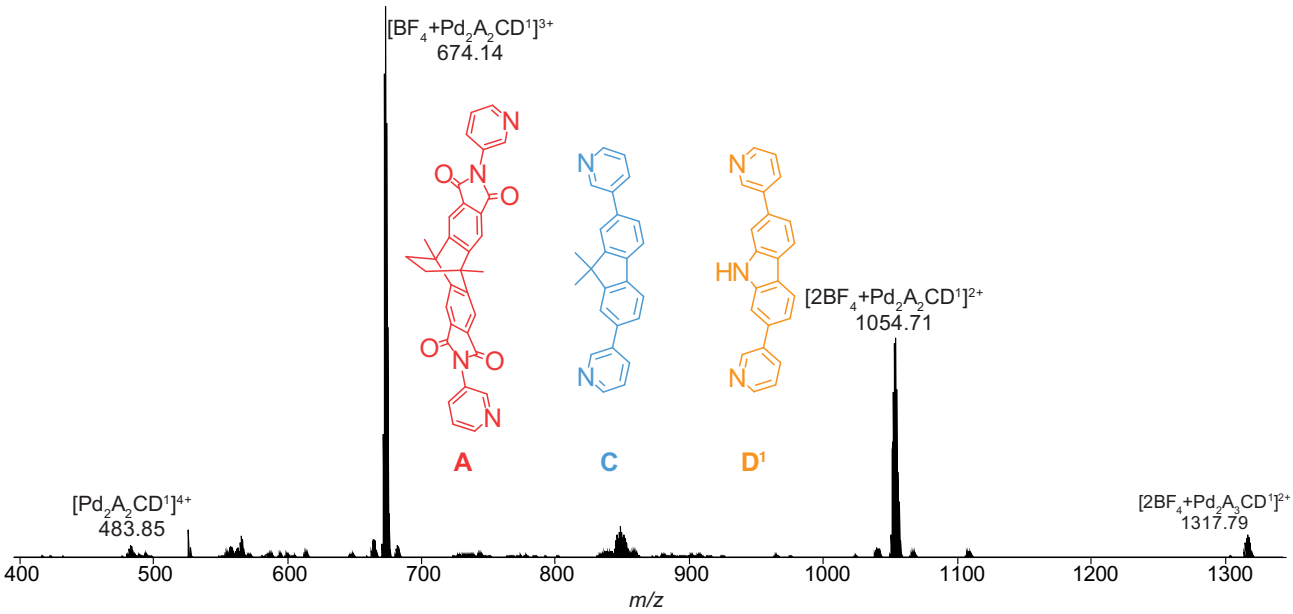

Supplementary Figure 152 | HR-ESI mass spectrum of heteroleptic cage $Pd_2\mathbf{A}_2\mathbf{CD}^{\mathbf{1}}$.

3.6.4. Self-assembly of heteroleptic cage $Pd_2B_2CD^1$

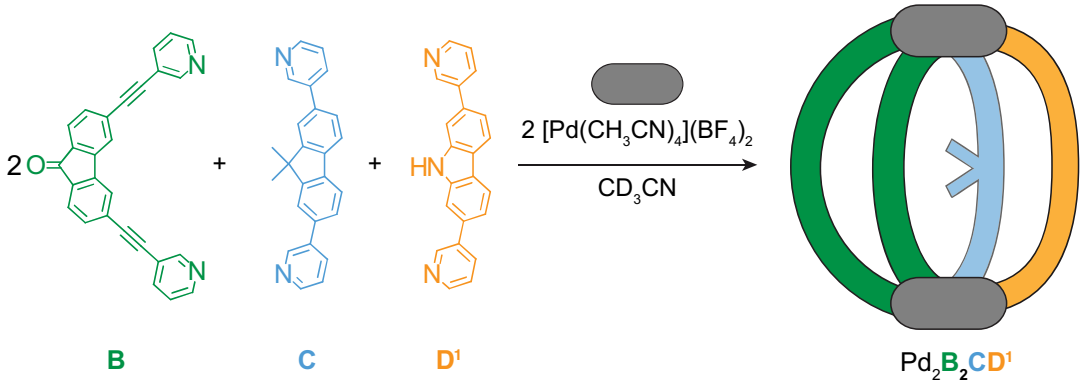

To a solution of **C** (60 µL, 3 mM, 0.18 µmol) and a suspension of **D¹** (60 µL, 3 mM, 0.18 µmol), **B** (120 µL, 3 mM, 0.36 µmol) in CD_3CN were added a stock solution of $[Pd(CH_3CN)_4](BF_4)_2$ (24 µL, 15 mM/CD_3CN, 0.36 µmol) and 186 µL additional CD_3CN. The mixture was heated at 80 °C for 8 h to give a 0.4 mM cage solution containing the shown cage as predominant species.

^{1}H NMR (700 MHz, 298 K, CD_3CN) δ 10.22 (s, 1H), 10.08 (d, J = 2.1 Hz, 2H), 9.69 (d, J = 1.8 Hz, 2H), 9.27 (d, J = 1.9 Hz, 2H), 9.23 (dd, J = 6.0, 1.4 Hz, 2H), 9.15 (dd, J = 5.9, 1.4 Hz, 2H), 9.05 (dd, J = 5.8, 1.2 Hz, 2H), 9.00 (dd, J = 5.9, 1.2 Hz, 2H), 8.69 (d, J = 1.7 Hz, 2H), 8.44 (dt, J = 7.8, 1.7 Hz, 2H), 8.34 (d, J = 7.9 Hz, 2H), 8.24 – 8.20 (m, 2H), 8.17 (tt, J = 7.8, 1.5 Hz, 2H), 8.13 (dt, J = 7.9, 1.6 Hz, 2H), 8.05 (s, 2H), 7.86 (d, J = 7.6 Hz, 2H), 7.72 (dt, J = 7.8, 5.4 Hz, 4H), 7.70 – 7.67 (m, 4H), 7.67 – 7.65 (m, 2H), 7.65 – 7.63 (m, 2H), 7.61 (d, J = 1.0 Hz, 4H), 7.58 – 7.55 (m, 2H), 7.50 (dd, J = 7.6, 1.8 Hz, 2H), 7.15 (d, J = 1.8 Hz, 2H), 1.70 (s, 3H), -0.06 (s, 3H).

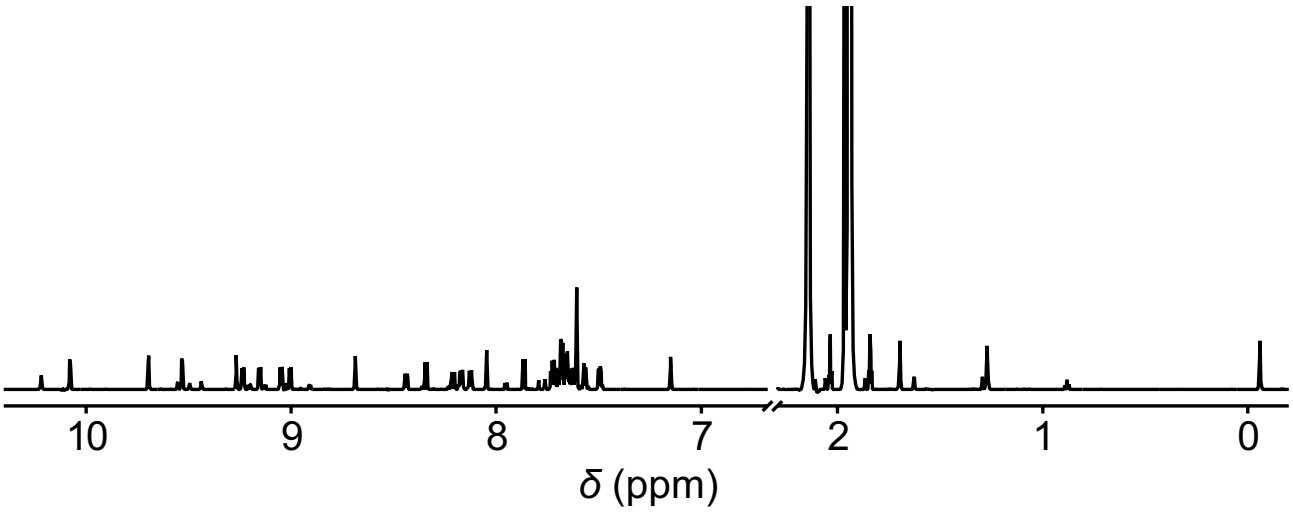

Supplementary Figure 153 | ^{1}H NMR spectrum (700 MHz, 298 K, CD_3CN) of heteroleptic cage $Pd_2B_2CD^1$.

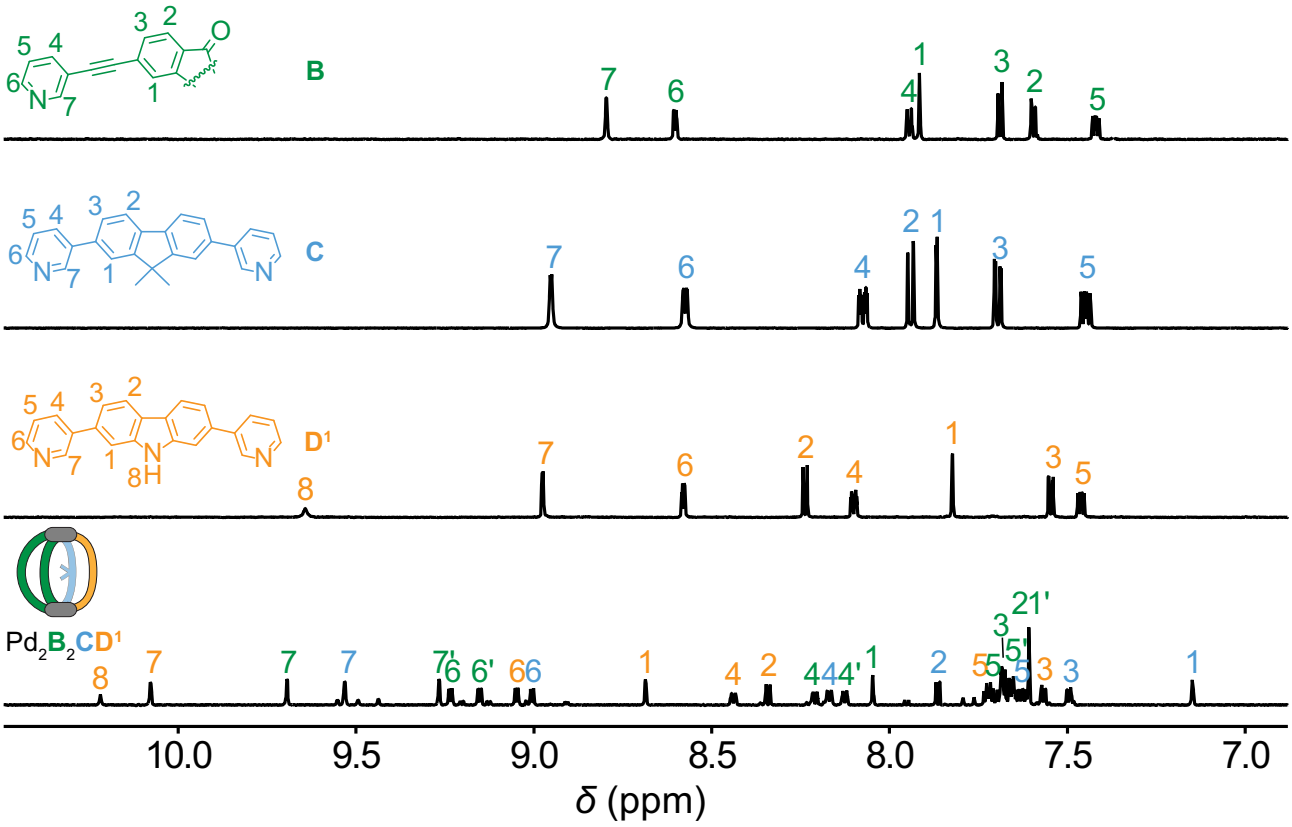

Supplementary Figure 154 | Partial ^{1}H NMR spectrum (700 MHz, 298 K, CD_3CN) comparison of ligand **B** (green), ligand **C** (blue), ligand **D¹** (yellow) and heteroleptic cage Pd_2**B**$_2$**CD¹**.

^{13}C NMR (151 MHz, 298 K, CD_3CN) δ 192.29, 192.15, 156.58, 153.88, 153.08, 152.81, 151.39, 151.24, 150.58, 150.42, 150.26, 150.05, 149.85, 144.96, 144.86, 144.71, 142.89, 142.54, 142.15, 140.20, 139.30, 139.03, 136.26, 136.12, 135.63, 135.52, 135.42, 134.25, 129.11, 128.67, 128.63, 128.43, 128.37, 128.36, 127.68, 125.16, 125.11, 125.11, 124.65, 124.52, 123.92, 123.17, 122.96, 122.86, 120.13, 111.13, 95.72, 95.68, 87.89, 87.48, 46.52, 30.37, 26.88.

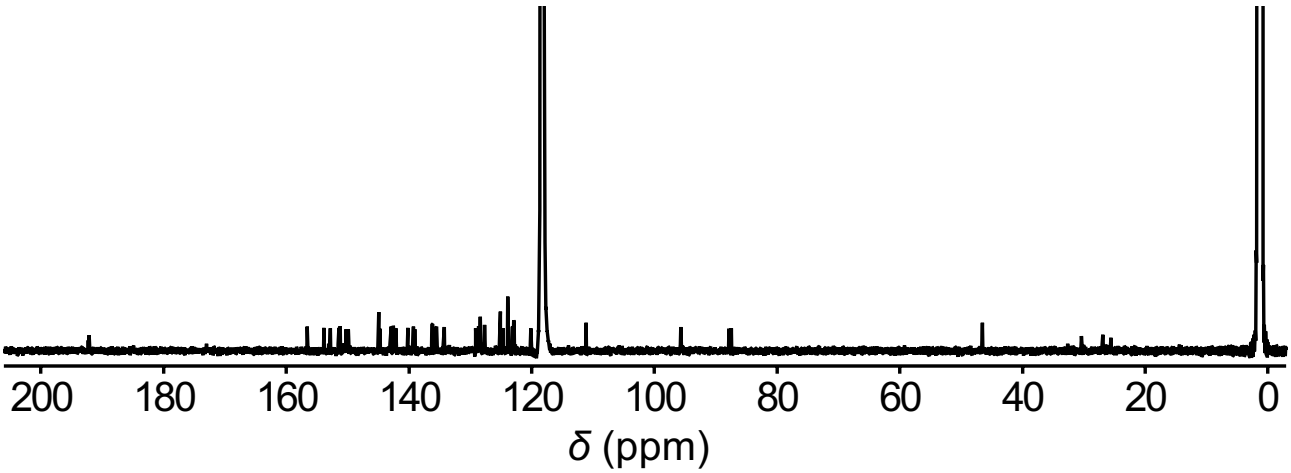

Supplementary Figure 155 | ^{13}C NMR spectrum (151 MHz, 298 K, CD_3CN) of heteroleptic cage Pd_2**B**$_2$**CD¹**.

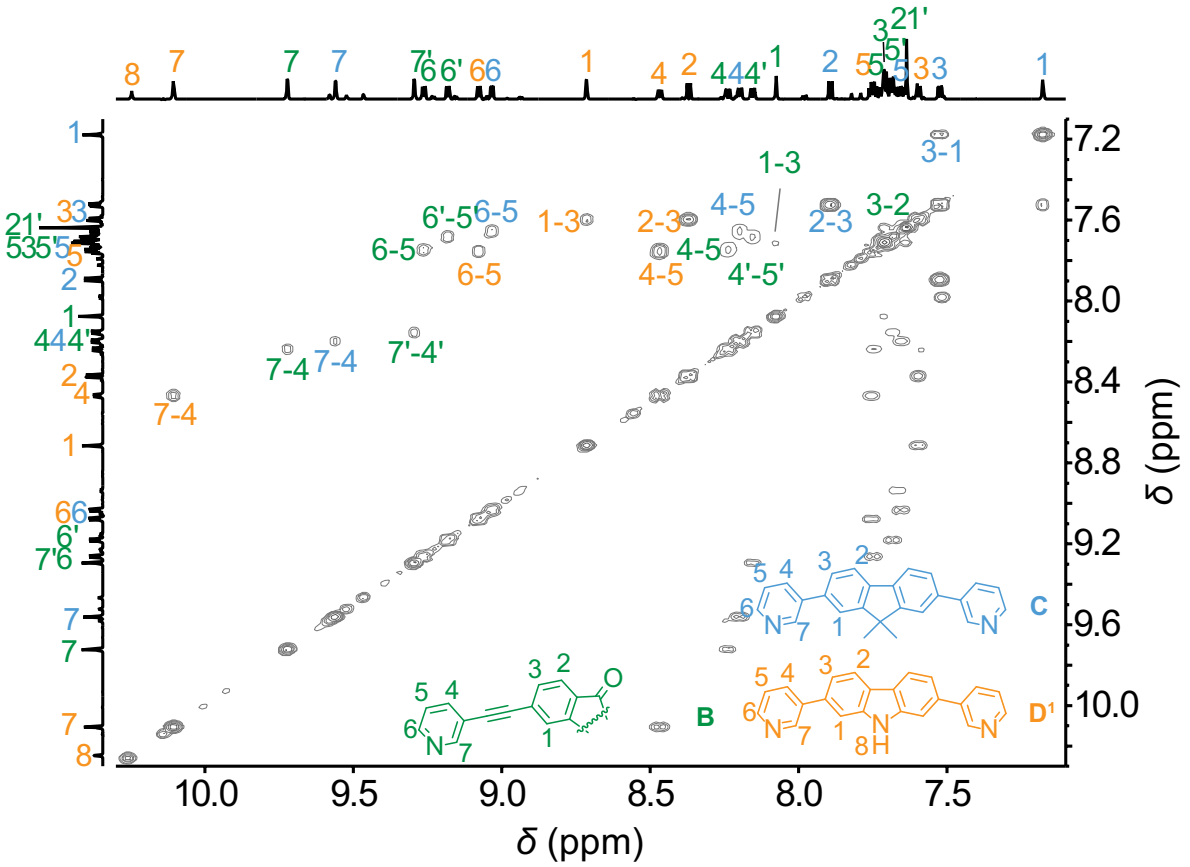

Supplementary Figure 156 | Partial ^{1}H–^{1}H COSY spectrum (500 MHz, 298 K, CD_3CN) of heteroleptic cage $Pd_2\mathbf{B}_2\mathbf{CD}^1$.

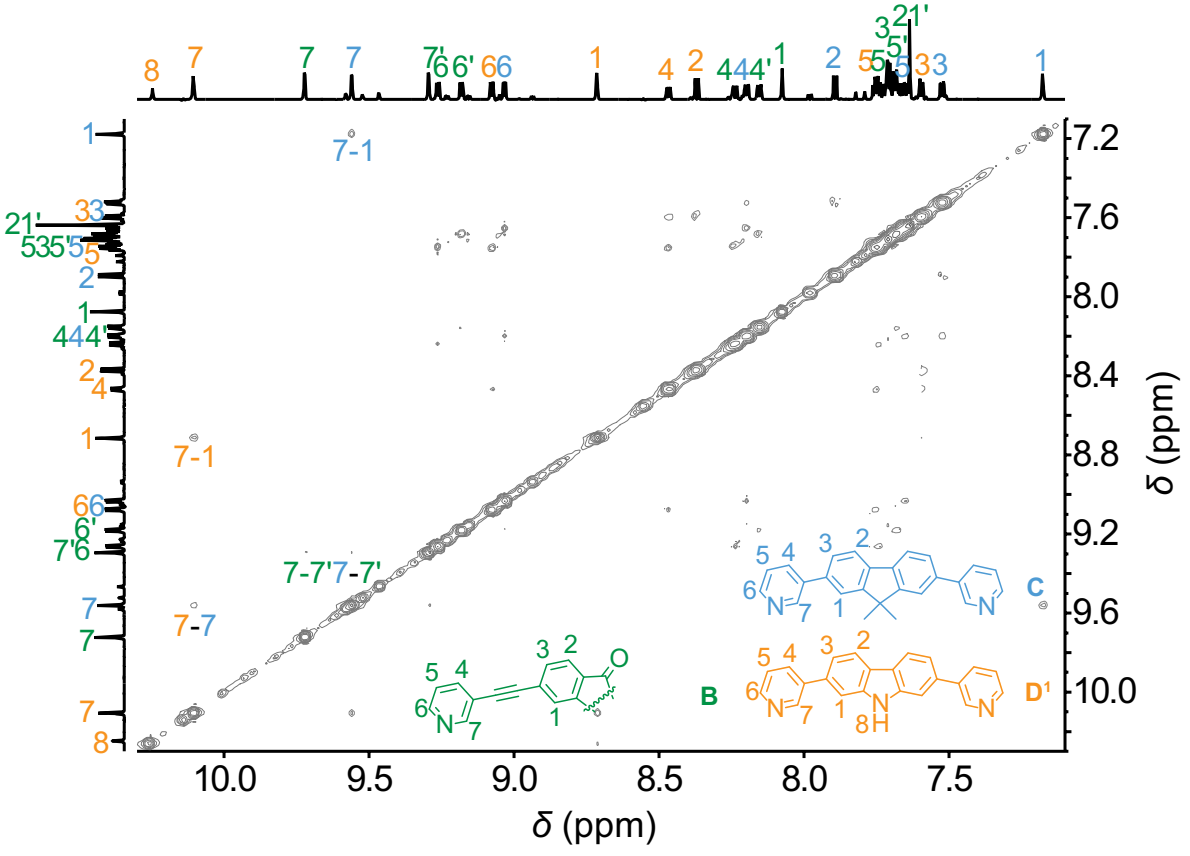

Supplementary Figure 157 | Partial ^{1}H–^{1}H NOESY spectrum (500 MHz, 298 K, CD_3CN) of heteroleptic cage $Pd_2\mathbf{B}_2\mathbf{CD}^1$. The composition of this heteroleptic cage is supported by a single crystal X-ray structure (details see below). The found NOE contacts in solution are in full accordance with the X-ray structure results.

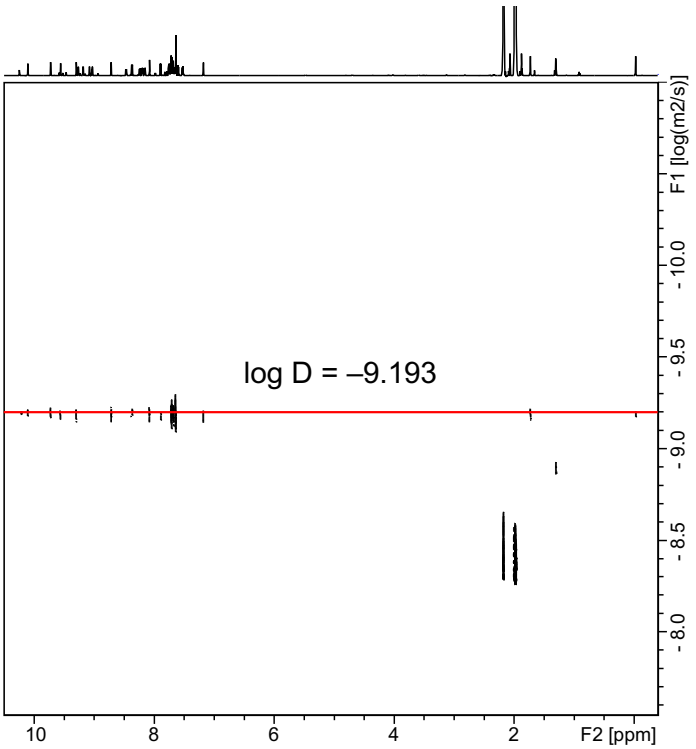

Supplementary Figure 158 | ^{1}H DOSY spectrum (500 MHz, 298 K, CD_3CN) of heteroleptic cage Pd_2**B**$_2$**CD**^{1}. Diffusion coefficient for Pd_2**B**$_2$**CD**^{1}: D = 6.412 × 10^{-10} m^2s^{-1}, log *D* = −9.193, r = 10.2 Å.

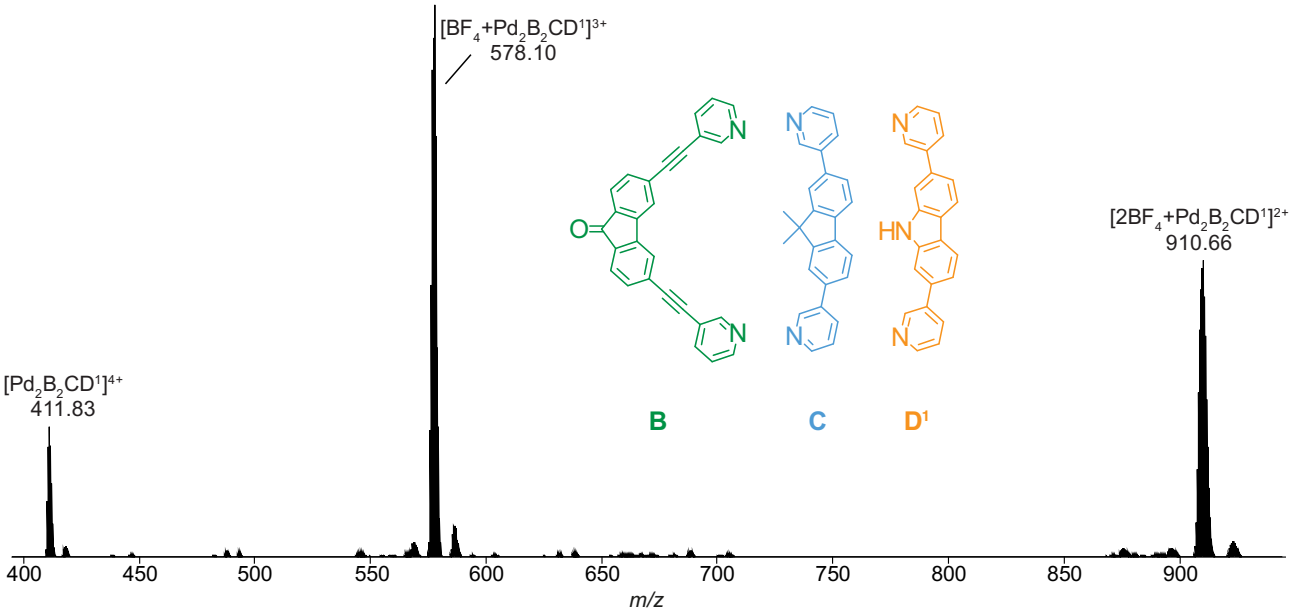

Supplementary Figure 159 | HR-ESI mass spectrum of heteroleptic cage Pd_2**B**$_2$**CD**^{1}.

*3.6.5. Self-assembly of heteroleptic cage Pd_2**ABD**$^1{}_2$*

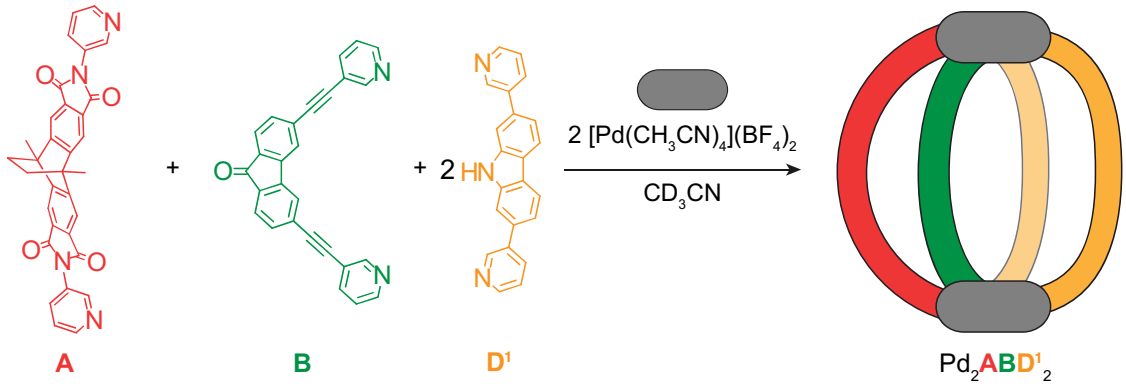

To a suspension of **B** (60 µL, 3 mM, 0.18 µmol) **D**^{1} (120 µL, 3 mM, 0.36 µmol) in CD_3CN and **A** (60 µL, 3 mM, 0.18 µmol) were added a stock solution of $[Pd(CH_3CN)_4](BF_4)_2$ (24 µL, 15 mM/CD_3CN, 0.36 µmol) and 186 µL additional CD_3CN. The mixture was heated at 80 °C for 8 h to give a 0.4 mM cage solution containing the shown cage as predominant species.

^{1}H NMR (700 MHz, 298 K, CD_3CN) δ 9.92 (d, J = 2.7 Hz, 4H), 9.61 (s, 2H), 9.48 (d, J = 2.1 Hz, 2H), 9.13 (d, J = 5.8 Hz, 2H), 8.96 – 8.92 (m, 4H), 8.89 (d, J = 5.7 Hz, 2H), 8.44 (s, 2H), 8.38 – 8.35 (m, 2H), 8.29 (d, J = 7.9 Hz, 2H), 8.22 (dt, J = 8.0, 1.5 Hz, 2H), 8.15 (dd, J = 11.2, 7.8 Hz, 4H), 8.13 – 8.08 (m, 4H), 7.84 (s, 2H), 7.81 – 7.75 (m, 6H), 7.75 (s, 2H), 7.71 – 7.61 (m, 6H), 7.56 (s, 2H), 7.51 (dd, J = 8.1, 1.6 Hz, 2H), 7.48 (dd, J = 7.5, 6.0 Hz, 2H), 2.04 (s, 3H), 1.84 (b, 4H), 1.73 (s, 4H).

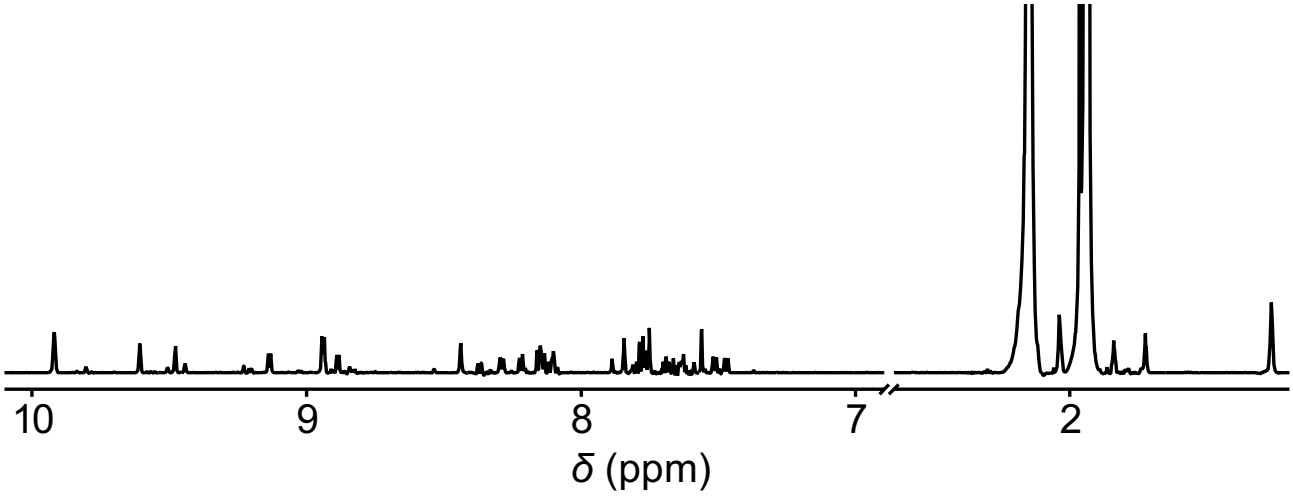

Supplementary Figure 160 | ^{1}H NMR spectrum (700 MHz, 298 K, CD_3CN) of heteroleptic cage Pd_2**ABD**$^1{}_2$.

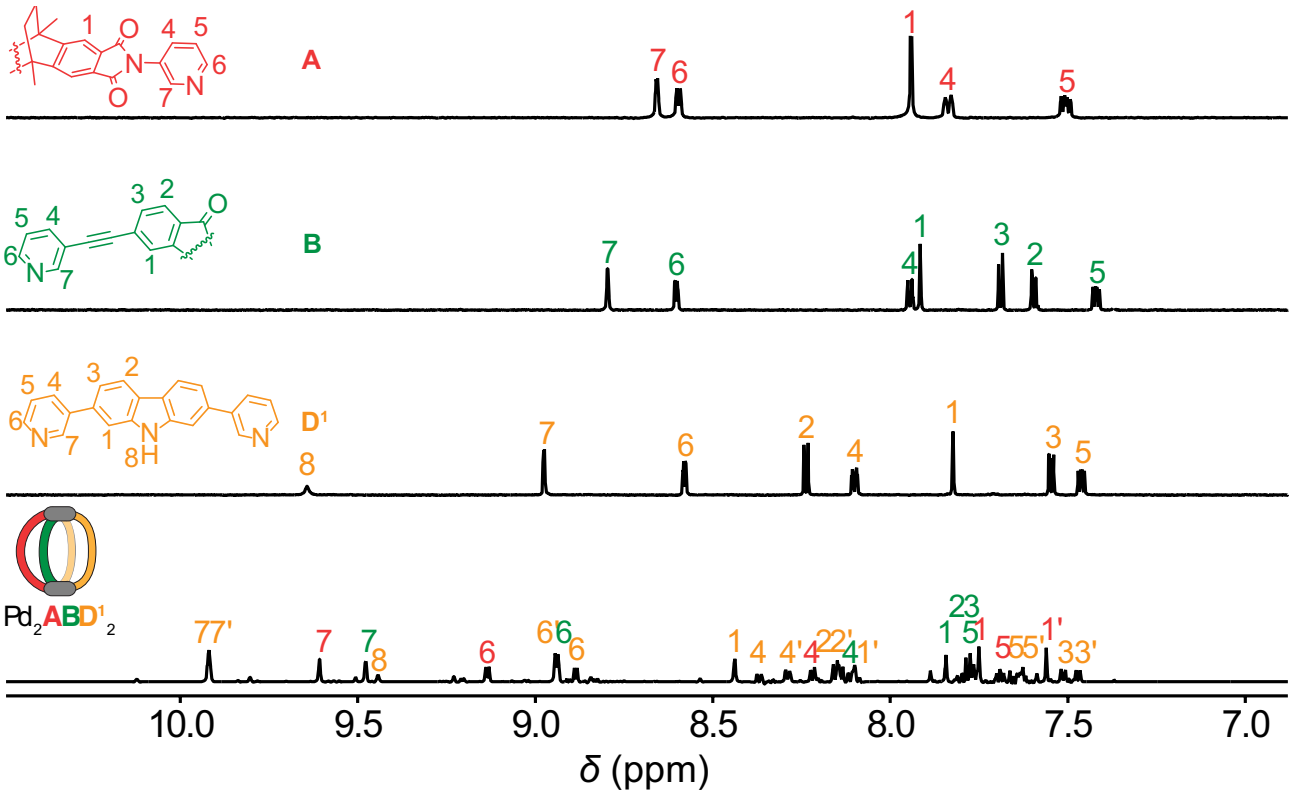

Supplementary Figure 161 | Partial ^{1}H NMR spectrum (700 MHz, 298 K, CD_3CN) comparison of ligand **A** (red), ligand **B** (green), ligand **D^{1}** (yellow) and heteroleptic cage Pd_2**ABD^{1}**$_2$.

^{13}C NMR (176 MHz, 298 K, CD_3CN) δ 192.31, 173.07, 166.94, 166.74, 154.82, 154.62, 153.75, 151.60, 150.35, 150.04, 149.94, 149.66, 149.62, 145.06, 144.68, 142.57, 142.17, 141.18 (d, J = 6.6 Hz), 138.91, 138.85, 138.76, 136.44, 135.56, 133.44, 133.22, 132.24, 130.64, 130.45, 129.43, 128.66, 128.58, 128.53, 128.25, 125.52, 124.79, 124.64, 124.51, 123.39, 122.93, 122.81, 119.51, 119.42, 117.18, 110.65, 110.47, 95.61, 87.97, 45.29, 44.90, 34.46, 33.97, 32.65, 30.37.

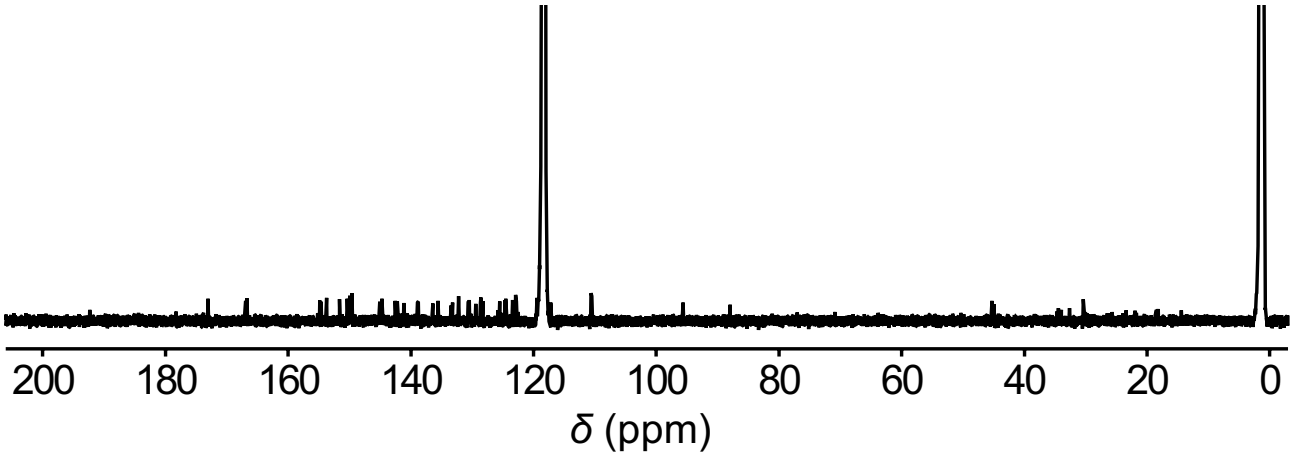

Supplementary Figure 162 | ^{13}C NMR spectrum (176 MHz, 298 K, CD_3CN) of heteroleptic cage Pd_2**ABD^{1}**$_2$.

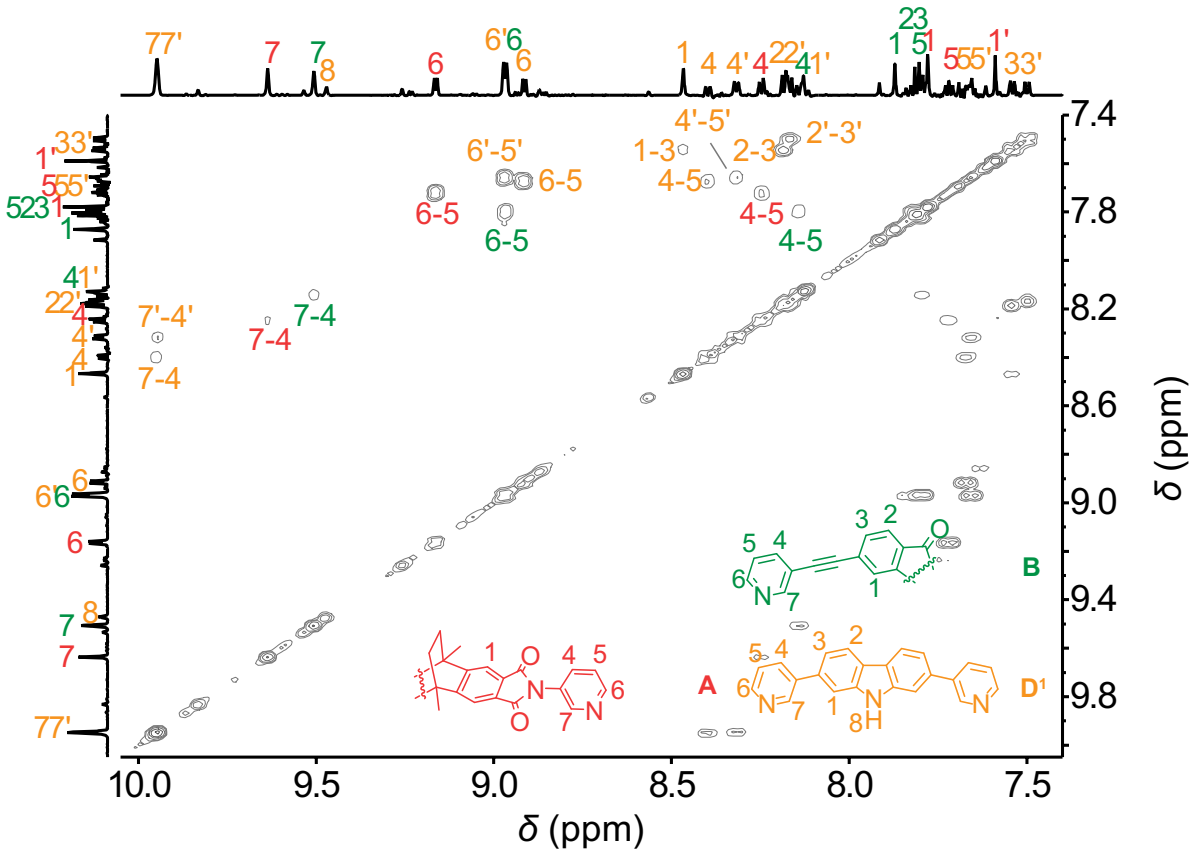

Supplementary Figure 163 | Partial ^{1}H–^{1}H COSY spectrum (500 MHz, 298 K, CD_3CN) of heteroleptic cage Pd_2**ABD**$^{1}_2$.

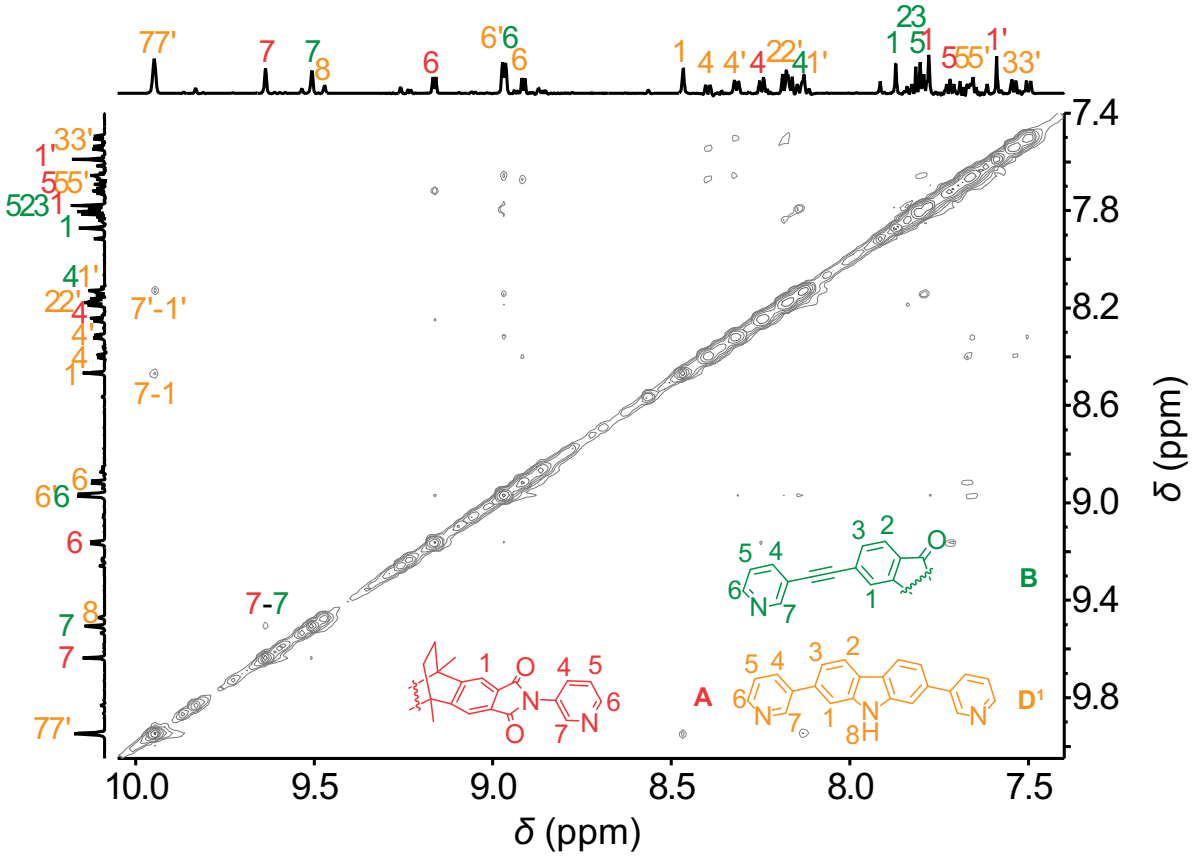

Supplementary Figure 164 | Partial ^{1}H–^{1}H NOESY spectrum (500 MHz, 298 K, CD_3CN) of heteroleptic cage Pd_2**ABD**$^{1}_2$.

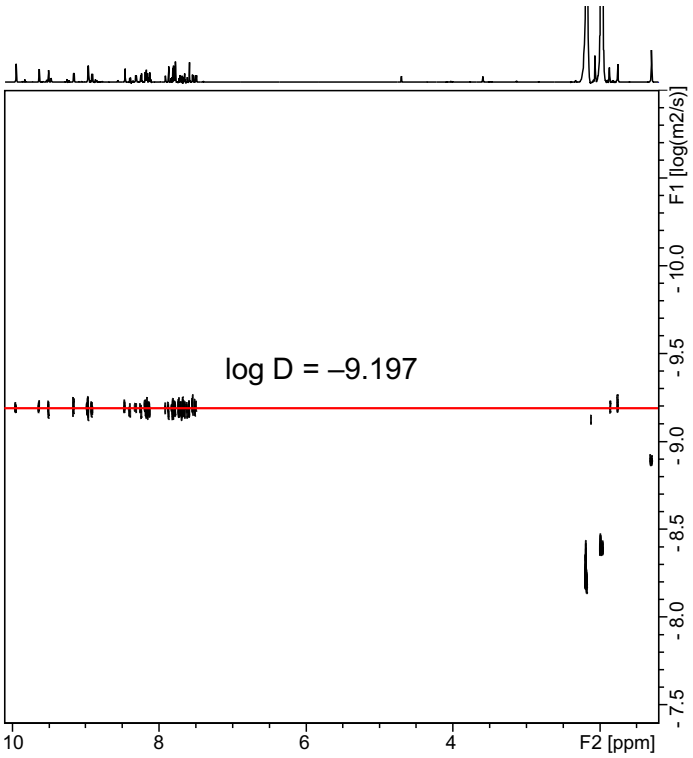

Supplementary Figure 165 | ^{1}H DOSY spectrum (500 MHz, 298 K, CD_3CN) of heteroleptic cage Pd_2**ABD**$^{1}{}_2$. Diffusion coefficient for Pd_2**ABD**$^{1}{}_2$: D = 6.353 × 10^{-10} m^2s^{-1}, log *D* = −9.197, r = 10.3 Å.

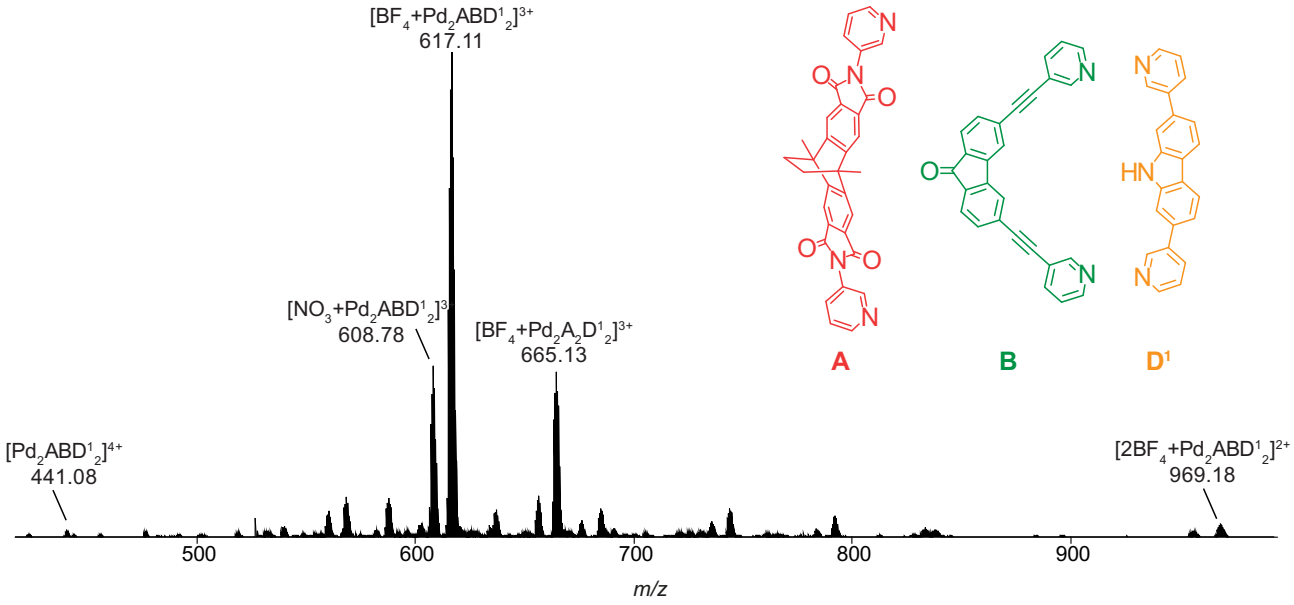

Supplementary Figure 166 | HR-ESI mass spectrum of heteroleptic cage Pd_2**ABD**$^{1}{}_2$.

*3.6.6. Self-assembly of heteroleptic cage Pd_2**ABCD**^{1}*

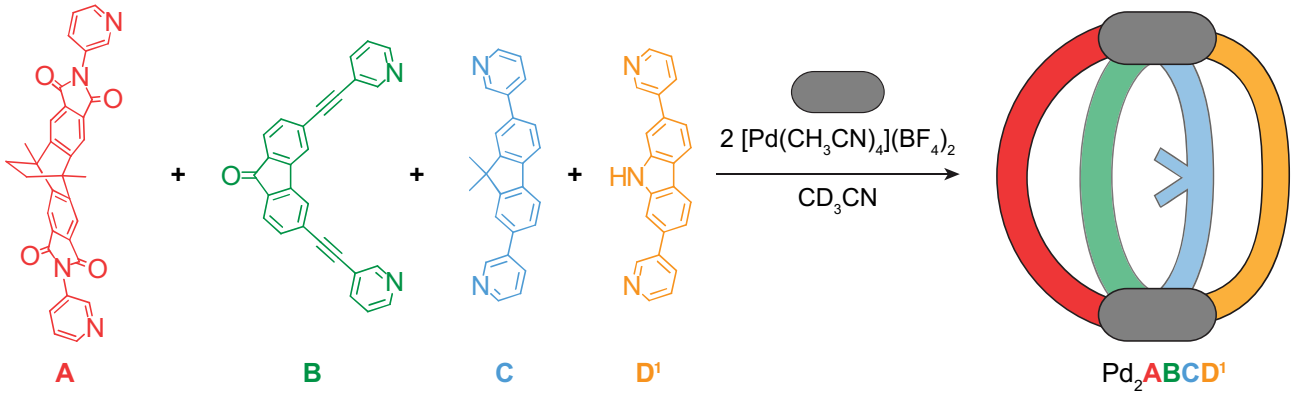

To a solution of **A** (60 µL, 3 mM, 0.18 µmol), **C** (60 µL, 3 mM, 0.18 µmol) and a suspension of **B** (60 µL, 3 mM, 0.18 µmol), **D**^{1} (60 µL, 3 mM, 0.18 µmol) were added a stock solution of $[Pd(CH_3CN)_4](BF_4)_2$ (24 µL, 15 mM/CD_3CN, 0.36 µmol) and additional 186 µL CD_3CN. The mixture was heated at 80 °C for 8 h to give a 0.4 mM cage solution containing the shown cage as predominant species.

^{1}H NMR (700 MHz, 298 K, CD_3CN) δ 9.94 (s, 2H), 9.59 (s, 1H), 9.45 (d, *J* = 2.0 Hz, 2H), 9.39 (s, 2H), 9.31 (s, 2H), 9.12 (d, *J* = 5.9 Hz, 2H), 9.01 (d, *J* = 6.0 Hz, 2H), 8.96 (d, *J* = 5.8 Hz, 2H), 8.80 (d, *J* = 6.0 Hz, 2H), 8.48 (d, *J* = 7.9 Hz, 2H), 8.44 (s, 2H), 8.33 (d, *J* = 7.9 Hz, 2H), 8.17 – 8.13 (m, 6H), 7.83 (d, *J* = 7.6 Hz, 2H), 7.76 – 7.73 (m, 3H), 7.73 – 7.69 (m, 7H), 7.69 – 7.66 (m, 3H), 7.63 (s, 2H), 7.62 (s, 2H), 7.54 (d, *J* = 7.9 Hz, 2H), 7.46 (d, *J* = 7.5 Hz, 2H), 7.02 (s, 2H), 1.91 (s, 3H), 1.89 (s, 3H), 1.78 (s, 4H), 1.42 (s, 3H), -0.21 (s, 3H).

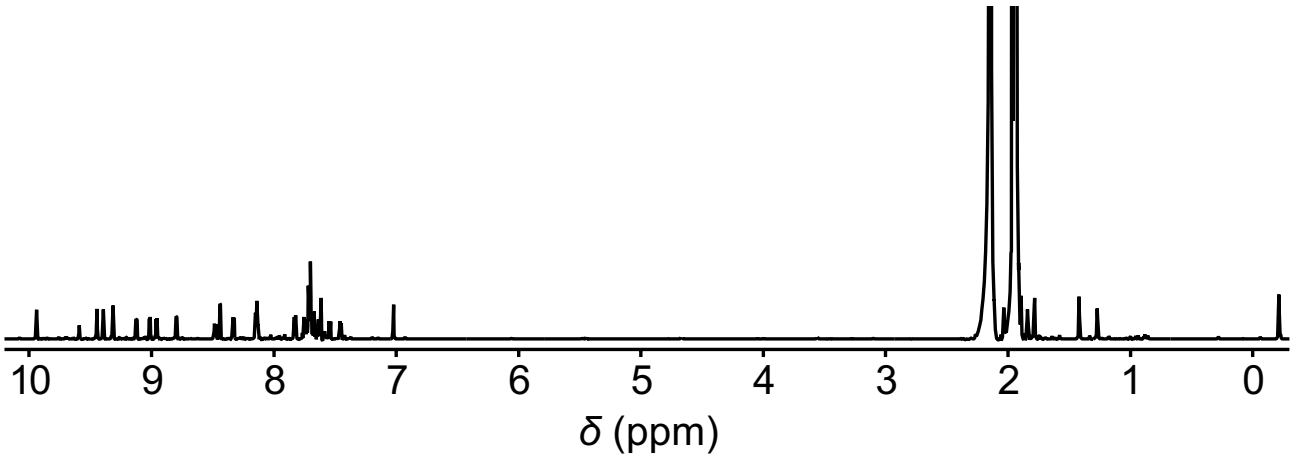

Supplementary Figure 167 | ^{1}H NMR spectrum (700 MHz, 298 K, CD_3CN) of heteroleptic cage Pd_2**ABCD**^{1}.

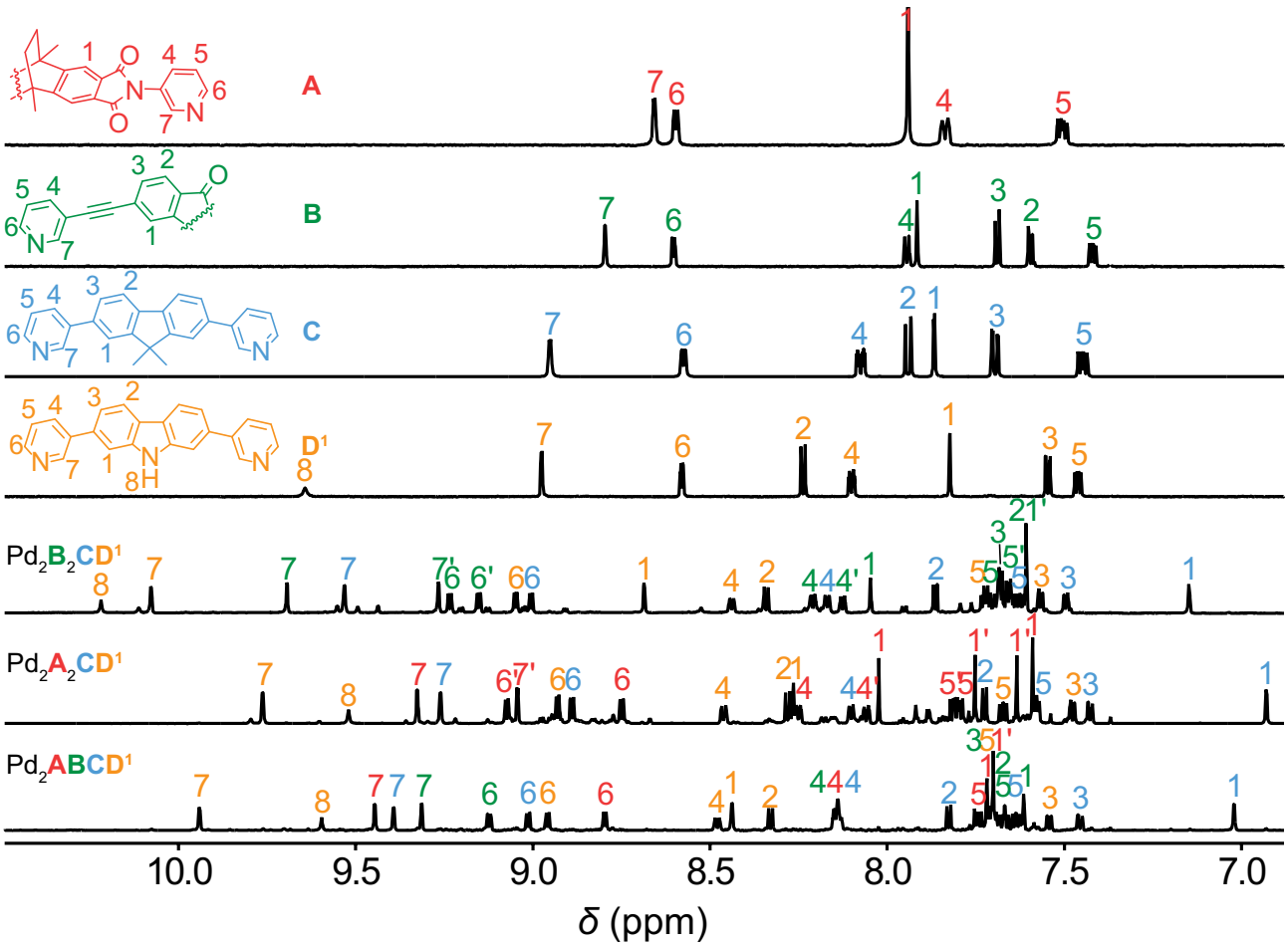

Supplementary Figure 168 | Partial ^{1}H NMR spectrum (700 MHz, 298 K, CD_3CN) comparison of ligands **A** (red), **B** (green), **C** (blue), **D**^{1} (yellow), heteroleptic cages Pd_2**B**$_2$**CD**^{1}, Pd_2**A**$_2$**CD**^{1} and Pd_2**ABCD**^{1}.

^{13}C NMR (176 MHz, 298 K, CD_3CN) δ 192.24, 173.05, 167.12, 167.01, 156.39, 154.79, 154.52, 153.67, 151.32, 150.28, 150.24, 150.21, 150.17, 150.02, 149.97, 144.87, 144.68, 143.42, 143.02, 141.94, 140.10, 139.58, 139.07, 138.67, 136.18, 135.58, 135.49, 134.51, 132.01, 130.99, 130.61, 128.98, 128.50, 128.45, 128.42, 127.60, 125.34, 125.13, 124.32, 123.56, 122.99, 122.79, 122.63, 120.51, 117.47, 111.36, 95.36, 87.46, 46.44, 45.15, 45.13, 34.34, 26.84, 25.19, 18.53, 18.31.

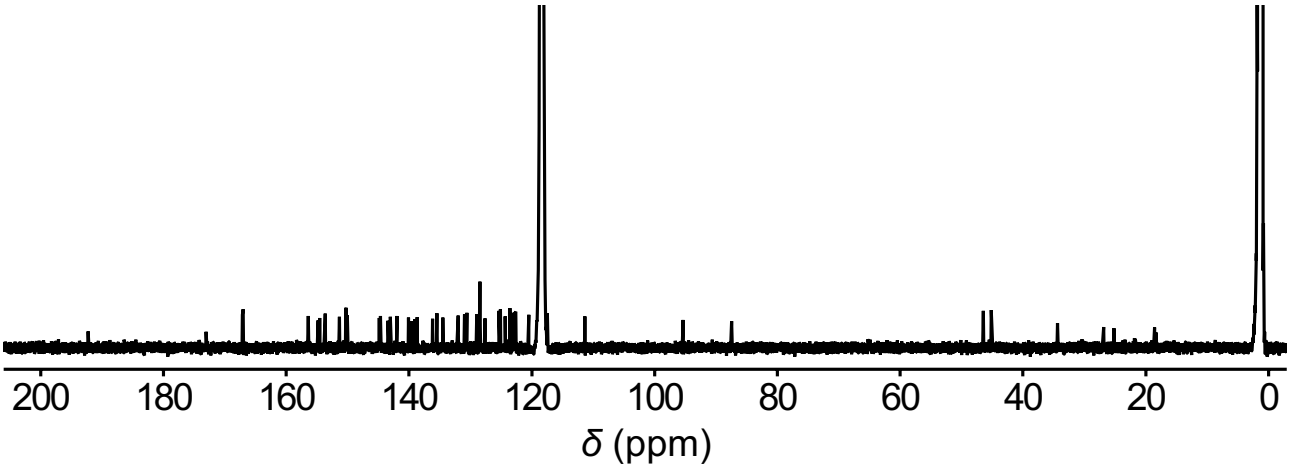

Supplementary Figure 169 | ^{13}C NMR spectrum (176 MHz, 298 K, CD_3CN) of heteroleptic cage Pd_2**ABCD**^{1}.

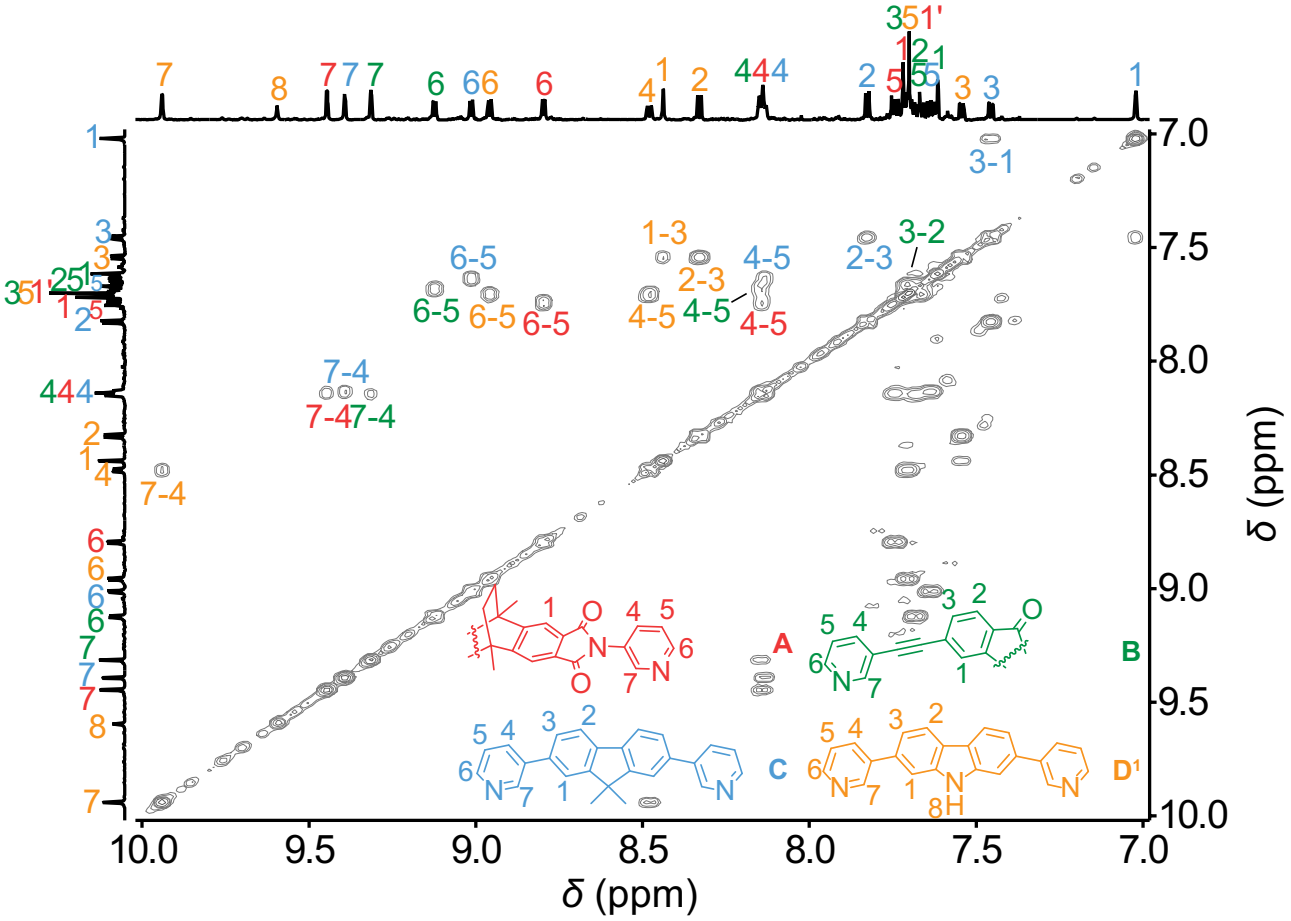

Supplementary Figure 170 | Partial ^{1}H–^{1}H COSY spectrum (500 MHz, 298 K, CD_3CN) of heteroleptic cage Pd_2**ABCD**^{1}.

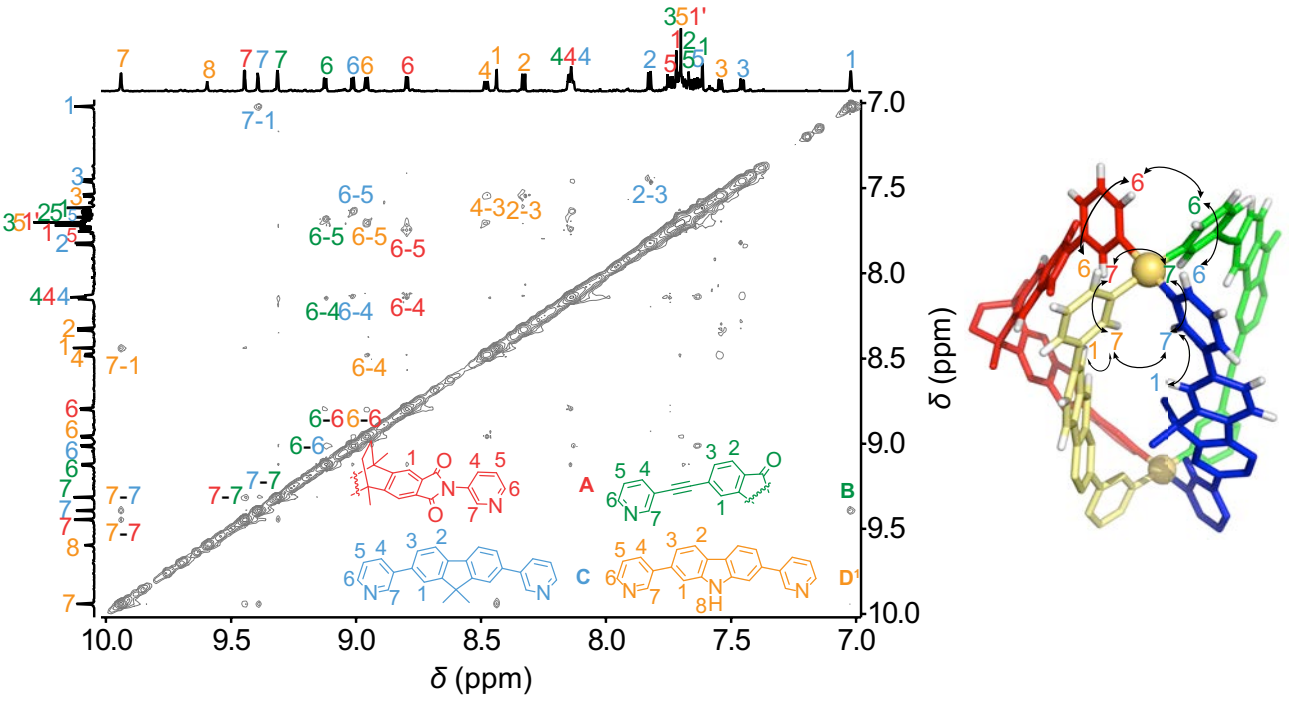

Supplementary Figure 171 | Partial ^{1}H–^{1}H NOESY spectrum (500 MHz, 298 K, CD_3CN) of heteroleptic cage Pd_2**ABCD**^{1}.

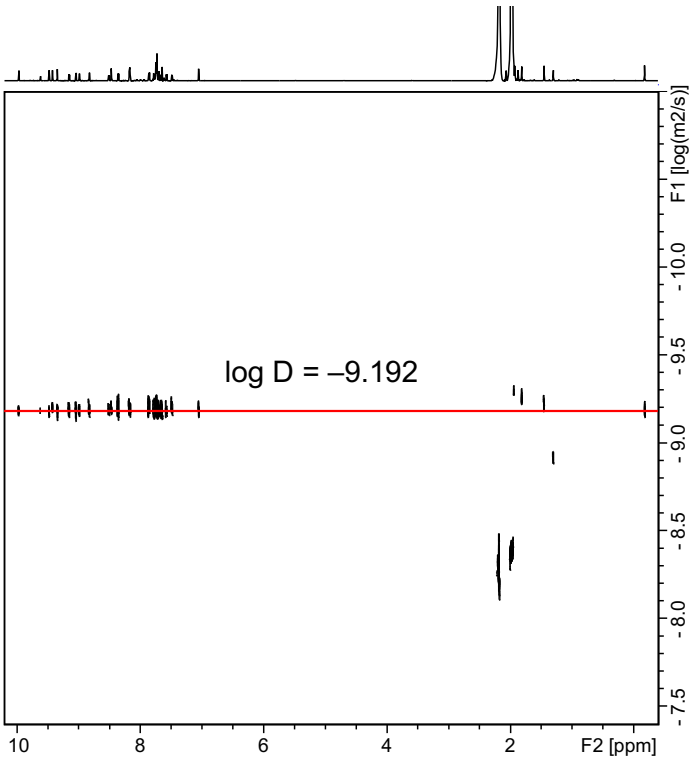

Supplementary Figure 172 | ^{1}H DOSY spectrum (500 MHz, 298 K, CD_3CN) of heteroleptic cage Pd_2**ABCD**^{1}. Diffusion coefficient for Pd_2**ABCD**^{1}: D = 6.427 × 10^{-10} m^2s^{-1}, log *D* = −9.192, r = 10.2 Å.

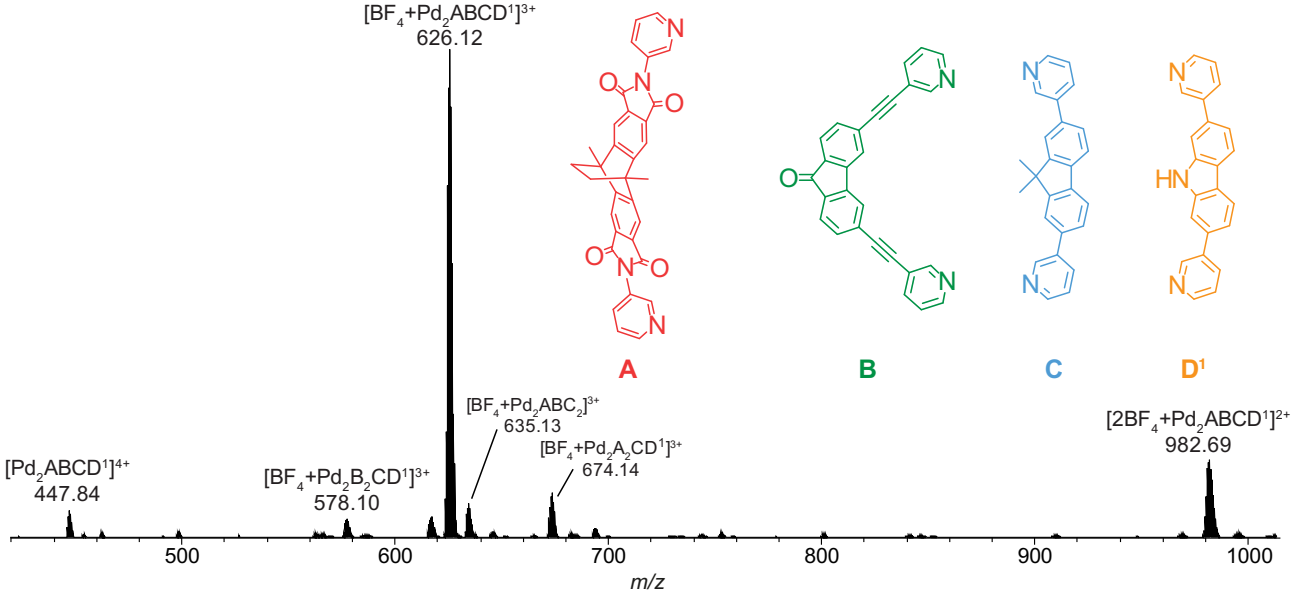

Supplementary Figure 173 | HR-ESI mass spectrum of heteroleptic cage Pd_2**ABCD**^{1}.

3.7. Evolution of heteroleptic cage Pd_2ABCD^{2}

3.7.1. Self-assembly of heteroleptic cage Pd_2***A***$_2$***D***^{2}$_2$

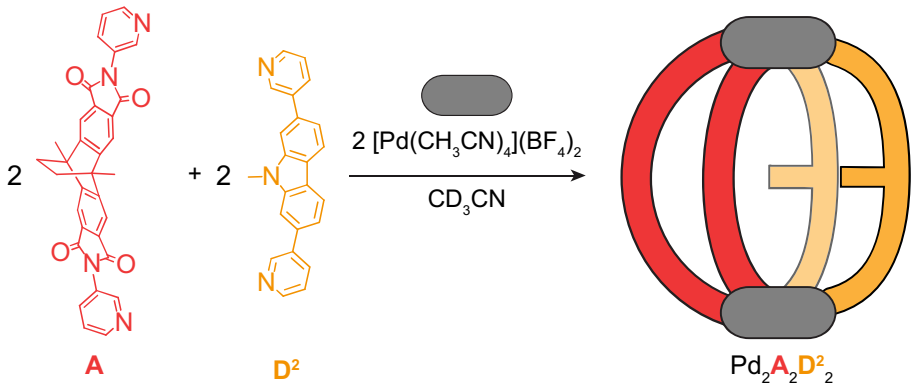

To a solution of **D²** (120 µL, 3 mM, 0.36 µmol) in CD_3CN and **A** (120 µL, 3 mM, 0.36 µmol) were added a stock solution of $[Pd(CH_3CN)_4](BF_4)_2$ (24 µL, 15 mM/CD_3CN, 0.36 µmol) and 186 µL additional CD_3CN. The mixture was heated at 80 °C for 8 h to give a 0.4 mM cage solution containing the shown cage as predominant species.

^{1}H NMR (500 MHz, 298 K, CD_3CN) δ 9.62 (s, 4H), 9.25 (d, J = 2.2 Hz, 4H), 8.93 (t, J = 5.4 Hz, 8H), 8.30 (d, J = 8.0 Hz, 4H), 8.20 – 8.13 (m, 8H), 7.89 (s, 4H), 7.81 (dd, J = 8.3, 5.7 Hz, 4H), 7.69 – 7.61 (m, 8H), 7.56 (s, 4H), 7.36 (dd, J = 8.0, 1.6 Hz, 4H), 2.93 (s, 6H), 2.18 (s, 6H), 1.90 (s, 6H), 1.75 (b, 8H).

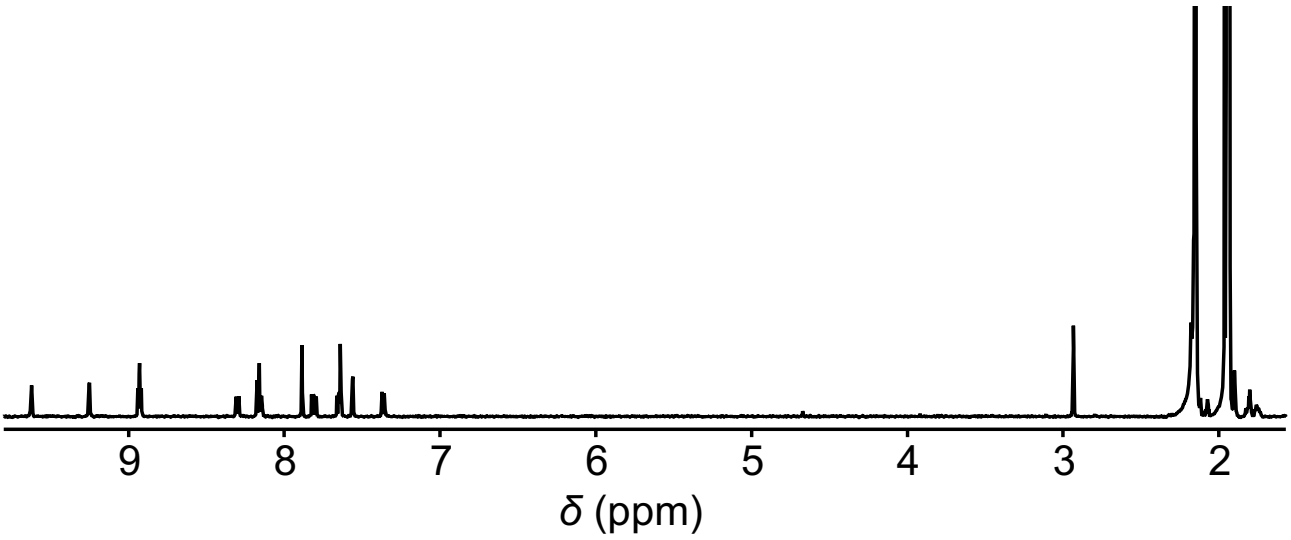

Supplementary Figure 174 | ^{1}H NMR spectrum (500 MHz, 298 K, CD_3CN) of heteroleptic cage $Pd_2\mathbf{A}_2\mathbf{D}^2_2$.

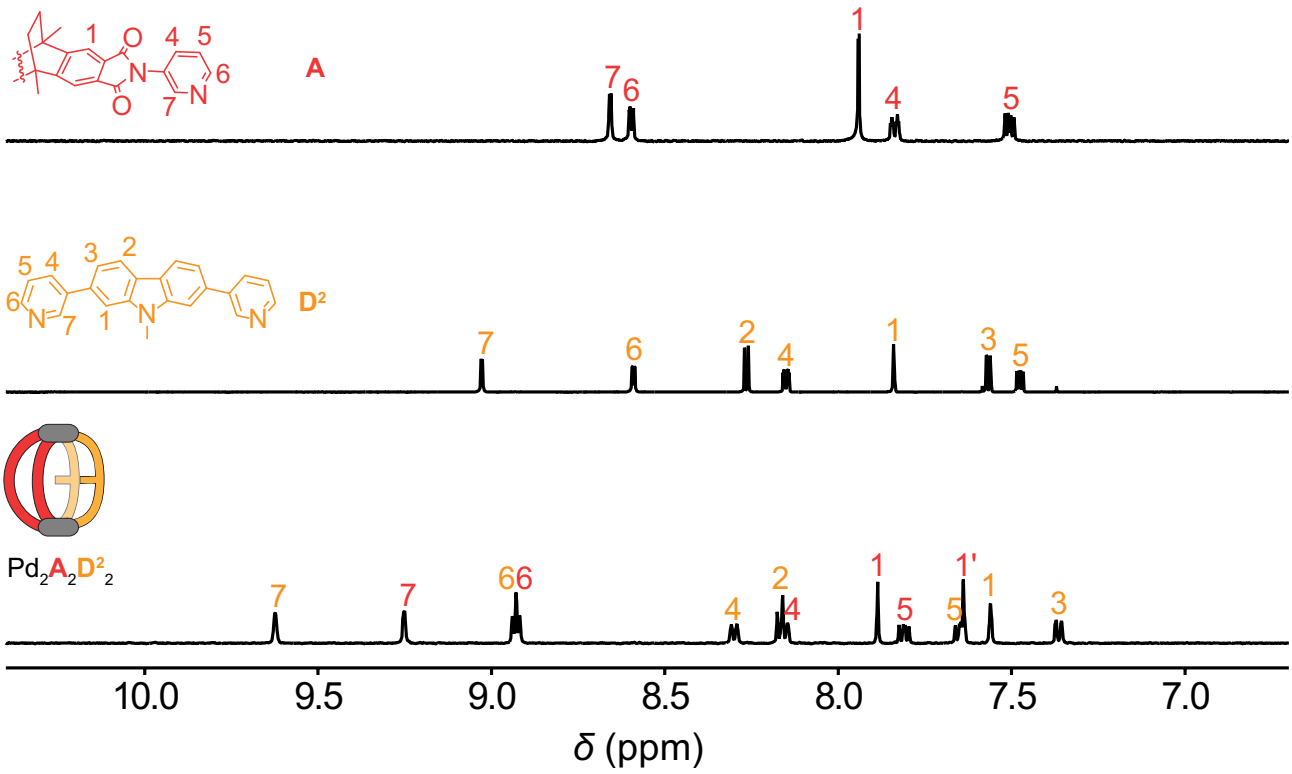

Supplementary Figure 175 | Partial ^{1}H NMR spectrum (700 MHz, 298 K, CD_3CN) comparison of ligand **A** (red), ligand **D²** (yellow) and heteroleptic cage $Pd_2\mathbf{A}_2\mathbf{D}^2_2$.

^{13}C NMR (126 MHz, 298 K, CD_3CN) δ 155.54, 154.74, 150.44, 150.26, 143.95, 143.30, 142.92, 140.60, 139.85, 139.05, 138.74, 134.55, 131.99, 130.50, 130.46, 128.63, 128.29, 123.58, 122.54, 120.18, 117.87, 117.33, 108.97, 57.16, 45.35, 33.96, 30.39, 28.58.

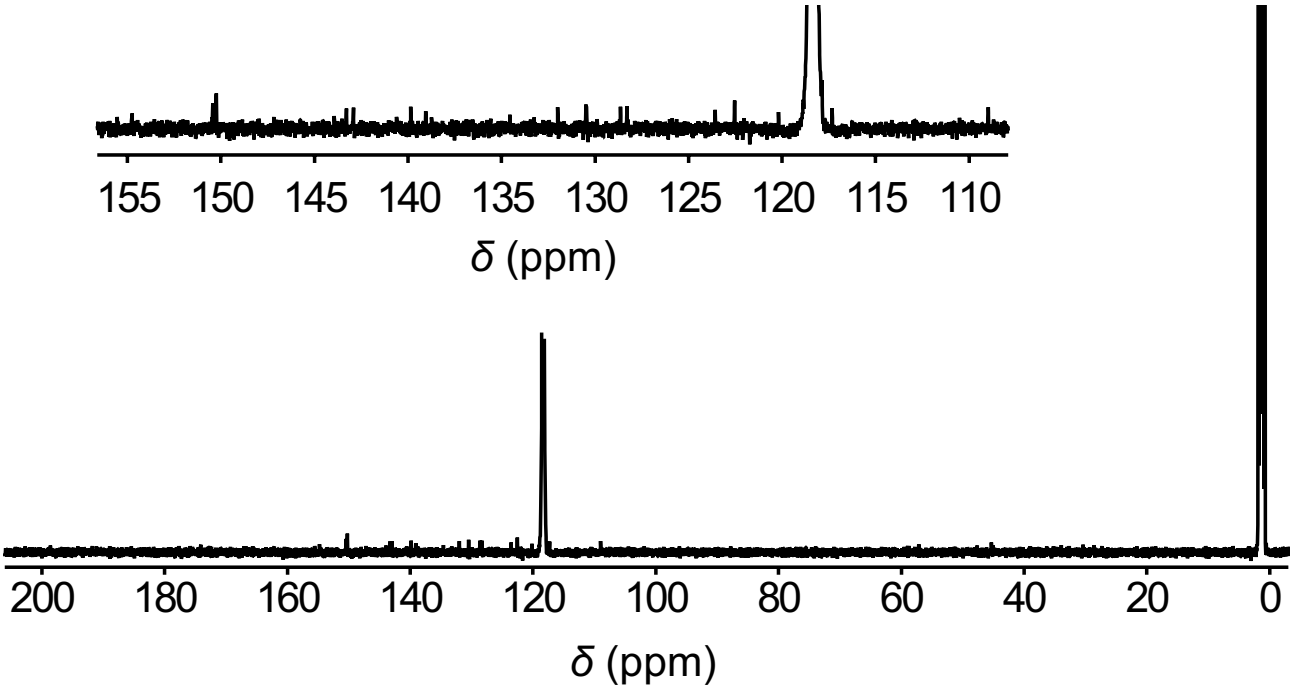

Supplementary Figure 176 | ^{13}C NMR spectrum (126 MHz, 298 K, CD_3CN) of heteroleptic cage $Pd_2\mathbf{A}_2\mathbf{D}^2_2$. The ^{13}C signals are quite weak, even using long measurement time, thus less than expected number of signals were observed.

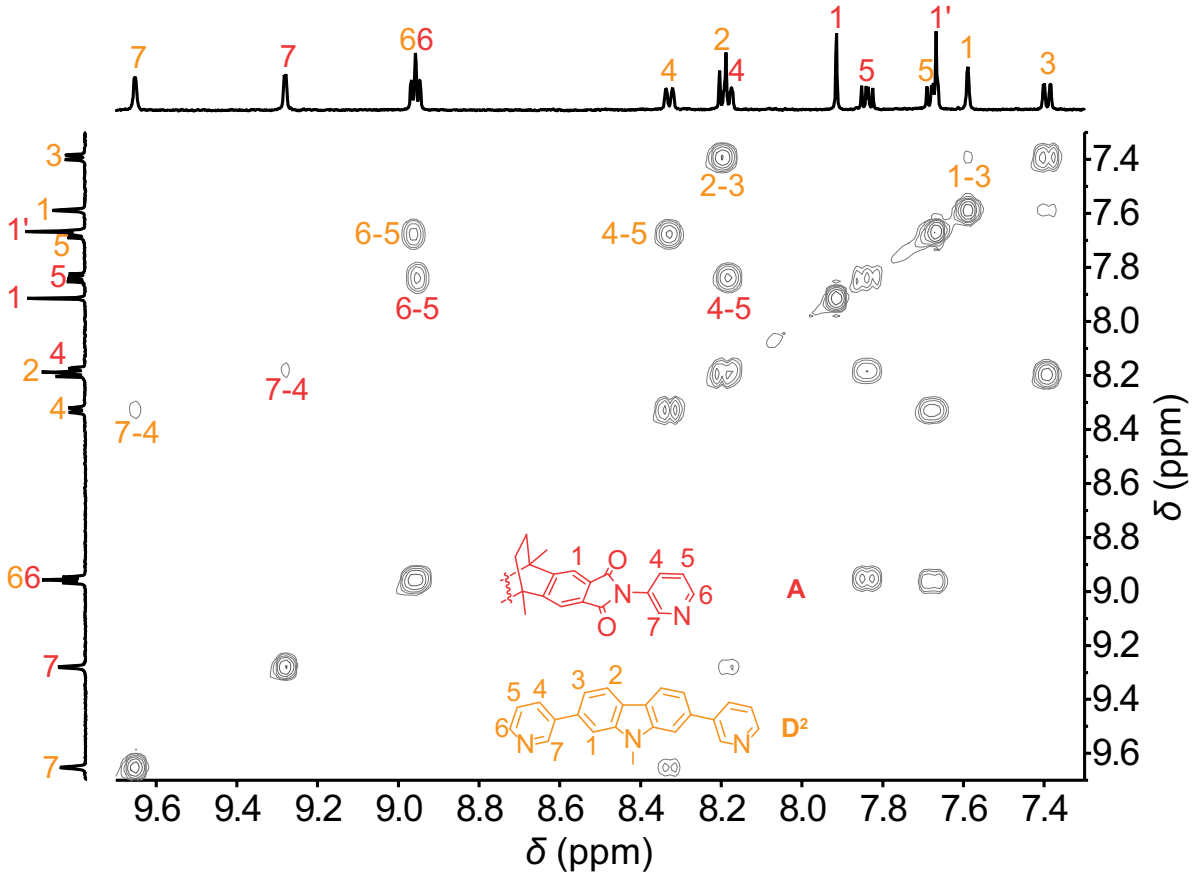

Supplementary Figure 177 | Partial ^{1}H–^{1}H COSY spectrum (500 MHz, 298 K, CD_3CN) of heteroleptic cage $Pd_2\mathbf{A}_2\mathbf{D}^2{}_2$.

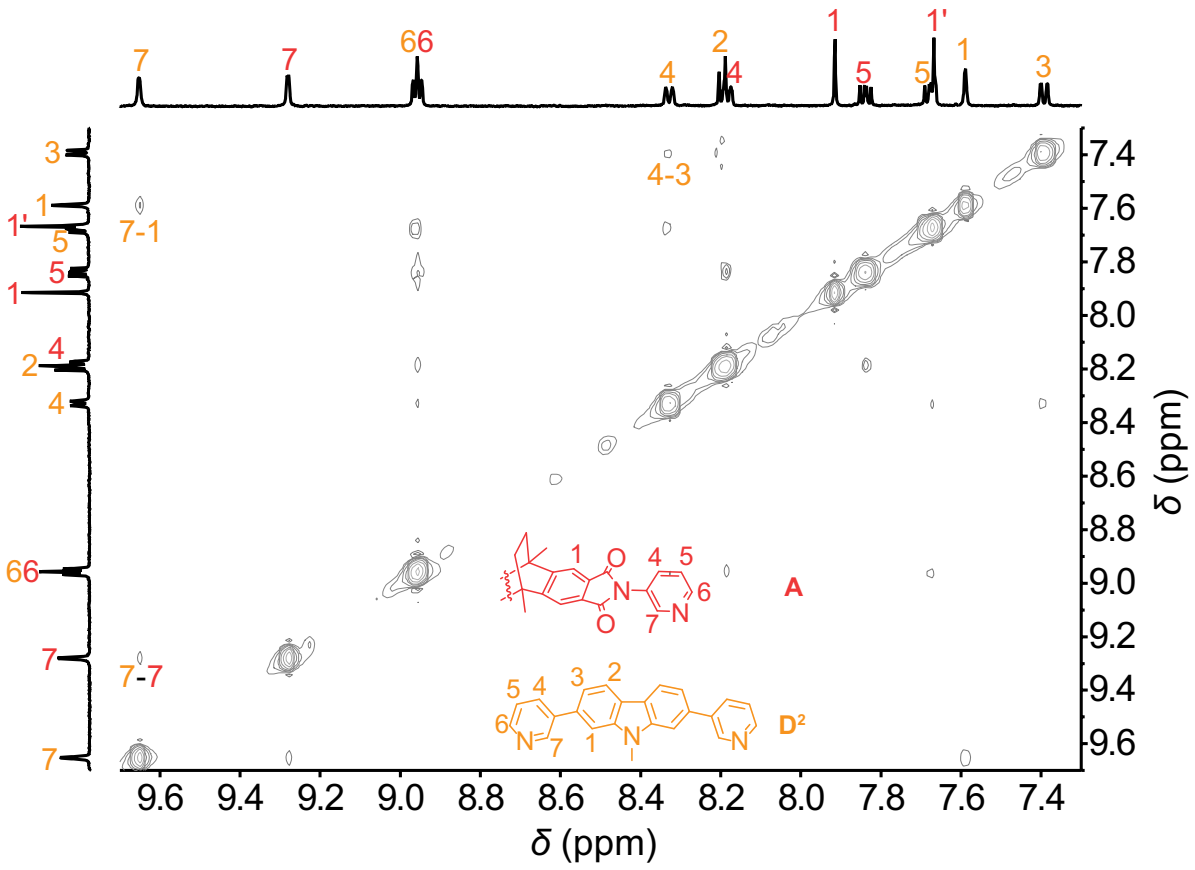

Supplementary Figure 178 | Partial ^{1}H–^{1}H NOESY spectrum (500 MHz, 298 K, CD_3CN) of heteroleptic cage $Pd_2\mathbf{A}_2\mathbf{D}^2{}_2$.

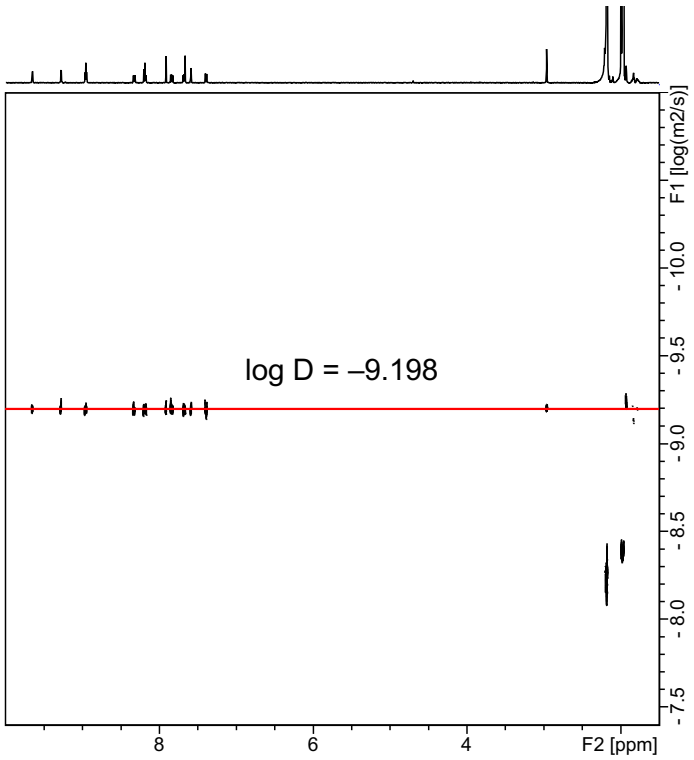

Supplementary Figure 179 | ^{1}H DOSY spectrum (500 MHz, 298 K, CD_3CN) of heteroleptic cage $Pd_2\mathbf{A}_2\mathbf{D}^2_2$. Diffusion coefficient for $Pd_2\mathbf{A}_2\mathbf{D}^2_2$: D = 6.339 × 10^{-10} m^2s^{-1}, log *D* = −9.198, r = 10.3 Å.

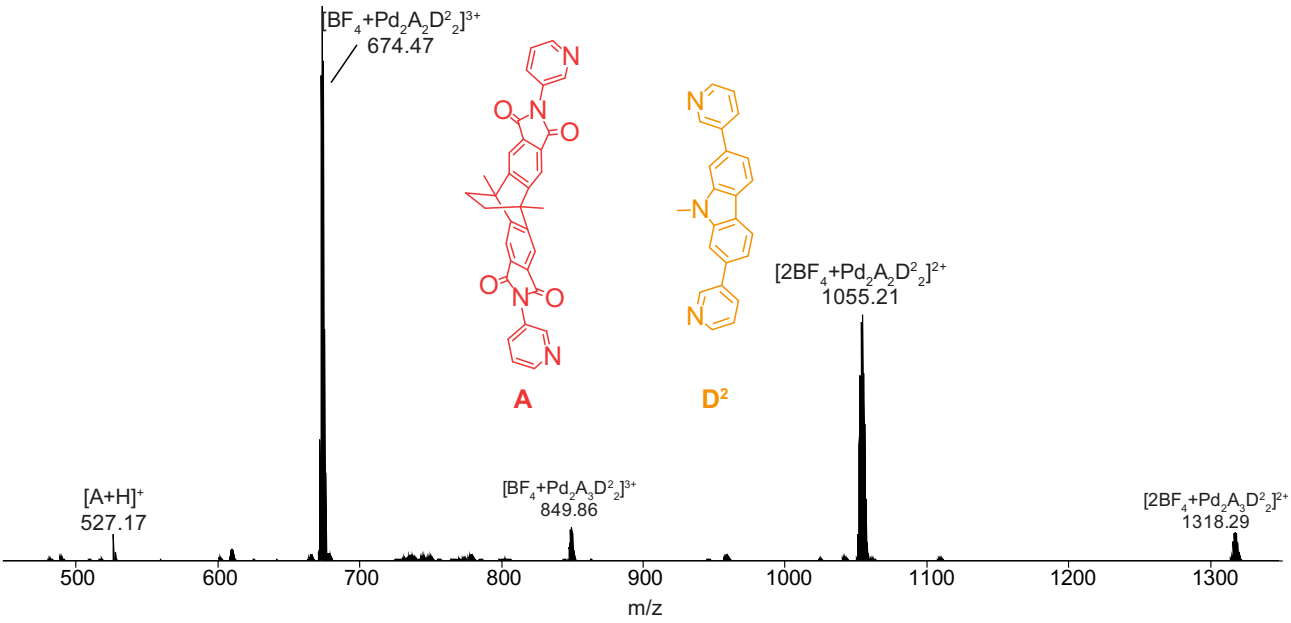

Supplementary Figure 180 | HR-ESI mass spectrum of heteroleptic cage $Pd_2\mathbf{A}_2\mathbf{D}^2_2$.

3.7.2. Self-assembly of heteroleptic cage $Pd_2\mathbf{B}_2\mathbf{D}^2_2$

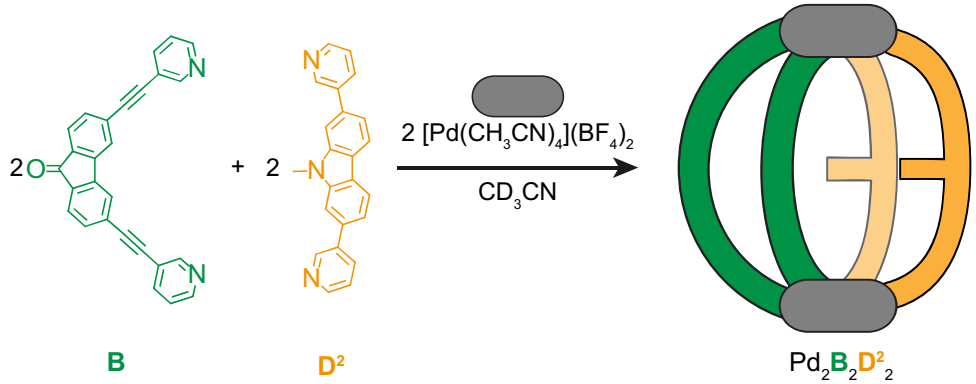

To a solution of **D²** (120 µL, 3 mM, 0.36 µmol) in CD_3CN and a suspension of **B** (120 µL, 3 mM, 0.36 µmol) were added a stock solution of $[Pd(CH_3CN)_4](BF_4)_2$ (24 µL, 15 mM/CD_3CN, 0.36 µmol) and 186 µL additional CD_3CN. The mixture was heated at 80 °C for 8 h to give a 0.4 mM cage solution containing the shown cage as predominant species.

^{1}H NMR (500 MHz, 298 K, CD_3CN) δ 9.92 (d, J = 2.0 Hz, 4H), 9.53 (d, J = 1.9 Hz, 4H), 9.19 (dd, J = 5.8, 1.4 Hz, 4H), 9.05 (dd, J = 5.7, 1.2 Hz, 4H), 8.36 – 8.31 (m, 4H), 8.25 (d, J = 8.0 Hz, 4H), 8.14 (d, J = 8.0 Hz, 4H), 7.87 (s, 4H), 7.69 (ddd, J = 10.5, 5.3, 2.2 Hz, 12H), 7.64 – 7.58 (m, 8H), 7.43 (dd, J = 8.0, 1.6 Hz, 4H), 3.75 (s, 6H).

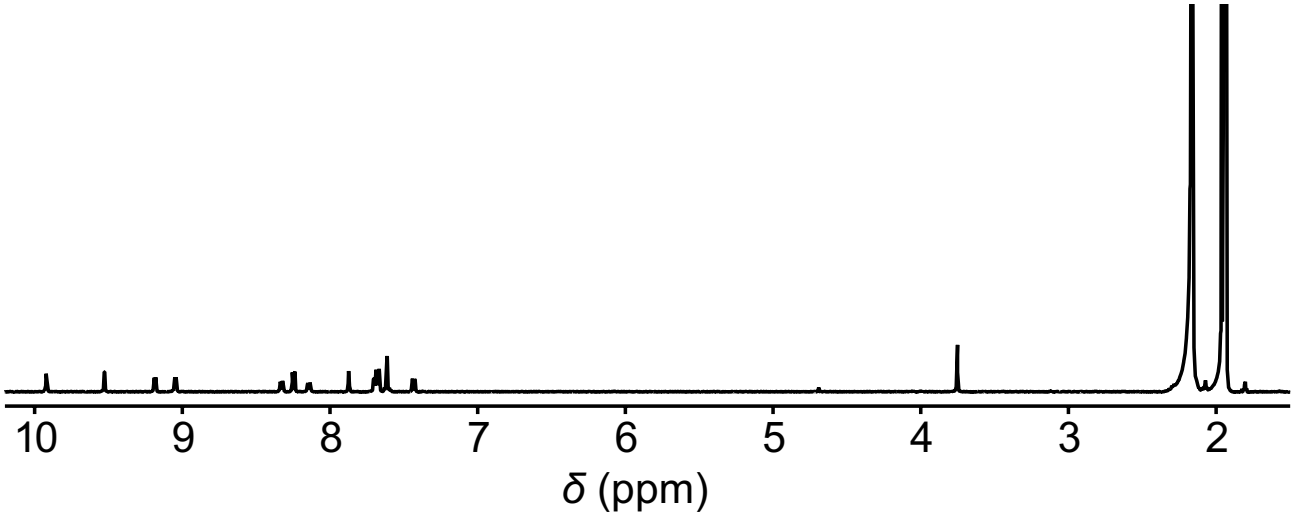

Supplementary Figure 181 | ^{1}H NMR spectrum (500 MHz, 298 K, CD_3CN) of heteroleptic cage $Pd_2\mathbf{B}_2\mathbf{D}^2{}_2$.

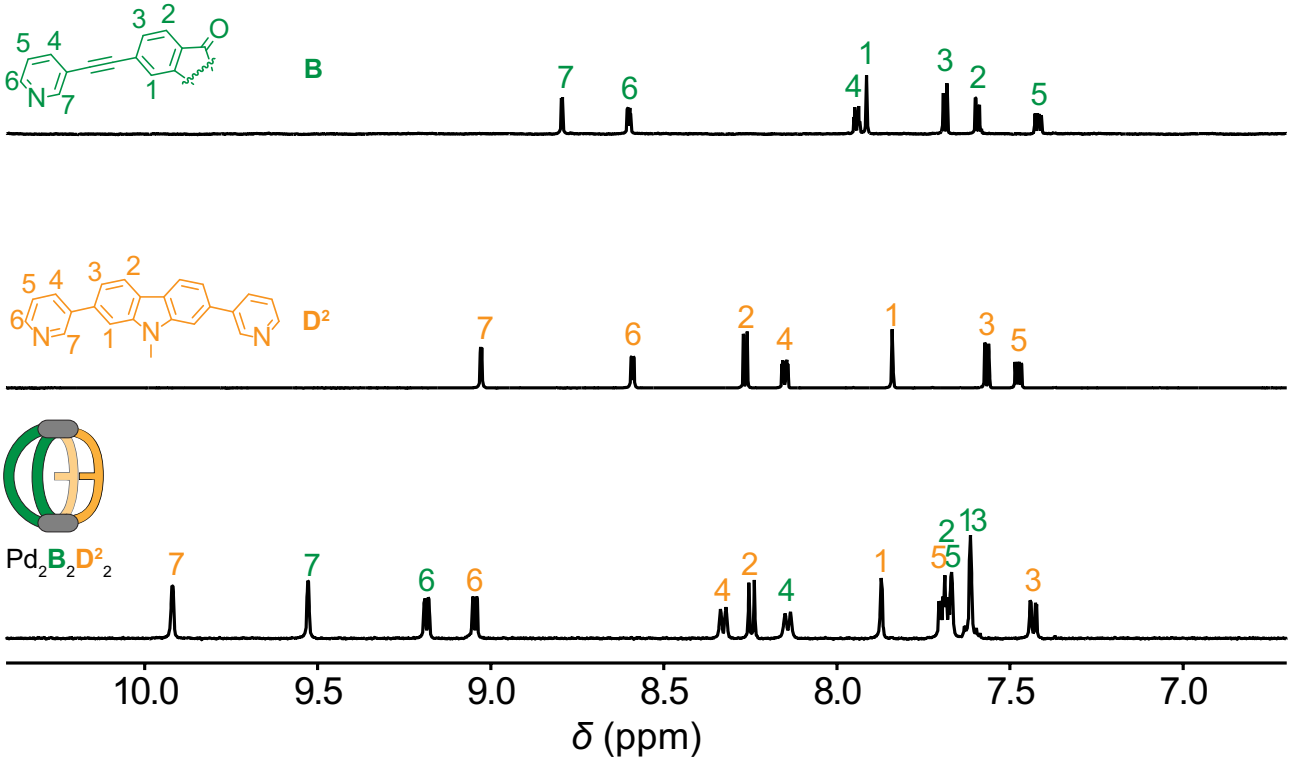

Supplementary Figure 182 | Partial ^{1}H NMR spectrum (700 MHz, 298 K, CD_3CN) comparison of ligand **B** (green), ligand **D²** (yellow) and heteroleptic cage $Pd_2\mathbf{B}_2\mathbf{D}^2_2$.

^{13}C NMR (126 MHz, 298 K, CD_3CN) δ 203.72, 153.62, 151.38, 150.71, 149.99, 144.81, 144.64, 143.26, 142.78, 139.47, 136.08, 135.40, 134.29, 128.82, 128.59, 128.32, 125.13, 124.53, 123.77, 123.75, 122.89, 119.85, 109.11, 95.56, 87.62, 30.37, 29.16.

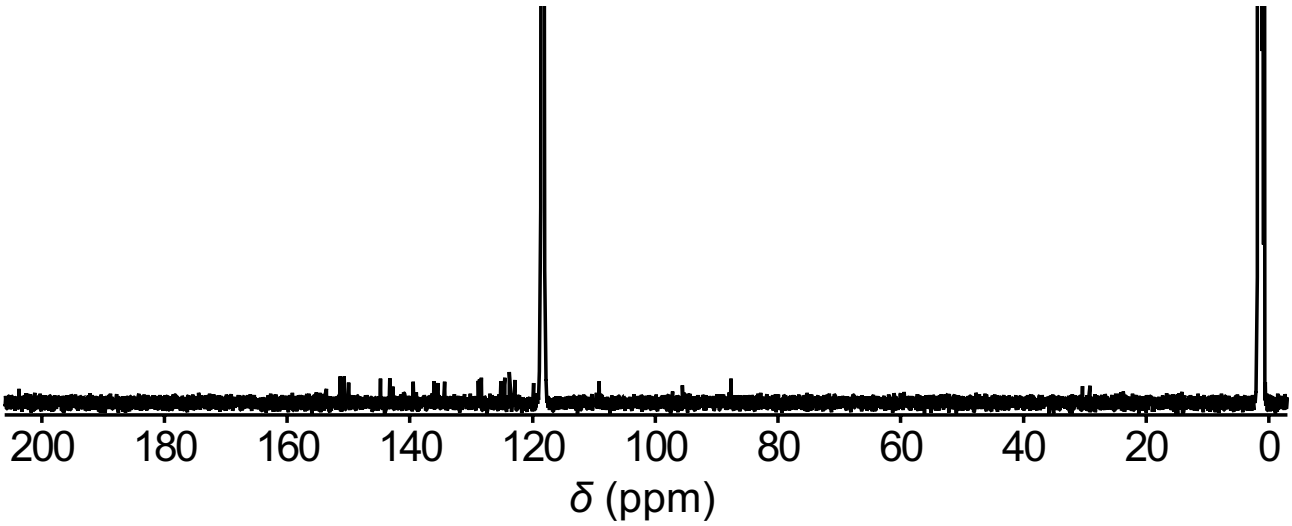

Supplementary Figure 183 | ^{13}C NMR spectrum (126 MHz, 298 K, CD_3CN) of heteroleptic cage $Pd_2\mathbf{B}_2\mathbf{D}^2_2$.

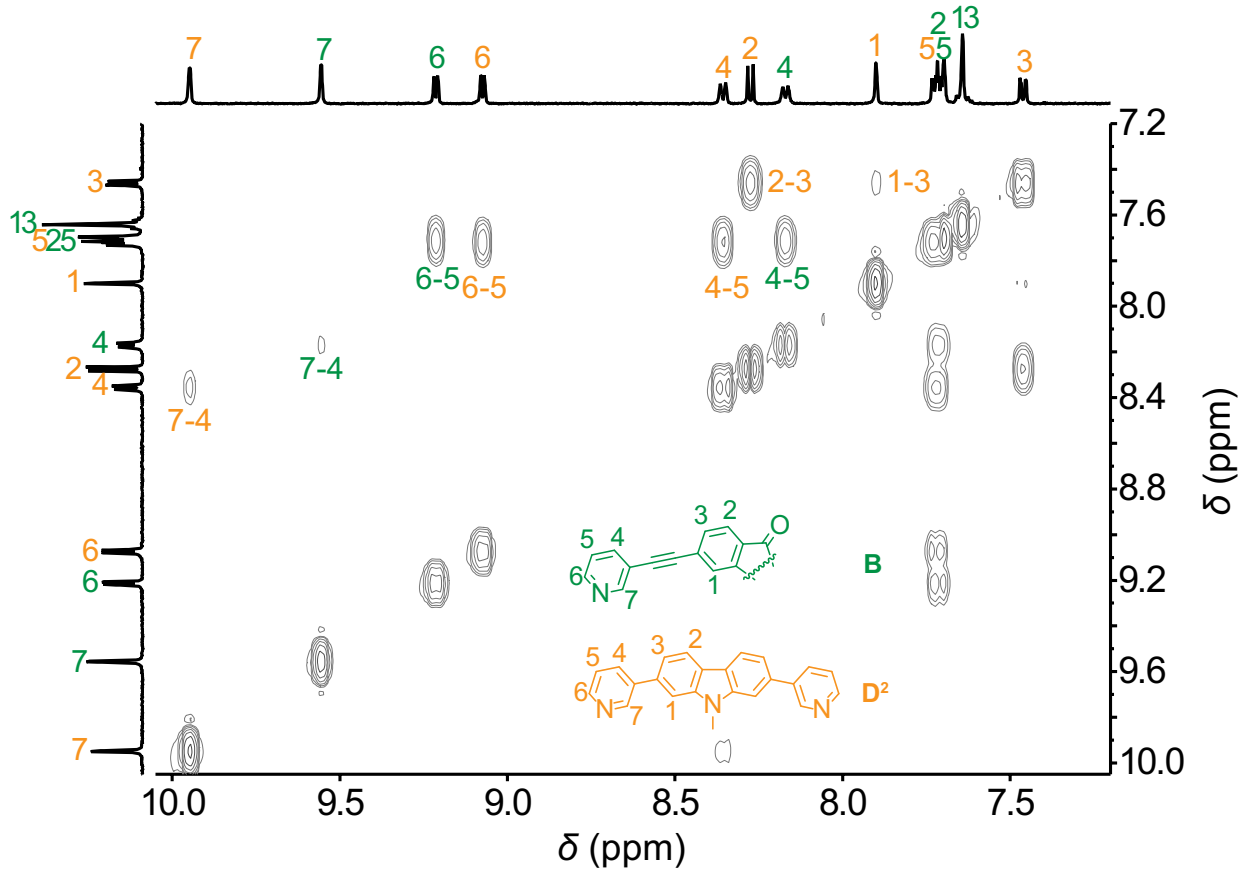

Supplementary Figure 184 | Partial ^{1}H–^{1}H COSY spectrum (500 MHz, 298 K, CD_3CN) of heteroleptic cage $Pd_2\mathbf{B}_2\mathbf{D}^2_2$.

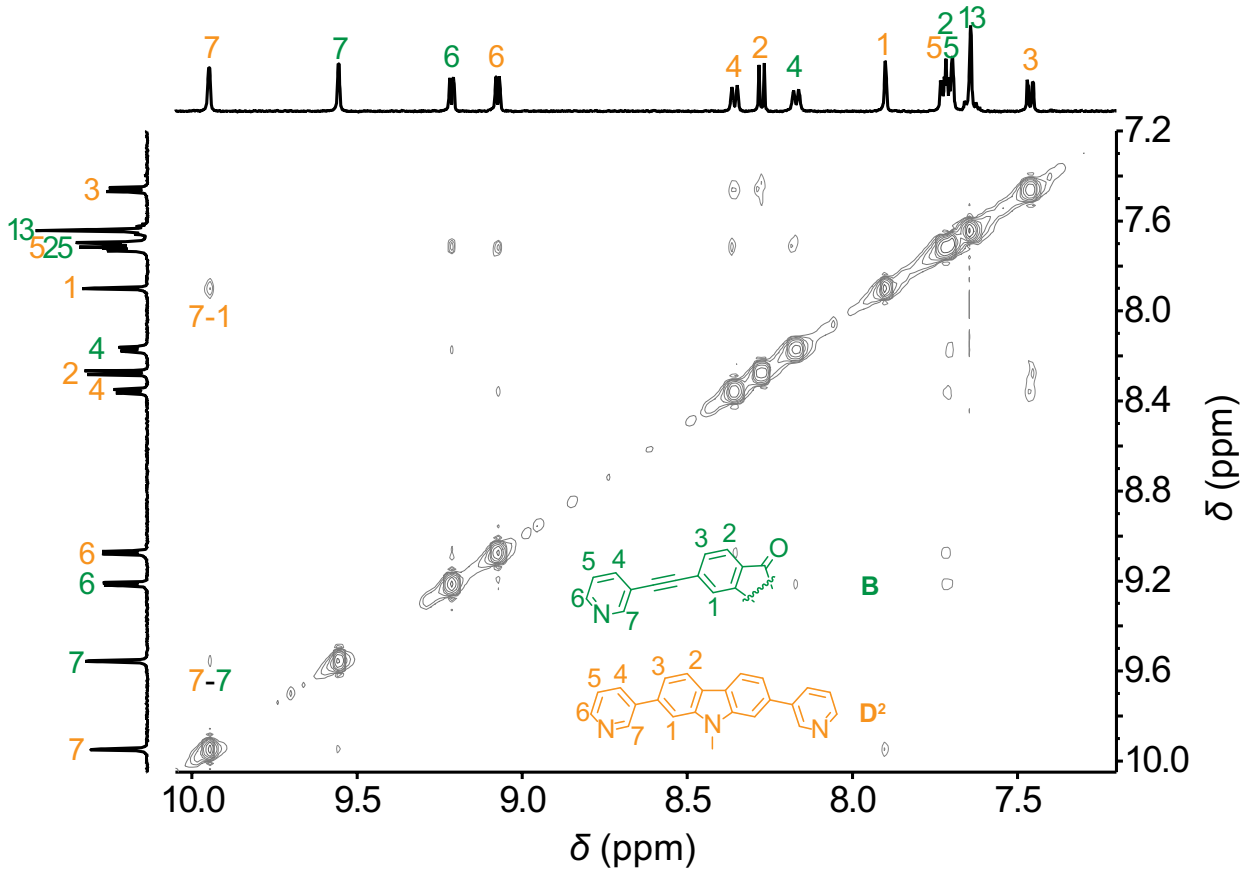

Supplementary Figure 185 | Partial ^{1}H–^{1}H NOESY spectrum (500 MHz, 298 K, CD_3CN) of heteroleptic cage $Pd_2\mathbf{B}_2\mathbf{D}^2_2$.

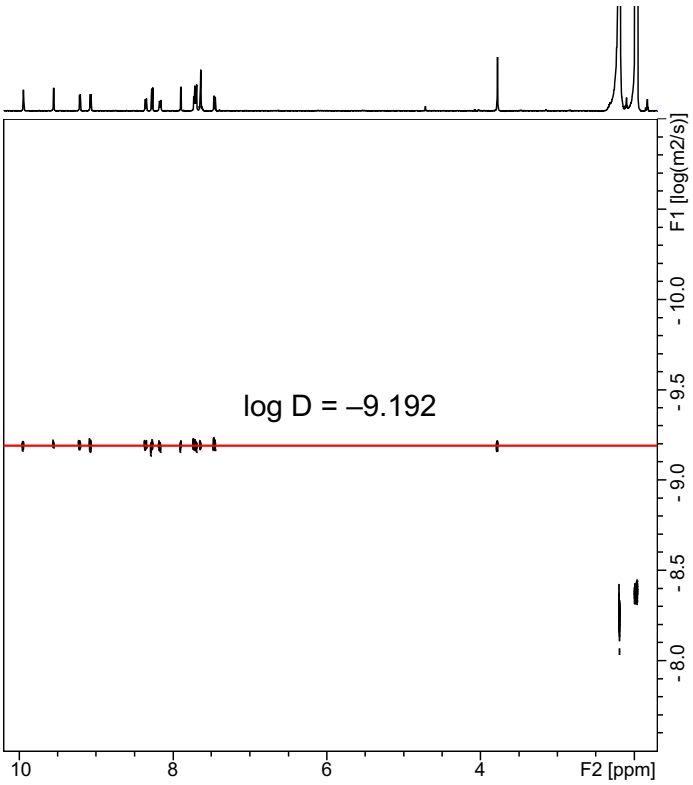

Supplementary Figure 186 | ^{1}H DOSY spectrum (500 MHz, 298 K, CD_3CN) of heteroleptic cage $Pd_2\mathbf{B}_2\mathbf{D}^2_2$. Diffusion coefficient for $Pd_2\mathbf{B}_2\mathbf{D}^2_2$: D = 6.427 × 10^{-10} m^2s^{-1}, log *D* = −9.192, r = 10.2 Å.

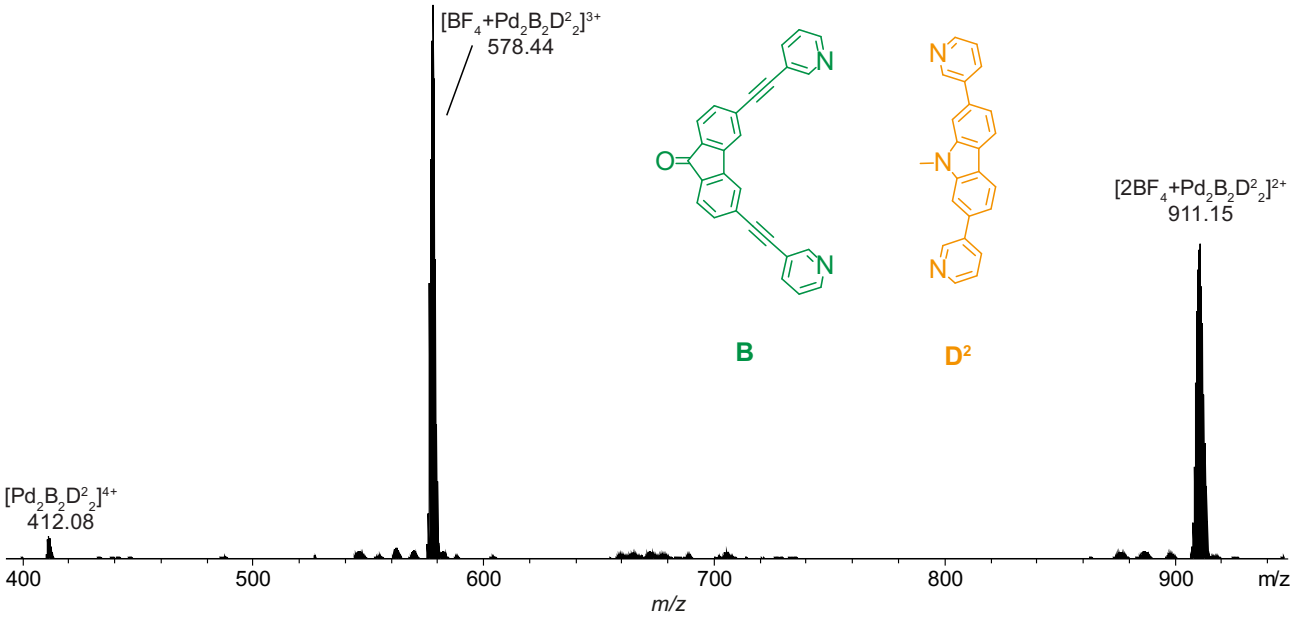

Supplementary Figure 187 | HR-ESI mass spectrum of heteroleptic cage $Pd_2\mathbf{B}_2\mathbf{D}^2_2$.

3.7.3. Self-assembly of heteroleptic cage $Pd_2A_2CD^2$

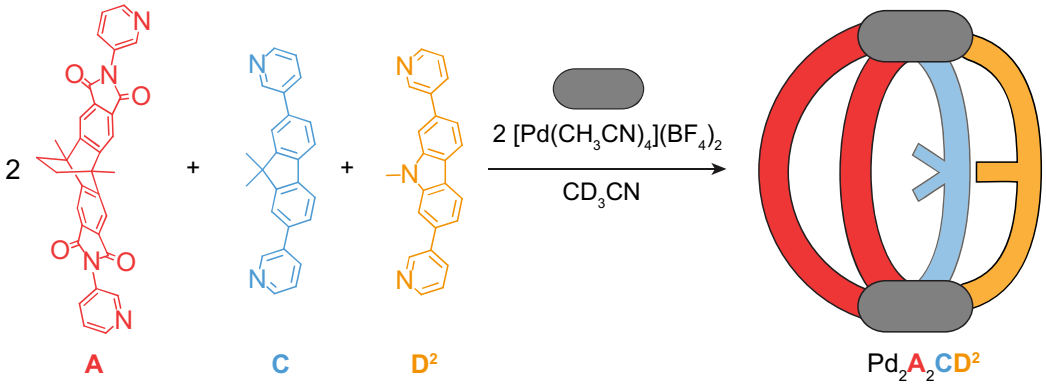

To a solution of **C** (60 µL, 3 mM, 0.18 µmol) and **D²** (60 µL, 3 mM, 0.18 µmol) in CD_3CN and **A** (120 µL, 3 mM, 0.36 µmol) were added a stock solution of $[Pd(CH_3CN)_4](BF_4)_2$ (24 µL, 15 mM/CD_3CN, 0.36 µmol) and 186 µL additional CD_3CN. The mixture was heated at 80 °C for 8 h to give a 0.4 mM cage solution containing the shown cage as predominant species.

^{1}H NMR (600 MHz, 298 K, CD_3CN) δ 9.80 (d, J = 2.1 Hz, 2H), 9.38 (d, J = 2.2 Hz, 2H), 9.19 (d, J = 2.1 Hz, 2H), 9.15 (d, J = 5.9 Hz, 2H), 9.04 (d, J = 2.1 Hz, 2H), 8.97 (d, J = 5.8 Hz, 2H), 8.90 (d, J = 5.7 Hz, 2H), 8.71 (d, J = 5.7 Hz, 2H), 8.48 (d, J = 8.0 Hz, 2H), 8.34 (d, J = 7.9 Hz, 2H), 8.26 (dd, J = 8.1, 1.8 Hz, 2H), 8.19 (s, 2H), 8.18 – 8.15 (m, 2H), 8.08 (s, 2H), 8.08 – 8.04 (m, 2H), 8.02 (dt, J = 8.6, 1.7 Hz, 2H), 7.81 (ddd, J = 14.2, 8.0, 5.8 Hz, 4H), 7.71 – 7.67 (m, 6H), 7.65 (s, 2H), 7.64 (d, J = 3.1 Hz, 2H), 7.59 – 7.55 (m, 2H), 7.48 (dd, J = 8.0, 1.6 Hz, 2H), 7.38 (dd, J = 7.7, 1.7 Hz, 2H), 6.77 (d, J = 1.8 Hz, 2H), 3.44 (s, 3H), 2.30 (s, 3H), 2.05 (s, 3H), 2.01 (s, 3H), 1.75 (s, 3H), 1.72 (s, 4H), 0.70 (s, 3H), -0.31 (s, 3H).

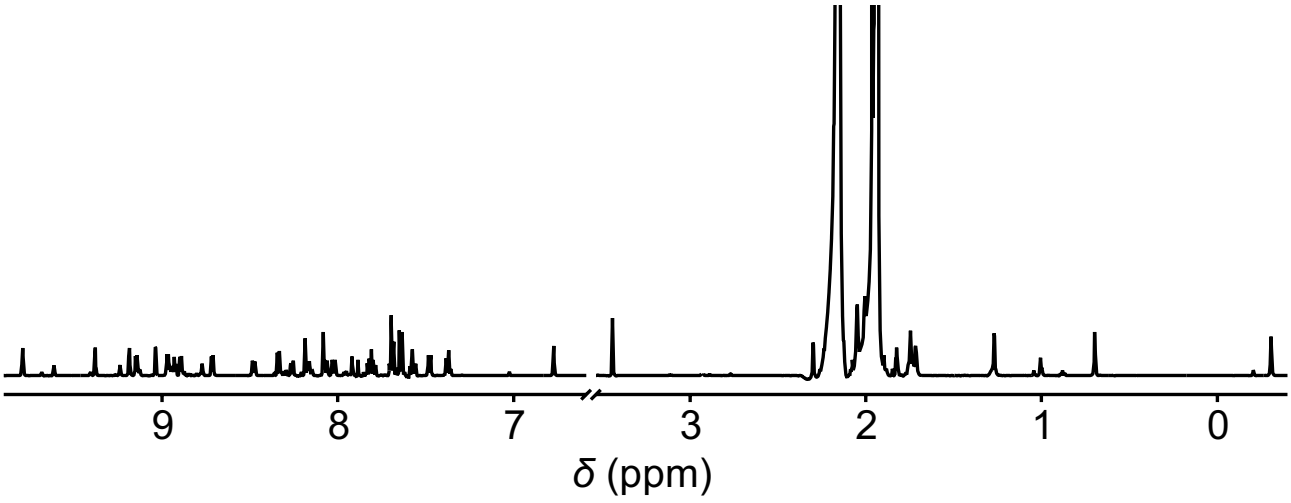

Supplementary Figure 188 | ^{1}H NMR spectrum (600 MHz, 298 K, CD_3CN) of heteroleptic cage $Pd_2A_2CD^2$.

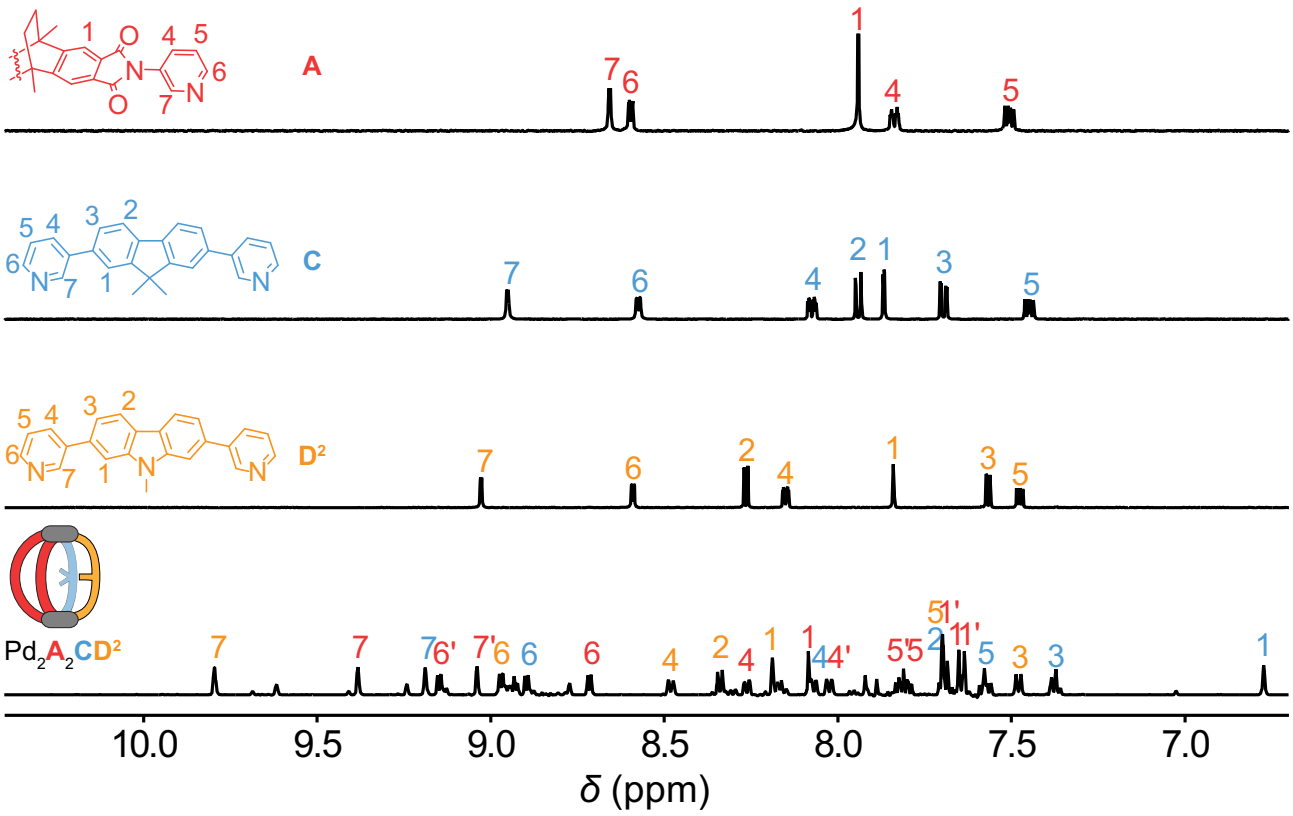

Supplementary Figure 189 | Partial ^{1}H NMR spectrum (700 MHz, 298 K, CD_3CN) comparison of ligand **A** (red), ligand **C** (blue), ligand **D²** (yellow) and heteroleptic cage $Pd_2\mathbf{A}_2\mathbf{CD}^2$.

^{13}C NMR (151 MHz, 298 K, CD_3CN) δ 173.01, 167.46, 166.91, 166.83, 166.51, 155.84, 155.01, 154.42, 154.37, 154.33, 151.06, 150.69, 150.55, 150.42, 150.31, 150.22, 150.10, 149.84, 144.54, 143.77, 142.03, 140.23, 139.76, 139.73, 139.23, 138.59, 135.49, 135.29, 132.21, 131.60, 130.82, 130.62, 130.36, 130.26, 128.86, 128.37, 128.33, 128.10, 127.46, 124.61, 122.94, 122.63, 122.22, 121.04, 117.67, 117.28, 116.94, 109.39, 46.34, 45.66, 45.35, 45.12, 45.08, 44.90, 34.83, 34.68, 29.81, 25.57.

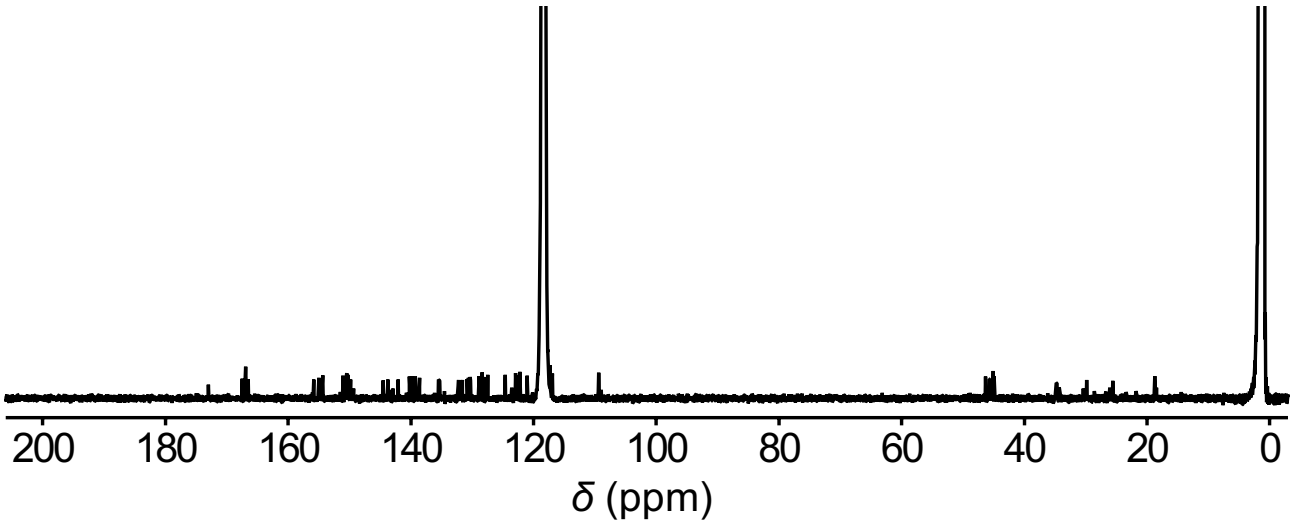

Supplementary Figure 190 | ^{13}C NMR spectrum (151 MHz, 298 K, CD_3CN) of heteroleptic cage $Pd_2\mathbf{A}_2\mathbf{CD}^2$.

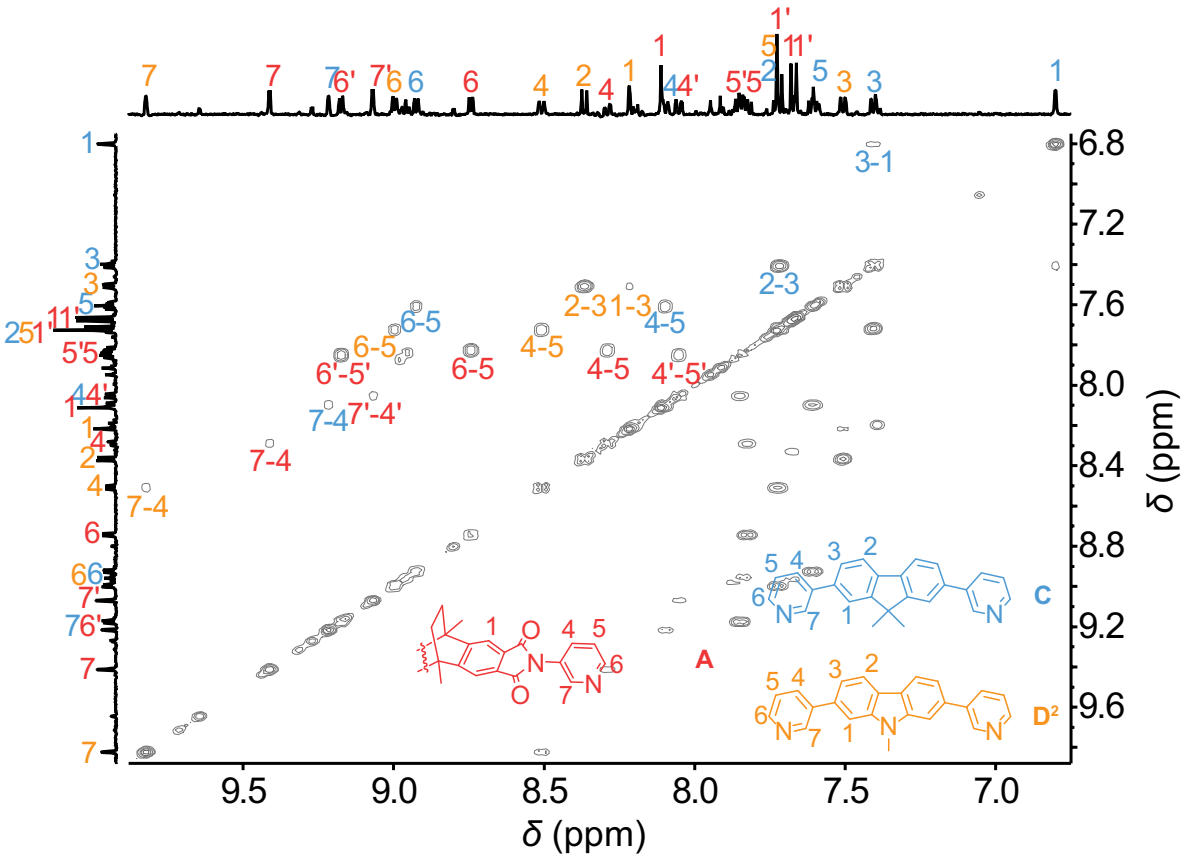

Supplementary Figure 191 | Partial ^{1}H–^{1}H COSY spectrum (500 MHz, 298 K, CD_3CN) of heteroleptic cage $Pd_2\mathbf{A}_2\mathbf{CD}^2$.

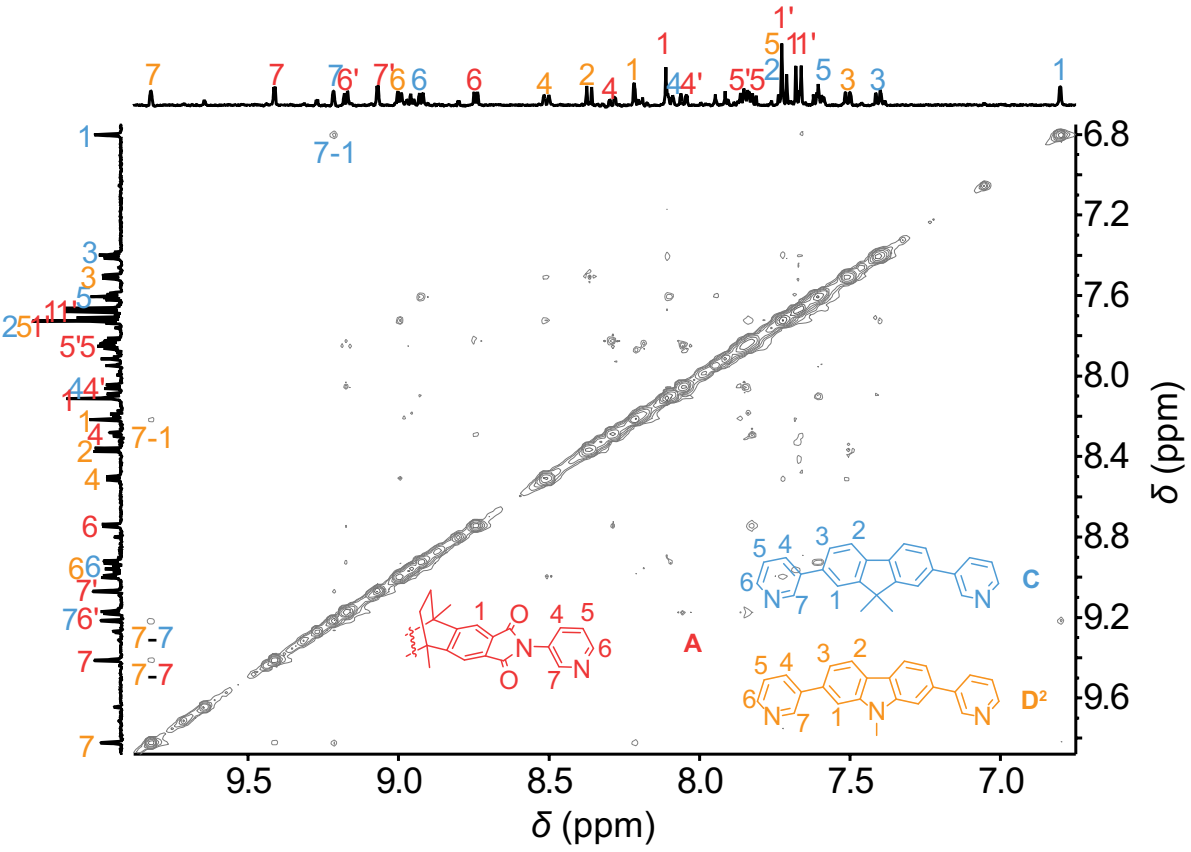

Supplementary Figure 192 | Partial ^{1}H–^{1}H NOESY spectrum (500 MHz, 298 K, CD_3CN) of heteroleptic cage $Pd_2\mathbf{A}_2\mathbf{CD}^2$.

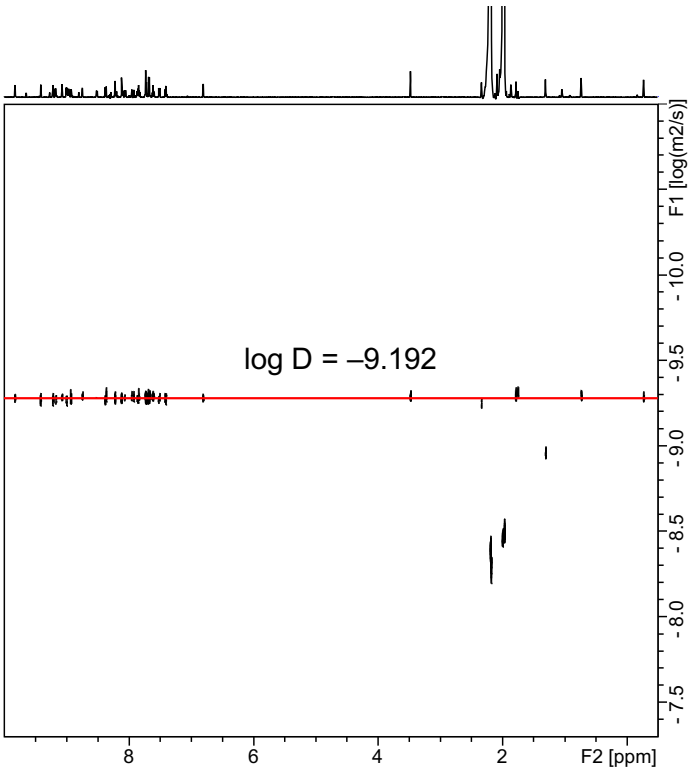

Supplementary Figure 193 | ^{1}H DOSY spectrum (500 MHz, 298 K, CD_3CN) of heteroleptic cage $Pd_2\mathbf{A}_2\mathbf{CD}^2$. Diffusion coefficient for $Pd_2\mathbf{A}_2\mathbf{CD}^2$: D = 6.427 × 10^{-10} m^2s^{-1}, log *D* = −9.192, r = 10.2 Å.

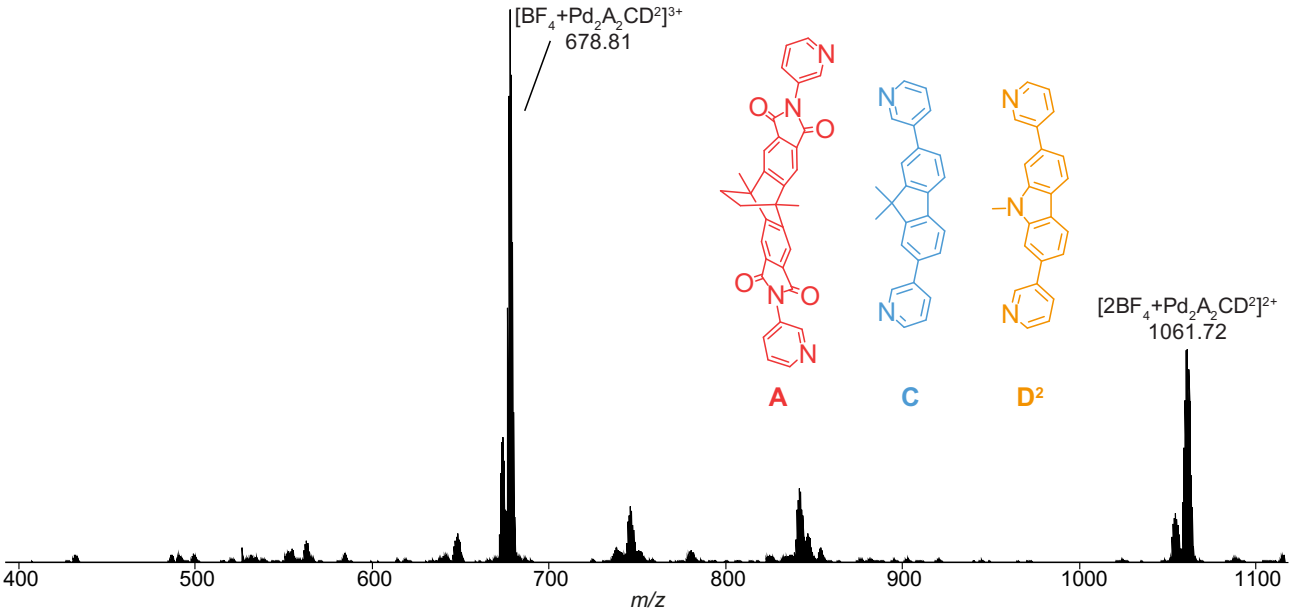

Supplementary Figure 194 | HR-ESI mass spectrum of heteroleptic cage $Pd_2\mathbf{A}_2\mathbf{CD}^2$.

3.7.4. Self-assembly of heteroleptic cage $Pd_2B_2CD^2$

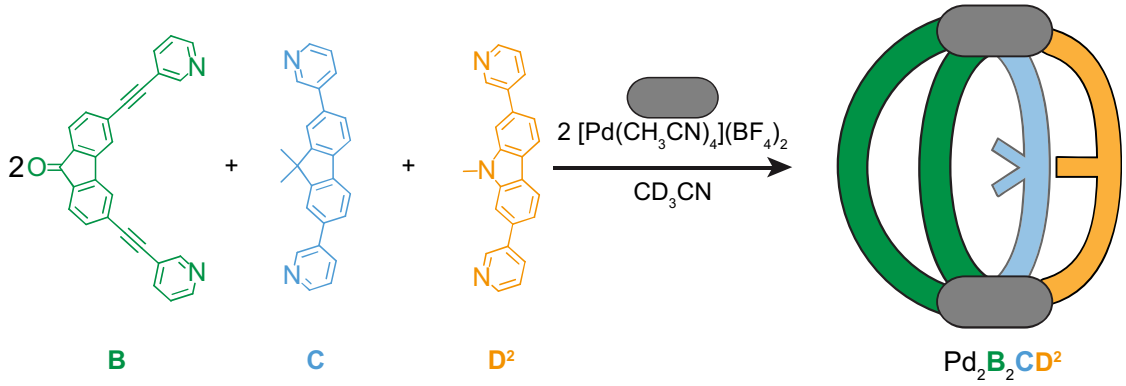

To a solution of **C** (60 µL, 3 mM, 0.18 µmol) and a suspension of **B** (120 µL, 3 mM, 0.36 µmol), **D²** (60 µL, 3 mM, 0.18 µmol) in CD_3CN were added a stock solution of $[Pd(CH_3CN)_4](BF_4)_2$ (24 µL, 15 mM/CD_3CN, 0.36 µmol) and 186 µL additional CD_3CN. The mixture was heated at 80 °C for 8 h to give a 0.4 mM cage solution containing the shown cage as predominant species.

^{1}H NMR (700 MHz, 298 K, CD_3CN) δ 10.06 (d, J = 2.0 Hz, 2H), 9.69 (d, J = 1.8 Hz, 2H), 9.49 (d, J = 2.0 Hz, 2H), 9.38 (d, J = 1.8 Hz, 2H), 9.16 (d, J = 5.8 Hz, 4H), 9.04 (d, J = 5.8 Hz, 2H), 9.00 (d, J = 5.8 Hz, 2H), 8.50 (s, 2H), 8.43 (d, J = 7.7 Hz, 2H), 8.36 (d, J = 7.8 Hz, 2H), 8.23 – 8.19 (m, 2H), 8.16 (dd, J = 7.6, 2.1 Hz, 2H), 8.12 (d, J = 8.0 Hz, 2H), 7.86 – 7.83 (m, 4H), 7.73 – 7.59 (m, 18H), 7.52 (dd, J = 7.8, 1.5 Hz, 2H), 7.47 (dd, J = 7.5, 1.7 Hz, 2H), 7.06 – 7.02 (m, 2H), 4.68 (s, 3H), 1.34 (s, 3H), 0.04 (s, 3H).

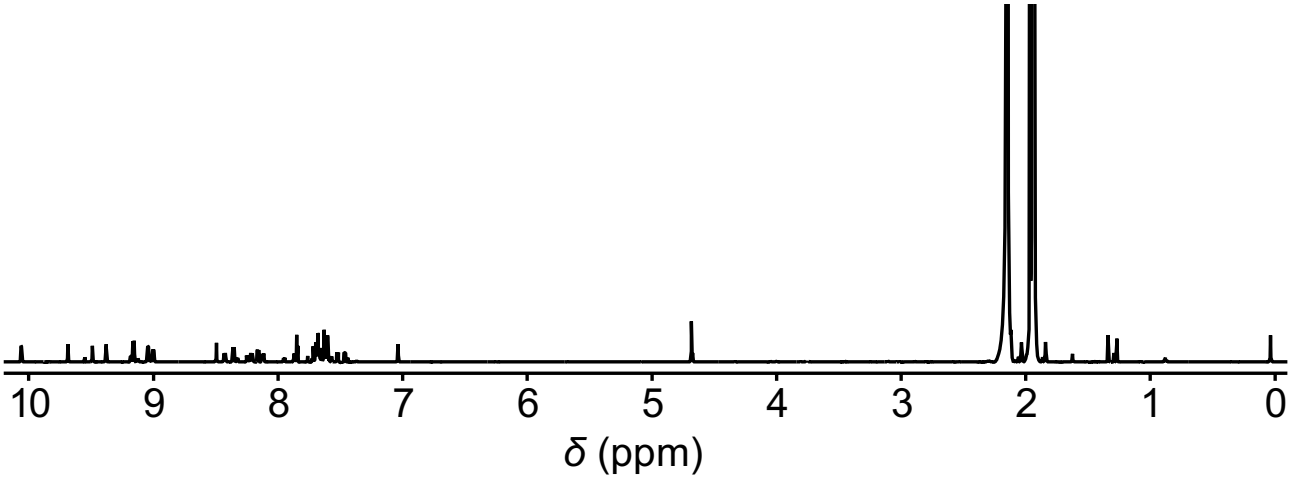

Supplementary Figure 195 | ^{1}H NMR spectrum (700 MHz, 298 K, CD_3CN) of heteroleptic cage $Pd_2B_2CD^2$.

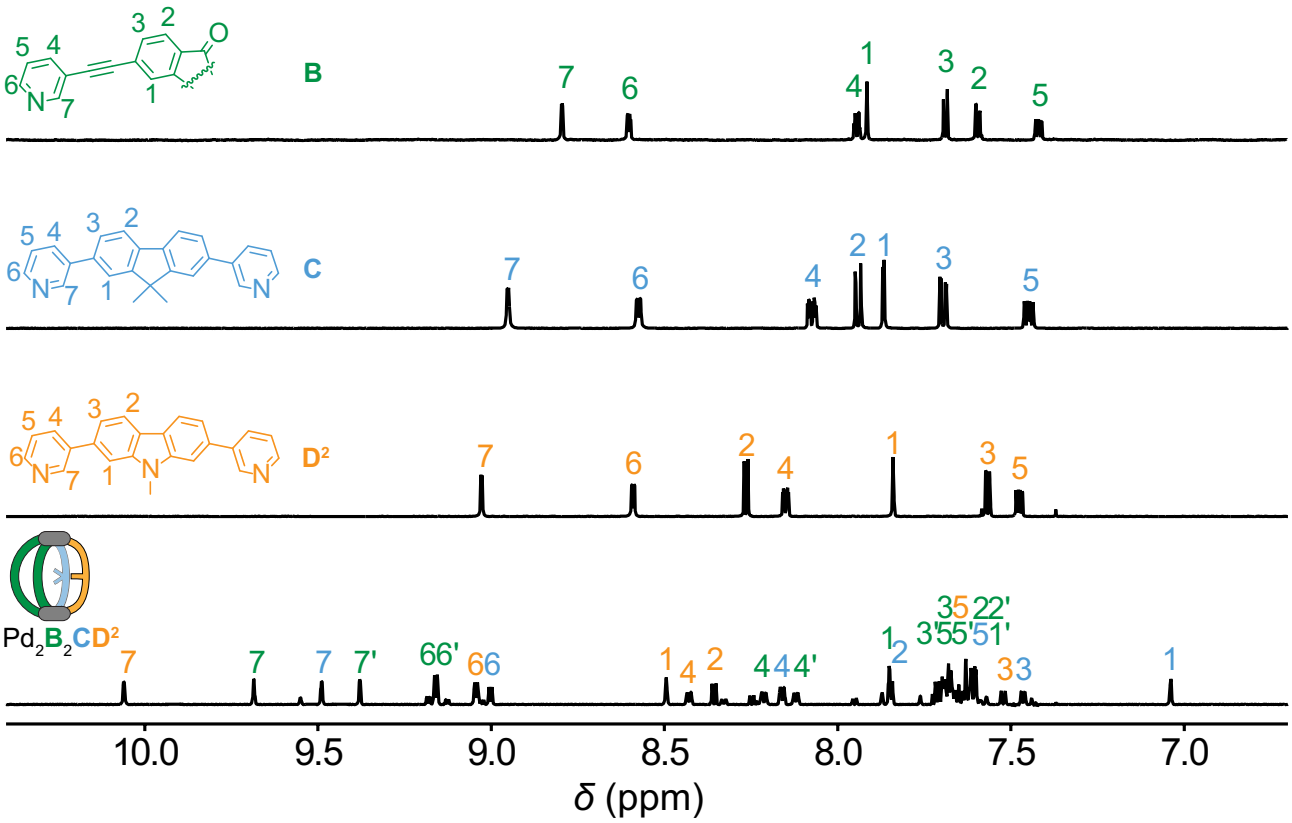

Supplementary Figure 196 | Partial ^{1}H NMR spectrum (700 MHz, 298 K, CD_3CN) comparison of ligand **B** (green), ligand **C** (blue), ligand **D** (yellow) and heteroleptic cage $Pd_2\mathbf{B}_2\mathbf{CD}^2$.

^{13}C NMR (176 MHz, 298 K, CD_3CN) δ 192.19, 192.16, 173.02, 156.38, 154.06, 153.64, 151.31, 151.22, 150.58, 150.43, 150.17, 149.97, 144.82, 144.03, 143.24, 142.30, 140.20, 139.71, 139.16, 136.24, 136.11, 135.68, 135.52, 135.43, 134.53, 129.06, 128.84, 128.72, 128.62, 128.44, 128.35, 128.29, 127.91, 125.22, 125.10, 124.54, 124.46, 124.33, 123.81, 123.76, 123.72, 123.09, 122.93, 122.69, 120.26, 109.23, 95.58, 95.50, 87.78, 87.51, 46.74, 30.47, 29.16, 26.35.

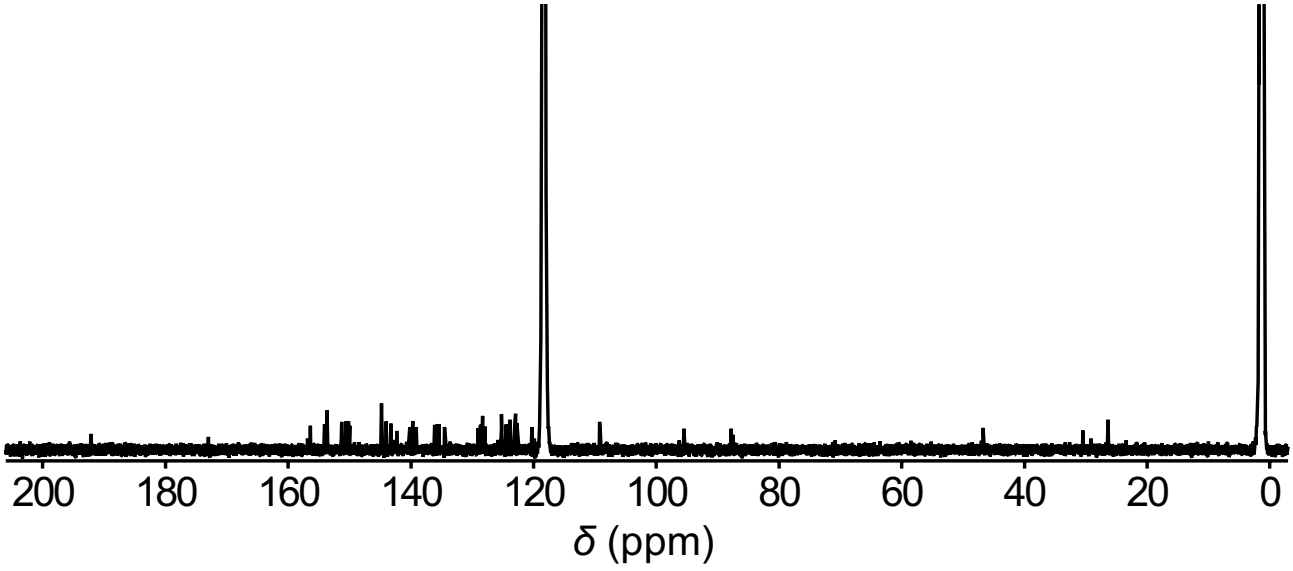

Supplementary Figure 197 | ^{13}C NMR spectrum (176 MHz, 298 K, CD_3CN) of heteroleptic cage $Pd_2\mathbf{B}_2\mathbf{CD}^2$.

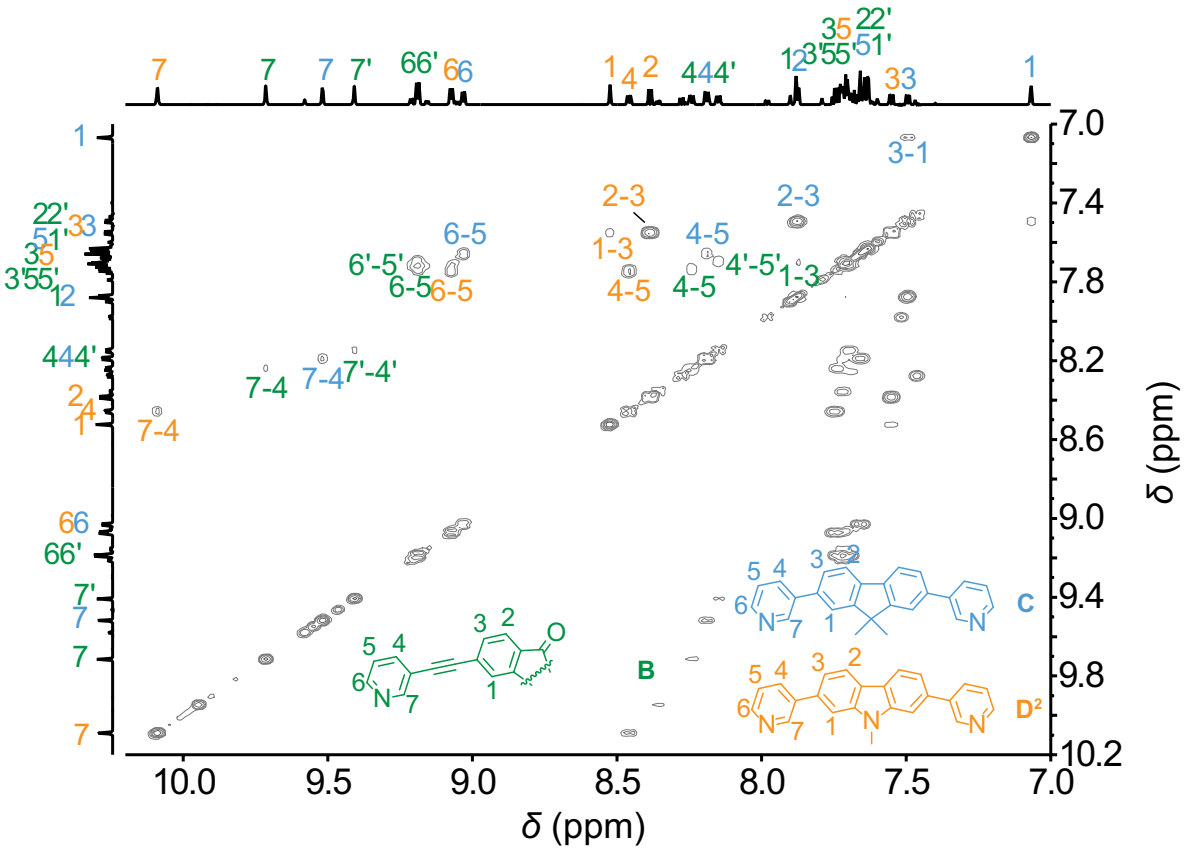

Supplementary Figure 198 | Partial ^{1}H–^{1}H COSY spectrum (500 MHz, 298 K, CD_3CN) of heteroleptic cage $Pd_2\mathbf{B}_2\mathbf{CD}^2$.

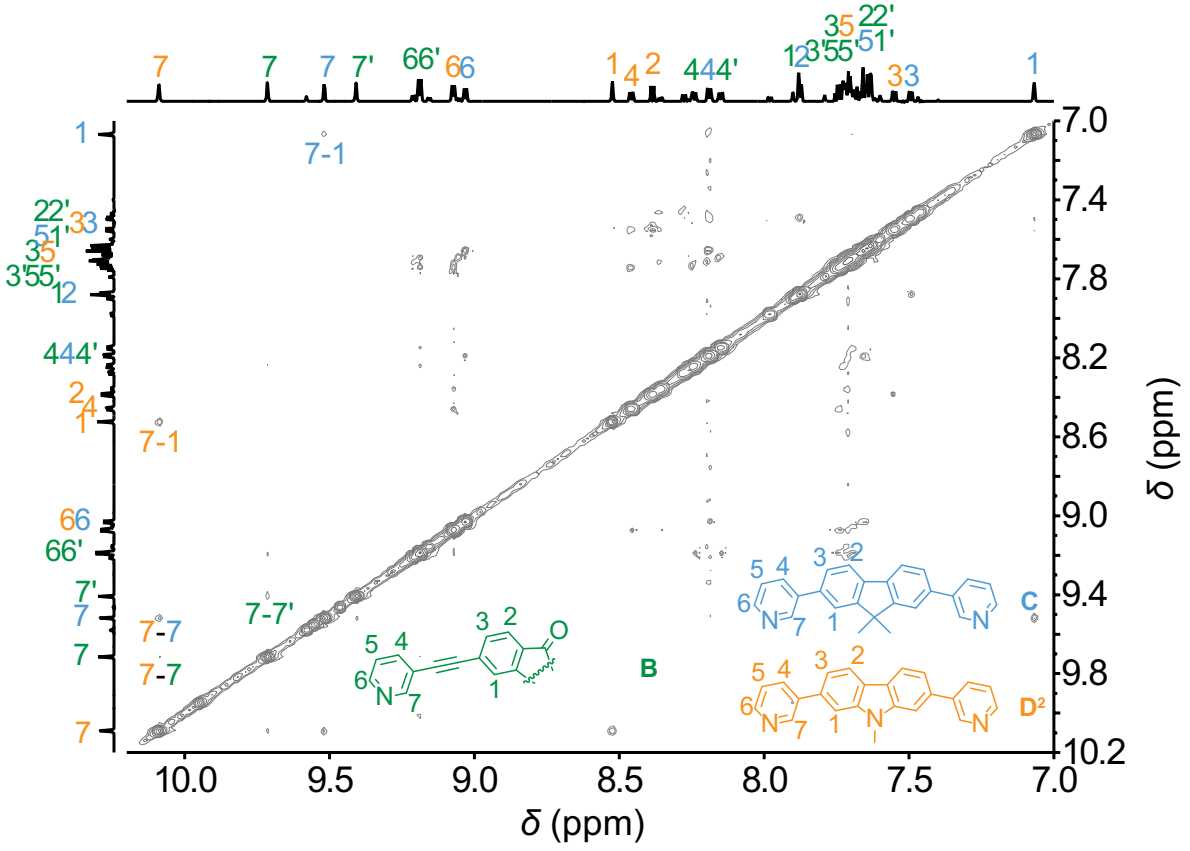

Supplementary Figure 199 | Partial ^{1}H–^{1}H NOESY spectrum (500 MHz, 298 K, CD_3CN) of heteroleptic cage $Pd_2\mathbf{B}_2\mathbf{CD}^2$.

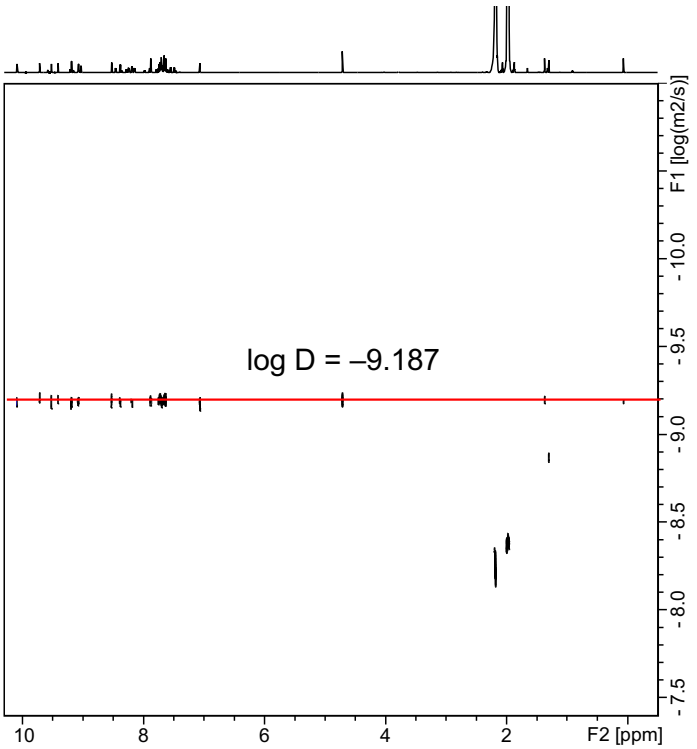

Supplementary Figure 200 | ^{1}H DOSY spectrum (500 MHz, 298 K, CD_3CN) of heteroleptic cage $Pd_2\mathbf{B}_2\mathbf{CD}^2$. Diffusion coefficient for $Pd_2\mathbf{B}_2\mathbf{CD}^2$: D = 6.501 × 10^{-10} m^2s^{-1}, log *D* = −9.187, r = 10.1 Å.

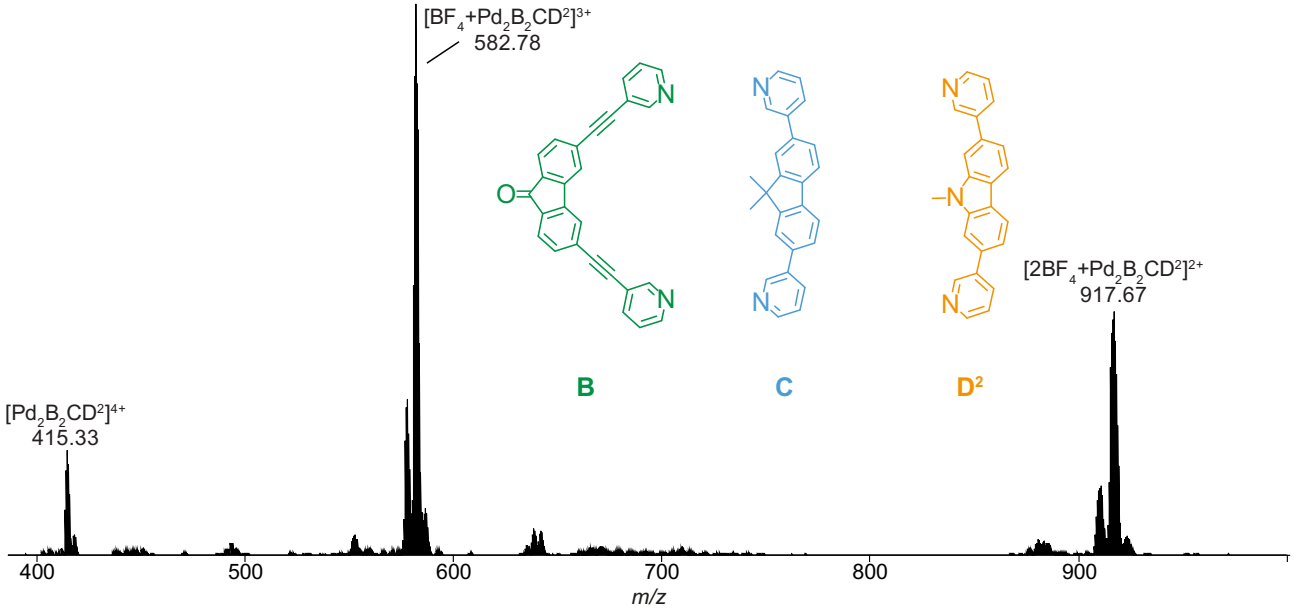

Supplementary Figure 201 | HR-ESI mass spectrum of heteroleptic cage $Pd_2\mathbf{B}_2\mathbf{CD}^2$.

*3.7.5. Self-assembly of heteroleptic cage Pd_2**ABD²**$_2$*

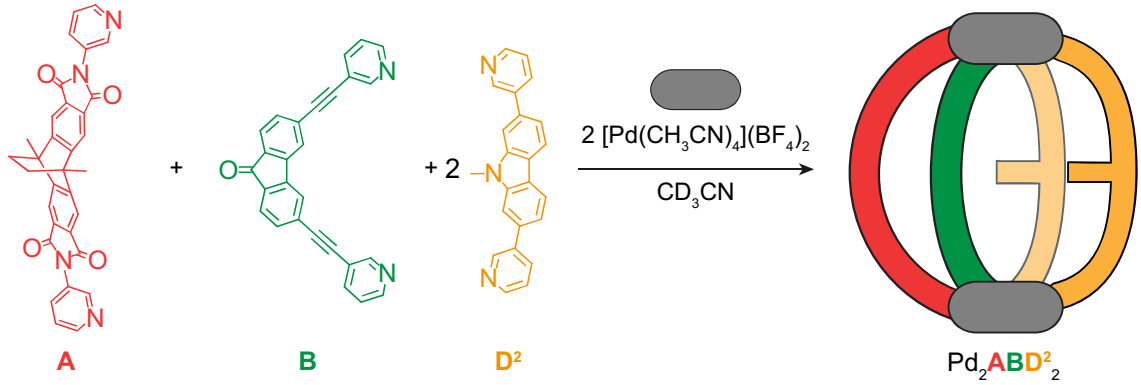

To a solution of **A** (60 µL, 3 mM, 0.18 µmol), **B** (60 µL, 3 mM, 0.18 µmol), **D²** (120 µL, 3 mM, 0.36 µmol) was added a stock solution of $[Pd(CH_3CN)_4](BF_4)_2$ (24 µL, 15 mM/CD_3CN, 0.36 µmol) and additional 186 µL CD_3CN. The mixture was heated at 80 °C for 8 h to give a 0.4 mM cage solution containing the shown cage as predominant species.

^{1}H NMR (700 MHz, 298 K, CD_3CN) δ 10.06 (d, J = 2.0 Hz, 2H), 9.69 (d, J = 1.8 Hz, 2H), 9.49 (d, J = 2.0 Hz, 2H), 9.38 (d, J = 1.8 Hz, 2H), 9.16 (d, J = 5.8 Hz, 4H), 9.04 (d, J = 5.8 Hz, 2H), 9.00 (d, J = 5.8 Hz, 2H), 8.50 (s, 2H), 8.43 (d, J = 7.7 Hz, 2H), 8.36 (d, J = 7.8 Hz, 2H), 8.23 – 8.19 (m, 2H), 8.16 (dd, J = 7.6, 2.1 Hz, 2H), 8.12 (d, J = 8.0 Hz, 2H), 7.86 – 7.83 (m, 4H), 7.73 – 7.59 (m, 18H), 7.52 (dd, J = 7.8, 1.5 Hz, 2H), 7.47 (dd, J = 7.5, 1.7 Hz, 2H), 7.06 – 7.02 (m, 2H), 4.68 (s, 3H), 1.34 (s, 3H), 0.04 (s, 3H).

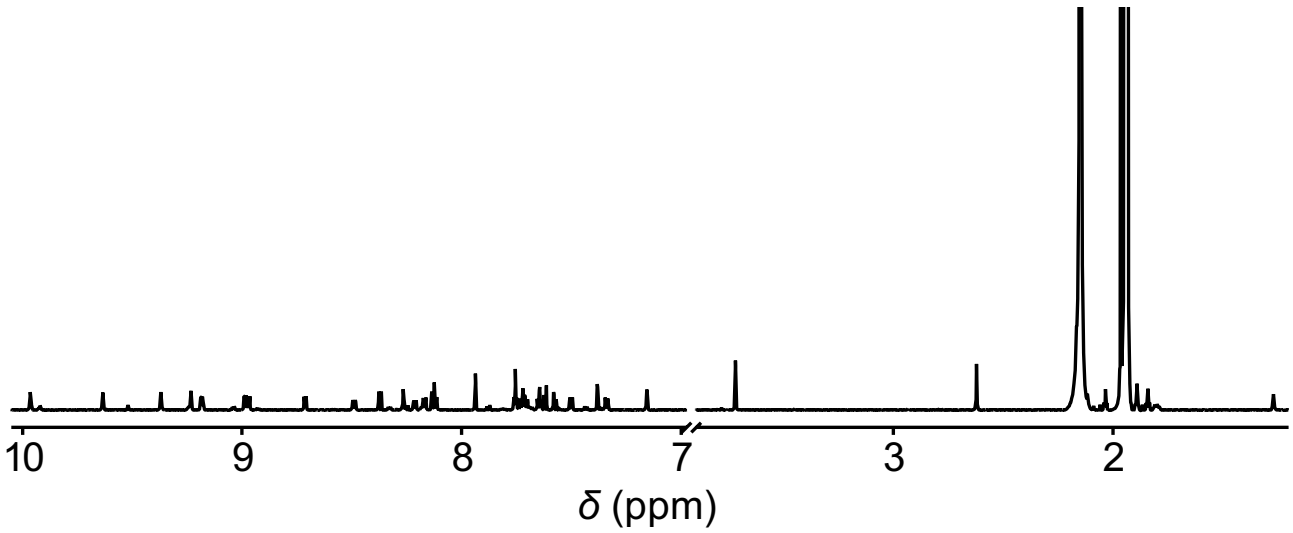

Supplementary Figure 202 | ^{1}H NMR spectrum (700 MHz, 298 K, CD_3CN) of heteroleptic cage Pd_2**ABD²**$_2$.

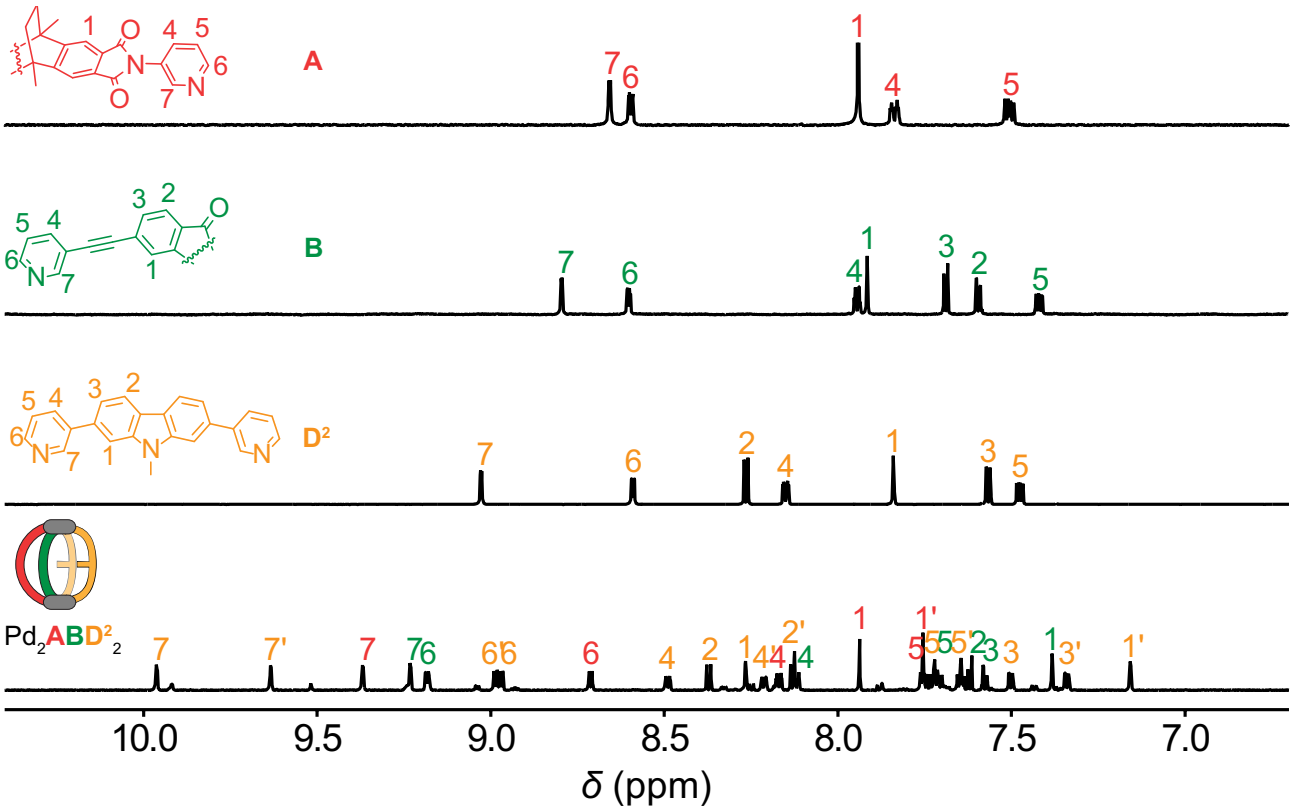

Supplementary Figure 203 | Partial ^{1}H NMR spectrum (700 MHz, 298 K, CD_3CN) comparison of ligand **A** (red), ligand **B** (green), ligand **D²** (yellow) and heteroleptic cage Pd_2**ABD²**$_2$.

^{13}C NMR (176 MHz, 298 K, CD_3CN) δ 192.17, 173.01, 167.40, 166.84, 155.07, 154.79, 154.05, 151.20, 151.02, 150.59, 150.33, 150.15, 150.12, 149.86, 144.74, 144.62, 144.31, 143.62, 142.73, 142.16, 140.03, 139.33, 138.77, 136.06, 135.43, 135.31, 133.96, 131.83, 130.82, 130.73, 128.59, 128.56, 128.51, 128.48, 128.28, 125.09, 124.15, 124.06, 123.71, 123.54, 122.84, 122.74, 121.04, 119.36, 117.11, 109.61, 108.40, 95.20, 87.38, 45.60, 45.07, 34.63, 34.12, 29.80, 27.71, 18.95, 18.51.

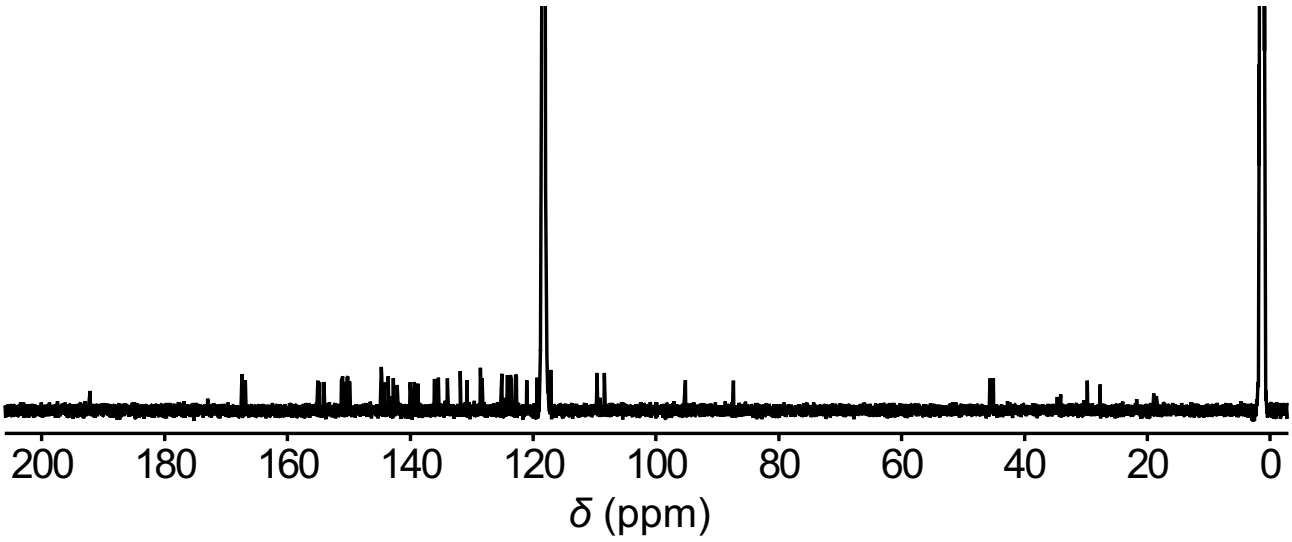

Supplementary Figure 204 | ^{13}C NMR spectrum (176 MHz, 298 K, CD_3CN) of heteroleptic cage Pd_2**ABD²**$_2$.

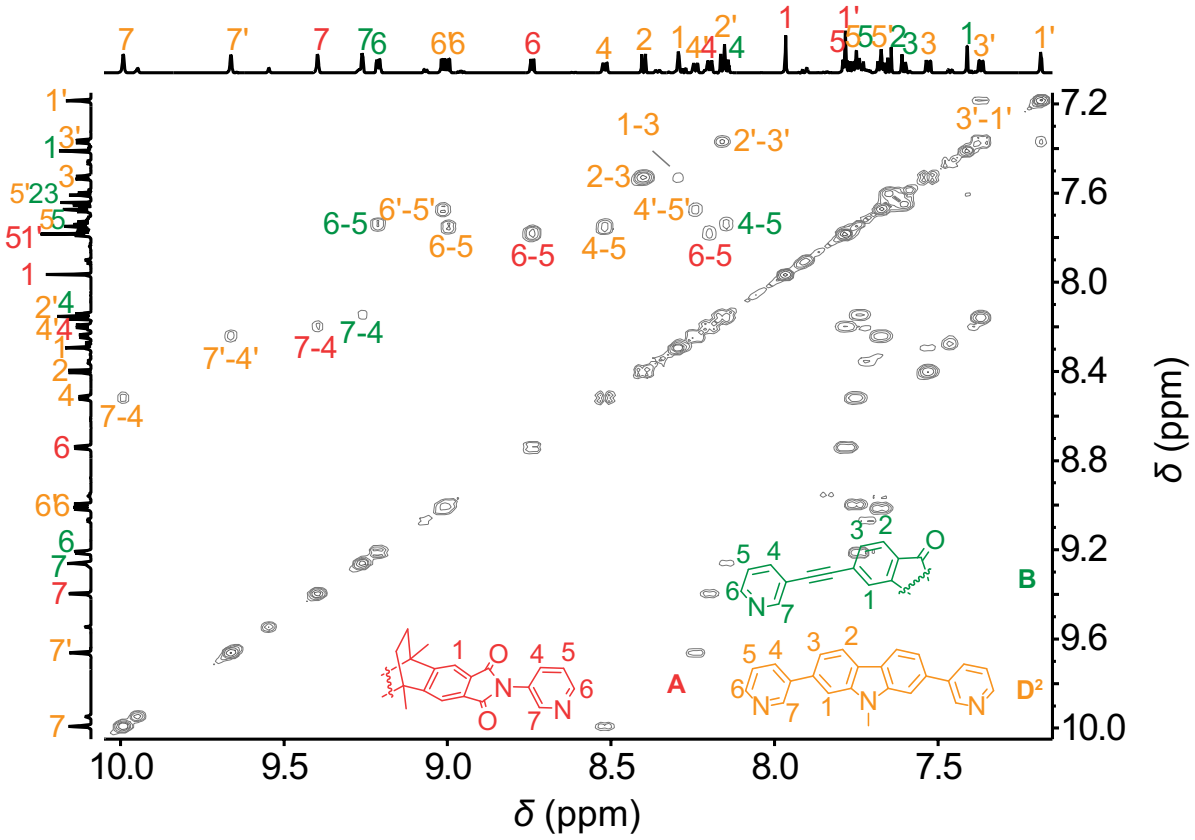

Supplementary Figure 205 | Partial ^{1}H–^{1}H COSY spectrum (500 MHz, 298 K, CD_3CN) of heteroleptic cage Pd_2**ABD²**$_2$.

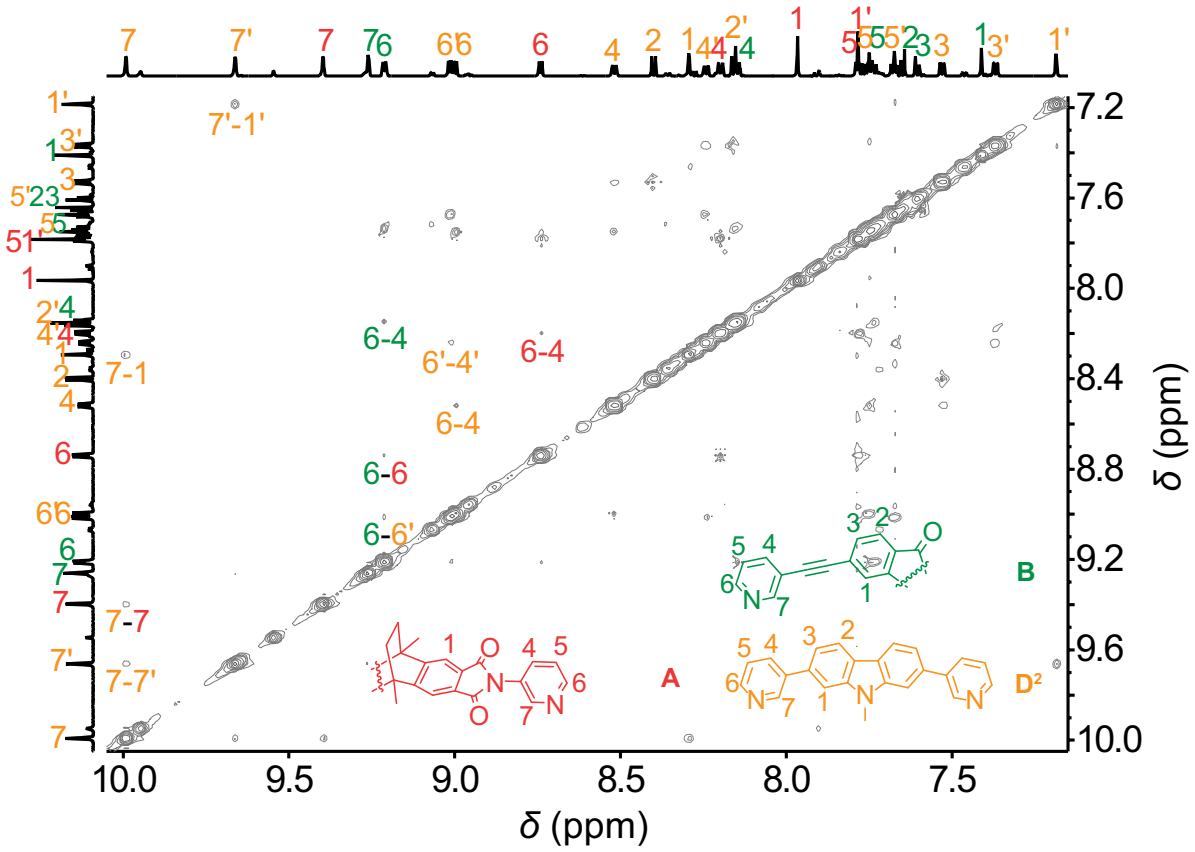

Supplementary Figure 206 | Partial ^{1}H–^{1}H NOESY spectrum (500 MHz, 298 K, CD_3CN) of heteroleptic cage Pd_2**ABD²**$_2$.

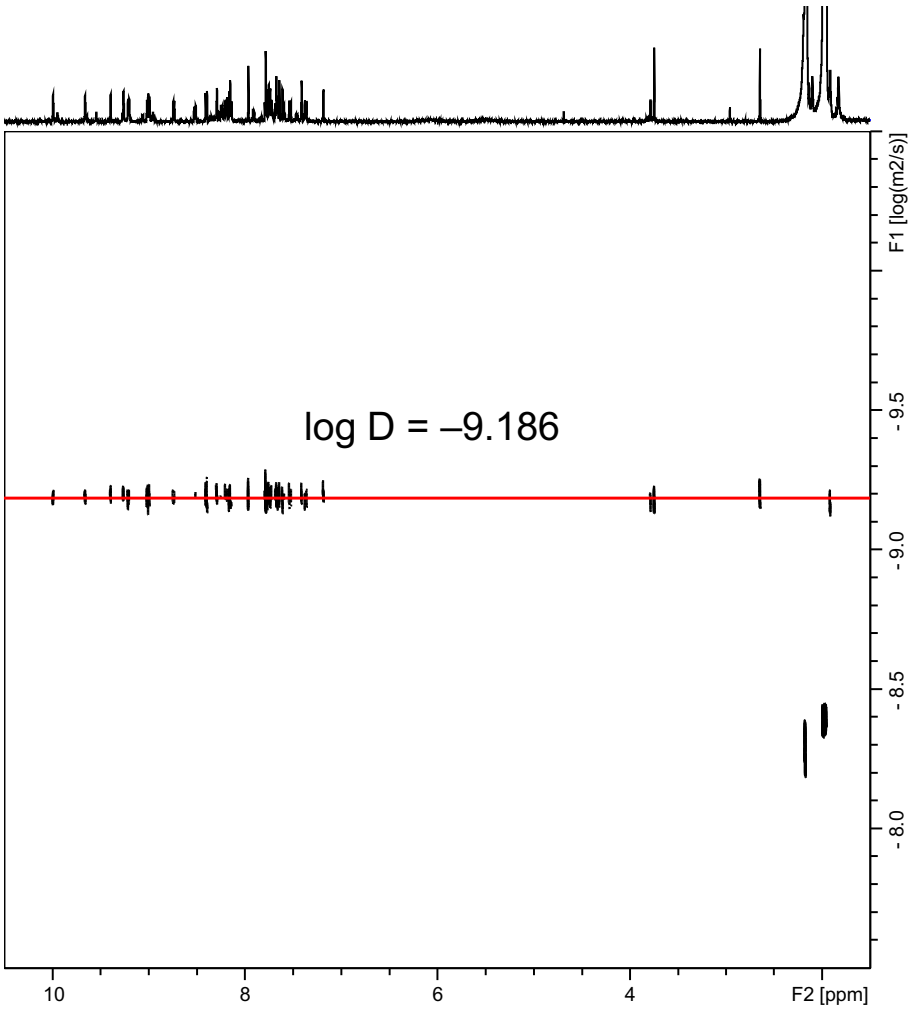

Supplementary Figure 207 | ^{1}H DOSY spectrum (500 MHz, 298 K, CD_3CN) of heteroleptic cage Pd_2**ABD²**$_2$. Diffusion coefficient for Pd_2**ABD²**$_2$: D = 6.516 × 10^{-10} m^2s^{-1}, log *D* = −9.186, r = 10.0 Å.

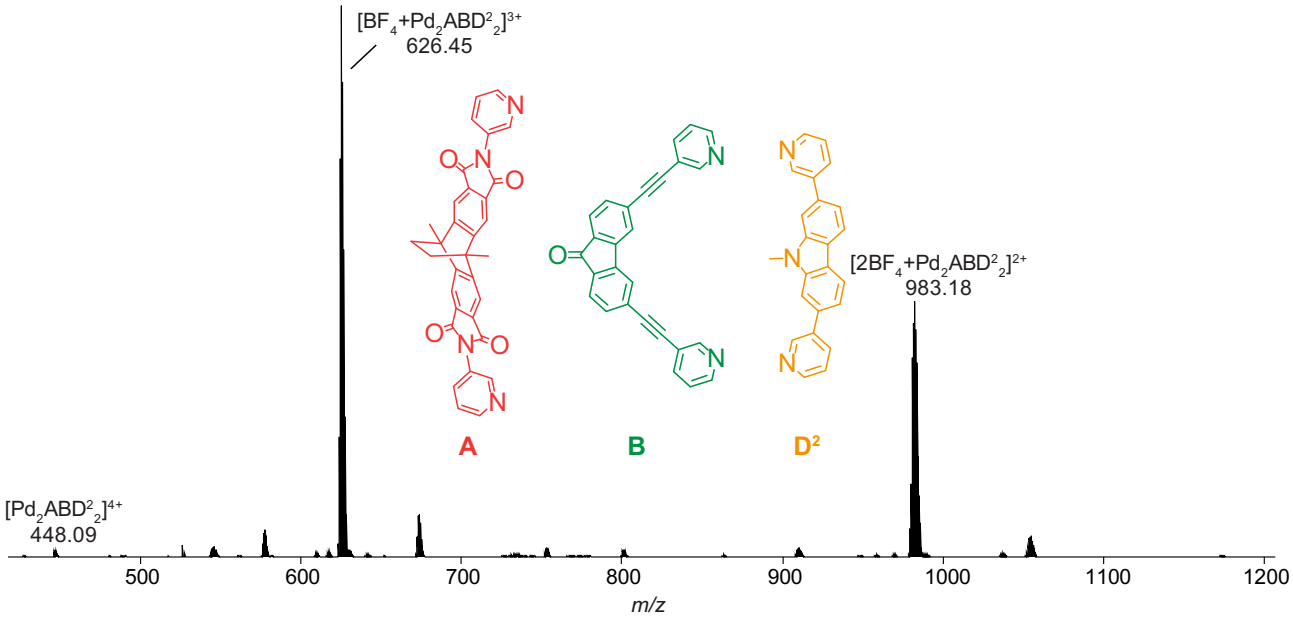

Supplementary Figure 208 | HR-ESI mass spectrum of heteroleptic cage Pd_2**ABD²**$_2$.

*3.7.6. Self-assembly of heteroleptic cage Pd_2**ABCD**^{2}*

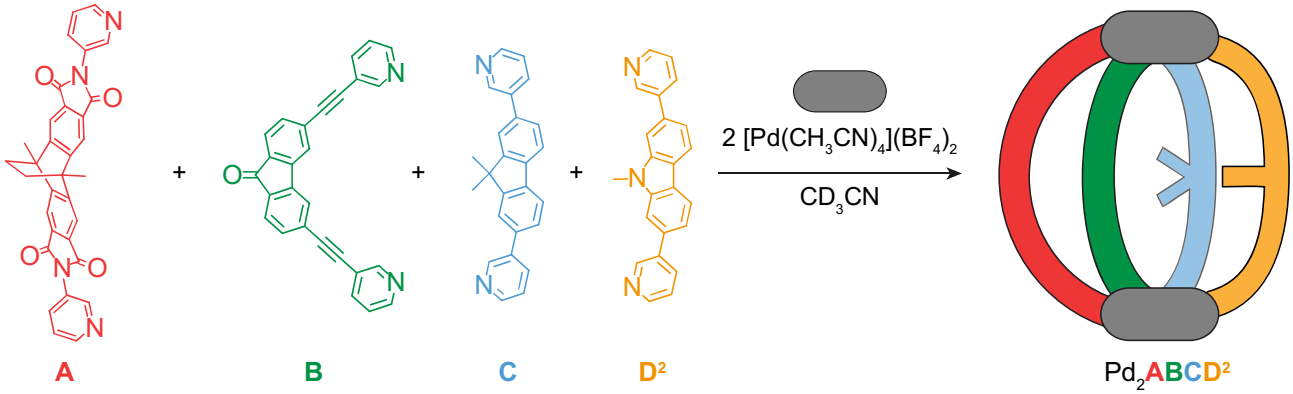

To a solution of **A** (60 µL, 3 mM, 0.18 µmol), **C** (60 µL, 3 mM, 0.18 µmol) and a suspension of **B** (60 µL, 3 mM, 0.18 µmol), **D**^{2} (60 µL, 3 mM, 0.18 µmol) was added a stock solution of $[Pd(CH_3CN)_4](BF_4)_2$ (24 µL, 15 mM/CD_3CN, 0.36 µmol) and additional 186 µL CD_3CN. The mixture was heated at 80 °C for 8 h to give a 0.4 mM cage solution containing the shown cage as predominant species.

^{1}H NMR (700 MHz, 298 K, CD_3CN) δ 10.00 (d, *J* = 2.0 Hz, 2H), 9.37 (d, *J* = 2.3 Hz, 2H), 9.33 (d, *J* = 2.1 Hz, 2H), 9.21 (d, *J* = 1.8 Hz, 2H), 9.18 (dd, *J* = 5.9, 1.4 Hz, 2H), 8.98 (dd, *J* = 6.0, 1.2 Hz, 2H), 8.95 (dd, *J* = 5.9, 1.2 Hz, 2H), 8.67 (dd, *J* = 6.0, 1.3 Hz, 2H), 8.53 (dt, *J* = 7.9, 1.7 Hz, 2H), 8.43 (d, *J* = 7.8 Hz, 2H), 8.37 (d, *J* = 1.6 Hz, 2H), 8.17 (ddd, *J* = 8.4, 2.2, 1.3 Hz, 2H), 8.11 (m, 4H), 7.96 (s, 2H), 7.79 (d, *J* = 7.7 Hz, 2H), 7.76 – 7.71 (m, 8H), 7.64 – 7.60 (m, 4H), 7.57 (ddd, *J* = 8.0, 3.7, 1.4 Hz, 4H), 7.41 (ddd, *J* = 10.0, 2.9, 1.1 Hz, 2H), 6.88 (d, *J* = 1.8 Hz, 2H), 3.71 (s, 2H), 2.20 (s, 3H), 1.89 (s, 4H), 1.82 (s, 3H), 1.05 (s, 3H), -0.15 (s, 3H).

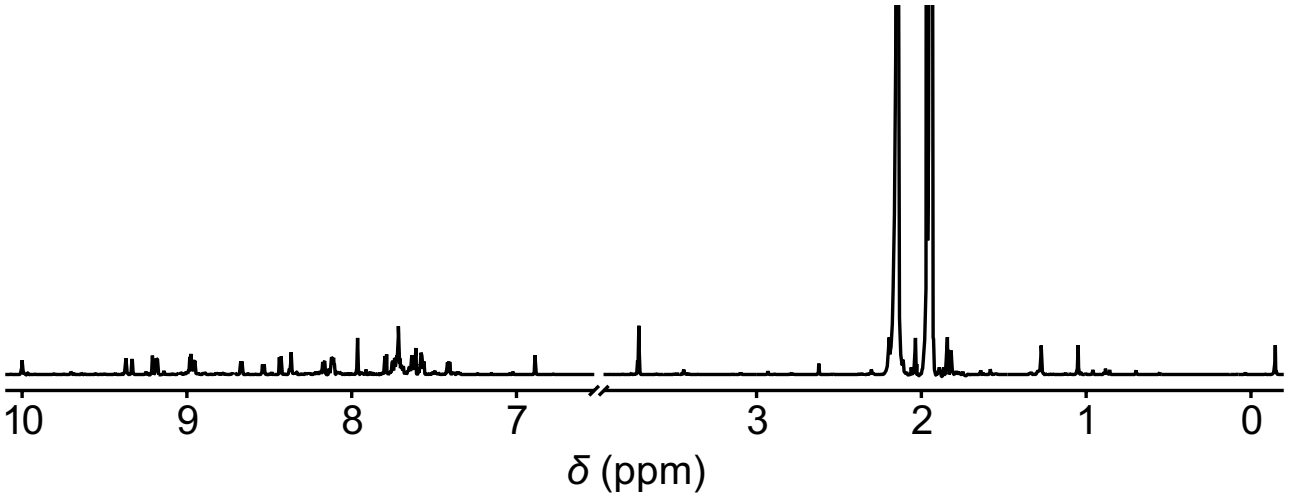

Supplementary Figure 209 | ^{1}H NMR spectrum (700 MHz, 298 K, CD_3CN) of heteroleptic cage Pd_2**ABCD**^{2}.

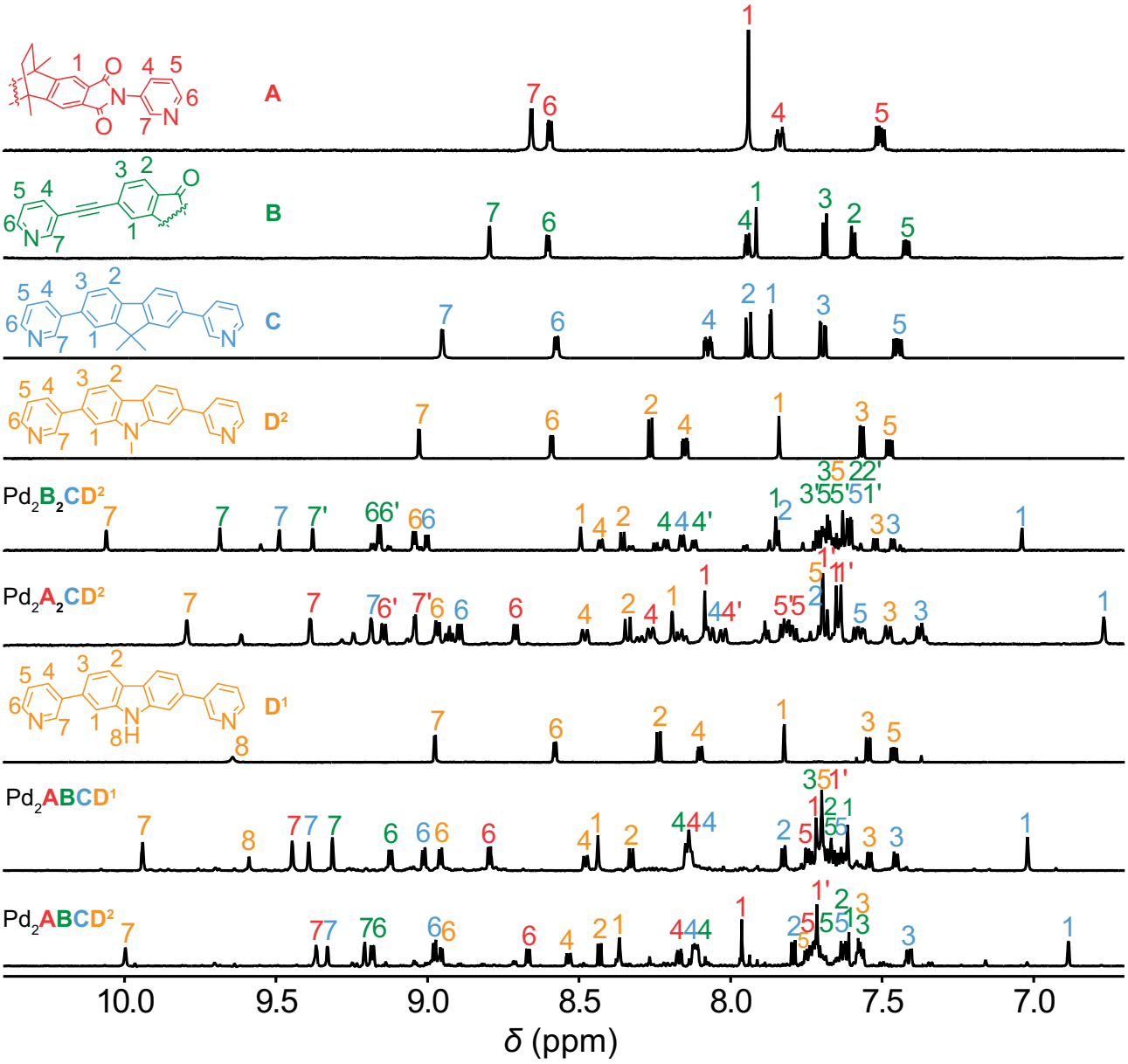

Supplementary Figure 210 | Partial ^{1}H NMR spectrum (700 MHz, 298 K, CD_3CN) comparison of ligands **A** (red), **B** (green), **C** (blue), **D²** (yellow), heteroleptic cages Pd_2**B**$_2$**CD²**, Pd_2**A**$_2$**CD²**, ligand **D¹**, and Pd_2**ABCD²**. (heteroleptic cage Pd_2**ABCD²** with very similar ligand **D^n** was also shown for comparison.)

^{13}C NMR (176 MHz, 298 K, CD_3CN) δ 192.19, 167.49, 166.82, 156.13, 155.02, 154.65, 154.14, 151.05, 150.79, 150.67, 150.34, 150.30, 149.95, 149.85, 144.78, 144.67, 144.53, 144.00, 142.01, 140.10, 140.05, 139.10, 138.60, 136.12, 135.65, 135.44, 135.37, 131.74, 130.93, 130.78, 128.58, 128.56, 128.49, 128.36, 128.20, 127.76, 125.09, 125.06, 124.81, 123.98, 123.72, 122.81, 122.63, 121.02, 116.97, 109.60, 95.19, 87.33, 46.53, 45.63, 44.98, 34.73, 34.12, 30.37, 30.03, 26.25, 25.73.

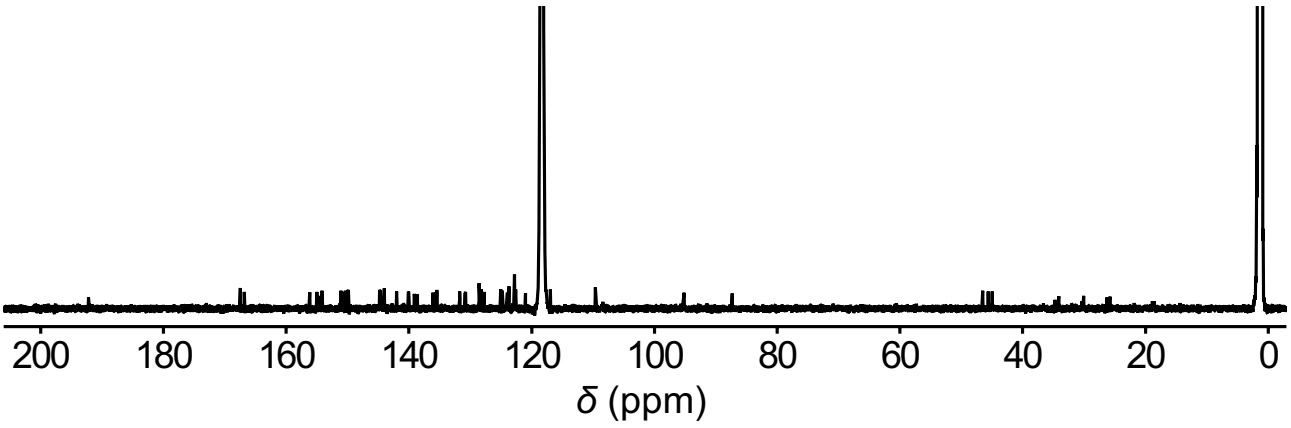

Supplementary Figure 211 | ^{13}C NMR spectrum (176 MHz, 298 K, CD_3CN) of heteroleptic cage Pd_2**ABCD²**.

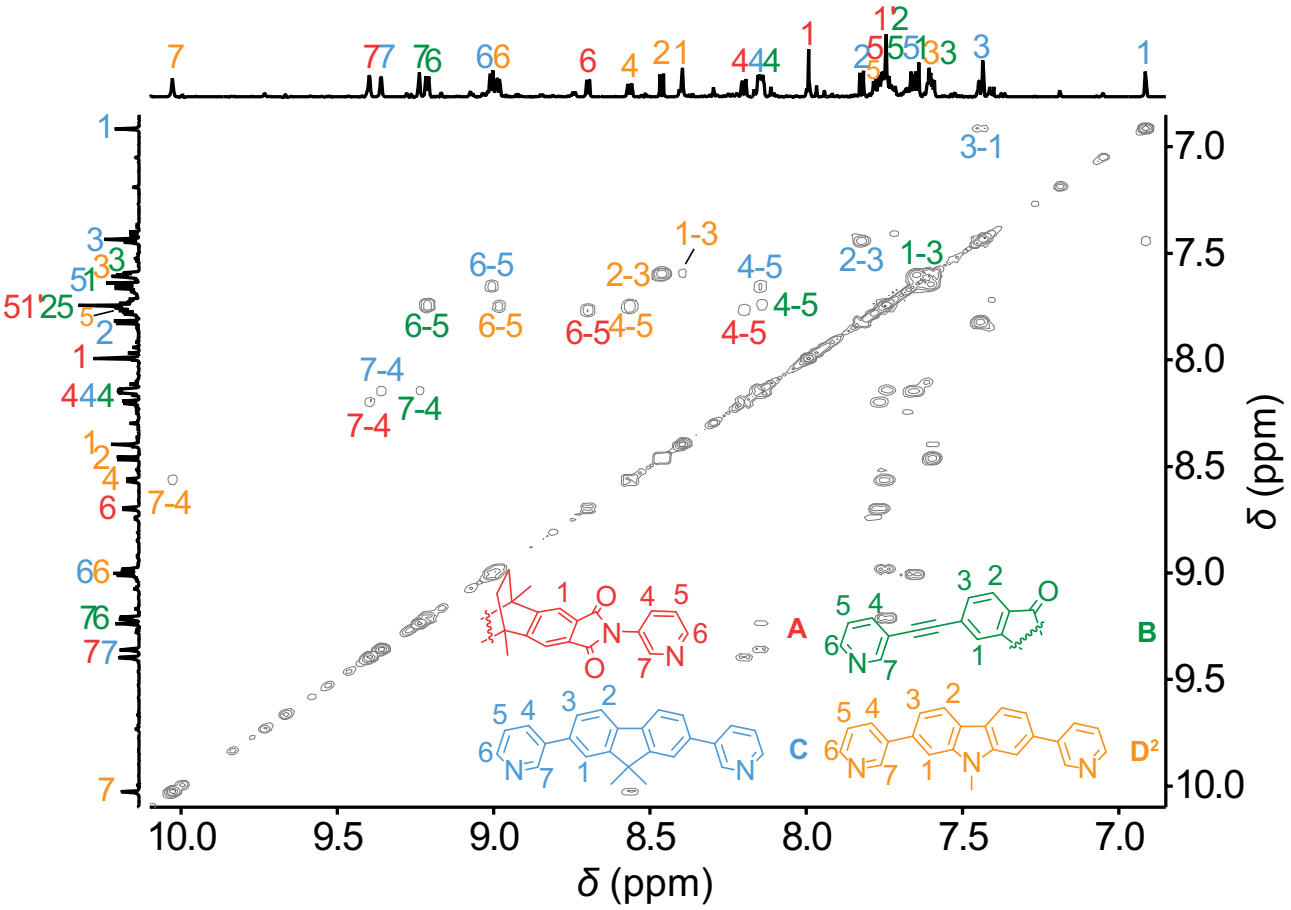

Supplementary Figure 212 | Partial ^{1}H–^{1}H COSY spectrum (500 MHz, 298 K, CD_3CN) of heteroleptic cage Pd_2**ABCD²**.

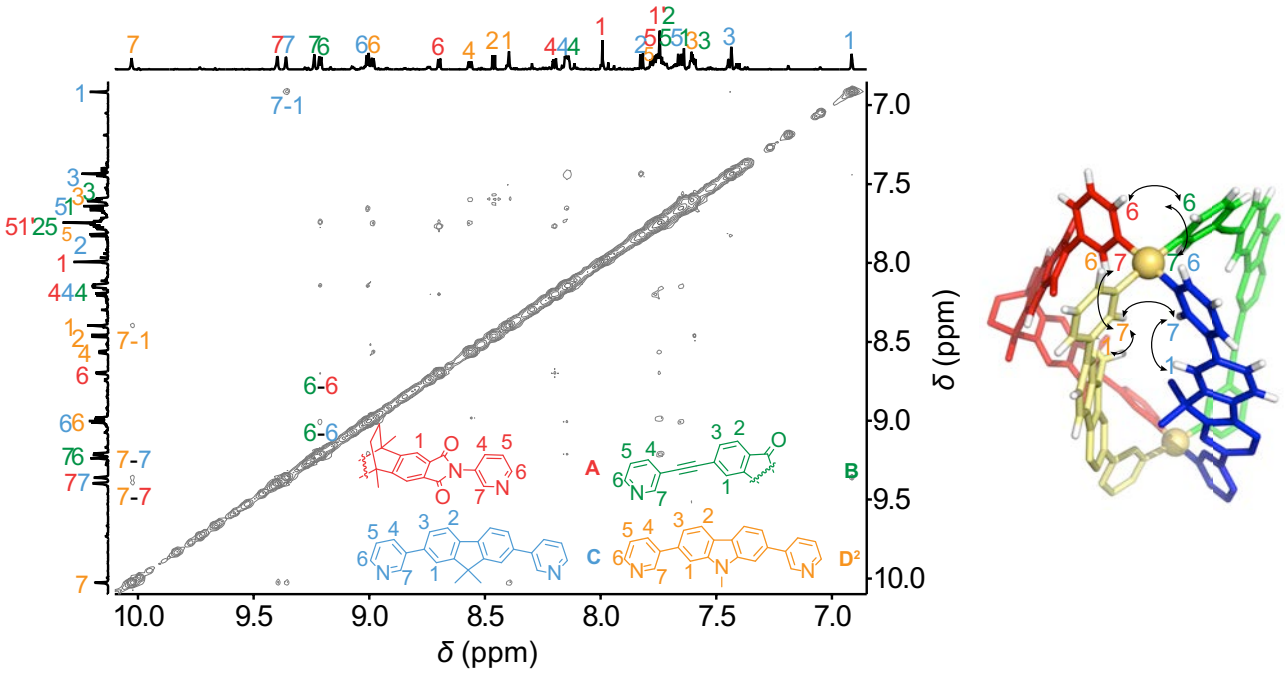

Supplementary Figure 213 | Partial ^{1}H–^{1}H NOESY spectrum (500 MHz, 298 K, CD_3CN) of heteroleptic cage Pd_2**ABCD**^{2}. The composition of this heteroleptic cage is supported by a single crystal X-ray structure (details see below). The found NOE contacts in solution are in full accordance with the X-ray structure results.

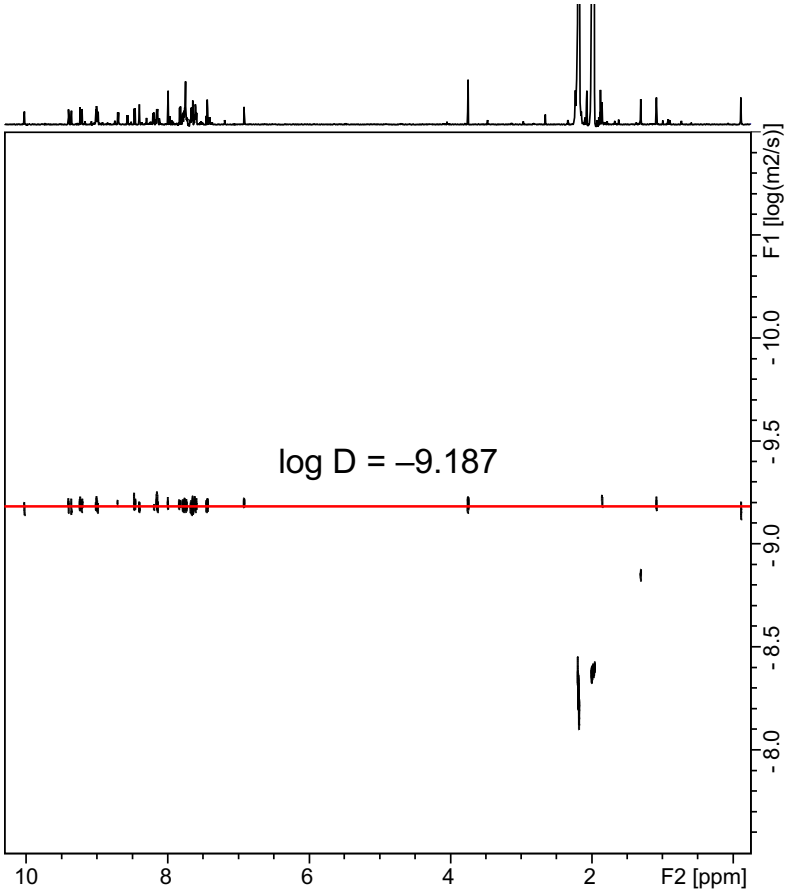

Supplementary Figure 214 | ^{1}H DOSY spectrum (500 MHz, 298 K, CD_3CN) of heteroleptic cage Pd_2**ABCD**^{2}. Diffusion coefficient for Pd_2**ABCD**^{2}: D = 6.187 × 10^{-10} m^2s^{-1}, log *D* = –9.187, r = 10.1 Å.

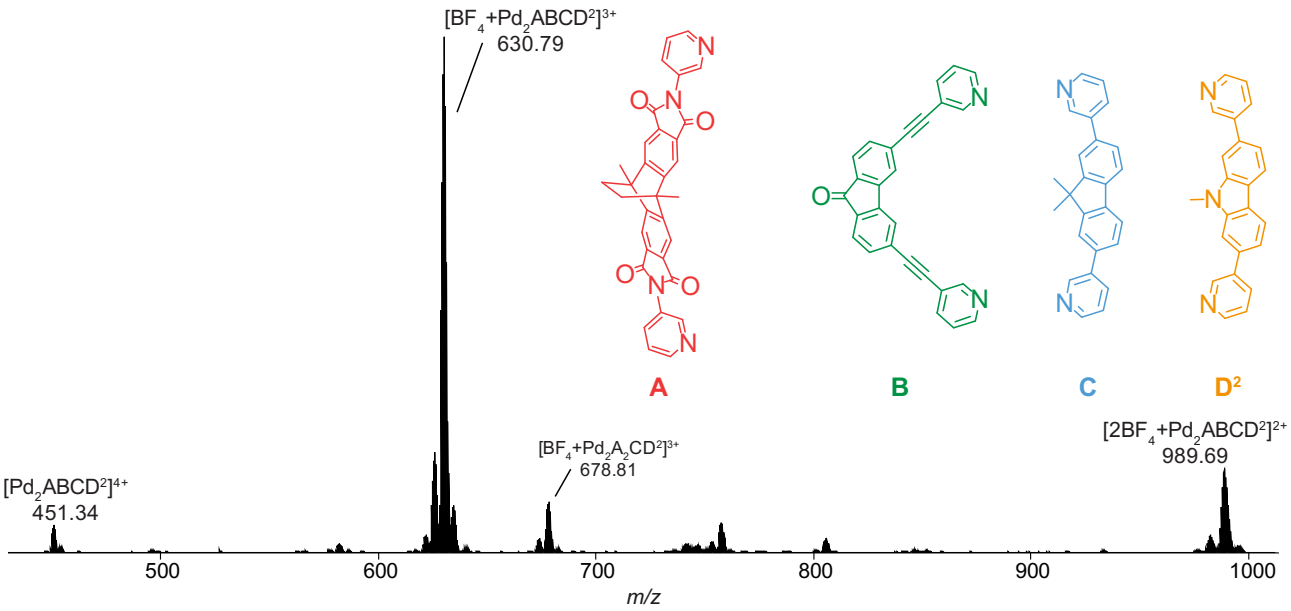

Supplementary Figure 215 | HR-ESI mass spectrum of heteroleptic cage Pd_2**ABCD**^{2}.

3.8. Evolution of heteroleptic cage Pd_2ABCD^3

3.8.1. Self-assembly of heteroleptic cage $Pd_2A_2CD^3$

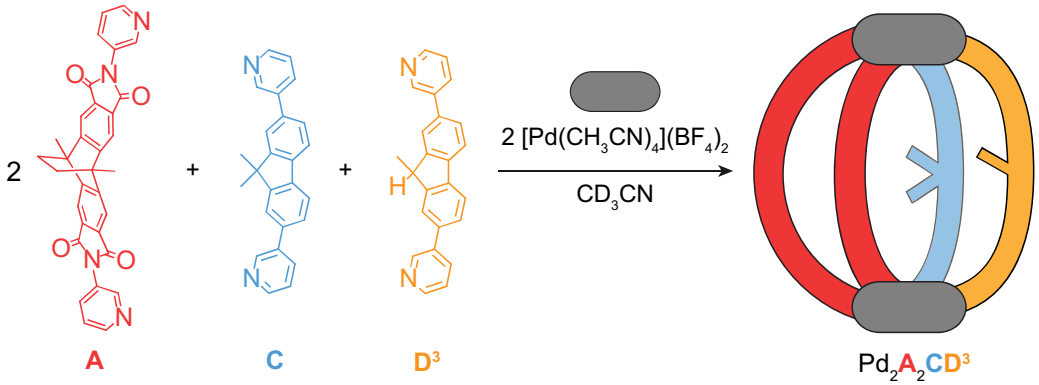

To a solution of **C** (60 µL, 3 mM, 0.18 µmol) and **D**^{2} (60 µL, 3 mM, 0.18 µmol) in CD_3CN and **A** (120 µL, 3 mM, 0.36 µmol) were added a stock solution of $[Pd(CH_3CN)_4](BF_4)_2$ (24 µL, 15 mM/CD_3CN, 0.18 µmol) and 186 µL additional CD_3CN. The mixture was heated at 80 °C for 8 h to give a 0.4 mM cage solution containing the shown cage as predominant species.

^{1}H NMR (700 MHz, 298 K, CD_3CN) δ 9.75 (d, J = 2.0 Hz, 2H), 9.31 (d, J = 2.1 Hz, 2H), 9.23 (d, J = 2.0 Hz, 2H), 9.10 (dd, J = 5.9, 1.3 Hz, 2H), 8.97 – 8.94 (m, 4H), 8.89 (ddd, J = 7.2, 5.8, 1.3 Hz, 4H), 8.41 (dt, J = 8.1, 1.5 Hz, 2H), 8.25 – 8.23 (m, 2H), 8.18 (ddd, J = 8.2, 2.2, 1.2 Hz, 2H), 8.14 (dt, J = 7.9, 1.6 Hz, 2H), 8.06 (s, 2H), 8.03 – 8.01 (m, 2H), 8.00 (d, J = 7.7 Hz, 2H), 7.82 – 7.79 (m, 4H), 7.76 (d, J = 7.7 Hz, 2H), 7.72 (s, 2H), 7.70 (s, 2H), 7.69 – 7.66 (m, 4H), 7.65 – 7.63 (m, 2H), 7.59 (s, 2H), 7.59 – 7.57 (m, 2H), 7.48 – 7.45 (m, 2H), 7.05 (d, J = 1.8 Hz, 2H), 4.20 (q, J = 7.3 Hz, 1H), 2.29 (s, 3H), 2.13 (s, 3H), 2.00 (s, 3H), 1.96 – 1.95 s, 3H), 1.76 (b, 8H), 1.17 (d, J = 7.4 Hz, 3H), 0.94 (s, 3H), 0.27 (s, 3H).

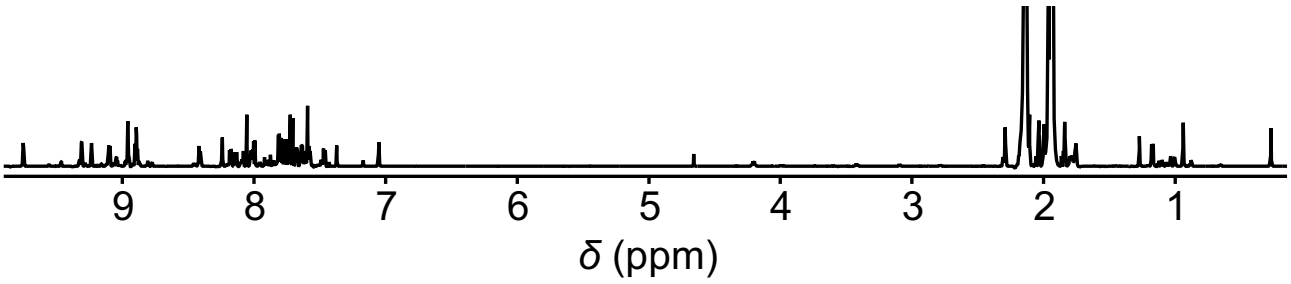

Supplementary Figure 216 | ^{1}H NMR spectrum (700 MHz, 298 K, CD_3CN) of heteroleptic cage $Pd_2\mathbf{A}_2\mathbf{CD}^3$.

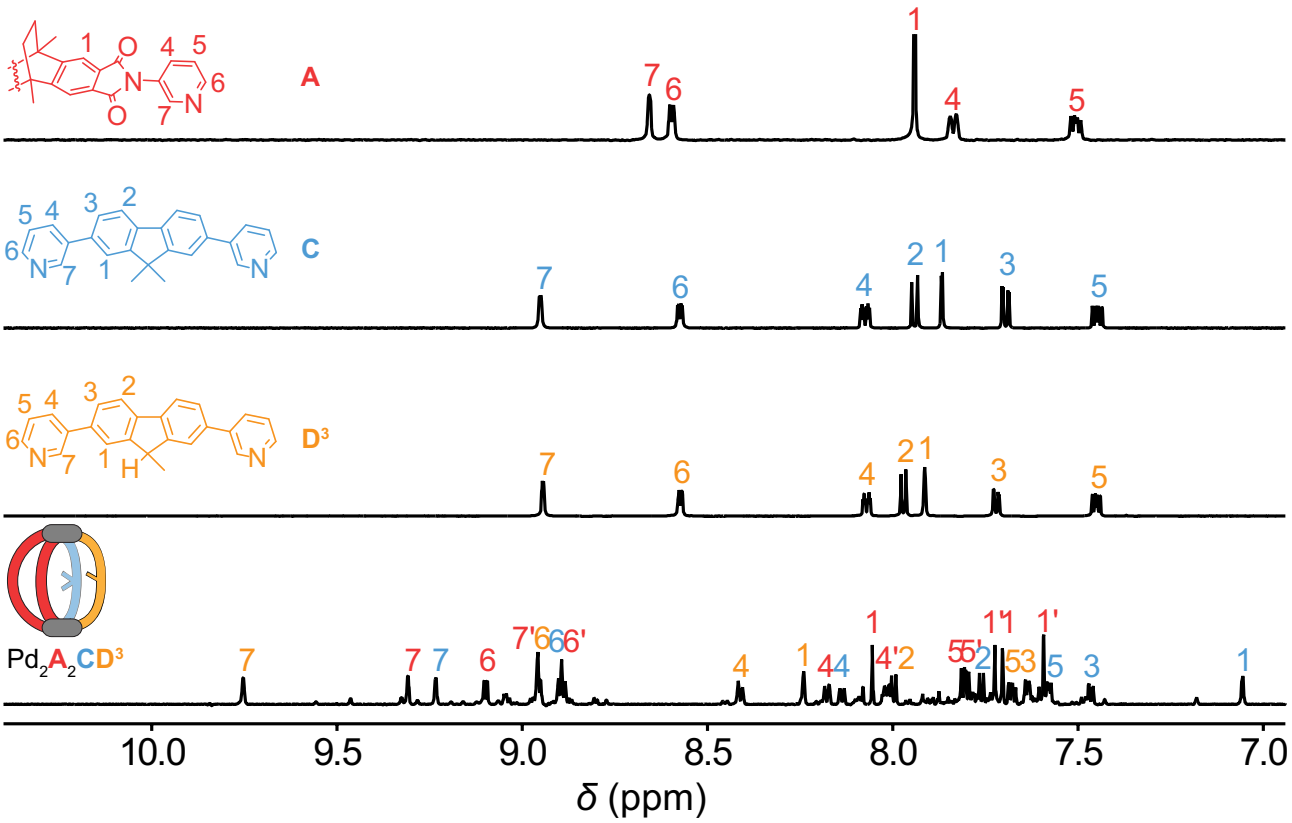

Supplementary Figure 217 | Partial ^{1}H NMR spectrum (700 MHz, 298 K, CD_3CN) comparison of ligands **A** (red), **C** (blue), **D**^{3} (yellow), heteroleptic cage $Pd_2\mathbf{A}_2\mathbf{CD}^3$.

^{13}C NMR (176 MHz, 298 K, CD_3CN) δ 172.96, 167.32, 166.93, 166.84, 166.40, 156.16, 154.91, 154.46, 154.41, 154.35, 152.26, 150.87, 150.82, 150.78, 150.56, 150.24, 150.07, 150.06, 149.99, 143.15, 142.37, 142.13, 140.14, 139.89, 139.80, 139.29, 139.17, 135.60, 135.43, 132.15, 132.06, 130.73, 130.59, 130.32, 128.85, 128.53, 128.30, 128.29, 127.54, 124.89, 122.93, 122.45, 122.39, 117.82, 117.59, 117.43, 46.54, 45.65, 45.25, 45.17, 45.07, 34.80, 34.65, 30.37, 27.02, 25.83, 20.92.

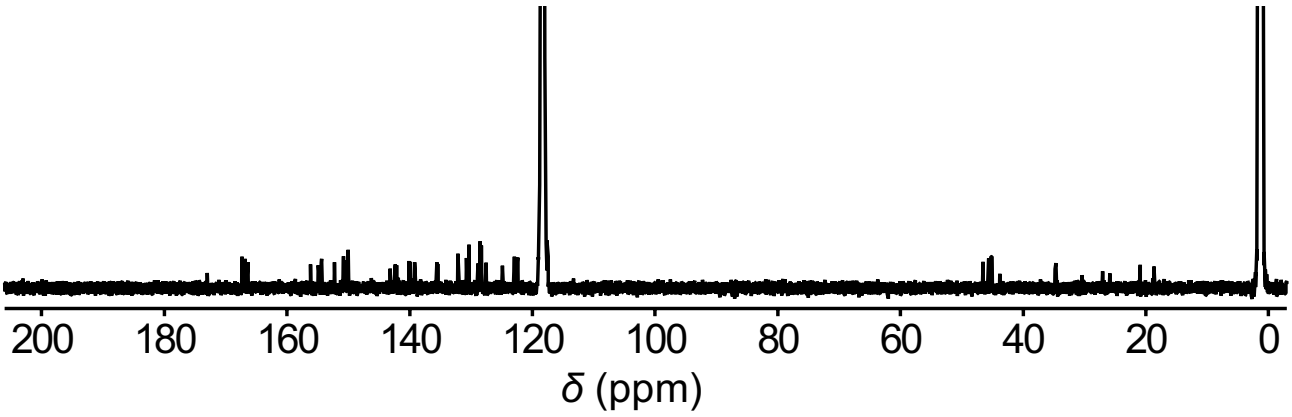

Supplementary Figure 218 | ^{13}C NMR spectrum (176 MHz, 298 K, CD_3CN) of heteroleptic cage $Pd_2\mathbf{A}_2\mathbf{CD}^3$.

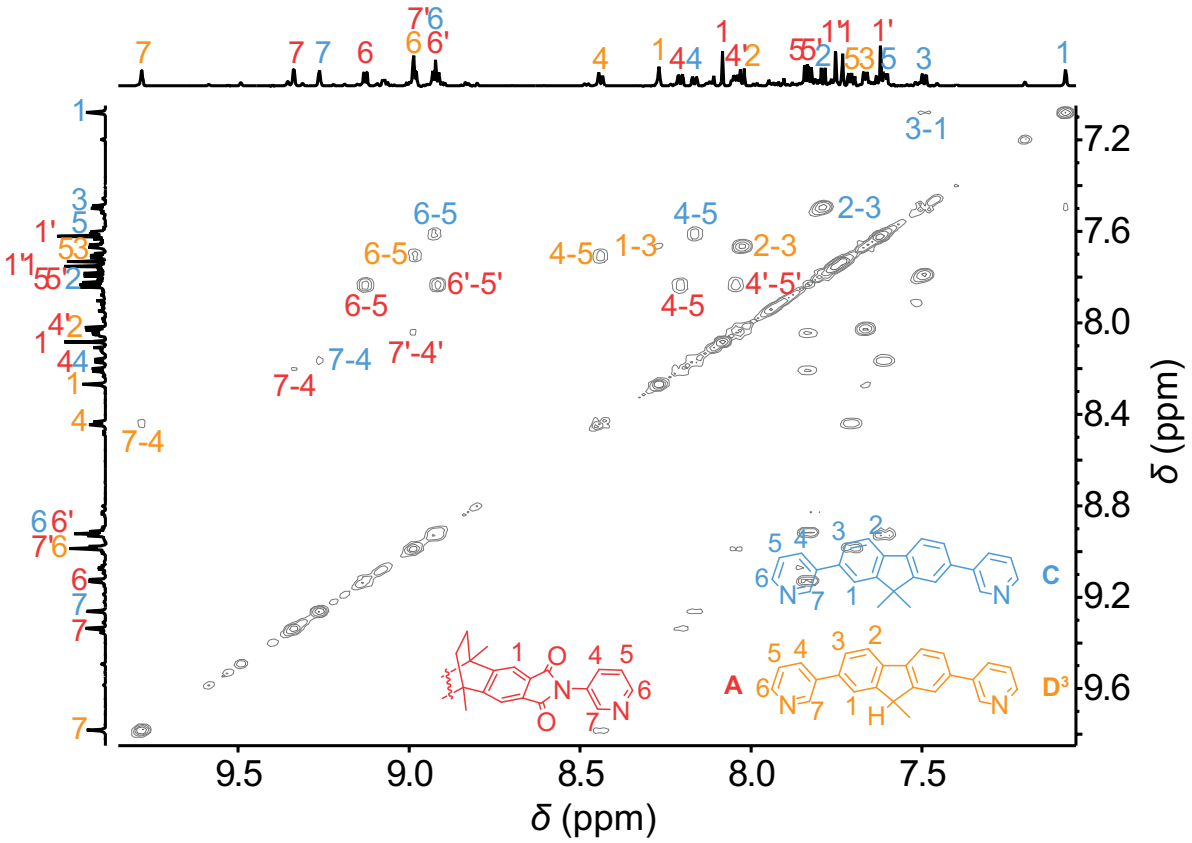

Supplementary Figure 219 | Partial ^{1}H–^{1}H COSY spectrum (500 MHz, 298 K, CD_3CN) of heteroleptic cage $Pd_2\mathbf{A}_2\mathbf{CD}^3$.

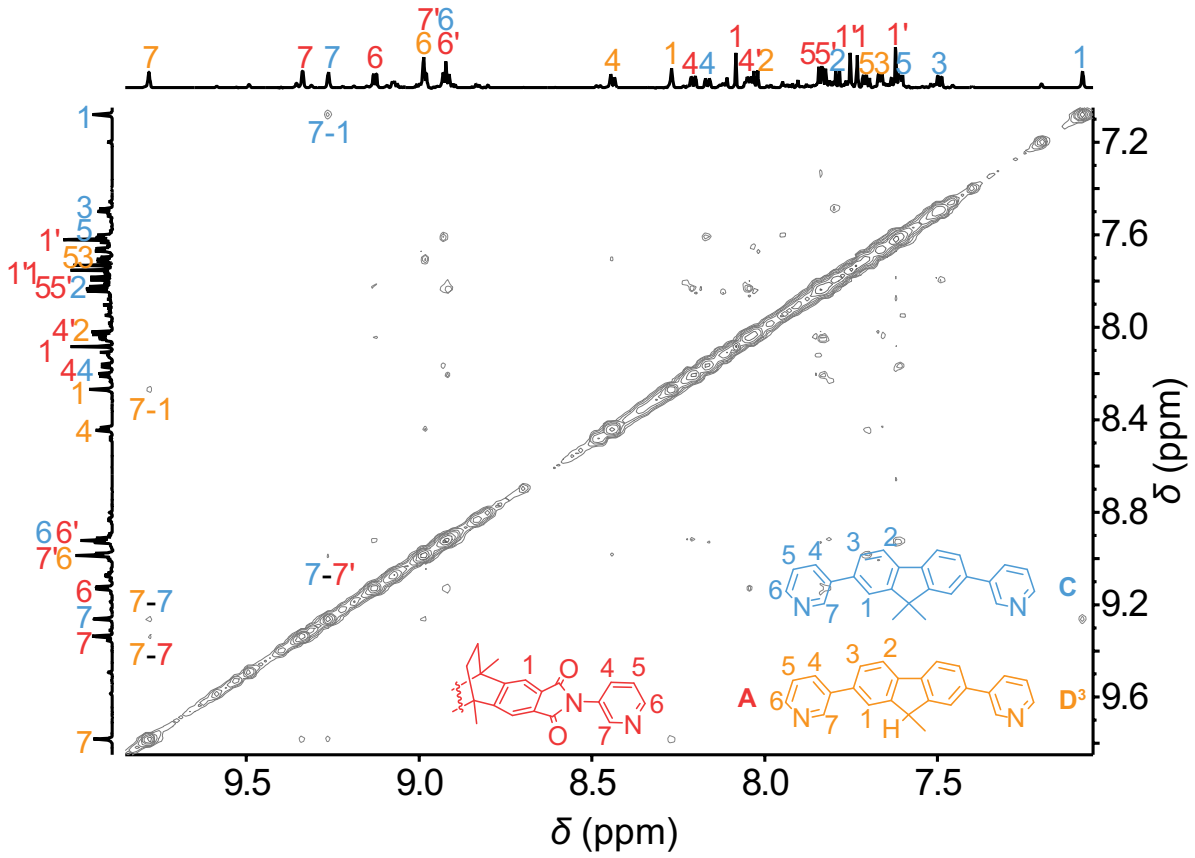

Supplementary Figure 220 | Partial ^{1}H–^{1}H NOESY spectrum (500 MHz, 298 K, CD_3CN) of heteroleptic cage $Pd_2\mathbf{A}_2\mathbf{CD}^{3}$.

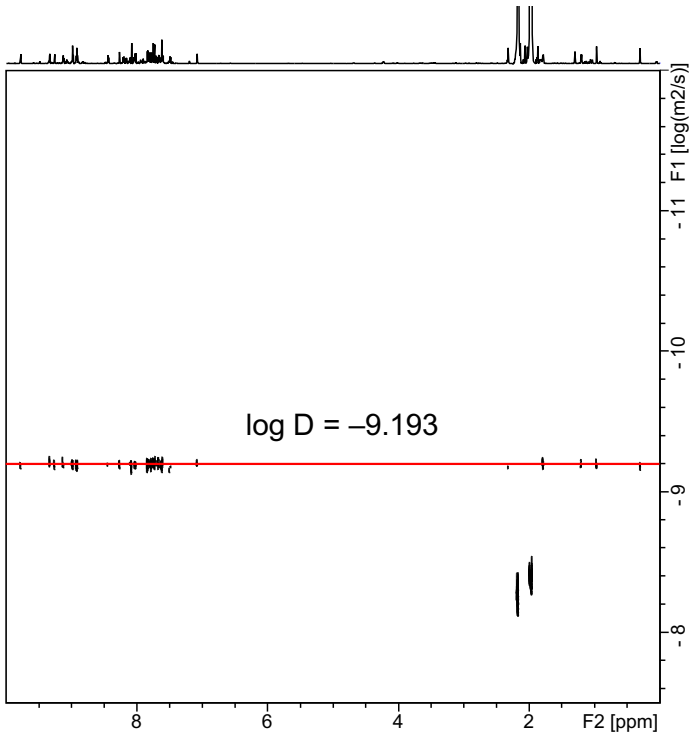

Supplementary Figure 221 | ^{1}H DOSY spectrum (500 MHz, 298 K, CD_3CN) of heteroleptic cage $Pd_2\mathbf{A}_2\mathbf{CD}^{3}$. Diffusion coefficient for $Pd_2\mathbf{A}_2\mathbf{CD}^{3}$: D = 6.412 × 10^{-10} m^2s^{-1}, log *D* = −9.193, r = 10.2 Å.

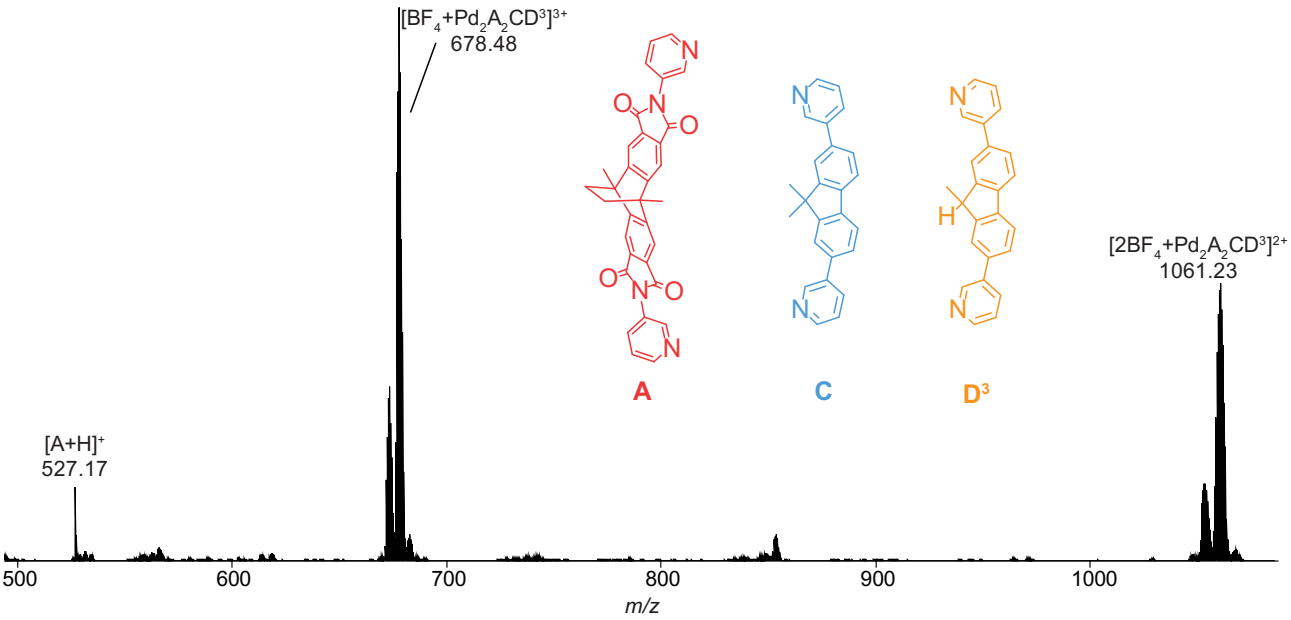

Supplementary Figure 222 | HR-ESI mass spectrum of heteroleptic cage $Pd_2\mathbf{A}_2\mathbf{CD}^3$.

3.8.2. Self-assembly of heteroleptic cage $Pd_2\mathbf{B}_2\mathbf{CD}^3$

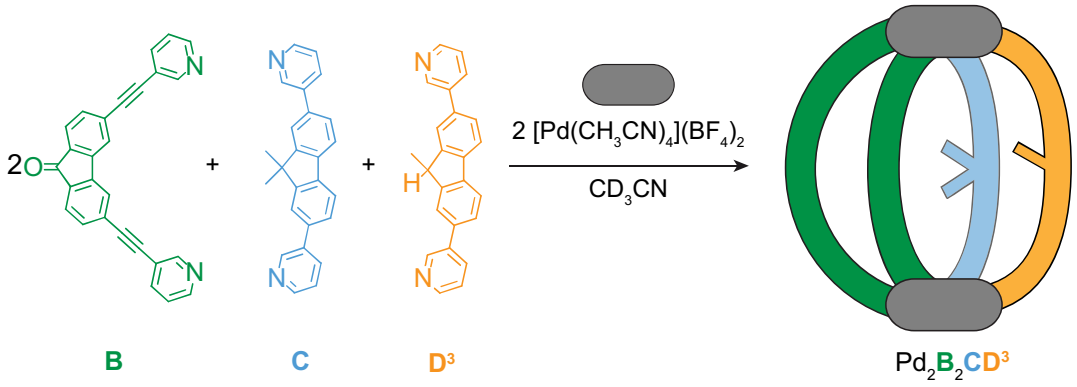

To a solution of **C** (60 µL, 3 mM, 0.18 µmol) and a suspension of $\mathbf{D}^2$ (60 µL, 3 mM, 0.18 µmol), **B** (120 µL, 3 mM, 0.36 µmol) in CD_3CN were added a stock solution of $[Pd(CH_3CN)_4](BF_4)_2$ (24 µL, 15 mM/CD_3CN, 0.18 µmol) and 186 µL additional CD_3CN. The mixture was heated at 80 °C for 8 h to give a 0.4 mM cage solution containing the shown cage as predominant species.

^{1}H NMR (700 MHz, 298 K, CD_3CN) δ 10.06 (d, J = 2.0 Hz, 2H), 9.67 (d, J = 1.8 Hz, 2H), 9.45 (d, J = 1.9 Hz, 2H), 9.32 (d, J = 1.8 Hz, 2H), 9.17 (dd, J = 5.9, 1.4 Hz, 2H), 9.09 – 9.07 (m, 2H), 9.02 (d, J = 5.6 Hz, 2H), 8.98 (dt, J = 6.0, 1.1 Hz, 2H), 8.61 (s, 2H), 8.36 (d, J = 7.9 Hz, 2H), 8.21 (dq, J = 7.9, 2.0 Hz, 2H), 8.17 (d, J = 7.6 Hz, 2H), 8.13 (dt, J = 8.0, 1.6 Hz, 2H), 8.07 (d, J = 7.6 Hz, 2H), 7.88 (d, J = 7.6 Hz, 2H), 7.85 (s, 2H), 7.72 – 7.64 (m, 18H), 7.63 – 7.60 (m, 2H), 7.49 (dd, J = 7.5, 1.7 Hz, 2H), 7.17 (d, J = 1.8 Hz, 2H), 1.90 (d, J = 7.6 Hz, 3H), 1.58 (s, 3H), 0.41 (s, 3H).

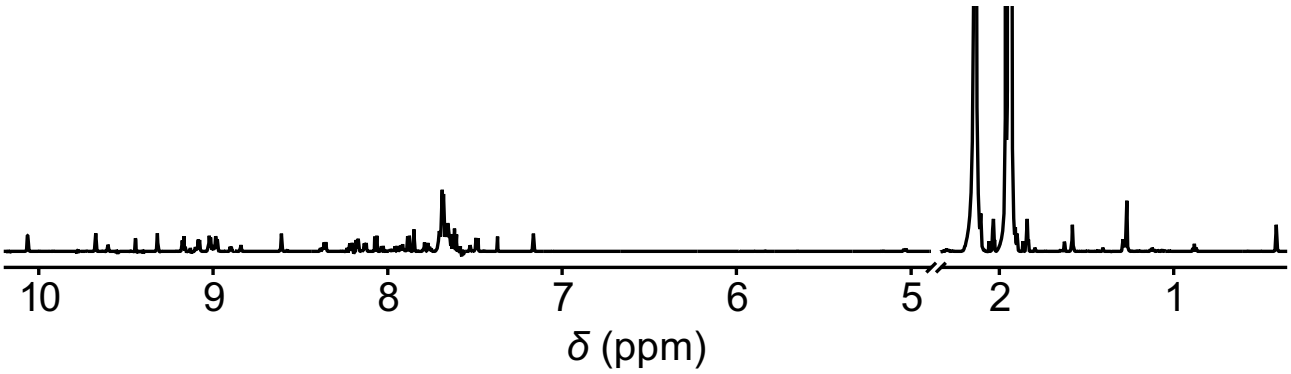

Supplementary Figure 223 | ^{1}H NMR spectrum (700 MHz, 298 K, CD_3CN) of heteroleptic cage $Pd_2\mathbf{B}_2\mathbf{CD}^3$.

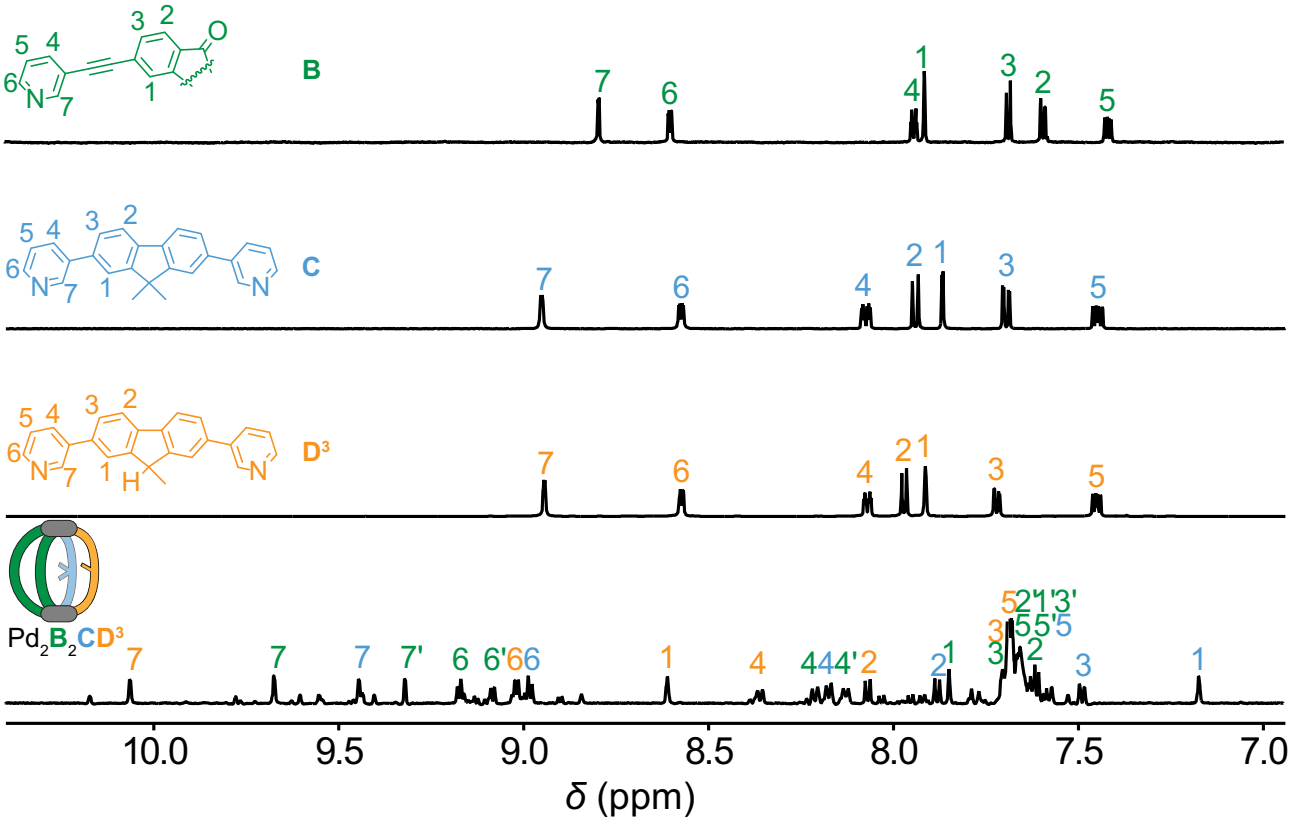

Supplementary Figure 224 | Partial ^{1}H NMR spectrum (700 MHz, 298 K, CD_3CN) comparison of ligands **B** (green), **C** (blue), $\mathbf{D}^3$ (yellow), heteroleptic cage $Pd_2\mathbf{B}_2\mathbf{CD}^3$.

^{13}C NMR (151 MHz, 298 K, CD_3CN) δ 192.20, 192.15, 172.97, 156.37, 153.80, 153.45, 152.49, 151.39, 151.23, 150.35, 150.25, 149.92, 144.87, 144.80, 144.74, 142.67, 142.55, 142.16, 140.23, 139.22, 139.16, 136.40, 136.03, 135.67, 135.56, 135.45, 129.07, 128.74, 128.59, 128.55, 128.49, 128.37, 128.29, 128.22, 127.94, 125.27, 125.10, 124.93, 124.49, 124.34, 123.87, 123.74, 123.35, 123.11, 122.78, 122.66, 95.52, 95.51, 87.85, 87.38, 46.85, 44.51, 30.39, 30.36, 27.45.

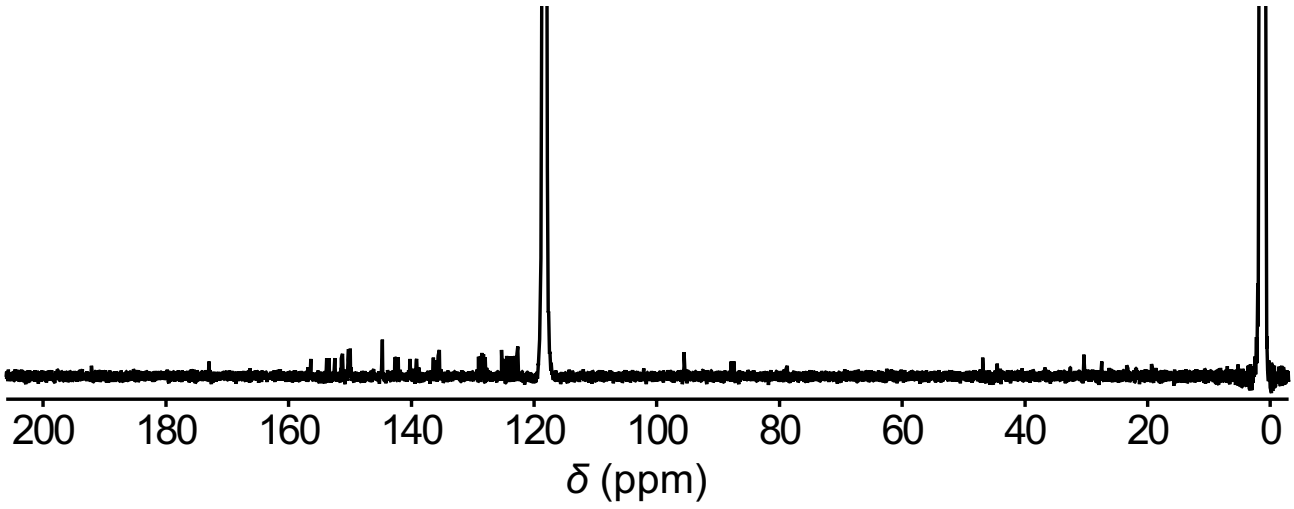

Supplementary Figure 225 | ^{13}C NMR spectrum (151 MHz, 298 K, CD_3CN) of heteroleptic cage $Pd_2\mathbf{B}_2\mathbf{CD}^3$.

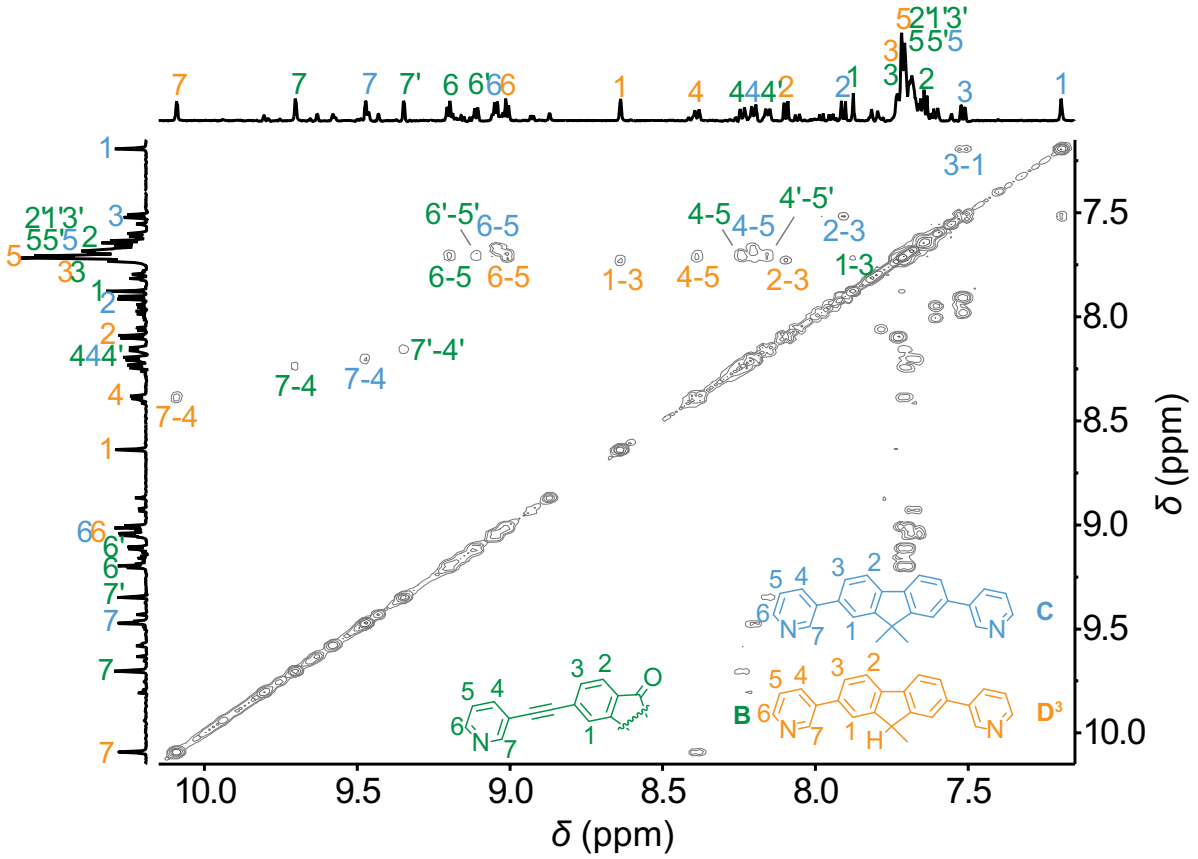

Supplementary Figure 226 | Partial ^{1}H–^{1}H COSY spectrum (500 MHz, 298 K, CD_3CN) of heteroleptic cage $Pd_2\mathbf{B}_2\mathbf{CD}^3$.

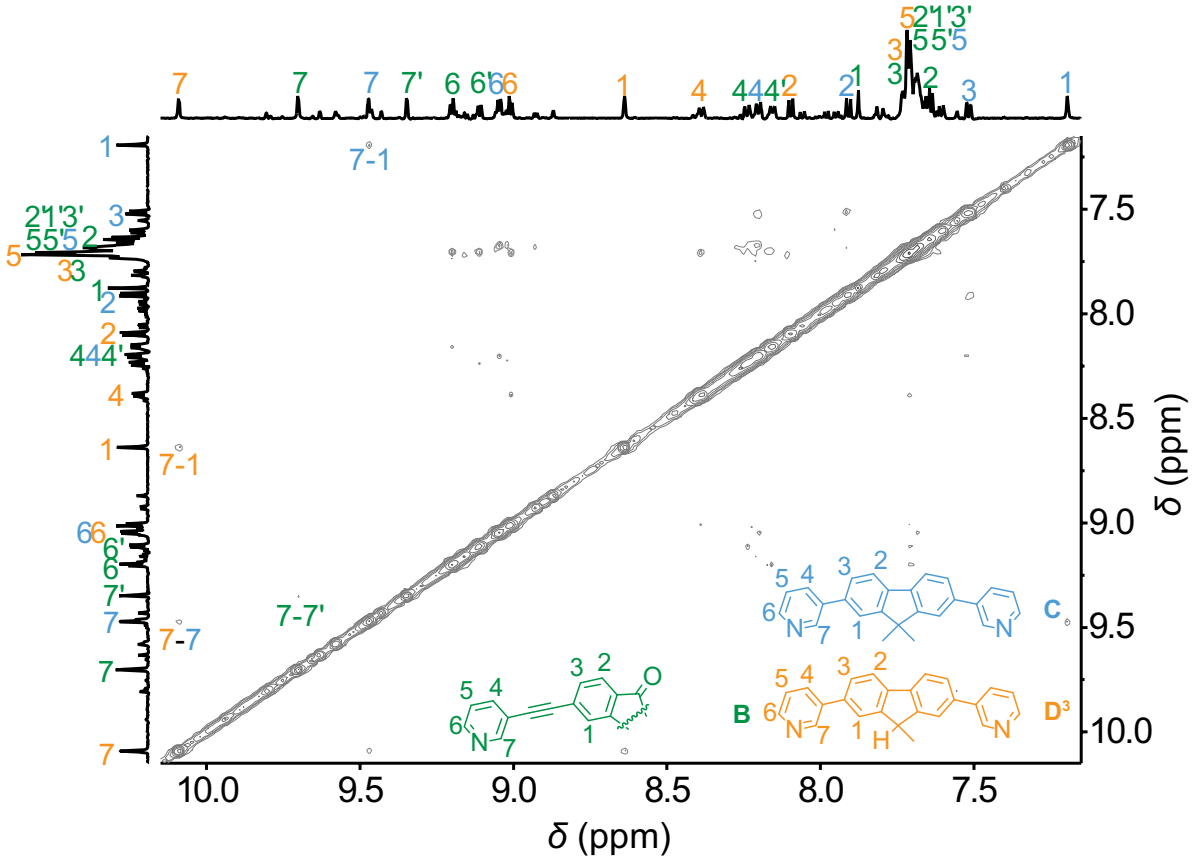

Supplementary Figure 227 | Partial ^{1}H–^{1}H NOESY spectrum (500 MHz, 298 K, CD_3CN) of heteroleptic cage $Pd_2\mathbf{B_2CD^3}$.

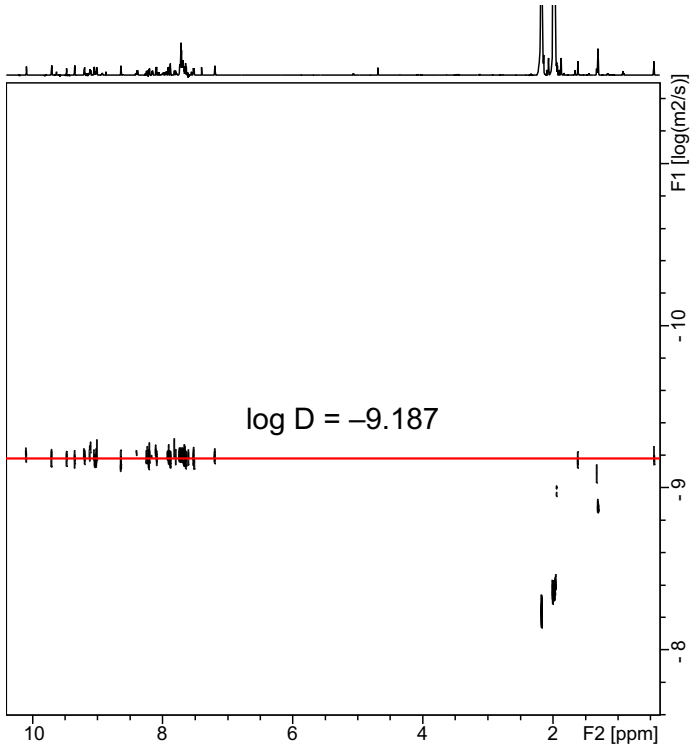

Supplementary Figure 228 | ^{1}H DOSY spectrum (500 MHz, 298 K, CD_3CN) of heteroleptic cage $Pd_2\mathbf{B_2CD^3}$. Diffusion coefficient for $Pd_2\mathbf{B_2CD^3}$: D = 6.501 × 10^{-10} m^2s^{-1}, log *D* = −9.187, r = 10.1 Å.

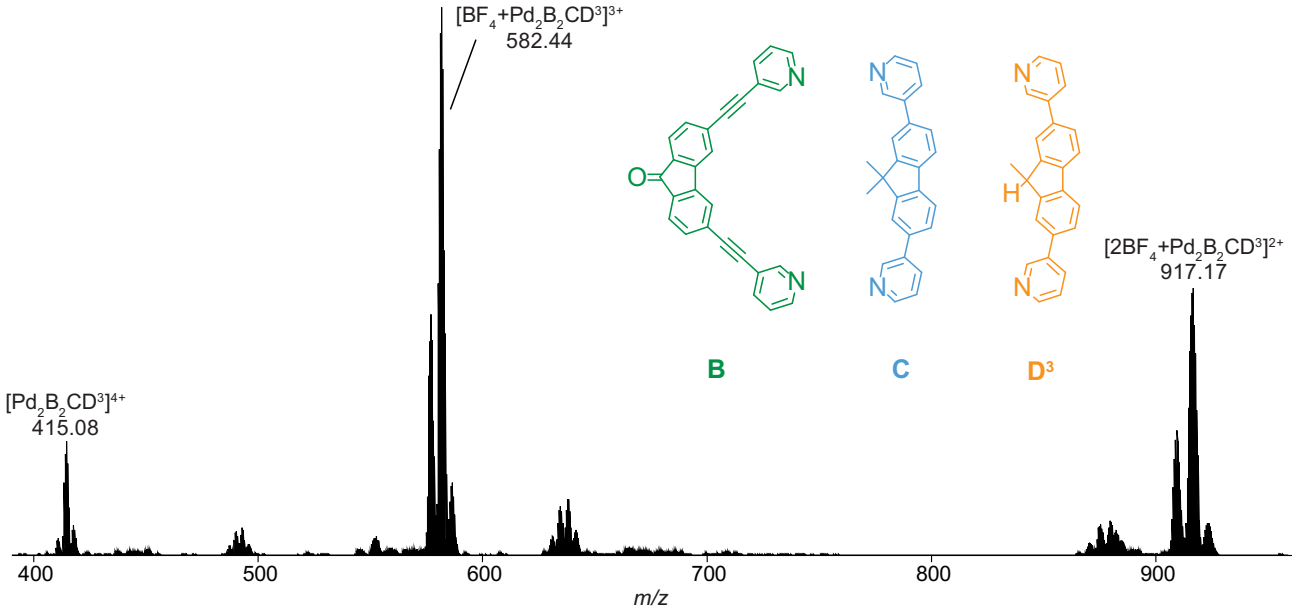

Supplementary Figure 229 | HR-ESI mass spectrum of heteroleptic cage Pd_2**B**$_2$**CD**^{3}.

*3.8.3. Self-assembly of heteroleptic cage Pd_2**ABCD**^{3}*

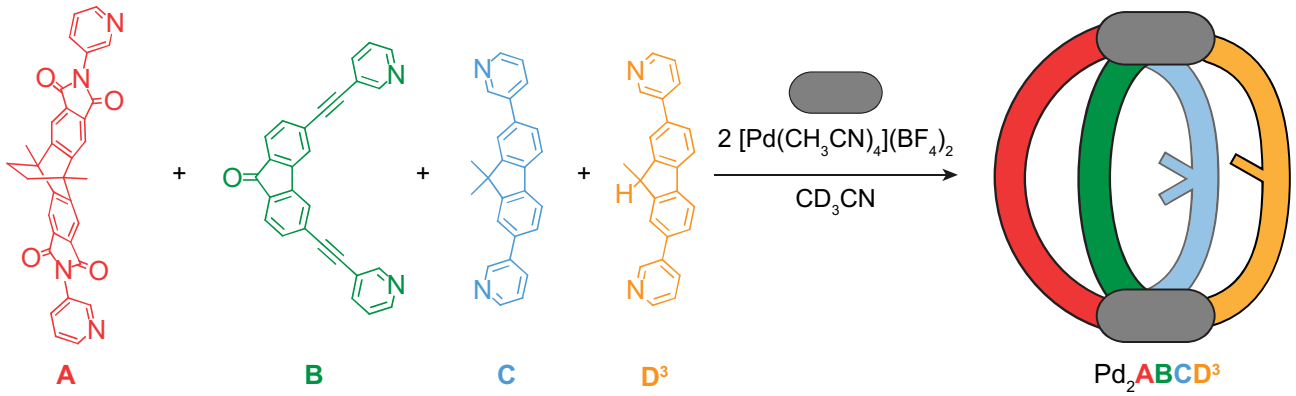

To a solution of **A** (60 µL, 3 mM, 0.18 µmol), **C** (60 µL, 3 mM, 0.18 µmol), **D**^{3} (60 µL, 3 mM, 0.18 µmol) and a suspension of **B** (60 µL, 3 mM, 0.18 µmol), was added a stock solution of $[Pd(CH_3CN)_4](BF_4)_2$ (24 µL, 15 mM/CD_3CN, 0.36 µmol) and additional 186 µL CD_3CN. The mixture was heated at 80 °C for 8 h to give a 0.4 mM cage solution containing the shown cage as predominant species.

^{1}H NMR (700 MHz, 298 K, CD_3CN) δ 9.97 (d, J = 2.0 Hz, 2H), 9.36 (d, J = 2.1 Hz, 2H), 9.28 (d, J = 2.1 Hz, 2H), 9.18 (dd, J = 5.9, 1.4 Hz, 2H), 9.13 (d, J = 1.8 Hz, 2H), 8.98 (dd, J = 6.0, 1.3 Hz, 2H), 8.96 (dd, J = 5.8, 1.2 Hz, 2H), 8.79 (dd, J = 6.1, 1.3 Hz, 2H), 8.45 (dt, J = 7.9, 1.7 Hz, 2H), 8.44 (s, 2H), 8.11 (m, 8H), 7.91 (d, J = 2.1 Hz, 2H), 7.82 (dd, J = 7.5, 3.2 Hz, 2H), 7.79 (s, 2H), 7.75 – 7.69 (m, 8H), 7.63 (ddd, J = 7.7, 2.2, 0.7 Hz, 4H), 7.59 (m, 2H), 7.44 – 7.42 (m, 4H), 7.01 (d, J = 1.8 Hz, 2H), 4.57 (q, J = 7.5 Hz, 1H), 2.16 – 2.15 (s, 3H), 2.02 (s, 3H), 1.82 (b, 4H), 1.42 (d, J = 7.4 Hz, 3H), 1.32 (s, 3H), 0.26 (s, 3H).

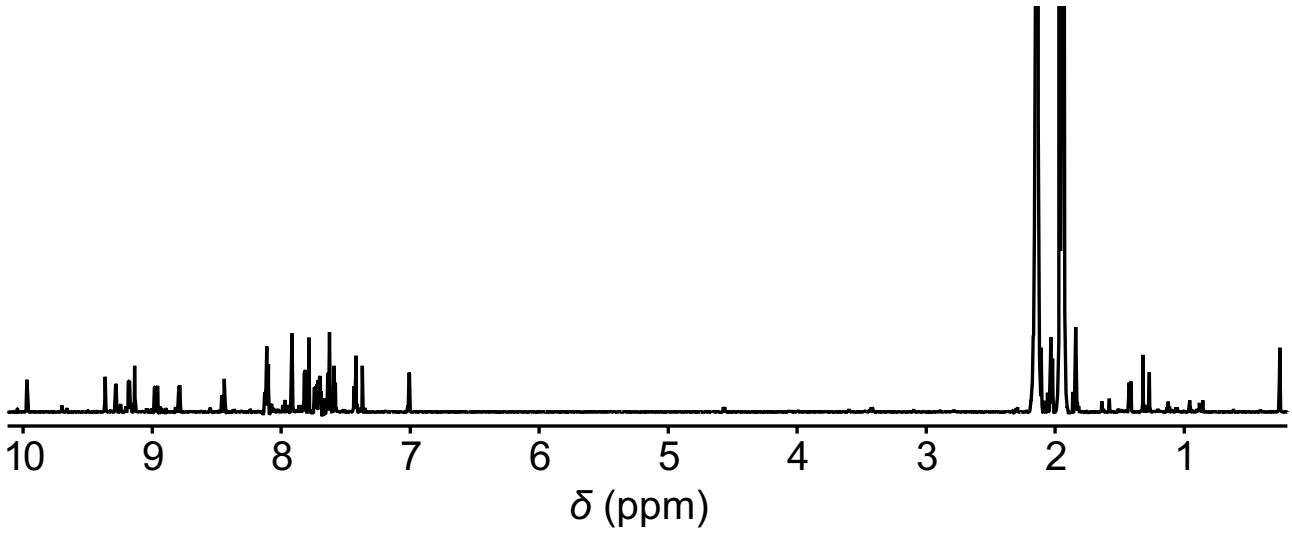

Supplementary Figure 230 | ^{1}H NMR spectrum (700 MHz, 298 K, CD_3CN) of heteroleptic cage Pd_2**ABCD**^{3}.

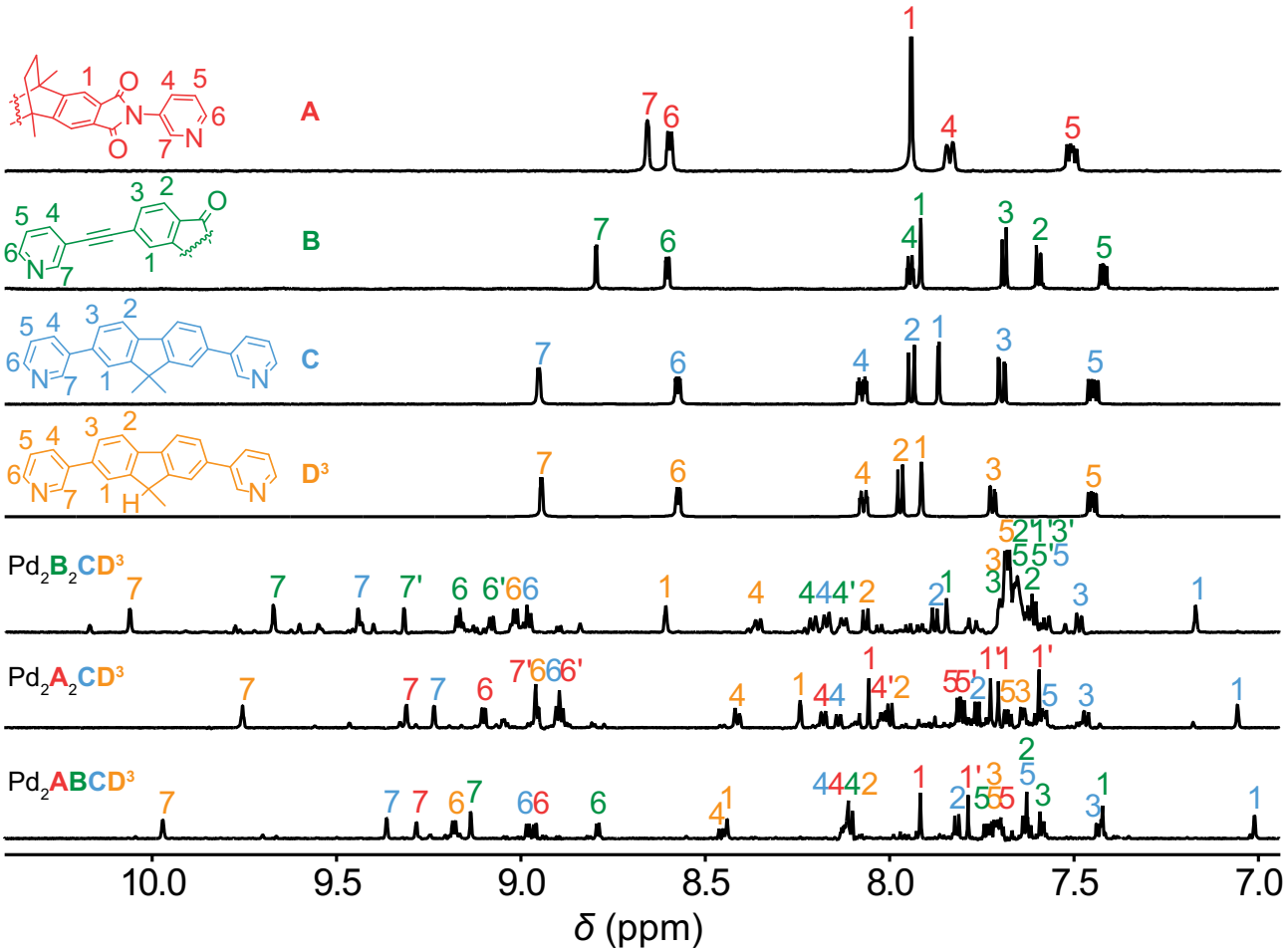

Supplementary Figure 231 | Partial ^{1}H NMR spectrum (700 MHz, 298 K, CD_3CN) comparison of ligands **A** (red), **B** (green), **C** (blue), **D**^{2} (yellow), heteroleptic cages Pd_2**B**$_2$**CD**^{3}, Pd_2**A**$_2$**CD**^{3} and Pd_2**ABCD**^{3}.

^{13}C NMR (176 MHz, 298 K, CD_3CN) δ 192.19, 172.98, 167.28, 167.02, 156.27, 154.87, 154.58, 153.80, 152.71, 151.07, 150.81, 150.67, 150.48, 150.44, 150.14, 149.84, 144.84, 144.64, 143.34, 142.63, 142.01, 140.14, 139.97, 139.23, 139.12, 136.05, 135.75, 135.65, 135.45, 132.35, 130.88, 130.85, 128.59, 128.54, 128.53, 128.48, 128.39, 128.37, 127.76, 125.42, 125.10, 124.04, 123.76, 122.96, 122.74, 122.57, 95.26, 87.26, 46.59, 45.58, 45.35, 44.11, 34.58, 34.45, 30.31, 27.28, 25.98, 21.50, 18.58.

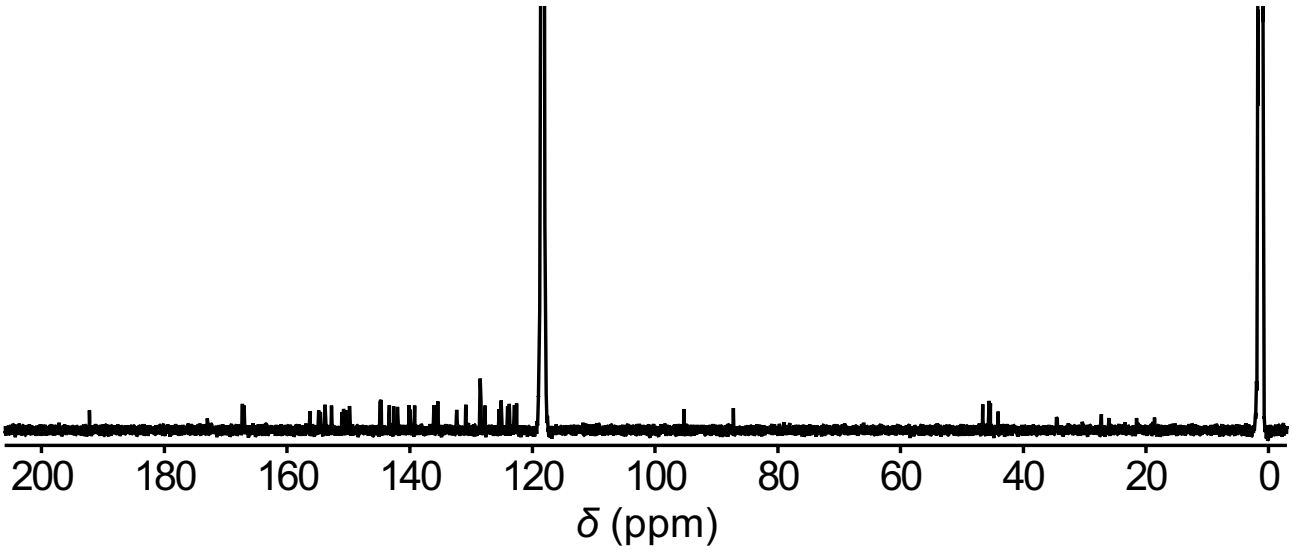

Supplementary Figure 232 | ^{13}C NMR spectrum (176 MHz, 298 K, CD_3CN) of heteroleptic cage Pd_2**ABCD**^{3}.

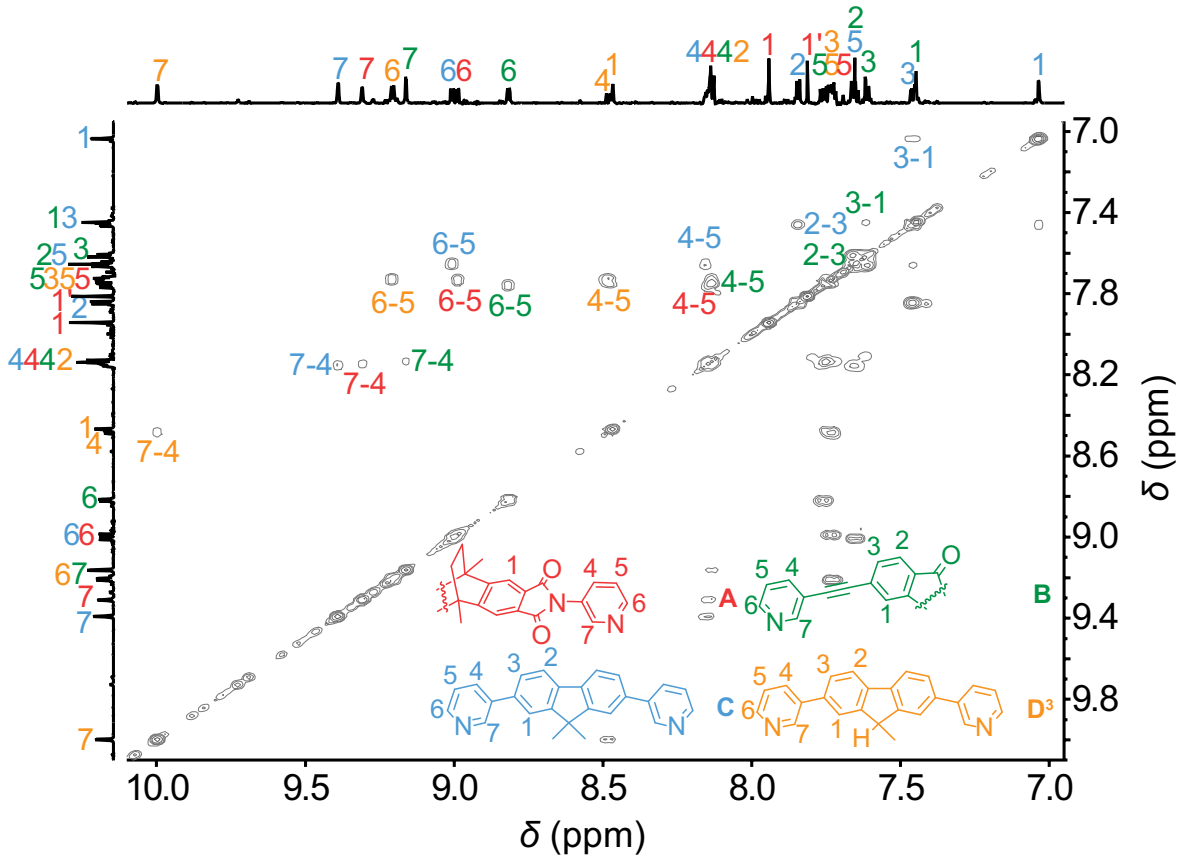

Supplementary Figure 233 | Partial ^{1}H–^{1}H COSY spectrum (500 MHz, 298 K, CD_3CN) of heteroleptic cage Pd_2**ABCD**^{3}.

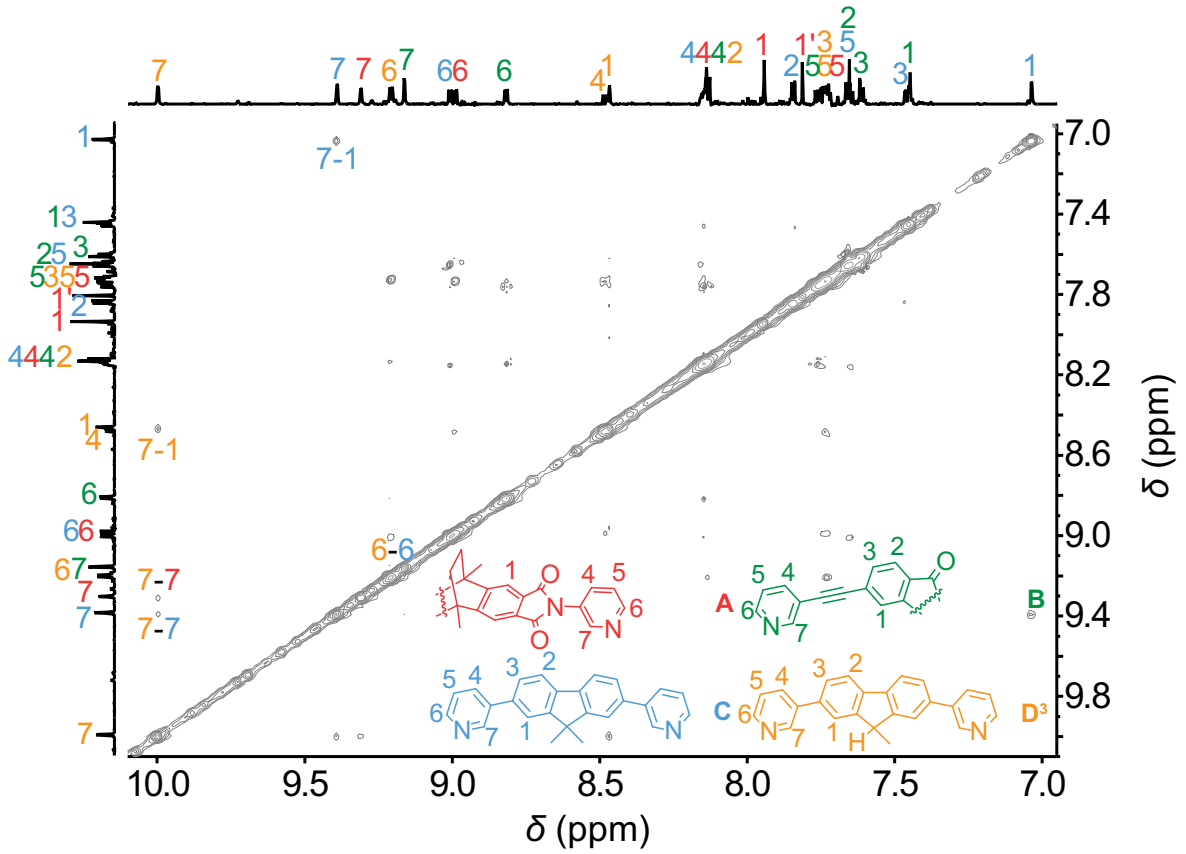

Supplementary Figure 234 | Partial ^{1}H–^{1}H NOESY spectrum (500 MHz, 298 K, CD_3CN) of heteroleptic cage Pd_2**ABCD**^{3}.

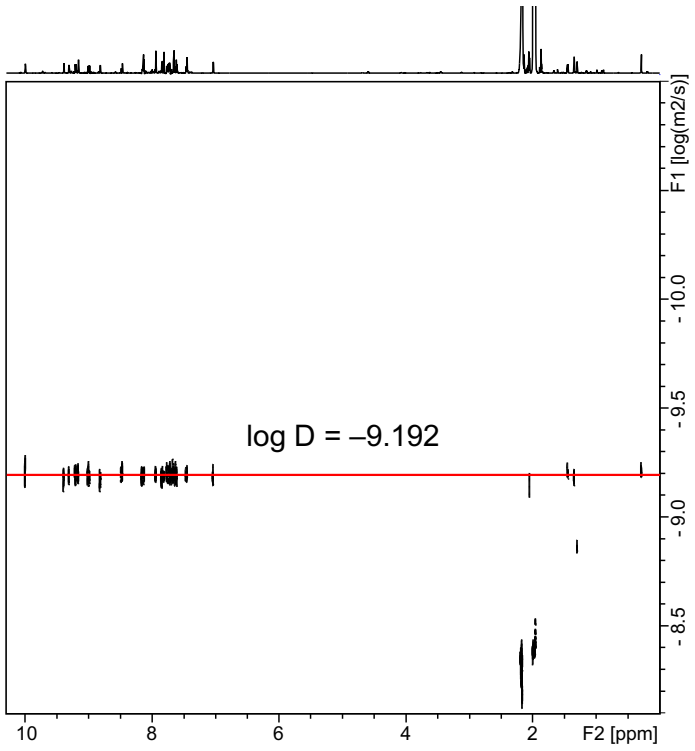

Supplementary Figure 235 | ^{1}H DOSY spectrum (500 MHz, 298 K, CD_3CN) of heteroleptic cage Pd_2**ABCD**^{3}. Diffusion coefficient for Pd_2**ABCD**^{3}: D = 6.427 × 10^{-10} m^2s^{-1}, log *D* = –9.192, r = 10.2 Å.

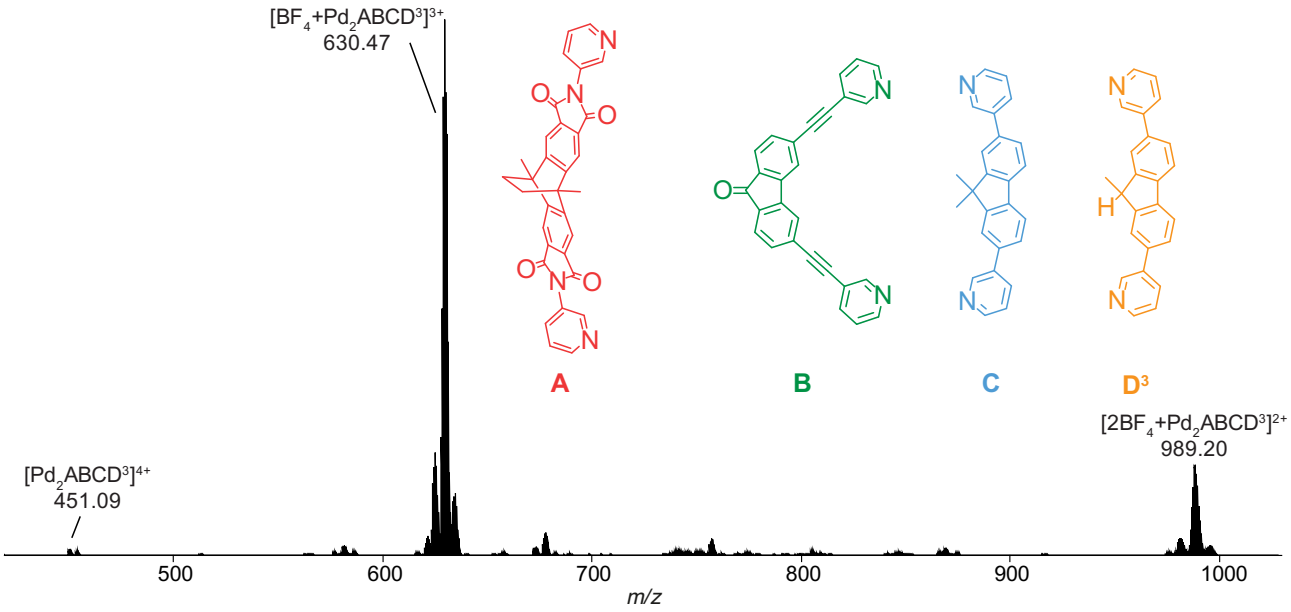

Supplementary Figure 236 | HR-ESI mass spectrum of heteroleptic cage Pd_2**ABCD**^{3}.

3.9. Evolution of heteroleptic cage Pd_2ABD^{4}C

For this particular combination of four distinguishable ligands, containing ligand **D**^{4} (notably having a much different structure than ligands **D**–**D**^{3}) a different ligand order was found concerning the arrangement around the Pd(II) centers, therefore this cage obeys to the formula Pd_2**ABD**^{4}**C** (not Pd_2**ABCD**^{4}). For a detailed discussion, see the main text.

3.9.1. Self-assembly of heteroleptic cage $Pd_2A_2D^4C$

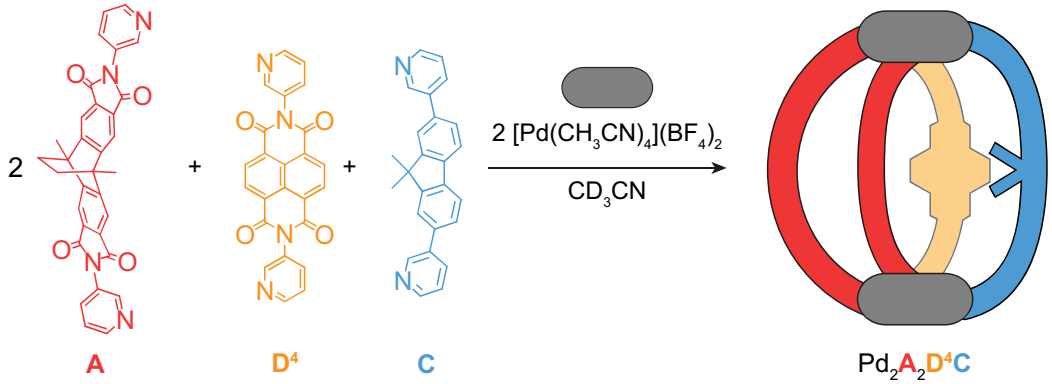

To a solution of **A** (120 µL, 3 mM, 0.36 µmol) and **C** (60 µL, 3 mM, 0.18 µmol) in CD_3CN and a suspension of **D**^{4} (60 µL, 3 mM, 0.18 µmol) were added a stock solution of $[Pd(CH_3CN)_4](BF_4)_2$ (24 µL, 15 mM/CD_3CN, 0.36 µmol) and 186 µL additional CD_3CN. The mixture was heated at 80 °C for 8 h to give a 0.4 mM cage solution containing the shown cage as predominant species.

^{1}H NMR (700 MHz, 298 K, CD_3CN) δ 9.27 (d, J = 2.0 Hz, 2H), 9.26 (d, J = 2.2 Hz, 2H), 9.14 (dd, J = 5.8, 1.3 Hz, 2H), 9.09 (d, J = 2.2 Hz, 2H), 9.02 (d, J = 2.2 Hz, 2H), 8.99 – 8.97 (m, 2H), 8.88 (dd, J = 5.8, 1.2 Hz, 2H), 8.75 (dd, J = 6.0, 1.3 Hz, 2H), 8.52 (dt, J = 7.7, 1.7 Hz, 2H), 8.50 (s, 2H), 8.33 (d, J = 7.6 Hz, 2H), 8.21 (ddd, J = 8.2, 2.2, 1.3 Hz, 2H), 8.08 (ddd, J = 8.2, 2.2, 1.2 Hz, 2H), 8.05 (s, 2H), 7.99 (ddd, J = 7.3, 2.3, 1.2 Hz, 2H), 7.93 – 7.90 (m, 2H), 7.88 – 7.86 (m, 2H), 7.80 – 7.77 (m, 6H), 7.75 (dd, J = 8.0, 6.0 Hz, 2H), 7.69 (dd, J = 7.8, 5.7 Hz, 2H), 7.62 (s, 2H), 7.55 (s, 2H), 6.87 (s, 2H), 2.27 (s, 3H), 2.11 (s, 3H), 2.04 (s, 3H), 1.88 (s, 3H), 1.74 – 1.71 (m, 8H), 0.92 (s, 3H), 0.63 (s, 3H).

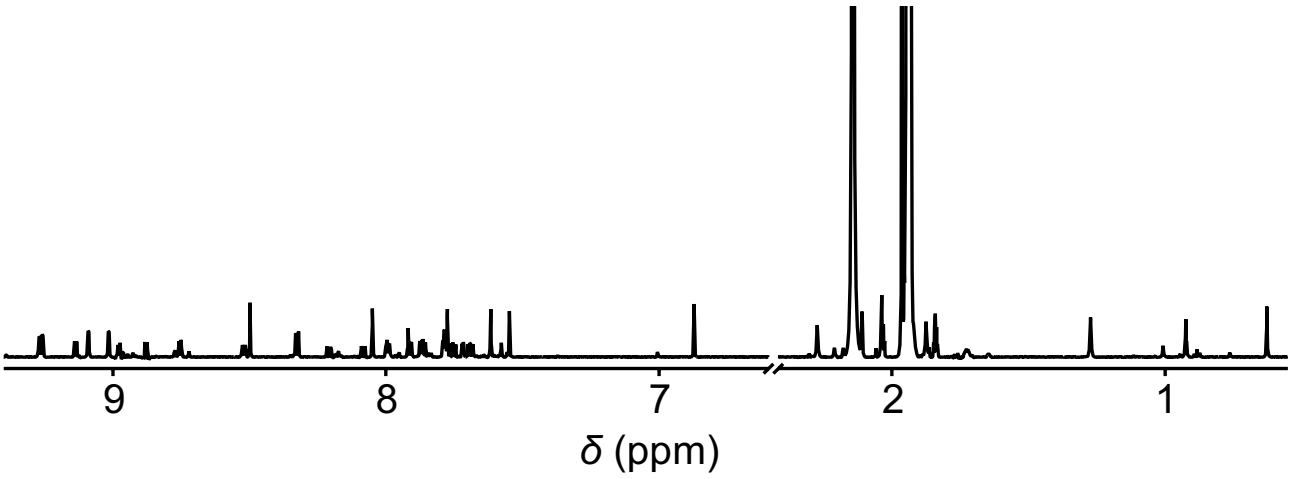

Supplementary Figure 237 | ^{1}H NMR spectrum (700 MHz, 298 K, CD_3CN) of heteroleptic cage $Pd_2\mathbf{A}_2\mathbf{D}^4\mathbf{C}$.

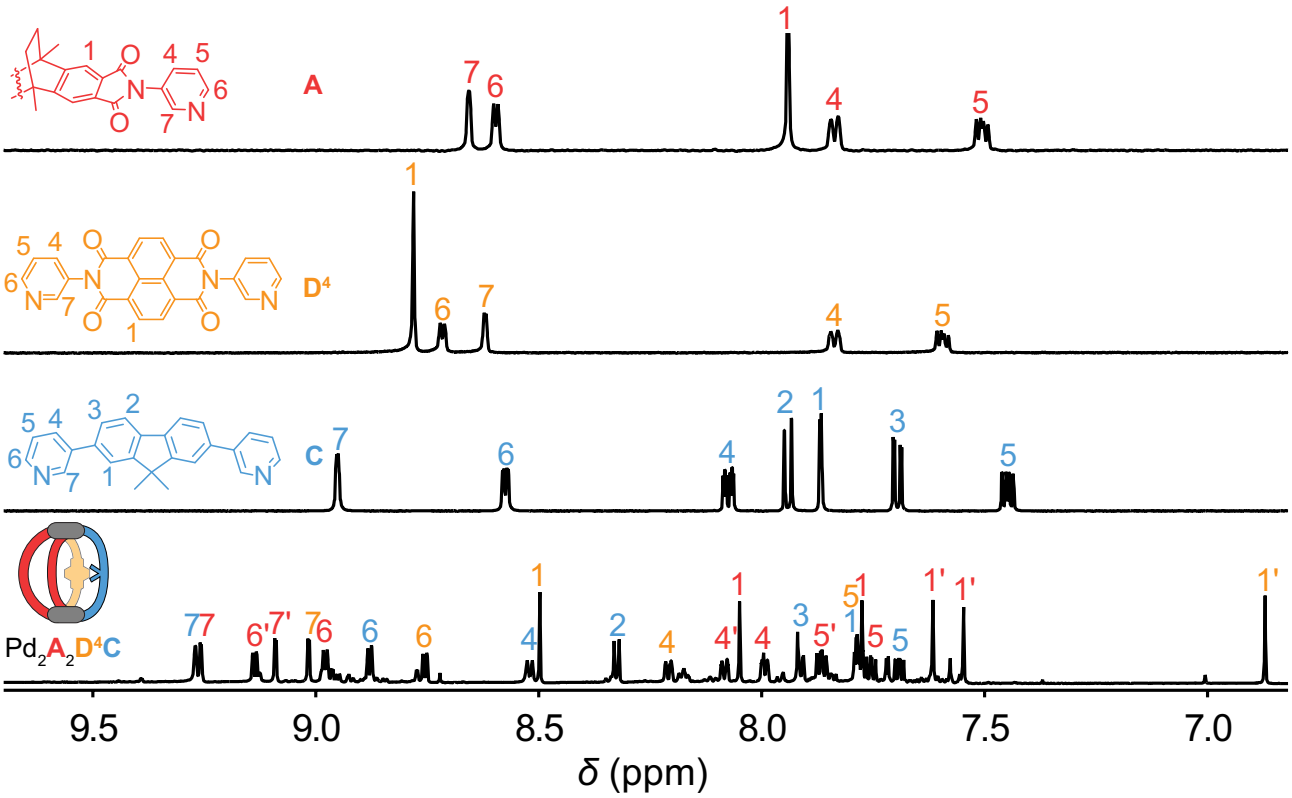

Supplementary Figure 238 | Partial ^{1}H NMR spectrum (700 MHz, 298 K, CD_3CN) comparison of ligands **A** (red), $\mathbf{D}^4$ (yellow), **C** (blue), heteroleptic cage $Pd_2\mathbf{A}_2\mathbf{D}^4\mathbf{C}$.

^{13}C NMR (176 MHz, 298 K, CD_3CN) δ 167.20, 167.10, 166.82, 166.79, 163.86, 162.39, 156.91, 155.01, 154.38, 154.34, 152.89, 151.48, 151.20, 150.90, 150.78, 150.16, 149.85, 149.36, 142.82, 142.17, 140.89, 139.95, 139.46, 139.43, 136.51, 135.22, 132.18, 132.09, 131.70, 131.68, 130.70, 130.38, 130.32, 130.29, 129.07, 128.82, 128.65, 128.24, 127.68, 127.61, 127.28, 126.81, 123.35, 122.72, 117.82, 117.73, 116.94, 47.79, 45.59, 45.29, 45.13, 45.02, 34.61, 29.78, 29.51, 25.07.

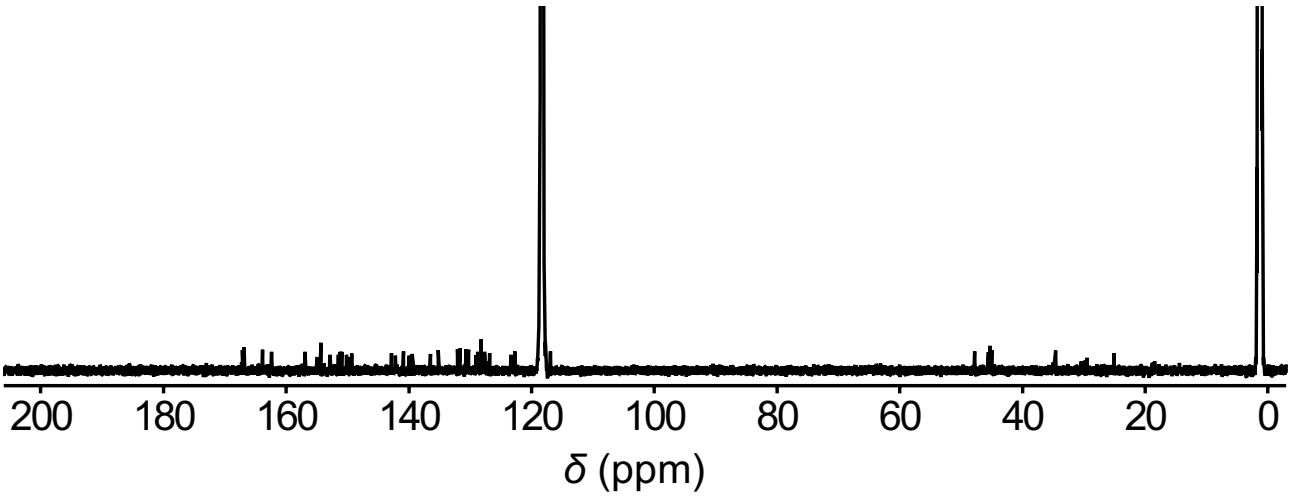

Supplementary Figure 239 | ^{13}C NMR spectrum (176 MHz, 298 K, CD_3CN) of heteroleptic cage $Pd_2\mathbf{A}_2\mathbf{D}^4\mathbf{C}$.

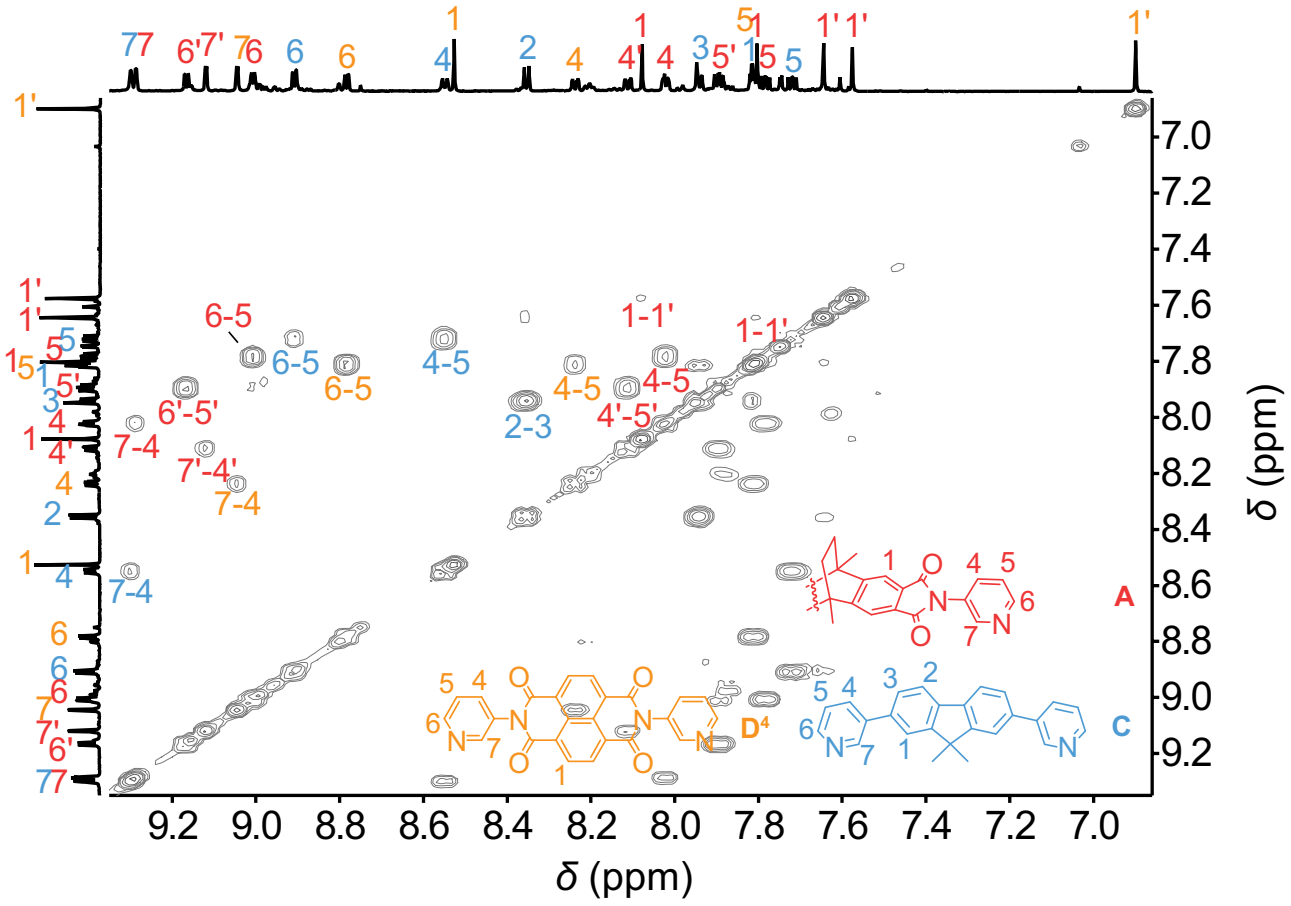

Supplementary Figure 240 | Partial ^{1}H–^{1}H COSY spectrum (500 MHz, 298 K, CD_3CN) of heteroleptic cage $Pd_2\mathbf{A}_2\mathbf{D}^4\mathbf{C}$.

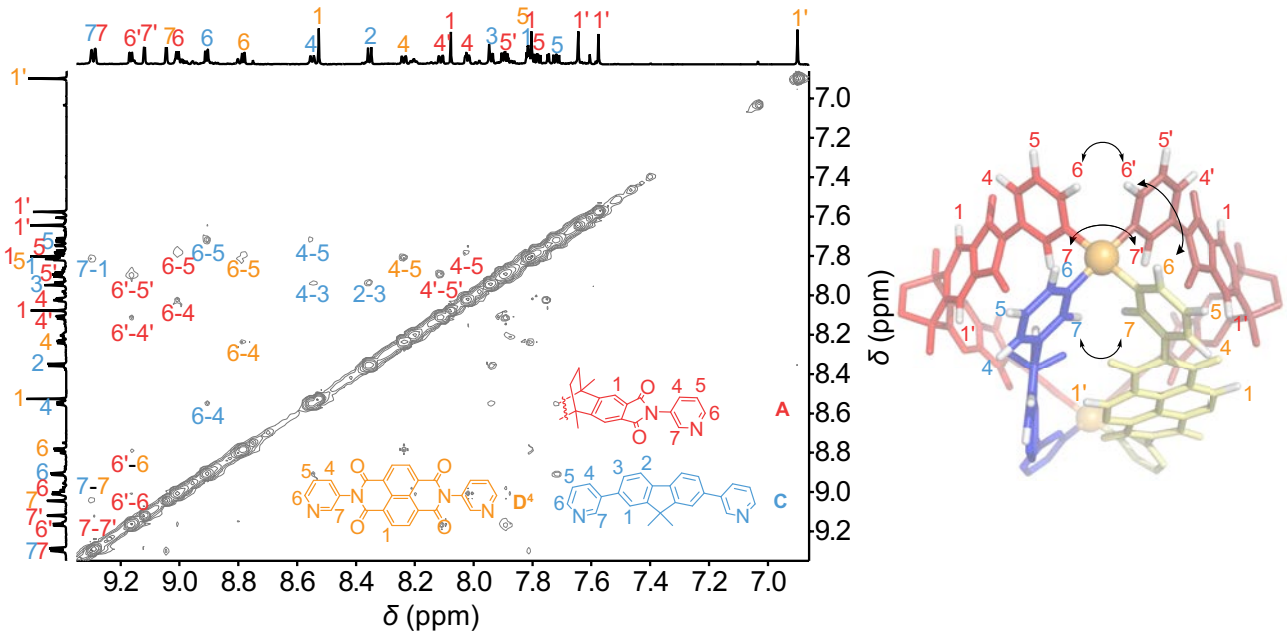

Supplementary Figure 241 | Partial ^{1}H–^{1}H NOESY spectrum (500 MHz, 298 K, CD_3CN) of heteroleptic cage $Pd_2\mathbf{A}_2\mathbf{D}^4\mathbf{C}$.

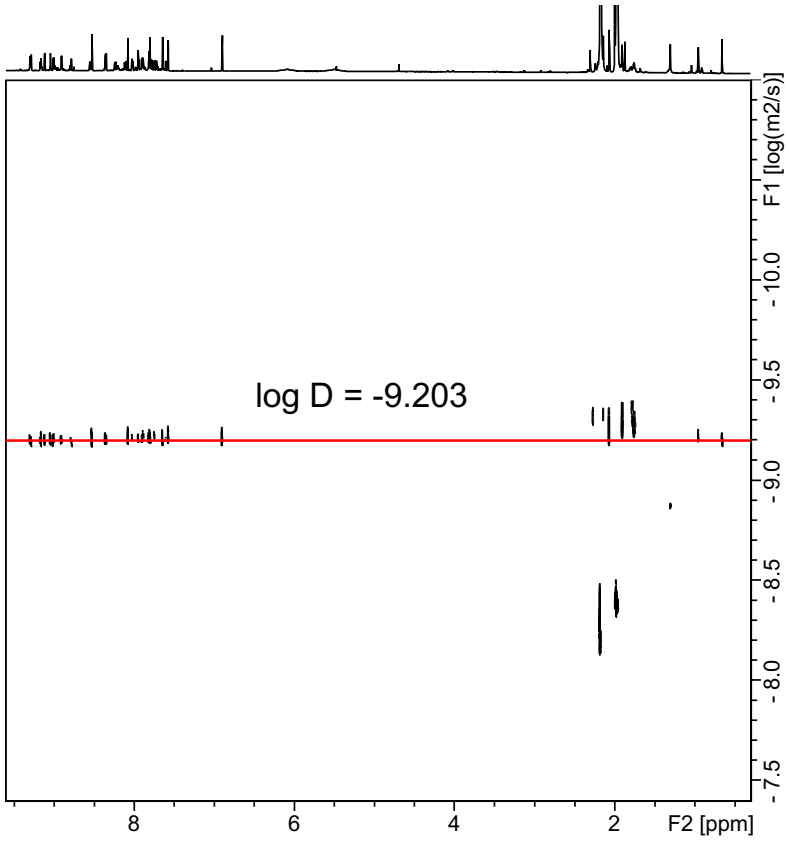

Supplementary Figure 242 | ^{1}H DOSY spectrum (500 MHz, 298 K, CD_3CN) of heteroleptic cage $Pd_2\mathbf{A}_2\mathbf{D}^4\mathbf{C}$. Diffusion coefficient for $Pd_2\mathbf{A}_2\mathbf{D}^4\mathbf{C}$: D = 6.266 × 10^{-10} m^2s^{-1}, log *D* = −9.203, r = 10.4 Å.

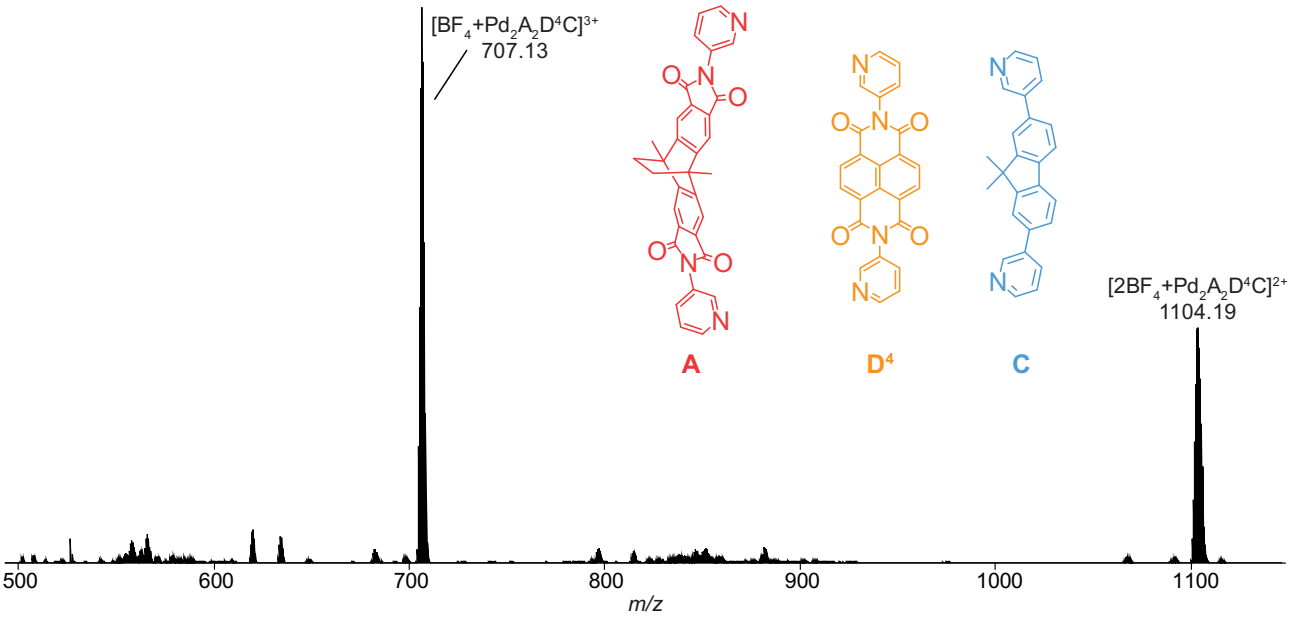

Supplementary Figure 243 | HR-ESI mass spectrum of heteroleptic cage $Pd_2\mathbf{A}_2\mathbf{D}^4\mathbf{C}$.

3.9.2. Self-assembly of heteroleptic cage $Pd_2\mathbf{B}_2\mathbf{D}^4\mathbf{C}$

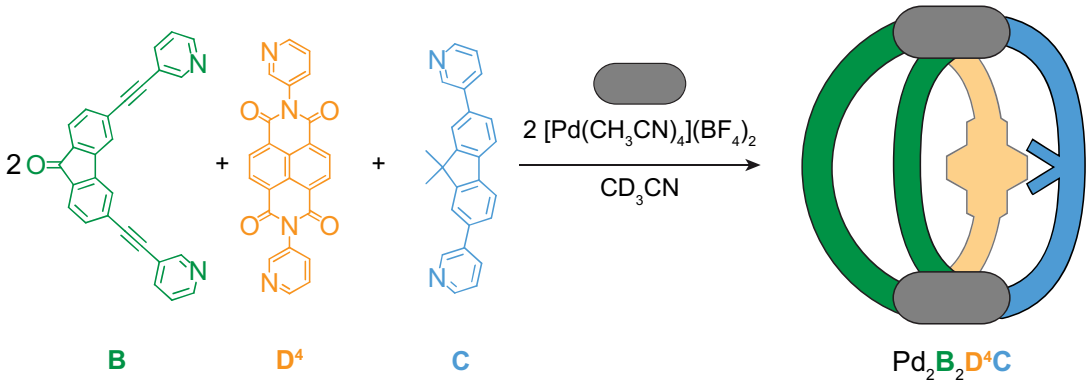

To a solution of **C** (60 µL, 3 mM, 0.18 µmol) in CD_3CN and a suspension of **B** (120 µL, 3 mM, 0.36 µmol) and $\mathbf{D}^4$ (60 µL, 3 mM, 0.18 µmol) were added a stock solution of $[Pd(CH_3CN)_4](BF_4)_2$ (24 µL, 15 mM/CD_3CN, 0.36 µmol) and 186 µL additional CD_3CN. The mixture was heated at 80 °C for 8 h to give a 0.4 mM cage solution containing the shown cage as predominant species and some impurities.

^{1}H NMR (700 MHz, 298 K, CD_3CN) δ 9.60 (d, J = 2.2 Hz, 2H), 9.54 (d, J = 2.0 Hz, 2H), 9.40 (d, J = 1.8 Hz, 2H), 9.29 (d, J = 1.8 Hz, 2H), 9.16 (d, J = 5.9 Hz, 2H), 9.09 (dd, J = 6.1, 1.4 Hz, 2H), 9.00 (d, J = 6.1 Hz, 2H), 8.92 (d, J = 5.8 Hz, 2H), 8.39 (dd, J = 7.9, 1.7 Hz, 2H), 8.27 (d, J = 7.6 Hz, 2H), 8.25 – 8.17 (m, 6H), 8.06 (d, J = 1.7 Hz, 2H), 7.87 – 7.84 (m, 2H), 7.84 (d, J = 1.1 Hz, 2H), 7.75 – 7.70 (m, 6H), 7.69 (dd, J = 1.8, 0.7 Hz, 2H), 7.69 – 7.64 (m, 6H), 1.74 (s, 3H), 1.58 (s, 3H).

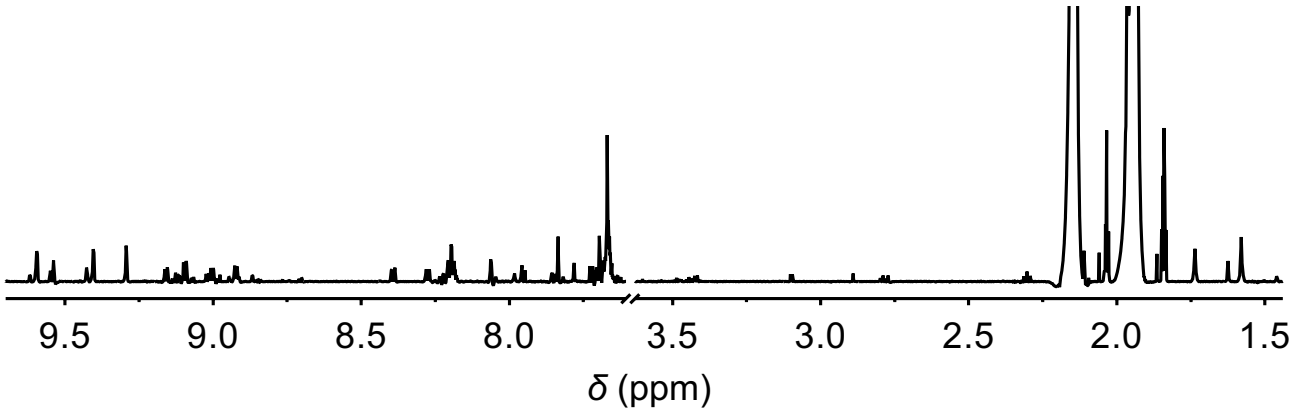

Supplementary Figure 244 | ^{1}H NMR spectrum (700 MHz, 298 K, CD_3CN) of heteroleptic cage Pd_2**B**$_2$**D**^{4}**C**.

^{13}C NMR (151 MHz, 298 K, CD_3CN) δ 192.18, 192.13, 172.99, 164.06, 162.84, 157.04, 154.12, 153.26, 153.06, 151.38, 151.31, 150.52, 150.15, 150.13, 145.02, 144.95, 144.76, 144.73, 143.13, 142.47, 140.79, 139.70, 139.29, 136.44, 136.37, 136.31, 135.55, 135.52, 135.29, 132.28, 132.05, 128.83, 128.41, 128.39, 125.29, 125.23, 124.39, 124.24, 124.16, 123.74, 123.49, 123.47, 123.40, 122.86, 95.61, 95.41, 87.81, 87.61, 48.19, 32.64, 30.36.

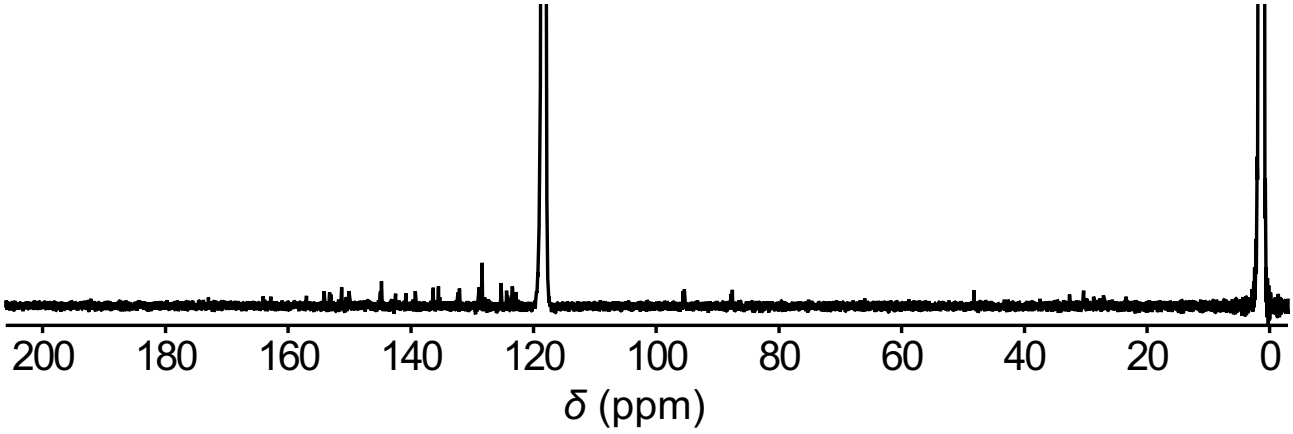

Supplementary Figure 245 | ^{13}C NMR spectrum (151 MHz, 298 K, CD_3CN) of heteroleptic cage Pd_2**B**$_2$**D**^{4}**C**.

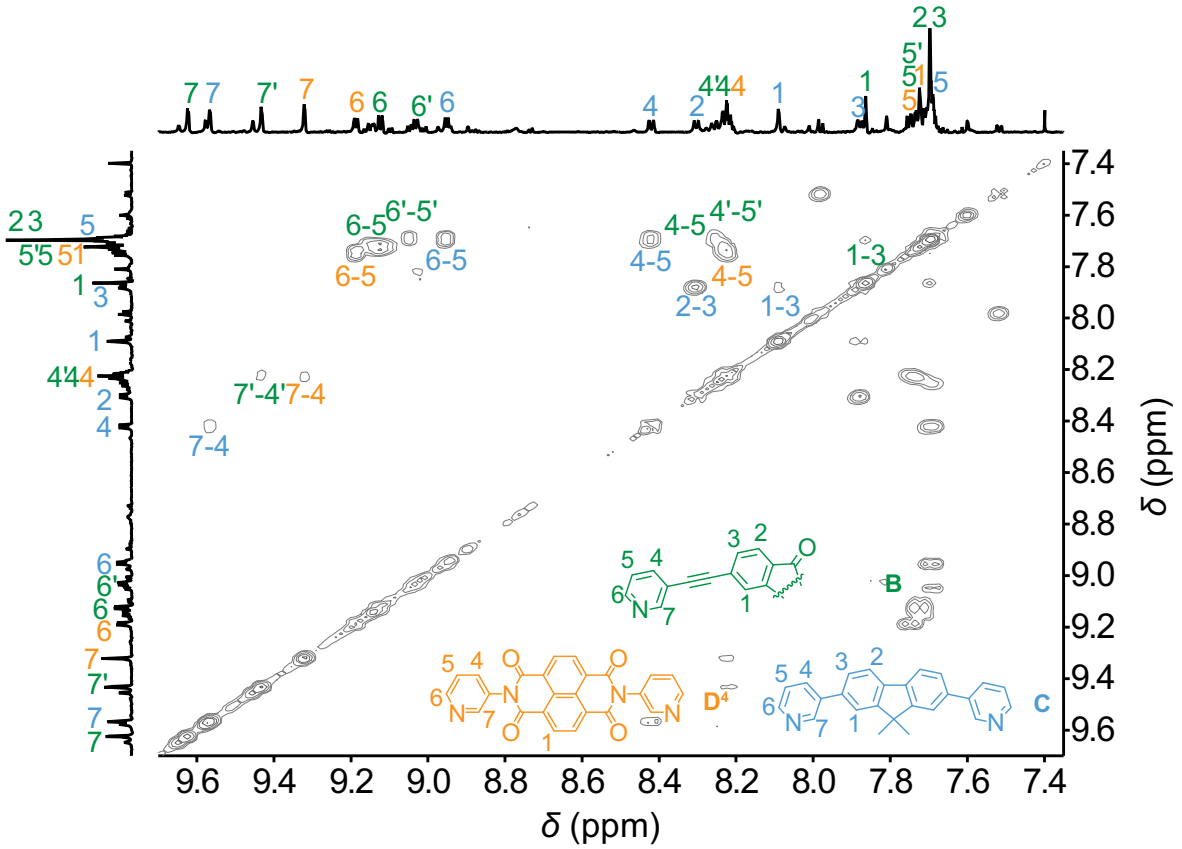

Supplementary Figure 246 | Partial ^{1}H–^{1}H COSY spectrum (500 MHz, 298 K, CD_3CN) of heteroleptic cage $Pd_2\mathbf{B}_2\mathbf{D}^4\mathbf{C}$.

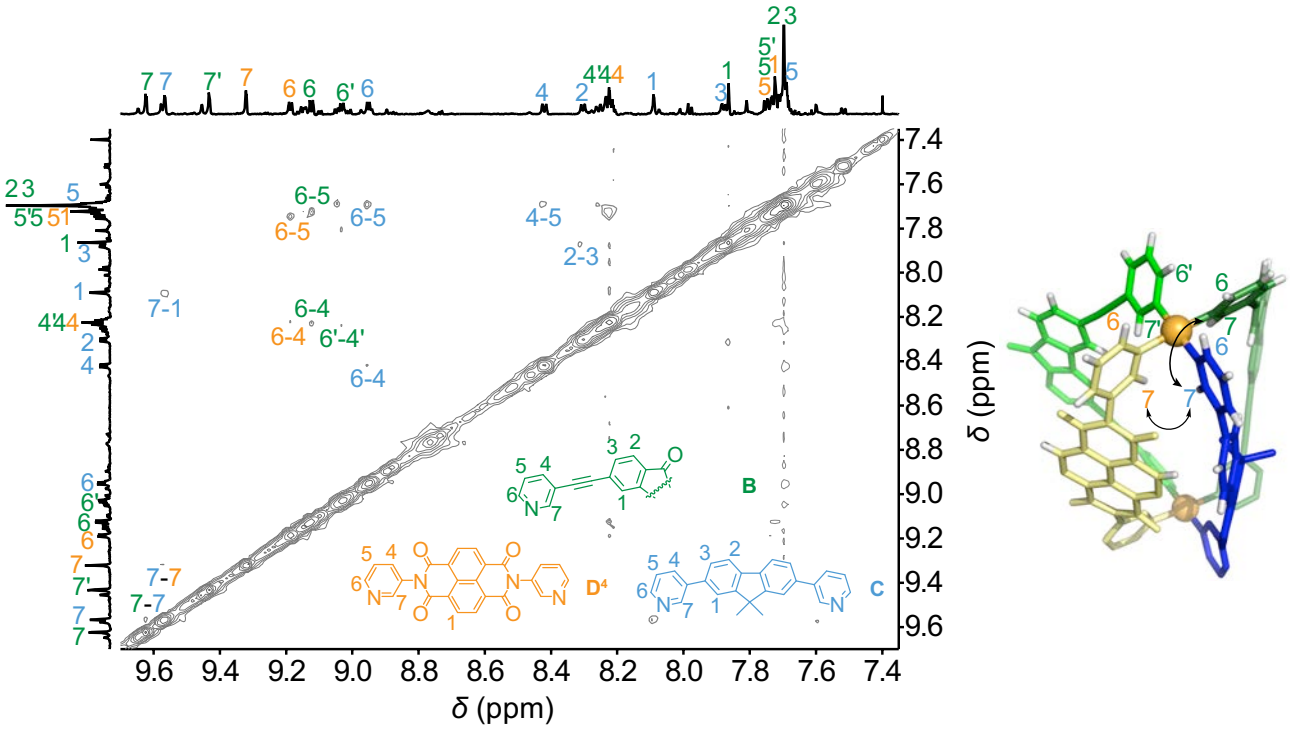

Supplementary Figure 247 | Partial ^{1}H–^{1}H NOESY spectrum (500 MHz, 298 K, CD_3CN) of heteroleptic cage $Pd_2\mathbf{B}_2\mathbf{D}^4\mathbf{C}$. The composition of this heteroleptic cage is supported by a single crystal X-ray structure (details see below). The found NOE contacts in solution are in full accordance with the X-ray structure results.

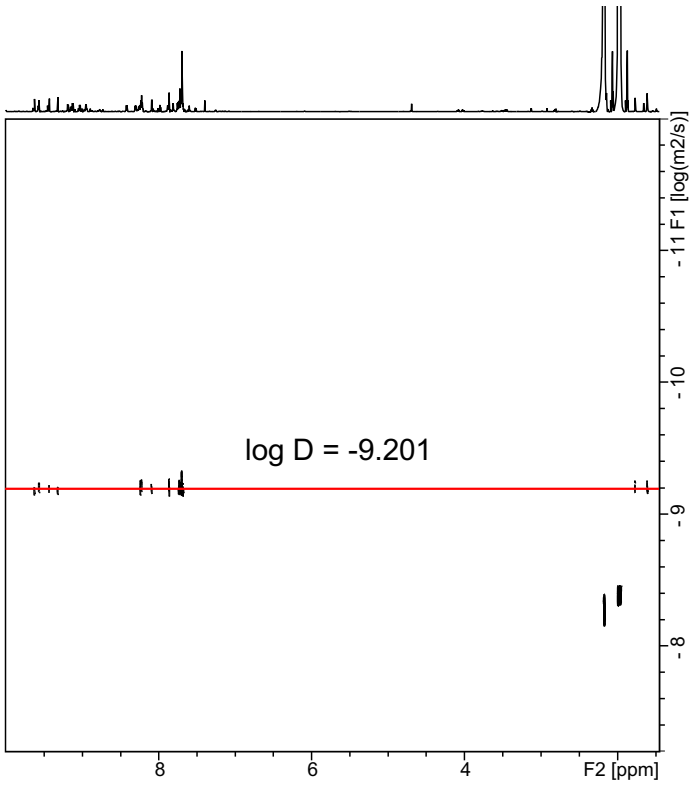

Supplementary Figure 248 | ^{1}H DOSY spectrum (500 MHz, 298 K, CD_3CN) of heteroleptic cage $Pd_2\mathbf{B}_2\mathbf{D}^4\mathbf{C}$. Diffusion coefficient for $Pd_2\mathbf{B}_2\mathbf{D}^4\mathbf{C}$: D = 6.295 × 10^{-10} m^2s^{-1}, log *D* = −9.201, r = 10.4 Å.

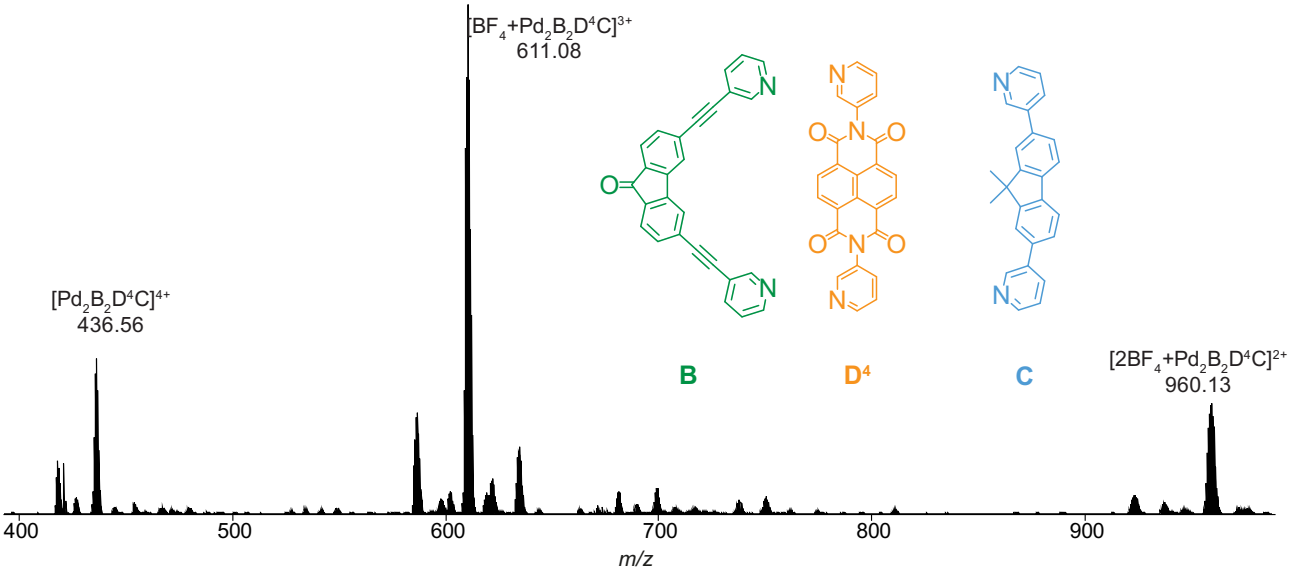

Supplementary Figure 249 | HR-ESI mass spectrum of heteroleptic cage $Pd_2\mathbf{B}_2\mathbf{D}^4\mathbf{C}$.

*3.9.3. Self-assembly of heteroleptic cage Pd_2**ABD^{4}C***

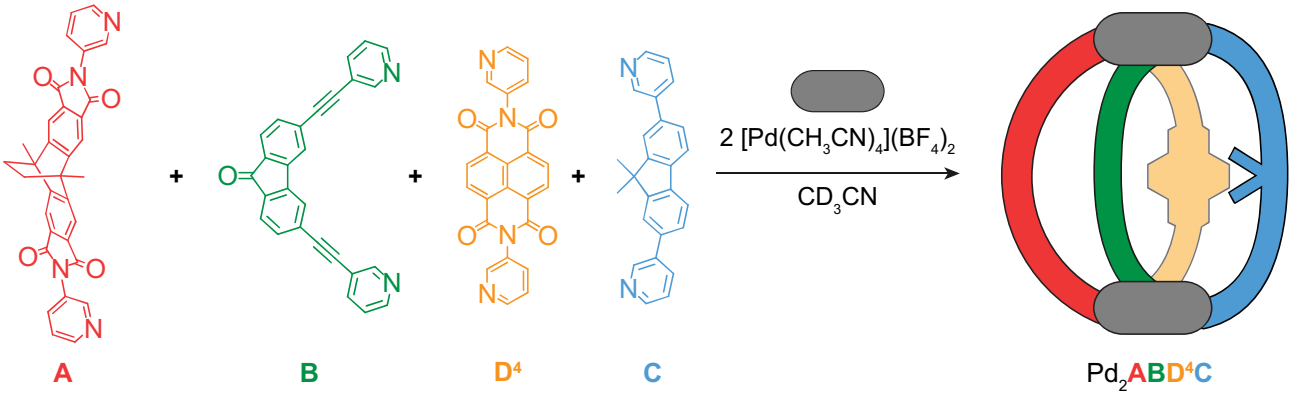

To a solution of **A** (60 µL, 3 mM, 0.18 µmol), **C** (60 µL, 3 mM, 0.18 µmol) and a suspension of **B** (60 µL, 3 mM, 0.18 µmol), **D^4** (60 µL, 3 mM, 0.18 µmol) were added a stock solution of $[Pd(CH_3CN)_4](BF_4)_2$ (24 µL, 15 mM/CD_3CN, 0.36 µmol) and additional 186 µL CD_3CN. The mixture was heated at 80 °C for 8 h to give a 0.4 mM cage solution containing the shown cage as predominant species.

^{1}H NMR (700 MHz, 298 K, CD_3CN) δ 9.52 (d, *J* = 2.0 Hz, 2H), 9.35 (d, *J* = 2.2 Hz, 2H), 9.25 (dd, *J* = 5.8, 1.3 Hz, 2H), 9.22 (d, *J* = 1.8 Hz, 2H), 9.06 (d, *J* = 2.2 Hz, 2H), 9.05 – 9.02 (m, 2H), 8.88 (d, *J* = 5.7 Hz, 2H), 8.76 (dd, *J* = 6.0, 1.2 Hz, 2H), 8.66 (s, 2H), 8.55 (d, *J* = 7.8 Hz, 2H), 8.39 (d, *J* = 7.6 Hz, 2H), 8.16 (dt, *J* = 7.9, 1.6 Hz, 2H), 8.09 (dt, *J* = 8.4, 1.7 Hz, 4H), 8.06 (d, *J* = 1.7 Hz, 2H), 7.98 (dd, *J* = 7.6, 1.7 Hz, 2H), 7.87 (s, 2H), 7.77 (m, 4H), 7.73 (dd, *J* = 8.2, 6.0 Hz, 2H), 7.71 – 7.69 (m, 2H), 7.65 (d, *J* = 7.5 Hz, 2H), 7.63 – 7.61 (m, 2H), 7.60 (s, 2H), 7.32 (s, 2H), 7.03 (s, 2H), 2.11 (s, 3H), 1.91 (s, 3H), 1.75 (s, 4H), 1.15 (s, 6H).

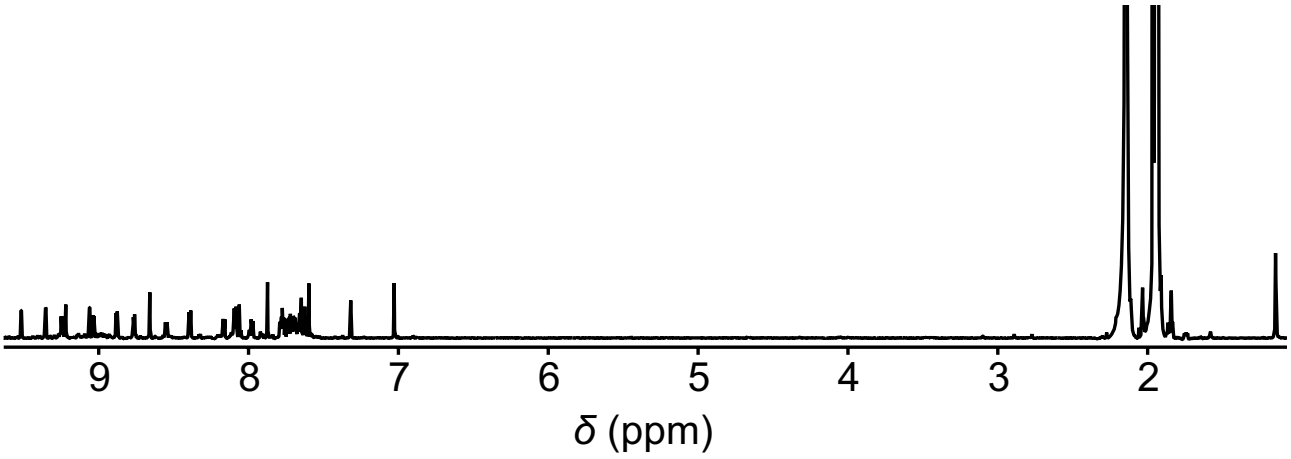

Supplementary Figure 250 | ^{1}H NMR spectrum (700 MHz, 298 K, CD_3CN) of heteroleptic cage Pd_2**ABD^{4}C**.

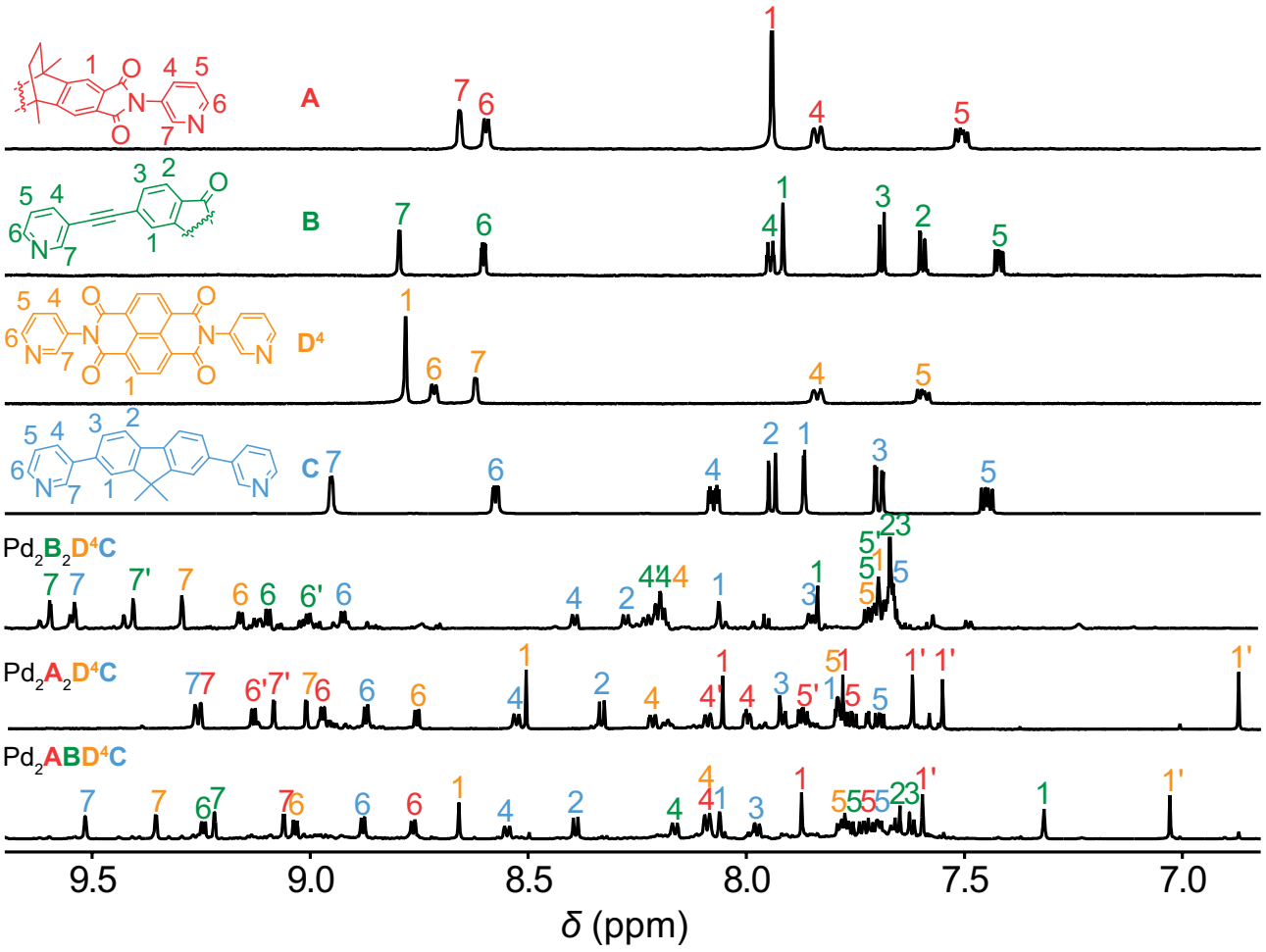

Supplementary Figure 251 | Partial ^{1}H NMR spectrum (700 MHz, 298 K, CD_3CN) comparison of ligands **A** (red), **B** (green), **D^4** (yellow), **C** (blue), heteroleptic cages Pd_2**B**$_2$**D^{4}C**, Pd_2**A**$_2$**D^{4}C** and Pd_2**ABD^{4}C**.

^{13}C NMR (151 MHz, 298 K, CD_3CN) δ 192.14, 172.98, 167.21, 166.89, 163.96, 162.57, 157.24, 154.74, 154.35, 154.24, 152.82, 151.46, 151.22, 150.64, 150.55, 150.43, 150.14, 145.03, 144.61, 142.81, 142.09, 140.93, 139.71, 139.18, 136.64, 136.44, 135.50, 135.20, 132.39, 132.11, 132.02, 130.82, 130.62, 128.68, 128.61, 128.40, 128.23, 128.16, 127.87, 127.77, 126.98, 125.12, 123.97, 123.87, 123.39, 122.82, 117.66, 95.26, 87.62, 47.87, 45.52, 45.12, 34.64, 34.38, 30.37, 28.98, 25.68.

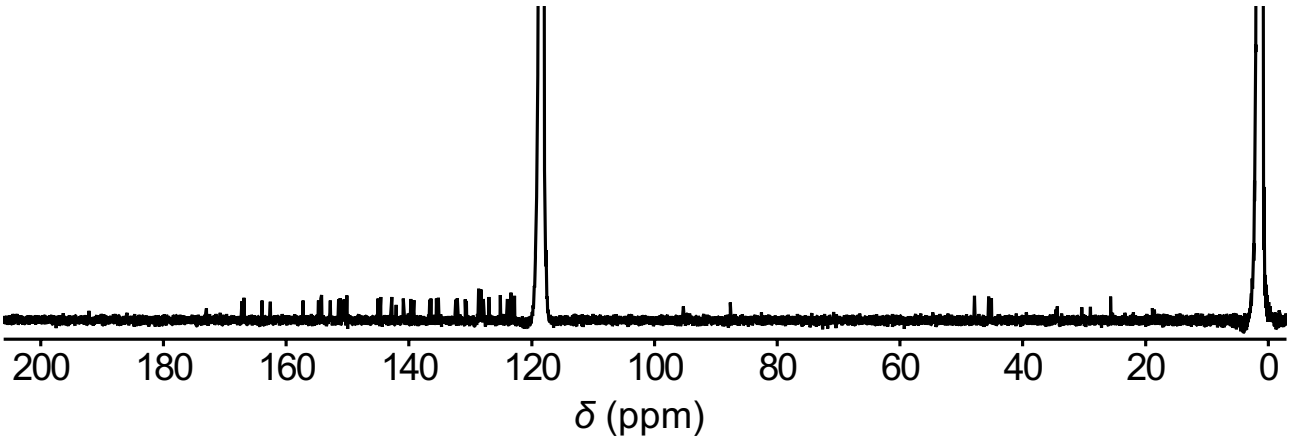

Supplementary Figure 252 | ^{13}C NMR spectrum (151 MHz, 298 K, CD_3CN) of heteroleptic cage Pd_2**ABD^{4}C**.

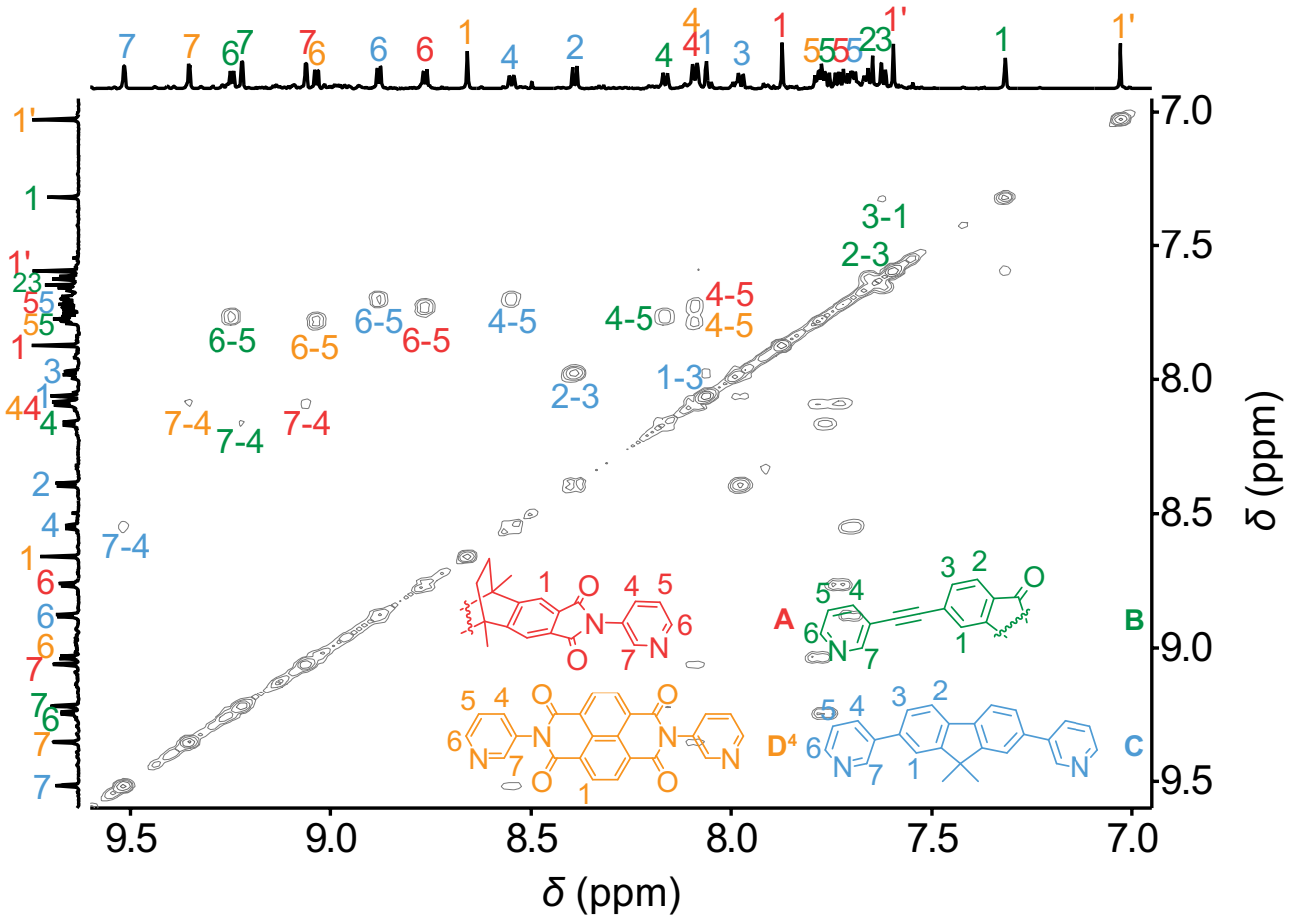

Supplementary Figure 253 | Partial ^{1}H–^{1}H COSY spectrum (500 MHz, 298 K, CD_3CN) of heteroleptic cage Pd_2**ABD⁴C**.

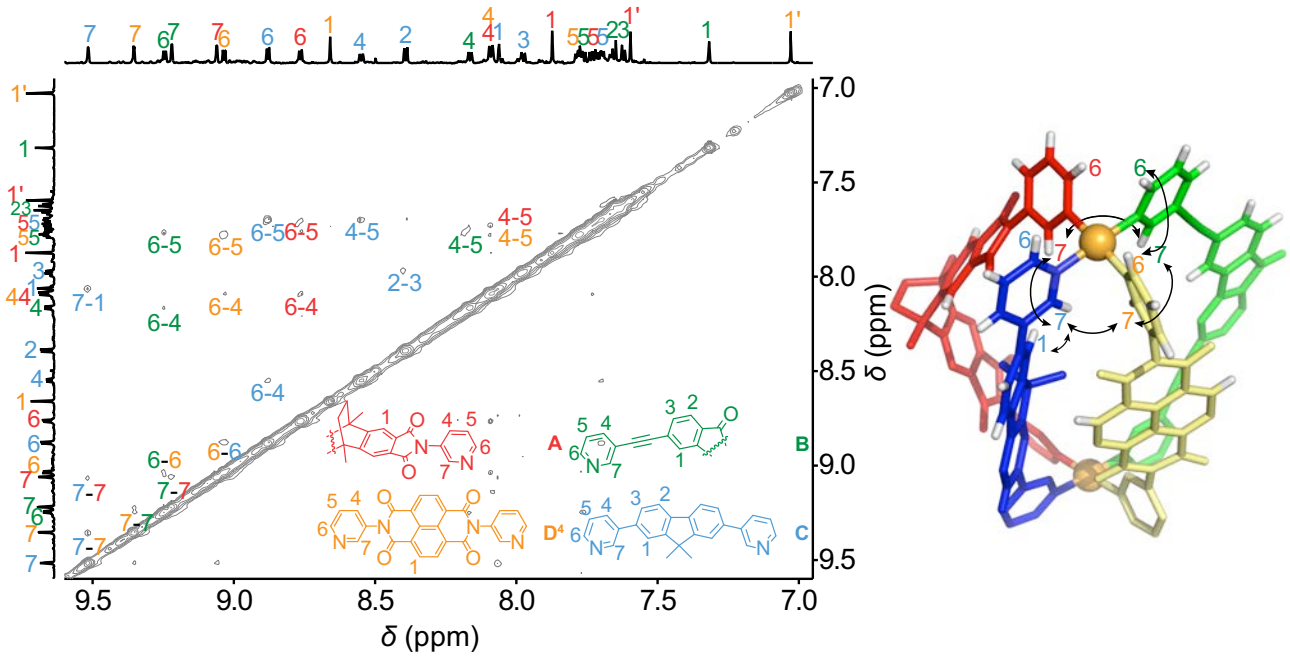

Supplementary Figure 254 | Partial ^{1}H–^{1}H NOESY spectrum (500 MHz, 298 K, CD_3CN) of heteroleptic cage Pd_2**ABD⁴C**. The composition of this heteroleptic cage is supported by a single crystal X-ray structure (details see below). The found NOE contacts in solution are in full accordance with the X-ray structure results.

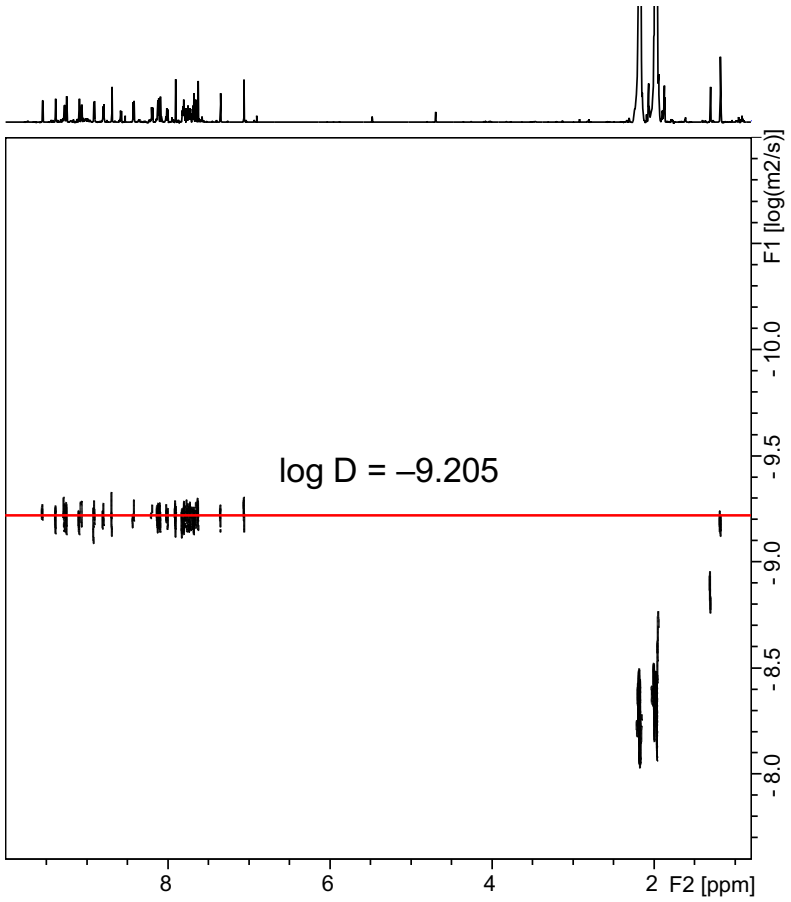

Supplementary Figure 255 | ^{1}H DOSY spectrum (500 MHz, 298 K, CD_3CN) of heteroleptic cage Pd_2**ABD^{4}C**. Diffusion coefficient for Pd_2**ABD^{4}C**: D = 6.240 × 10^{-10} m^2s^{-1}, log *D* = −9.205, r = 10.5 Å.

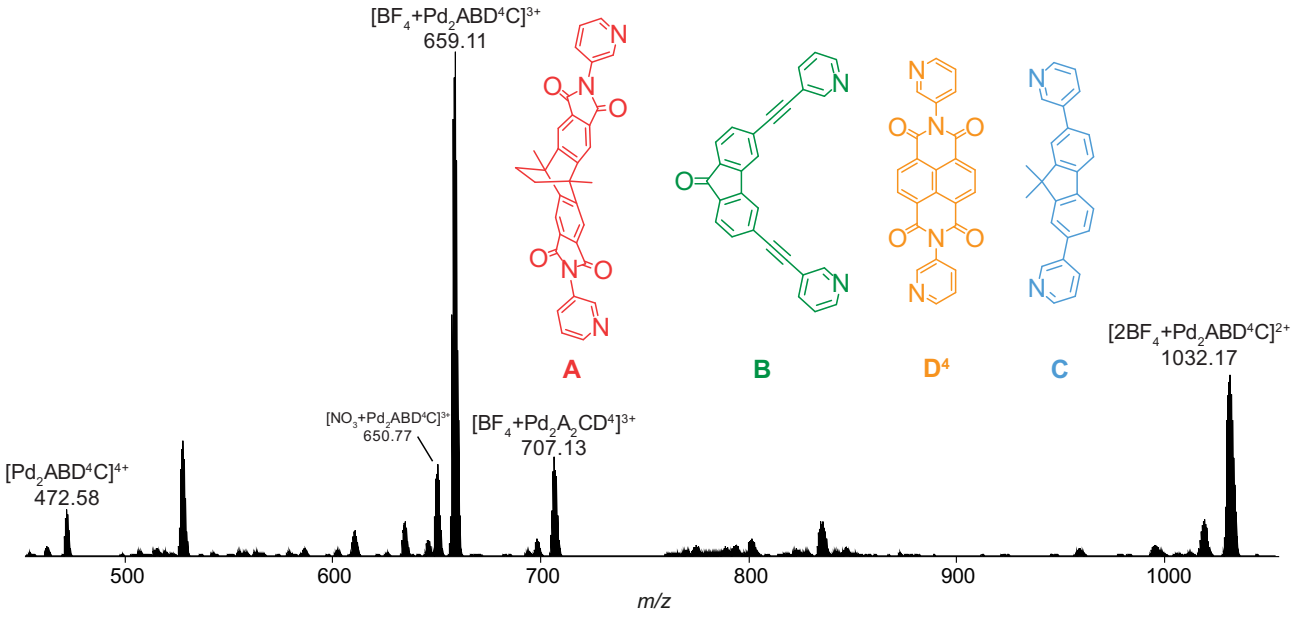

Supplementary Figure 256 | HR-ESI mass spectrum of heteroleptic cage Pd_2**ABD^{4}C**.

4. Cage-to-cage transformation kinetics

4.1. Reaction of homoleptic to heteroleptic cages with two different ligands

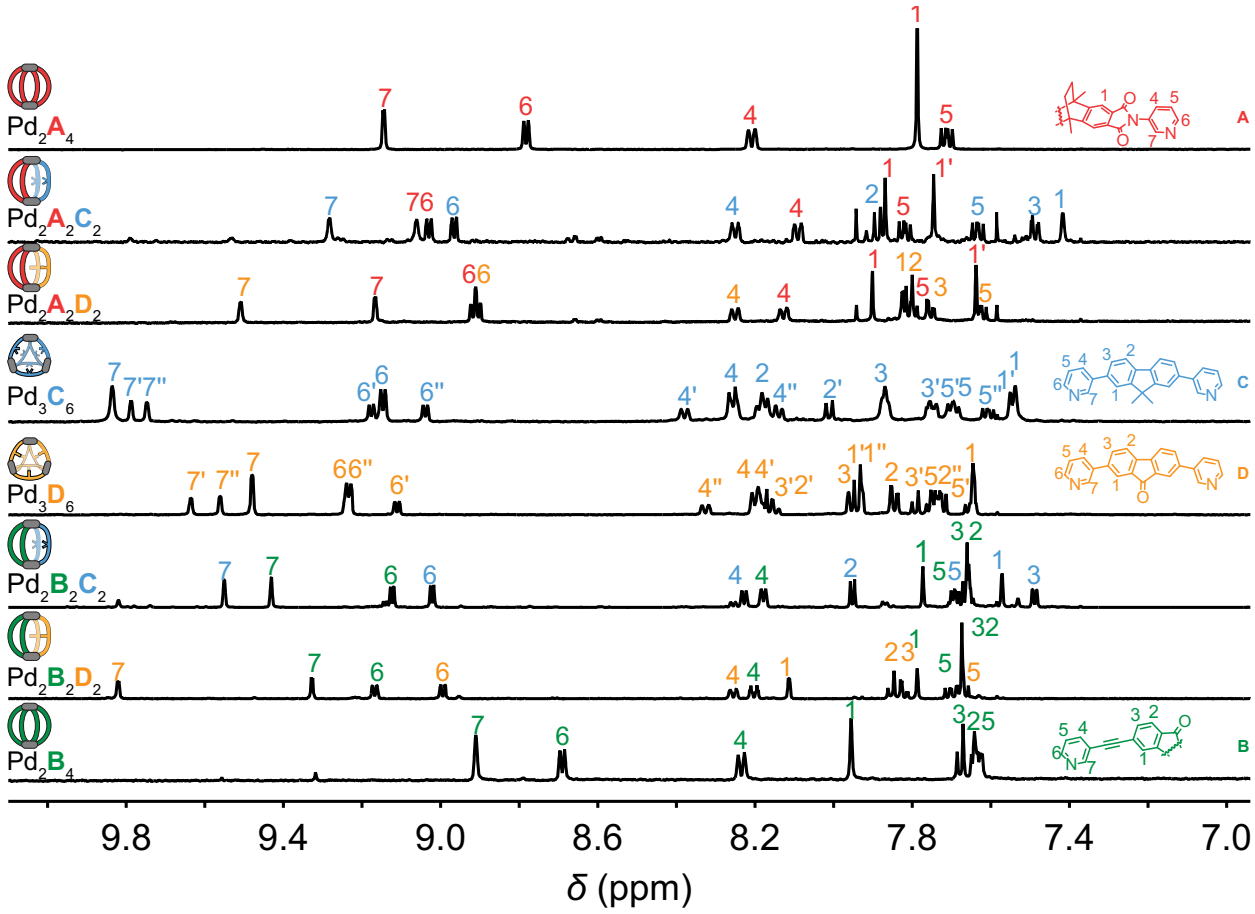

Supplementary Figure 257 | Overview of ^{1}H NMR spectra (500 MHz, 298 K, CD_3CN) of the cage-to-cage transformation inputs and results from the reaction of homoleptic cages to heteroleptic cages with two chemically different ligands after heating at 80 °C. In each case, the homoleptic cages (either existing as defined Pd_2L_4 species or mixtures of rings and cages) as acetonitrile solutions were combined in a 1:1 ratio with respect to the ligand stoichiometry to obtain heteroleptic cages $Pd_2L_2L'_2$.

4.2. Cage-to-cage reaction: $Pd_2\mathbf{A}_2\mathbf{C}_2 + Pd_2\mathbf{A}_2\mathbf{D}_2 = 2Pd_2\mathbf{A}_2\mathbf{CD}$

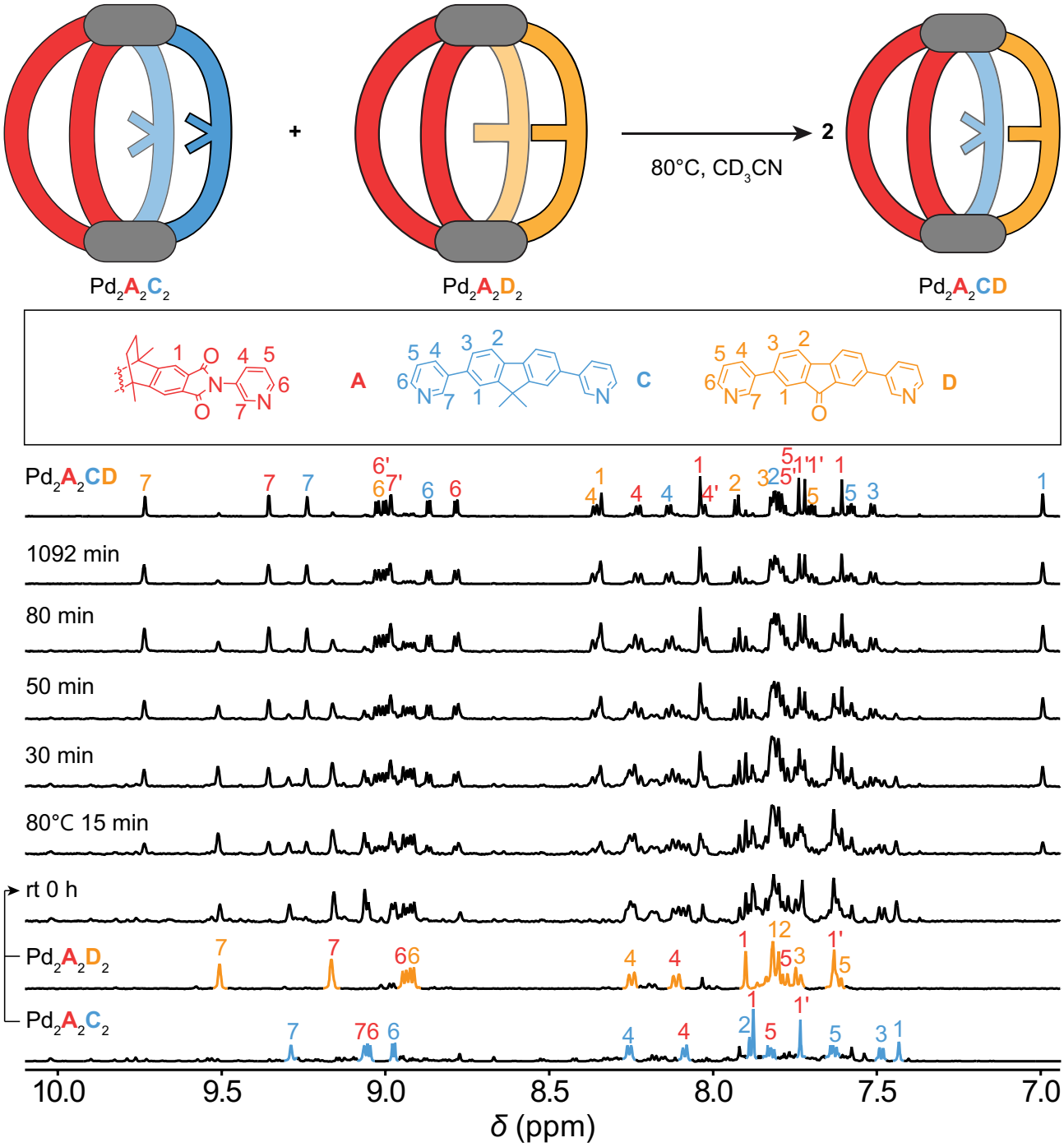

Supplementary Figure 258 | ^{1}H NMR monitoring (500 MHz, 298 K, CD_3CN) of the cage-to-cage transformation process from heteroleptic cages $Pd_2\mathbf{A}_2\mathbf{C}_2$ and $Pd_2\mathbf{A}_2\mathbf{D}_2$ to cage $Pd_2\mathbf{A}_2\mathbf{CD}$ after heating at 80 °C. The top spectrum shows heteroleptic cage $Pd_2\mathbf{A}_2\mathbf{CD}$ formed from mixing the ligands with Pd(II).

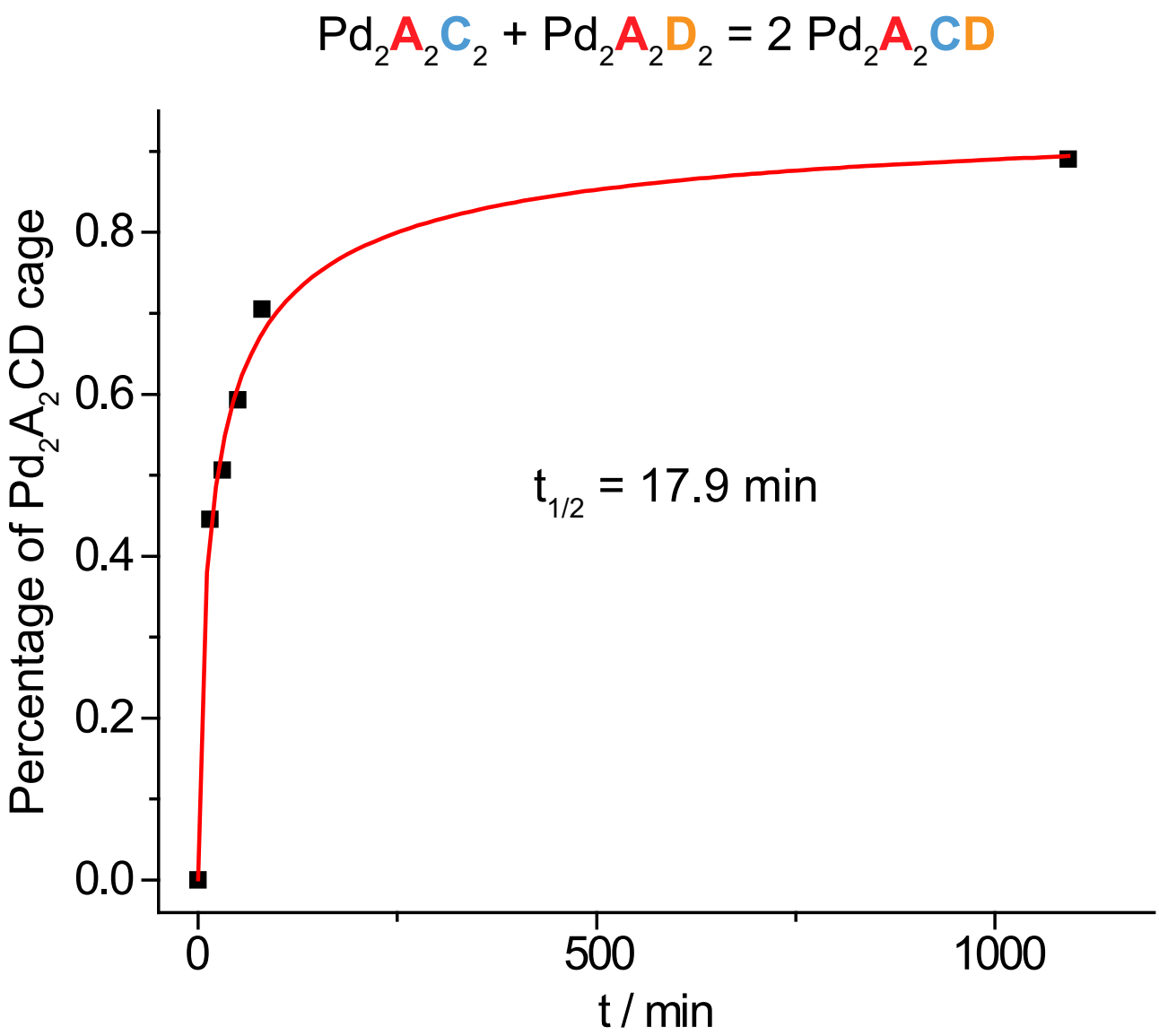

Supplementary Figure 259 | Plot of cage-to-cage transformation from heteroleptic cages $Pd_2\mathbf{A}_2\mathbf{C}_2$ and $Pd_2\mathbf{A}_2\mathbf{D}_2$ to heteroleptic cage $Pd_2\mathbf{A}_2\mathbf{CD}$ after heating at 80 °C over time, $t_{1/2}$ = 17.9 min.

4.3. Cage-to-cage reaction: $Pd_2\mathbf{B}_2\mathbf{C}_2 + Pd_2\mathbf{B}_2\mathbf{D}_2 = 2Pd_2\mathbf{B}_2\mathbf{CD}$

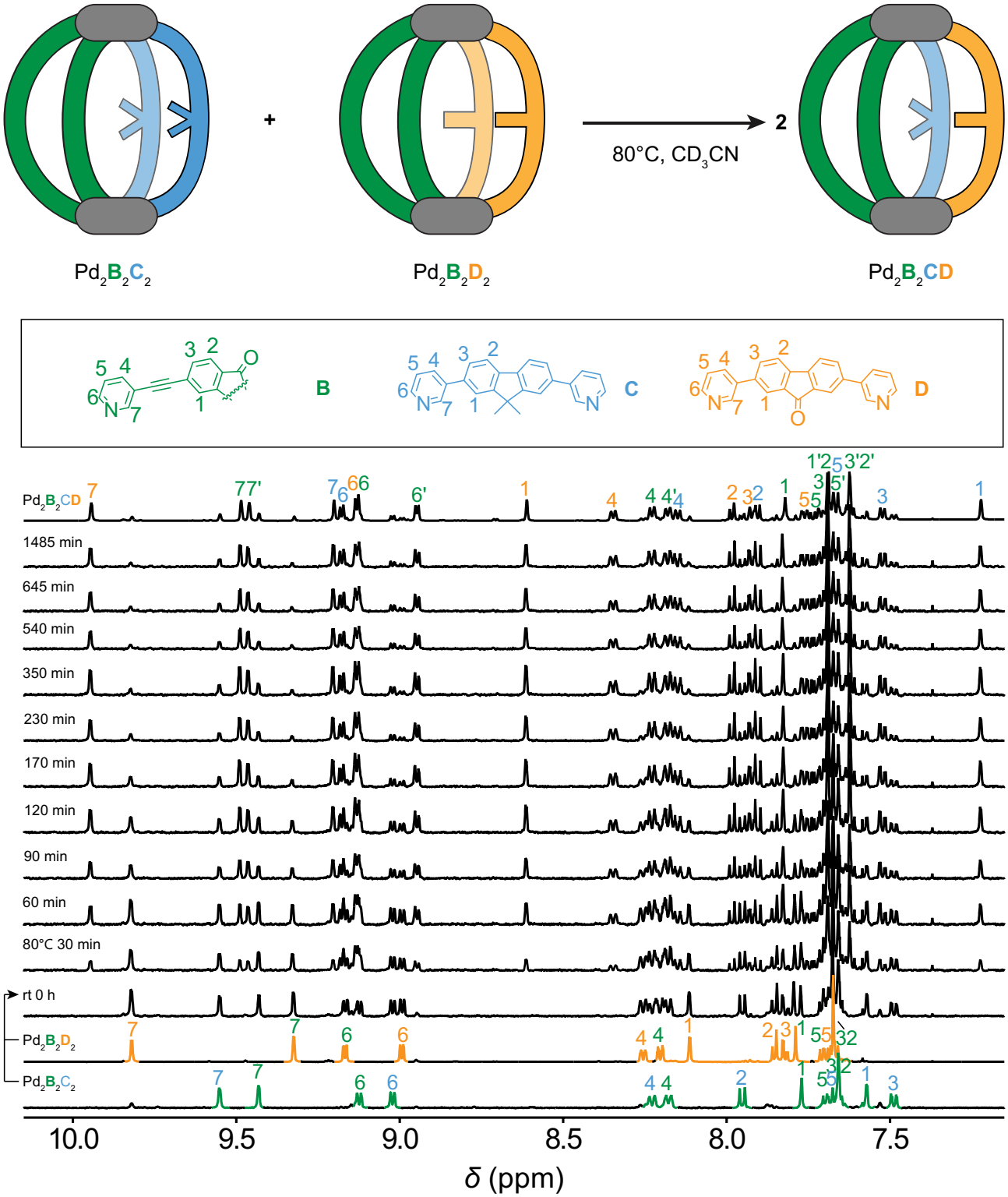

Supplementary Figure 260 | ^{1}H NMR spectra (500 MHz, 298 K, CD_3CN) of cage-to-cage transformation from heteroleptic cages $Pd_2\mathbf{B}_2\mathbf{C}_2$ and $Pd_2\mathbf{B}_2\mathbf{D}_2$ to heteroleptic cage $Pd_2\mathbf{B}_2\mathbf{CD}$ after heating at 80 °C. The top spectrum shows cage $Pd_2\mathbf{B}_2\mathbf{CD}$ formed from mixing the ligands with Pd(II).

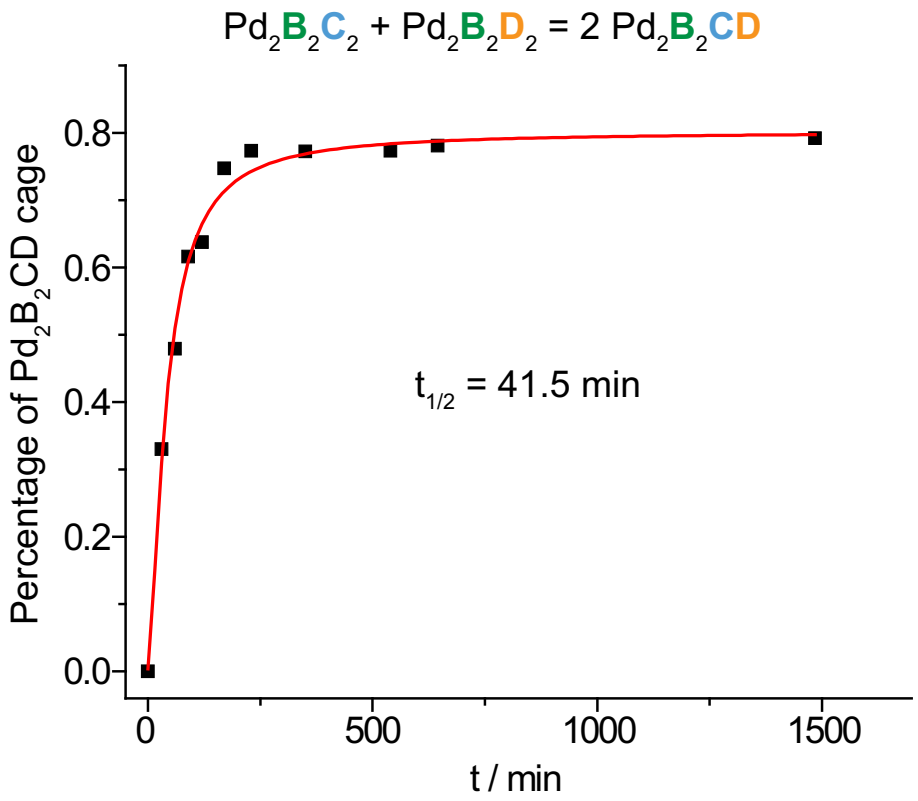

Supplementary Figure 261 | Plot of cage-to-cage transformation from Pd_2**B**$_2$**C**$_2$ and Pd_2**B**$_2$**D**$_2$ to cage Pd_2**B**$_2$**CD** after heating at 80 °C over time, $t_{1/2}$ = 41.5 min.

4.4. Cage-to-cage reaction: $Pd_2B^0{}_2C_2 + Pd_2B^0{}_2D_2 = 2Pd_2B^0{}_2CD$

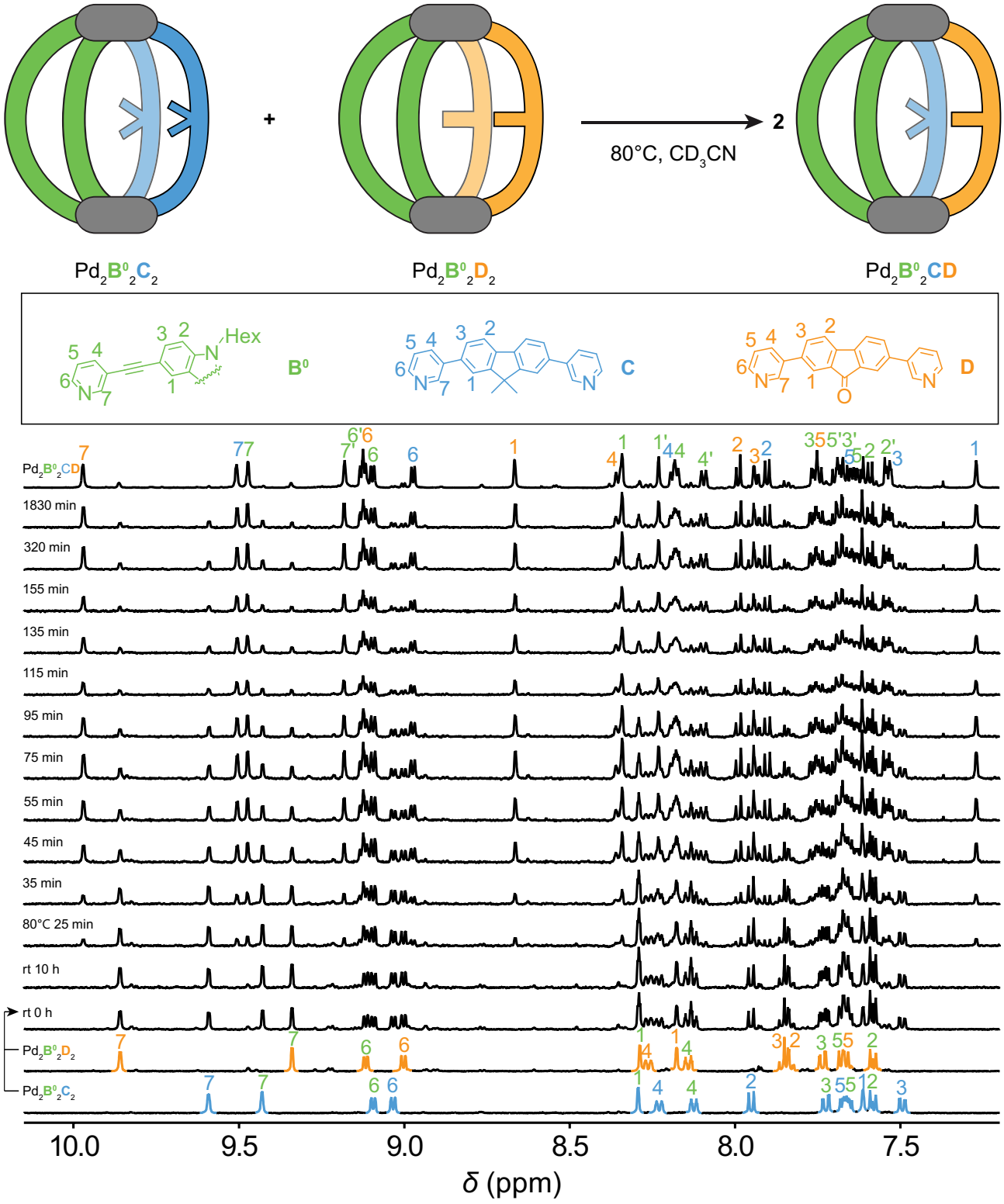

Supplementary Figure 262 | ^{1}H NMR monitoring (500 MHz, 298 K, CD_3CN) the cage-to-cage transformation process from heteroleptic cages $Pd_2B^0{}_2C_2$ and $Pd_2B^0{}_2D_2$ to cage $Pd_2B^0{}_2CD$ cage after heating at 80 °C. The top spectrum shows cage $Pd_2B^0{}_2CD$ formed from mixing the ligands with Pd(II).

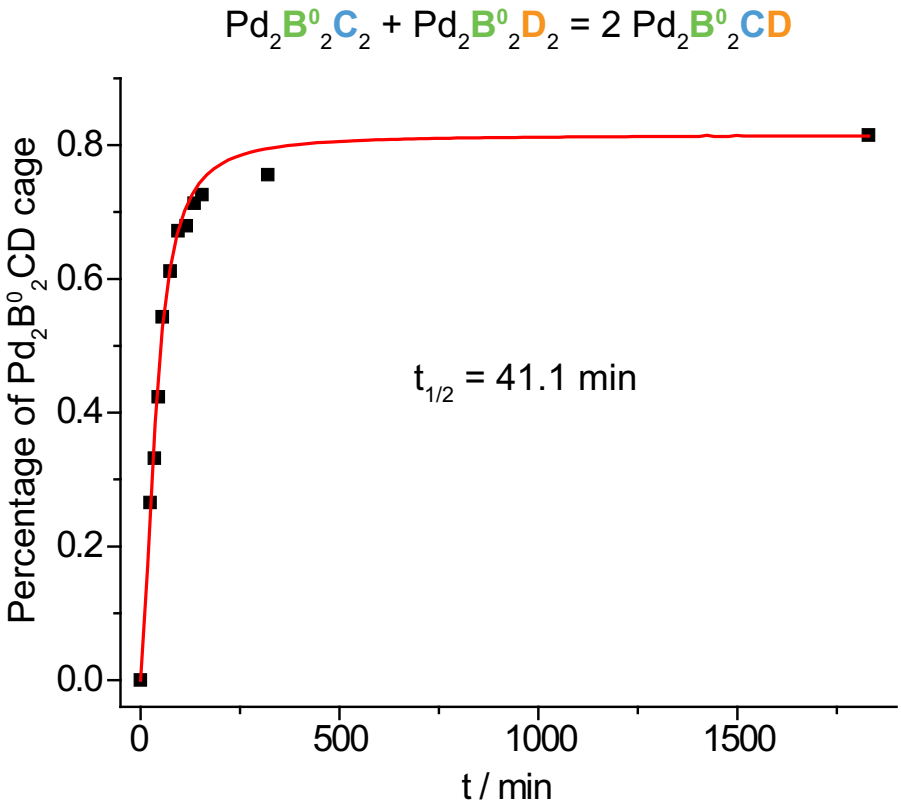

Supplementary Figure 263 | Plot of cage-to-cage transformation from $Pd_2\mathbf{B^0}_2\mathbf{C}_2$ and $Pd_2\mathbf{B^0}_2\mathbf{D}_2$ to cage $Pd_2\mathbf{B^0}_2\mathbf{CD}$ after heating at 80 °C over time, $t_{1/2}$ = 41.1 min.

4.5. Cage-to-cage reaction: $Pd_2\mathbf{A}_2\mathbf{CD} + Pd_2\mathbf{B}_2\mathbf{CD} = 2Pd_2\mathbf{ABCD}$

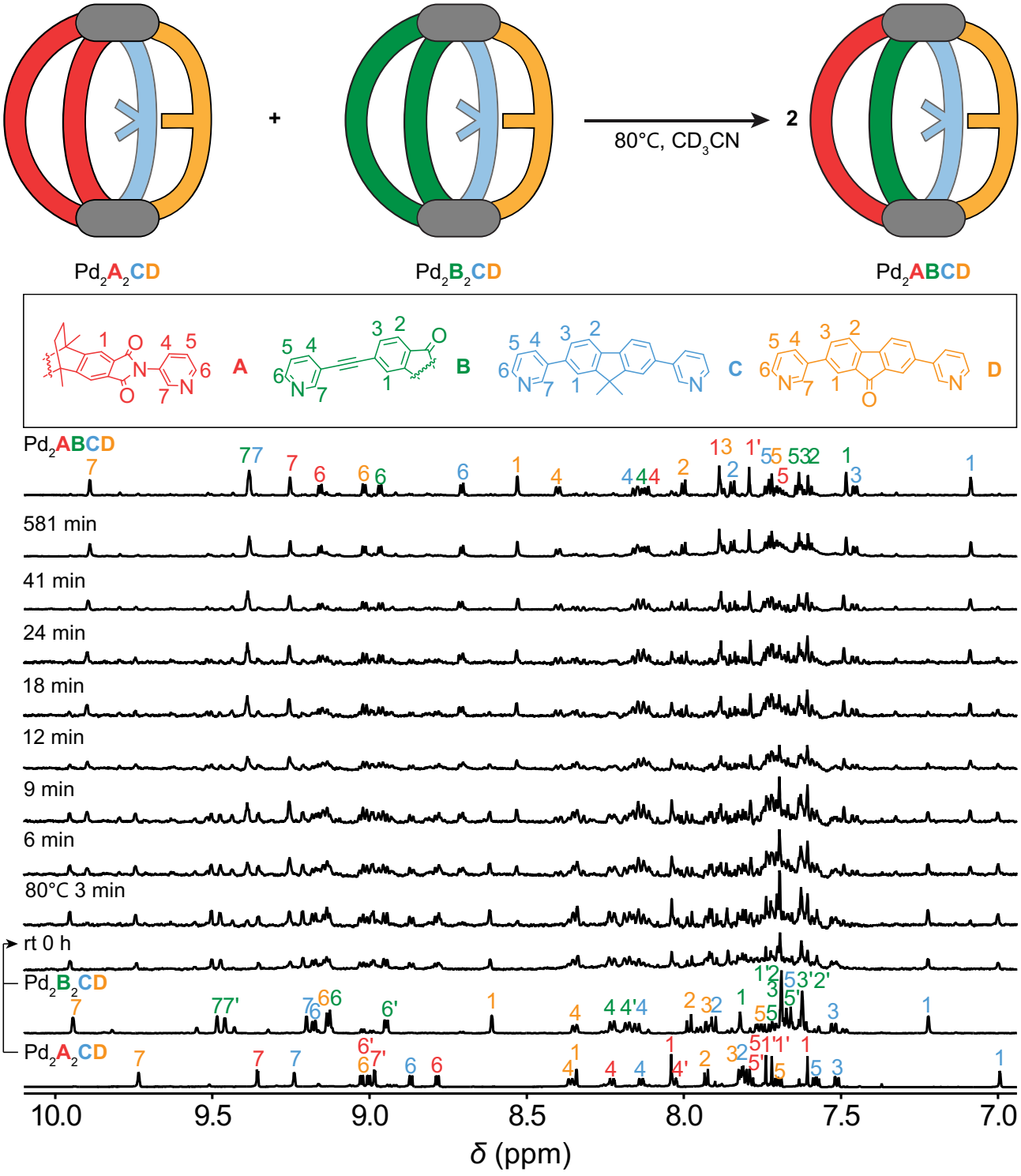

Supplementary Figure 264 | ^{1}H NMR spectra (500 MHz, 298 K, CD_3CN) of cage-to-cage transformation from heteroleptic cages $Pd_2\mathbf{A}_2\mathbf{CD}$ and $Pd_2\mathbf{B}_2\mathbf{CD}$ to heteroleptic cage $Pd_2\mathbf{ABCD}$ after heating at 80 °C. The top spectrum shows cage $Pd_2\mathbf{ABCD}$ formed from mixing the ligands with Pd(II). The top spectrum shows cage $Pd_2\mathbf{ABCD}$ formed from mixing the ligands with Pd(II).

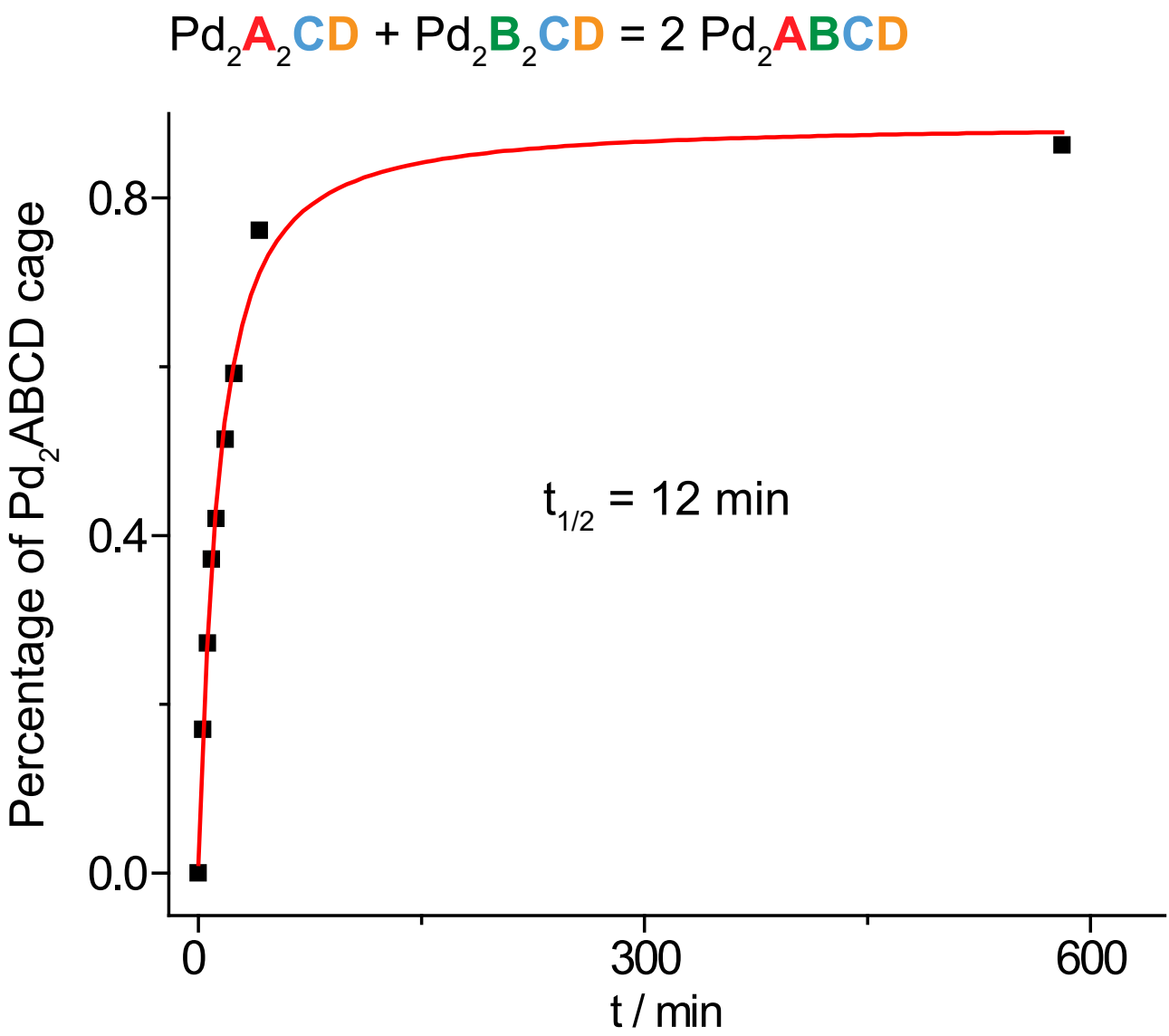

Supplementary Figure 265 | Plot of cage-to-cage transformation from Pd_2**A**$_2$**CD** and Pd_2**B**$_2$**CD** to cage Pd_2**ABCD** after heating at 80 °C over time, $t_{1/2}$ =12 min.

4.6. Cage-to-cage reaction: Pd_2**ABC**$_2$ + Pd_2**ABD**$_2$ = 2Pd_2**ABCD**

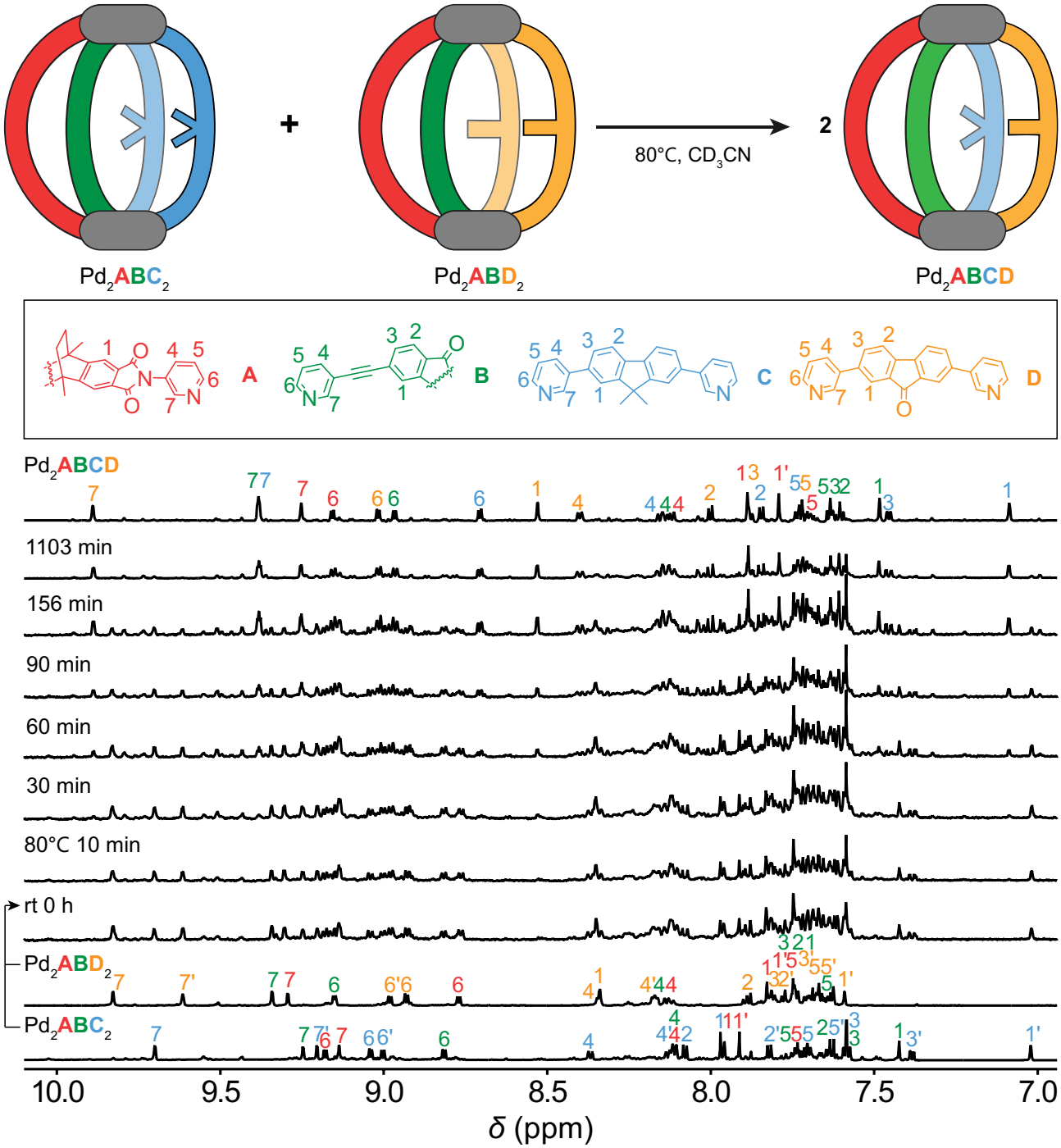

Supplementary Figure 266 | ^{1}H NMR spectra (500 MHz, 298 K, CD_3CN) of cage-to-cage transformation from heteroleptic cages Pd_2**ABC**$_2$ and Pd_2**ABD**$_2$ to heteroleptic cage Pd_2**ABCD** after heating at 80 °C. The top spectrum shows cage Pd_2**ABCD** formed from mixing the ligands with Pd(II). The top spectrum shows cage Pd_2**ABCD** formed from mixing the ligands with Pd(II).

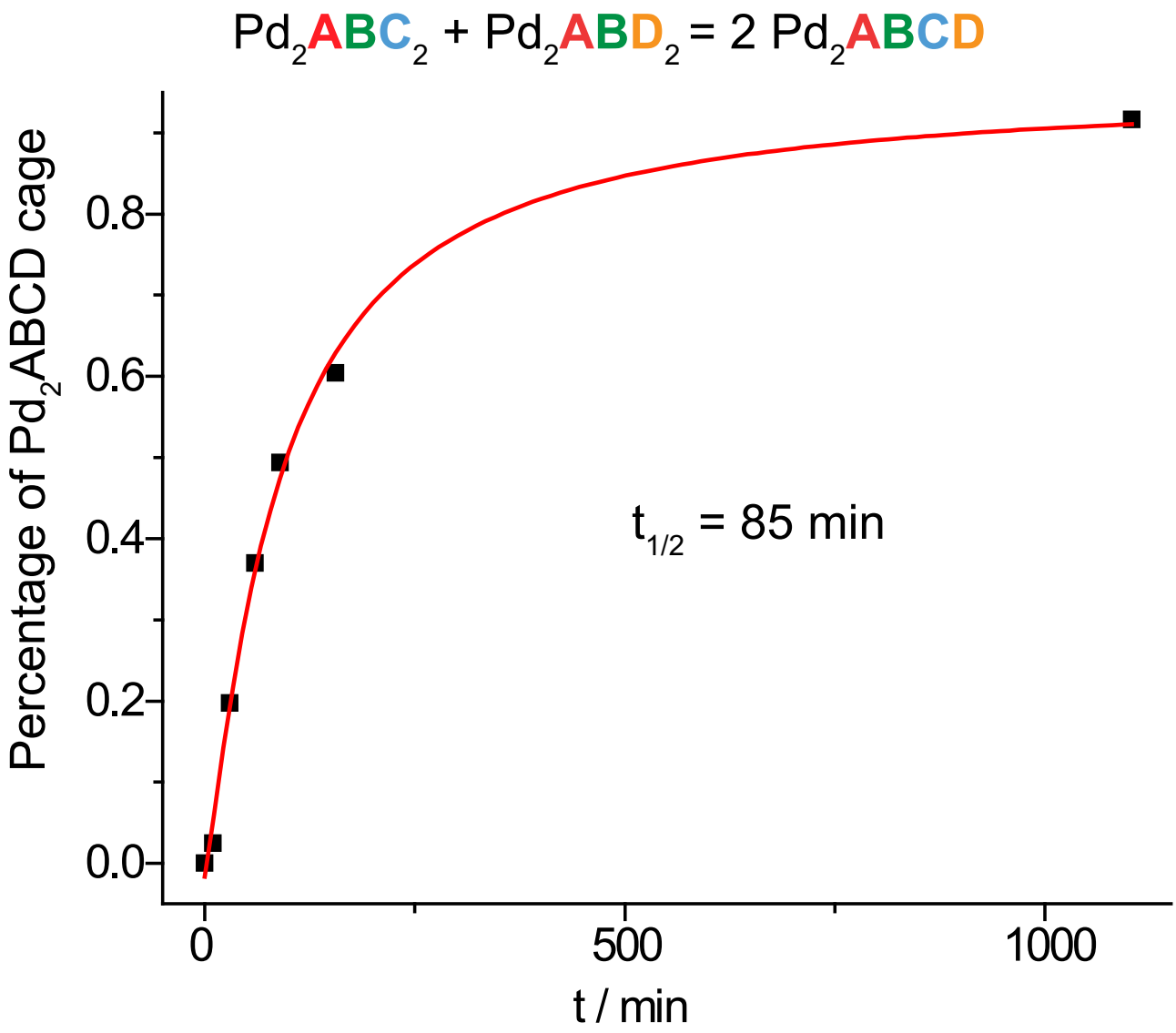

Supplementary Figure 267 | Plot of cage-to-cage transformation from Pd_2**ABC**$_2$ and Pd_2**ABD**$_2$ to cage Pd_2**ABCD** after heating at 80 °C over time, $t_{1/2}$ = 85 min.

Supplementary Table 1. Summary of half-times $t_{1/2}$ of cage-to-cage transformation. The half-time for cage-to-cage transformation from heteroleptic cages with two different ligands to three different ligands is shorter when ligand **A** is present (instead of **B**; e.g for $[Pd_2\mathbf{A}_2\mathbf{C}_2]^{4+}$ + $[Pd_2\mathbf{A}_2\mathbf{D}_2]^{4+}$ → 2 $[Pd_2\mathbf{A}_2\mathbf{CD}]^{4+}$: $t_{½}$ = 17.9 min vs. $[Pd_2\mathbf{B}_2\mathbf{C}_2]^{4+}$ + $[Pd_2\mathbf{B}_2\mathbf{D}_2]^{4+}$ → 2 $[Pd_2\mathbf{B}_2\mathbf{CD}]^{4+}$: $t_{½}$ = 41.5 min), which may be explained by the higher structural flexibility of ligand **A**, facilitating ligand exchange from/to the square-planar Pd^{II} centers in the constrained 3D assembly.

	$t_{1/2}$ [min]
$Pd_2\mathbf{A}_2\mathbf{C}_2$ + $Pd_2\mathbf{A}_2\mathbf{D}_2$ = 2 $Pd_2\mathbf{A}_2\mathbf{CD}$	17.9
$Pd_2\mathbf{B}_2\mathbf{C}_2$ + $Pd_2\mathbf{B}_2\mathbf{D}_2$ = 2 $Pd_2\mathbf{B}_2\mathbf{CD}$	41.5
$Pd_2\mathbf{B}^0{}_2\mathbf{C}_2$ + $Pd_2\mathbf{B}^0{}_2\mathbf{D}_2$ = 2 $Pd_2\mathbf{B}^0{}_2\mathbf{CD}$	41.1
$Pd_2\mathbf{A}_2\mathbf{CD}$ + $Pd_2\mathbf{B}_2\mathbf{CD}$ = 2 Pd_2**ABCD**	12
$Pd_2\mathbf{ABC}_2$ + $Pd_2\mathbf{ABD}_2$ = 2 Pd_2**ABCD**	85

4.7. Cage-to-cage reaction: Homoleptic cages to heteroleptic cage Pd_2**ABCD**

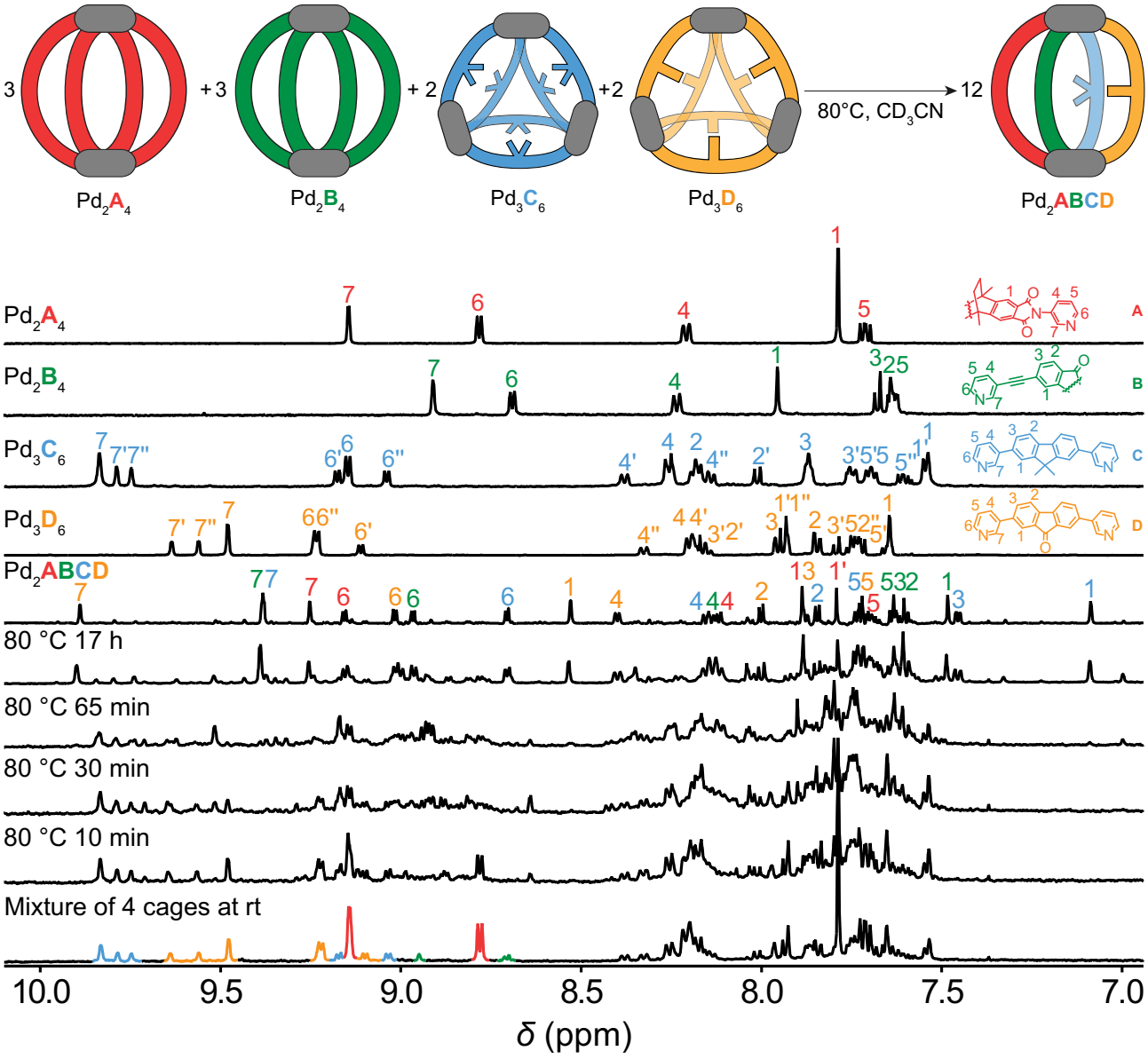

Supplementary Figure 268 | ^{1}H NMR spectra (500 MHz, 298 K, CD_3CN) of cage-to-cage transformation from all the four homoleptic cages Pd_2**A**$_4$, Pd_2**B**$_4$, Pd_3**C**$_6$, Pd_3**D**$_6$ to heteroleptic cage Pd_2**ABCD** (the solubility of homoleptic cages Pd_2**B**$_4$ and Pd_3**D**$_6$ in CD_3CN is low, resulting in weak NMR signals). Homoleptic cage assembled with ligand **C** contains a mixture of Pd_3**C**$_6$ triangular ring and Pd_4**C**$_8$ tetrahedron in a 1.6:1 ratio. Similar for ligand **D** with Pd_3**D**$_6$: Pd_4**D**$_8$ = 2.2:1. The fifth spectrum from top shows cage Pd_2**ABCD** formed from mixing the ligands with Pd(II).

4.8. Monitoring heteroleptic cage Pd_2**ABCD**^{1} formation

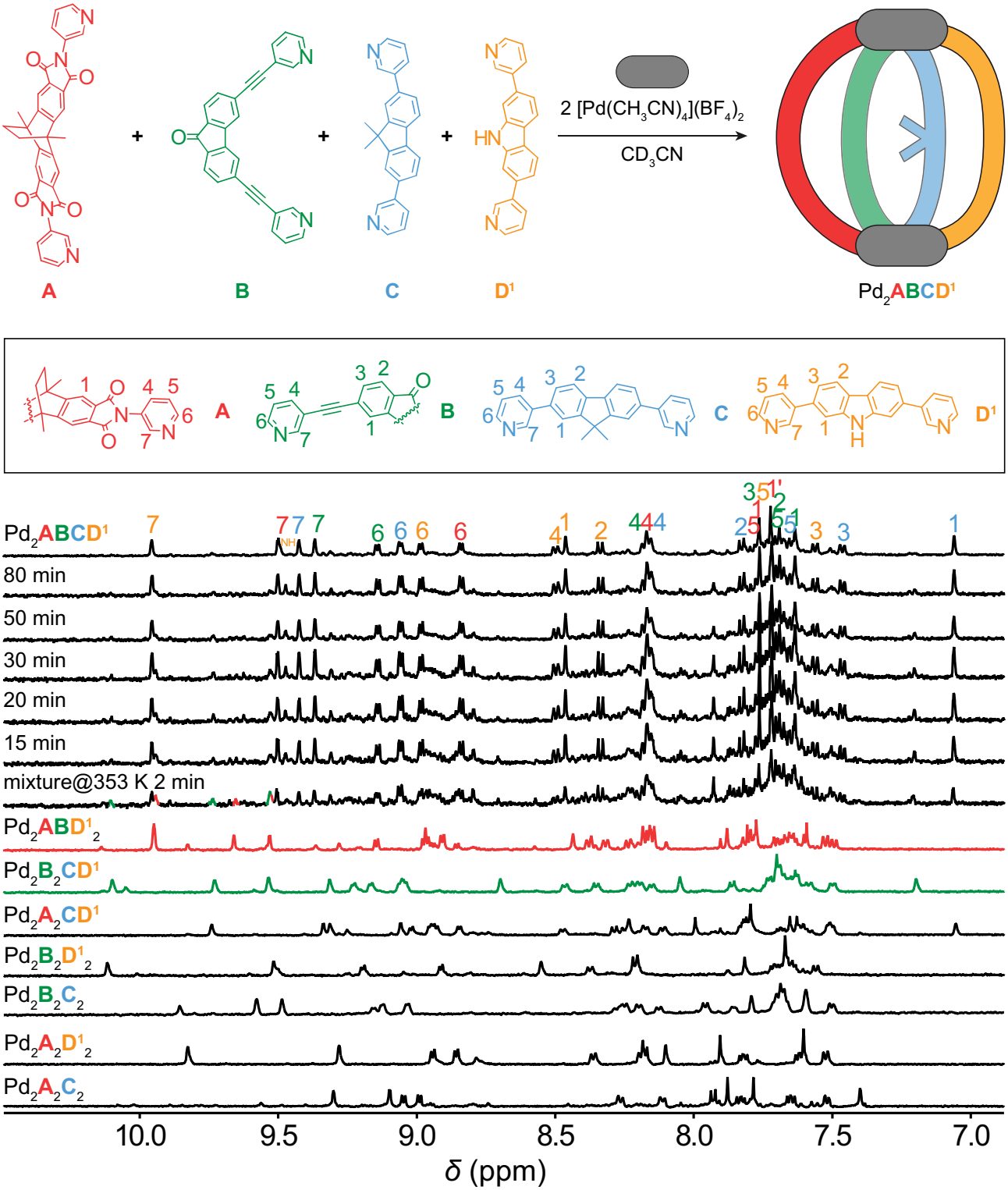

Supplementary Figure 269 | ^{1}H NMR spectra (500 MHz, 353 K, CD_3CN) monitoring the formation of heteroleptic cage Pd_2**ABCD**^{1} from all the four ligands and Pd(II). To monitor the intermediates during the formation of the heteroleptic cage with four different ligands, cage derivative Pd_2**ABCD**^{1} was chosen, due to its very clean NMR spectrum. As can be seen from the result, at the early stage of heating the ligands and Pd(II) mixture, no homoleptic cages can be found, and heteroleptic cages with three different ligands and Pd_2**ABCD**^{1} already appear. Procedure: All the four ligands in CD_3CN and Pd^{II} stock solution were added in the correct stoichiometry to an NMR tube containing CD_3CN at rt and NMR machine was set to 353 K before inserting the NMR tube and starting the measurement, then the shown spectra were recorded at different time intervals. Heteroleptic cages with two and three different ligands were formed from mixing the ligands with Pd(II) as reference, the spectra were measured at 353 K.

4.9. Competitive experiment between heteroleptic cages Pd_2**ABD^{4}C** and Pd_2**ABCD**

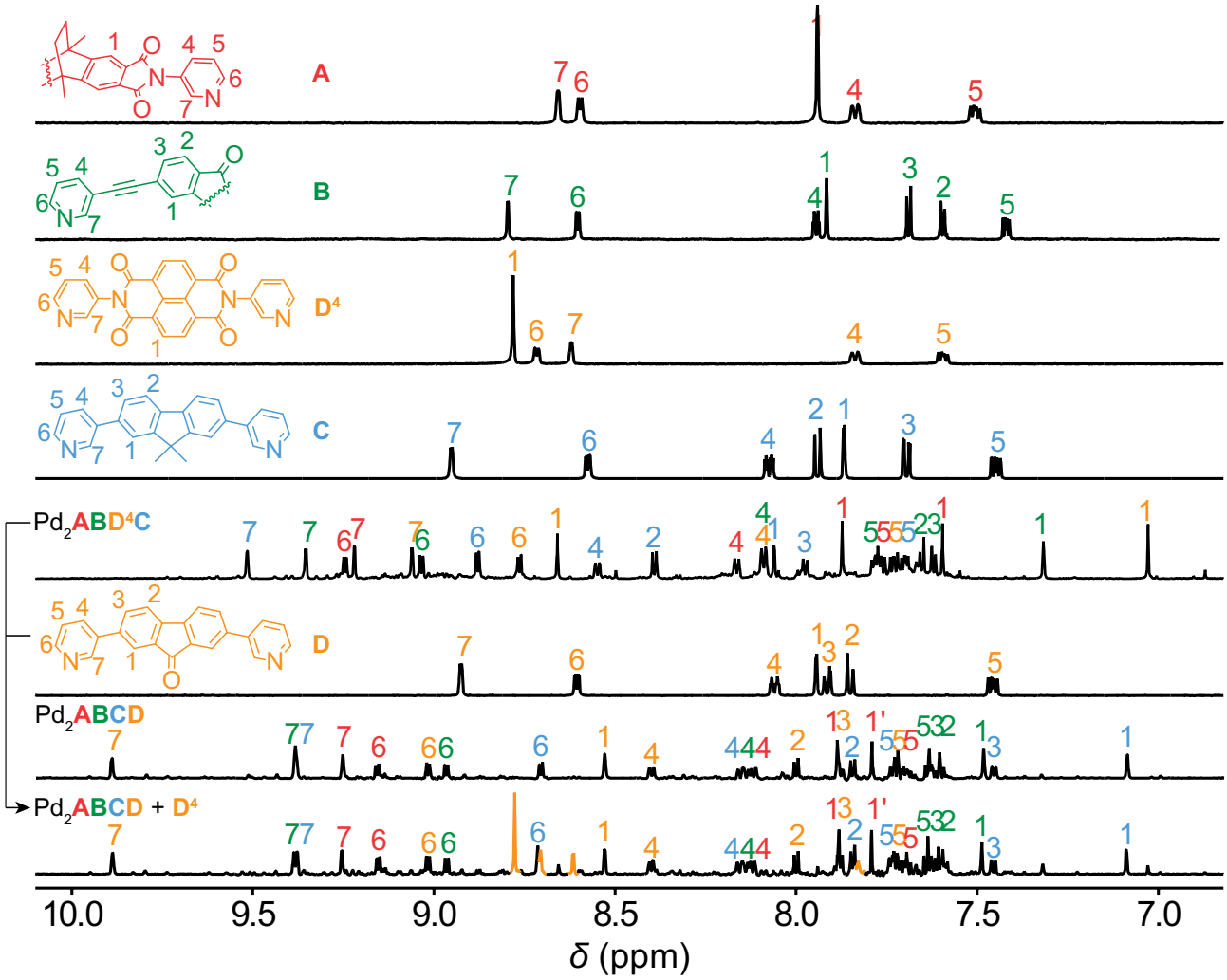

Supplementary Figure 270 | ^{1}H NMR spectra (500 MHz, 298 K, CD_3CN) of the competitive formation of heteroleptic cage Pd_2**ABCD** over cage Pd_2**ABD^{4}C**. The preformed heteroleptic cage Pd_2**ABD^{4}C** and ligand **D** was added in an NMR tube with a 1:1 ratio at rt and heated at 353 K for 8 h, resulting in the exclusive formation of cage Pd_2**ABCD** with released free ligand **D^4**.

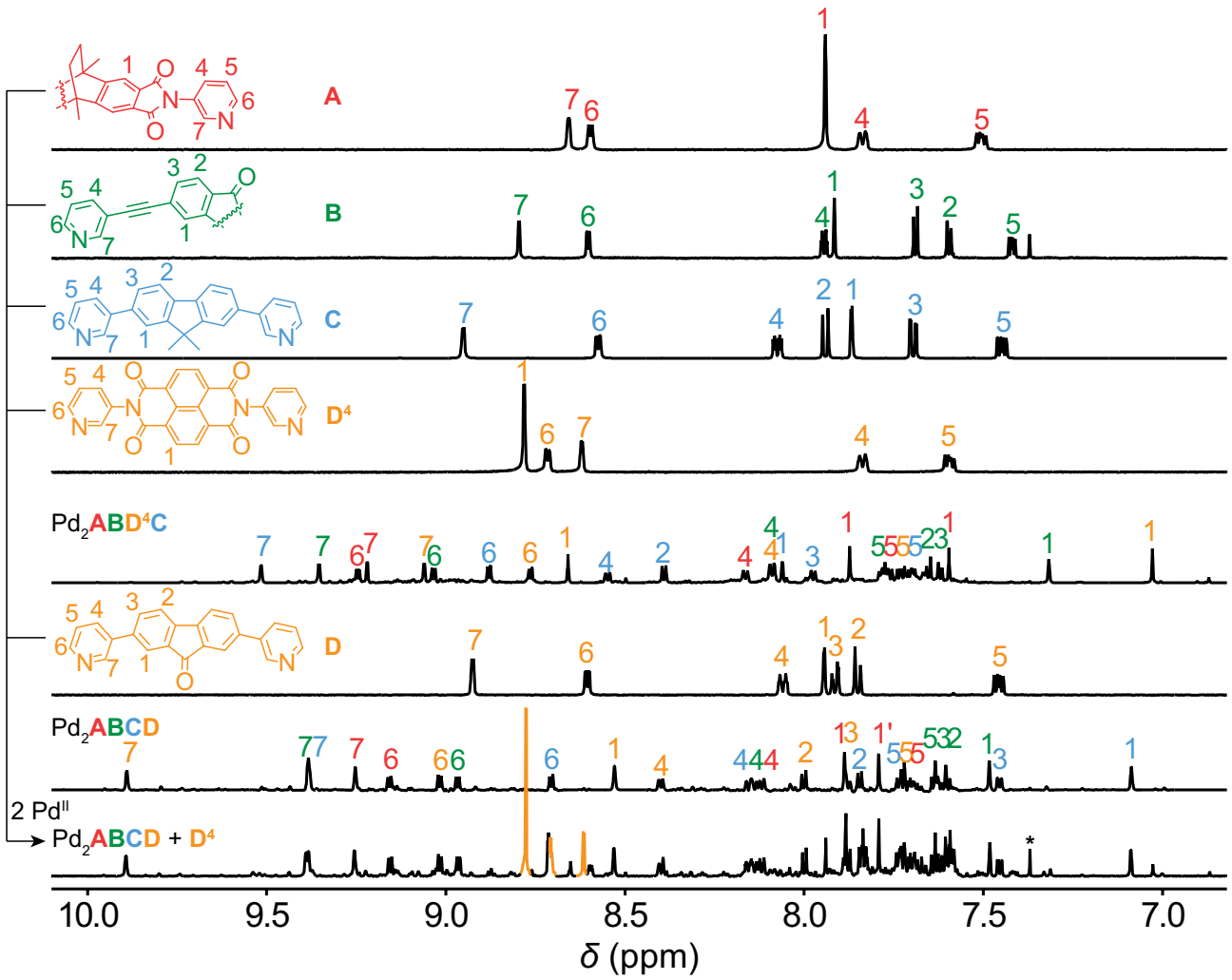

Supplementary Figure 271 | ^{1}H NMR spectra (500 MHz, 298 K, CD_3CN) of the selective formation of heteroleptic cage Pd_2**ABCD** over cage Pd_2**ABD^{4}C**. All the five ligands and Pd^{II} were added in an NMR tube with a 1:1:1:1:1:2 ratio at rt and heated at 353 K for 8 h, resulting in the exclusive formation of $[Pd_2$**ABCD**$]^{4+}$ cage with free ligand **D^4** ($CHCl_3$ residual was marked with an asterisk).

5. Thermodynamic study of cage-to-cage transformations

For each of the following experiments, an equimolar amount of two matching heteroleptic cages was mixed and heated at the indicated temperature for 12 h until the equilibrium towards formation of the resulting heteroleptic cage was reached. The equilibrated concentration for each cage was obtained by NMR signal integration and used to calculate the equilibrium constant $\ln K_{eq}$ at the respective temperature. Thermodynamic parameters were obtained by plotting $\ln K_{eq}$ values over 1/T, fitting the data by linear regression and applying the Van 't Hoff equation (**Eq. 4**).

$$K_{eq} = \frac{[\text{Cage 3}]^2}{[\text{Cage 1}][\text{Cage 2}]} \qquad \textbf{Eq. 1}$$

$$\Delta G = \Delta H - T\Delta S \qquad \textbf{Eq. 2}$$

$$\Delta G = -RT\ln K_{eq} \qquad \textbf{Eq. 3}$$

$$\ln K_{eq} = -\frac{\Delta H}{R}\cdot\frac{1}{T} + \frac{\Delta S}{R} \qquad \textbf{Eq. 4}$$

5.1. Cage-to-cage reaction: $Pd_2A_2C_2 + Pd_2A_2D_2 = 2Pd_2A_2CD$

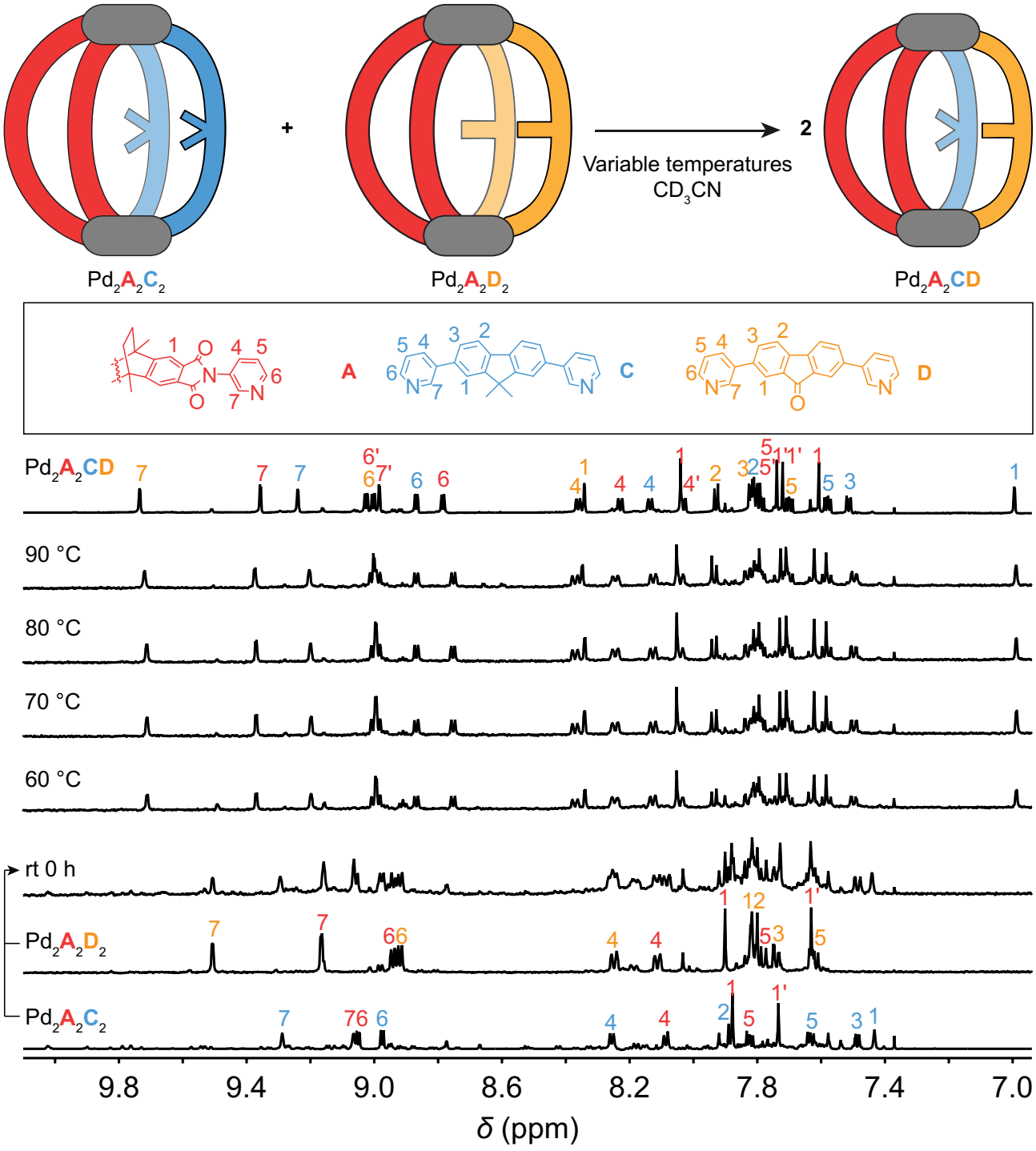

Supplementary Figure 272 | ^{1}H NMR spectra (500 MHz, 298 K, CD_3CN) of cage-to-cage transformation from heteroleptic cages $Pd_2A_2C_2$ and $Pd_2A_2D_2$ to heteroleptic cage Pd_2A_2CD at different temperatures (each of the heteroleptic $Pd_2A_2C_2$ and $Pd_2A_2D_2$ cage samples were mixed in an NMR tube, and heated at corresponding temperature for 12 h to reach equilibrium. The spectrum measured at rt for 0 h is not equilibrated and only serves as reference for the cage mixture prior to thermal equilibration). The top spectrum shows cage Pd_2A_2CD formed from mixing the ligands with Pd(II).

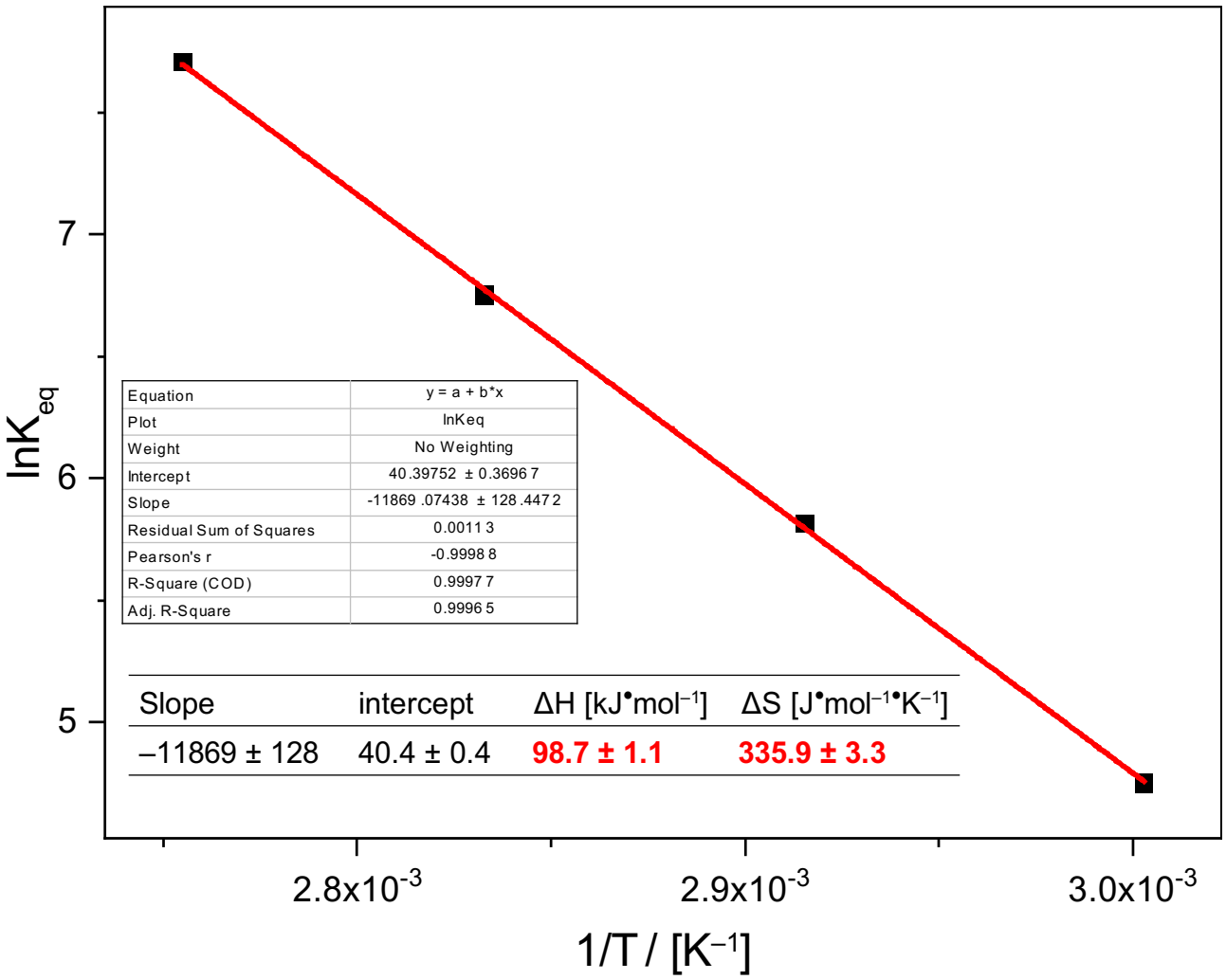

Supplementary Figure 273 | Van't Hoff plot of cage-to-cage transformation from heteroleptic cages $Pd_2\mathbf{A}_2\mathbf{C}_2$ and $Pd_2\mathbf{A}_2\mathbf{D}_2$ to heteroleptic cage $Pd_2\mathbf{A}_2\mathbf{CD}$ at different temperatures.

5.2. Cage-to-cage reaction: $Pd_2B_2C_2 + Pd_2B_2D_2 = 2Pd_2B_2CD$

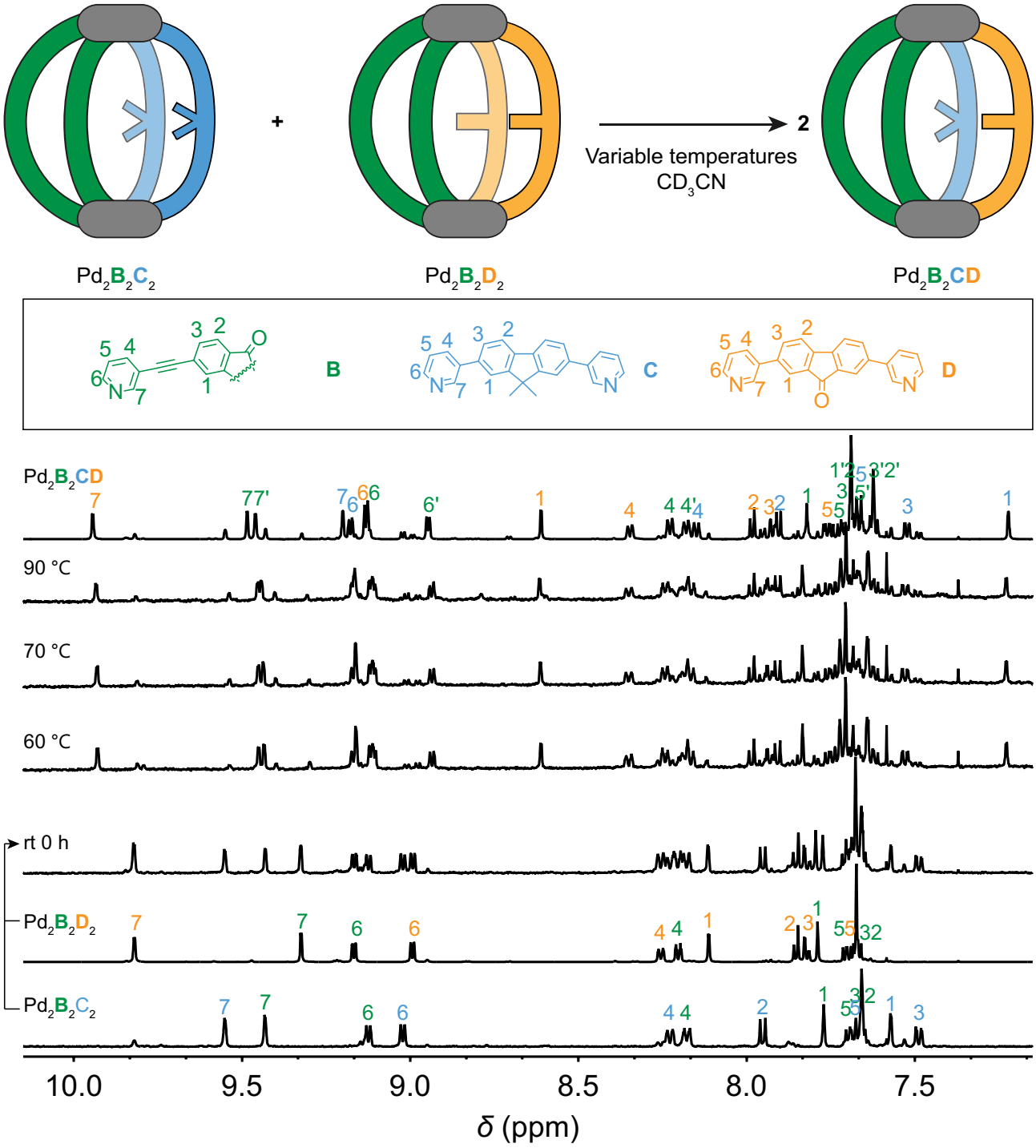

Supplementary Figure 274 | ^{1}H NMR spectra (500 MHz, 298 K, CD_3CN) of cage-to-cage transformation from heteroleptic cages $Pd_2B_2C_2$ and $Pd_2B_2D_2$ to heteroleptic cage Pd_2B_2CD at different temperatures (each of the heteroleptic $Pd_2B_2C_2$ and $Pd_2B_2D_2$ cage samples were mixed in an NMR tube, and heated at corresponding temperature for 12 h to reach equilibrium. The spectrum measured at rt for 0 h is not equilibrated and only serves as reference for the cage mixture prior to thermal equilibration). The top spectrum shows cage Pd_2B_2CD formed from mixing the ligands with Pd(II).

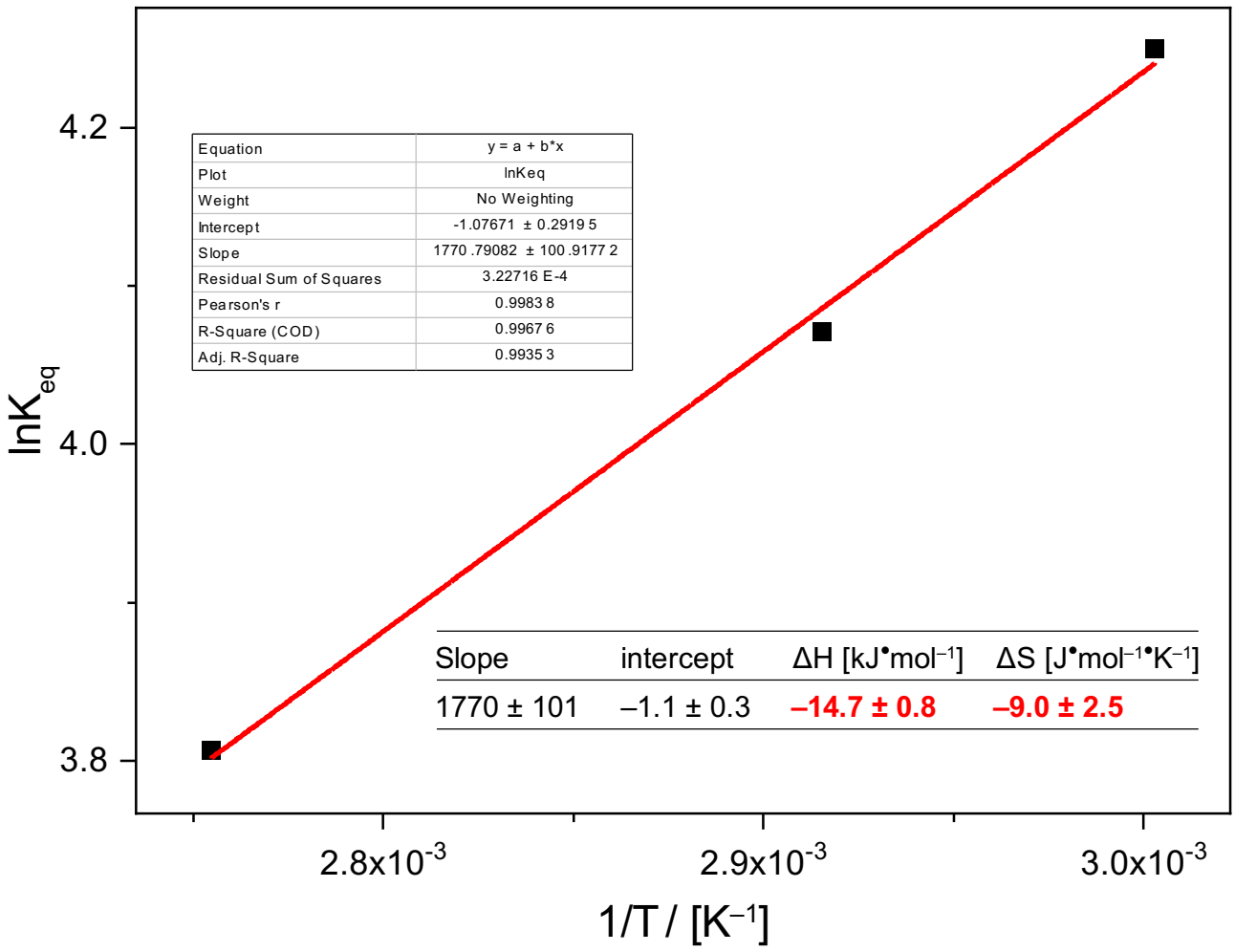

Supplementary Figure 275 | Van't Hoff plot of cage-to-cage transformation from heteroleptic cages Pd_2**B**$_2$**C**$_2$ and Pd_2**B**$_2$**D**$_2$ to heteroleptic cage Pd_2**B**$_2$**CD** at different temperatures.

5.3. Cage-to-cage reaction: $Pd_2\mathbf{A}_2\mathbf{C}_2 + Pd_2\mathbf{B}_2\mathbf{C}_2 = 2Pd_2\mathbf{ABC}_2$

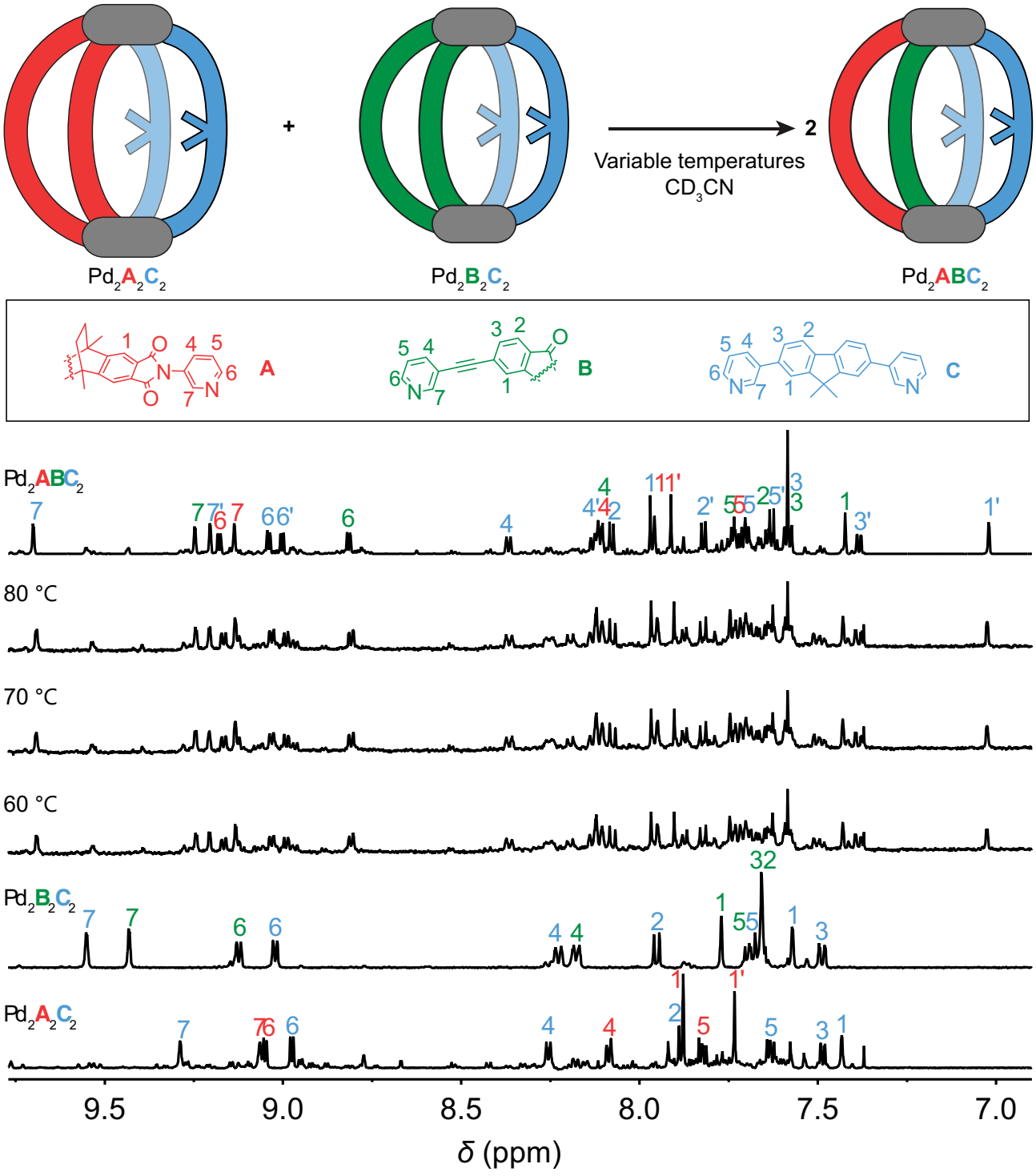

Supplementary Figure 276 | ^{1}H NMR spectra (500 MHz, 298 K, CD_3CN) of cage-to-cage transformation from heteroleptic cages $Pd_2\mathbf{A}_2\mathbf{C}_2$ and $Pd_2\mathbf{B}_2\mathbf{C}_2$ to heteroleptic cage $Pd_2\mathbf{ABC}_2$ at different temperatures (each of the heteroleptic $Pd_2\mathbf{A}_2\mathbf{C}_2$ and $Pd_2\mathbf{B}_2\mathbf{C}_2$ cage samples were mixed in an NMR tube, and heated at corresponding temperature for 12 h to reach equilibrium). The top spectrum shows cage $Pd_2\mathbf{ABC}_2$ formed from mixing the ligands with Pd(II).

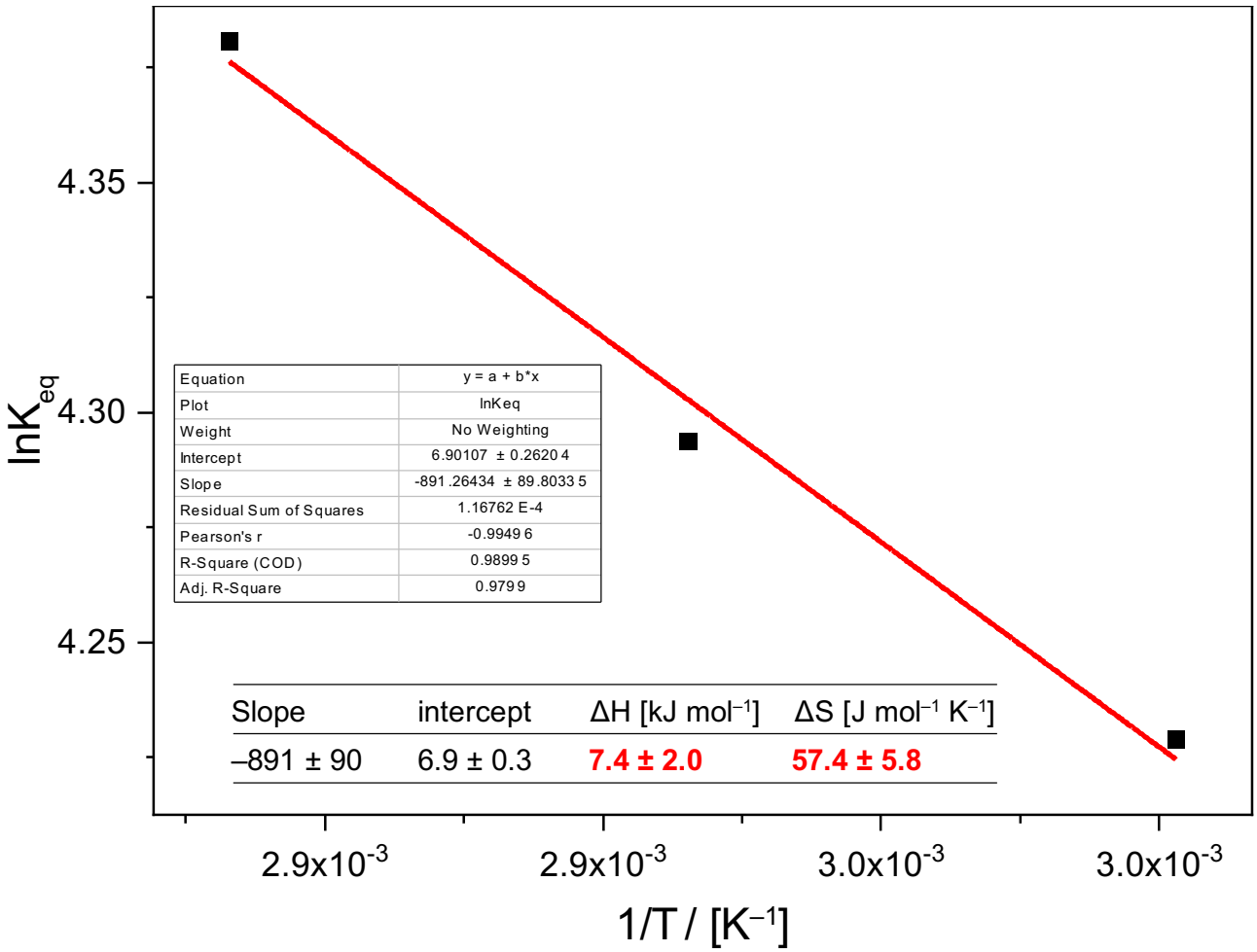

Supplementary Figure 277 | Van't Hoff plot of cage-to-cage transformation from heteroleptic cages $Pd_2\mathbf{A}_2\mathbf{C}_2$ and $Pd_2\mathbf{B}_2\mathbf{C}_2$ to heteroleptic cage $Pd_2\mathbf{ABC}_2$ at different temperatures.

5.4. Cage-to-cage reaction: $Pd_2\mathbf{A}_2\mathbf{D}_2 + Pd_2\mathbf{B}_2\mathbf{D}_2 = 2Pd_2\mathbf{ABD}_2$

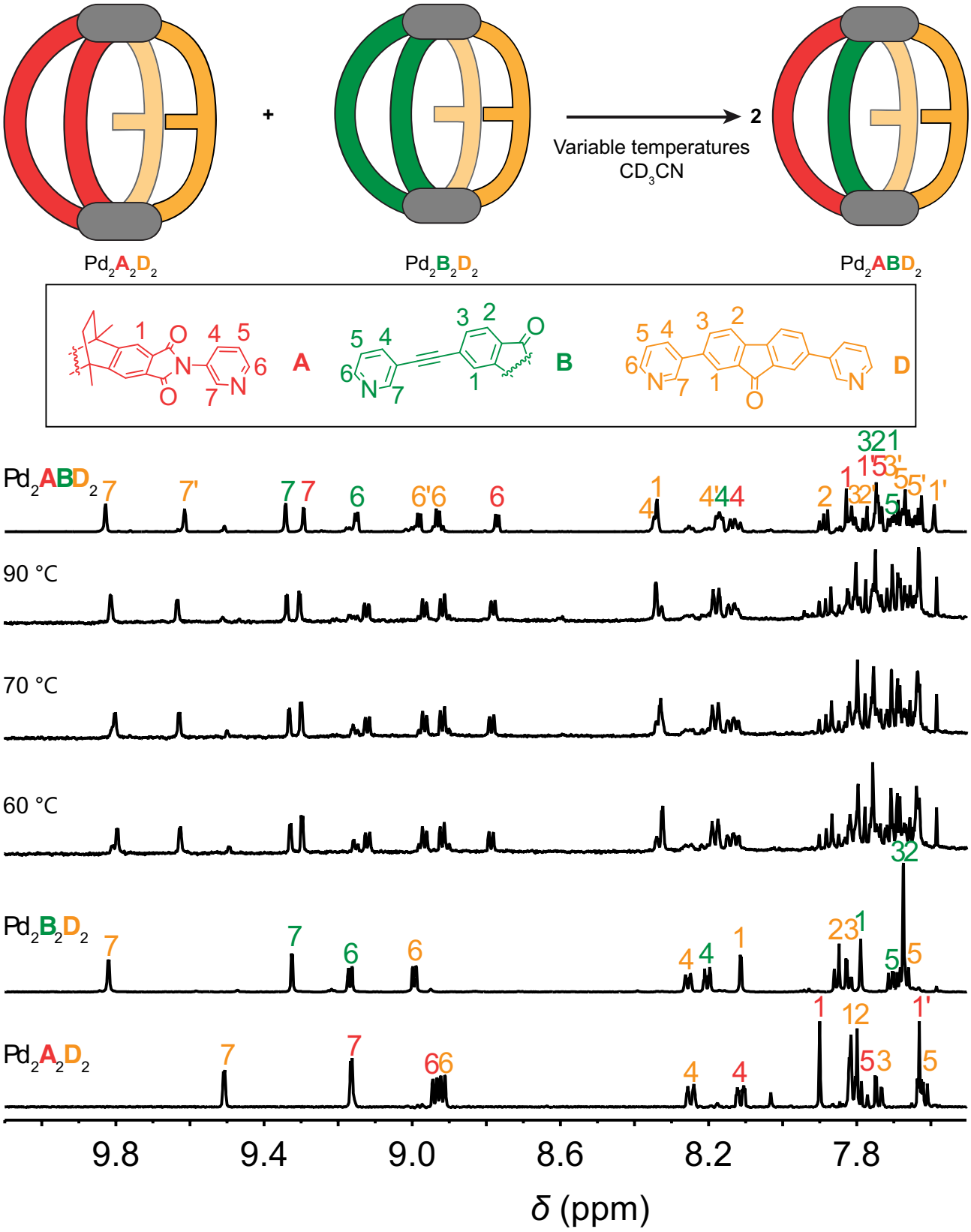

Supplementary Figure 278 | ^{1}H NMR spectra (500 MHz, 298 K, CD_3CN) of cage-to-cage transformation from heteroleptic cages $Pd_2\mathbf{A}_2\mathbf{D}_2$ and $Pd_2\mathbf{B}_2\mathbf{D}_2$ to heteroleptic cage $Pd_2\mathbf{ABD}_2$ at different temperatures (each of the heteroleptic $Pd_2\mathbf{A}_2\mathbf{D}_2$ and $Pd_2\mathbf{B}_2\mathbf{D}_2$ cage samples was mixed in an NMR tube, and heated at corresponding temperature for 12 h to reach equilibrium). The top spectrum shows cage $Pd_2\mathbf{ABD}_2$ formed from mixing the ligands with Pd(II).

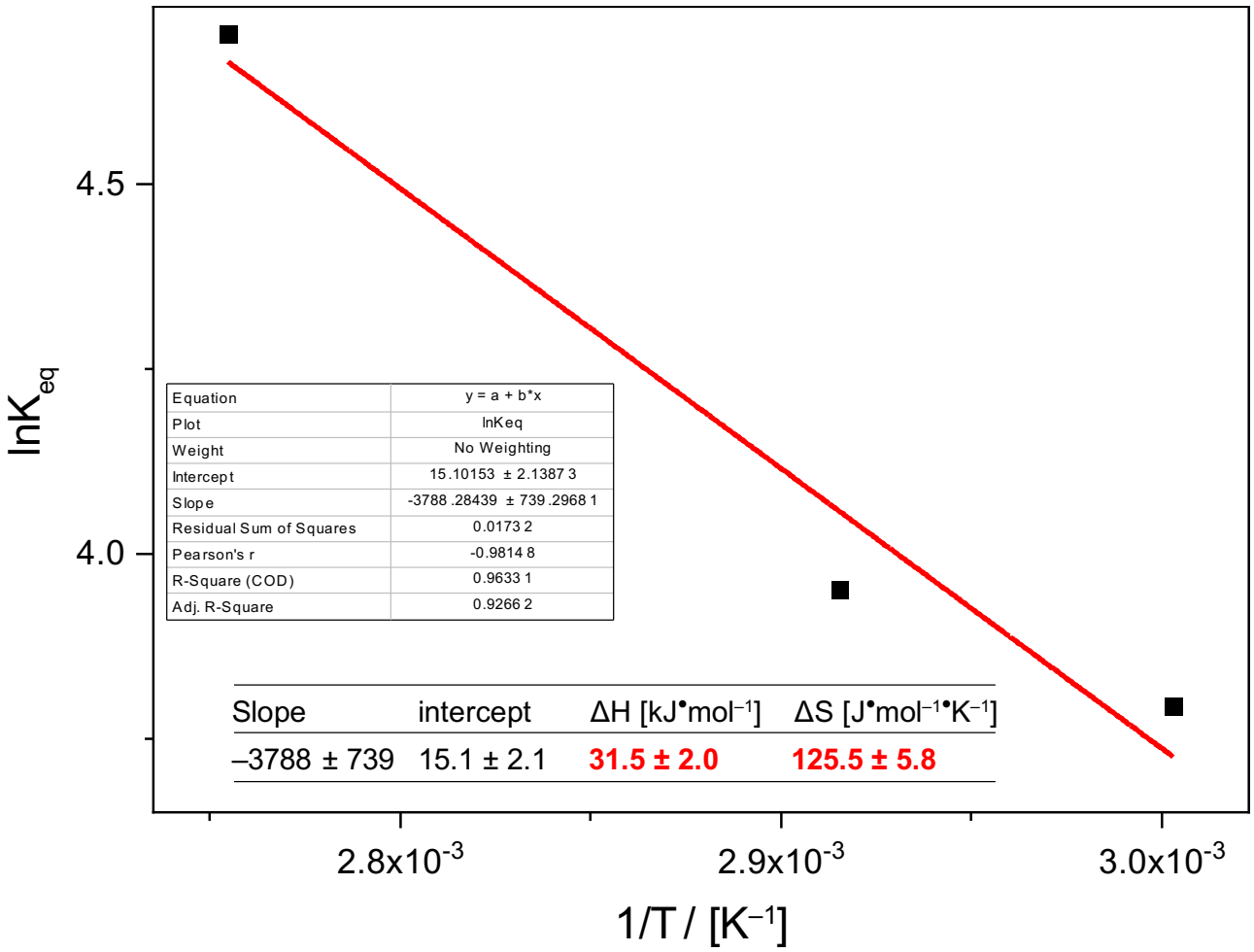

Supplementary Figure 279 | Van't Hoff plot of cage-to-cage transformation from heteroleptic cages $Pd_2\mathbf{A}_2\mathbf{D}_2$ and $Pd_2\mathbf{B}_2\mathbf{D}_2$ to heteroleptic cage $Pd_2\mathbf{ABD}_2$ at different temperatures.

5.5. Cage-to-cage reaction: $Pd_2\mathbf{A}_2\mathbf{CD} + Pd_2\mathbf{B}_2\mathbf{CD} = 2Pd_2\mathbf{ABCD}$

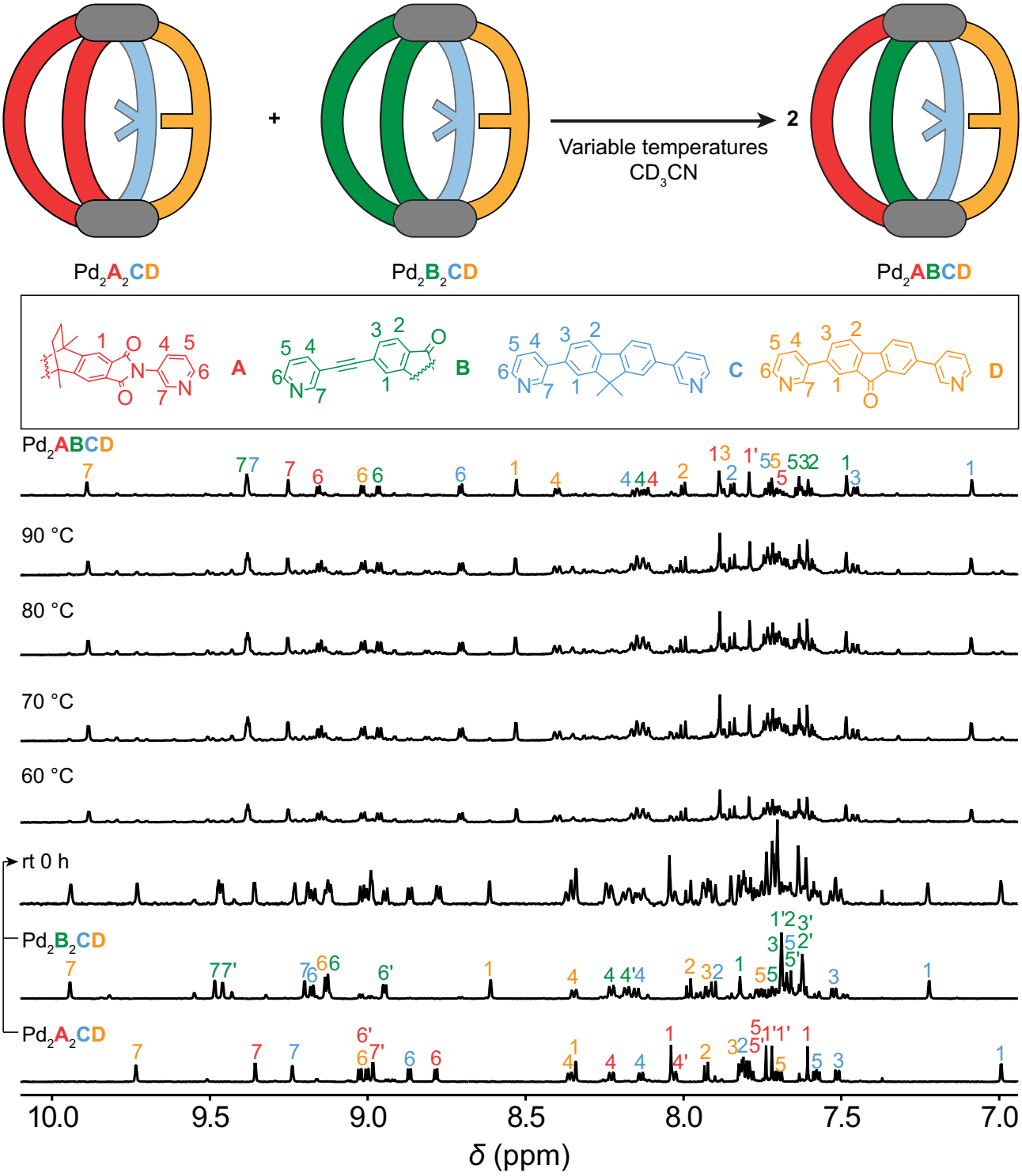

Supplementary Figure 280 | ^{1}H NMR spectra (500 MHz, 298 K, CD_3CN) of cage-to-cage transformation from heteroleptic cages $Pd_2\mathbf{A}_2\mathbf{CD}$ and $Pd_2\mathbf{B}_2\mathbf{CD}$ to heteroleptic cage $Pd_2\mathbf{ABCD}$ at different temperatures (each of the heteroleptic $Pd_2\mathbf{A}_2\mathbf{CD}$ and $Pd_2\mathbf{B}_2\mathbf{CD}$ cage samples were mixed in an NMR tube, and heated at corresponding temperature for 12 h to reach equilibrium. The spectrum measured at rt for 0 h is not equilibrated and only serves as reference for the cage mixture prior to thermal equilibration). The top spectrum shows cage $Pd_2\mathbf{ABCD}$ formed from mixing the ligands with Pd(II).

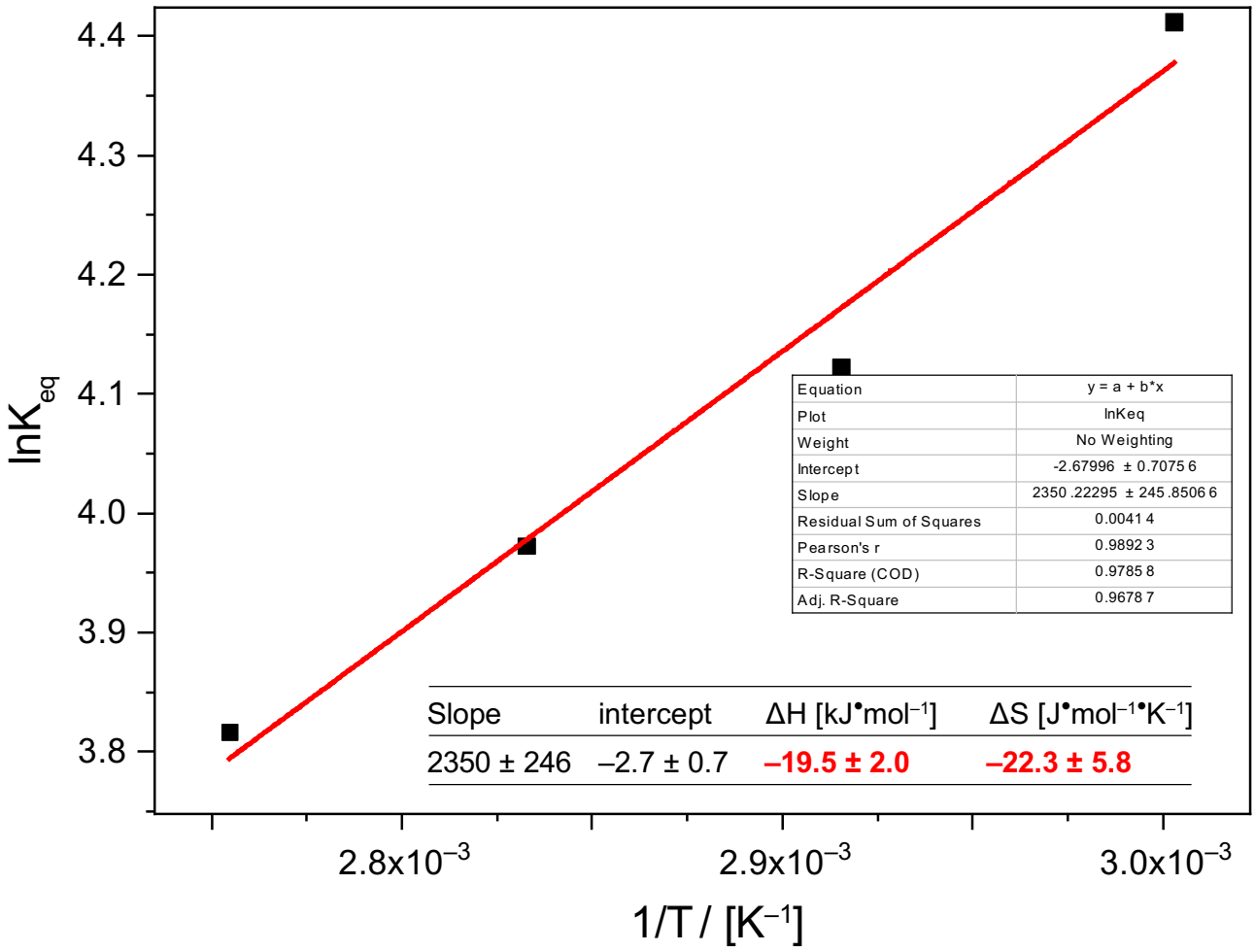

Supplementary Figure 281 | Van't Hoff plot of cage-to-cage transformation from heteroleptic cages Pd_2**A**$_2$**CD** and Pd_2**B**$_2$**CD** to heteroleptic cage Pd_2**ABCD** at different temperatures.

5.6. Cage-to-cage reaction: Pd_2**ABC**$_2$ + Pd_2**ABD**$_2$ = 2Pd_2**ABCD**

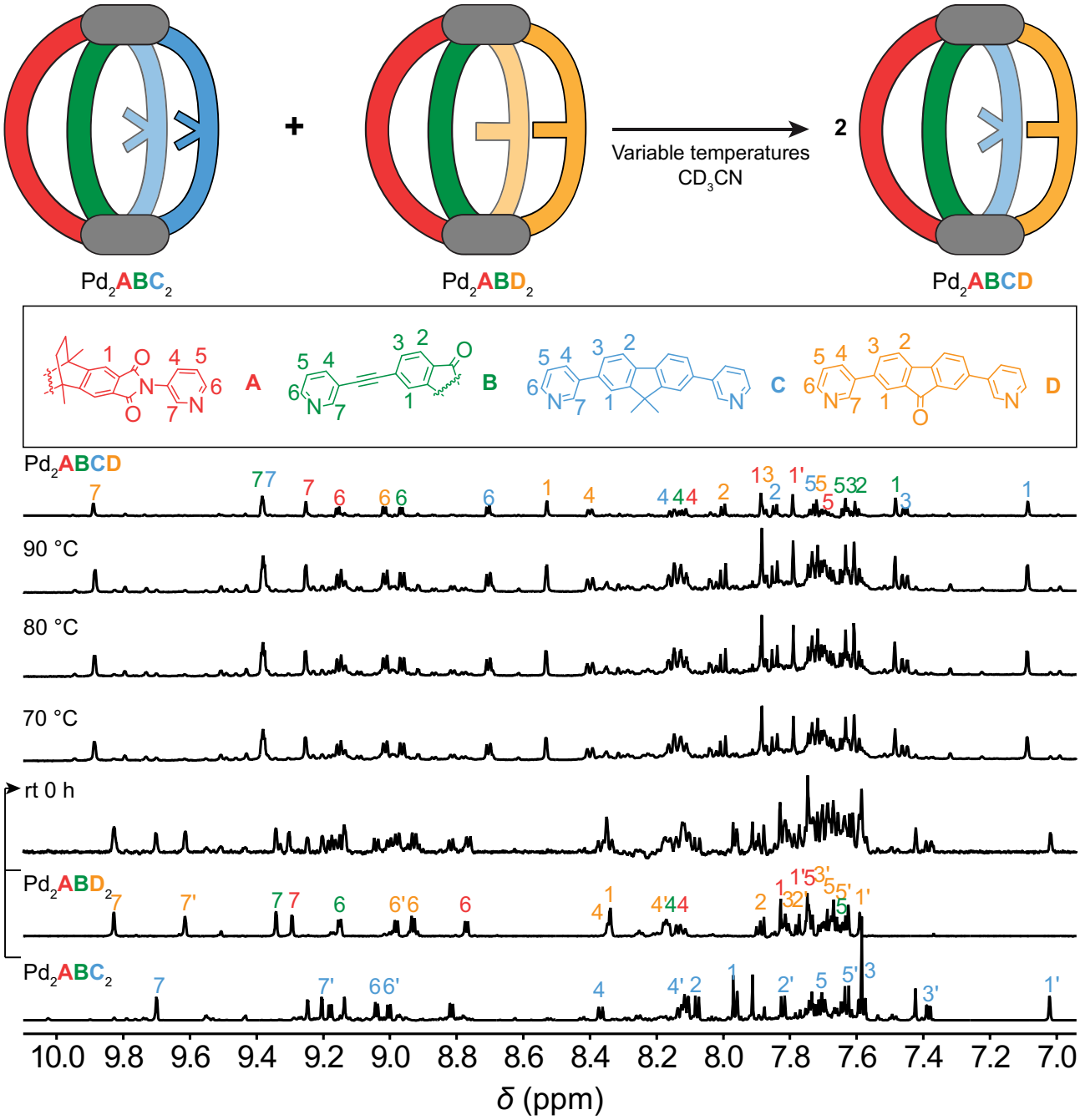

Supplementary Figure 282 | ^{1}H NMR spectra (500 MHz, 298 K, CD_3CN) of cage-to-cage transformation from heteroleptic cages Pd_2**ABC**$_2$ and Pd_2**ABD**$_2$ to heteroleptic cage Pd_2**ABCD** at different temperatures (each of the heteroleptic Pd_2**ABC**$_2$ and Pd_2**ABD**$_2$ cage samples were mixed in an NMR tube, and heated at corresponding temperature for 12 h to reach the equilibrium. The spectrum measured at rt for 0 h is not equilibrated and only serves as reference for the cage mixture prior to thermal equilibration). The top spectrum shows cage Pd_2**ABCD** formed from mixing the ligands with Pd(II).

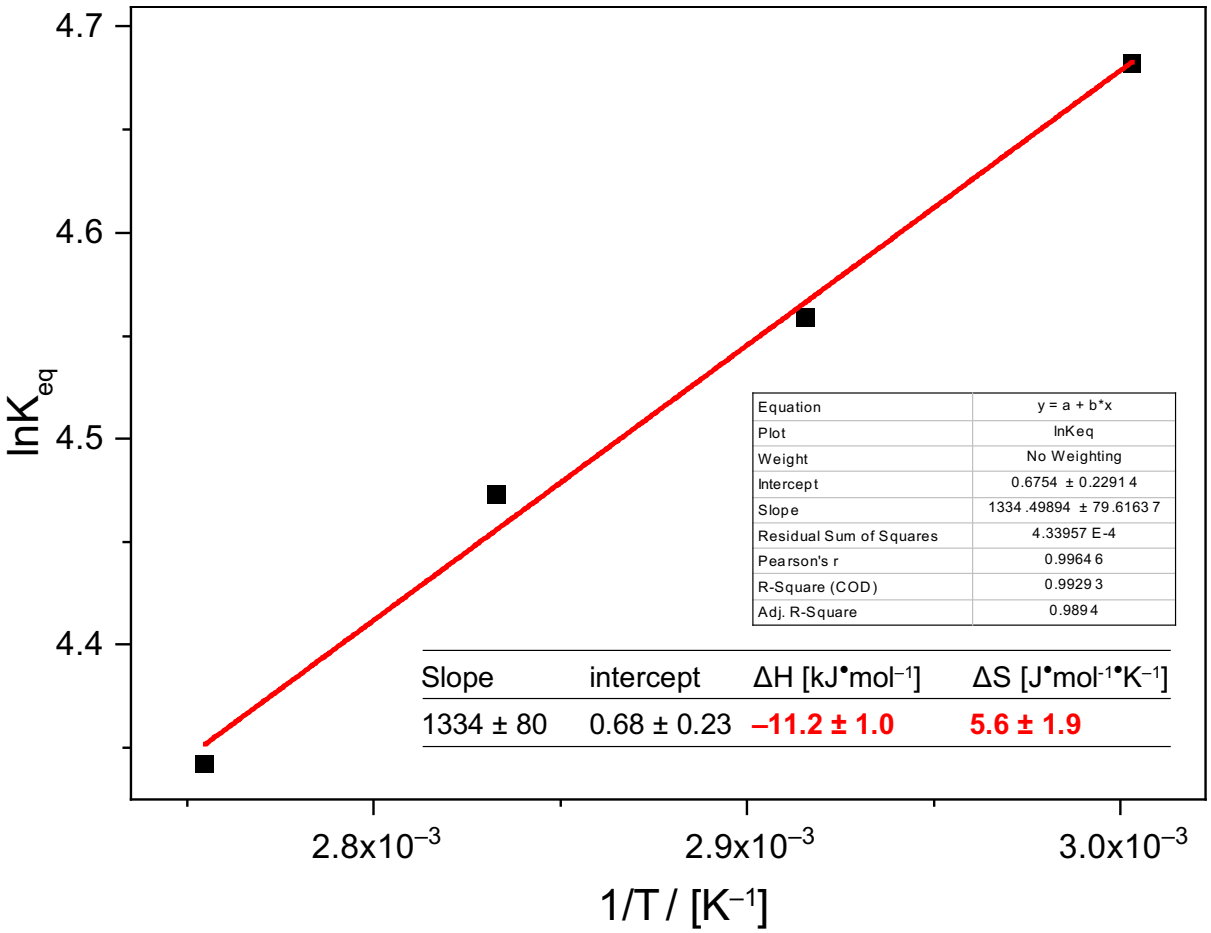

Supplementary Figure 283 | Van't Hoff plot of cage-to-cage transformation from heteroleptic cages Pd_2**ABC**$_2$ and Pd_2**ABD**$_2$ to heteroleptic cage Pd_2**ABCD** at different temperatures.

5.7. Cage-to-cage reaction: $Pd_2\mathbf{A}_2\mathbf{C}_2 + Pd_2\mathbf{B}_2\mathbf{D}_2 = 2Pd_2\mathbf{ABCD}$

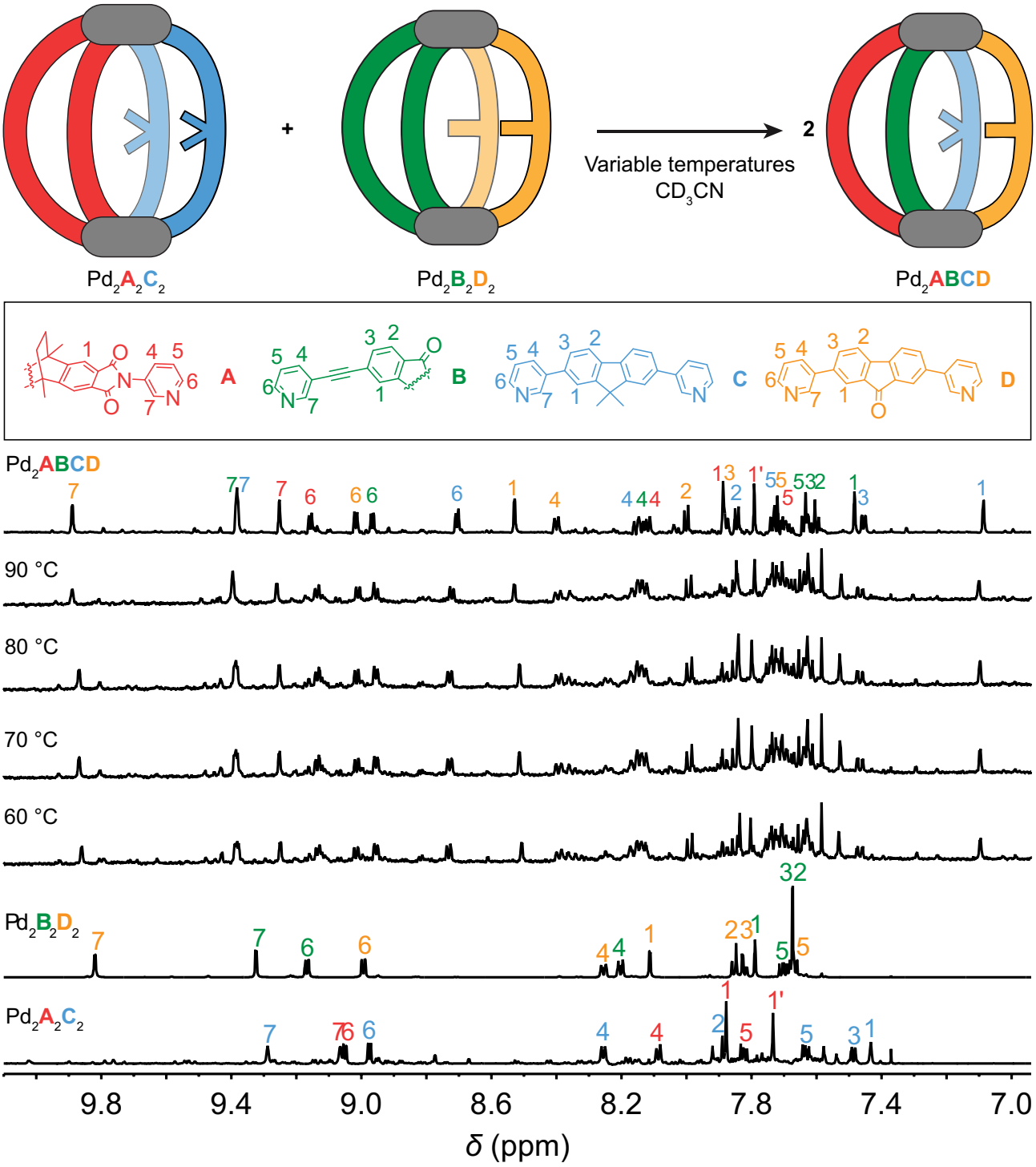

Supplementary Figure 284 | ^{1}H NMR spectra (500 MHz, 298 K, CD_3CN) of cage-to-cage transformation from heteroleptic cages $Pd_2\mathbf{A}_2\mathbf{C}_2$ and $Pd_2\mathbf{B}_2\mathbf{D}_2$ to heteroleptic cage $Pd_2\mathbf{ABCD}$ at different temperatures (each of the heteroleptic $Pd_2\mathbf{A}_2\mathbf{C}_2$ and $Pd_2\mathbf{B}_2\mathbf{D}_2$ cage samples were mixed in an NMR tube, and heated at corresponding temperature for 12 h to reach equilibrium). The top spectrum shows cage $Pd_2\mathbf{ABCD}$ formed from mixing the ligands with Pd(II).

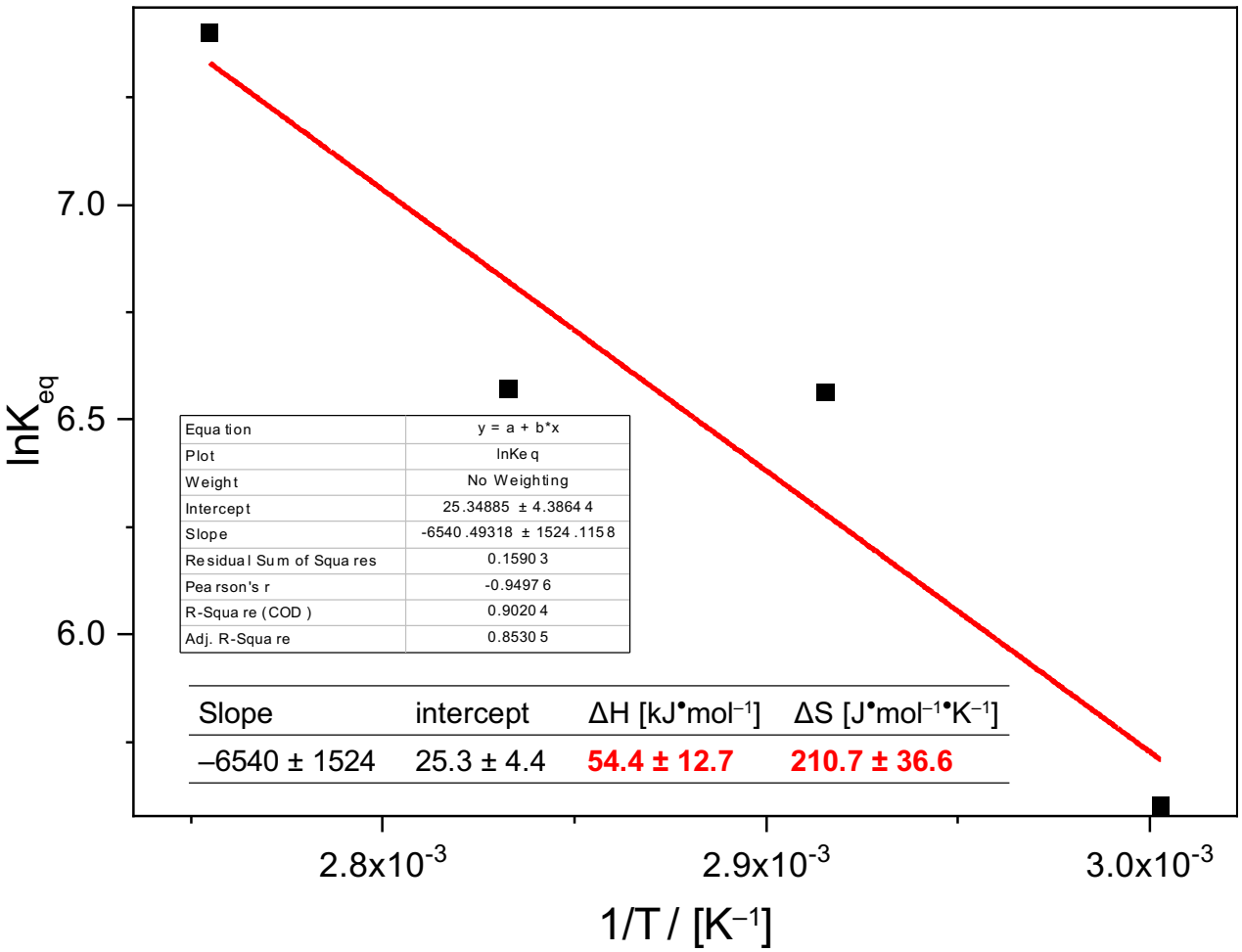

Supplementary Figure 285 | Van't Hoff plot of cage-to-cage transformation from heteroleptic cages Pd_2**A**$_2$**C**$_2$ and Pd_2**B**$_2$**D**$_2$ cages to heteroleptic cage Pd_2**ABCD** at different temperatures.

Supplementary Table 2. Summary of thermodynamic parameters of the examined cage-to-cage transformations.

	ΔH [kJ mol^{-1}]	ΔS [J mol^{-1} K^{-1}]	ΔG$^{353\ K}$ [kJ mol^{-1}]
Pd_2**A**$_2$**C**$_2$ + Pd_2**A**$_2$**D**$_2$ = 2 Pd_2**A**$_2$**CD**	98.7	335.9	–19.8
Pd_2**B**$_2$**C**$_2$ + Pd_2**B**$_2$**D**$_2$ = 2 Pd_2**B**$_2$**CD**	–14.7	–9.0	–11.5
Pd_2**A**$_2$**C**$_2$ + Pd_2**B**$_2$**C**$_2$ = 2 Pd_2**ABC**$_2$	7.4	57.4	–12.9
Pd_2**A**$_2$**D**$_2$ + Pd_2**B**$_2$**D**$_2$ = 2 Pd_2**ABD**$_2$	31.5	125.5	–12.8
Pd_2**A**$_2$**CD** + Pd_2**B**$_2$**CD** = 2 Pd_2**ABCD**	–19.5	–22.3	–11.7
Pd_2**ABC**$_2$ + Pd_2**ABD**$_2$ = 2 Pd_2**ABCD**	–11.2	5.6	–13.2
Pd_2**A**$_2$**C**$_2$ + Pd_2**B**$_2$**D**$_2$ = 2 Pd_2**ABCD**	54.4	210.7	–20.0

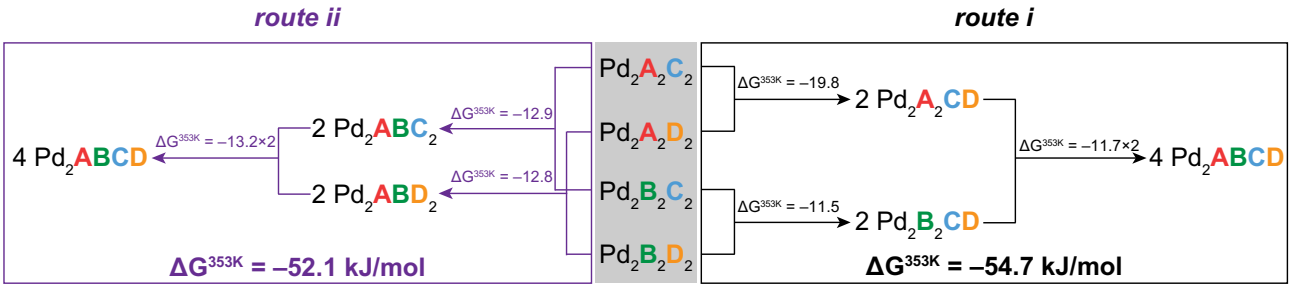

Supplementary Figure 286 | Gibbs free energy change at 353 K in the process of cage-to-cage transformation starting from four heteroleptic cages with two different types of ligands to the final Pd_2**ABCD** cage through two different routes *i* and *ii*.

5.8. Cage-to-cage reaction: $Pd_2\mathbf{A}_2\mathbf{D}_2 + Pd_2\mathbf{B}_2\mathbf{C}_2 = 2Pd_2\mathbf{ABCD}$

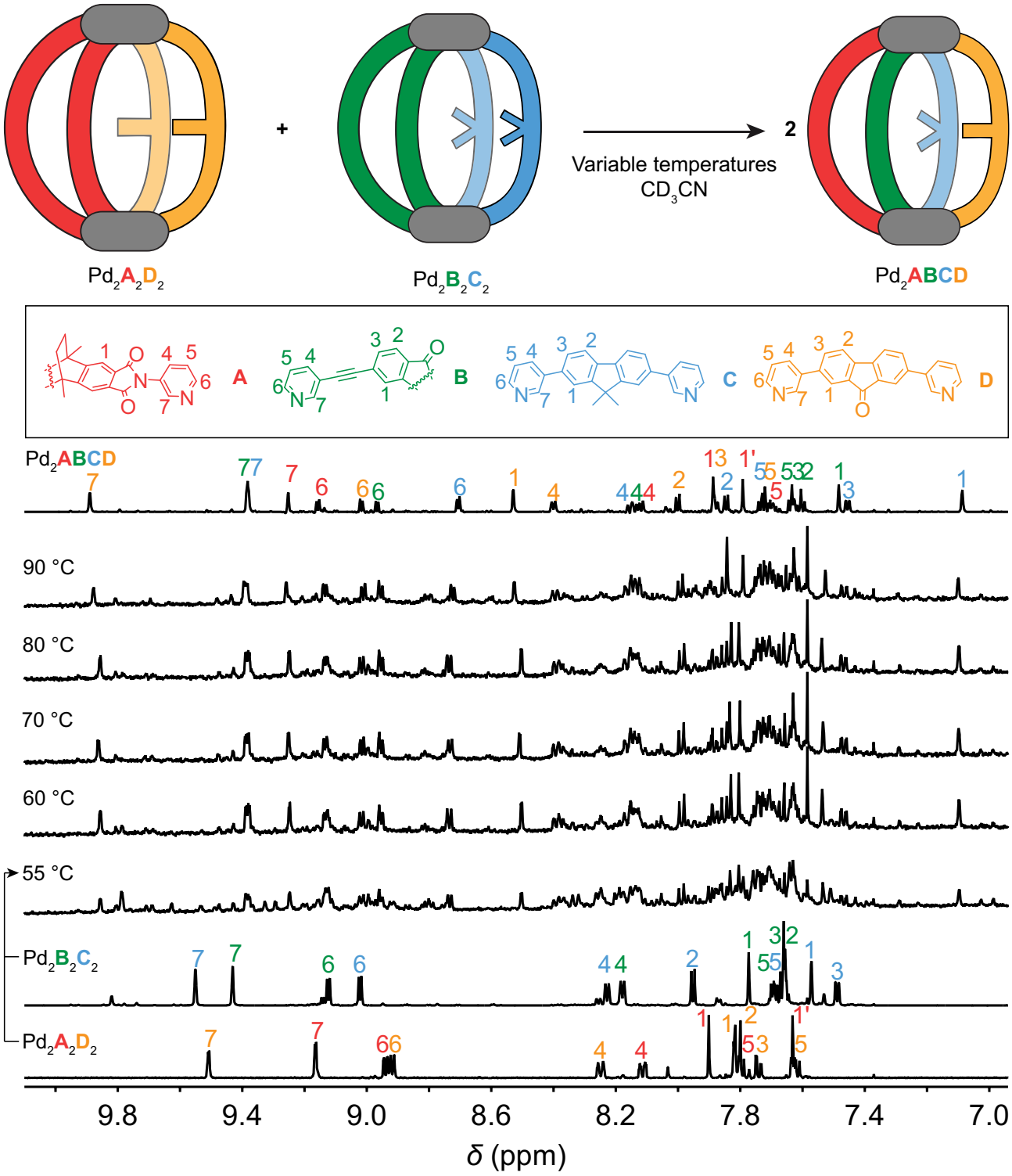

Supplementary Figure 287 | ^{1}H NMR spectra (500 MHz, 298 K, CD_3CN) of cage-to-cage transformation from heteroleptic cages $Pd_2\mathbf{A}_2\mathbf{D}_2$ and $Pd_2\mathbf{B}_2\mathbf{C}_2$ to heteroleptic cage $Pd_2\mathbf{ABCD}$ at different temperatures (each of the heteroleptic $Pd_2\mathbf{A}_2\mathbf{D}_2$ and $Pd_2\mathbf{B}_2\mathbf{C}_2$ cage samples were mixed in an NMR tube, and heated at corresponding temperature for 12 h to reach equilibrium). The signals for $Pd_2\mathbf{A}_2\mathbf{D}_2$ and $Pd_2\mathbf{B}_2\mathbf{C}_2$ cages could not be integrated accurately, thus thermodynamic parameters were not calculated in this case. The top spectrum shows cage $Pd_2\mathbf{ABCD}$ formed from mixing the ligands with Pd(II).

6. DFT calculations

6.1. Cage-to-cage transformations

All models were constructed using Wavefunction SPARTAN[10] and were first optimized on a PM6 level of theory (charge = +4, multiplicity = singlet, no counterions were included). The resulting models were further optimized by DFT calculations using SPARTAN, Method: ωB97X-D, Basis set: DEF2-SV(P) in the gas-phase. The final energy differences were calculated as Σ products – Σ reactants.

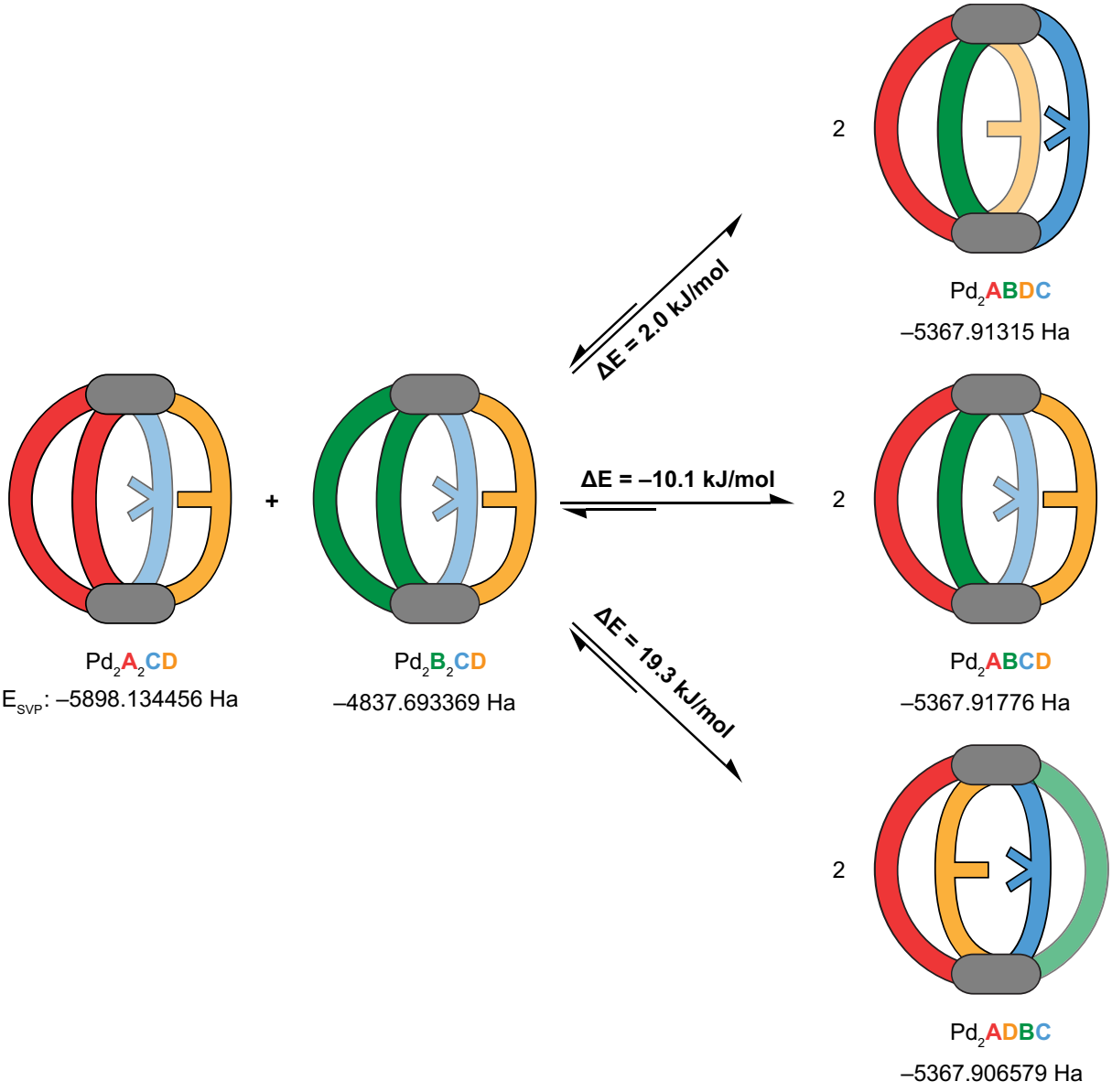

$\Delta E(\mathbf{ABDC}) = \sum products - \sum reactants = \mathbf{2}\times[Pd_2\mathbf{ABDC}] - [Pd_2\mathbf{A}_2\mathbf{CD}] - [Pd_2\mathbf{B}_2\mathbf{CD}]$
$= (-2\times 5367.91315 + 5898.134456 + 4837.693369)\times 2625.5$ kJ/mol
$= 4.0$ kJ/mol ($\mathbf{2}\times[Pd_2\mathbf{ABDC}]^{4+}$)
$= 2.0$ kJ/mol ($\mathbf{1}\times[Pd_2\mathbf{ABDC}]^{4+}$)

$\Delta E(\mathbf{ABCD}) = \sum products - \sum reactants = \mathbf{2}\times[Pd_2\mathbf{ABCD}] - [Pd_2\mathbf{A}_2\mathbf{CD}] - [Pd_2\mathbf{B}_2\mathbf{CD}]$
$= (-2\times 5367.91776 + 5898.134456 + 4837.693369)\times 2625.5$ kJ/mol
$= -20.2$ kJ/mol ($\mathbf{2}\times[Pd_2\mathbf{ABCD}]^{4+}$)
$= -10.1$ kJ/mol ($\mathbf{1}\times[Pd_2\mathbf{ABCD}]^{4+}$)

$\Delta E(\mathbf{ADBC}) = \sum products - \sum reactants = \mathbf{2}\times[Pd_2\mathbf{ADBC}] - [Pd_2\mathbf{A}_2\mathbf{CD}] - [Pd_2\mathbf{B}_2\mathbf{CD}]$
$= (-2\times 5367.906579 + 5898.134456 + 4837.693369)\times 2625.5$ kJ/mol
$= 38.51$ kJ/mol ($\mathbf{2}\times[Pd_2\mathbf{ADBC}]^{4+}$)
$= 19.25$ kJ/mol ($\mathbf{1}\times[Pd_2\mathbf{ADBC}]^{4+}$)

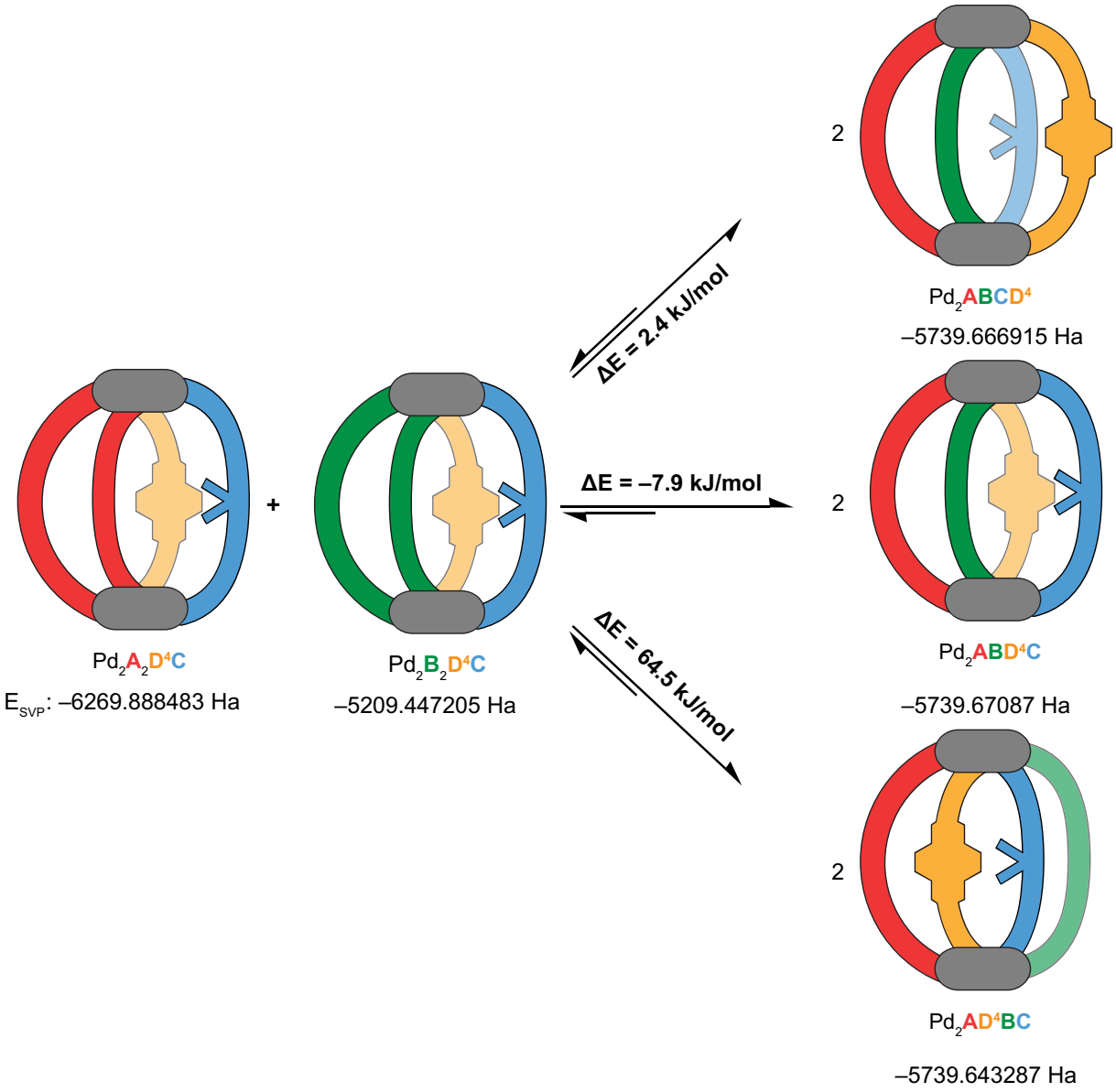

$\Delta E(\mathbf{ABCD^4}) = \sum\text{products} - \sum\text{reactants} = \mathbf{2}\times[Pd_2\mathbf{ABCD^4}] - [Pd_2\mathbf{A_2CD^4}] - [Pd_2\mathbf{B_2CD^4}]$
$= (-2\times 5739.666915 + 6269.888483 + 5209.447205)\times 2625.5 \text{ kJ/mol}$
$= 4.88 \text{ kJ/mol } (\mathbf{2}\times[Pd_2\mathbf{ABCD^4}]^{4+})$
$= 2.44 \text{ kJ/mol } (\mathbf{1}\times[Pd_2\mathbf{ABCD^4}]^{4+})$

$\Delta E(\mathbf{ABD^4C}) = \sum\text{products} - \sum\text{reactants} = \mathbf{2}\times[Pd_2\mathbf{ABD^4C}] - [Pd_2\mathbf{A_2CD^4}] - [Pd_2\mathbf{B_2CD^4}]$
$= (-2\times 5739.67087 + 6269.888483 + 5209.447205)\times 2625.5 \text{ kJ/mol}$
$= -15.89 \text{ kJ/mol } (\mathbf{2}\times[Pd_2\mathbf{ABD^4C}]^{4+})$
$= -7.94 \text{ kJ/mol } (\mathbf{1}\times[Pd_2\mathbf{ABD^4C}]^{4+})$

$\Delta E(\mathbf{AD^4BC}) = \sum\text{products} - \sum\text{reactants} = \mathbf{2}\times[Pd_2\mathbf{AD_4BC}] - [Pd_2\mathbf{A_2CD^4}] - [Pd_2\mathbf{B_2CD^4}]$
$= (-2\times 5739.643287 + 6269.888483 + 5209.447205)\times 2625.5 \text{ kJ/mol}$
$= 128.95 \text{ kJ/mol } (\mathbf{2}\times[Pd_2\mathbf{AD_4BC}]^{4+})$
$= 64.47 \text{ kJ/mol } (\mathbf{1}\times[Pd_2\mathbf{AD_4BC}]^{4+})$

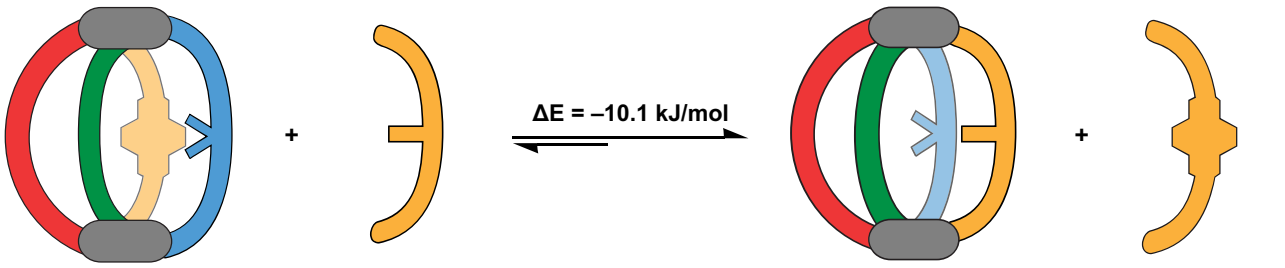

Pd_2ABD^4C + D ⇌ Pd_2ABCD + D^4

E_{SVP}: –5739.670870 Ha + –1068.458153 Ha ⇌ –5367.91776 Ha + –1440.215108 Ha

$\Delta E(ABCD) = \sum products - \sum reactants = ([Pd_2ABCD]+[D^4]) - ([Pd_2ABD^4C]+[D])$
$= \{(-5367.917760 - 1440.215108) - (-5739.670870 - 1068.458153)\} \times 2625.5$ kJ/mol
$= -10.09$ kJ/mol

Supplementary Table 3. Summary of energy differences for cage-to-cage transformations by DFT calculations. The formation of Pd_2**ABCD** and Pd_2**ABD⁴C** stereoisomers are energetically more favoured, consistent with experimental results.

reactants		products	ΔE [kJ mol^{-1}]
Pd_2A_2CD	Pd_2B_2CD	Pd_2ABDC	2.0
		Pd_2ABCD	**–10.1**
		Pd_2ADBC	19.3
$Pd_2A_2CD^4$	$Pd_2B_2CD^4$	Pd_2ABCD^4	2.4
		Pd_2ABD^4C	**–7.9**
		Pd_2ADBC	64.5
Pd_2ABD^4C	D	Pd_2ABCD	–10.1

6.2. Computation of ESP (Electrostatic Surface Potential) maps

ESP maps were computed using Wavefunction SPARTAN[10] on the ω97X-D/6-311+G*-geometry-optimized ligands (Iso value 0.002, min/max property range in kJ/mol as indicated in color legend). Relevant values as picked on the molecular surface are given in the figure.

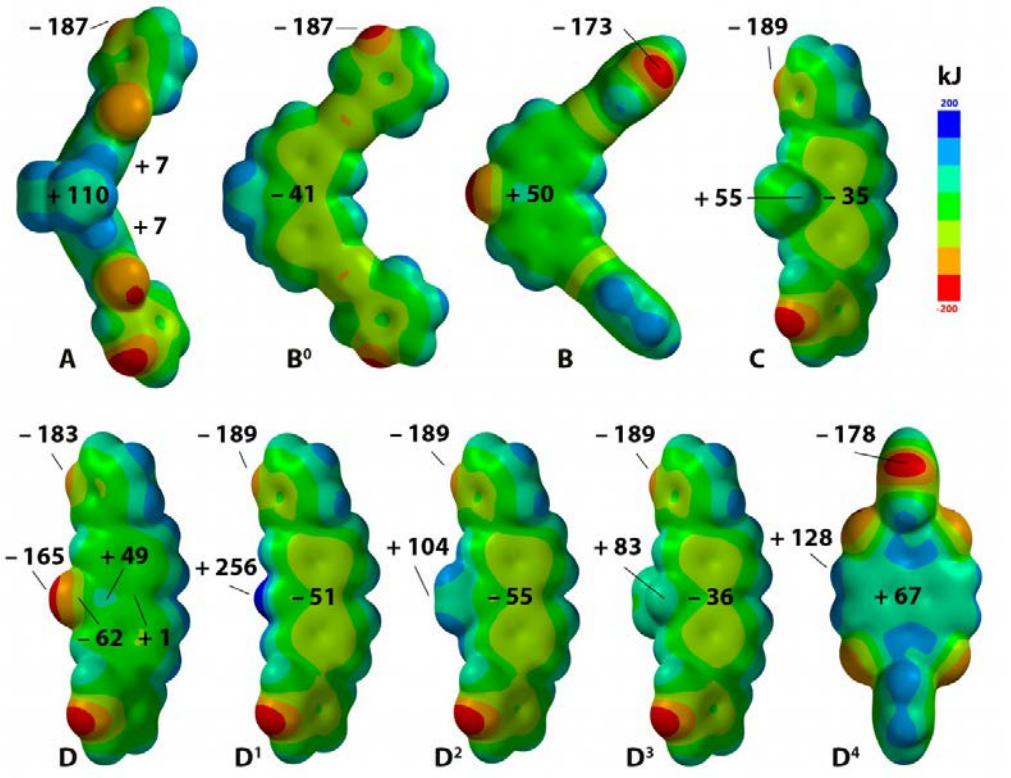

Supplementary Figure 288 | ESP maps for the ligand library.

The obtained values show that while the donor strengths (pyridine N-lone pair values) are similar for all ligands (with a slight drop for the electron-poor fluorenone and NDI ligands), the relative donor/acceptor character in the central plane and rim regions of the ligands differ significantly. These values serve to explain certain structural features found experimentally in a number of the formed heteroleptic cages, e.g. concerning the relative ligand arrangement in cage Pd_2**ABCD** vs. cage Pd_2**ABD^{4}C**: in the former one ligand **C** prefers to make CH_3-π interactions with the π-planes of ligands **D** and **D$^{1–3}$**. In Pd_2**ABD^{4}C**, however, **C**'s methyl groups refrain to point to the positively polarized NDI-π surface and instead the NDI's CH substituents now point towards the π-surface of **C**. The resulting structural flip also seems to affect the shape-complementarity with the oppositely arranged ligands, leading to the observed change in the ligand order.

7. Ion Mobility Mass Spectrometry

Ion mobility measurements were performed on a Bruker timsTOF instrument combining a trapped ion mobility (TIMS) with a time-of-flight (TOF) mass spectrometer in one instrument.

In contrast to the conventional drift tube method to determine mobility data, where ions are carried by an electric field through a stationary drift gas, the TIMS method is based on an electric field ramp to hold ions in place against a carrier gas pushing them in the direction of the analyzer. Consequently, larger sized ions that experience more carrier gas impacts leave the TIMS units first and smaller ions elute later. This method offers a much higher mobility resolution despite a smaller device size.

Briefly, in trapped ion mobility spectrometry (TIMS) the ions are held by an electric field gradient (EFG) while exposed to a constant N_2 flow. The source of the flow is a pressure difference (Δp) between the entrance and the exit of the TIMS-tunnel. Lowering the EFG results in the elution of the analyte according to its inverse mobility ($1/K_0$). Depending on the difference between start-EFG and end-EFG (ΔEFG) as well as the duration

of this reduction (ramp time = t_r), rather high ion mobility resolutions can be achieved. Resolutions of 200 and higher was targeted in all the experiments using custom mode of measurement. In front of the trapping part of the TIMS-tunnel, a second ramp accumulates the ions for a given period of time (accumulation time = t_a) in order to enhance the overall duty cycle.

Since TIMS doesn't operate on first principles, a calibration is necessary. For calibration, Agilent Tune-Mix™ was used as purchased and the reported drift tube $^{DT}CCS_{N2}$ values published by Stow et al. have been used.[11] TIMS determines (calibrated) inverse mobilities which were converted to the tabulated $^{TIMS}CCS_{N2}$ values following Mason-Schamp equation:

$$\mathbf{CCS} = \left(\frac{\mathbf{3}}{\mathbf{16}\boldsymbol{N}}\right)\left(\frac{\mathbf{2}\boldsymbol{\pi}}{\boldsymbol{kT}}\right)^{\mathbf{0.5}} \frac{\boldsymbol{q}}{\sqrt{\mu}} \frac{\mathbf{1}}{\boldsymbol{K_0}}$$

where, q is the charge of the ion, N the number density of the collision gas, μ is the reduced mass of the ion and the N_2 collision gas, k the Boltzmann's constant, T the temperature in Kelvin. Both the analyte solution and the calibrants have been electrosprayed in cationic mode with the same experimental conditions. Therefore, the first part of the equation is constant for every ions measured in the same condition. The constant was found by calculating the reduced mobility of the calibrant ions and plotting them against their reported CCS. The plot was fitted using linear fit with fixed intercept at 0. The slope is the constant for the specific experiment. The $1/K_0$ found from the experiment was then multiplied as per the equation.

Optimized parameters: After the generation of ions by electrospray ionisation (ESI, analyte concentration: 0.1 mg/mL solvent: Acetonitrile, capillary voltage: 2000V, end plate offset voltage: 150 V, nebulizer gas pressure: 0.3 bar, dry gas flow rate: 3.0 L/min, dry temperature: 75 °C) the desired ions were orthogonally deflected into the TIMS cell consisting of an entrance funnel, the TIMS analyser (carrier gas: N_2, temperature: 305 K, entrance pressure: 2.72 mbar, exit pressure: 0.96 mbar, Δp = 1.77 mbar, t_r = 450 ms, t_a = 5 ms, a stepwise reduction of the electric field strength leads to a release of ion packages separated by their mobility. After a subsequent focusing, the separated ions are transferred to the TOF-analyser.[12-14]

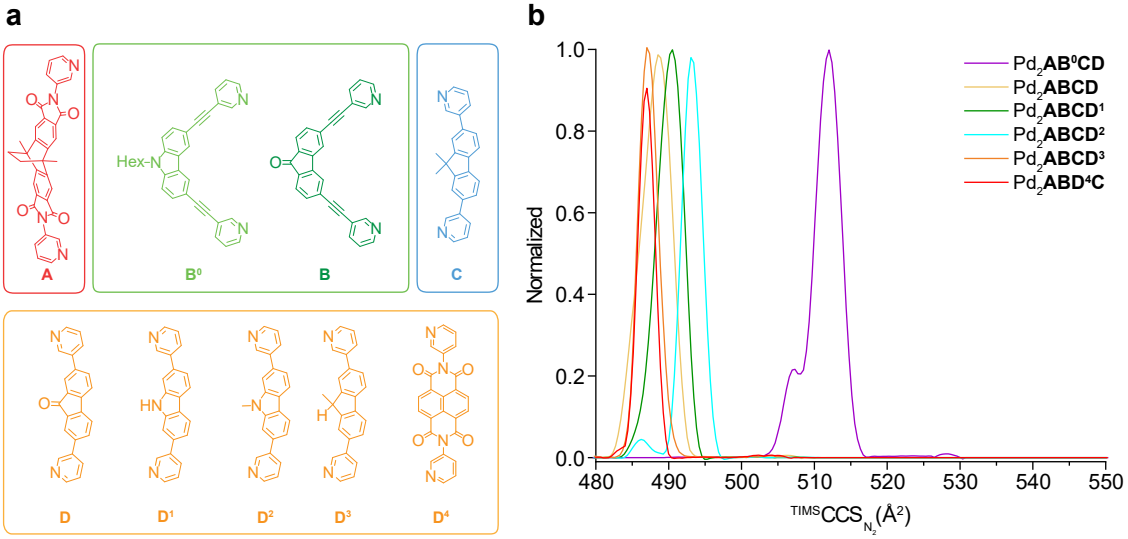

Supplementary Figure 289 | Overlap comparison of the CCS values of different heteroleptic cages with four chemically different ligands, revealing a narrow peak for each cage.

8. X-ray Crystallography

8.1. Crystal structures of *trans*-[$Pd_2A_2B_2$]$(BF_4)_4$, [Pd_2A_2CD]$(BF_4)_4$, [$Pd_2B_2CD^1$]$(BF_4)_4$.

Supplementary Table 4. Crystallographic data of *trans*-[Pd_2**A**$_2$**B**$_2$]$(BF_4)_4$, [Pd_2**A**$_2$**CD**]$(BF_4)_4$, [Pd_2**B**$_2$**CD**^{1}]$(BF_4)_4$.

Compound	***trans*-[$Pd_2A_2B_2$]$(BF_4)_4$**	**[Pd_2A_2CD]$(BF_4)_4$**	**[$Pd_2B_2CD^1$]$(BF_4)_4$**
Identification code	kw90i_sq	kw71i_sq	kw92i_sq
CCDC number	2207621	2207623	2207622
Empirical formula	$C_{162}H_{144}B_4F_{16}N_{30}O_{12}Pd_2$	$C_{122}H_{93}B_4F_{16}N_{17}O_9Pd_2$	$C_{105}H_{73}B_4F_{16}N_9O_3Pd_2$
Formula weight	3263.10	2501.17	2068.76
Temperature [K]	100(2)	120(2)	100(2)
Crystal system	triclinic	triclinic	triclinic
Space group (number)	$P\bar{1}$ (2)	$P\bar{1}$ (2)	$P\bar{1}$ (2)
a [Å]	14.0126(4)	14.0567(4)	16.641(2)
b [Å]	16.5365(4)	14.7152(4)	17.205(2)
c [Å]	19.3847(6)	29.3022(9)	20.842(3)
α [°]	105.584(2)	88.946(2)	84.862(5)
β [°]	101.884(2)	86.990(2)	67.757(5)
γ [°]	103.511(2)	77.742(2)	87.523(6)
Volume [Å^3]	4030.1(2)	5914.6(3)	5500.6(12)
Z	1	2	2
ρ_{calc} [g cm^{-3}]	1.345	1.404	1.249
μ [mm^{-1}]	2.532	3.221	3.290
F(000)	1678	2544	2092
Crystal size [mm^3]	0.100 × 0.100 × 0.100	0.100 × 0.100 × 0.100	0.100 × 0.100 × 0.050
Crystal colour	yellow	yellow	yellow
Crystal shape	needle	block	needle
Radiation	CuK_α (λ=1.54178 Å)	CuK_α (λ=1.54178 Å)	CuK_α (λ=1.54178 Å)
2θ range [°]	4.94 to 136.78 (0.83 Å)	3.02 to 136.88 (0.83 Å)	4.59 to 68.88 (1.36 Å)
Index ranges	–16 ≤ h ≤ 16 –19 ≤ k ≤ 19 –23 ≤ l ≤ 23	–16 ≤ h ≤ 16 –17 ≤ k ≤ 17 –35 ≤ l ≤ 35	–11 ≤ h ≤ 12 –12 ≤ k ≤ 9 –15 ≤ l ≤ 15
Reflections collected	84134	114547	14107
Independent reflections	14743 R_{int} = 0.0753 R_{sigma} = 0.0433	21599 R_{int} = 0.0685 R_{sigma} = 0.0440	4439 R_{int} = 0.1387 R_{sigma} = 0.2072
Completeness to θ = 67.679°	100.0 %	99.6 %	97.5 %
Data / Restraints / Parameters	14743/1967/1096	21599/3533/1679	4439/2624/1300
Goodness-of-fit on F^2	1.066	1.064	1.208
Final *R* indexes [$I \geq 2\sigma(I)$]	R_1 = 0.0823 wR_2 = 0.2419	R_1 = 0.0619 wR_2 = 0.1577	R_1 = 0.1209 wR_2 = 0.3132
Final *R* indexes [all data]	R_1 = 0.0988 wR_2 = 0.2614	R_1 = 0.0705 wR_2 = 0.1648	R_1 = 0.2221 wR_2 = 0.3676
Largest peak/hole [eÅ^{-3}]	1.97/–1.27	1.95/–0.83	0.54/–0.41

(a) *trans*-$[Pd_2A_2B_2](BF_4)_4$

Yellow needle-shaped crystals of *trans*-$[Pd_2\mathbf{A}_2\mathbf{B}_2](BF_4)_4$ were grown by slow vapor diffusion of Et_2O into a solution of the cage in CD_3CN.

The crystals were prone to a loss of solvent after removal from the mother liquor and rapid handling in NVH oil prior to flash cooling in liquid nitrogen was required to collect data. Data were collected in-house on a Bruker D8 venture diffractometer equipped with an INCOATEC microfocus sealed tube (Iμs 3.0) using CuK_α radiation at 100 K. The data was integrated with APEX3 and the structure was solved by intrinsic phasing/direct methods using SHELXT[15] and refined with SHELXL[16] for full-matrix least-squares routines on F^2 and ShelXle[17] as a graphical user interface.

Specific refinement details

Stereochemical restraints for the ligands **A**, **B** were generated by the GRADE program using the GRADE Web Server (http://grade.globalphasing.org) and applied in the refinement. A GRADE dictionary for SHELXL contains target values and standard deviations for 1,2-distances (DFIX) and 1,3-distances (DANG), as well as restraints for planar groups (FLAT). All displacements for non-hydrogen atoms were refined anisotropically. The refinement of ADP's for carbon, nitrogen and oxygen atoms was enabled by a combination of similarity restraints (SIMU) and rigid bond restraints (RIGU). The contribution of the electron density from disordered counterions and solvent molecules, which could not be modeled with discrete atomic positions were handled using the SQUEEZE routine in PLATON[18]. The solvent mask file (.fab) computed by PLATON was included in the SHELXL refinement via the ABIN instruction leaving the measured intensities untouched.

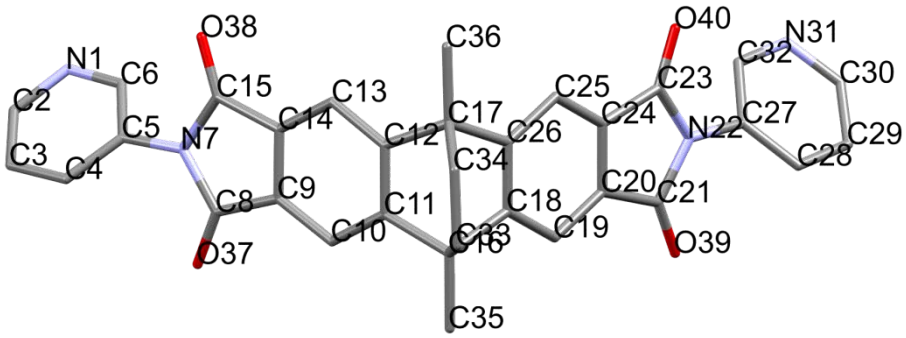

Supplementary Figure 290 | Atomic numbering scheme of residue ETP (ligand **A**).

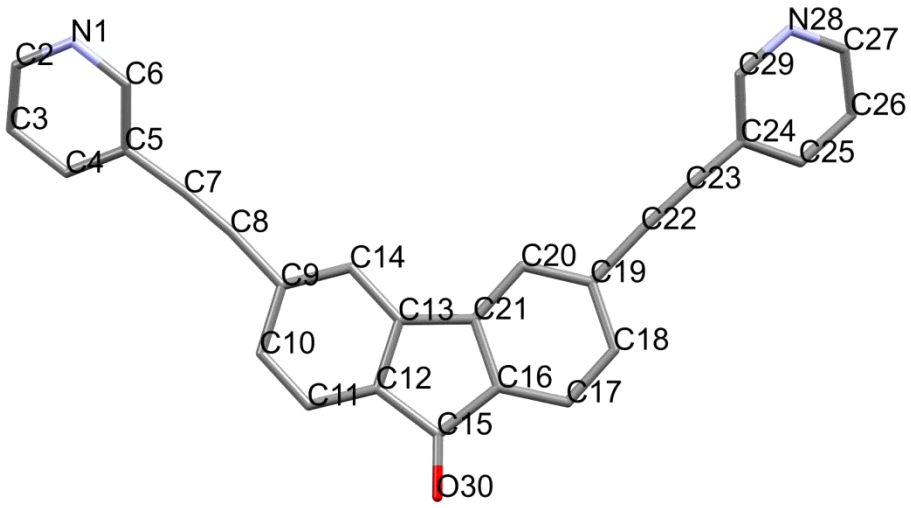

Supplementary Figure 291 | Atomic numbering scheme of residue IFP (ligand **B**).

(b) [Pd_2A_2CD]$(BF_4)_4$

Yellow needle-shaped crystals of [Pd_2**A**$_2$**CD**]$(BF_4)_4$ were grown by slow vapor diffusion of Et_2O into a solution of the cage in CD_3CN.

The crystals employed immediately lost solvent after removal from the mother liquor and rapid handling in NVH oil prior to flash cooling in liquid nitrogen was required to collect data. Data were collected in-house on a Bruker D8 venture diffractometer equipped with an INCOATEC microfocus sealed tube (Iμs 3.0) using CuK_α radiation at 120 K. The data was integrated with APEX3 and the structure was solved by intrinsic phasing/direct methods using SHELXT[15] and refined with SHELXL[16] for full-matrix least-squares routines on F^2 and ShelXle as a graphical user interface.

Specific refinement details

Stereochemical restraints for the ligands **A**, **C**, **D** were generated by the GRADE program using the GRADE Web Server (http://grade.globalphasing.org) and applied in the refinement. A GRADE dictionary for SHELXL contains target values and standard deviations for 1,2-distances (DFIX) and 1,3-distances (DANG), as well as restraints for planar groups (FLAT). All displacements for non-hydrogen atoms were refined anisotropically. The refinement of ADP's for carbon, nitrogen and oxygen atoms was enabled by a combination of similarity restraints (SIMU) and rigid bond restraints (RIGU). The contribution of the electron density from disordered counterions and solvent molecules, which could not be modeled with discrete atomic positions were handled using the SQUEEZE routine in PLATON[18]. The solvent mask file (.fab) computed by PLATON was included in the SHELXL refinement via the ABIN instruction leaving the measured intensities untouched.

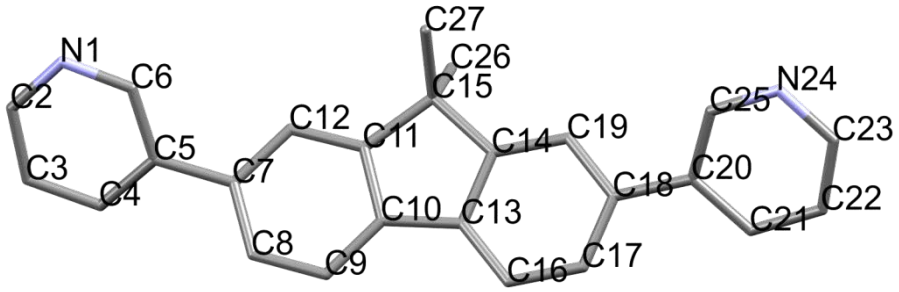

Supplementary Figure 292 | Atomic numbering scheme of residue LFP (ligand **C**).

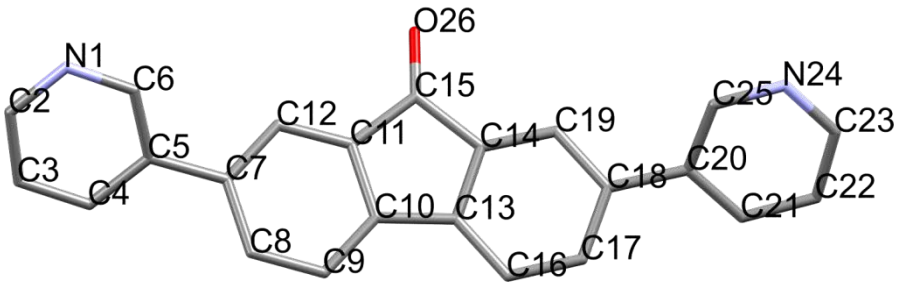

Supplementary Figure 293 | Atomic numbering scheme of residue LFO (ligand **D**).

(c) [$Pd_2B_2CD^1$]$(BF_4)_4$

Yellow needle-shaped crystals of [Pd_2**B**$_2$**CD**^{1}]$(BF_4)_4$ were grown by slow vapor diffusion of Et_2O into a solution of the cage in CD_3CN.

The crystals were prone to a loss of solvent after removal from the mother liquor and rapid handling in NVH oil prior to flash cooling in liquid nitrogen was required to collect data. Despite these measures and the use of copper source, few reflections at greater than 1.36 Å resolution were observed and the data were trimmed accordingly. Data were collected in-house on a Bruker D8 venture diffractometer equipped with an INCOATEC microfocus sealed tube (Iμs 3.0) using CuK_α radiation at 100 K. The data was integrated with APEX3 and the structure was solved by intrinsic phasing/direct methods using SHELXT[15] and refined with SHELXL[16] for full-matrix least-squares routines on F^2 and ShelXle as a graphical user interface.

Specific refinement details

Stereochemical restraints for the ligands **B**, **C**, **D**[1] were generated by the GRADE program using the GRADE Web Server (http://grade.globalphasing.org) and applied in the refinement. A GRADE dictionary for SHELXL contains target values and standard deviations for 1,2-distances (DFIX) and 1,3-distances (DANG), as well as restraints for planar groups (FLAT). All displacements for non-hydrogen atoms were refined anisotropically. The refinement of ADP's for carbon, nitrogen and oxygen atoms was enabled by a combination of similarity restraints (SIMU) and rigid bond restraints (RIGU). The contribution of the electron density from disordered counterions and solvent molecules, which could not be modeled with discrete atomic positions were handled using the SQUEEZE routine in PLATON[18]. The solvent mask file (.fab) computed by PLATON was included in the SHELXL refinement via the ABIN instruction leaving the measured intensities untouched.

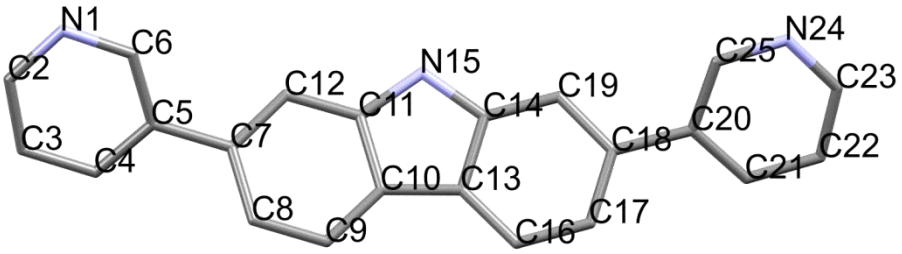

Supplementary Figure 294 | Atomic numbering scheme of residue FNH (ligand **D**[1]).

8.2. Crystal structure of $[Pd_2B_2D^4C](BF_4)_4$, $[Pd_2AB^0CD](BF_4)_4$, $[Pd_2ABCD](BF_4)_4$

Supplementary Table 5. Crystallographic data of $[Pd_2\mathbf{B}_2\mathbf{D}^4\mathbf{C}](BF_4)_4$, $[Pd_2\mathbf{AB}^0\mathbf{CD}](BF_4)_4$, $[Pd_2\mathbf{ABCD}](BF_4)_4$.

Compound	$[Pd_2B_2D^4C](BF_4)_4$	$[Pd_2AB^0CD](BF_4)_4$	$[Pd_2ABCD](BF_4)_4$
Identification code	kw81i_sq	kw72i_sq	kw66b1_sq
CCDC number	2207624	2207626	2207625
Empirical formula	$C_{113}H_{75}B_4F_{16}N_{15}O_6Pd_2$	$C_{118}H_{92}B_4F_{16}N_{14}O_5Pd_2$	$C_{137}H_{100}B_4F_{16}N_{10}O_6Pd_2$
Formula weight	2298.92	2346.09	2542.30
Temperature [K]	100(2)	120(2)	120(2)
Crystal system	triclinic	triclinic	triclinic
Space group (number)	$P\bar{1}$ (2)	$P\bar{1}$ (2)	$P\bar{1}$ (2)
a [Å]	14.458(2)	14.9522(15)	15.9726(7)
b [Å]	20.195(3)	21.132(3)	20.6968(10)
c [Å]	21.445(3)	21.447(2)	22.0756(10)
α [°]	99.846(9)	69.034(5)	98.449(3)
β [°]	94.538(9)	76.140(5)	105.381(3)
γ [°]	110.881(9)	87.552(6)	109.609(3)
Volume [Å^3]	5696.7(16)	6136.7(11)	6400.8(5)
Z	2	2	2
ρ_{calc} [g cm^{-3}]	1.340	1.270	1.319
μ [mm^{-1}]	3.271	3.036	2.952
F(000)	2324	2388	2592
Crystal size [mm^3]	0.100 × 0.050 × 0.050	0.050 × 0.050 × 0.050	0.100 × 0.100 × 0.050
Crystal colour	yellow	yellow	yellow
Crystal shape	block	block	needle
Radiation	CuK_α (λ=1.54178 Å)	CuK_α (λ=1.54178 Å)	CuK_α (λ=1.54178 Å)
2θ range [°]	4.23 to 100.94 (1.00 Å)	4.55 to 76.52 (1.24 Å)	4.30 to 84.19 (1.15 Å)
Index ranges	–14 ≤ h ≤ 14 –20 ≤ k ≤ 20 –21 ≤ l ≤ 21	–9 ≤ h ≤ 11 –16 ≤ k ≤ 16 –14 ≤ l ≤ 17	–13 ≤ h ≤ 13 –17 ≤ k ≤ 17 –19 ≤ l ≤ 19
Reflections collected	54306	28971	48125
Independent reflections	11587 R_{int} = 0.0974 R_{sigma} = 0.0788	6493 R_{int} = 0.0927 R_{sigma} = 0.1042	8597 R_{int} = 0.0976 R_{sigma} = 0.0695
Completeness to θ = 50.468°	97.0 %	97.6 %	97.5 %
Data / Restraints / Parameters	11587/2677/1380	6493/2858/1440	8597/3442/1718
Goodness-of-fit on F^2	1.016	1.070	1.377
Final R indexes [I≥2σ(I)]	R_1 = 0.1337 wR_2 = 0.3386	R_1 = 0.0863 wR_2 = 0.2233	R_1 = 0.1148 wR_2 = 0.3201
Final R indexes [all data]	R_1 = 0.1738 wR_2 = 0.3707	R_1 = 0.1278 wR_2 = 0.2495	R_1 = 0.1534 wR_2 = 0.3480
Largest peak/hole [eÅ^{-3}]	1.41/–0.90	0.57/–0.69	1.02/–0.90

(a) $[Pd_2B_2D^4C](BF_4)_4$

Yellow block-shaped crystals of $[Pd_2\mathbf{B}_2\mathbf{D}^4\mathbf{C}](BF_4)_4$ were grown by slow vapor diffusion of Et_2O into a solution of the cage in CD_3CN.

The crystals were prone to a loss of solvent after removal from the mother liquor and rapid handling in NVH oil prior to flash cooling in liquid nitrogen was required to collect data. Despite these measures and the use of copper source few reflections at greater than 1.0 Å resolution were observed and the data were trimmed accordingly. Data were collected in-house on a Bruker D8 venture diffractometer equipped with an INCOATEC microfocus sealed tube (Iμs 3.0) using CuK_α radiation at 100 K. The data was integrated with APEX3 and the structure was solved by intrinsic phasing/direct methods using SHELXT[15] and refined with SHELXL[16] for full-matrix least-squares routines on F^2 and ShelXle as a graphical user interface.

Specific refinement details

Stereochemical restraints for the ligands **B**, **D**^{4}, **C** were generated by the GRADE program using the GRADE Web Server (http://grade.globalphasing.org) and applied in the refinement. A GRADE dictionary for SHELXL contains target values and standard deviations for 1,2-distances (DFIX) and 1,3-distances (DANG), as well as restraints for planar groups (FLAT). All displacements for non-hydrogen atoms were refined anisotropically. The refinement of ADP's for carbon, nitrogen and oxygen atoms was enabled by a combination of similarity restraints (SIMU) and rigid bond restraints (RIGU). The contribution of the electron density from disordered counterions and solvent molecules, which could not be modeled with discrete atomic positions were handled using the SQUEEZE routine in PLATON[18]. The solvent mask file (.fab) computed by PLATON was included in the SHELXL refinement via the ABIN instruction leaving the measured intensities untouched.

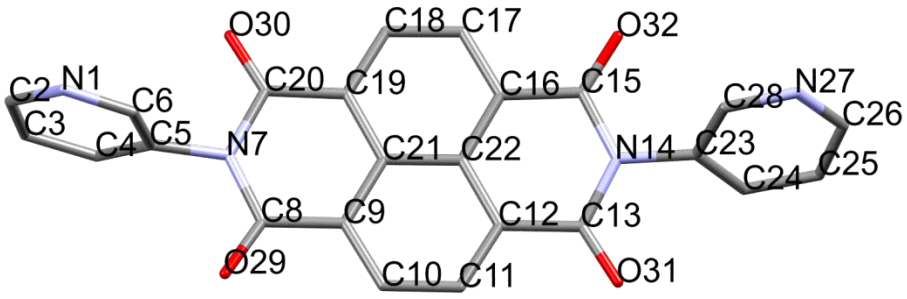

Supplementary Figure 295 | Atomic numbering scheme of residue NDI (ligand **D**^{4}).

(b) $[Pd_2AB^0CD](BF_4)_4$

Yellow block-shaped crystals of $[Pd_2\mathbf{AB}^0\mathbf{CD}](BF_4)_4$ were grown by slow vapor diffusion of Et_2O into a solution of the cage in CD_3CN.

The crystals were prone to a loss of solvent after removal from the mother liquor and rapid handling in NVH oil prior to flash cooling in liquid nitrogen was required to collect data. Despite these measures and the use of copper source, few reflections at greater than 1.24 Å resolution were observed and the data were trimmed accordingly. Data were collected in-house on a Bruker D8 venture diffractometer equipped with an INCOATEC microfocus sealed tube (Iμs 3.0) using CuK_α radiation at 120 K. The data was integrated with APEX3 and the structure was solved by intrinsic phasing/direct methods using SHELXT[15] and refined with SHELXL[16] for full-matrix least-squares routines on F^2 and ShelXle as a graphical user interface.

Specific refinement details

Stereochemical restraints for the ligands **A**, **B**^{0}, **C**, **D** were generated by the GRADE program using the GRADE Web Server (http://grade.globalphasing.org) and applied in the refinement. A GRADE dictionary for SHELXL contains target values and standard deviations for 1,2-distances (DFIX) and 1,3-distances (DANG), as well as restraints for planar groups (FLAT). All displacements for non-hydrogen atoms were refined anisotropically. The refinement of ADP's for carbon, nitrogen and oxygen atoms was enabled by a combination of similarity restraints (SIMU) and rigid bond restraints (RIGU). The contribution of the electron density from disordered counterions and solvent molecules, which could not be modeled with discrete atomic positions were handled using the SQUEEZE routine in PLATON[18]. The solvent mask file (.fab) computed by PLATON was included in the SHELXL refinement via the ABIN instruction leaving the measured intensities untouched.

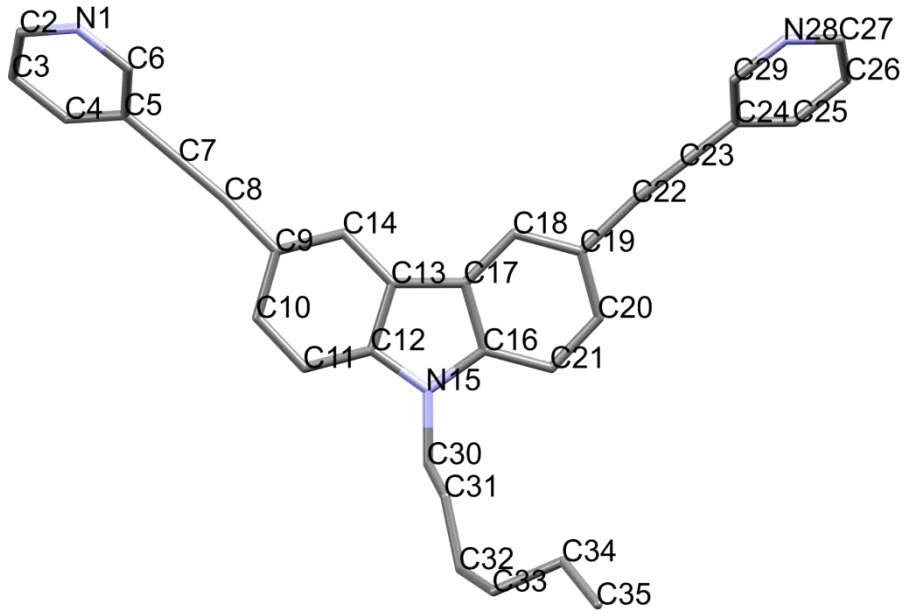

Supplementary Figure 296 | Atomic numbering scheme of residue CHP (ligand $\mathbf{B^0}$).

(c) [Pd_2ABCD]$(BF_4)_4$

Yellow needle-shaped crystals of [Pd_2**ABCD**]$(BF_4)_4$ were grown by slow vapor diffusion of benzene into a solution of the cage in CD_3CN.

The crystals were prone to a loss of solvent after removal from the mother liquor and rapid handling in NVH oil prior to flash cooling in liquid nitrogen was required to collect data. Despite these measures and the use of copper source, few reflections at greater than 1.15 Å resolution were observed and the data were trimmed accordingly. Data were collected in-house on a Bruker D8 venture diffractometer equipped with an INCOATEC microfocus sealed tube (Iμs 3.0) using CuK_α radiation at 120 K. The data was integrated with APEX3 and the structure was solved by intrinsic phasing/direct methods using SHELXT and refined with SHELXL for full-matrix least-squares routines on F^2 and ShelXle as a graphical user interface.

Specific refinement details

Stereochemical restraints for the ligands **A**, **B**, **C**, **D** were generated by the GRADE program using the GRADE Web Server (http://grade.globalphasing.org) and applied in the refinement. A GRADE dictionary for SHELXL contains target values and standard deviations for 1,2-distances (DFIX) and 1,3-distances (DANG), as well as restraints for planar groups (FLAT). All displacements for non-hydrogen atoms were refined anisotropically. The refinement of ADP's for carbon, nitrogen and oxygen atoms was enabled by a combination of similarity restraints (SIMU) and rigid bond restraints (RIGU). The contribution of the electron density from disordered counterions and solvent molecules, which could not be modeled with discrete atomic positions were handled using the SQUEEZE routine in PLATON. The solvent mask file (.fab) computed by PLATON was included in the SHELXL refinement via the ABIN instruction leaving the measured intensities untouched.

8.3. Crystal structure of $[Pd_2ABCD^2](BF_4)_4$, $[Pd_2ABD^4C](BF_4)_4$, $[Pd_2ABD^2D](BF_4)_4$.

Supplementary Table 6. Crystallographic data of $[Pd_2\mathbf{ABCD^2}](BF_4)_4$, $[Pd_2\mathbf{ABD^4C}](BF_4)_4$, $[Pd_2\mathbf{ABD^2D}](BF_4)_4$.

Compound	$[Pd_2ABCD^2](BF_4)_4$	$[Pd_2ABD^4C](BF_4)_4$	$[Pd_2ABD^2D](BF_4)_4$
Identification code	kw88b_sq	kw80b_sq	kw91i_sq
CCDC number	2207629	2207627	2207628
Empirical formula	$C_{131}H_{97}B_4F_{16}N_{11}O_5Pd_2$	$C_{149}H_{116}B_4F_{16}N_{19}O_9Pd_2$	$C_{113}H_{83}B_4F_{16}N_{13}O_7Pd_2$
Formula weight	2465.23	2876.64	2294.96
Temperature [K]	100(2)	100(2)	100(2)
Crystal system	triclinic	triclinic	triclinic
Space group (number)	$P\bar{1}$ (2)	$P\bar{1}$ (2)	$P\bar{1}$ (2)
a [Å]	15.8663(7)	19.8224(4)	16.0274(9)
b [Å]	20.6139(10)	20.5363(4)	20.0502(12)
c [Å]	22.1792(11)	20.7178(4)	22.3286(13)
α [°]	98.759(3)	67.5680(10)	97.045(3)
β [°]	104.463(2)	68.2250(10)	105.235(3)
γ [°]	109.354(2)	63.1880(10)	109.333(3)
Volume [Å^3]	6404.1(5)	6752.4(2)	6357.2(7)
Z	2	2	2
ρ_{calc} [g cm^{-3}]	1.278	1.415	1.199
μ [mm^{-1}]	2.929	2.904	2.930
F(000)	2512	2942	2328
Crystal size [mm^3]	0.100 × 0.100 × 0.100	0.100 × 0.100 × 0.100	0.200 × 0.100 × 0.100
Crystal colour	yellow	yellow	yellow
Crystal shape	block	block	block
Radiation	CuK_α (λ=1.54178 Å)	CuK_α (λ=1.54178 Å)	CuK_α (λ=1.54178 Å)
2θ range [°]	5.47 to 81.57 (1.18 Å)	4.75 to 133.28 (0.84 Å)	4.80 to 83.30 (1.16 Å)
Index ranges	–13 ≤ h ≤ 13 –17 ≤ k ≤ 17 –18 ≤ l ≤ 18	–21 ≤ h ≤ 23 –24 ≤ k ≤ 24 –24 ≤ l ≤ 24	–13 ≤ h ≤ 13 –17 ≤ k ≤ 17 –19 ≤ l ≤ 19
Reflections collected	45824	119144	42565
Independent reflections	8136 R_{int} = 0.1049 R_{sigma} = 0.0892	23551 R_{int} = 0.0847 R_{sigma} = 0.0595	8478 R_{int} = 0.1007 R_{sigma} = 0.0906
Completeness to θ = 40.784°	99.6 %	98.6 %	99.3 %
Data / Restraints / Parameters	8136/3038/1544	23551/3570/1887	8478/2659/1399
Goodness-of-fit on F^2	1.040	1.031	1.114
Final R indexes [I≥2σ(I)]	R_1 = 0.0836 wR_2 = 0.2313	R_1 = 0.0645 wR_2 = 0.1611	R_1 = 0.0933 wR_2 = 0.2701
Final R indexes [all data]	R_1 = 0.1351 wR_2 = 0.2659	R_1 = 0.0811 wR_2 = 0.1740	R_1 = 0.1349 wR_2 = 0.3009
Largest peak/hole [eÅ^{-3}]	0.89/–0.41	1.55/–0.77	1.16/–0.67

(a) [Pd_2 $\mathbf{ABCD^2}$**](BF_4)$_4$**

Yellow needle-shaped crystals of [Pd_2**$\mathbf{ABCD^2}$**](BF_4)$_4$ were grown by slow vapor diffusion of benzene into a solution of the cage in CD_3CN.

The crystals were prone to a loss of solvent after removal from the mother liquor and rapid handling in NVH oil prior to flash cooling in liquid nitrogen was required to collect data. Despite these measures and the use of copper source, few reflections at greater than 1.18 Å resolution were observed and the data were trimmed accordingly. Data were collected in-house on a Bruker D8 venture diffractometer equipped with an INCOATEC microfocus sealed tube (Iμs 3.0) using CuK_α radiation at 100 K. The data was integrated with APEX3 and the structure was solved by intrinsic phasing/direct methods using SHELXT and refined with SHELXL for full-matrix least-squares routines on F^2 and ShelXle as a graphical user interface.

Specific refinement details

Stereochemical restraints for the ligands **A**, **B**, **C**, $\mathbf{D^2}$ were generated by the GRADE program using the GRADE Web Server (http://grade.globalphasing.org) and applied in the refinement. A GRADE dictionary for SHELXL contains target values and standard deviations for 1,2-distances (DFIX) and 1,3-distances (DANG), as well as restraints for planar groups (FLAT). All displacements for non-hydrogen atoms were refined anisotropically. The refinement of ADP's for carbon, nitrogen and oxygen atoms was enabled by a combination of similarity restraints (SIMU) and rigid bond restraints (RIGU). The contribution of the electron density from disordered counterions and solvent molecules, which could not be modeled with discrete atomic positions were handled using the SQUEEZE routine in PLATON. The solvent mask file (.fab) computed by PLATON was included in the SHELXL refinement via the ABIN instruction leaving the measured intensities untouched.

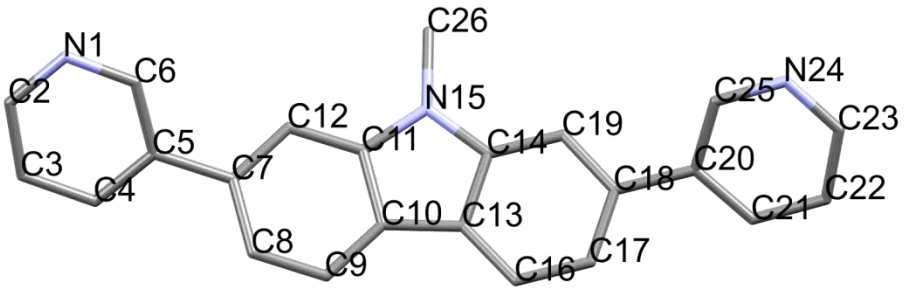

Supplementary Figure 297 | Atomic numbering scheme of residue FNC (ligand $\mathbf{D^2}$).

(b) [Pd_2 $\mathbf{ABD^4C}$**](BF_4)$_4$**

Yellow needle-shaped crystals of [Pd_2**$\mathbf{ABD^4C}$**](BF_4)$_4$ were grown by slow vapor diffusion of benzene into a solution of the cage in CD_3CN.

Data were collected in-house on a Bruker D8 venture diffractometer equipped with an INCOATEC microfocus sealed tube (Iμs 3.0) using CuK_α radiation at 100 K. The data was integrated with APEX3 and the structure was solved by intrinsic phasing/direct methods using SHELXT and refined with SHELXL for full-matrix least-squares routines on F^2 and ShelXle as a graphical user interface.

Specific refinement details

Stereochemical restraints for the ligands **A**, **B**, $\mathbf{D^4}$, **C** were generated by the GRADE program using the GRADE Web Server (http://grade.globalphasing.org) and applied in the refinement. A GRADE dictionary for SHELXL contains target values and standard deviations for 1,2-distances (DFIX) and 1,3-distances (DANG), as well as restraints for planar groups (FLAT). All displacements for non-hydrogen atoms were refined anisotropically. The refinement of ADP's for carbon, nitrogen and oxygen atoms was enabled by a combination of similarity restraints (SIMU) and rigid bond restraints (RIGU). The contribution of the electron density from disordered counterions and solvent molecules, which could not be modeled with discrete atomic positions were handled using the SQUEEZE routine in PLATON. The solvent mask file (.fab) computed by PLATON was included in the SHELXL refinement via the ABIN instruction leaving the measured intensities untouched.

(c) [Pd_2 $\mathbf{ABD^2D}$**](BF_4)$_4$**

Yellow needle-shaped crystals of [Pd_2**$\mathbf{ABD^2D}$**](BF_4)$_4$ were grown by slow vapor diffusion of Et_2O into a solution of the cage in CD_3CN.

The crystals employed immediately lost solvent after removal from the mother liquor and rapid handling in NVH oil prior to flash cooling in liquid nitrogen was required to collect data. Despite these measures and the use of copper source, few reflections at greater than 1.16 Å resolution were observed and the data were trimmed accordingly. Data were collected in-house on a Bruker D8 venture diffractometer equipped with an INCOATEC microfocus sealed tube (Iμs 3.0) using CuK_α radiation at 100 K. The data was integrated with APEX3 and the structure was solved by intrinsic phasing/direct methods using SHELXT and refined with SHELXL for full-matrix least-squares routines on F^2 and ShelXle as a graphical user interface.

Specific refinement details

Stereochemical restraints for the ligands **A**, **B**, **D²**, **D** were generated by the GRADE program using the GRADE Web Server (http://grade.globalphasing.org) and applied in the refinement. A GRADE dictionary for SHELXL contains target values and standard deviations for 1,2-distances (DFIX) and 1,3-distances (DANG), as well as restraints for planar groups (FLAT). All displacements for non-hydrogen atoms were refined anisotropically. The refinement of ADP's for carbon, nitrogen and oxygen atoms was enabled by a combination of similarity restraints (SIMU) and rigid bond restraints (RIGU). The contribution of the electron density from disordered counterions and solvent molecules, which could not be modeled with discrete atomic positions were handled using the SQUEEZE routine in PLATON. The solvent mask file (.fab) computed by PLATON was included in the SHELXL refinement via the ABIN instruction leaving the measured intensities untouched.

Supplementary Table 7. Summary of structural parameters of heteroleptic cage crystal structures. Ligand twist refers to the dihedral angles between ligand backbone core and the pyridyl motifs.

	$Pd_2A_2B_2$	Pd_2A_2CD	$Pd_2B_2CD^1$	$Pd_2B_2D^4C$	Pd_2AB^0CD	Pd_2ABCD	Pd_2ABCD^2	Pd_2ABD^4C	Pd_2ABD^2D
α	0	33.97	19.00	13.73	25.32	20.54	21.02	24.13	17.75
Pd–Pd distance	14.16	14.33	13.59	13.21	13.73	13.67	13.57	13.99	13.54
ligand **C** twist	-	34.87	36.51	41.75	40.03	37.57	36.61	39.8	32.42
ligand $\mathbf{D^n}$ twist	-	31.17	33.94	54.44	48.57	39.87	36.75	76.42	38.66

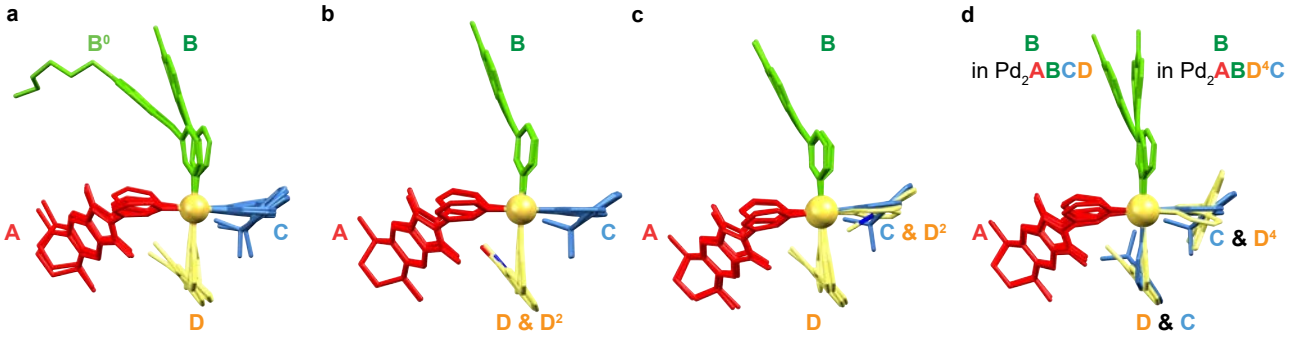

Supplementary Figure 298 | Top view of the overlapped crystal structures. **a,** $[Pd_2\mathbf{ABCD}](BF_4)_4$ and $[Pd_2\mathbf{AB^0CD}](BF_4)_4$, **b,** $[Pd_2\mathbf{ABCD}](BF_4)_4$ and $[Pd_2\mathbf{ABCD^2}](BF_4)_4$, **c,** $[Pd_2\mathbf{ABCD}](BF_4)_4$ and $[Pd_2\mathbf{ABD^2D}](BF_4)_4$, **d,** $[Pd_2\mathbf{ABCD}](BF_4)_4$ and $[Pd_2\mathbf{ABD^4C}](BF_4)_4$.

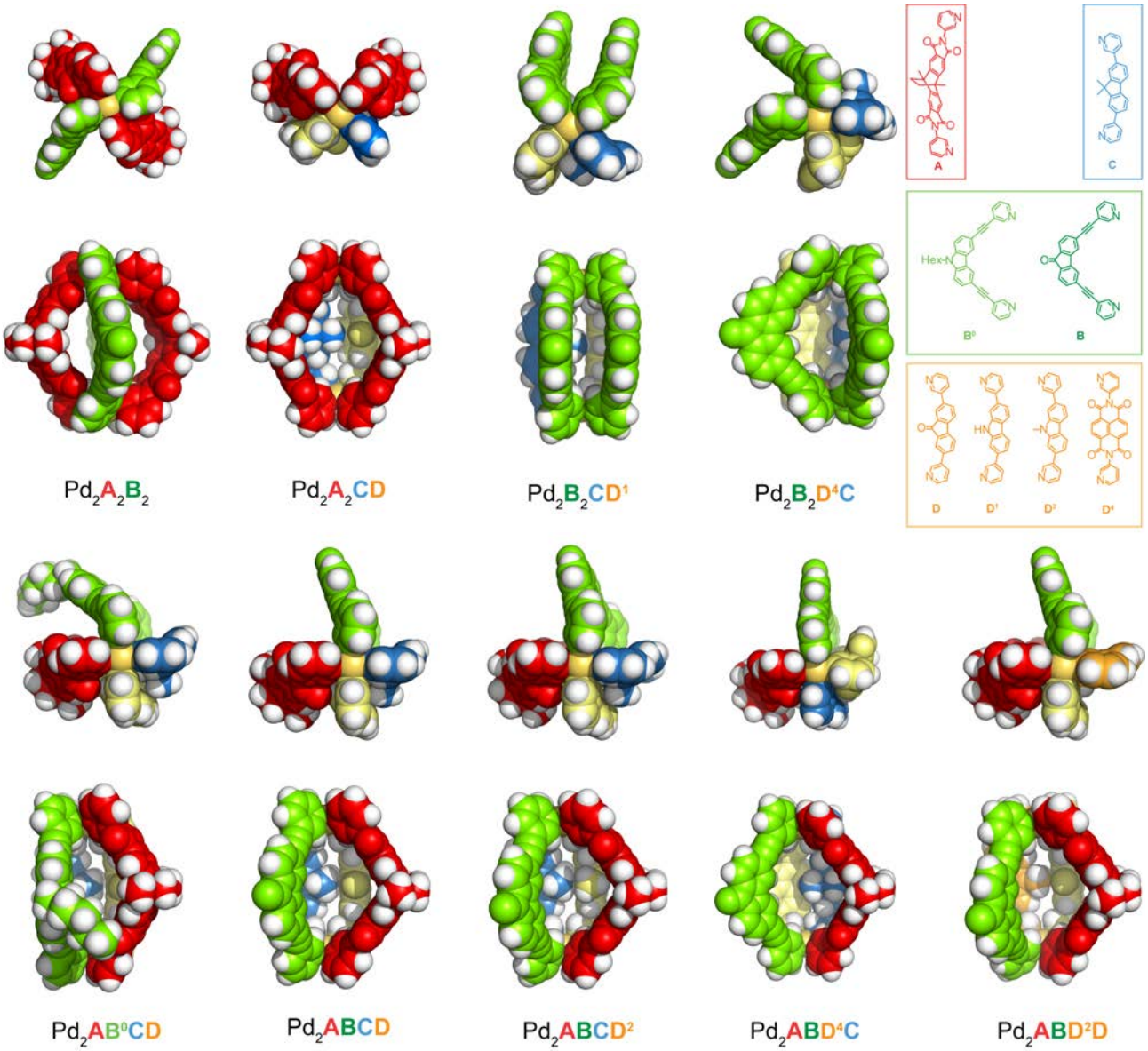

Supplementary Figure 299 | Top view and side view of the crystal structures in space-filling mode, revealing interligand interactions. Ligands **A**, **B**^{0}, **B**, **C**, **D**^{n}, and Pd^{II} are shown in red, green, blue and yellow, and brown, respectively.

9. References

1. Platzek, A. et al. Endohedrally Functionalized Heteroleptic Coordination Cages for Phosphate Ester Binding. *Angew. Chem., Int. Ed.*, DOI: 10.1002/anie.202209305 (2022).
2. Bordwell, F. G. & Hughes, D. L. Direct relationship between nucleophilicity and basicity in SN2 reactions of fluorenyl anions with benzyl chloride in dimethyl sulfoxide solution. *The Journal of Organic Chemistry* **45**, 3314–3320 (1980).
3. Chen, B., Holstein, J. J., Horiuchi, S., Hiller, W. G. & Clever, G. H. Pd(II) Coordination Sphere Engineering: Pyridine Cages, Quinoline Bowls, and Heteroleptic Pills Binding One or Two Fullerenes. *J. Am. Chem. Soc.* **141**, 8907–8913 (2019).
4. Rongmei, Z., Jens, L., Birger, D. & H., C. G. Stepwise Halide-Triggered Double and Triple Catenation of Self-Assembled Coordination Cages. *Angew. Chem., Int. Ed.* **54**, 2796–2800 (2015).
5. Croué, V. et al. A self-assembled M2L4 cage incorporating electron-rich 9-(1,3-dithiol-2-ylidene)fluorene units. *New J. Chem.* **41**, 3238–3241 (2017).
6. Wu, K., Zhang, B., Drechsler, C., Holstein, J. J. & Clever, G. H. Backbone-Bridging Promotes Diversity in Heteroleptic Cages. *Angew. Chem., Int. Ed.* **60**, 6403–6407 (2021).

7. Tessarolo, J., Lee, H., Sakuda, E., Umakoshi, K. & Clever, G. H. Integrative Assembly of Heteroleptic Tetrahedra Controlled by Backbone Steric Bulk. *J. Am. Chem. Soc.* **143**, 6339–6344 (2021).
8. Koshkakaryan, G. et al. Alternative Donor−Acceptor Stacks from Crown Ethers and Naphthalene Diimide Derivatives: Rapid, Selective Formation from Solution and Solid State Grinding. *J. Am. Chem. Soc.* **131**, 2078–2079 (2009).
9. Ebbert, K. E. et al. Resolution of minor size differences in a family of heteroleptic coordination cages by trapped ion mobility ESI-MS. *Dalton Trans.* **48**, 11070–11075 (2019).
10. Spartan 08 Version 1.2.0, Wavefunction, Inc., Irvine, CA, 2009.
11. Stow, S. M. et al. An Interlaboratory Evaluation of Drift Tube Ion Mobility–Mass Spectrometry Collision Cross Section Measurements. *Anal. Chem.* **89**, 9048–9055 (2017).
12. Hernandez, D. R. et al. Ion dynamics in a trapped ion mobility spectrometer. *Analyst* **139**, 1913–1921 (2014).
13. Greisch, J.-F. et al. Correlation of the structural information obtained for europium-chelate ensembles from gas-phase photoluminescence and ion-mobility spectroscopy with density-functional computations and ligand-field theory. *Phys. Chem. Chem. Phys.* **19**, 6105–6112 (2017).
14. Fernandez-Lima, F. A., Kaplan, D. A. & Park, M. A. Note: Integration of trapped ion mobility spectrometry with mass spectrometry. *Rev. Sci. Instrum.* **82**, 126106 (2011).
15. Sheldrick, G. M. SHELXT–Integrated space-group and crystal-structure determination. *Acta Crystallogr. Sect. A* **71**, 3–8 (2015).
16. Sheldrick, G. M. Crystal structure refinement with SHELXL. *Acta Crystallogr. Sect. C* **71**, 3–8 (2015).
17. Hubschle, C. B., Sheldrick, G. M. & Dittrich, B. ShelXle: a Qt graphical user interface for SHELXL. *J. Appl. Crystallogr.* **44**, 1281–1284 (2011).
18. Spek, A. L. PLATON SQUEEZE: a tool for the calculation of the disordered solvent contribution to the calculated structure factors. *Acta Crystallogr. Sect. C* **71**, 9–18 (2015).